ACTA CHIMICA

ACADEMIAE SCIENTIARUM HUNGARICAE

TOMUS 96 FASCICULUS 1

AKADÉMIAI KIADÓ, BUDAPEST

1978

ACTA CHIM. ACAD. SCI. HUNG. ACASA2 96 (1) 1–81 (1978)

ACTA CHIMICA

A MAGYAR TUDOMÁNYOS AKADÉMIA KÉMIAI TUDOMÁNYOK OSZTÁLYÁNAK IDEGEN NYELVŰ KÖZLEMÉNYEI

Acta Chimica is a journal for the publication of papers on all aspects of chemistry in English, German, French and Russian.

Acta Chimica is published in 4 volumes per year. Each volume consists of 4 issues of varying size.

Manuscripts should be sent to

Acta Chimica
H-1521 Budapest, Hungary

Correspondence with the editors should be sent to the same address. Manuscripts are not returned to the authors.

Subscription: $ 36.00 per volume.

Hungarian subscribers should order from Akadémiai Kiadó, 1363 Budapest, P.O. Box 24. Account No. 215 11488.

Orders from other countries are to be sent to "Kultura" Foreign Trading Company (H-1389 Budapest 62, P.O. Box 149. Account No. 218 10990) or its representatives abroad.

ACTA CHIMICA

ACADEMIAE SCIENTIARUM HUNGARICAE

TOMUS 96

AKADÉMIAI KIADÓ, BUDAPEST

1978

ACTA CHIMICA

TOMUS 96

FASCICULUS 1
FASCICULUS 2
FASCICULUS 3
FASCICULUS 4

INDEX

Acta Chimica Academiae Scientiarum Hungaricae, Tomus 96 (1), pp. 1—12 (1978)

ELECTROHYDROGENATION AND HYDROGENATION OF SIMPLE ALIPHATIC KETONES IN ACIDIC MEDIA

S. SZABÓ and GY. HORÁNYI

(Central Research Institute of Chemistry, Hungarian Academy of Sciences, Budapest)

Received January 12, 1976

The electrohydrogenation and hydrogenation of some simple ketones (2-butanone, 3-pentanone, 3-methyl-2-butanone and 2-pentanone) were investigated on a platinum catalyst in acidic media. Hydrocarbons were always formed during these reactions but whereas butanone gave mainly hydrocarbons, in the case of pentanones the corresponding secondary alcohol was the main product. The results and literature data permit the conclusion that in the electrohydrogenation of ketones the alcohol and the hydrocarbon are not formed *via* two independent paths but are rather the products of a branching reaction. The rate determining step occurs prior to branching.

In earlier communications [1, 2] we discussed hydrogenation and electrohydrogenation of acetone on a platinum catalyst and a platinum electrode. It was found, in accordance with the experimental results of other authors [3—7], that under given experimental conditions propane is the only product of hydrogenation or electrohydrogenation. In contrast to this, no gaseous product is formed in alkaline media, and also the rate is significantly lower than in acidic media. In the present work, in connection with the hydrogenation and electrohydrogenation of some simple aliphatic ketones: 2-butanone (ethyl methyl ketone), 2-pentanone (methyl propyl ketone), 3-pentanone (diethyl ketone), 3-methyl-2-butanone (isopropyl methyl ketone) in acidic media, we intend to find out whether the regularities observed in the case of acetone may be considered as general.

Experimental

The method applied was essentially the same as that used by us earlier. Prior to use, the ketones were purified by distillation. 1 *M* $HClO_4$ served as background solution. The gaseous products were analyzed by gas chromatography.

Results

In the case of all ketones examined, also gaseous components were found among the products of hydrogenation and electrohydrogenation. The composition of the gaseous products is illustrated in Fig. 1. It appears from

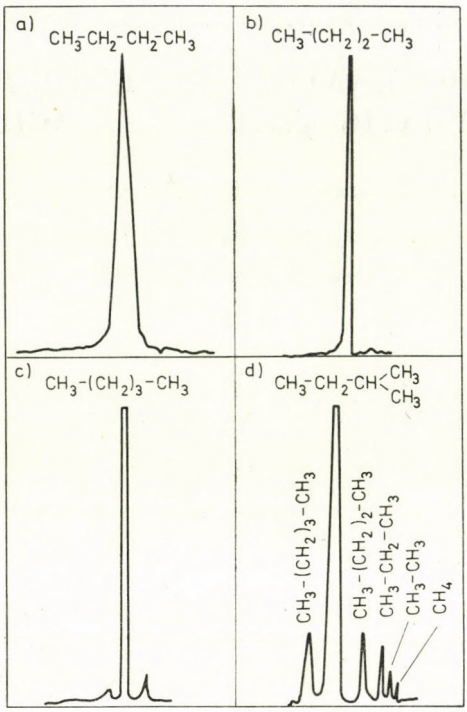

Fig. 1. Gas chromatogram of the gaseous products for the electrohydrogenation of (a) 2-butanone; (b) 2-pentanone; (c) 3-pentanone; (d) 3-methyl-2-butanone

Fig. 1 that besides the hydrocarbon which can be expected on the basis of the reaction

$$R - \underset{\underset{O}{\|}}{C} - R' + 2H_2 \longrightarrow R - CH_2 - R' + H_2O$$

other hydrocarbons are formed in considerable amounts only in the case of 3-methyl-2-butanone.

Consequently, in the case of 3-methyl-2-butanone, methane, ethane, propane, butane and *n*-pentane are present in addition to 2-methylbutane, the latter being the predominant component of the gaseous product.

Accordingly, in addition to the hydrogenation of the oxo-group, also reductive cleavage of the carbon chain and an intramolecular rearrangement take place. It is however conspicuous that isobutane is not present among the products, indicating that no splitting occurs in the carbon chain of 3-methyl-2-butanone between C_1 and C_2.

Presumably the rearrangement resulting in *n*-pentane and the rupture of the carbon chain take place with some of the intermediates of the hydrogenation reaction.

Theoretically it could be imagined that the splitting reaction is preceded by the rearrangement. However, the fact that in the case of 3-pentanone and 2-pentanone, whose chains are unbranched, the hydrogenation reaction is not accompanied by a considerable chain rupture, contradicts this assumption.

The formation of *n*-butane, provided that chain splitting is not preceded by rearrangement, can be imagined in a way that the methyl group attached to the main chain is split off in a reductive manner:

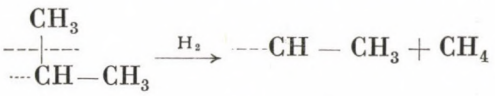

For the formation of propane and ethane the reaction scheme

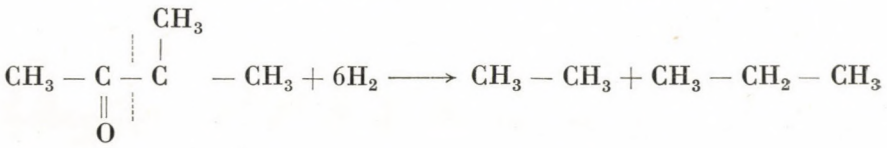

can be given.

This indicates that the reaction of 3-methyl-2-butanone is significantly more complex than those of simpler ketones, which, similarly to acetone, give only a single hydrocarbon. Therefore, in the following we shall discuss in detail only the problems concerning the hydrogenation of 2-butanone, 3-pentanone and 2-pentanone.

The fact that the gaseous products are of uniform nature does not mean it in itself that no other products are actually formed during hydrogenation or electrohydrogenation. Whereas in case of acetone we could maintain experimental conditions under which propane was the sole product of the reaction, this could not be attained in the case of the other ketones investigated. With the lengthening of the carbon chain of the ketone the formation of the corresponding secondary alcohols begins to predominate. In the case of 2-butanone the current efficiency during electrohydrogenation was only about 70—80% referred to butane, as supported by the results obtained by the method applied also earlier. At the same electrode hydrogen was evolved without 2-butanone at the same current density as that applied in the electrohydrogenation of 2-butanone, and the volume of the hydrogen evolved was measured as a function of time.

The current efficiency can be determined from the ratio of the slopes of the straight lines obtained upon plotting the volume of hydrogen evolved *vs.* time taking into account that according to the reaction

$$2\,H^+ + 2\,e^- \rightarrow H_2$$

a charge of 2F is required for the evolution of 1 mol hydrogen, whereas 4F are required for the formation of 1 mol butane. The volume *vs.* time curves are shown in Fig. 2.

Catalytic hydrogenations carried out on powdered platinum gave similar results. The product retained in the liquid phase proved to be 2-butanol. (Some experiments were carried out in a preparative hydrogenation apparatus in which 1/2 mol of ketone was hydrogenated. The products in the liquid

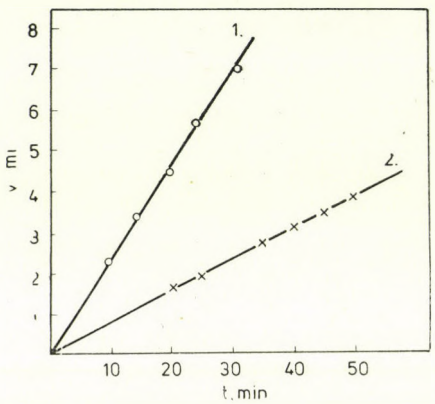

Fig. 2. Volume *vs.* time curves for (1) hydrogen evolution; (2) reduction of 2-butanone (i = = 30 mA)

phase were obtained by extraction with ether followed by drying, and the product was processed by microdistillation after the removal of ether.) In the case of C_5 ketones the product composition was shifted more and towards the alcohols. From 80—90% of the ketone converted, the corresponding secondary alcohol was formed.

The shape of the polarization curves in the case of the investigated ketones deviates to certain extent from that obtained in the presence of acetone.

The rather wide limiting current section observed for acetone became shorter to such an extent that sometimes it could not be distinguished. Under identical experimental conditions the apparent rate of electrohydrogenation, the current passing through the system showed the highest values generally in the case of acetone; at potentials of about 70—100 mV the following order given was observed:

$$\text{acetone} > \text{2-butanone} > \text{2-pentanone} > \text{3-pentanone}$$

The polarization curves of the various ketones are shown in Fig. 3.

On applying a suitable anodic prepolarization, polarization curves best resembling that of acetone were obtained in the case of 2-butanone.

Thus, *e.g.* the maximum and minimum values appearing in the limiting current section can be observed also in this case as indicated by Fig. 4. The decrease of the limiting current, as already discussed in connection with acetone, can be ascribed presumably to more extensive formation of alcohol [1].

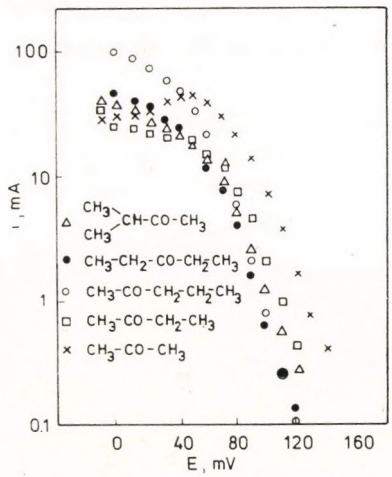

Fig. 3. Polarization curves of various ketones

The similarity observable in the polarization properties of acetone and 2-butanone can be understood because in both cases the formation of the hydrocarbon is the predominant process.

In the case of various pentanones the assumption of the limiting current appears already slightly forced though the slope of the *i vs. E* curves undoubtedly decreases to certain extent on changing the potential in the negative direction. Thus, certain similarity remains in the nature of the

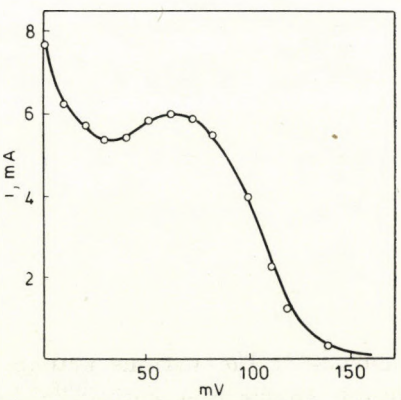

Fig. 4. Polarization curve of 2-butanone at a butanone concentration of 0.2 mol/l

polarization curves though, as already shown, the formation of the hydrocarbon is rather suppressed in the case of these compounds.

It should be noted that the comparison of the polarization curves of the various ketones is justified only to a limited extent because the current (i) can be correlated with the consumption rate or the ketone (w_k) only on taking into account the composition of the product. If the product is not uniform or when various reactions are possible, *e.g.* when hydrocarbon and alcohol are formed at the same time, the measured current will be

$$i = z_1 F w_1 + z_2 F w_2$$

where

$$w_1 = \frac{dn_1}{dt}, \qquad w_2 = \frac{dn_2}{dt}$$

is the amount (in mol) formed in unit time from one and the other product. In the steady state, the rate of ketone consumption is $w_k = w_1 + w_2$. On denoting by α the ratio of the rates of formation of the two types of products, *i.e.*

$$\alpha = \frac{w_1}{w_2}$$

we obtain that

$$i = z_1 F \alpha w_2 + z_2 F w_2$$

Since for alcohol formation $z_1 = 2$ and for hydrocarbon formation $z_2 = 4$,

$$i = 2 F w_2(\alpha + 2)$$

and

$$i = 2Fw_k \frac{(\alpha + 2)}{1 + \alpha}$$

Thus, the rate of consumption of the ketone is given by

$$w_k = \frac{(1 + \alpha)}{\alpha + 2} \frac{i}{2F}$$

It appears from this equation that even in the case of identical values of w_k, various currents can be measured, depending on the size of α. The theoretically possible values are located in the interval $2 F w_k - 4 F w_k$. The changes appearing in the limiting current of acetone were discussed on the basis of similar considerations [1].

As both reactions are presumably preceded by the adsorption of the ketone and since it is conceivable that the reactions leading to alcohol and

hydrocarbon have a common intermediate, it is of interest to investigate the relationships existing between the measured currents and the rate of ketones consumption.

In the literature there are studies on butanone, where both the current and the product distribution were examined simultaneously [5]. These investigations related to aging processes taking place under given experimental

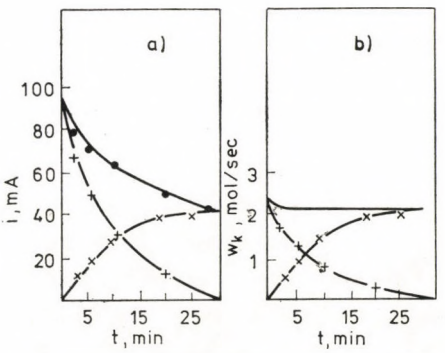

Fig. 5. (a) Current of electrohydrogenation plotted against time for 2-butanone. ● Overall current; + current corresponding to butane formation; × current corresponding to 2-butanol formation; (b) values of Fig. 5a expressed as rates of ketone consumption. The curve without dots is the resultant rate curve

conditions, are shown in Fig. 5a. According to Fig. 5a, under pote ntiostatic conditions the current passing through system, when plotted against time, shows a monotonous decrease, and in parallel to this, also the amount of the formed hydrocarbon decreases. At the same time the quantity of secondary butanol formed will be gradually greater and it will finally become the sole product of the reaction. The decrease of the current is explained by the deactivation, or aging, of the electrode. On calculating, from the current *vs.* time curves corresponding to the various products, the rates of formation of butane and butanol, respectively, referred to butanone consumed in the reaction, the curves in Fig. 5b are obtained. It appears from this figure that no significant change takes place in the rate of butanone consumption, though appreciable variations occur in the product composition.

The fact that though no changes occur in the rate of reaction, the selectivity is altered to a significant extent, prompts one to investigate whether the routes leading to hydrocarbon and alcohol may be independent of each other. Namely, according to certain assumptions [5], the formation of alcohol is connected with a reaction involving interstitial hydrogen in the platinum lattice. At the same time it is as sumed that the adsorption properties of platinum are modified by this hydrogen, resulting in a decrease of ketone adsorption and together with that, in a decrease of the reaction rate.

On the basis of the above results and the considerations outlined, it is rather difficult to suppose that the rates of the reaction of butanone *via* two independent routes would be the same. On the basis of Fig. 5b it is more likely that the initial steps, and presumably also the rate-determining step, are identical in both cases. The change observed in selectivity would then be due to the fact that the branch of the reaction leading to the hydrocarbon is gradually suppressed for reasons unknown as yet.

The above considerations are justified not only in the case of butanone. It is known from the literature that the composition of products changes also in the electrohydrogenation of acetone, depending on the nature of catalyst. The electrohydrogenation of acetone was investigated by SEMENOVA *et al.* [6] in the presence of platinum–iridium skeleton catalysts. It was found that at a given potential the current efficiency referred to isopropanol rises with increasing iridium content of the catalyst but at the same time also the current required for electrohydrogenation decreases. Table I was constructed on the basis of the data and curves given by SEMENOVA *et al.* [6].

The current resulting in the formation of hydrocarbon can be calculated from the data given in Table I in the following way:

$$i_{\text{hydrocarbon}} = i\left(1 - \frac{p}{100}\right)$$

Table I

Electrohydrogenation of acetone on Pt–Ir skeleton catalysts at 100 mV [6]

Composition of catalyst	Current efficiency referred to isopropanol, p (%)	Current, i (mA)
Pt	6.3	1.8
90% Pt–Ir	11	1.7
75% Pt–Ir	29	1.5
50% Pt–Ir	48	1.4
40% Pt–Ir	56	1.15
25% Pt–Ir	70	1.0
10% Pt–Ir	80	0.83
Ir	80	0.71

and the rate of reaction is:

$$w_k = \frac{i_p}{2F100} + i\left(1 - \frac{p}{100}\right)\frac{1}{4F} = \frac{i}{4F}\left(1 + \frac{p}{100}\right)$$

The rates of reaction calculated for skeleton catalysts of various compositions are summarized in Table II. The rates corresponding to the formation of propane and the alcohol are plotted in Fig. 6 against the concentration of iridium in the catalyst. The overall rate given also in Table II does not show appreciable changes even at high iridium concentrations, and it increases rather than decreases. A considerable decrease in the rate was observed only at iridium contents above 60%. Thus, the increase of the proportion of alcohol in the product is in this case not accompanied by a decrease of reaction rates. Similarly to butanone, data are available also concerning the electrohydrogenation of acetone on a platinum electrode. These data show changes in the composition of the product.

Table II

Reaction rate referred to acetone consumption as a function of the catalyst composition [6]

Composition of catalyst	w_k $10^{-9}w$(mol/sec)
Pt	4.96
90% Pt–Ir	4.89
75% Pt–Ir	5.01
50% Pt–Ir	5.37
40% Pt–Ir	4.65
25% Pt–Ir	4.40
10% Pt–Ir	3.87
Ir	3.31

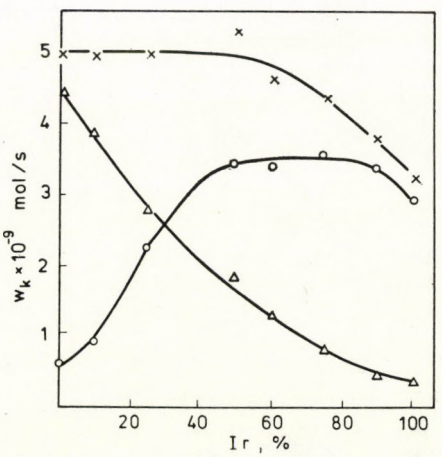

Fig. 6. Electrohydrogenation of acetone on Pt–Ir alloys. Rate of the formation of propane ($\Delta\,\Delta$) and of propanol (o o) *vs.* the Ir concentration at 100 mV

The values calculated on the basis of the experimental data given by DE HEMPTINNE *et al.* [3] are presented in Table III, using the symbols applied above. These values indicate that w_k (the amount of acetone consumed in unit time) did not decrease even after 3.5 hrs, whereas the value of α (the alcohol to hydrocarbon ratio) increased by a full order of magnitude.

Table III

Changes in the rate of the electrohydrogenation of acetone and isopropanol to propane ratio as a function of time

t (brs)	α	i (A)	w_k (mol/sec)
0	0.18	0.165	4.6×10^{-7}
0.5	0.26	0.16	4.6×10^{-7}
1	0.42	0.155	4.7×10^{-7}
1.5	0.50	0.15	4.6×10^{-7}
2	0.66	0.145	4.7×10^{-7}
2.5	0.88	0.142	4.8×10^{-7}
3	1.22	0.13	4.6×10^{-7}
3.5	1.80	0.125	4.7×10^{-7}

In accordance with the above discussion also these data confirm that the formation of alcohol and hydrocarbon cannot be processes completely independent of each other.

On the basis of the present observations and the literature data we may attempt a qualitative interpretation of the phenomena occurring during the stationary processes. Let us assume that one or several initial steps of the series of reactions leading to hydrocarbon and alcohol are identical, and that at the beginning of the measurements the rate determining step is one of these. The overall reaction can be characterized by the scheme

$$A \xrightarrow{k_1} B \begin{array}{l} \xrightarrow{k_2} C(\text{hydrocarbon}) \\ \xrightarrow[k_3]{} D(\text{alcohol}) \end{array}$$

where routes $A \rightarrow$, $B \rightarrow C$ and $B \rightarrow D$ denote reactions which may comprise also several elementary steps and which can be characterized by the apparent rate constants k_1, k_2 and k_3. If $k_1 \ll k_2$, $k_1 \ll k_3$ and $k_1 \ll k_2 + k_3$, then the rate determining step is in route $A \rightarrow B$. The ratio of products will depend on the k_2 to k_3 ratio. If $k_2 \gg k_3$, then the product will be practically pure hydrocarbon.

If however effects affecting (*e.g.* decreasing) the relative and absolute values of k_2 and k_3, occur the overall rate under otherwise identical conditions will remain stable until the above inequalities for k_1, k_2 and k_3 are still valid. At the same time if k_2 and k_3 are not changing to the same extent (*e.g.* k_2 decreases faster than k_3), the proportion of hydrocarbons in the product will decrease. Accordingly, the phenomena observed by us can be explained by the decrease of the value of apparent rate constants k_2 and k_3 belonging to reaction routes $B \rightarrow C$ and $B \rightarrow D$ (k_2 decreasing to a greater extent that k_3). As was discussed above, this does not imply that the rate of the overall process should change at the same time though the product will be already practically pure alcohol if $k_3 \gg k_2$. However, k_3 and k_2 may decrease further to such an extent that k_1 will be only slightly smaller than k_3 or eventually commensurable with k_1 or even smaller than k_1, and thus the rate of the overall process will be determined ever more by process $B \rightarrow D$, and this rate will be already lower than at the beginning of the measurements.

In our opinion the phenomena observed in the electroreduction of 2-butanone and acetone can be adequately interpreted in this way. Only hypotheses can be set up concerning the causes leading to changes in selectivity, *e.g.* the irreversible adsorption of the oxo-compound or of the products of its reduction, *e.g.* of the alcohol. These problems require still further investigations. Anyhow, we succeeded in pointing out that extreme care is needed in the interpretation of the processes taking place during the electrohydrogenation of ketones.

The same can be stated concerning the comparison of the polarization curves of various ketones because in this case currents and current densities belonging to the various potentials are being compared.

However, it is quite obvious from what has been said that this comparison is justifiable only if the alcohol to hydrocarbon ratio is also identical, which occurs very rarely.

Polarization curves reflect in an unequivocal way the reduction of ketones only if only one product may be formed or if both products may be formed but the ratio of the products does not change with the potential and with the experimental conditions. In the case of acetone, it was possible to draw the kinetic conclusions described earlier [1, 2] because under given conditions only propane was formed. On generalizing the results referring to acetone and 2-butanone [2—5], the relationship

$$w_k = \frac{Bc_k}{1 + Dc_k 10^{bE}}$$

can be given for the value of w_k, whereas the polarization curve can be described by the relationship

$$i = zF \frac{Bc_k}{1 + Dc_k 10^{bE}}$$

where B, D and b are constants, c_k is the concentration of the ketone, E is the potential and

$$z = 2\,\frac{\alpha + 2}{\alpha + 1}$$

If α depends on the potential and on the lifestory of the electrode (and, as we have shown, this is frequently the case), the polarization curve may exhibit very diversified shapes.

REFERENCES

[1] HORÁNYI, G., SZABÓ, S., SOLT, J., NAGY, F.: Acta Chim. Acad. Sci. Hung., **68,** 205 (1971); HORÁNYI, GY., SOLT, J., SZABÓ, S., NAGY F.: Magy. Kém. Folyóirat, **76,** 333 (1970); HORÁNYI, GY., SZABÓ, S., SOLT, J., NAGY, F.: Magy. Kém. Folyóirat **77,** 568 (1971)
[2] HORÁNYI, G., SZABÓ, S., SOLT, J., NAGY, F.: Acta Chim. (Budapes) **71,** 239 (1972); SOLT, J., SZABÓ, S., HORÁNYI, GY., NAGY, F.: Magy. Kém. Folyóirat, **77,** 17 (1971)
[3] DE HEMPTINNE, X., SCHUNCK, K.: Ann. Soc. Sci. Bruxelles, **80,** 289 (1966)
[4] DE HEMPTINNE, X., SCHUNCK, K.: Trans. Faraday Soc., **65,** 591 (1969)
[5] FLOREQUIN, P., LARMUSEAU, H., DE HEMPTINNE, X.: Ann. Soc. Sci. Bruxelles, **88,** 241 (1974)
[6] SEMENOVA, A. D., KROPOTOVA, N. V., VOVCHENKO, G. D.: Elektrokhimiya, **10,** 1233 (1974)
[7] SEMENOVA, A.D., KROPOTOVA, N. V., VOVCHENKO, G. D.: Elektrokhimiya, **10,** 621 (1974)

György HORÁNYI
Sándor SZABÓ
} H-1525 Budapest Pf. 17.

Acta Chimica Academiae Scientiarum Hungaricae, Tomus 96 (1), pp. 13—18 (1978)

APPLICATION OF FLORY'S THEORY FOR CALCULATING EXCESS THERMODYNAMIC FUNCTIONS OF THE SYSTEMS PIPERIDINE–TETRAHYDROPYRANE; PIPERIDINE–CYCLOHEXANE AND TETRAHYDRO-PYRANE–CYCLOHEXANE

J. D. PANDEY and R. L. MISHRA

(Department of Chemistry, University of Allahabad)

Received June 28, 1976
In revised form January, 15, 1977

Statistical theory due to FLORY has been applied to the systems: piperidine–tetrahydropyrane; piperidine–cyclohexane and tetrahydropyrane–cyclohexane. Excess thermodynamic functions as a function of temperature and composition have been evaluated and results were used to examine the theory.

Introduction

Successful attempts [1—6] have been made to test FLORY's theory in the light of excess thermodynamic functions [7, 8] using thermodynamic data. Very few attempts [9] have been made to study the excess thermodynamic functions in the light of FLORY's theory using ultrasonic measurements. In the present investigation excess volume (V^E), excess enthalpy (H^E), excess isothermal compressibility ($\varkappa_T^E$), excess thermal pressure coefficient (γ^E) and excess entropy (TS^E) were studied in the light of FLORY's theory for associated mixtures of piperidine–tetrahydropyrane, piperidine–cyclohexane and tetrahydropyrane–cyclohexane using ultrasonic velocity and compressibility data of MOELWYN-HUGHES and THORPE [10].

Theoretical

The numerical evaluation of characteristic parameters V^*, T^* and P^* and reduced parameter $\tilde{V}$, $\tilde{T}$ and $\tilde{P}$ for each of the pure components and corresponding parameters as well as segment fractions (Φ_1 and Φ_2), site fraction (θ_2) and reduced excess volume ($\tilde{V}^E$) of the mixture were made according to the procedure adopted by FLORY [11, 12]. Experimental excess volumes were used in the present investigation to calculate energy parameter

X_{12}. The excess functions were calculated using the following equations:

$$V^E = (x_1 V_1^* + x_2 V_2^*)\tilde{V}^E \tag{1}$$

$$H^E = x_1 V_1^* P_1^* \left(\frac{1}{\tilde{V}_1} - \frac{1}{\tilde{V}}\right) + x_2 V_2^* P_2^* \left(\frac{1}{\tilde{V}_2} - \frac{1}{\tilde{V}}\right) + \frac{x_1 V_1^* \theta_2 X_{12}}{\tilde{V}} \tag{2}$$

$$\varkappa_T^E = \frac{3\tilde{V}^2(\tilde{V}^{1/3} - 1)}{P^*[1 - 3(\tilde{V}^{1/3} - 1)]} - \frac{1}{\tilde{V}}(\Phi_1 \tilde{V}_1 \varkappa_{T,1} + \Phi_2 \tilde{V}_2 \varkappa_{T,2}) \tag{3}$$

$$-TS^E = 3x_1 V_1^* \tilde{T}_1 P_1^* \ln (\tilde{V}_1^{1/3} - 1)/(\tilde{V}^{1/3} - 1) + \\ + 3x_2 V_2^* \tilde{T}_2 P_2^* \ln (\tilde{V}_2^{1/3} - 1)/(\tilde{V}^{1/3} - 1) \tag{4}$$

Excess thermal pressure coefficient was calculated using the relation:

$$\gamma^E = \gamma - (x_1\gamma_1 + x_2\gamma_2) \tag{5}$$

The calculated thermal pressure coefficient γ was obtained from P^* for the solution, as given by the equation:

$$P^* = (\Phi_1 P_1^* + \Phi_2 P_2^* - \Phi_1 \theta_2 X_{12}) = \frac{T\tilde{V}^{4/3}}{(\tilde{V}^{1/3} - 1)} \times \left[\frac{\Phi_1 P_1^*}{T_1^*} + \frac{\Phi_2 P_2^*}{T_2^*}\right] \tag{6}$$

by resort to equation

$$P^* = \gamma\, T\, \tilde{V}^2 \tag{7}$$

Results and discussion

Values of characteristic parameters are listed in Table I. Here and throughout this paper, mole fractions are those of the first named component of each system. The abbreviations P, T and C respectively denote piperidine, tetrahydropyrane and cyclohexane.

Table I

Parameters for the pure liquids

T °K	V C.C. mol^{-1}	$\varkappa_T \times 10^6$ atm^{-1}	$\alpha \times 10^3$ deg^{-1}	γ (calcd.) Cal CC^{-1} deg^{-1}	$\tilde{V}$	V^* C.C. mol^{-1}	T^* °K	P^* Cal CC^{-1}
				Piperidine				
293	98.86	79.8	1.055	0.320	1.2554	78.7478	5037.8	147.7
313	100.98	91.8	1.077	0.284	1.2653	78.8071	5250.0	142.3
				Tetrahydropyrane				
293	97.44	93.4	1.123	0.292	1.2695	76.7546	4864.7	137.8
313	99.69	108.1	1.155	0.258	1.2896	77.3030	4965.0	134.3
				Cyclohexane				
293	108.08	111.6	1.224	0.265	1.2875	83.9456	4669.3	128.7
313	110.79	130.4	1.254	0.232	1.3100	84.5725	4772.0	124.6

The excess volume

The $V^E_{(\text{calcd.})}$ are subject to vitiation by errors in T^* and P^* for the pure components. The former parameter depends on the thermal expansion coefficient α, the latter is mainly determined by the thermal pressure coefficient γ.

According to the relationship given by FLORY [11], the effect on $V^E_{(\text{calcd.})}$ of an error in α_2 is approximately proportional to $(P^*_2 - P^*_1)\ x\ (P^*_2 + P^*_1)^{-1}$ and sensitivity of V^E to γ_2 is proportional to the difference $(\tilde{T}_2 - \tilde{T}_1)$. Because the comparatively large difference between the thermal expansion coefficients and less difference between the thermal pressure coefficients, the effect on $V^E_{(\text{calcd.})}$ of an error in γ is larger than the effect of an error in α, in the present systems under investigation. An examination of Table II shows that $V^E_{(\text{exptl.})}$ are in good agreement in sign but not in magnitude with FLORY's value. The lower value of $V^E_{(\text{calcd.})}$ is due to making the approximation that $P^*_1 = P^*_2$ and $\theta_2 X_{12} \approx 0$ in Eq. (5), so that $\tilde{T}$ is given by $\tilde{T} = \Phi_1 \tilde{T}_1 + \Phi_2 \tilde{T}_2$.

The excess enthalpy and excess entropy

Theoretical values of H^E have been calculated using X_{12} values derived from experimental excess volume [11, 12] and are shown in Table II. Largest discrepancy is seen in the system *P–C*. Agreement on the whole is quite satisfactory within the limits of error. An examination of Table II shows that the 'equation of state' contribution of H^E is positive for all the systems under investigation. This contribution depends [12, 14] not only on the reduced volume of the mixture and, therefore, on the excess volume but also on the difference between reduced volumes $\tilde{V}_1$ and $\tilde{V}_2$ of the pure components. The 'contact interaction term' $x_1 \theta_2 V^*_1 X_{12}/2 \tilde{V}$ is dominant, thereby rendering the enthalpy of mixing positive. The positive H^E values of the systems under investigation suggest that the systems are formed endothermally. $H^E_{(\text{exptl.})}$ for *P–C* is greater than that for *P–T* showing that N—H — — — O hydrogen bonds formed in the second systems are weaker than the N—H — — — N bonds solely present in the first. $H^E_{(\text{calcd.})}$ values also show the same trend. TS^E values are all positive for the systems under investigation.

The excess isothermal compressibility and the excess thermal pressure coefficient

Excess isothermal compressibilities have been calculated using X_{12} values evaluated from experimental excess volume [10] and experimental excess enthalpy [13]. $\varkappa^E_T$, using X_{12} values evaluated from H^E could not be

Table II

Comparison of calculated and observed excess quantities

Systems	Mole fraction	X_{12} Cal. cc. evaluated using expt. V^E		V calcd.		Eq. of state contribution to H^E cal. mol^{-1}		H^E cal mol^{-1}				V^Ecc mol^{-1}				TS^E cal mol^{-1} cald.	
								20 °C		40 °C		20 °C		40 °C			
		20 °C	40 °C	20 °C	40 °C	20 °C	40 °C	Cald.	Expt.	Cald.	Expt.	Cald.	Expt.	Cald.	Expt.	20 °C	40 °C
P–T	0.1990	4.70	5.50	1.2685	1.2865	13.5	14.1	59.7	56.9	47.3	47.0	0.02	0.14	0.02	0.15	14.4	11.2
	0.3516	3.61	1.86	1.2670	1.2835	19.4	20.3	82.4	85.8	40.1	69.0	0.01	0.20	0.02	0.21	20.1	8.7
	0.5072	1.89	2.32	1.2650	1.2799	21.6	22.5	69.3	94.2	58.2	79.6	0.02	0.22	0.01	0.23	15.9	12.9
	0.6732	2.84	5.59	1.2625	1.2758	19.8	21.6	115.0	80.4	136.3	67.1	0.58	0.20	0.01	0.22	27.5	33.0
	0.8252	1.24	2.22	1.2597	1.2714	14.9	15.6	65.9	48.5	71.6	71.3	0.33	0.15	0.02	0.16	14.3	16.3
P–C	0.2090	2.78	9.14	1.2833	1.3034	19.3	23.0	48.7	190.2	81.6	—	0.01	0.18	0.15	0.20	10.5	19.0
	0.3078	4.05	12.17	1.2789	1.2970	23.1	12.2	74.3	241.7	127.5	—	0.01	0.25	0.000	0.28	8.1	23.2
	0.5088	3.09	7.46	1.2747	1.2914	30.3	35.5	127.8	254.6	153.0	—	0.01	0.25	0.003	0.29	23.6	34.1
	0.6478	2.83	3.56	1.2698	1.2848	26.8	32.8	117.6	200.0	104.6	—	0.11	0.21	0.007	0.26	25.5	14.0
	0.8322	1.92	1.80	1.2622	1.2746	13.0	17.4	92.5	139.5	64.5	—	0.08	0.09	0.001	0.12	20.8	12.5
T–C	0.2548	3.44	19.42	1.2855	1.3123	16.6	46.4	56.2	108.8	188.0	—	0.02	0.19	0.00	0.60	13.6	51.9
	0.4833	2.80	15.49	1.2819	1.3112	20.2	74.4	81.6	140.2	289.6	—	0.008	0.22	0.01	0.94	19.9	78.8
	0.5236	2.25	10.77	1.2812	1.3104	20.3	68.0	73.8	138.7	280.8	—	0.006	0.22	0.02	0.86	17.0	73.1
	0.7383	1.75	5.23	1.2763	1.3043	14.0	58.0	72.7	98.4	169.7	—	0.022	0.14	0.008	0.71	17.2	45.2

Table III

Comparison of calculated and observed excess isothermal compressibility

System	Mole fraction	$\varkappa_T^E \times 10^6$ atm^{-1}						$-Y^E \times 10^2$ calcd. Cal cc^{-1} deg^{-1}	
		20 °C			40 C°				
		Calcd. using X_{12} from expt. V^E	Calcd. using X_{12} from expt. H^E	Expt.	Calcd. using $\varkappa_{12}$ from expt. V^E	Calcd. using $\varkappa_{12}$ from expt. H^E	Expt.	20 °C	40 °C
$P-T$	0.1990	1.5	0.6	0.6	0.7	0.7	0.5	0.245	0.185
	0.3516	1.55	0.9	0.8	0.1	0.2	0.7	0.340	0.176
	0.5072	1.6	1.8	0.9	0.2	0.4	0.7	0.299	0.239
	0.6732	2.4	2.1	0.8	1.1	0.3	0.7	0.454	0.486
	0.8252	1.1	1.4	0.4	— 1.1	— 1.4	0.4	0.272	0.266
$P-C$	0.2090	0.3	0.8	0.3	0.8	—	0.6	0.283	0.367
	0.3078	1.3	2.0	0.6	2.5	—	0.5	0.137	0.334
	0.5088	1.1	1.0	0.5	0.56	—	0.5	0.549	0.651
	0.6478	1.3	1.1	0.4	— 2.0	—	0.3	0.569	0.497
	0.8322	1.0	0.8	0.1	— 2.7	—	0.0	0.414	0.302
$T-C$	0.2548	1.7	1.7	1.4	8.9	—	2.1	0.283	0.737
	0.4833	2.4	2.2	2.1	13.3	—	2.6	0.399	0.115
	0.5236	2.1	2.1	2.0	10.4	—	2.7	0.375	0.962
	0.7383	1.9	1.5	1.6	7.4	—	2.2	0.351	0.752

calculated for P–C and T–C at 40 °C due to unavailability of experimental H^E at this temperature. The two sets of the theoretical $\varkappa_T^E$ values shown in Table III are in good agreement with each other as well as with $\varkappa_{T(\text{exptl.})}^E$. This agreement indicates that there is no esssential difference between the two procedures of evaluation of X_{12}. When there is an increase in the volume due to mixing, the solution can be compressed to a greater extent leading to an increase in the compressibility of the mixture *i.e.* V^E and $\varkappa_T^E$ should be of the same sign. Results presented in Tables II and III show that like experimental V^E and $\varkappa_T^E$, theoretical V^E and $\varkappa_T^E$ also have the same sign in all the systems under investigation with the exception of P–T and P–C at 40 °C when the mole fraction of piperidine is $x_1 = 0.8252$ and 0.8322, respectively. This may be attributed to the predominancy of the errors effective in the computation of P^* values for this set. A perusal of Table III shows that $\varkappa_{T(\text{exptl.})}^E$ values for the systems under investigation are in the order P–$C < P$–$T < T$–C, at the same temperature and corresponding mole fractions, this trend is also observed in $\varkappa_{T(\text{calcd.})}^E$ values. The greater the hydrogen bonding, the smaller is the intermolecular spacing, and hence lesser is the extent to which it can be compressed. Thus N—H — — — O hydrogen

bonds formed in the *P–T* system are weaker than N—H — — — N bonds solely present in the *P–C* system. Nuclear magnetic resonance spectra have provided evidence for the formation of these hydrogen bonds. In the systems *P–T* and *T–C*, $\varkappa^E_{T(\text{exptl.})}$ varies symmetrically with the composition of the mixture but the variation of $\varkappa^E_{T(\text{exptl.})}$ is unsymmetrical in the case of *P–C*, the maximum being displaced towards lower piperidine concentrations. The same sequence is observed in $\varkappa^E_{T(\text{calcd.})}$

Excess thermal pressure coefficients for the systems under investigation are negative at both temperatures. The theory fails to predict $\gamma^E = \gamma^E(x)$. However, in view of the inaccuracy in the values of P^* and α, it is difficult to offer any specific comments on this aspect.

*

The authors are grateful to Prof. R. D. TEWARI for providing electronic calculating machine.

REFERENCES

[1] JAIN, D. V. S., GUPTA, V. K., LARK, B. S.: Ind. J. Chem., **8,** 815 (1970)
[2] RASTOGI, R. P., JAGAN NATH, MISHRA, J.: J. Phys. Chem., **71,** 1277 (1967)
[3] NIGAM, R. K., SINGH, R. P.: Trans. Faraday Soc., **65,** 950 (1969)
[4] HOCKER, H., FLORY, P. J.: Trans. Faraday Soc., **65,** 1188 (1968)
[5] DELMAS, G., TURRELL, S.: Trans. Faraday Soc., **70,** 572 (1974)
[6] GORGE CALADO, C. G., GERALD, A. G., STAVELY, L. A. K.: Trans. Faraday Soc., **70,** 1445 (1974)
[7] ROWLINSON, J. S.: Liquids and Liquid Mixtures, Butterworths 1959
[8] GUGGENHEIM, E. A.: Mixtures, O. U. P. 1952
[9] HYDER KHAN, V., SUBRAHMANYAM, S. V.: Trans. Faraday Soc., **67,** 2282 (1971)
[10] MOELWYN-HUGHES, E. A., THORPE, P. L.: Proc. Roy. Soc., **277A,** 423 (1964)
[11] FLORY, P. J.: J. Amer. Chem. Soc., **82,** 1833 (1965)
[12] ABE, A., FLORY, P. J.: J. Amer. Chem. Soc., **87,** 1838 (1965)
[13] MOELWYN-HUGHES, E. A., THORPE, P. L.: Proc. Roy. Soc., **277A,** 423 (1964)
[14] FLORY, P. J., ORWOLL, R. A., VRIJ, A.: J. Amer. Chem. Soc., **86,** 3515 (1964)

J. D. PANDEY
R. L. MISHRA
Department of Chemistry, University of Allahabad, Allahabad-211002 India.

Acta Chimica Academiae Scientiarum Hungaricae, Tomus 96 (1), pp. 19—26 (1978)

STUDIES ON THE CHELATES OF SOME LESS COMMON TRANSITION METALS III

RU(III), RH(III), IR(III) AND PT(IV)

R. K. UPADHYAY* M. L. SINGHAL and A. K. BAJPAI

(Department of Chemistry and Department of Physics N. R. E. C. College, Khurja, India)

Received February 1, 1977

Electronic spectral studies of some less common transition metal complexes with four ketoanil ligands have been carried out in conjugation with ligand field theory for d–d and charge transfer transitions. Low spin octahedral stereochemistry established spectroscopically was verified magnetically. Abnormal paramagnetic behaviour exhibited by Rh(III), Ir(III) and Pt(IV) complexes has been accounted for second order Zeeman effect. Infrared spectral studies were employed, to investigate sites of co-ordination in ligands, and to elucidate complex structures. Electron repelling tendency of *para*-substituted groups of ligands has been found to exert direct influence on complex stability. Stability orders of the complexes (ligand or metal wise) have also been established and have been substantiated by 10 *Dq* values.

Introduction

Several attempts [1—8] have been made during last decade to investigate electronic spectra of platinum metal ions involving d^5 and d^6 configurations under the influence of octahedrally arranged ligands of different field strengths, but references [9—14] on these configurations under the perturbing fields of ketoanil ligands are scanty and hardly any attempt [11] has been made so far to investigate ketoanil–Ru(III) complex. The present communication in continuation to our previous work describes quantitatively in conjugation with ligand field theory the electronic spectral and magnetic features of some platinum metal ions, *viz.* Ru(III), Rh(III), Ir(III) and Pt(IV) complexed with four ketoanil ligands (abbreviated as *A*, *B*, *C* and *D*). Unusual paramagnetic behaviour of Rh(III), Ir(III) and Pt(IV) complexes established magnetically and verified spectroscopically has been explained in terms of second order Zeeman effect. Infrared spectral studies of complexes and ligands have also been carried out in order to elucidate their structures, to mark the sites of co-ordination and to establish their stability sequence and its substantiation by electronic spectral results.

A = *p*-Dimethylaminoanil of phenyl glyoxal
B = *p*-Diethylaminoanil of phenyl glyoxal
C = *p*-Bromoanil of phenyl glyoxal
D = *p*-Iodoanil of phenyl glyoxal

* Postal address: R. K. UPADHYAY, 57, Chhatta Street, Khurja, 203131, India.

Table I

Electronic spectral and magnetic characteristics

Complex	Bands cm^{-1}	Assignments	$10Dq$ (mm^{-1})	Racah's Parameters	L.F.S.E. (K/Cal. mol^{-1})	μ_{eff} B.M.	Nitrogen (%)		Metal (%)	
							Calc.	Found	Calc.	Found
RuA_2Cl_3	13333	$^2T_{2g} \rightarrow {}^4T_{1g}$	27833.25	B = 545.75	73.286	1.62	7.94	7.78	14.33	14.18
	17699	$\rightarrow {}^4T_{2g}$		C = 2183.00						
	18182	$\rightarrow {}^2A_{1g}$								
	21505	$\rightarrow {}^2A_{2g}$								
	23529	$\rightarrow 2\,{}^2E_g$								
	25000	$\rightarrow 2\,{}^2T_{1g}$								
	31250	—								
	40000	$L \rightarrow M$ Charge transfer								
RuD_2Cl_3	12987	$^2T_{2g} \rightarrow {}^4T_{1g}$	22580.25	B = 442.75	59.454	1.72	3.60	3.49	12.99	12.82
	16529	$\rightarrow {}^4T_{2g}$		C = 1771.00						
	18182	$\rightarrow {}^2A_{1g}$								
	21053	$\rightarrow {}^2A_{2g}$								
	24691	$\rightarrow 2\,{}^2E_g$								
	26667	$\rightarrow 2\,{}^2T_{1g}$								
	32258	—								
	40816	$L \rightarrow M$ Charge transfer								
RhA_2Cl_3	13514	$^1A_{1g} \rightarrow {}^3T_{1g}$	27924.50	B = 508.06	74.450	0.48	7.91	7.77	14.53	14.42
	20408	$\rightarrow {}^3T_{2g}$		C = 4803.5		(0.43)				
	23121	$\rightarrow {}^1T_{1g}$								
	31250	$\rightarrow {}^1T_{2g}$								
	41667	$\rightarrow a, {}^1T_{1u}$ $L \rightarrow M$ Charge transfer $\pi \rightarrow e_g$								
IrA_2Cl_3	18692	$^1A_{1g} \rightarrow {}^3T_{1g}$	28154.00	B = 453.62	114.49	0.36	7.02	6.92	24.10	24.00
	25000	$\rightarrow {}^1T_{1g}$		C = 3154.00		(0.42)				
	26315	—								
	32258	$\rightarrow {}^1T_{2g}$								
	37736	$\rightarrow a, {}^1T_{1u}$ $L \rightarrow M$ Charge transfer $\pi \rightarrow e_g$								

IrD_2Cl_3	14925	$^1A_{1g} \rightarrow {}^3T_{1g}$	23150.00	B = 413.69	90.17	0.37	3.22	3.12	22.12	22.02
	20408	$\rightarrow {}^1T_{1g}$		C = 2741.50		(0.47)				
	25641	—								
	27027	$\rightarrow {}^1T_{2g}$								
	34482	$\rightarrow a, {}^1T_{1u}$								
	40000	$\rightarrow b, {}^1T_{1u}$								
		$L \rightarrow M$ Charge transfer $\pi \rightarrow e_g$, $\sigma \rightarrow e_g$								
$PtACl_4$	19231	$^1A_{1g} \rightarrow {}^3T_{1g}$	29345.50	B = 459.94	117.59	0.36	4.77	4.68	33.27	33.12
	22222	$\rightarrow {}^3T_{2g}$		C = 3372.50		(0.41)				
	25974	$\rightarrow {}^1T_{1g}$								
	33333	$\rightarrow {}^1T_{2g}$								
	38462	$\rightarrow a, {}^1T_{1u}$								
		$L \rightarrow M$ Charge transfer $\pi \rightarrow e_g$								
$PtBCl_4$	19044	$^1A_{1g} \rightarrow {}^3T_{1g}$	28939.70	nB = 446.63	116.66	0.37	4.55	4.41	31.75	31.63
	22727	$\rightarrow {}^3T_{2g}$		C = 3298.70		(0.42)				
	25641	$\rightarrow {}^1T_{1g}$								
	32787	$\rightarrow {}^1T_{2g}$								
	38462	$\rightarrow a, {}^1T_{1u}$								
		$L \rightarrow M$ Charge transfer $\pi \rightarrow e_g$								
$PtDCl_4$	18868	$^1A_{1g} \rightarrow {}^3T_{1g}$	28540.00	nB = 433.87	115.81	0.40	2.25	2.18	31.16	31.28
	25316	$\rightarrow {}^1T_{1g}$		C = 3224.00		(0.42)				
	32258	$\rightarrow {}^1T_{2g}$								
	40000	$\rightarrow a, {}^1T_{1u}$								
		$L \rightarrow M$ Charge transfer $\pi \rightarrow e_g$								
$PtECl_4$	17544	$^1A_{1g} \rightarrow {}^3T_{1g}$	26316.00	nB = 417.69	107.65	0.43	2.09	1.98	29.15	29.00
	19231	$\rightarrow {}^3T_{2g}$		C = 2924.00		(0.44)				
	23392	$\rightarrow {}^1T_{1g}$								
	27778	—								
	30075	$\rightarrow {}^1T_{2g}$								
	40000	$\rightarrow a, {}^1T_{1u}$								

Values in parentheses are calculated spectroscopically

Experimental

Preparation of ligands and complexes

All the ligands and complexes under study were prepared and purified following the methods reported [15, 16] earlier. Chemicals used in these preparations were B. H. D. or J. M. (London) products.

Table II

Infrared frequencies with their tentative assignments

Ligand A	RuA_2Cl_3	RhA_2Cl_3	IrA_2Cl_3	$PtACl_4$	Ligand B	$PtBCl_4$
1748m	1668s, sh	1660m, sh	1625s	1620m, b	1738s	1622s
1680s	1622s	1612s	1590s	1590m	1668s, b	1590s
1618s	—	—	—	—	1618s	—
1588s	—	—	1568s	—	—	1553s
1558s, sh	1556s, sh	1550m	—	1558m, sh	—	—
1528s	1523s	1520s	1528s	1518m	1523s	1518s
820 s	810s	812s	808s	804s	817s	802s,
—	552m b	560m, b	560m, b	622m, b	—	582s
—	330m	334s	334m	342s	—	330 m
—	277m	265m	272m	274m	—	277m

Ligand	RuD_2Cl_3	IrD_2Cl_3	$PtDCl_4$	Ligand E	$PtECl_4$	Assignment
1684s	1628s, b	1622s, b	1618m	1635s	1598m, b	C = O str.
1648s	1608b	1606s	1604s	1600s	1563m	C = N str.
1603s	1588s	—	—	—	—	
—	1568m	1548s	1563s	—	—	C = C str.
—	1553m	—	—	—	—	
—	1498s	1518s	—	—	—	
817s	810m	810m	812s	817m, sh	812m, sh	C—H bending adjacent H atoms + 1 : 4 disubstitution
—	487w	487m	492s	—	484s	M—N str.
—	317m	317s	322s	—	322m	M — Cl str.
—	277m	277s, b	277m,	—	277m	M — O str.

Physical measurements and analyses:

Infrared spectra of ligands and their complexes were recorded in the range of 200 cm^{-1} to 4000 cm^{-1} in Nujol mull using CsF optics on a Perkin Elmer-621 spectrophotometer. Principal infrared frequencies with their tentative assignments are noted in Table II. Electronic spectral measurements were made on Beckman DU-2 spectrophotometer on acetonitrile solutions of complexes in the 200—800 nm range in 5 nm steps. Magnetic measurements on the pulverized complexes were performed on a Gouy' balance. The results are compiled in Table I.

Results and discussion

The magnetic moments (1.62 B .M. and 1.72 B. M.) of Ru(III) complexes at room temperature are quite near to spin-only value 1.73 B. M. Low experimental values may be accounted for high spin-orbit coupling. These results

show the presence of only one unpaired electron and deviation from the HUND's rule of maximum multiplicity in Ru(III) ion complexes in under study. Ru(III) complexes of similar magnetic behaviour generally form low spin octahedral stereochemistry involving d^2sp^3 hybridization.

A perusal of electronic spectral reports on Ru(III) complexes reveals that on account of strong charge transfer bands spreading over a wide range of wave length bands corresponding to *d–d* transitions have been difficult to identify. Another difficulty experienced in the assignment of *d–d* type transitions has arisen owing to their intermixing as they appeared within a relatively narrow range of energy. Although the TANABE and SUGANO diagram [17] predicts eight transitions from the ground state $(t_{2g})^5$ to the doublet states of configuration $(t_{2g})^4(e_g)^1$, yet all the bands have not necessarily appeared and assigned in the spectra of Ru(III) complexes. In the present complexes eight bands have been observed in each case which have been assigned to various spin-forbidden and spin-allowed *d–d* and charge-transfer transitions. The last band with very high extinction coefficient and energy (~ 40000 cm^{-1}) could only be assigned to $L \rightarrow M$ charge transfer while next broad peak with relatively very low extinction coefficient and energy could be considered to have arisen on account of *d–d* $^2T_{2g} \rightarrow 2\ ^2T_{2g}$ transition coupled with $L \rightarrow M$ charge transfer. All the remaining six bands with very low extinction coefficients have been assigned to spin-forbidden and spin-allowed *d–d* type transitions on the basis of TANABE and SUGANO predictions. Making the use of following equations [18]:

$$^4T_{2g} - {}^4T_{1g} = 8\ B$$
$$Dq/B = 5.1$$

and

$$C = 4\ B$$

The values of 10 *Dq*, *B* and *C* have been calculated and are noted in Table I.

A comparison of electronic spectra of Rh(II), Ir(III) and Pt(IV) complexes with those of isoelectronic (d^6) Co(III) and Ru(III) octahedral strong field complexes shows an analogy in the band-splitting pattern. This indicates that complexes under study are octahedral, strong field cases. Further, in the present complexes ligand field bands show expected shift arrangement according to an increasing number of transition series $5d^n > 4d^n > 3d^n$ (with relative values of function 1.75 : 1.45 : 1.00) and according to increasing oxidation numbers $+4 > +3 > +2$, being obtained in isoelectronic ions. Four to six bands observed in the electronic spectra of complexes have been assigned on the comparison basis to K_2PtCl_6. All the *d–d* transitions have taken place from the ground term $^1A_{1g}$ of substate $(t_{2g})^6$ to the excited terms $^3T_{1g}$, $^3T_{2g}$, $^1T_{1g}$ and $^1T_{2g}$ of substate $(t_{2g})^5$ $(e_g)^1$; first two transitions are spin forbidden while remaining two are spin allowed. Some of the ligand field

parameters, *viz.* B and C (Racah's interelectronic repulsion parameters), Dq (field strength parameter of SCHLAPP and PENNEY), 10 Dq (splitting energy). L. F. S. E. etc. have been calculated for each complex by employing the following equations:

$$^3T_{1g} = 10\ Dq - 3C$$
$$^1T_{1g} = 10\ Dq - C$$
and
$$^1T_{2g} = 10\ Dq + 16\ B - C$$

and values are noted in Table I. One band (unassigned) observed in the ligand field spectra, very near to spin-allowed band $^1A_{1g} \rightarrow {}^1T_{2g}$ in some complexes have been considered a part of $^1A_{1g} \rightarrow {}^1T_{2g}$ band. Splitting of $^1A_{1g} \rightarrow {}^1T_{2g}$ band may be accounted for high spin orbit coupling. Last band with very high extinction coefficient appeared at ~ 40000 cm^{-1} invariably in all the spectra except in the spectrum of the Ir(III)–D complex (at ~ 34482 cm^{-1}) has been assigned to $L \rightarrow M$ charge-transfer (allowed) transition $\pi \rightarrow e_g$ from $^1T_{1u}$ ground term. The next higher band appearing at 40000 cm^{-1} only in Ir(III)–D complex corresponds to $\sigma \rightarrow e_g$.

Very small values of magnetic moments (Table I) are exhibiting feeble paramagnetism in the Rh(III), Ir(III) and Pt(IV) complexes under study, however, are not accountable for the presence of any free electron in their d-configuration. Thus these results infer spin paired d^6 octahedral configuration to the complexes. The unusual magnetic behaviour verified spectroscopically [19] may be explained in terms of second order Zeeman effect.

Principal infrared frequencies with their assignments [20—22] for the ligands and complexes are noted in Table II. A perusal of infrared spectral data reveals the lowering in C=O and C=N stretching frequencies of parent ligands on complexation. This lowering indicates the participation of these groups in co-ordination. Appearance of new bands in the spectra of complexes corresponding to M–O and M–N bonds infer the same conclusion arrived at earlier. The perturbation, appearance or disappearance of peaks corresponding to C=C (aromatic) stretching vibrations evidently show the rearrangement or shifting of double bonds in ligand molecules during complexation. If doublet band at ~ 817 cm^{-1} is considered due to 1 : 4 disubstitution (*para* substitution) of ligands then lowering in its value and its change to singlet will lead to the change of benzenoid structures of ligands to quinonoid in complexes involving rearrangement of double bonds. A new band appearing at ~ 317——342 cm^{-1} in the complexes has been assigned [22] to M–Cl stretching vibrations. The M–N stretching frequency orders (metal and ligand wise) substantiated by 10 Dq values clearly show the direct influence of electron repelling tendency (falling in identical order) of ligands *para* substituents on the complex stabilities.

Considering the inferences as arrived at above the tentative structure of complexes with possible mechanism may be shown as follows:

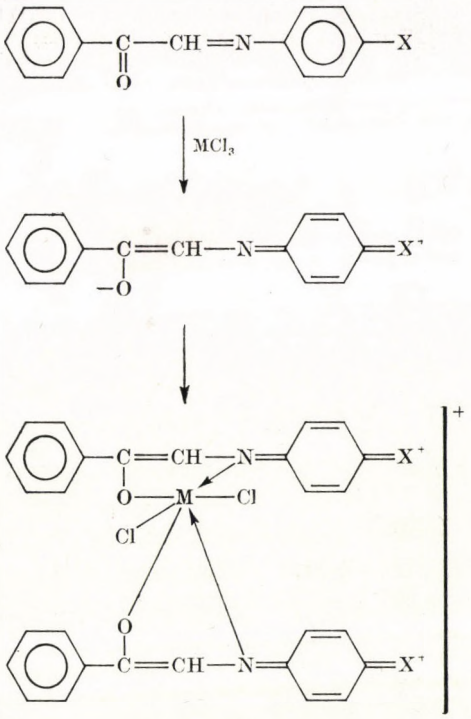

where M = Ru(III), Rh(III) or Ir(III) and X = $N(CH_3)_2$, $N(C_2H_5)_2$, Br or I.

In Pt(IV) complexes Pt(IV) : ligand ratio is 1 : 1, four chlorine atoms are in the co-ordination sphere.

*

We are highly indebted to Prof. W. U. Rehman, Head of the Chemistry Department, A. M. University, Aligarh and Ex. Prof. W. U. Malik, Head of the Chemistry Department, Roorkee University, Roorkee for providing facilities for the electronic spectral and magnetic mesurements, respectively. Thanks are also due to other friends of our group who have helped in this work.

REFERENCES

[1] Rastogi, D. K.: Ph. D. Thesis, Agra Univ., Agra (1970)
[2] Rastogi, D. K., Shrivastava, A. K., Jain, P. C., Agrawal, B. R.: J. inorg. nucl. Chem. **34,** 1449 (1972)
[3] Jain, P. C., Nigam, H. L., Mehra, A.: J. inorg. nucl. Chem. **32,** 2933 (1970)
[4] Jorgensen, C. K.: Acta Chem. Scand. **10,** 500 (1956)
[5] Jorgensen, C. K.: Acta Chem. Scand. **11,** 151 (1957)
[6] Dewedi, J. S., Agrawal, U.: Indian J. Chem. **10,** (1972)
[7] Jorgensen, C. K.,: Acta Chem. Scand. **10,** 518 (1956)
[8] Rastogi, D. K., Shrivastava, A. K., Jain, P. C., Agrawal, B. R.: J. Less Common Metals. **24,** 383 (1971)

[9] UPADHYAY, R. K.: Ph. D. Thesis, Meerut Univ., Meerut (1974)
[10] SHARMA, R. R.: Ph. D. Thesis, Meerut Univ., Meerut (1974)
[11] MAHESHWARI, S. C.: Ph. D. Thesis, Meerut Univ., Meerut (1975)
[12] VERMA, H. P. S.: Ph. D. Thesis, Meerut Univ., Meerut (1976)
[13] UPADHYAY, R. K., SINGH, V. P.: Acta Chimica (Budapest) in press
[14] UPADHYAY, R. K., KUMAR, A.: Acta Chimica (Budapest) in press
[15] UPADHYAY, R. K., SINGHAL, M. L.: Monatshefte für Chemie, in press
[16] UPADHYAY, R. K., KUMAR, A.: Monatshefte für Chemie, in press
[17] TANABE, Y., SUGANO, S.: J. Phys. Soc. Japan **9,** 753, 766 (1954)
[18] SCHLAFER, H. L., GLIEMANN, G.: Basic Principles of Ligand Field Theory, Wiley, Interscience, New York 1969
[19] FIGGIS, B. N.: Introduction to Ligand Fields, Interscience, John Wiley & Sons, London 1966
[20] DYER, J. R.: Applications of Absorption Spectroscopy of Organic Compounds, Prentice Hall of India, Pvt. Ltd., New Delhi (1969)
[21] SAXENA, R. N., PANDEY, K. K.: J. Indian Chem. Soc. **49,** 782 (1972)
[22] NAKAMOTO, K.: Infrared Spectra of Inorganic and Coordination Compounds, John Wiley & Co., New York (1968)

R. K. UPADHYAY
M. L. SINGHAL
A. K. BAJPAI

Department of Chemistry, and Department of Physics
N.R.E.C. College, Khurja, 203131, India

Acta Chimica Academiae Scientiarum Hungaricae, Tomus 96 (1), pp. 27—37 (1978)

REACTIONS OF SOME ALKANES ON PALLADIUM BLACK CATALYST

A. SÁRKÁNY, L. GUCZI and P. TÉTÉNYI

(Institute of Isotopes of the Hungarian Academy of Sciences)

Received February 8, 1977

Adsorption of methane and ethane, deuterium exchange of methane, ethane, *n*-butane, and 2,2-dimethylpropane, and the hydrogenolysis and isomerization of ethane, butanes and 2,2-dimethylpropane on a palladium black catalyst have been studied. Data on adsorption of methane and ethane suggest different adsorption forms. The 'weak' irreversible adsorption may play an important role in deuterium exchange, whereas the 'strong' interaction leads to rupture of the C–C bond and to poisoning of the catalyst. The hindrance of formation of $\alpha\alpha$ bonds is revealed not only by the abundance of the $[^2H_1]$ alkane among the initial products but also by the well-defined separation of deuterium exchange and hydrogenolysis. Kinetic parameters of hydrogenolysis and isomerization as well as product distributions have been determined as a function of temperature and hydrogen pressure. The results suggest that different surface intermediates are responsible for isomerization and hydrogenolysis.

The mechanism of isomerization and hydrogenolysis of saturated hydrocarbons on palladium films [1—4] and blacks [5, 8], as well as on silica [6, 7] and alumina [9] supported catalysts has been extensively investigated. Comprehensive studies [1, 2, 5] have shown that Pd is much less in isomerization active than Pt. Another interesting feature of Pd catalysts is the lack of isomer production in case of neopentane [1, 2, 8] and of other hydrocarbons [4, 11] containing a quaternary carbon atom. MULLER and GAULT [4] has explained this phenomenon by suggesting a π-bonded Pd intermediate $\pi(\alpha, \beta), \gamma$ in bond shift rearrangements as well as in the hydrogenolysis of the C–C bond.

In this work we present results in the catalytic properties of Pd-black. For better understanding of the nature of active sites, we have studied the adsorption of methane, ethane and the deuterium exchange of methane, ethane, *n*-butane and neopentane. This paper is also concerned with the hydrogenolysis of ethane, butanes and neopentane, and especially with the effect of hydrogen pressure on the selectivity of hydrogenolysis and isomerization. A comparison is made between the catalytic hehaviour of Pd and Pt [12, 13].

Experimental

Adsorption of methane and ethane was measured gravimetrically using a Sartorius vacuum microbalance. The composition of hydrocarbons irreversibly bonded was determined by thermodesorption in a flow system at atmospheric pressure. Details have been given elsewhere [13].

Hydrogenolysis and deuterium exchange were investigated in a circulation apparatus [12] with a total volume of 0.153 l.

Deuterium exchange and the consumption of 'light' hydrocarbon were followed on an AEI MS 10 C2 mass spectrometer connected to the circulating system through a fine capillary leak. Procedures for natural ^{13}C and for fragmentation patterns, as well as the calculation of product distribution have been described [14].

Products of hydrogenolysis were separated gas chromatographically at room temperature on a column 5 m in length, filled with 20 w/w% squalane on Chromosorb W. Calibration was performed with mixtures of the products.

Palladium black catalyst was prepared from H_2PdCl_6 by reduction with formaldehyde at room temperature in an alkaline medium, followed by careful washing and drying. Two types of catalysts were used. Catalyst I was prepared from the freshly deposited sample by sintering (original surface area 14.3 $m^2\ g^{-1}$) with repeated oxygen-hydrogen treatment at 423 K. The surface area of the sample was 3—3.5 $m^2\ g^{-1}$. The mean crystallite size, as measured by X-ray diffraction, was 35 nm. Catalyst II was prepared from Catalyst I: some *n*-butane hydrogenolysis runs were carried out above 573 K during which the activity of Catalyst I decreased. The drop in the hydrogenolysis activity of Catalyst I is about one order in magnitude. The surface area of the sample and the mean crystallite size remained practically the same as before.

Results

Adsorption

Adsorption of methane and ethane on presintered Pd-black was investigated in the temperature range of 196—533 K *via* adsorption isotherms and isobars. Temperature dependence of the amount of total and irreversible adsorption at a pressure of 26.67 kNm^{-2} is presented in Fig. 1.

In the temperature range between 196 and 473 K, where reversible and irreversible adsorption can be separated, adsorption isotherms were recorded. From the isotherms, isosteric heats and the entropy of adsorption were determined. Typical results are shown in Table I, which includes also the surface area occupied by an adsorbed molecule, as calculated from $V_{m,HC}/V_{m,N_2}$ (BET). It should be emphasized that the values in Table I were calculated for a 'poisoned' surface (weight of the amount adsorbed irreversibly, $V_{HC}^{irrev.}$ is in parenthesis), where the most active sites are occupied by substrates bonded irreversibly.

Irreversible adsorption of CH_4 and C_2H_6 takes place above 359 and 295 K, respecitvely. The amount of ethane bonded irreversibly was measured in a hydrogen flow at atmospheric pressure either at the temperature of adsorption or using temperature-programmed heating. The ethane retained irreversibly can be removed in original form by hydrogen treatment at the temperatures of chemisorption between 196—453 K. Above 453 K, part of the ethane chemisorbed leaves the surface in the form of methane. Results are shown in Fig. 1. Typical runs for the temperature-programmed desorption of chemisorbed ethane are presented in Fig. 2.

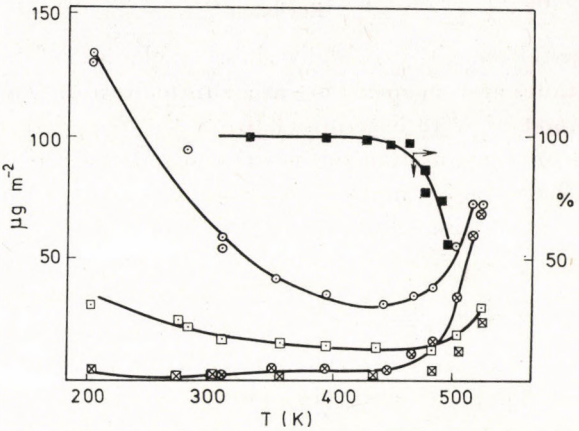

Fig. 1. Temperature dependence of methane and ethane adsorption at 26.6 kNm^{-2} (CH_4 : : □-total, ⊠-irreversible adsorption; C_2H_6 : ○-total, ⊗-irreversible adsorption; ■ — percentage of desorbed ethane formed from irreversibly adsorbed ethane in hydrogen flow at the temperature of adsorption)

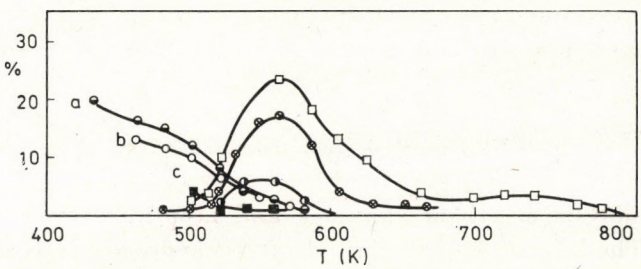

Fig. 2. Thermodesorption of irreversibly bonded ethane in H_2, (a) — adsorption at 423 K (93% is removed as ethane at the temperature of adsorption) ◒ — C_2H_6, ◑ — CH_4; (b) adsorption at 458 K (74% is removed as ethane at 458 K) ○ — C_2H_6, ⊗ — Ch_4; (c) adsorption at 493 K (49% is removed as C_2H_6, 39% as CH_4 at 493 K) ■ — C_2H_6, □ — CH_4. Heating rate $\simeq 10°\ min^{-1}$; flow rate of $H_2 \simeq 10$ ml min^{-1}

Table I

Data on adsorption of CH_4 and C_2H_6 on Pd-black

		CH_4	C_2H_6
Isotherm		F	F
$-\Delta H_a$ (kJ mol^{-1})	194—273 K	—	17.9
($\Theta_{rev.} = 0.05$)	273—423 K	32.5	51.3
Surface area/	194—273 K	18.2	23.1
adsorbed molecule	273—333 K	24.1(1.9)*	38.5(3.2)
10^{-20} (m^2)	333—393 K	36.2(8.6)	64.1(8.8)
$-\Delta S$ (J mol^{-1} K^{-1})	333—410 K	—	100.3

F – Freundlich
* Weight of the irreversibly adsorbed substrate (10^6 gm^{-2})

Exchange

Experimental results on deuterium exchange of methane, ethane, propane, *n*-butane and neopentane are summarized in Tables II and III. Arrhenius parameters were determined from the temperature dependence of the initial rate of consumption of 'light' hydrocarbons ($-w_{d_0}$) in the temperature range between 333 and 443 K using 10 : 1 deuterium to hydrocarbon mixtures unless otherwise stated.

Deuterium exchange of methane and neopentane can be satisfactorily described by the stepwise exchange of hydrogen atoms in agreement with KEMBALL's [15] and MCKEE and NORTON's [16] results. At 438 K the ratio of single to multiple exchange is 20.9 and 18.8 for methane and neopentane, respectively. The apparent activation energies of the formation of multiple deuterated isomers methane-d_4, neopentane-d_3 and -d_4 are 182 ± 25 and 176 ± 30 kJ mol^{-1}, respectively.

In the case of ethane and propane, a maximum appears at d_1 and d_2 isomers, but with rising temperature, the distribution is shifted towards ethane-d_6 and propane-d_8. In the temperature range of 338—393 K multiply deuterated isomers prevail in the deuterium distribution pattern of *n*-butane.

Hydrogenolysis and isomerization

Hydrogenolysis of ethane, butanes and neopentane was investigated above 513 K. The logarithm of the initial rate of hydrogenolysis as a function of the hydrogen pressure is plotted in Fig. 3 for 558 ± 3 K. The hydrogen pressures at which hydrogenolysis and isomer formation show maxima, along with the kinetic order in hydrogen before and after the maximum rate, are collected in Table IV.

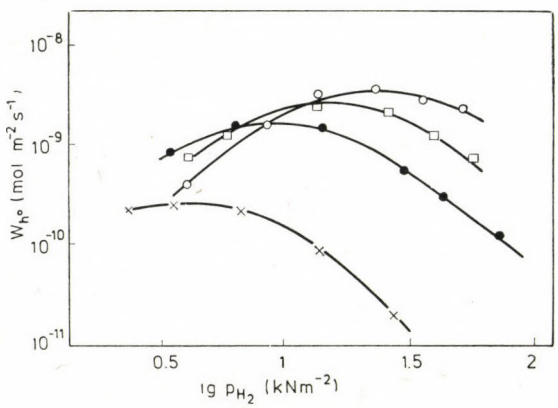

Fig. 3. Rate of hydrogenolysis as a function of hydrogen pressure at 558 ± 3 K; p (hydrocarbon) = 1.33 kNm^{-2}, × — ethane, ● — neopentane, □ — *i*-butane, ○ — *n*-butane

Table II

Data on deuterium exchange of ethane, propane and n-butane on palladium black

	lg A(molecules $m^{-2} s^{-1}$)	E (kJ mol^{-1})	T (K)	Initial per cent distribution										$\bar{M}$
				d_1	d_2	d_3	d_4	d_5	d_6	d_7	d_8	d_9	d_{10}	
			360	42.3	32.1	4.3	8.1	7.4	5.8					2.23
C_2H_6	24.97	71	395	30.7	35.46	8.0	10.2	8.0	7.5					2.51
			428	22.7	21.0	7.8	7.2	18.2	23.1					3.46
			356	28.2	24.3	2.1	2.0	3.7	4.8	16.6	18.3			4.00
C_3H_8	23.81	58	380	10.6	18.6	1.5	8.1	1.1	1.5	21.5	36.6			5.42
			399	8.2	7.8	0.2	6.4	5.3	12.1	24.6	35.4			6.04
			341	3.0	3.4	0.8	2.1	0.3	4.1	10.2	18.3	24.2	33.6	8.18
n–C_4H_{10}	23.88	54	355	1.7	2.5	2.1	3.4	2.9	5.1	7.6	15.8	26.0	32.47	8.10
			370	2.1	1.3	0.2	0.3	1.1	2.0	8.5	18.5	28.2	37.8	8.63
C_2H_6**	24.42	70	399	38.31	27.2	13.6	14.1	4.0	2.8					2.26
C_3H_8**	23.52	58	380	34.3	28.6	12.1	3.2	4.3	7.2	6.2	3.9			2.81

Arrhenius parameters were measured in the temperature range 333—443 K using a mixture of 1.33 kNm^{-2} hydrocarbon and 13.3 kNm^{-2} deuterium

** Exchange on catalyst II

Table III

Results on deuterium exchange of methane and neopentane

	1 g A (molecules $m^{-2} s^{-1}$)	E (kJ mol^{-1})	T (K)		Initial per cent distribution									
					d_0	d_1	d_2	d_3	d_4	d_5	d_6	d_7	d_8	d_9
CH_4	27.60	111	438	obs.	84.12	10.31	1.32	0.17	0.21					
			$\Phi = 14.32$	calc.	86.43	12.83	0.71	0.02	0.00					
			456	obs.	81.86	17.12	0.96	0.06	0.00					
			$\Phi = 19.21$	calc.	82.13	16.57	1.25	0.04	0.00					
			485	obs.	80.96	15.88	2.03	0.50	0.63					
			$\Phi = 23.97$	calc.	78.09	19.91	1.90	0.08	0.00					
neo–C_5H_{12}*	24.98	85	435	obs.	88.77	10.00	0.84	0.13	0.26	—	—	—	—	—
			$\Phi = 13.11$	calc.	87.62	11.65	0.68	0.02	0.00	0.00	0.00	0.00	0.00	0.00
			460	obs.	92.55	6.82	0.37	0.23	0.03	—	—	—	—	—
			$\Phi = 8.36$	calc.	91.94	7.75	0.29	0.00	0.00	0.00	0.00	0.00	0.00	0.00
			480	obs.	73.25	21.30	4.36	1.01	0.08	—	—	—	—	—
			$\Phi = 33.37$	calc.	71.35	24.53	3.75	0.33	0.02	0.00	0.00	0.00	0.00	0.00

Arrhenius parameters were determined from the initial consumption of "light" hydrocarbon (1.33 kNm^{-2} hydrocarbon, 13.3 kNm^{-2} deuterium)

* Deuterium distribution in $C_4H_9^+$ fragment

Table IV

Kinetic data on hydrogenolysis and isomerization

HC	T(K)		$p_{H_2}^{max}$ (kNm^{-2})	a	b	lg A(mol m^{-2} s^{-1})	E (kJ mol^{-1})
C_2H_6	558		2.6—4	— 2.4	+0.2	34.72	222
	606		6—8	— 2.0	+0.35		
neo-C_5H_{12}	558	A	8—11	— 1.5	0.67	35.46	224
		B	57	— 0.1	0.98	—	—
	585	A	14.6—20	— 1.35	1.1		
		B	73	—	1.35		
i-C_4H_{10}	537	A	10—15	— 1.6	0.97	30.23	162
		B	16—20	— 1.5	1.11	28.20	152[d]
	558	A	18—24	— 1.6	1.35		
		B	27—33	— 1.5	1.63		
	589	A	31—36	— 1.1	1.63		
		B	45—51	— 0.6	2.35		
i-C_4H_{10}[c]		A				31.26	163
n-C_4H_{10}	537	A	18—23	— 1.63	1.12	29.60	155
		B	32—35	— 1.41	1.20	27.54	143
	558	A	24—28	— 1.45	1.45		
		B	35—40	— 1.2	1.51		
	589	A	44—47	— 0.8	1.63		
		B	54.5—57	— 0.9	2.18		
n-C_4H_{10}[c]		A				29.40	144

A — hydrogenolysis; B — isomerization; c — experiments on Catalyst I; d — Arrhenius plots bend down; a and b are the reaction orders in hydrogen after (a) and before (b) the maximum rate of reaction

The maximum rate of hydrogenolysis is shifted towards higher hydrogen pressures with increasing carbon chain length (compare ethane and *n*-butane) and with decreasing branching (see neopentane, isobutane, *n*-butane). An opposite trend is observed for the maxima of isomer formation. At higher temperatures the maximum rates of hydrogenolysis and isomerization are shifted towards higher pressures of hydrogen. The same phenomenon has been observed for transformations of saturated hydrocarbons catalyzed by platinum [12, 17].

The selectivity as a function of hydrogen pressure and temperature can be seen in Figs 4 and 5 and in Table V for *n*-butane, isobutane and neopentane, respectively.

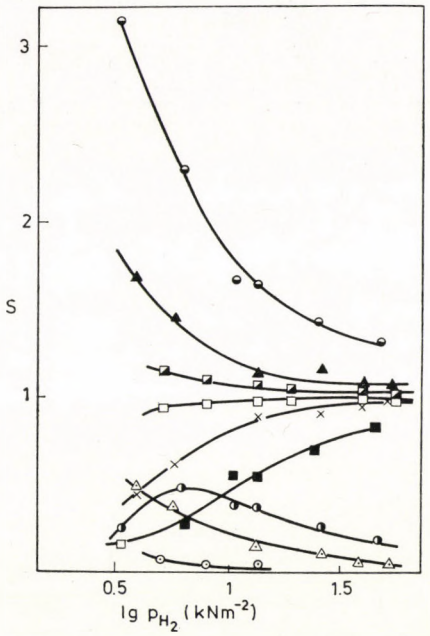

Fig. 4. Selectivity of hydrogenolysis of 2-methylpropane as a function of hydrogen pressure. P_{HC}= 1.33 kNm^{-2}; at 538 K ◪—CH_4; ○ — C_2H_6; □ — C_3H_8; at 558 K ▲ — CH_4; △— C_2H_6; ⊠— C_3H_8; at 588 K ◒ — CH_4; ◑ — C_2H_6; ■ — C_3H_8

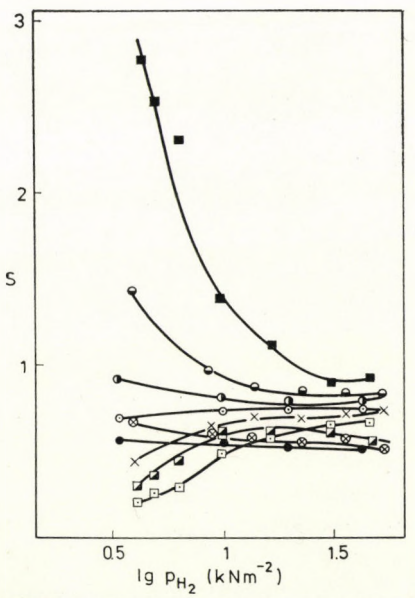

Fig. 5. Selectivities for the hydrogenolysis of *n*-butane as a function of hydrogen pressure P_{HC}= 1.33 kNm^{-2}; at 537 K ◑—CH_4; ⊗—C_2H_6; ○ — C_3H_8; at 558 K ◒ — CH_4; × — C_2H_6; × — C_3H_8; at 589 K ■ — CH_4; ◪ — C_2H_6; □ — C_3H_8

Table V

Hydrogenolysis product distribution and selectivity of isomerization for neopentane on Pd-black

T(K)	p_2(kNm^{-2})	Product distribution					S_i w_i^0/w_h^0
		Met	Et	Pr	*n*-But	*i*-But	
558	73.6	57.2	1.7	3.36	3.33	34.6	0.035
	42.3	56.3	3.75	2.63	4.12	33.2	0.023
	29.2	58.6	4.3	2.7	3.9	30.5	0.012
	15.0	68.3	12.3	5.2	1.9	12.2	0.005
585	75.1	58.2	1.12	2.81	4.63	33.5	0.037
	58.5	62.3	3.41	2.11	3.5	28.6	0.018
	44.5	67.7	4.12	2.7	2.8	22.7	traces

At hydrogen pressures of 26.6—66.5 kNm^{-2} and between 513—573 K, the hydrogenolysis of isobutane approaches selective propane formation ($S_{C_3H_8} \simeq 1$). The selectivity of terminal bond rupture is 0.75 in *n*-butane. Under identical conditions the rupture of neopentane to isobutane is less selective and secondary products such as *n*-butane, propane, are always formed.

The maximum ratio of isomerization to hydrogenolysis is observed under conditions of selective rupture as shown in Fig. 6.

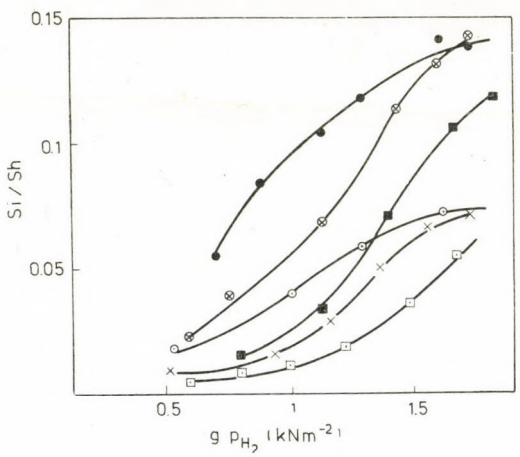

Fig. 6. Isomerization to hydrogenolysis ratio as a function of hydrogen pressure. $p_{HC} = 1.33$ kNm^{-2}; *n*-butane ○ — 537 K; × — 558 K; □ — 589 K; 2-methylpropane ● — 537 K; ⊗ — 558 K; ■ — 589 K

* S is the selectivity given by the equation: [12]: $S_i = \dfrac{n\, w_i^0}{\sum_{i=1}^{n-1} i\, w_i^0}$ where w^0 is the initial rate of product formation

Data on kinetic investigations with 10 : 1 hydrogen to ethane, and 20 : 1 hydrogen to hydrocarbon mixtures for butanes and neopentane are also collected in Table V. The catalytic activities of Pd and Pt blacks were compared in the hydrogenolysis of ethane at 563 K, using a standard mixture of ethane and hydrogen. Rates for Pd and Pt are 2.69×10^{-9} and 1.83×10^{-10} mol m^{-2} sec^{-1}, respectively. The reaction rate decreased in subsequent runs. After the sixt runs the rates are lower by 94.14 and 84.03%, while the surface area diminishes only by 20.3 and 36.3% for Pd and Pt, respectively.

Discussion

The results obtained provide further evidence for the different adsorption forms of hydrocarbons [12] and for the importance of 'weak' and 'strong' interactions [18] in deuterium exchange and hydrogenolysis.

The reversible adsorption of methane and ethane at 194 K suggests physical sorption. The area occupied by adsorbed molecules is in good agreement with the geometrical cross sections [19] of 18×10^{-20} and 24×10^{-20} m^2 for methane and ethane, respectively. In the 273—423 K range reversible adsorption may not be regarded as pure physical adsorption. This is clearly shown by the value of the isosteric heat of adsorption and by the surface area occupied by adsorbed ethane molecules. Data on the entropy of ethane adsorption are nearly equal to the entropy change on losing one translational degree of freedom [20]. This observation is valid also for Pt, for which the entropy change between 405—465 K, as calculated from data in Ref. [13], corresponds to -68 J mol^{-1} K^{-1}. Comparing the data on Pt and Pd, we suggest that the loss of the degree of freedom is more extensive on Pd than on Pt. This activated form of adsorption can be considered as a precursor of dissociative chemisorption.

Irreversible adsorption of methane and ethane occurs above 359 and 295 K, respectively. Its value increases with increasing temperature in the range between 360 and 533 K. In the presence of hydrogen, the irreversibly bonded ethane can be removed in its original form from the Pd surface between 295—463 K. This type of chemisorption (irreversible 'weak' adsorption) may play an important role in the deuterium exchange of hydrocarbons. Above 453 K the part of irreversibly bonded ethane leaves the surface as methane. From the temperature-programmed desorption experiments it is clear that part of the irreversibly bonded substrate comes off only at elevated temperatures. These results indicate a 'strong' metal–hydrocarbon interaction which may be responsible for the self-poisoning of the catalyst. (The formation of on interstitial surface carbide cannot be excluded.) This process occurs at lower temperatures on Pd than on Pt, in agreement with the hydrogenolysis activity ethane on these metals.

Exchange of deuterium in ethane, propane and *n*-butane proceeds easily. In agreement with results on Pt [12] there are large amounts of the d_1 and d_2 isomers among the initial products in ethane and propane. The preferred formation of the d_2-isomer can be explained by the simultaneous elimination of eclipsed hydrogens. Indeed, deuterium atoms enter into ethane symmetrically [13], confirming the importance of 1,2-bonded intermediates in the exchange, as proved for exchange on Ni and Pt. In contrast to Pt, where the formation of deuterated methane isomers shows a rather 'uniform' distribution, Pd gives a monodeuterated product. The hindrance to the formation of multiply deuterated products is caused by the apparent activation energy of d_4 formation with respect to d_1. The results presented are in agreement with those reported by KEMBALL [15] and MCKEE and NORTON [16] for films and powders.

The formation bonded multiply carbon atoms [21], considered as intermediates in hydrogenolysis, requires higher temperatures in agreement with the adsorption results. This phenomenon seems to be supported not only by kinetic results on the multiple exchange of deuterium in methane and neopentane but also by the well-defined separation of the temperature ranges for exchange hydrogenolysis. The ratios of deuterium exchange and hydrogenolysis rates for ethane at a temperature where the rate of hydrogenolysis is 10^{15} mol m^{-2} s^{-1} are 5.8×10^3 and 3.7×10^4 for Pd and Pt, respectively. This points to the easier transformation of the 'weak' form of adsorption into a 'strongly' bonded one on Pd.

The presence of hydrogen affects the "strength" of interaction as pointed out earlier [22]. The volcano-shaped kinetic curves as well as the product distribution pattern can be interpreted in terms of numbers of working active sites. (For the sake of simplicity the change in the rate of turnover is neglected.) At high hydrogen pressures, *i.e.* with more hydrogen on the surface, the dissociation of C–H bonds is hindered, resulting in a negative order in hydrogen and of the selective rupture of the C–C bond. At low hydrogen pressures, Pd behaves as a reactant; the hydrocarbons are more strongly adsorbed and presumably more extensively dissociated species are formed, decreasing the number of working active sites. The reaction rate is governed then by the rate of product desorption [23].

According to Table V, the location of maxima shows a correlation with the reactivity sequence for hydrogenolysis, while an opposite trend can be observed for bond-shift isomerization. This observation is valid also for product selectivities.

This phenomenon underlines our earlier proposal that a less dehydrogenated surface species participates [12] in isomerization. Experiments on self-poisoned Pd surface [24] can also be explained from this standpoint; upon poisoning of the catalyst, the rate of hydrogenolysis decreases more

rapidly than that of isomerization. This means that isomerization is favoured on the less active sites, which are also less sensitive for self-poisoning.

In contrast to ANDERSON's and BOUDART's works [2, 8] certain isomerization activity has been found also for neopentane. It is clear, however, that a high hydrogen pressure is required to maintain the conditions required for isomerization. In fact, neopentane suffers deeper fragmentation than butanes for similar reaction rates and hydrogen pressures.

The difference in the isomerization selectivity for neopentane on Pd and Pt is striking. On Pt black at 573 K, w_i/w_h is 1.52, while on Pd under similar conditions it is in the range of 10^{-2}. To explain this feature of Pt, one has to assume that on Pt the double bond is attached to single Pt sites while on Pd the formation of a bridged intermediate occurs. This phenomenon would explain the differences in deuterium distribution for methane in accordance with the higher isomerization activity of Pt.

REFERENCES

[1] ANDERSON, J. R., AVERY, N. R.: J. Catal., **2,** 542 (1963)
[2] ANDERSON, J. R., AVERY, N. R.: J. Catal., **5,** 446 (1966)
[3] KEMBALL, C.: Catal. Rev., **1,** (1971)
[4] MULLER, J. M., GAULT, F. G : J. Catal., **24,** 361 (1972)
[5] CARTER, J. L., CUSUMANO, J. A., SINFELT, J. H.: J. Catal., **20,** 223 (1971)
[6] KIKUCHI, E., TSUSUNI, M., MORITA, Y.: J. Catal., **22,** 226 (1971)
[7] SINFELT, J. H.: Catal. Rev., **3,** 175 (1969)
[8] BOUDART, M., PTAK, L. D.: J. Catal., **16,** 90 (1970)
[9] BRUNELLE, J. P., MONTARNAL, R. E., SUGIER, A. A.: VIth Internat. Congress on Catalysis, London 1976, Paper, B24
[10] SINFELT, J. H.: Adv. Catal., **23,** 91 (1973)
[11] MULLER, J. M., GAULT, F. G.: IVth Internat. Congress on Catalysis, Moscow, 1968: Symposium "Mechanism and Kinetics of Complex Catalytic Reations", Paper 15.
[12] GUCZI, L., SÁRKÁNY, A., TÉTÉNYI, P.: J. C. S. Faraday I, **70,** 1971 (1974)
[13] BABERNICS, L., GUCZI, L., MATUSEK, K., SÁRKÁNY, A., TÉTÉNYI, P.: VIth Internat. Congress on Catalysis, London 1976, Paper A36.
[14] GUCZI, L., SHARAN, K. M., TÉTÉNYI, P.: Monatshefte, **102,** 187 (1971)
[15] KEMBALL, C.: Proc. Roy. Soc., **A217,** 376 (1953)
[16] MCKEE, D. W., NORTON, F. J.: Catal., **3,** 252 (1964)
[17] PAÁL, Z., MATUSEK, K., TÉTÉNYI, P.: Acta Chim. (Budapest), **94,** 119 (1977)
[18] GUCZI, L., TÉTÉNYI, P.: Ann. N. Y. Acad. Sci., **213,** 173 (1973)
[19] MCCLELLAN, A. L., HARUSBERGER, H. R.: J. Coll. Interface Sci., **23,** 577 (1967)
[20] KEMBALL, C.: Adv. Catal., **2,** 233 (1950)
[21] KEMBALL, C.: Proc. 4th Internat. Congress on Catalysis, Vol. 1, p. 224, 1971
[22] TÉTÉNYI, P., GUCZI, L., PAÁL, Z.: Acta Chim. (Budapest), **83,** 37 (1974)
[23] GUCZI, L., SÁRKÁNY, A., TÉTÉNYI, P.: Proc. 5th Internat. Congress on Catalysis, Vol. 2, 1122, 1973
[24] SÁRKÁNY, A.: unpublished results

Antal SÁRKÁNY
László GUCZI
Pál TÉTÉNYI
H-1525 Budapest 114, P. O. Box 77.

Acta Chimica Academiae Scientiarum Hungaricae, Tomus 96 (1), pp. 39—44 (1978)

WET REFINING OF PHOSPHATIC YELLOW CAKE TO URANIUM TETRAFLUORIDE

M. R. ZAKI, S. A. EL-FEKEY and M. Y. FARAH

(Atomic Energy Authority, Cairo, Egypt)

Received January 10, 1977
In revised form March 15, 1977

The photolytic refining-reduction method applied to precleaned phosphatic yellow cake has been extended to uranium tetrafluoride preparation. In this study, the effect of precipitation and washing of the product on its texture and density was examined and the Debyegrams were recorded. Nuclear purity tetrafluoride was obtained, as confirmed by emission spectroscopy.

Introduction

In addition to dry methods for the preparation of uranium tetrafluoride, wet procedures have also been tried, in which hexavalent uranium is reduced to the tetravalent state, followed by the precipitation of the tetrafluoride. The characteristics of the fluoride prepared, which play a major role in the metal production process, vary remarkably with the procedure of preparation. With regard to the reduction of U(VI) to U(IV), many methods have been reported; in most of these there is serious contamination by the reductant used. The difficulties pertaining to contamination were overcome by means of organic reductants. Photolytic reduction of uranyl solutions in the presence of organic reducing agents has been known since long time [1] and various mechanisms were suggested to interpret this phenomenon [2—3]. GAL [4] has reported a method for the preparation of uranium tetrafluoride by insolation of uranyl nitrate solution in the presence of ethanol. The tetrafluoride obtained had the composition $UF_4 . 1.2\ H_2O$ after drying at 105 °C and standing for several days. DADAPE and PRASAD [5] prepared ammonium uranium fluoride by the photochemical reduction of ammonium uranyl fluoride solution, which was subsequently decomposed to anhydrous tetrafluoride. PATNAIK and SHAO [6] described a method for the preparation of U(IV) oxyformate based on photolysis. The oxyformate was then treated with 30—40% hydrofluoric acid to give uranium tetrafluoride. The reduction of pure uranyl nitrate, sulfate or chloride solutions *via* ethanol photolysis has been investigated [7]. It was found that (a) U(IV) could be reduced by solar irradiation to completion with excess ethanol and 4×10^{-2} *M* acidified uranyl sulfate solution, as long as the hydrogen ion concentration

was higher than twice that of uranium; (b) for more concentrated uranyl sulfates, an extra addition of small quantities of hydrazine sulfate was needed to complement photoreduction; (c) 20% ethanol is the recommended reductant for up to 70 g/l uranium solutions.

In the present work, studies on the precipitation of uranium tetrafluoride from completely reduced (photolysis and hydrazine) pure uranyl sulfate solutions have been carried out. Moreover, attempts have been made at preparing the tetrafluoride from actual sulfate process liquors either after direct reduction or after iron and phosphate precleaning. The green cakes prepared were subjected to chemical, mechanical, X-ray and spectrographic analysis.

Experimental

Solar irradiation experiments were carried out in various seasons, however, the results reported here pertain to autumn, whereby the average monthly bright sunshine was 318 hrs, the maximum temperature 33.2 °C, and the solar and sky radiation 532.0 cal cm^{-2}. Emphasis is placed on the autumn experiments, because in winter, at an average temperature of 17.7 °C, a monthly bright sunshine of 227.3 hrs, and solar and sky radiation of 286.6 cal cm^{-2} reduction was only half complete. In summer, at an average temperature temperature of 36.8 °C, monthly bright sunshine of 268.7 hrs, and solar and sky radiation of 690.9 cal cm^{-2}, reduction was two-third of that in autumn. The maximum average temperature was recorded 1.5 m above ground; the solar and sky radiation was obtained from meteorological records, using a Robitz Actinograph compared with an Epply pyrheliometer, whose elements were placed one meter above ground.

UF_4 preparation from pure uranyl sulfate solutions

Two series of experiments were carried out. In the first series, the hydrofluoric acid was added before insolation, while in the second it was added afterwards, with continuous stirring during precipitation. The uranyl sulfate solutions subjected to solar irradiation were 3×10^{-1} and 0.5 *M* with respect to uranium and free sulfuric acid, respectively. To these solutions, appropriate amounts of reducing agents were added (20 vol-% ethanol and 2% hydrazine sulfate). Insolation was carried out in polyethylene beakers of 50 cm cross-section. The depth of solutions varied between 1.3 and 3.75 cm. The time for complete reduction was 90 min. Hydrofluoric acid was used in a 10% excess over the stoichiometric amount as recommended by several authors [8].

We have studied effect of stirring speed, precipitation temperature and mode of washing of the precipitates, in order to define the optimal conditions for obtaining tetrafluoride with appropriate tap density. Precipitation was carried out either at room temperature or at 98 °C under nitrogen. Precipitates were washed with 1% HF till sulfate-free, then with ethanol or acetone before filtration and drying in air. The "green cakes" were then analyzed as mentioned before

Total fluorides were determined following the procedure described by SPOREK [9]. The tetrafluoride was dissolved in NaOH + H_2O_2, diluted and passed through an ion exchange column charged with Amberlite IRA–120 in the hydrogen form. The liberated hydrofluoric acid in the effluent was titrated against standard soda using methyl red as indicator. The percentage of F^- was then calculated.

The uranium in the 'green cake' was determined by dissolution in $HClO_4$–HNO_3, evaporation to dryness, redissolution of the residue in dilute nitric acid, precipitation as ammonium uranate, followed by ignition and weighing as U_3O_8 [10].

Green cake from actual process liquors

The process sulfate liquor containing foreign elements (11,400 ppm P, 8700 ppm Fe, 400 ppm Na, 200 ppm Zn, 50 ppm Pb, 25 ppm Sn, V, Cr, Cd) was either insolated directly after adjustment of the uranyl ion concentration and the free acidity (70 g U/l, 0.5 *M* H_2SO_4) and addition of the appropriate amounts of ethanol and hydrazine sulfate, or treated, while hot (85 °C), with aqueous ammonia until pH 2.7 for the skimming of iron and phosphate. Uranium and free acid concentrations were adjusted in the filtrate and the appropriate quantities of reducing agents were added before insolation for sufficient periods. The "green cake" was precipitated in nitrogen atmosphere from the hot (98 °C), reduced uranium solution by the addition of 40% hydrofluoric acid while stirring. The tetrafluoride obtained was thoroughly washed, air-dried and analyzed spectrographically.

Results and discussion

The uranium tetrafluoride prepared from pure sulfate solutions by the addition of hydrofluoric acid before and after insolation were subjected to various modes of precipitation and washing. From the results shown in Table I, it is obvious that the tetrafluoride precipitated during insolation and washed with 1% HF solution and acetone possesses the lowest tap density amounting to 1.62 g/m³. Tetrafluorides with the highest tap density of around 3 g/cm³ are precipitated from strongly stirred hot solutions. Stirring during precipitation leads to a marked increase in tap density. It should be noted that the tap density of double uranium fluoride also obtained photolytically [7] was 1.48 and 1.85 g/cm³ upon precipitation at 30 and 60 °C, respectively.

Table I

Effect of precipitation conditions and mode of washing on the tap density

UF_4 precipitated during* insolation without stirring[a]			UF_4 precipitated after insolation, while stirring[b]	
Mode of washing	Tap density (g/cm³)	Temp. (°C)	Stirring speed (rpm)	Tap density (g/cm³)
1% HF	1.57	20	—	2.1
1% HF, ethanol	1.60	20	100	1.4
1% HF, acetone	1.62	20	250	2.5
		20	500	2.8
		98	—	2.5
		98	100	2.8
		98	250	3.0

[a] Precipitation without heating

[b] Washing with 1% HF and acetone

* Personal communication; NABIL ROFAIL (M. Sc. Thesis).

Stirring at a speed of 250 °C rpm also increased the density. In the dry process involving the fluorination of UO_2 by Freon 12, the tap density of the (UF_4 + + UO_2F_2) was found to fluctuate between 2.15 and 3.04 g/cm³ for fluorination temperatures between 250 and 500 °C, and its durations between 30 and 240 min.

Regarding the screen analysis of the tetrafluoride obtained, it is clear from the data reported in Table II that (a) the density of tetrafluorides precipitated after insolation depend more or less on their texture; the finer the precipitate the higher its tap density; (b) the fluoride of the lowest tap density precipitated during insolation. It is therefore difficult to determine the dependence of density, on the particle size, as observed by PETROW [11].

The chemical and X-ray diffraction analyses (Table III) reveal that precipitates of low tap density (ca.) 1.6 (g/cm³) have the approximate composition $UF_4 \cdot 2H_2O$, while those of high density (ca.) 3 g (cm³) correspond to $UF_4 \cdot {}^3/_4\, H_2O$. The X-ray patterns show the characteristic intensities for $UF_4 \cdot 2^1/_2\, H_2O$ and $UF_4 \cdot {}^3/_4\, H_2O$ in the ASTM cards 11—623 and 10—95, respectively.

Finally, to ascertain the feasibility of a dual purpose photolytic reduction and refining, the actual yellow cake from phosphatic ores was dissolved in sulfuric acid for the simulation of process sulfate liquors obtained from autunite or uranium bearing apatite leaching. This solution was subjected to ethanol insolation followed by tetrafluoride precipitation. From Table IV,

Table II

Screen analysis of uranium tetrafluoride

Temp. (°C)	Stirring (rpm)	HF addition	Tap density (g/cm³)	Weight % (mesh)					
				+ 80	+ 120	+ 170	+ 200	+ 270	— 270 mesh
20	—	before insolation	1.62	0.9	1.0	1.1	0.2	7.0	89.2
20	—	after insolation	2.1	36.0	11.13	5.41	2.36	1.99	42.9
20	100	after insolation	2.4	23.0	7.9	6.1	4.8	3.8	53.5
20	250	after insolation	2.5	13.1	3.0	3.2	0.4	0.7	78.8
20	500	after insolation	2.8	11.0	3.8	3.5	1.5	1.9	77.3
98	—	after insolation	2.5	traces	traces	3.86	4.34	19.43	72.26
98	100	after insolation	2.8	traces	traces	3.02	4.40	16.38	76.04
98	250	after insolation	3.0	traces	traces	traces	3.20	3.14	93.65
98	500	after insolation	3.1	traces	traces	traces	3.32	3.60	92.99

Table III

X-ray diffraction analysis of uranium tetrafluoride

UF_4 (tap density 1.62 g/cm³)				UF_4 (tap density 3.1 g/cm³)			
d	I	d	I	d	I	d	I
8.45	100	2.82	40	11.64	23	1.41	30
5.96	50	2.71	40	6.92	25		
5.15	40	2.33	40	4.23	100		
4.75	40	2.02	80	4.06	40		
4.38	70			3.67	70		
4.21	60			2.08	40		
3.51	60			2.01	80		
3.48	70			1.87	30		
3.19	60			1.72	20		
2.91	40			1.44	30		

Table IV

Spectroscopic analysis of green cake

Element	Impurity in liquor (ppm)	UF_4 precipitated without precleaning		UF_4 precipitated after precleaning	
		Impurities (ppm)	Decontamination factor	Impurities (ppm)	Decontamination factor
Cd	5	0.5	10	0.1	50
B	5	0.5	10	0.1	50
P	11400	15	760	15	760
Al	25	15	2	15	2
Cu	20	5	4	5	4
Cr	5	3	2	3	2
Fe	8700	15	580	15	580
Pb	50	20	2.5	20	2.5
Mg	20	20	1	10	2
Ag	2	1	2	0.5	4
Zn	200	20	10	20	10
Na	400	200	2	20	20
Sn	5	2	1	2	2.5
V	5	5	1	5	1

it is evident that better decontamination is reached when ferric iron and phosphate are removed by precipitation at pH 2.7 and hot filtration before insolation at the optimal parameters previously defined.

By this means, cascade grade tetrafluoride can be obtained in mines. If the tetrafluoride is to be used for the production of metallic uranium by calcium or magnesium reduction, it has to be dehydrated by heating gradually up to 400 °C in a dry stream of nitrogen [12] or HF. Double fluoride has also been separated as an alternative [13] to dehydration for the preparation of UO_2F_2- free metal.

Nuclear purity uranium tetrafluoride has been prepared from photolytically reduced sulfate process liquor. Products of various tap density, texture and composition are obtained under different precipitation conditions. The approximate composition of the products with low tap density is UF_4--$2H_2O$ and UF_4, $^3/_4$ H_2O; for high density products dehydration is also feasible.

REFERENCES

[1] MELLOR, J. W.: A Comprehensire Treatise on Inorganic and Theoretical Chemistry Vol. XII, Longmans 1961
[2] HEIDT, L. J., MOON, K. A.: J. Am. Chem. Soc.; **75,** 5803 (1953)
[3] CARROLL, J. L., BURNS, R. E., WARREN, H. D.: AEC research and development HW-70543 (1961) Manford Labs. USA
[4] IVAN GAL: Recueil de travaux de l'institut de recherches sur la structure de la matière, Vol. 2, 1961 Belgrade
[5] DADAPE, V. V., KRISHNA PRASAD, N. S.: 2nd Int. Conf. on Peaceful Uses of Atomic Energy, Geneva, vol. 4, p. 130 (1958)
[6] PATNAIK, D., SAHOO, B.: Proc. Indian Acad. Sci. Sec. A 49, 200—2, April (1959)
[7] ZAKI, M. R., FARAH, M. Y,. EL-FEKEY, S. A.: Acta Chim. (Budapest) **80,** 167 (1974)
[8] NEILL, W. J., HIGGINS, I. R.: Report ORNL-2469 (1958) USAEC
[9] SPOREK, K. F.: Anal. Chem.: **30,** 1030—2 (1958
[10] CUNNUNGHAM, J. E., WALL, G. P., WELLS, I.: AERE-CE/R 2052 Part 2 (1958) United Kingdom
[11] PETROW, H. G.: Report WIN-90 (1958) USAEC
[12] HIGGINS, I. R., NEILL, W. J., MC NEESE, L. E.: 2nd Int. Conf. on Peaceful Uses of Atomic Energy, Geneva, P/506 (1958)
[13] EL-FEKEY, S. A., ZAKI, M. R., FARAH, M. Y.: Arab Journal of Nuclear Sciences and Applications; January 8,9 (1975) Cairo, Egypt.

M. R. ZAKI
S. A. EL-FEKEY
M. Y. FARAH
Atomic Energy Authority, Cairo, Egypt.

Acta Chimica Academiae Scientiarum Hungaricae, Tomus 96 (1), pp. 45–54 (1978)

SYNTHESIS OF IPECACUANHA ALKALOIDS, IV*

SYNTHESIS OF THE ETHOXY ANALOGUE OF EMETINE

J. ROHÁLY and CS. SZÁNTAY

(Institute of Organic Chemistry, Technical University, Budapest, and Central Research Institute for Chemistry, Hungarian Academy of Sciences, Budapest)

Received November 18, 1976

The analogue of emetine containing ethoxyl groups has been synthesized (**1b**). The ORD and PMR properties of emetine (**1a**), isoemetine (**9a**) and their ethoxy analogues (**1b** and **9b**) have been studied.

In the application of emetine (**1a**), exhibiting an excellent amoebicide activity [1], its relatively strong toxicity, must always be considered.

Therefore, it appears rewarding to attempt the synthesis of analogues having more favourable therapeutic indices than that of the natural product.

Exchange of methoxyl groups attached to the aromatic nucleus of alkaloids against ethoxyl has often brought about favourable changes in the physiological properties of the substance (*e.g.*, papaverine → perparine). Therefore, the aim of the present work was to synthesize the ethoxy analogue (**1b**) of emetine.

As described in an earlier paper [2], 6,7-diethoxy-3,4-dihydroisoquinoline (**2**) yields the benzoquinolizidine derivative **3a** with ethylbutenone [8], and this product was converted further with alkoxycarbonylmethylphosphonic acid dialkyl ester [3] under the conditions applied in the synthesis of emetine.

According to our earlier experience [3], the formation of three isomers (**3b**, **4a**, **5a**) can be expected. The main product (55% yield) was the crystalline compound **3b**. The IR spectrum of this product indicated the presence of a conjugated ester group, and its steric structure was proved by its successful conversion into **1b**.

By means of TLC, a fourth isomer could also be detected in the mother liquor, in addition to the three isomers mentioned (**3b**, **4a**, **5a**). This substance is **6a**, with the double bond in endocyclic position. This is confirmed by the conversion of all the other isomers uniformly into **6a** on heating with sodium methoxide, which treatment is known to catalyze the exo → endo double bond migration [4].

Catalytic reduction of **3b** yielded the saturated ester **7a** in a satisfactory yield (90%). Another substance could be detected in the mother liquor by means of TLC; this is probably the C-2 epimer.

* Part III. M. BÁRCZAI-BEKE, J. JELINEK, CS. SZÁNTAY: Acta Chim. Acad. Sci. Hung. **95**, 77 (1977).

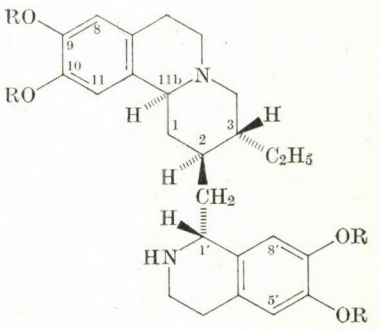

1a R = CH_3

1b R = C_2H_5

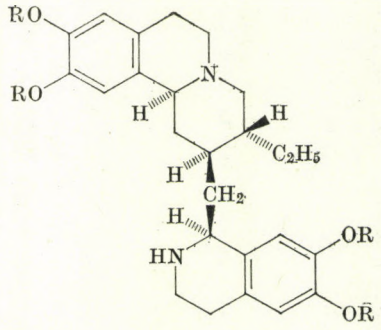

9a R = CH_3

9b R = C_2H_5

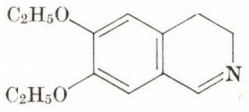

2

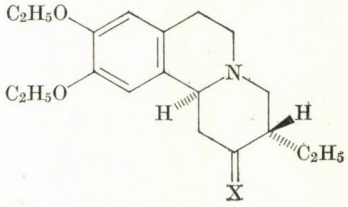

3a X = O

3b X = $CH_3O_2C—\ddot{C}—H$

3c X = $C_2H_5O_2—\ddot{C}—H$

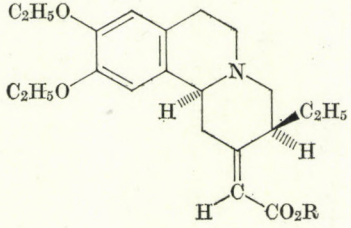

4a R = CH_3

4b R = C_2H_5

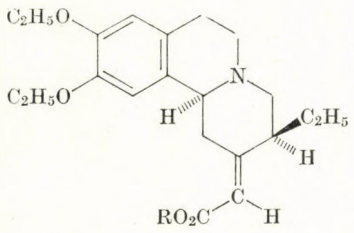

5a R = CH_3

5b R = C_2H_5

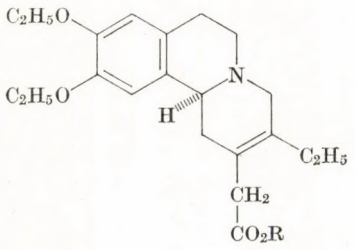

6a R = CH_3

6b R = C_2H_5

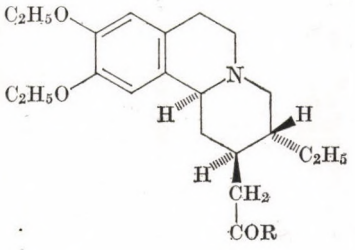

7a R = OCH_3

7b R = $NH(CH_2)_2—C_6H_3—(OC_2H_5)_2$

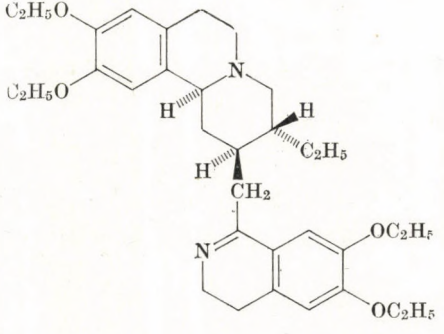

8

On the analogy of the procedure applied by OPENSHAW and WHITTAKER [5] in the synthesis of emetine, **7a** was converted into the acid amide (**7b**) with diethoxyphenylethylamine and subjected to cyclization with phosphorus oxychloride to obtain the ethoxy analogue (**8**) of O-methylpsychotrine.

Catalytic reduction of this product yielded **1b** and the isomeric **9b**. The two structures were distinguished by means of the ORD curves applied by VAN TAMELEN *et al.* [6] for making distinction between emetine (**1a**) and isoemetine (**9a**). This, of course, required isolation of the substances, which was achieved by the use of N-acetyl-L-(—)-leucine applied to **8**. Reduction of **8** in the resolved state, gave the optically active (—)-**1b** and (—)-**9b**, and their antipodes.

Since the difference between emetine (**1a**) and **1b** appears only in the alkoxyl groups located far from the chiral centres, it is justified to assume that similar rotation values correspond to similar absolute configurations.

The ORD curves (Figs 1 and 2) could be recorded in a broader wave length range than in the work of VAN TAMELEN *et al.* [6], thus even more characteristic differences were observed between the ethoxy analogues **1b** (Fig. 1) and **9b** (Fig. 2) than between emetine (**1a**) and isoemetine (**9a**).

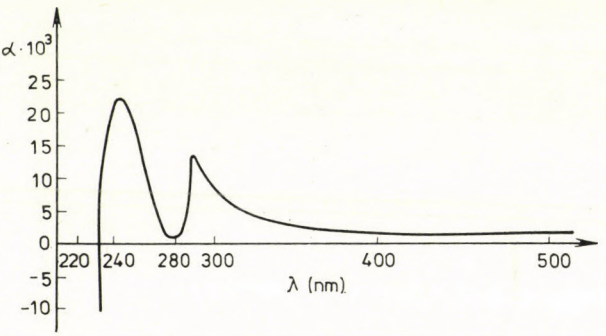

Fig. 1. ORD curve of the ethoxy analogue of emetine, **1b**.HBr; c = 0.103 (625—244 nm) in water

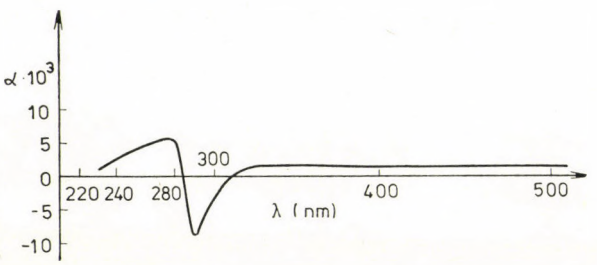

Fig. 2. ORD curve of the ethoxy analogue of isoemetine, **9b**-HBr c = 0.1505 (625—280 nm); c = 0.0752 (285—232 nm), in water

In view of the course of the ORD curves and after comparison with the ORD curves [6] of emetine (**1a**) and isoemetine (**9a**), the compounds are, in all probability, represented by structures **1b** and **9b**. The PMR spectra of the compounds epimeric at C-1' also show characteristic differences (Table I).

Table I

Chemical shifts of the aromatic protons of emetine (**1a**), *its ethoxy analogue* (**1b**), *isoemetine* (**9a**), *and its ethoxy analogue* (**9b**) *in deuterochloroform solution**

Compound	Aromatic protons		
	C-8, C-5' and C-8'		C-11
Emetine **1a**	6.64	6.6 shoulder	6.82
Ethoxy analogue of emetine **1b**	6.64	6.6 shoulder	6.82
Isoemetine **9a**	6.58		6.69
Ethoxy analogue of isoemetine **9b**	6.60		6.70

* Chemical shift values are given in δ units

In the spectra of **1a** and **1b**, one single aromatic proton appears separately, while the other three are found very near to one another. It is very probable that the conformation represented by the formula in the usual form (**1**) is not the real state of the substance in chloroform solution. It can be observed by the examination of models that a strong interference exists between the ethyl group at C-3 and the isoquinoline ring.

It seems to be more probable that the two aromatic rings are located rather near to each other in such a manner that one of the aromatic protons will reach the deshielding region of the other aromatic ring.

In the PMR spectra of isoemetine (**9a**) and its analogue (**9b**), the displacement of the special aromatic proton signal from the signals of the other aromatic protons is much smaller (0.12 pp), while this value is 0.22 ppm in the spectra of emetine (**1a**) and of its ethoxy analogue (**1b**).

Similar observations have been made in the case of (±)-2,3-didehydroemetine and (±)-2,3-didehydroisoemetine and their ethoxy analogues, too [7].

The assumed structures of compounds **1b** and **9b** have also been confirmed by the biological investigations. It was established earlier [1] that of emetine isomers a notable, amoebicide action was exerted only by the one possessing structure **1a**.

Substance **1b** had essentially the same activity as emetine, while the isomeric **9b** proved to be inactive.

The biological activity will be discussed in another paper.

Experimental

β-(3,4-Diethoxyphenyl)ethylamine was supplied by Chinoin Pharmaceutical and Chemical Works, Budapest.

UV spectra were recorded with a Unicam SP 800 spectrophotometer and the IR spectra (in KBr pellets) with a Spectromom 2000 instrument. The PMR spectra were obtained with a Perkin—Elmer R12 (60 MHz) spectrophotometer; the chemical shift values (δ) are given as ppm units; the internal standard was TMS.

The ORD curves were recorded with a Opton REPM 12 instrument.

In the qualitative thin-layer chromatographic tests Kieselgel G (Merck) adsorbent was used. The developing solvent was benzene–methanol (9 : 1). Iodine vapour was applied for detection.

3,4-Dihydro-6,7-diethoxyisoquinoline (2)

β-(3,4-Diethoxyphenyl)ethylamine (12.8 g; 61 mmoles) was dissolved in formic acid (70 ml) and refluxed for 5 hrs. The excess of formic acid was evaporated in vacuum. The residue was dissolved in dry benzene (75 ml), phosphorus oxychloride (11.85 g; 7.1 ml; 78 mmoles) was added with stirring, and the mixture was refluxed for 2 hrs. The solvent and excess phosphorus oxychloride were then evaporated in vacuum. The residue was dissolved in water (50 ml) and made alkaline with 10*N* NaOH. The aqueous solution was extracted with benzene ($2\delta \times 20$ ml). The combined benzene solution was dried over $MgSO_4$, filtered, and the benzene evaporated. The residual oil was dissolved in methanol (20 ml), acidified with conc. hydrochloric acid (4.5 ml) while cooling in ice, refrigerated, and the yellow crystals which deposited were filtered off. The hydrochloride of **2** (8.7 g; 56%) had m.p. 223—224 °C.

$C_{13}H_{18}NO_2Cl$ (255.73). Calcd. C 61.06; H 7.09; N 5.48; Cl 13.86. Found C 61.15; H 7.07; N 6.09; Cl 13.93%.

UV: λ_{max}^{water} (log ε): 246 nm (3.92), 307 (3.67), 353 (3.61).

IR (KBr): partial maxima in the 1800 cm^{-1} range; 1650 cm^{-1} (C=NH—).

The hydrochloride of **2** (2.55 g; 10 mmoles) was dissolved in water (20 ml) and made alkaline with 10*N* NaOH, then extracted with ether (4×10 ml). The combined ethereal solution was dried over $MgSO_4$, filtered and the ether evaporated. The oily residue was dissolved in hot petroleum ether (20 ml) then refrigerated. The solvent was decanted from the white needles which deposited. The crystals were dried over paraffin chips and solid KOH in a vacuum desiccator.

Compound **2** was thus obtained in the form of colourless crystals (1.0 g), m.p. 46—47 °C.

$C_{13}H_{17}NO_2$ (219.27). Calcd. C 71.2; H 7.82; N 6.39. Found C 71.06; H 7.80; N 6.64%.

UV λ_{max}^{EtOH} (log ε): 234 nm (4.27); 285 (3.85); 312 (3.79).

IR (KBr): 1630 cm^{-1} (C=N—).

PMR ($CDCl_3$): 1.45 (t, 6H, $J = 6.66$, $OCH_2—CH_3$); 2.64 (t, 2H, $J = 8$, $—CH_2—CH_2—N=$); 3.74 (t, 2H, $J = 6.66$, $CH_2—CH_2—N=$); 4.1 (q, 2H, $J = 13.5$, $J = 7.32$, $O—CH_2—CH_3$); 4.22 (q, 2H, $J = 13.5$, $J = 7.32$, $O—CH_2—CH_3$); 6.68 (s, 1H, aromatic proton); 6.84 (s, 1H, aromatic proton); 8.22 (s, 1H, CH=N—).

2-Oxo-3α-ethyl-9,10-diethoxy-1,2,3,4,6,7-hexahydro-11bαH-benzo(a)-quinolizine (3a)

The hydrochloride of **2** (25.57 g; 100 mmoles) and ethylbutenone [8] (14.47 g; 147 mmoles) were refluxed in 93% ethanol (75 ml) on a water bath for 24 hrs. The alcohol was evaporated and the residue dissolved in water (200 ml), made alkaline with solid Na_2CO_3, then refrigerated overnight. The crystals were filtered off, washed with ice-water ($2\delta \times 20$ ml), and dried in air. The solid product (25 g) was recrystallized from acetone (50 ml) to obtain **3a** (19.3 g; 62%). m.p. 120—122° C (lit. [9] m.p. 117—118 °C.

UV λ_{max}^{EtOH} (log ε): 212 nm (4.045), 281 (3.474), 224 (inflection).

IR (KBr): 2760 and 2800 cm^{-1} (Bohlmann bands), 1710 cm^{-1} (C=O, ketone).

PMR ($CDCl_3$): 1.0 (t, 3H, $J = 6.0$, $CH_2—CH_3$); 1.44 (t, 6H, $J = 6.6$, $O—CH_2—CH_3$); 2.1—3.8 (m, 12H, Cl, C3, C4, C6, C7, C11b, $C4—CH_2—$: aliphatic protons) 4.067; 4.078 (q, 4H, $J = 6.0$, $O—CH_2—CH_3$); 6.55, 6.61 (s, 2H, aromatic protons).

E-Methyl[3α-ethyl-9,10-diethoxy-1,3,4,6,7,11bα-hexahydro-2H--benzo(a)quinolizinylidene-2]-acetate (3b)

Potassium *t*-butoxide (6.72 g; 60 mmoles) and diethyl methoxycarbonylmethylphosphonate [3] (16.0 g; 76 mmoles) were dissolved in anhydrous dimethylformamide (19.2 ml). A solution of **3a** (8.6 g; 21 mmoles) in anhydrous dimethylformamide (43 ml) was added, and the mixture was allowed to stand at room temperature for 72 hrs. The solution was added to ice-water (500 ml) by drops, and the aqueous phase was extracted with ether (4×50 ml). The combined ethereal solution was extracted with saturated aqueous $NaHSO_3$ solution (20 ml) and with water (2×20 ml). Th ethereal solution was dried over $MgSO_4$, filtered, and the ether evaporated. The syrupy residue (10.15 g) was dissolved in methanol (6.5 ml) and refrigerated overnight. The crystals were filtered off yielding **3b** (5.6 g; 55%); m.p. 77—78 °C.

After recrystallization from methanol, the m.p. was 80—81 °C.

$C_{22}H_{31}NO_4$ (373.478). Calcd. C 70.75; H 8.37; N. 3.75. Found C 70.80; H 8.35; N 3.81%.

IR (KBr): 2745, 2765, 2805 (Bohlmann bands); 1720 cm^{-1} (C=O ester); 1640 cm^{-1} (C=C—C=O).

PMR ($CDCl_3$): 0.98 (t, 3H, $CH_2—CH_3$); 1.41 (t, 6H, J = 6.66, O—CH_2—CH_3); 2.0—3.4 (m, 11H, Cl, C3 C4, C6, C7, C3—CH_2—, aliphatic protons); 3.76 (s, 3H, CO_2CH_3); 4.054, 4.11 (q, 4H, J = 14.7, J = 7.32, O—CH_2—CH_3); 4.51 (q, 1H, J = 13.3, J = 3.3; Cl—H *equ*); 5.65 (s, 1H, $CH_3O_2C—CH=C$); 6.6, 6.86 (s, 2H, aromatic protons).

E-Ethyl [3α-ethyl-9,10-diethoxy-1,3,4,6,7,11bα-hexahydro-2H--benzo(a)quinolizinylidene-2]-acetate (3c)

The substance was prepared as described for **3b**, using diethyl ethoxycarbonylmethylphosphonate [3]. M.p. of **3c**: 97—98 °C (from ethanol).

$C_{23}H_{33}NO_4$ (387.508). Calcd. C 71.28; H 8.59; N 3.61. Found C 71.27; H 8.51; N 3.33%.

IR (KBr): 2745 and 2795 cm^{-1} (Bohlmann bands); 1715 cm^{-1} (C=O ester); 1536 cm^{-1} (C=C—CO).

Methyl [3-ethyl-9,10-diethoxy-1,6,7,11bα-tetrahydro-4H-benzo(a)quinolizinyl--2]-acetate (6a)

After having prepared **3b** as described above and isolating the pure compound, the methanolic mother liquor containing 4.5 g (12 mmoles) of **3b**, **4a** and **5a** was mixed with a solution of sodium methoxide (3.95 g; 73 mmoles) in methanol (25 ml) and refluxed in nitrogen atmosphere for 2 hrs.; the methanol was then evaporated in vacuum, under nitrogen. The residue was dissolved in ice-water (20 ml), and the aqueous solution was extracted with benzene (5×10 ml). The combined benzene solution was dried over $MgSO_4$, filtered and the solvent evaporated in vacuum. The residue was a pale yellow oil, **6a** (4.5 g; 100%).

IR (KBr): film, 2800, 2755, 2730 cm^{-1} (Bohlmann bands); 1740 cm^{-1} (C=O ester). According to TLC, the product was homogeneous and suitable for use in the further synthetic steps.

Methyl [3α-ethyl-9,10-diethoxy-1,3,4,6,7,11bα-hexahydro-2H-benzo(a)quinolizinyl--2]-acetate (7a)

Compound **3b** (10 g; 26.5 mmoles), prepared as described above, was dissolved in methanol (90 ml) and, after the addition of methanol (6 ml) containing hydrochloric acid (0.98 g; 26.8 mmoles), it was hydrogenated in the presence of Pd/C catalyst (1.5 g) at a pressure of 6 atm. After the absorption of the calculated amount of hydrogen (2 hrs) the solution was filtered from the catalyst and evaporated to dryness in vacuum. The residue was dissolved in water (50 ml) and made alkaline with conc. NH_4OH (14 ml). A sticky material separated, which was dissolved in ether (60 ml). The ethereal solution was dried over $MgSO_4$, filtered, and the ether evaporated. The oily residue was dissolved in petroleum ether (18 ml) and refrigerated overnight. White crystals of **7a** separated (8.84 g; 89%), m.p. 74—75 °C.

$C_{22}H_{33}NO_4$ (375.494). Calcd. C 70.35; H 8.86; N 3.73. Found C 70.51; H 8.80; N 3.66%.

IR (KBr): 2794 and 2745 cm^{-1} (Bohlmann bands); 1735 cm^{-1} (C=O ester).

PMR ($CDCl_3$): 0.96 (t, 3H, —CH_2—CH_3); 1.42 (t, 6H, J = 6.66, —OCH_2—CH_3); 1.9—3.3 (m, 15H, Cl, C2, C3, C4, C6, C7, C2—CH_2—, C3—CH_2— aliphatic protons); 3.72 (s, 3H, CH_3—CO); 4.06 (q, 4H, J = 6.66, O—CH_2—CH_3); 6.6 (s, 1H, aromatic proton); 6.72 (s, 1H, aromatic proton).

3α-Ethyl-9,10-diethoxy-1,3,4,6,7,11bα-hexahydro-2H-benzo(a)quinolizinyl--2β-acetic acid N-[β-(3',4'-diethoxyphenyl)]-ethylamide (7b)

A mixture of β-(2,3-diethoxyphenyl)ethylamine (15.8 g; 76 mmoles) and **7a** (9.46 g; 25 mmoles) was maintained at 170 °C for 14 hrs in nitrogen atmosphere. After cooling, the product was mixed with ethyl acetate (30 ml) and refrigerated. The pale yellow crystals were filtered off and washed with some cold ethyl acetate to obtain compound **7b** (11.77 g; 84%), m.p. 142—146 °C.

The substance was sufficiently pure for direct use in the further synthetic steps.

A sample recrystallized from ethyl acetate (10 ml solvent per g) had m.p. 152—153 °C.

$C_{33}H_{48}N_2O_5$ (552.73). Calcd. C 71.75; H 8.75; N 5.07. Found C 71.51; H 8.82; N 5.08%.

IR (KBr): 2810 and 2750 cm^{-1} (Bohlmann bands); 1640 cm^{-1} (Amide I); 1558 and 1562 (Amide II); 1260 and 1230 cm^{-1} (C—O—C).

(±)-2β[(6',7'-Diethoxy-3',4'-dihydro-1'-isoquinolinyl)-methyl]--3α-ethyl-1,3,4,6,7,11bα-hexahydro-9,10-diethoxy-2H-benzo(a)quinolizine (8)

Compound **7b** (11.7 g; 21.2 mmoles) was dissolved in anhydrous benzene (250 ml). $POCl_3$ (8.2 g; 4.9 ml; 53.2 mmoles) was added to the solution dropwise under stirring and the mixture was refluxed for 1 hr. The solvent was evaporated in vacuum and the residue dissolved in water (100 ml). The aqueous solution was made alkaline with conc. NH_4OH (20 ml) under cooling in ice-water. The sticky substance which separated from the aqueous solution was dissolved in chloroform (100 ml), dried over $MgSO_4$, filtered and the chloroform was evaporated. The residue was dissolved in methanol (14 ml) and crystalline oxalic acid (5.5 g; 43.6 mmoles) in methanol (12 ml) was added to the solution.

The methanol solution was mixed with ether (30 ml) and refrigerated. The crystalline oxalic acid salt was obtained by decanting the mother liquor and recrystallizing the salt from a mixture of methanol (15 ml) and ether (25 ml). The crystals were filtered off and dried in air to obtain the dioxalic acid salt of (±)-**8** (12.5 g; 79%), m.p. 150—152 °C.

$C_{33}H_{46}N_2O_4 \cdot 2\ C_2H_2O_4 \cdot 1.5\ H_2O$ (741.824). Calcd. C 59.9; H 7.2; N 3.78; H_2O 3.64. Found C 60.1; H 7.19; N 3.81; H_2O 4.0%.

The oxalate of **8** (12.5 g) was dissolved in water (100 ml) and made alkaline with conc. NH_4OH while cooling in ice-water. The white solid was filtered off, washed with water (3×10 ml) and dried over solid KOH in a vacuum desiccator, then dissolved in boiling anhydrous ether (100 ml). (±)-**8** crystallized from the ethereal solution after cooling in a refrigerator (8.6 g; 76%), m.p. 94—95 °C.

$C_{33}H_{46}N_2O_4$ (534.717). Calcd. C 74.11; H 8.67; N 5.24. Found C 74.3; H 8.98; N 5.21%.

UV λ_{max}^{EtOH} (log ε): 231 (4.38), 281 (3.93), 310 (3.71).

UV $\lambda_{max}^{0.1\ N\ HCl}$ (log ε) 213 (4.20), 251 (4.40); 2.90 (3.85), 309 (3.93); 348 (3.84).

IR (KBr): 2790 and 2740 cm^{-1} (Bohlmann bands); 1623 cm^{-1} (C=N); 1265 and 1230 cm^{-1} (C—O—C).

PMR ($CDCl_3$): 1.02 (t, 3H, CH_2—CH_3); 1.43 (dec., 12H, O—CH_2—CH_3); 1.8—3.8 (m, 19H, aliphatic protons); 4.07 (dec., 8H, O—CH_2—CH_3); 6.58 (s, 2H, aromatic protons); 6.7 and 7.1 (s, 2H, aromatic protons).

(±)-2β-[(6',7'-Diethoxy-3',4'-dihydro-1'-isoquinolinyl)-methyl]-3α-ethyl--1,3,4,6,7,11bα-hexahydro-9,10-diethoxy-2H-benzo(a)quinolizine ((+)-8) di-N-acetyl-L-(—)-leucine salt

Compound (±)-**8** (5.34 g; 10 mmoles) and N-acetyl-L-(—)-leucine (3.46 g; 20 mmoles) were dissolved in warm ethyl acetate (50 ml). The solution was cooled to room temperature, ether (550 ml) was added and the mixture was allowed to stand in a refrigerator for 24 hrs. The solvent was decanted and the crystals were washed with a mixture of dry ethyl acetate and ether (1 : 10) at 0 °C, to obtain the di-N-acetyl-L-(—)-leucine salt of (+)-**8** (4.8 g; 4.36 mmoles), m.p. 68—70 °C. After recrystallization from ethyl acetate (23 ml), the compound had m.p. 70—71 °C; $[\alpha]_D^{20}$ + 25.5 ±1° (c = 4, methanol).

$C_{33}H_{26}N_2O_4 \cdot 2C_8H_{15}NO_3 \cdot 3H_2O$ (935.21). Calcd. C 62.92; H 8.83; N 5.99; H_2O 5.78. Found C 62.85; H 8.7; N 6.16; H_2O 5.22%.

(+)-2β-[(6',7'-Diethoxy-3',4'-dihydro-1'-isoquinolinyl)-methyl]-3α-ethyl--1,3,4,6,7,11bα-hexahydro-9,10-diethoxy-2H-benzo(a)quinolizine ((+)-8)

The di-N-acetyl-L-(—)-leucine salt of (+)-**8** (1.0 g; 1.07 mmoles) was dissolved in water (10 ml). The solution was made alkaline with conc. NH_4OH and extracted with ether (3×10 ml). The combined ethereal solution was dried over $MgSO_4$, filtered, and the ether evaporated. The residual oil (0.5 g) was dissolved in anhydrous ether (1.3 ml) and petroleum ether was added (1.3 ml) to the solution. The crystals which separated on refrigeration were filtered off to yield (+)-**8** (0.3 g; 52%), m.p. 50—52 °C; $[\alpha]_D^{20}$ + 42.6° ±1° (c = 1.85, ethyl alcohol).

$C_{33}H_{46}N_2O_4$ (534.717). Calcd. C 74.11; H 8.67; N 5.24. Found C 74.08; H 8.67; N 5.24%.

UV λ_{max}^{EtOH} (log ε): 232 (4.31), 260 (3.91,) 280 (4.01), 308 (3.80).

UV $\lambda_{max}^{0.1\,N\,HCl}$ (log ε): 213 (4.21), 245 (4.22), (290 (3.84), 307 (3.91), 352 (3.87).

PMR ($CDCl_3$): 1.03 (t, 3H, CH_2—CH_3); 1.48 (dec., 12H O—CH_2—CH_3); 4.1 (dec., 8H, O—CH_2—CH_3); 6.57; 6.59; 6.75; 7.09 (s, 4H, aromatic protons).

(—)-2β-[6',7'-Diethoxy-1'β,2',3',4'-tetrahydro-1'-isoquinolinyl)-methyl]-3α-ethyl-1,3,4, 6,7,11bα-hexahydro-9,10-diethoxy-2H-benzo(a)quinolizine (1b) and (—)-2β-[(6',7'- -diethoxy-1'α,2',3',4'-tetrahydro-1'-isoquinolinyl(-methyl]-3α-ethyl-1,3,4,6,7,11bα- -hexahydro-9,10-diethoxy-2H-benzo(a)quinolizine (9b)

Raney nickel catalyst (21 g), washed previously with water and ethanol, was suspended in ethanol (40 ml). A solution of (+)-**8** (8.0 g; 15 mmoles) and sodium ethoxide (19 g; 280 mmoles) in ethanol (125 ml) was added to the suspension. The alcoholic suspension was subjected to hydrogenation at 15 atm pressure. After the absorption of 1 mole of hydrogen (16 hrs) the catalyst was filtered off and the alcohol evaporated in vacuum. The residue was dissolved in water (60 ml) at room temperature and extracted with ether (3×40 ml). The combined ethereal solution was dried over $MgSO_4$, filtered, and the solvent evaporated. The residual sticky substance (8 g) was mixed with anhydrous oxalic acid (3.1 g; 34.5 mmoles) and dissolved in hot methanol (9 ml). The solution was allowed to stand at room temperature for about 2 hrs. The white crystals were filtered off, washed with cold methanol (7 ml), and dried; 6.4 g, m.p. 193—195 °C. After recrystallization from methanol (100 ml), the dioxalate of **1b** (3.83 g; 35%) had m.p. 195—198 °C.

$C_{33}H_{48}N_2O_4 \cdot 2C_2H_2O_4$ (716.813). Calcd. C 62.0; H 7.31; N 3.91. Found C 61.75; H 7.27; N 4.14%.

The dioxalate of **1b** (3.8 g) was dissolved in water (30 ml) and the solution was made alkaline with conc. NH_4OH. Base **1b** separating from the aqueous solution was dissolved in ether (20 ml), dried over $MgSO_4$, filtered, and the ether was evaporated. The residue was dissolved in ethanol (5 ml) and, after the addition of ethanol containing an equivalent amount of hydrochloric acid, it was evaporated to dryness in vacuum. The solid residue (3.31 g) was dissolved in chloroform (3 ml), ethyl acetate (6 ml) was added and the mixture was allowed to stand in a refrigerator. The crystals were filtered off and dried to give **1b**. $2HCl \cdot 2.5H_2O$ (2.5 g; 25.8%), m.p. 210—215 °C; $[\alpha]_D^{22}$ + 44.5° ±1° (c = 1.01, $CHCl_3$).

$C_{33}H_{48}N_2O_4 \cdot 2HCl \cdot 2.5H_2O$ (652.40). Calcd. C 60.52; H 8.47; N 4.28; Cl 10.83; H_2O 6.88. Found C 60.44; H 8.65; N 4.42; Cl 10.93; H_2O 6.93%.

UV $\lambda_{max}^{H_2O}$ (log ε): 211 (4.21); 230 (4.08); 282 nm (3.75).

1b. $2HCl \cdot 2.5H_2O$ (0.2 g; 0.3 mmole) was dissolved in water (10 ml) and, with cooling in ice-water, the solution was made alkaline by the addition of conc. NH_4OH. The white amorphous precipitate was filtered off, washed with water (2×5 ml) and dried over solid KOH in a vacuum desiccator. Compound (—)-**1b** (0.15 g; 0.275 mmole) was obtained as a white amorphous powder, $[\alpha]_D^{22}$ —49.70° ±1° (c = 2.009, $CHCl_3$).

$C_{33}H_{48}N_2O_4 \cdot 1/2H_2O$ (545.442). Calcd. C 72.66; H 9.05; N 5.14; H_2O 1.65. Found C 72.69; H 8.91; N 5.12; H_2O 1.49%.

UV λ_{max}^{EtOH} (log ε): 226 (4.15); 285 nm (3.83).

PMR ($CDCl_3$): 0.98 (t, 3H, CH_2—CH_3); 1.39 and 1.41 (t, 12H, J = 7.32, O—CH_2—CH_3); 1.8—3.3 (m, 21H, aliphatic protons and NH proton); 4.05 and 4.06 (q, 8H, J = 18 and J = 7.32 O—CH_2—CH_3); 6.64, 6.6 (sh.), (3H, aromatic protons); 6.82 (1H, aromatic proton).

The methanolic mother liquor obtained after filtering off the crystalline dioxalate of **1b** (6.4 g) was evaporated to dryness in vacuum. The solid residue (4.5 g) was crystallized from methanol (16 ml). The crystals were rapidly filtered off and recrystallized from a mixture

of methanol and water (16 : 1). The crystalline substance obtained was the dioxalate of (—)-**9b** (1.2 g; 18.6%), m.p. 145—146 °C.

$C_{33}H_{48}N_2O_4 \cdot 2C_2H_2O_4 \cdot H_2O$. Calcd. C 60.48; H 7.14; N 3.81; H_2O 2.45. Found C 60.55; H 7.25; N 3.84; H_2O 2.55%.

Isolation of the base (—)-**9b** was accomplished as described for (—)-**1b**, starting from the dioxalate (—)-**9b**.

Compound (—)-**9b** is a white amorphous powder, $[\alpha]_D^{25}$ —25° ±1° (c = 1.18, $CHCl_3$).

PMR ($CDCl_3$): 1.01 (t, 3H, CH_2—CH_3); 1.41 (t, 12H, J = 7, O—CH_2—CH_3); 1.8—3.5 (m, 21H, aliphatic protons and NH proton); 4.04 and 4.05 (q, 8H, J = 16, J = 6, —O—CH_2—CH_3); 6.6 (3H, aromatic protons); 6.7 (1H, aromatic proton).

*

The authors' thanks are due to Chinoin Pharmaceutical and Chemical Works for supporting the present work; to Dr. M. VAJDA (Organic Chemical Institute of the Eötvös L. University, Budapest) for recording the ORD curve; to Dr. P. KOLONITS for recording the PMR spectra and to Dr. I. BALOGH-BATTA for the microanalyses. Valuable technical assistance by Mr. I. JAKSA is acknowledged.

REFERENCES

[1] VEDDER,: J. Trop. Med., **15,** 313 (1912)
[2] BEKE, D., SZÁNTAY, Cs.: Ber., **95,** 2132 (1962) Magyar Kém. Foly., **68,** 426 (1962); Hung. Pat. 150168
[3] SZÁNTAY, Cs., TŐKE, L., KOLONITS, P.: J. Org. Chem., **31,** 1447 (1966); Magyar Kém. Foly., **73,** 293 (1967)
[4] WHITTAKER, N.: J. Chem. Soc. (C), **1969**, 94
[5] OPENSHAW, H. T., WHITTAKER, N.: J. Chem. Soc., **1963,** 1461
[6] VAN TAMELEN, E. E., ALDRICH, P. E., HESTER, J. B: J. Am. Chem. Soc., **81,** 6214 (1959)
[7] SZÁNTAY, Cs., ROHÁLY, J.: Acta Chim. (Acad. Sci. Hung.) **96**, 55 (1978)
[8] SZÁNTAY, Cs., ROHÁLY, J.: Ber., **96,** 1788 (1963); Magyar Kém. Foly., **69,** 390 (1963)
[9] BROSSI, A., LINDLAR, H., WALTER, M., SCHNIEDER, O.: Helv. Chim. Acta, **41,** 119 (1958)

János ROHÁLY
Csaba SZÁNTAY
H-1521 Budapest, Műegyetem.

Acta Chimica Academiae Scientiarum Hungaricae, Tomus 96 (1), pp. 55—60 (1978)

SYNTHESIS OF IPECACUANHA ALKALOSID, V*

A NEW SYNTHESIS OF DEHYDROEMETINE AND ITS ETHOXY ANALOGUE

Cs. SZÁNTAY and J. ROHÁLY

(Institute of Organic Chemistry, Technical University, Budapest and Central Research Institute for Chemistry, Hungarian Academy of Sciences, Budapest)

Received November 18, 1976

The synthesis of dehydroemetine (**1a**) has been achieved through dehydroprotoemetine (**3b**) by means of the Pictet—Spengler type cyclization procedure. In the preparation of the ethoxy analogue of dehydroemetine (**1b**) the Bischler—Napieralski cyclization reaction was used.

Dehydroemetine (**1a**) is a drug with an excellent amoebicide activity. Its first synthesis was reported by BROSSI *et al.* [1].

In the hope of reducing the toxic side effects of both emetine and dehydroemetine, the ethoxy analogue of dehydroemetine (**1b**) was also synthesized, following a synthesis of the ethoxy analogue of emetine [3]. A new reaction path was simultaneously developed for the preparation of dehydroemetine (**1a**).

Since in our earlier emetine synthesis [2] the stereoselectivity of the last step was successfully enhanced by the application of the Pictet—Spengler cyclization procedure, this reaction was favoured in the preparation of dehydroemetine (**1a**), too.

The synthesis of the ethoxy analogue of dehydroemetine (**1b**) was achieved by using the Bischler—Napieralski cyclization reaction.

On the analogy of the method given for the preparation of the dimethoxy derivative **2a** [4], the exo → endo isomerization of the double bond of the unsaturated ester **2b** [3] was effected again with sodium methoxide [3].

In the course of the new synthesis of dehydroemetine (**1a**), the ester **3a** [4] was reduced with di-isobutylaluminium hydride yielding dehydroprotoemetine (**3b**), which was then converted with β-(3-hydroxy-4-methoxyphenyl)-ethylamine into dehydrocephaeline (**1c**) and its epimer, **5c**, by the Pictet—Spengler method. These reaction products were converted into dehydroemetine (**1a**) and dehydroisoemetine (**5a**) with diazomethane, without previous separation.

In order to prepare the ethoxy analogue of dehydroemetine (**1b**), the ester **3c** [3] was converted into the acid amide **3d** with diethoxyphenylethyl-

* Part IV: ROHÁLY, J., SZÁNTAY, Cs.: Acta Chim. Acad. Sci. Hung. **96**, 45 (1978)

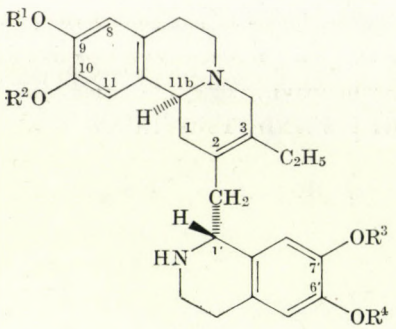

1a $R^1 = R^2 = R^3 = R^4 = CH_3$

1b $R^1 = R^2 = R^3 = R^4 = C_2H_5$

1c $R^1 = R^2 = R^3 = CH_3$ $R^4 = H$

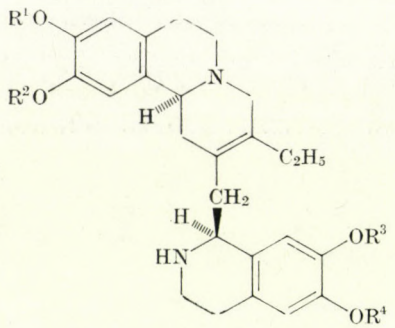

5a $R^1 = R^2 = R^3 = R^4 = CH_3$

5b $R^1 = R^2 = R^3 = R^4 = C_2H_5$

5c $R^1 = R^2 = R^3 = CH_3$ $R^4 = H$

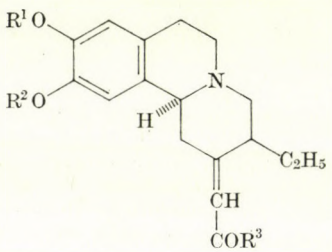

2a $R^1 = R^2 = CH_3$ $R^3 = OC_2H_5$

2b $R^1 = R^2 = C_2H_5$ $R^3 = OCH_3$

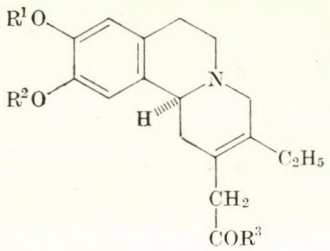

3a $R^1 = R^2 = CH_3$ $R^3 = OC_2H_5$

3b $R^1 = R^2 = CH_3$ $R^3 = H$

3c $R^1 = R^2 = C_2H_5$ $R^3 = OCH_3$

3d $R^1 = R^2 = C_2H_5$ $R^3 = NH-(CH_2)_2-C_6H_3(OC_2H_5)_2$

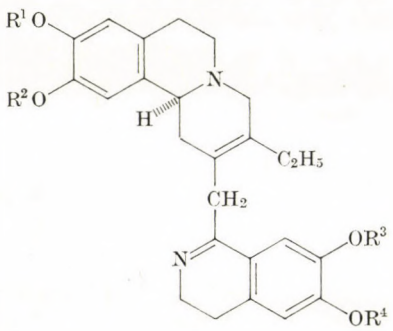

4

$R^1 = R^2 = R^3 = R^4 = C_2H_5$

amine, according to the method suggested by OPENSHAW and WHITTAKER [5]. Cyclization of the reaction product with phosphorus oxychloride gave the ethoxy analogue of 2,3-didehydro-O-methylpsyhotrine (**4**), and this yielded **1b** and the isomeric **5b** on reduction with zinc in hydrochloric acid.

Compounds **1b** had near the same antiamoebic properties towards *Entamoeba hystolytica* strains as emetine or dehydroemetine (**1a**), at the same time the lethal dose (LD_{50}) was 1000 mg/kg, in contrast with about 80 mg/kg of emetine and dehydroemetine, in subcutaneous administration to mice. Similar differences amounting to an order of magnitude in favour of **1b** were observed in the chronic toxicity tests.

Experimental

The IR spectra were recorded in KBr pellets with a Spectromom 2000 instrument. The UV spectra were taken with a Unicam SP 800 spectrophotometer, and the PMR spectra were obtained with a Perkin—Elmer R12 (60 MHz) instrument. Chemical shifts are given in δ (ppm) units; the internal standard was TMS. β-(3,4-Diethoxyphenyl)ethylamine was supplied by Chinoin Pharmaceutical and Chemical Works.

2,3-Didehydroprotoemetine (3b)

Ethyl [3-ethyl-9,10-dimethoxy-1,6,7-11bα-tetrahydro-4H-benzo(a)quinolizinyl-2]-acetate (**3a**) [4] (2.6 g; 7.25 mmoles) was dissolved in anhydrous toluene (53 ml). The solution was cooled to —65 °C with stirring in dry nitrogen atmosphere, and di-isobutylaluminium hydride (1.2 g; 1.5 ml; 8.5 mmoles) was added to it. The solution was stirred at —65 °C for 2 hrs. A saturated solution of sodium hydrogen sulfite was then added, while maintaining the temperature below —40 °C.

After the addition of the $NaHSO_3$ solution, the temperature of the mixture was allowed to rise to room temperature. The precipitate was filtered off and dissolved in water (100 ml). Toluene was separated from the aqueous $NaHSO_3$ solution. The aqueous phases were combined and extracted with ether (40 ml). The aqueous solution was then made alkaline (pH = 9) with 2*N* NaOH, while cooling in an ice salt mixture: the temperature of the solution must not exceed 0 °C. The precipitate produced by the addition of the alkali was dissolved in ether (60 ml), and the aqueous phase was extracted with ether (3×30 ml).

The combined ethereal solution was dried over $MgSO_4$, filtered, and the solvent was removed at room temperature in vacuum in a stream of nitrogen. The residue was a pale yellow solid, **3b** (1.4 g; 64%).

PMR ($CDCl_3$): 1.04 (t, 3H, J = 7.2, CH_2—CH_3); 1.9—3.5 (m, 13H, aliphatic protons); 3.84 (s, 6H, O—CH_3); 6.58 and 6.61 (2×s, 2H, aromatic protons); 9.68 (t, 1H, CHO).

The substance was subjected to analysis in the form of the perchlorate. Compound **3b** (0.157 g; 0.5 mmole) was dissolved in ethanol (1 ml) and perchloric acid (0.17 ml; 70%) was added dropwise. The perchlorate was then precipitated by the addition of water. The perchlorate **3b** (0.175 g; 0.405 mmole) was dissolved in hot methanol (3.2 ml), cooled to room temperature, a few drops of water were added until the solution became turbid and the mixture was refrigerated. The crystals were filtered off to obtain the perchlorate of **3b**. H_2O (0.076 g; 0.176 mmole), m.p. 198—200 °C, analytically pure.

$C_{19}H_{25}NO_3 \cdot HClO_4 \cdot H_2O$ (433.86). Calcd. C 52.6; H 6.5; N 3.23; Cl 8.17; H_2O 4.52. Found C 52.11; H 6.6; N 3.13; Cl 7.82; H_2O 4.15%.

2,3-Didehydroemetine (1a), 2,3-didehydroisoemetine (5a) and 2,3-didehydrocephaeline (1c)

Compound **3b** (1.3 g; 4.34 mmoles) and β-(3-hydroxy-4-methoxyphenyl)ethylamine hydrochloride (1.71 g; 8.15 mmoles) were suspended in water (36 ml) and glacial acetic acid (3 ml) was added. The solution (pH 4.5) was allowed to stand in nigtrogen atmosphere at

room temperature for 5 days. The pH of the solution was then adjusted to 9 by the addition of solid Na_2CO_3. A pale brown precipitate separated; this was filtered off, washed with some water and dried over P_2O_5 in a vacuum desiccator. Raw 2,3-didehydrocephaeline (**1c**) and its epimer (**5c**) (1.55 g; 81%) were obtained. The products were dissolved in ethanol (35 ml), diazomethane (3.5 g; 83.5 mmoles) in ether (300 ml) was added to the solution, and the mixture was allowed to stand at room temperature for 2 days. The solvents were removed on a water bath at 35 °C in vacuum.

The oily residue was dissolved in ether (75 ml) and extracted with 2*N* NaOH (20 ml) and water (5×20 ml). The ether solution was dried over $MgSO_4$, filtered, and the ether was evaporated in vacuum. The residue was a mixture (1 : 1) of 2,3-didehydroemetine (**1a**) and 2,3-didehydroisoemetine (**5a**) (1.5 g; 75%).

The mixture was dissolved in methanol (2.7 ml) and a solution of anhydrous oxalic acid (0.6 g; 6.65 mmoles) in methanol (1.6 ml) was added to the solution. After seeding with the oxalate of 2,3-didehydroisoemetine (**5a**), the solution was allowed to stand at room temperature for one day. The oxalate of 2,3-didehydroisoemetine (**5a**) crystallized (0.9 g; 1.35 mmoles), m.p. 175—177 °C (lit. [1] m.p. 175—178 °C).

The filtrate was then evaporated to dryness in vacuum, the residue was dissolved in water (20 ml), clarified with carbon and made alkaline with 10*N* NaOH (1 ml). The precipitate was dissolved in benzene (40 ml). The benzene solution was extracted with water (3×20 ml), dried over $MgSO_4$, filtered and acidified with ethanol, which contained hydrochloric acid, then evaporated to dryness in vacuum. The residue (0.8 g) was crystallized from a mixture of methanol (15 ml) and ether (40 ml) to obtain the dihydrochloride of 2,3-didehydroemetine (**1a**) (0.75 g; 1.3 mmoles), m.p. 252—254 °C (lit. [1] m.p. 248—250 °C).

[3-Ethyl-9,10-diethoxy-1,6,7,11bα-tetrahydro-4H-benzo(a)quinolizinyl-2]-acetic acid N-[β-(3',4'-diethoxyphenyl)]ethyl amide (3d)

Methyl [3-ethyl-9,10-diethoxy-1,6,7,11bα-tetrahydro-4H-benzo(a)quinolizinyl-2]-acetate (**3c**) [3] (4.5 g; 12 mmoles) and β-(3,4-diethoxyphenyl)ethylamine (6.2 g; 29.6 mmoles) were heated under nitrogen atmosphere at 170 °C for 4 hrs. The excess of β-(3,4-diethoxyphenyl)ethylamine was then evaporated in a stream of nitrogen in vacuum. The residue was recrystallized from ethyl acetate (7 ml) to obtain **3d** (5.2 g; 78%), m.p. 115—116 °C.

This product was sufficiently pure for use in the following synthetic steps.

A sample recrystallized from ethyl acetate (5 ml) for analysis had m.p. 122—124 °C.

$C_{33}H_{46}N_2O_5$(550.717). Calcd. C 71.97; H 8.42; N 5.09. Found C 71.44; H 8.31; N 5.04%.

IR (KBr): 3320 (NH); 1645 (Amide I); 1560 cm^{-1} (Amide II).

(±)-2-[(6',7'-Diethoxy-3',4'-dihydro-1'-isoquinolinyl)-methyl]-3-ethyl-1,6,7,11bα-tetrahydro-9,10-diethoxy-4H-benzo(a)quinolizine (4)

Compound **3d** (5.5 g; 10 mmoles) was dissolved in anhydrous benzene (60 ml). Phosphorus oxychloride (3.85 g; 2.3 ml; 25 mmoles) was added with stirring, and the solution was refluxed for 1 hr. The solvent was evaporated in vacuum and the residue dissolved in water (60 ml). The aqueous solution was made alkaline with conc. NH_4OH (7.5 ml) while cooling in ice-water. The precipitate was extracted with benzene (4×20 ml). The combined benzene solution was dried over $MgSO_4$, filtered, and the benzene was evaporated in vacuum. The oily residue was dissolved in methanol (5 ml) and acidified with methanol containing hydrochloric acid. Cooling in ice-water was applied meanwhile. The methanolic solution was mixed with ether (30 ml) and refrigerated. Compound **4** · 2HCl · 4 · H_2O was thus obtained (5.53 g; 81%), m.p. 136—138 °C.

$C_{33}H_{44}N_2O_4$ · 2HCl · 4.5 H_2O (686.802). Calcd. C 57.83; H 8.08; N 4.08; Cl 10.32; H_2O 11.80. Found C 57.80; H 7.92; N 3.81; Cl 10.37; H_2O 11.30%.

UV λ_{max}^{water} (log ε): 213 (4.17), 242 (4.14), 290 (3.83), 307 (3.87), 353 nm (3.87).

Compound **4** · 2HCl (1 g) was dissolved in water (20 ml) and made alkaline with conc. NH_4OH while cooling in ice-water. The yellow precipitate was filtered off, washed with water and dried over KOH at room temperature in a vacuum desiccator to obtain a yellow powder, **4** (0.7 g).

$C_{33}H_{44}N_2O_4$ · 1/2H_2O (543.725). Calcd. C 73.14; H 8.14; N 5.17; H_2O 1.66. Found C 73.15; H 8.37; N 4.8; H_2O 1.14%.

UV λ_{max}^{EtOH} (log ε): 232 (4.28), 282 (4.03), 310 nm (3.82).

IR (KBr): 2790, 2750, 2730 (Bohlmann bands); 1623 (C=N); 1255 and 1225 cm^{-1} (C—O—C).

PMR ($CDCl_3$): 1.09 (t, 3H, $J = 7.32$, $CH_2—CH_3$); 1.4, 1.405 (t, 12H, $O—CH_2—CH_3$); 1.9—3.8 (m, 17H, alipathic protons); 4.06 (q, 8H, $O—CH_2—CH_3$); 6.59 (s, 2H, aromatic protons); 6.69 (s, 1H, aromatic proton); 7.15 (s, 1H, aromatic proton).

(±)-2-[(6',7'-Diethoxy-1'β,2',3',4'-tetrahydro-1'-isoquinolinyl)-methyl]-3-ethyl-1,6,7,11bα--tetrahydro-9,10-diethoxy-4H-benzo(a)quinolizine (1b) and (±)-2-[(6',7'-diethoxy--1'α,2',3',4'-tetrahydro-1'-isoquinolinyl)-methyl]-3-ethyl-1,6,7,11bα-tetrahydro-9,10-diethoxy-4H-benzo(a)quinolizine (5b)

The dihydrochloride of **4** (4 g; 5.8 mmoles) was dissolved in aqueous alcoholic (1 : 1) 2*N* HCl solution (65 ml). The solution was heated and stirred on a water bath, and zinc powder was added (4.0 g; 61 mmoles) by half-hour periods in 1-g portions. Stirring of the solution was continued on the water bath for 5 hrs. The alcohol was evaporated and the aqueous solution made strongly alkaline while cooling in ice-water, then extracted with benzene (4×30 ml). The combined benzene solution was acidified to pH 6 with methanol containing hydrochloric acid, and evaporated to dryness in vacuum. The residue was dissolved in methanol (17.5 ml), and ether (35.5 ml) was added; the mixture was then refrigerated. The crystals were filtered off, washed with a small amount of a mixture of methanol and ether (1 : 2) at 0 °C, and dried over $CaCl_2$ in a vacuum desiccator,. The dihydrochloride of **1b** with 1 mole of water of crystallization was obtained (1.52 g; 41%), m.p. 210—212 °C.

$C_{33}H_{46}N_2O_4 \cdot 2HCl \cdot H_2O$ (625.66). Calcd. C 63.34; H 8.06; N 4.48; Cl 11.34; H_2O 2.88. Found C 63.48; H 8.30; N 4.4; Cl 11.11; H_2O 2.96%.

UV $\lambda_{max}^{H_2O}$ (log ε): 213 (4.19), 230 (4.09), 282.5 nm (3.79).

IR (KBr): 2600 cm^{-1} ($\overset{+}{N}H_2$).

The dihydrochloride of **1b** (1 g) was dissolved in water (10 ml) and the solution was made alkaline with conc. NH_4OH while cooling in ice-water. The resulting white precipitate was filtered off, washed with water, and dried over KOH in a vacuum desiccator to obtain **1b** as a white powder (0.7 g).

$C_{33}H_{46}N_2O_4 \cdot 1/2H_2O$ (543.726). Calcd. C 72.88; H 8.62; N 5.15; H_2O 1.65. Found C 73.05; H 8.48; N 5.19; H_2O 1.52%.

IR (KBr): 2795, 2755, 2735 cm^{-1} (Bohlmann bands).

PMR ($CDCl_3$): 1.0 (t, 3H, $J = 7.3$, $CH_2—CH_3$); 1.4 (t, 12H, $J = 6.66$, $O—CH_2—CH_3$); 1.7—3.6 (m, 19H, aliphatic protons); 4.08 (q, 8H, $J = 6.66$, $O—CH_2—CH_3$); 6.63 (s, 2H, aromatic protons); 6.7 and 6.76 (s, 2H, aromatic protons).

After the isolation of **1b** · 2HCl, ether (35.5 ml) was added to the mother liquor of crystallization. The solvent mixture was decanted from the precipitate and the residue (0.38 g) was dissolved in methanol (1.3 ml). A few drops of ether were added, and the mixture was allowed to stand at room temperature. The crystals which deposited were filtered off to obtain **5b** · 2HCl (0.21 g; 5.52%), m.p. 175—177 °C.

$C_{33}H_{46}N_2O_4 \cdot 2HCl \cdot 2.5H_2O$ (652.78). Calcd. C 60.70; H 8.12; N 4.29; Cl 10.86; H_2O 6.94. Found C 60.89; H 8.29; N 4.2; Cl 10.61; H_2O 6.86%.

UV $\lambda_{max}^{H_2O}$ (log ε): 213 (4.21), 230 (4.11), 282 nm (3.77).

IR (KBr): 2550 cm^{-1} ($\overset{+}{N}H_2$).

The base liberated from **5b** · 2HCl was obtained in the form of an amorphous powder.

$C_{33}H_{46}N_2O_4 \cdot 1/2H_2O$ (543.725). Calcd. C 72.88; H 8.62; N 5.15; H_2O 1.65. Found C 72.81; H 8.43; N 5.32; H_2O 1.32%.

IR (KBr): 2795 and 2735 cm^{-1} (Bohlmann bands).

PMR ($CDCl_3$): 1.04 (t, 3H, $J = 7.3$, $CH_2—CH_3$); 1.45 (t, 12H, $J = 6.66$, $O—CH_2—CH_3$); 1.5—3.6 (m, 19H, aliphatic protons, NH); 4.1 (q, 8H, $J = 6.66$, $O—CH_2—CH_3$); 6.67 (s, 2H, aromatic protons), 6.76 and 6.8 (s, 2H, aromatic protons).

*

The authors' thanks are due to Chinoin Pharmaceutical and Chemical Works for supporting the present work; to Dr. P. KOLONITS for recording the IR and PMR spectra; and to Mrs. Dr. L. BALOGH for the microanalyses. Valuable help by Mr. I. JAKSA in the experimental work is gratefully acknowledged.

REFERENCES

[1] Brossi, A., Baumann, M., Chopard-dit-Jean, L. H., Würsch, J., Schneider, F., Schnider, A.: Helv. Chim. Acta, **42,** 772 (1959)
[2] Szántay, Cs., Tőke, L., Kolonits, P.: J. Org. Chem., **31,** 1447 (1966); Magyar Kém. Foly., **73,** 293 (1967)
[3] Rohály, J., Szántay, Cs.: Acta Chim. Acad. Sci. Hung. **96,** 45 (1978)
[4] Whittaker, N.: J. Chem. Soc. (C), **1969,** 94
[5] Openshaw, H. T., Whittaker, N.: J. Chem. Soc., **1963,** 1461

Csaba Szántay
János Rohály
H-1521 Budapest, Műegyetem.

Acta Chimica Academiae Scientiarum Hungaricae, Tomus 96 (1), pp. 61—74 (1978)

QUANTUM CHEMICAL INVESTIGATIONS ON PYRIDO- AND QUINOLINO-*AS*-TRIAZINES, I

PYRIDO-*as*-TRIAZINE UNSUBSTITUTED SYSTEMS

Z. DINYA, P. BENKÓ*, Á. I. KISS**, L. PALLOS*, E. BERÉNYI*, P. JÉKEL*** and SZ. ROCHLITZ****

(Institute of Organic Chemistry, Kossuth Lajos University, Debrecen, United Works of Pharmaceutical and Dietetic Products, Budapest, Department of Physical Chemistry, Technical University, Budapest**, Computational Centre, Kossuth Lajos University, Debrecen*** and Department of Computational Science, Deb recen****)*

Received November 15, 1976

The characteristics of the electronic structure and the UV spectral properties of pyrido-*as*-triazines and benzo-*as*-triazine were investigated by the use of different semiempirical methods (PPP, CNDO). The reactivity properties of the molecules were studied on the basis of calculations. It is concluded that the UV spectral and electronic structural properties are decided by the position of the pyrido-N-atom.

In the recent years several biologically active compounds have been found among pyrido- and quinolino-*as*-triazines characterized by formulas **I** and **II**, respectively. For an interpretation of the results

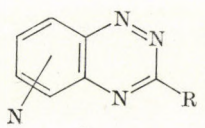

I

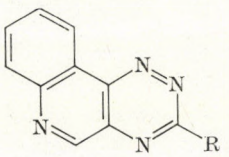

II

relating to reactivity and biological activity, an investigation on the electronic structure of these compounds is necessary. In continuation of our earlier work [1—6], in the present paper we report the results of quantum chemical investigations on pyrido-*as*-triazine skeletons (**III**—**VI**) and on benzo-*as*-triazine (**VII**),

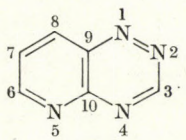

(2,3-e)
III

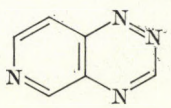

(3,4-e)
IV

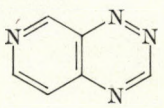

(4,3-e)
V

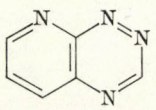

(3,2-e)
VI

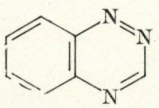

VII

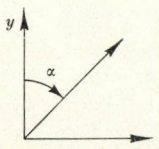

of the four possible unsubstituted **VII** pyrido-*as*-triazines (**III**—**VI**) the following are known: 3,4e (**IV**), 3,2-e (**VI**) and 4,3-e (**V**). In each type several derivatives have been prepared.

Relatively little quantum chemical work has been done on azanaphthalenes containing more than one nitrogen atoms. First FAVINI *et al.* [7] investigated the electronic transition spectra of azanaphthalenes by the Pariser—Parr—Pople (PPP) method. These authors were also the first to examine the benzo-*as*-triazine (**VII**) molecule. In 1966 WAIT and WESLEY [8] carried out Hückel molecular orbital (HMO) calculations for azanaphthalenes, including pyrido-*as*-triazines. They gave the HMO charge density data and the value of the excitation energy calculated for the first $\pi \rightarrow \pi^*$ transition in benzo-*as*-triazine. For azanaphthalenes containing one or two N atoms in one ring some further PPP calculations are also known [9—10b]. All-valence electron (CNDO, INDO) calculations have also been reported for these compounds [11]. The non-condensed *as*-triazine molecule was theoretically investigated by several workers [7, 12—14].

Calculations

The calculations were carried out by the use of the CNDO/2 [15] and PPP [16, 17] methods. In the CNDO calculations the original program and parametrization have been employed [15].

The PPP method was applied in the SCF—MO—LCAO—CI form with ZDO approximation [16—17]. In the calculation of configurational interaction (CI) first excited configurations were taken into account. The γ_{ii} and γ_{ij} integrals were obtained by the PARISER—PARR [17] and NISHIMOTO—MATAGA [18] approximations, respectively. The values for the ionization potential (I_i) and electron affinity (A_i), both referred to the valence state, were taken from the work of HINZE and JAFFE [19]. In the course of our calculations, including also those by the CNDO method, all molecules were supposed to have planar structure and all valence angles were taken as nearly 120°. The

Table I

Bond distances used in the calculations

Bond	Distance (Å)	Ref.
C = C	1.39	[17]
C = N	1.36	[20]
N = N	1.33	[13]
C — H	1.08	[21]

Table II

Initial data for PPP calculations

Atom	I_i(eV)[13]	A_i(eV)[19]		$-\beta_{ij}$(eV)	Ref.
$C(t_r t_r t_r \pi, V_3)$	11.16	0.03	$\dot{C} = \dot{C}$	2.39	[17]
$\dot{N}(t_r^2 t_r t_r \pi, V_2)$	14.12	1.78	$\dot{C} = \dot{N}$	2.58	[20]
			$\dot{N} = \dot{N}$	2.20	[22]

applied bond distance (R_{ij}) data are shown in Table I. The atomic parameters (A_i, I_i) and bond parameters (resonance integral, β_{ij}) are shown in Table II.

The UV spectra were recorded on a UNICAM SP-800 instrument in ethanol solution. The experimental oscillator strength values [23] were determined from the log ε data.

Results and discussion

The values for the first four singulet-singulet π—π^* electronic transition energies (ΔE), (PPP method), the wave length values (λ) and the oscillator strength data, together with the experimental values determined in the present work, are shown in Table III.

It is seen that there is a good agreement between the experimental and theoretical values for the transition energies. For the oscillator strength (f) the deviation is larger, but for the main bands the values are acceptable. In the case of benzo-*as*-triazine (**VII**) the data given by FAVINI *et al.* [7] are also shown. It is seen that the data calculated in the present work are in better agreement with the experimental results than those of the previous authors. The reason for that lies in the choice of the value for the $\beta_{N=N}$ integral. In the present work the $\beta_{N=N}$ value (Table II) was determined by a spectrum-fitting technique which means, that $\beta_{N=N}$ was varied as a parameter until the best fit between the experimental and theoretical data was obtained. This $\beta_{N=N}$ value was then used in the case of the pyrido-*as*-triazines.

Pyrido(3,4-e)-*as*-triazine (**IV**) and pyrido(3,2-e)-*as*-triazine (**VI**) were prepared first by LEWIS and SHEPHERD [24]. They also gave UV data for these compounds (with which our data are in perfect agreement). Each compound can be characterized by a three-band UV spectrum, in agreement with the statement of PAUL and RODDA [25] concerning pyrido-pyridazines. On the basis of our theoretical results, these bands belong to π—π^* transitions. (The $n \rightarrow \pi^*$ band appears at about 470 nm).

It is seen from the data in Table III that the UV spectral data show a dependence on the position of the N atom in the pyrido-ring. At the first

Table III

Calculated and experimental electronic transition spectra

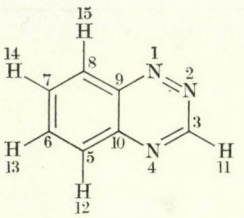

Compound	Theoretical					Experimental (EtOH)		
	ΔE^{s-s}(eV)	λ [nm]	f	α***	φ_i^j $i \rightarrow j$	ΔE(eV)	λ (nm)	f**
	3.932	315	0.176	205.9	5 → 6			
	(3.817)*	325	(0.154)*					
	4.150	299	0.200	120	4 → 6	4.137	300	0.066
VII	(4.105)*	302	(0,116)*		5 → 7			
	5.739	216	0.881	259.3	5 → 8	5.413	229	0.767
	(5.741)*	216	(0.183)*		5 → 7			
	6.041	205	0.019	333.1				
	(5.811)*	213	(0.456)*					
	4.024	308	0.245	165.4	5 → 6			
	4.451	279	0.249	323.4	5 → 6			
III					5 → 7			
(2,3-e)	5.975	208	0.104	249.8	3 → 6			
	6.102	203	0.137	268.6	4 → 6			
	3.748	331	0.187	195.6	5 → 6	3.735	332	0.065
	4.397	282	0.073	293.4	4 → 6			
IV	5.630	220	1.008	271.6	5 → 7	5.486	226	0.472
(3,4-e)					4 → 7			
	6.030	206	0.069	179.5	5 → 6			
	3.966	313	0.199	330	5 → 6			
	4.199	295	0.054	255.4	4 → 6			
V	5.606	221	1.023	221.2	5 → 7			
(4,3-e)					4 → 6			
	6.128	202	0.029	149.5	3 → 6			
	4.107	302	0.260	347.2	5 → 6	3.936	315	0.136
					5 → 7			
VI	4.419	281	0.222	152.3	5 → 6	4.065	305	0.157
(3,2-e)					4 → 6			
	5.930	209	0.670	77.6	5 → 7	5.904	210	0.700
	6.084	204	0.017	288.4	4 → 7			

* data by FAVINI *et al.* [7], ** $f = \frac{\varepsilon}{41700}$ [23]

*** α: polarization angle measured from y (grades)

$\pi \rightarrow \pi^*$ transition band (350—290 nm) the wave length sequence is the following:

$$\lambda^{\pi-\pi^*}_{(3,4-e)} > \lambda^{\pi-\pi^*}_{(4,3-e)} > \lambda^{\pi-\pi^*}_{(2,3-e)} > \lambda^{\pi-\pi^*}_{(3,2-e)}$$

In all cases for this band, the dominating transition is φ_n^{n+1} ($n = 5$), with the exception of the ring (3,2-e) (**VI**), where φ_n^{n+2} transition also contributes significantly. In the above mentioned cases, the band is polarized in the Y-direction.

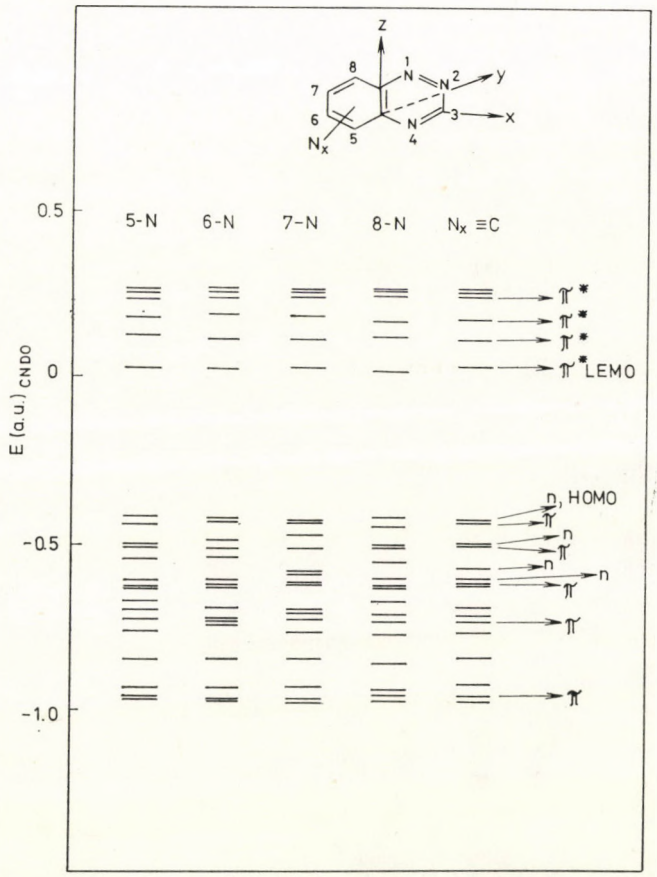

Fig. 1. Partial energy diagrams for CNDO MO's

The position of the band appearing at about 220 nm is also influenced by the position of the pyrido-N-atom. This band is polarized in the x-direction, and the φ_n^{n+2} electronic transition has a significant role in its appearance. In comparison with benzo-*as*-triatine it is found that the introduction of a new nitrogen atom — with the exception of pyrido(3,4-e)-*as*-triazine (**IV**) —

Table IV

Total energies and HOMO and LEMO orbital energies calculated by the PPP method

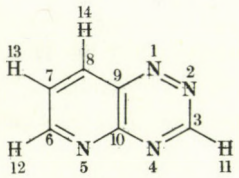

PPP-π-energies (eV)			
Compound	Total π-energy	HOMO*	LEMO**
III (2,3-e)	— 318.77329	— 10.55186	— 3.26150
IV (3,4-e)	— 318.40316	— 10.05678	— 3.28738
V (4,3-e)	— 318.44582	— 10.12894	— 3.22315
VI (3,2-e)	— 318,7338	— 10.53008	— 3.28806

* Highest Occupied Molecular Orbital.
** Lowest Empty Molecular Orbital.

does not cause a significant change in the π—π^* transition energies. This is in accordance with the general observation that replacement of sp^2 carbon atoms by $\dot{N}(t_r^2, t_r t_r, \pi, V_2)$ does not change markedly the structure of the UV spectra, thus when compared with the spectra of unsubstituted hydrocarbons, in our case naphthalene, no additional π—π^* bands can be observed.

It was found further that the UV features of the two pyrido-*as*-triazine pairs, (3,4-e)–(4,3-e) and (2,3-e)–(3,2-e), are similar to each other. The lowest π—π^* transition energies are seen in the (3,4-e) and (4,3-e) fused rings, thus their π-electron system can easily be excited. This is confirmed by the values of the all-π-electron energies (Table IV) indicating the stability the π-electron system in these compounds, and by the energy diagram for the CNDO molecular orbital shown in Fig. 1.

It can be inferred from the PPP-π-energy values and from Fig. 1 that the stability of the π-system is the smallest in the case of the pyrido-*as*-triazines (3,4-e) and (4,3-e) (**IV** and **V**, respectively).

Figure 1 shows the CNDO molecular orbital energy values for the compounds examined. (The energy diagram is not complete, because of the possible 44 orbitals the energy values for only orbitals No. 9—30 are shown.) The character of the different MO's was determined from the orbital coefficients. (Those MO's for which the *n*-character is greater than 60%, are denoted by *n* [26].

It appears that in all cases the highest occupied orbital (HOMO) has *n*-character, while the lowest empty MO (LEMO) has π-character. It is seen that for compounds (2,3-e) and (3,2-e) the HOMO energies are higher com-

Table V

Total energies calculated by the CNDO method

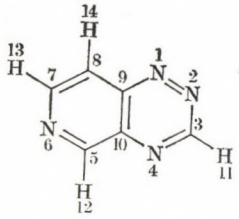

Compound	Total energy (a.u.) CNDO
III (2,3-e)	— 92.19951
IV (3,4-e)	— 92.19186
V (4,3-e)	— 92.20722
VI (3,2-e)	— 92.20643

pared with those of the analogous compounds (3,4-e) and (4,3-e), respectively. In the case of the highest occupied π-orbital the situation is reversed. A further difference between the pyrido-*as*-triazine pairs (3,2-e)–(2,3-e) and (4,3-e)–(3,4-e) is that in the former it is orbital No. 20, while in the latter orbital No. 22, which has *n*-character. This fact can be rationalized by suggesting that the single electron pair of the pyrido-N-atom is more delocalized into the ring for (3,4-e) and (4,3-e) linkage, than for (3,2-e) and (2,3-e) linkage.

The CNDO total energy values (Table V) are informative regarding the general stability features of these compounds. From these data it can be inferred that the stability is the lowest for the pyrido(4,3-e)-*as*-triazine (**IV**) skeleton, and the stability sequence obtained by CNDO calculations differ from the sequence for the π-system obtained by the PPP method.

Besides the UV spectral properties, we also examined the electron distribution of the molecules. The data for the ground state electron distribution calculated by the CNDO method are shown in Tables VI—X. The π-electron densities were determined by WAIT and WESLEY [8] using the HMO method, thus we can use their data as the only reference for comparison with our CNDO and PPP results, as we did in Fig. 2 for pyrido(2,3-e)-*as*--triazine (**III**).

It is seen that the various approximation methods yield data of the same character but differing in numerical value. The values obtained by the HMO and PPP methods are, however, also numerically near to each other. In the interpretation of reactivity features, the σ-electron densities cannot be neglected; in this respect the CNDO results are therefore more valuable.

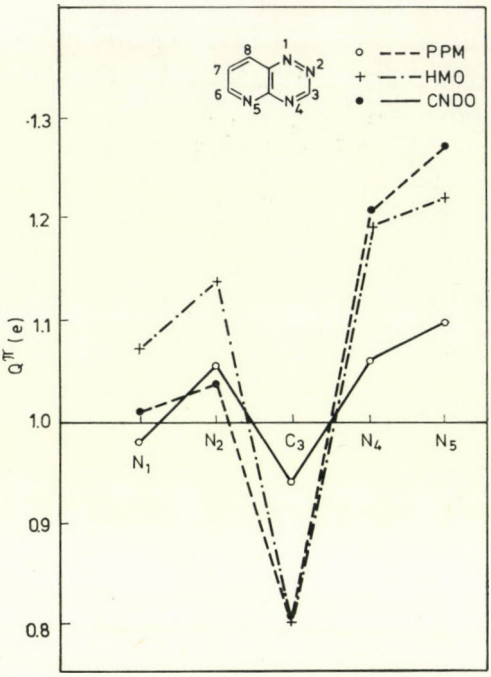

Fig. 2. π-electron density data for some atoms of pyrido-*as*-triazines calculated by different methods

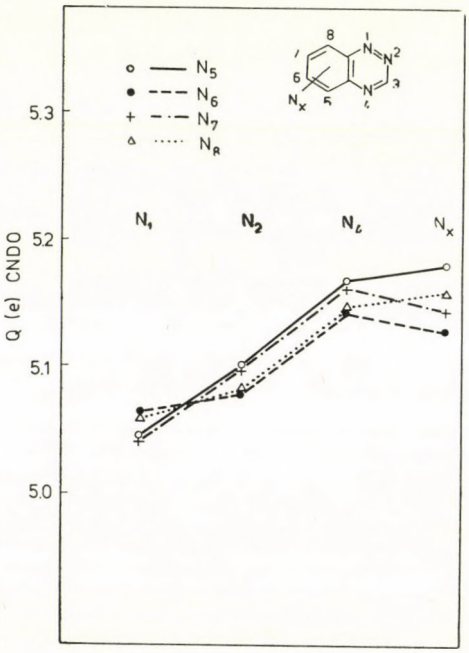

Fig. 3. CNDO electron density data for the N atoms of pyrido-*as*-triazines

Table VI

Electron and charge densities for Compound **VII**

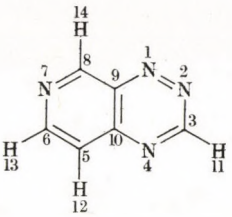

Atom	Bonding type	Total	Charge
N (1)	σ 4.0596 π 0.9963	5.0559	— 0.0559
N (2)	σ 4.0505 π 1.0443	5.0948	— 0.0948
C (3)	σ 2.9010 π 0.9576	3.8586	0.1414
N (4)	σ 4.1127 π 1.0453	5.1580	— 0.1580
C (5)	σ 3.0044 π 1.0242	4.0286	— 0.0286
(6)	σ 3.0021 π 0.9789	3.9810	0.0190
C (7)	σ 2.9940 π 1.0034	3.9974	0.0026
C (8)	σ 3.0084 π 0.9963	4.0047	— 0.0047
C (9)	σ 2.9408 π 0.9958	3.9366	0.0634
C (10)	σ 2.9202 π 0.9579	3.8781	0.1219
H (11)	σ 1.0029	1.0029	— 0.0029
H (12)	σ 0.9969	0.9969	0.0031
H (13)	σ 1.0040	1.0040	— 0.0040
H (14)	σ 1.0035	1.0035	— 0.0035
H (15)	σ 0.9990	0.9990	0.0010

On the basis of data for the π-electron systems of all pyrido-*as*-triazines, the most negative — thus the most basic — N atom is the one in the pyrido-ring. From the CNDO total electron density ($\sigma + \pi$) values it can be seen (Fig. 3), however, that the electron densities on the N atoms and on the C-3 atom depend on the position of the pyrido-N-atom. It is also shown that

Table VII

Electron and Charge Densities for Compound **III**

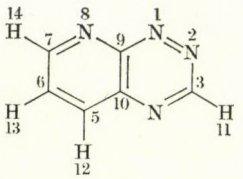

Atom	Bonding type	Total	Charge
N (1)	σ 4.0681 π 0.9793	5.0474	— 0.0474
N (2)	σ 4.0459 π 1.0562	5.1021	— 0.1021
C (3)	σ 2.9035 π 0.9426	3.8461	0.1539
N (4)	σ 4.1080 π 1.0622	5.1702	— 0.1702
N (5)	σ 4.0836 π 1.0977	5.1813	— 0.1813
C (6)	σ 2.9532 π 0.9379	3.8911	0.1089
C (7)	σ 3.0026 π 1.0320	4.0346	— 0.0346
C (8)	σ 3.0178 π 0.9440	3.9618	0.0382
C (9)	σ 2.9504 π 1.0064	3.9568	0.0432
C (10)	σ 2.8588 π 0.9417	3.8005	0.1995
H (11)	σ 1.0005	1.0005	— 0.0005
H (12)	σ 1.0069	1.0069	— 0.0069
H (13)	σ 0.9997	0.9997	0.0003
H (14)	σ 1.0010	1.0010	— 0.0010

in all cases it is the N-1 atom which has the smallest charge. The most negative nitrogen atom of the *as*-triazine ring is N-4. The CNDO results reveal — contradicting the PPP and HMO data — that the pyrido-N atom is not found to be the most negative in all cases. In the case of the compounds (2,3-e) and (3,2-e), in accordance with the PPP and HMO calculations, the largest neg-

Table VIII

Electron and charge densities for Compound **IV**

Atom	Bonding type	Total	Charge
N (1)	σ 4.0499 π 1.0155	5.0654	— 0.0654
N (2)	σ 4.0622 π 1.0203	5.0825	— 0.0825
C (3)	σ 2.8952 π 0.9706	3.8658	0.1342
N (4)	σ 4.1199 π 1.0253	5.1452	— 0.1452
C (5)	σ 2.9513 π 0.9871	3.9384	0.0616
N (6)	σ 4.0947 π 1.0366	5.1313	— 0.1313
C (7)	σ 2.9329 π 0.9869	3.9198	0.0802
C (8)	σ 3.0118 π 1.0143	4.0261	— 0.0261
C (9)	σ 2.9417 π 0.9665	3.9082	0.0918
C (10)	σ 2.9314 π 0.9771	3.9085	0.0915
H (11)	σ 1.0008	1.0008	— 0.0008
H (12)	σ 0.9999	0.9999	0.0001
H (13)	σ 1.0064	1.0064	— 0.0064
H (14)	σ 1.0017	1.0017	— 0.0017

ative charge is located on the pyrido-N-atom, but for pyrido(3,4-e)- and (4,3-e)-*as*-triazines the largest negative charge is on the N-4-atom of the *as*-triazine ring. The reason for this difference lies in the different extent of delocalization of the single *n*-electron pair of the pyrido-N-atom, because this electron pair is more localized on the N atom in the (2,3-e) and (3,2-e) molecules, than in the two other cases.

At present we have no experimental data for the dipole moment. On the basis of the CNDO results the values for dipole moment vary in the following sequence:

μ (D) 4.02 2.3 2.01 0.31

(3,2-e) $\gg$ (2,3-e) $>$ (4,3-e) $\gg$ (3,4-e)

Table IX

Electron and charge densities for Compound **V**

Atom	Bonding type	Total	Charge
N (1)	σ 4.0639 π 0.9778	5.0417	— 0.0417
N (2)	σ 4.0425 π 1.0554	5.0979	— 0.0979
C (3)	σ 2.9084 π 0.9399	3.8483	0.1517
N (4)	σ 4.1080 π 1.0561	5.1641	— 0.1641
C (5)	σ 3.0126 π 1.0483	4.0609	— 0.0609
C (6)	σ 2.9436 π 0.9561	3.8997	0.1003
N (7)	σ 4.0778 π 1.0696	5.1474	— 0.1474
C (8)	σ 2.9562 π 0.9527	3.9089	0.0911
C (9)	σ 2.9542 π 1.0134	3.9676	0.0324
C (10)	σ 2.9239 π 0.9308	3.8547	0.1453
H (11)	σ 1.0011	1.0011	— 0.0011
H (12)	σ 0.9925	0.9925	0.0075
H (13)	σ 1.0074	1.0074	— 0.0074
H (14)	σ 1.0080	1.0080	— 0.0080

Thus on theoretical grounds the (3,2-e) pyrido-triazine system is the most polar, while the (3,4-e) is the least polar.

From our data it can be inferred that the C-3 atom of the *as*-triazine ring is unequivocally favoured in respect to nucleophilic attacks. The carbon atoms of the pyrido-ring have electrophilic character. These conclusions are in agreement with the experimental facts.

An interpretation of the different reactivity properties of C_3-substituted derivatives [1—6] will be given in forthcoming publications.

Table X

Electron and charge densities for Compound **VI**

Atom	Bonding type	Total	Charge
N (1)	σ 4.0512 π 1.0106	5.0618	— 0.0618
N (2)	σ 4.0471 π 1.0368	5.0839	— 0.0389
C (3)	σ 2.8976 π 0.9668	3.8644	0.1356
N (4)	σ 4.1165 π 1.0336	5.1491	— 0.1491
C (5)	σ 3.0169 π 0.9770	3.9939	0.0061
C (6)	σ 3.0130 π 0.9999	4.0139	— 0.0129
C (7)	σ 2.9462 π 0.9561	3.9023	0.0877
N (8)	σ 4.0929 π 1.0692	5.1621	— 0.1621
C (9)	σ 2.8872 π 0.9832	3.8704	0.1296
C (10)	σ 2.9318 π 0.9669	3.8987	0.1013
H (11)	σ 1.0002	1.0002	— 0.0002
H (12)	σ 0.9966	0.9966	0.0034
H (13)	σ 0.9985	0.9985	0.0015
H (14)	σ 1.0052	1.0052	— 0.0052

Conclusions

According to our investigations, the results of different semiempirical methods properly reflect the experimental characteristics of unsubstituted pyrido-*as*-triazine compounds. About the electronic structures of pyrido-*as*-triazines it can be established that the introduction of a new nitrogen atom, as compared with the case of benzo-*as*-triazines does not cause significant changes in the UV spectral properties and in electron distribution. The observed differences are mainly due to the different positions of the pyrido-N-atom. In determining the reactivity of the molecules, the dominating factor is the strong nucleophilic character of the C-3 atom.

*

The authors are grateful to the United Works of Pharmaceutical and Dietetic Products (EGYT) Budapest, for supporting the present work.

REFERENCES

[1] BENKÓ, P., GELLÉRI, A., MESSMER, A., PALLOS, L.: Magyar Kém. Foly., **82,** 166 (1976)
[2] MESMER, A., GELLÉRI, A., BENKÓ, P., PALLOS, L.: Magy. Kém. Foly., **82,** 173 (1976)
[3] BERÉNYI, E., BENKÓ, P., PALLOS, L.: Magy. Kém. Foly., **82,** 179 (1976)
[4] BERÉNYI, E., BENKÓ, P., PALLOS, L.: Magy. Kém. Foly., **82,** 180 (1976)
[5] BENKÓ, P., BERÉNYI, E., MESSMER, A., HAJÓS, GY., PALLOS, L.: Magy. Kém. Foly., **82,** 183 (1976)
[6] BENKÓ, P., PALLOS, L.: Magy. Kém. Foly., **82,** 187 (1976)
[7] FAVINI, G., VANDONI, I., SIMONETTA, M., Theoret. chim. Acta (Berlin), **3,** 45 (1965)
[8] WAIT, S. C. Jr. WESLEY, J. W.: J. Mol. Spectr., **19,** 25 (1966)
[9] TINLAND, B.: Theoret. chim. Acta (Berlin), **8,** 361 (1967)
[10] FAVINI, G., BUENI, G.: Theoret. chim. Acta (Berlin), **13,** 79 (1969)
[10a] NÁRAY-SZABÓ, G., DUDAR, E., HORVÁTH, G.: Acta Chim. (Budapest), **74,** 281 (1972)
[10b] DUDAR, E., KISS, A. I., HORVÁTH, G.: Acta Chim. (Budapest), **78,** 253 (1973)
[11] RIDLEY, J. E., ZERNER, M. C.: J. Mol. Spectr., **50,** 457 (1974)
[12] DEWAR, M. J. S., GLEICHNER, G. J.: J. Chem. Phys., **44,** 759 (1966)
[13] PUKANIC, G. W., FORSHEY, D. R., WEGENER, B. J. D., GREENSHIELDS J. B.: Theoret. chim. Acta (Berlin), **10,** 240 (1968
[14] PALMER, M. H., GASKELL, A. J., FINDLAY, R. H.: Tetrahedron Lett., **173,** 4659
[15] POPLE, J. A., BEVERIDGE, D. L.: Approximate Molecular Orbital Theory, McGraw-Hill, New York 1970
[16] POPLE, J. A.: Trans. Faraday Soc., **49,** 1375 (1953)
[17] PARISER, R., PARR, R. G.: J. Chem. Phys., **21,** 466, 767 (1953)
[18] MATAGA, N., NISHIMOTO, K.: Z. physik. Chem. N. F., **13,** 140 (1957)
[19] HINZE, J. JAFFE, H. H.: J. Amer. Chem. Soc., **84,** 540 (1962)
[20] LINDNER, P., MANNE, R., MARTENSSON, O.: Theoret. chim. Acta (Berlin), **5,** 406 (1966)
[21] SUTTON, L. E., Ed.: Tables of Interatomic Distances and Configuration in Molecules and Ions, Chem. Soc., London, 1958
[22] DINYA, Z.: Private communication
[23] ALLINGER, N. L., STUART, T. W., TAI, J. C.: J. Am. Chem. Soc., **90,** 2819 (1968)
[24] LEWIS, A., SHEPHERD, R. G.: J. Heterocycl. Chem., **8,** 41, 47 (1971)
[25] PAUL, D. P., RODDA, H. J.: Austral. J. Chem., **21,** 1291 (1968)
[26] CHEN, S—Y.: Ph. D. Dissertation, Texas, A—M. University 1972, University Microfilms Ann Arbor, Michigan, Order No. 73 — 12246

Zoltán DINYA
Pál BENKÓ
H-4010 Debrecen
United Works of Pharmaceutical and Dietetic Products, Budapest

Árpád I. KISS
László PALLOS
Edit BERÉNYI
H-1521 Budapest
United Works of Pharmaceutical and Dietetic Products, Budapest

Pál JÉKEL
Szilveszter ROCHLITZ
H-4010 Debrecen

RECENSIONES

M. SITTIG: *Toxic Metals.* Pollution Control and Worker Protection

Pollution Technology Review, No. 30, pp. 300.
Noyes Data Corp., Park Ridge, New Jersey, U.S.A. 1976

Mass poisoning with tragical outcome, *e.g.* Minimata illness in Japan, have proved that metals which are toxic already in low doses endanger not only those who work with them but, if they find their way into the environment, endanger also the population.

The aim of the author in this work is to offer some guiding principles concerning the elimination of the possibly poisonous effects of toxic metals, through organization of prevention and testing. This book is a comprehensive survey of the latest information which bears upon preventive measures at work sites and in the environment. The bulk of this information consists of reports, patent specifications and communications in competent journals, derived from studies financed or sanctioned by governing bodies.

Each in a separate chapter of its own, the following metals are discussed: antimony, arsenic, barium, beryllium, boron, cadmium, chromium, copper, indium, lead, manganese, mercury, molybdenum, nickel, selenium, tin, vanadium and zinc. Lucidity is enhanced by all the substances being treated uniformly and with regard to the following features: toxicity, incidence and the extent of exposition to the substance, detection in air, water and in biological media, the standards of tolerability in the environment, prescribed methods of treatment, removal of the substance from air and from water, solid waste disposal, economic effects and consequences of measures of control. References are given at the end of each chapter.

This book is a recommended item on the bookshelves of specialists who work as environmental engineers, industrial sanitary personnel, toxicologists and chemists.

J. MOLNÁR

E. CLEMENTI: *Determination of Liquid Water Structure.* Coordination Numbers for Ions and Solvation for Biological Molecules

pp. 107. Springer Verlag, Berlin, Heidelberg, New York 1976

The structure of water, the solvation of ions and molecules are important problems of present day chemical physics. This second volume of the series "Lecture Notes in Chemistry" acquaints the reader with the quantum-mechanical treatment of these. The work done in the last five years by the author and his team, well known for their extensive quantum-chemical calculations, is reported in thirteen parts in the Journal of Chemical Physics, forming the core of this book. The 107 pages carry 3 chapters; in them we find 23 tables, 32 figures, with 122 references to the literature.

The chapters are: 1. Description of a Chemical System as a Set of m Fixed Nuclei and n Electrons; 2. Structure of Liquid Water as a Test Case; 3. Co-ordination Numbers and Solvation Shells.

The first chapter is an introduction into the quantum-mechanics of molecular aggregates. The SCF—LCAO—MO approximation used is explained in detail. The advantages of the choice of basic sets and the electron population analyses and bond energy analyses in molecules and in molecular complexes are discussed. It is especially useful that the physical and chemical meaning of the quantities which constitute the classical final results of quantum-mechanical calculations, *viz.* electron density, total energy, orbital energies are underlined. Considering the subject matter of this chapter and its volume of 56 pages, the unusually high number of examples, numerical data, and comparative tables render this discussion most enjoyable.

The second chapter shows the application of the method in the study of the structure of liquid water. The determination, based upon the Hartree—Fock potentials, of the energy contours of the water dimer is discussed and results are compared with those obtained by the em-

pirical Ben Naim—Stillinger and Rowlinson potentials. From the analysis of the stabilization energy of many different $(H_2O)_n$-type aggregates of various configurations theconclusion is drawn that none of the individual clusters shows favoured stability. This is contrary to various mixture models of liquid water for which the properties of water are explained in terms of small, regular polymers. The existence of clusters nearly equivalent energetically but rather different in geometrical structure suggests that the exact geometry of the clusters is of little importance and that the probability distribution of the clusters with various structures is physically the more significant parameter Finally, in this chapter the pair correlation functions determined by Monte-Carlo calculations based upon Hartree—Fock pair potentials of liquid water are compared with results of X-ray and neutron-diffraction experiments.

The third chapter shows the applications of quantum mechanics in the study of ion–water aggregates and of ion hydration. The results of Monte-Carlo calculations, based upon Hartree—Fock pair potentials, for the hydration of alkali and halide ions as well as for ion pairs are shown. The role of three-particle forces in the case of H_2O–Li–F is discussed and at the end of the chapter, briefly the study of the solvation of amino acids and of other biologically interesting systems is dealt with.

The text reads easily and affords the fundamentals for a more thorough study, for both expert and beginner. By dedicating this work its author has paid tribute to Prof. Per-Olov LÖWDIN at his 60th birthday. Finally the reviewer wishes to note that this book fully achieves the purpose of the Series, which is: "to report new developments in chemical research and teaching — quickly, informally and at a high level".

E. KÁLMÁN

Structure and Bonding, Vol. 30

pp. 197. Springer Verlag, Berlin, Heidelberg, New York 1976

The task continuously to keep up with progress even in a narrow field of science is made even more burdensome by the proliferation of scientific communications, both in respect of numbers and volume. Also this is a reason why publications that give a comprehensive account of the actual state of a narrowly defined domain of problems are especially welcome. "Structure and Bonding" contains such summaries; these significantly facilitate inquiry into a certain field and help to review the most important recent achievements.

Volume 30 is already the fourth in a series which deals with the chemistry of the rare earths: a fact which points to the importance attributed and the interest accorded to both theory and practice in connection with this group of elements and their compounds.

This volume contains four reviews. The first is the work of S. P. SINHA, entitled "A Systematic Correlation of the Properties of the *f*-Transition Metal Ions". Several parameters that describe properties of lanthanides and actinides, *viz.* spectroscopic parameters, oxidation potentials, constants of formation, crystallographic data, linear complete angular momentum, show an L-dependence. However, in many cases a linear function emerges only if J is taken into consideration. Such cases are: atomic number, extraction data, Racah-parameters, spin orbital coupling parameter, etc. The great number of data collected shows that the J-dependence permits the realization of really well manageable linear correlations, though deviations occur also in these cases. This review refers the reader to 98 items of the literature; the possibilities of illustration are shown by 67 figures.

The second article, by R. REISFELD, deals with "Excited States and Energy Transfer from Donor Cations to Rare Earths in the Condensed Phase". Here it is demonstrated how the probability of energy transfer in microscopic and in macroscopic dimensions can be calculated. Resonance transition plays hardly any role; however, the diffusion of energy must be taken into account together with 'phonon-assisted' energy transfer. As a technique, selective laser excitation combined with 'time-resolved' spectroscopy is proposed. The donor ion can be excited selectively and from the time-resolved emission of the rare earth acceptor the energy rate, increasing with time, is obtainable. Optical characteristics are well interpretable by the nephelauxetic effect found by JØRGENSEN and by electronegativity according to PAULING. 74 items of literature are cited, 10 figures and 10 tables illustrate the text.

M. CAMPAGNA, G. K. WERTHEIM, and E. BUCHER wrote the third review, its title is "Spectroscopy of Homogeneous Mixed Valence Rare Earth Compounds". The 4*f*-photoemission of the rare earths can be adequately discussed on the basis of intensity and mul-

tiplet structures. As reflected by the results of the electron spectroscopic method, the electron structure of homogeneous mixed valence compounds is expounded in quite a new way. The phenomenon is discussed in consideration of the results of X-ray photoemission, XPS, of ultraviolet photoemission, UPS, and of electronic energy-loss spectroscopy, ELS. Spectroscopic results are shown in 27 figures; 76 items of literature are cited.

C. K. JØRGENSEN is the author of the fourth review, entitled "Deep-lying Valence Orbitals and Problems of Degeneracy and Intensities in Photoelectron Spectra". Here the validity of s–p separation, the overlap of neighbouring atoms of the same element, the role of 5p and 6p shells in post-transition elements, the Gelius-effect, electron transition and the type of information to be gained for the ground state from the final ionization state are discussed. All these questions are answered on the basis of results gathered by photoelectron spectroscopy. 224 items of the literature are germane to this highly concise treatment of the subject.

All the four articles in this book attest that the exacting standards set in the edition of this series have been fully adhered to. The reader is given four very succinct summaries and is helped to significant information about spectroscopic and theoretical studies concerning lanthanides and actinides, the electronic states and the structures of their compounds.

J. CSÁSZÁR

Contact Catalysis, Vols 1 and 2

pp. 1019. Editor-in-chief Z. G. SZABÓ, Assistant editor D. KALLÓ
Akadémiai Kiadó, Budapest, and Elsevier Publishing Co., Amsterdam 1976

This work, issued as a joint venture of the two publishing houses, is a revised version in English of the Hungarian "Kontakt katalízis" written by a team of authors from the Hungarian Catalysis Club. Each of the authors is a specialist in some field, thus what the reader holds in his hands is a fully comprehensive treatment of the entire science of contact catalysis. In the first volume primarily a theoretical approach to catalysis and the disciplines pertinent to it is offered; the second volume deals with practical problems of the preparation of catalysts and with reactor design. This work certainly is a remarkable attempt at the creation of a handbook: the reader is given if not the answer to, then at least an instruction for the solving of, every problem in connection with contact catalysis.

The first chapter (J. LADIK and F. SOLYMOSI) is about the electronic structure of metals and semiconductors. Not only the most modern approaches of solid state physics to the structure of metals and semiconductors are shown here but also the application, still in an initial phase, of quantum-mechanical methods to the calculation of the surface states of solids are treated. Good approaches are shown to the band structures of metals and semiconductors, to the theories about defects in semiconductors. The defect structures of the most important *n*- and *p*-conductors, further those of the intrinsic conductor oxides are discussed separately. There is only one topic the omission of which is perhaps regrettable: theoretical considerations concerning alloys.

The second chapter (P. FEJES) treats the adsorption of gases on the surface of solids. Here we get the phenomenological description of the interaction of adsorbent and adsorbate, the derivation and the interpretation of the established isotherms, *viz.* LANGMUIR, FREUNDLICH, TEMKIN, etc. After the expounding of the thermodynamics of adsorption, the changes in enthalpy and in entropy, the heat of chemisorption, the mobility of the absorbed layer, theories concerning the rate of sorption, energy, considerations of geometrical features and the determination of the rate constant of desorption are discussed. The methods used for the determination of rates of adsorption and desorption also belong here. The chapter concludes with a critical review of theories relating to the mechanism of chemisorption.

The third chapter (D. KALLÓ and F. SOLYMOSI) is devoted to questions of catalyst structure and activity. Not only the effects of geometrical and of energy factors are thoroughly and critically discussed, but also the theory of processes which occur at energetically heterogeneous surfaces; *e.g.* the rule of compensation, is considered, further an introduction to the electron theory of catalysis is given. The mechanisms of the most important catalytic reactions and the effect of changes in the catalyst upon the mechanism of the process were reviewed according to types of catalysts, *i.e.* metal, semiconductor, supporter and insulator catalysts.

The kinetics of heterogeneous catalytic reactions form the subject of the fourth chapter (F. NAGY and D. KALLÓ), where the most important problems of reaction kinetics are dealt with in a logical order. Thus, we read about the concepts of reaction rate, the elementary steps of heterogeneous catalytic reactions, the rate-determining process and the transport processes. Various static and dynamic reactors are described; these can be used for the laboratory determination of the rates of processes. The calculations for the solution of kinetic equations which represent the catalytic processes $A \rightarrow B$, $A \rightarrow B_1 + B_2$ and $A_1 + A_2 \rightarrow B$ are summarized. At the end of this chapter we find examples of how to solve rate and kinetic equations derived from work with various laboratory reactors.

In the fifth chapter (J. PETRÓ) heterogeneous catalysts are described: operations in the preparation of a catalyst, *viz.* precipitation, impregnation, washing, drying, forming, activation, etc. A separate part is devoted to the modification of catalysts, to promoter effects, to carrier effects and to the alteration of catalyst selectivity with the help of catalyst poisons. Finally the various types of catalysts are discussed.

The physical testing of catalysts is treated in the sixth chapter (K. SASVÁRI, K. IBRÁNYI M. ÁRKOSI, G. MENYHÁRT, A. GERGELY, F. TUNGLER, J. SOLYMOSI, S. KIRÁLY, S. HOLLY and L. RADICS). This chapter describes X-ray diffraction methods used for the determination of the structure of a catalyst. Electron optical studies, *i.e.* electron microscopy, electron diffraction, LEED and Auger spectroscopy, give information about the morphology of surfaces. The efficiency of the latter two techniques places them uncontestably in the foremost rank among those suitable for use in the study of the composition and the structure of a catalyst surface.

The study of magnetic properties reveals the ways of interactions; at present, however, it is successfully used for the determination of the dispersity of metal catalysts. Electrical characteristics, *e.g.* conductivity and Hall effect are important primarily in the case of semiconductor catalysts.

One of the dominant features of a catalyst is its surface: the part about adsorption deals with the techniques suitable for the determination of this feature. The BET equation, Harkins—Jura method, their criticism, their limits of applicability are all mentioned. Infrared spectroscopy isf accorded a separate part; unfortunately this is not detailed enough, considering the signiicance of this method. The series of experimental methods closes with the application of EPR. In the cases of insulator and oxide- type catalysts the importance of these methods is considerable. Also it is regrettable that no space could be found for the ever more often applied ESCA method and for Mössbauer spectroscopy.

The last chapter (M. BAKOS) comprises the practical realization of heterogeneous catalytic processes. Here not only the transport processes, *i.e.* heat and material transport occurring together with a catalytic process, are shown but also the methods used for the determination of the most important parameters of the catalytic process itself, *viz.* rate equations, order of reaction, apparent reaction rate, etc. Besides this, the estimation of the parameters most important for engineering design calculations is shown, *i.e.* catalyst volume, length of catalyst bed, reactor diameter, etc. and the use of these data in the design of various reactor types is discussed.

L. GUCZI

NMR: Basic Principles and Progress

Ed. P. DIEHL, E. FLUCK, R. KOSFELD,

Vol. 11, pp. 246. M. MEHRING (University of Dortmund): High Resolution NMR Spectrosopy in Solids. Springer Verlag, Berlin, Heidelberg, New York 1976

As well known by chemists, in the NMR spectrum of a liquid sample sharp lines emerge; these have, however, a width that corresponds to about 0.1—1 Hz, due to the inhomogeneity of the magnetic field and to spin relaxation. Hamiltonian interactions manifest themselves in isotropic chemical shifts and in scalar spin–spin interactions. Owing to rapid isotropic molecular motion, all other anisotropic interactions, *e.g.* chemical shift anisotropy, dipole–dipole or quadrupole interaction are averaged to zero. In the solid state, however, these anisotropic interactions prevail and ought to furnish interesting information in respect of features of symmetry and in electron configurations. Since most often, *e.g.* with ^1H, ^{19}F nuclei, in the case of the generally applied magnetic field, that is with 1 to 6 Tesla, the dipole–dipole inter-

action dominates, in the NMR spectrum of a solid sample very broad, featureless bands will appear and from these no conclusions on local symmetry and electron distribution can be drawn. Therefore the fundamental purpose of high resolution NMR spectroscopy of solid psamles is the elaboration of methods suppressing unwelcome dipolar interactions responsible for the broadening of the bands and leave, more or less, unaffected the anisotropies of chemical shifts and the scalar interactions. The chief objective of this book is to acquaint its readers with the recent methods evolved for this purpose. This topic is treated in seven chapters with 283 references.

1. The introduction is a short survey of the most important methods and results of high-resolution NMR spectroscopy of solids.

2. In the chapter "Nuclear Spin Interactions in Solids" the discussion in terms of tensors, of spin interactions is given. Here the rotation about the 'magic' angle $\vartheta_m = 54°44'8''12'''$, *i.e.* the "specimen rotation method" is explained: the result of this is that dipolar interactions and shielding anisotropy average out to zero. The isotropic chemical shift, Knight-shift and scalar coupling thus become accessible besides. In addition to metal powders, this methods has been successfully applied to polymers and to biologically interesting compounds. These measurements have proved that in the solid state, especially in organic solids, rapid molecular re-orientation may occur even at not too high (100—500 °K) temperatures.

3. Multiple Pulse NMR Experiments. This chapter deals in detail with multiple pulse tests applied in cycles, among these with the so-called WHH-4 four-pulse sequence. This fundamental method, which operates in the spin space, brings about the averaging of dipole and quadrupole interactions but does not interfere with shift interactions. It has the advantage that the broadening of bands due to shift interaction and paramagnetic contaminants becomes amenable to study. The limit of this method is set chiefly by pulse imperfections.

4. Double Resonance Experiments. Since dipole interactions are inversely proportional to the third power of the distance r between spins, the suppression of band diffusion due to homonuclear dipole–dipole interactions is possible also through a dilution of the spin system. Thus *e.g.* in the case of ^{13}C, ^{15}N, ^{43}Ca nuclei, rarely met with in nature, homonuclear interactions are rather negligible; the interaction with the surrounding ^{1}H, ^{19}F, etc. nuclei which abound in nature, can be eliminated by decoupling techniques, consequently, a high resolution spectrum is obtained. Since the ^{13}C, ^{15}N, etc. nuclei give very weak signals, the reservoir furnished by commonly available spins is used for the enhancement of sensitivity. This may be achieved in two ways, *viz.* (1) by the indirect method where rare spins are detected through their effect upon the common spins, or (2) by the direct method where the rare spins are polarized by the common ones. This is the method known as proton enhanced nuclear induction spectroscopy or cross-polarization experiment. The latter of the two has been found the more advantageous for practical applications.

5. The chapter about Magnetic Shielding Tensors is a review of the various shielding tensors, determined by various methods, for ^{1}H, ^{19}F, ^{13}C, etc. nuclei. Not only the actual measure, but also the symmetries of these tensors are important since this also is a function of the structure of a molecule or a crystal.

6. Spin–Lattice Relaxation in Line Narrowing Experiments. This chapter treats the physics and a few useful applications of spin-lattice relaxation processes hitherto not considered as very important in the high-resolution NMR spectroscopy of solids.

7. The book ends with an Appendix: here the author summarizes all the theoretical aspects which he has utilized in the preceding chapters.

Due to the method of discussion and the deductions which require a relatively high level of mathematical knowledge, this book is designed chiefly for physicists and for specialists in NMR spectroscopy; nevertheless, it allows also chemists and organic chemists to catch glimpses of some possibilities of collecting information relevant to structures of molecules and crystals with the help of high-resolution NMR spectroscopy of solid specimens. This is important also because this branch of science, regarded as a curiosity at present, may furnish an important research tool applicable to a wide range of problems, thanks to the rapid development of instrumentation and techniques.

G. TÓTH

Cs. Szántay and L. Novák: "*Prosztaglandinok szintézise*" *(Synthesis of Prostaglandins)*

Akadémiai Kiadó, Budapest, 1976. pp. 317. Cloth. Ft 49.—

This book, the 33rd volume in the series: "A kémia újabb eredményei" (New Results in Chemistry), offers an evaluative and comprehensive review, interspersed with comments based on experimental work done by the authors themselves active in this field, of the chemistry of a group of compounds which is highly interesting from a biological point of view. Researches in the syntheses of prostaglandins have enriched chemical theory as well as methodology. Beyond the factual communication of results, Szántay and Novák discuss the why and how of the chemical reactions and, in connexion with given processes, throw light upon several general regularities. Owing to this, their book is of interest not only for those who are engaged in the study of prostaglandin chemistry, but also for those who wish to keep pace with the development of organic chemistry. Copious references to the literature at the end of each chapter render this volume an indispensable source book for those actively engaged in this field, while those about to enter it will find that these references will spare them much time and labour.

Attractive type and printing, clearly and carefully reproduced formulae highly facilitate perusal without weariness. It is a very great pity that the binding is by cheap sticking at the spine: this breaks after short use and allows the pages fall apart. Such a fundamental book which certainly will be thumbed very often ought to have been given some much more lasting form.

Considering the high professional level of this work, the not too rare and more than once rather sense-distorting misprints weigh heavily, *viz.* on p. 86 phosphonate is formed from a phosphonium salt by alkyllithium; on p. 99 thorium nitrate is printed instead of thallium nitrate; on p. 105 the reference number to an item in the literature is erroneous etc. At least a list of errors should have been provided.

The information-content of some figures showing synthetic routes is open to censure. For instance, on p. 107, Fig. 2.10 is one of simple reaction steps which are clear even when given in a contracted form; in contrast, the illustration of the Prins reaction which comprises complicated rearrangements of bonds is not provided with even a single arrow for pointing out electron shifts, though formulae 2.127 and 2.128 are drawings of the fundamental skeleton from different points of view.

The detailed Table of Contents placed at the beginning of the book seems to be quite a lucky device and helps to find one's in this concrete domain better than would a subject index of minute particulars.

The structural division of this book follows the topics dealt with. An Introduction, five pages altogether, delineates the importance, history of research of prostaglandins, and where these compounds are to be found in nature.

The first chapter is about the structure, nomenclature, physical properties of prostaglandins, and about how to convert one into another.

In the second chapter the linear variants of syntheses are explained, thus the Corey-syntheses, grouped according to the types of prostaglandins; then the methods according to Corey for the preparation of lactone-aldehydes; the variant according to Woodward; and the syntheses which start from norbornadiene, and from bicyclohexyl derivatives. There was no time to include a later method developed in the laboratories of the Chemical and Pharmaceutical Works Chinoin, Budapest.

The third chapter contains a discussion of the convergent variants of the synthesis of prostaglandins. The methods proposed for the synthesis of cyclopentenone derivatives which serve as synthones, are dealt with in detail, then less convergent transformations (addition of cyano compounds, nitromethane) follow; after these the high degree of convergence and stereoselectivity to be achieved by the addition of organometallic compounds, *i.e.* Grignard reagents, copper compounds, is illustrated with a number of examples very much to the point. In its concluding part this chapter treats the regionally selective ring, cleavage of epoxy-cyclopentane derivatives; the way of planning syntheses with a computer is then outlined.

Chapter 4 starts with an exposition of the concepts of chirality and asymmetrical synthesis. This part has a smack of a textbook: beyond technical terms precisely and concisely explained, scarcely anything else is offered here; this review is a useful refresher, but it is not really needed for the comprehension of what this chapter intends to convey.

The discussion of the brilliant synthesis worked out by Uskokovic *et al.* is perhaps too laconic. The designation "pseudo-symmetrical meso-compound" used in the description

of Fischli's synthesis is not very well chosen since in the meso-compound (which has a plane of symmetry) not the symmetry but the asymmetry is 'pseudo', thus the meso-compound is 'pseudo-asymmetrical'. The concluding part of this chapter deals with the microbiological reductions reported by SIH *et al.*

In the fifth chapter we find syntheses of prostaglandin derivatives and analogues. Perhaps this is the field where progress is most rapid and most diversified at the present time; this is also the part of their book where the authors' sense of proportion is most happily in evidence. The examples discussed comprise the syntheses of methyl-, oxa-, and thia-prostaglandin analogues.

In the sixth chapter the biosyntheses of prostaglandins and their recovery from natural sources are described. Unfortunately the recently published achievements of biosyntheses, *viz.* thromboxanes, prostacycline, could not be included, though, as a formula, *i.e.* 6.23 on p. 300, the so-called TX_2B, even if under another name, is to be found here.

The Appendix which concludes this work gives an outline of the chemical analysis methods used in connexion with prostaglandins.

I. TÖMÖSKÖZI

A. ROMANOV (editor): *Modified Polymers, their Preparation and Properties*

Pergamon Press, Oxford—New York—Toronto—Sydney—Paris—Frankfurt, 1977 (70 pages)

The volume contains the main lectures presented at the 4th Bratislava Conference on Polymers 1—4 July, 1975.

It includes the following papers:

J. DOBÓ: Radiation cross-linking of PVC with ethylene glycol dimethacrylate

P. REMPP: Recent results on chemical modification of polymers

A. A. ASKADSKIJ: Influence of chemical structure on the properties of polymers

W. JAEGER and G. REINISCH: Mikrogebildung durch thermische Aktivierung

N. G. GAYLORD and T. TOMONO: Alternating copolymer graft copolymers — XI. Grafting through matrix polymerization

A. D. JENKINS: Acrylonitrile block and graft copolymers

N. A. PLATÉ: Problems of polymer modification and the reactivity of functional groups of macromolecules

H. INAGAKI, T. KOTAKA and T. I. MIN: Separation and characterization of block and graft copolymers by thin-layer chromatography

The content of the book is identical with that of the periodical Pure and Applied Chemistry, Vol. 46, No. 1, pp. 1—70 (1976).

I. GÉCZY

INDEX

PHYSICAL AND INORGANIC CHEMISTRY

ORGANIC CHEMISTRY

Printed in Hungary

A kiadásért felel az Akadémiai Kiadó igazgatója. Műszaki szerkesztő: Zacsik Annamária

A kézirat nyomdába érkezett: 1977. X. 7. — Terjedelem: 7,35 (A/5) ív, 27 ábra

78.5029 Akadémiai Nyomda, Budapest — Felelős vezető: Bernát György

ACTA CHIMICA

ТОМ 96—ВЫП. 1

РЕЗЮМЕ

Электрогидрирование и гидрирование простых алифатических кетонов в кислых средах

Ш. САБО и ДЬ. ХОРАНИ

Электрогидрирование и гидрирование некоторых простых кетонов (2-бутанон 3-пентанон, 3-метил-2-бутанон и 2-пентанон) было исследовано на платиновом катализаторе в кислой среде. Углеводороды всегда образуются в этой реакции. Однако, если в, случае бутанона основным продуктом является углеводород, то в случае пентанонов основным продуктом является соответствующий вторичный спирт. На основе результатов исследований и литературных данных можно сделать заключение, что при электрогидрировании кетонов спирты и углеводороды образуются не в двух независимых ступенях реакции, а являются продуктами разветвленной реакции. Ступенью, лимитирующей скорость является та, которая предшествует ответвлению.

Применение теории Флори к расчету избыточных термодинамических функций систем пиперидин–тетрагидропиран, пиперидин–циклогексан и тетрагидропиран–циклогексан

ДЖ. Д. ПАНДЕЙ и Р. Л. МИШРА

Статистическая теория флори была применена к системам: пиперидин-тетрагидрофуран, пиперидин–циклогексан и тетрагидропиран–циклогексан. Избыточные термодинамические функции были определены в зависимости от температуры и состава, а результаты были использованы для проверки теории.

Исследование хелатов некоторых менее распространенных переходных металлов, II

Ru(III), Rh(III), Ir(III) и Pt(IV)

Р. К. УПАДХАЙ и М. Л. СИНГАЛ

Исследования электронных спектров комплексов некоторых менее распространенных переходных металлов с четырьмя кетонильними лигандами были проведены в связи с теорией лигандного поля для d—d переходов переноса заряда. Низкоспинная октаэдрическая стереохимия, определенная спектроскопически, была доказана магнитным путем. Абнормальное парамагнитное поведение комплексов Rh(III), Ir(III) и Pt(IV) было приписано эффекту Зе-мана второго порядка. ИК спектроскопические исследования были использованы для определения мест координации в лигандах и для определения структуры комплексов. Было найдено, что электро-донорные свойства пара-замещенных групп лигандов оказывают прямое влияние на стабильность комплекса. Был определен порядок стабильности комплексов (по лиганду и по металлу), который подтверждается их величинами 10Dq.

Реакции некоторых алканов на катализаторе палладиевой черни

А. ШАРКАНЬ, Л. ГУЦИ и П. ТЕТЕНИ

Была исследована адсорбция метана и этана, реакции дейтерийного обмена метана, этана, н-бутана и 2,2-диметилпропана а также гидрогенолиз и изомеризация этана, бутанов и 2,2-диметилпропана на палладиевой черни. Исходя из данных адсорбции метана и этана можно полагать различные формы адсорбции. «Слабая» необратимая адсорбция может играть важную роль в реакциях дейтерийного обмена, в то время как «сильное» взаимодействие приводит к разрыву связи С—С и к отравлению катализатора. Стерические препятсвия в образовании связей α были обнаружены не только на основе данных по обогащению начальных продуктов алканами [$^2H_1$], но также и на основе хорошо определенного разделения дейтерийного обмена от гидрогенолиза. Кинетические параметры гидрогенолиза и изомеризации, а также распределение продуктов были определены в зависимости от температуры и давления водорода. Результаты указывают на то, что различные поверхностные промежуточные продукты принимают участие в реакциях изомеризации и гидрогенолиза.

Мокрое рафинирование фосфатной желтой лепешки до тетрафтористого урана

М. Р. ЗАКИ, С. А. ИЛЬ-ФЕКЕЙ и М. Й. ФАРАХ

Метод фотолитического рафинирования — восстановления, применяемый для предварительно очищенных фосфатных фильтр-прессных лепешок, был распространен и для получения тетрафтористого урана. Был исследован эффект высаждения и промывки продукта на его текструру и плотность, а также на его Дебайграмы. Был получен тетрафторид с ядерной чистотой, как это было подтверждено его спектром эмиссии.

Синтез алкалоидов ипекакуаны, IV
Синтез этокси-аналога эметина

Я. РОХАЙ и Ч. САНТАИ

Был синтезирован аналог эметина, содержащий этоксигруппу *(1b)*. Эметин *(1a)* и изоэметин *(9a)*, а также их этокси-аналоги *(1b)* и *(9b)* были исследованы методами ОРД и ПМР.

Синтез алкалоидов ипекакуаны, V
Новый путь получения дегидроэметина и его этокси-аналога

Ч. САНТАИ и Я. РОХАЙ

Был осуществлен синтез дегидроэметина *(1a)* через дегидропротонэметин *(3b)* с помощью циклизации типа Пиктет—Шпенглера. Дгя синтеза этокси-аналога дегидроэметина *(1b)* использовали циклизацию типа Бишлер—Напиральского.

Квантовохимические исследования пиридо- и хинолино-астриазинов, I
Модельные соединения пиридо-ас-триазина

З. ДИНЯ, П. БЕНКО, А. И. КИШ, Л. ПАЛЛОШ, Э. БЕРЕНИ, П. ЕКЕЛ и С. РОХЛИЦ

С помощью различных полуэмпирических методов (ППП, КНДО) были исследованы электроноструктурные и УФ-спектроскопические данные пиридо-ас-триазина и бензо-ас-триазина. На основе результатов расчета были обсуждены данные реактивности. Было установлено, что УФ-спектральные и электроноструктурные характеристики изменяются в зависимости от положения пиридо-N-атома.

Les Acta Chimica paraissent en français, allemand, anglais et russe et publient des mémoires du domaine des sciences chimiques.

Les Acta Chimica sont publiés sous forme de fascicules. Quatre fascicules seront réunis en un volume (4 volumes par an).

On est prié d'envoyer les manuscrits destinés à la rédaction à l'adresse suivante:

Acta Chimica
H-1521 Budapest, Hongrie

Toute correspondance doit être envoyée à cette même adresse.

La rédaction ne rend pas de manuscript.

Le prix de l'abonnement: $ 36,00 par volume.

Abonnement en Hongrie à l'Akadémiai Kiadó (1363 Budapest, P. O. B. 24, C. C. B. 215 11488), à l'étranger à l'Entreprise du Commerce Extérieur « Kultura » (H-1389 Budapest 62, P. O. B. 149 Compte-courant No. 218 10990) ou chez représentants à l'étranger.

Die Acta Chimica veröffentlichen Abhan5lungen aus dem Bereich der chemischen Wissenschaften in deutscher, englischer, französischer und russischer Sprache.

Die Acta Chimica erscheinen in Heften wechselnden Umfanges. Vier Hefte bilden einen Band. Jährlich erscheinen 4 Bände.

Die zur Veröffentlichung bestimmten Manuskripte sind an folgende Adresse zu senden:

Acta Chimica
H-1521 Budapest, Ungarn

An die gleiche Anschrift ist jede für die Redaktion bestimmte Korrespondenz zu richten.

Manuskripte werden nicht zurückerstattet.

Abonnementspreis pro Band: $ 36,00.

Bestellbar für das Inland bei Akadémiai Kiadó (1363 Budapest, Postfach 24, Bankkonto Nr. 215 11488), für das Ausland bei »Kultura« Außenhandelsunternehmen (H-1389 Budapest 62, P. O. B. 149. Bankkonto Nr. 218 10990) oder seinen Auslandsvertretungen.

«Acta Chimica» издают статьи по химии на русском, английском, французском и немекком языках.

«Acta Chimica» выходит отдельными выпусками разного объекта, 4 выпуска составляют один тдм и за год выходят 4 тома.

Предназначенные для публикации рукописи следует направлять по адресу:

Acta Chimica
H-1521 Budapest, BHP

Всякую корреспонденцию в редакцию направляйте по этому же адресу.

Редакция рукописей не возвращает.

Подписная цена — $ 36,00 за том.

Отечественные подписчики направляйте свои заявки по адресу Издательства Академии Наук (1363 Budapest, P. O. B. 24, Текущий счет 215 11488), а иностранные подписчики через организацию по внешней торговле «Kultura» (H-1389 Budapest 62, P. O. B. 149. Текущий счет 218 10990) или через ее заграничные представительства и уполномеченных.

Reviews of the Hungarian Academy of Sciences are obtainable at the following addresses:

AUSTRALIA
C.B.D. LIBRARY AND SUBSCRIPTION SERVICE, Box 4886, G.P.O., *Sydney N.S.W. 2001*
COSMOS BOOKSHOP, 135 Ackland Street, *St. Kilda (Melbourne), Victoria 3182*

AUSTRIA
GLOBUS, Höchstädtplatz 3, *1200 Wien XX*

BELGIUM
OFFICE INTERNATIONAL DE LIBRAIRIE, 30 Avenue Marnix, *1050 Bruxelles*
LIBRAIRIE DU MONDE ENTIER, 162 Rue du Midi, *1000 Bruxelles*

BULGARIA
HEMUS, Bulvar Ruszki 6, *Sofia*

CANADA
PANNONIA BOOKS, P.O. Box 1017, Postal Station "B", *Toronto, Ontario M5T 2T8*

CHINA
CNPICOR, Periodical Department, P.O. Box 50, *Peking*

CZECHOSLOVAKIA
MAD'ARSKÁ KULTURA, Národní třida 22, *115 66 Praha*
PNS DOVOZ TISKU, Vinohradská 66, *Praha 2*
PNS DOVOZ TLAČE, *Bratislava 2*

DENMARK
EJNAR MUNKSGAARD, Norregade 6, *1165 Copenhagen*

FINLAND
AKATEEMINEN KIRJAKAUPPA, P.O. Box 128, *SF-00101 Helsinki 10*

FRANCE
EUROPERIODIQUES S.A., 41 Avenue de Versailles, *78170 La Celle St.- Cloud*
LIBRAIRIE LAVOISIER, 11 rue Lavoisier, *75008 Paris*
OFFICE INTERNATIONAL DE DOCUMENTATION ET LIBRAIRIE, 38 rue Gay-Lussac, *75240 Paris Cedex 05*

GERMAN DEMOCRATIC REPUBLIC
HAUS DER UNGARISCHEN KULTUR, Karl-Liebknecht-Strasse 9, *DDR-102 Berlin*
DEUTSCHE POST ZEITUNGSVERTRIEBSAMT, Strasse der Pariser Kommüne 3—4, *DDR-104 Berlin*

GERMAN FEDERAL REPUBLIC
KUNST UND WISSEN ERICH BIEBER, Postfach 46, *7000 Stuttgart 1*

GREAT BRITAIN
BLACKWELL'S PERIODICALS DIVISION, Hythe Bridge Street, *Oxford OX1 2ET*
BUMPUS, HALDANE AND MAXWELL LTD., Cowper Works, *Olney, Bucks MK46 4BN*
COLLET'S HOLDINGS LTD., Denington Estate, *Wellingborough, Northants NN8 2QT*
W.M. DAWSON AND SONS LTD., Cannon House, *Folkestone, Kent CT19 5EE*
H. K. LEWIS AND CO., 146 Gower Street, *London WC1E 6BS*

GREECE
KOSTARAKIS BROTHERS, International Booksellers, 2 Hippokratous Street, *Athens-143*

HOLLAND
MEULENHOFF-BRUNA B.V., Beulingstraat 2, *Amsterdam*
MARTINUS NIJHOFF B.V., Lange Voorhout 9—11, *Den Haag*
SWETS SUBSCRIPTION SERVICE, 347b Heereweg, *Lisse*

INDIA
ALLIED PUBLISHING PRIVATE LTD., 13/14 Asaf Ali Road, *New Delhi 110001*
150 B-6 Mount Road, *Madras 600002*
INTERNATIONAL BOOK HOUSE PVT. LTD., Madame Cama Road, *Bombay 400039*
THE STATE TRADING CORPORATION OF INDIA LTD., Books Import Division, Chandralok, 36 Janpath, *New Delhi 110001*

ITALY
EUGENIO CARLUCCI, P.O. Box 252, *70100 Bari*
INTERSCIENTIA, Via Mazzé 28, *10149 Torino*
LIBRERIA COMMISSIONARIA SANSONI, Via Lamarmora 35, *50121 Firenze*
SANTO VANASIA, Via M. Macchi 58, *20124 Milano*
D.E.A., Via Lima 28, *00198 Roma*

JAPAN
KINOKUNIYA BOOK-STORE CO. LTD., 17-7 Shinjuku-ku 3 chome, Shinjuku-ku, *Tokyo 160-91*
MARUZEN COMPANY LTD., Book Department, P.O. Box 5056 Tokyo International, *Tokyo 100-31*
NAUKA LTD., IMPORT DEPARTMENT, 2-30-19 Minami Ikebukuro, Toshima-ku, *Tokyo 171*

KOREA
CHULPANMUL, *Phenjan*

NORWAY
TANUM-CAMMERMEYER, Karl Johansgatan 41—43, *1000 Oslo*

POLAND
WĘGIERSKI INSTYTUT KULTURY, Marszałkowska 80, *Warszawa*
CKP I W ul. Towarowa 28 *00-985 Warsaw*

ROMANIA
D. E. P., *Bucureşti*
ROMLIBRI, Str. Biserica Amzei 7, *Bucureşti*

SOVIET UNION
SOJUZPETCHATJ — IMPORT, *Moscow*
and the post offices in each town
MEZHDUNARODNAYA KNIGA, *Moscow G-200*

SPAIN
DIAZ DE SANTOS, Lagasca 95, *Madrid 6*

SWEDEN
ALMQVIST AND WIKSELL, Gamla Brogatan 26, *S-101 20 Stockholm*
GUMPERTS UNIVERSITETSBOKHANDEL AB, Box 436, *401 25 Göteborg 1*

SWITZERLAND
KARGER LIBRI AG, Petersgraben 41, *4011 Basel*

USA
EBSCO SUBSCRIPTION SERVICES, P.O. Box 1943, *Birmingham, Alabama 35201*
F. W. FAXON COMPANY, INC., 15 Southwest Park, *Westwood, Mass, 02090*
THE MOORE-COTTRELL SUBSCRIPTION AGENCIES, *North Cohocton, N. Y. 14868*
READ-MORE PUBLICATIONS, INC., 130 Cedar Street, *New York, N. Y. 10006*
STECHERT-MACMILLAN, INC., 7250 Westfield Avenue, *Pennsauken N. J. 08110*

VIETNAM
XUNHASABA, 32, Hai Ba Trung, *Hanoi*

YUGOSLAVIA
JUGOSLAVENSKA KNJIGA, Terazije 27, *Beograd*
FORUM, Vojvode Mišića 1, *21000 Novi Sad*

10. IV. 1978 HU ISSN 0001—5407 Index: 26.007

ACTA CHIMICA

ACADEMIAE SCIENTIARUM HUNGARICAE

TOMUS 96 FASCICULUS 2

AKADÉMIAI KIADÓ, BUDAPEST

1978

ACTA CHIM. ACAD. SCI. HUNG. ACASA2 96 (2) 83–187 (1978)

ACTA CHIMICA

A MAGYAR TUDOMÁNYOS AKADÉMIA KÉMIAI TUDOMÁNYOK OSZTÁLYÁNAK IDEGEN NYELVŰ KÖZLEMÉNYEI

Acta Chimica is a journal for the publication of papers on all aspects of chemistry, in the English, German, French and Russian.

Acta Chimica is published in 4 volumes per year. Each volume consists of 4 issues of varying size.

Manuscripts should be sent to

Acta Chimica
H-1521 Budapest, Hungary

Correspondence with the editors should be sent to the same address. Manuscripts are not returned to the authors.

Subscription: $ 36.00 per volume.

Hungarian subscribers should order from Akadémiai Kiadó, 1363 Budapest, P.O. Box 24. Account No. 215 11488.

Orders from other countries are to be sent to "Kultura" Foreign Trading Company (H-1389 Budapest 62, P.O. Box 149. Account No. 218 10990) or its representatives abroad.

Acta Chimica Academiae Scientiarum Hungaricae, Tomus 96 (2), pp. 83—94 (1978)

A STUDY OF THE DISSOLUTION OF TUNGSTEN AND MOLYBDENUM IN MIXTURES COMPOSED OF SULPHURIC ACID, NITRIC ACID AND WATER

A. B. KISS and É. SZALÁNCZY

(Research Institute of the United Incandescent Lamps and Electric Co. Ltd., Budapest)

Received April 6, 1976

The rates of dissolution of tungsten and molybdenum in mixtures composed of sulphuric acid, nitric acid and water have been studied. Based on rates of dissolution as measured, the concentration-domains in triangular diagrams, characteristic of the two metals, have been delimited. Due to the vigorous oxidizing effect of the reaction products formed when molybdenum goes into solution, the corrosion of tungsten increases significantly, *i.e.* when these two metals are placed into the acid mixture at the same time. When molybdenum is also present in the acid mixture, the location and the shape of the concentration domains in the triangular diagrams, characteristic of the rate of solution of tungsten, will aproximate those characteristic of molybdenum rather than of tungsten. Generally the extent of corrosion of tungsten is proportional to the mass of molybdenum gone into solution at the same time. A method is proposed for the calculation of dissolution rates when the two metals are in inseparable mechanical combination in the sample and thus their initial masses cannot be determined by weighing, only by calculation from the $m_1^W + m_2^{Mo}$ total initial weight. The relative error of the calculation of the initial weight of tungsten is expressed as a function of the relative error in the measurement of the common density ϱ_{1+2} of the composite sample.

Introduction

Metals, *e.g.* tungsten or molybdenum, which form acidic oxides, can be dissolved both in acidic or alkaline media if oxidative conditions are secured. Many various acidic or alkaline solvents that contain some oxidative agent are known [1, 2], several among these attained considerable practical importance. Under the head of acidic oxidant nitric acid might be considered as the most important one; in order to reduce its aggressiveness it is admixed also with sulphuric acid, thus, in fact, one has to deal with a ternary system composed of nitric acid, sulphuric acid and water. It is well known [3] that in the corrosion of tungsten a significant increase of this will be effected by reaction products which form when some other metal *e.g.* molybdenum is also dissolved in the same medium, in other words, when these two metals are put at the same time into the acidic mixture. This experience justifies that the rate of dissolution

of tungsten be studied in a system where also molybdenum is dissolved at the same time, apart from the study of the processes that take place when these metals are dissolved separately.

Experimental

Variously composed mixtures of sulphuric acid (specific weight 1.84), nitric acid (sp.w. 1.40 and 1.52), and water were kept at temperatures between 60 and 100 °C, ± 0.5 °C, then weighed pieces of tungsten and molybdenum were placed into the mixtures. After a certain period of time the metal pieces were removed from the acid, rinsed, dried, then the weight losses were determined and referred to the initial surface of the pieces and to unit time.

In order to remove the oxide layer from the surface, the metals were kept for some time in a 10 per cent solution of sodium hydroxide and the weight of the samples thus pre-treated was accepted as the initial weight. In the case of some compositions of the acid mixture the weight of the tungsten sample became higher than its initial weight; this was due to the formation of an oxide, visible to the naked eye. Therefore these samples, weighed after rinsing and drying, were stripped of oxide in a warm, 10 per cent solution of sodium hydroxide and weighed again.

Since the rate of dissolution of tungsten is very low, a piece of a given mass had to be worked so as to present the largest possible surface that an accurately measurable loss of weight be recorded. Pieces of spirals of incandescent lamp filament were most suitable for this purpose. The surface F (in cm^2) of a spiral piece of the filament 0.005 cm in diameter was calculated according to the equation

$$F = \frac{4m}{d\varrho} = 41.343 \cdot m$$

where m stands for the mass of the spiral (in grammes), d for the diameter of the filament, and ϱ for the density of tungsten (19.35). Since the solubility of molybdenum is higher by several orders of magnitude, from this metal platelets 10 by 10 by 0.25 mm were used.

In tests which involved the simultaneous dissolution of the two metals, 15 pieces of tungsten spirals were fitted tightly around a 50 mm length of a molybdenum wire of 2 mm diameter. With the geometrical arrangement of the samples always the same, well defined conditions were assured for the contact between nitrous gases and tungsten spirals.

Since the acids commercially available were of various concentrations we thought it better to express the composition of their mixtures uniformly as per cents by weight, *i.e.* grammes of acid in 100 grammes of the acid mixture, and not as per cents by volume of acids of ascertained specific weight.

Results and discussion

1. *Dissolving of tungsten*

No measurable quantities of tungsten dissolved at temperatures below 100 °C, therefore tests were carried out at this temperature. Since besides nitric acid also sulphuric acid can be an active component, first the binary systems sulphuric acid and water, respectively, nitric acid and water were studied (*cf.* Fig. 1). In disagreement with the statement of VAN LIEMPT [1] we have

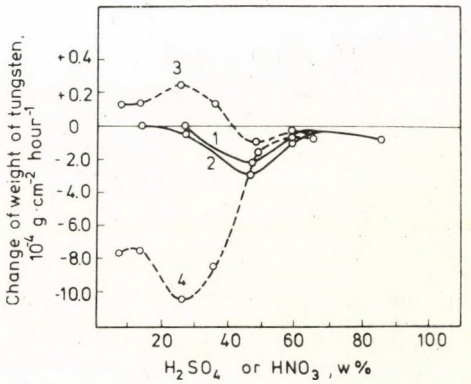

Fig. 1. Change of weight of tungsten in sulphuric acid and water, respectively in nitric acid and water systems. 1. After treatment in sulphuric acid. 2. After treatment in sulphuric acid and subsequent alkaline removal of oxide. 3. After treatment in nitric acid. 4. After treatment in nitric acid and subsequent removal of oxides by alkali

found that sulphuric acid dissolves tungsten slightly. The maximum rate of dissolution is at the concentration of 45 per cent (Curve 1). After the acid treatment a slight layer of oxide is formed on the surface of the metal: the measure of this formation as a function of the concentration of the acid is shown by Curve 2 plotted with data gathered after alkaline boiling. In nitric acid the weight of the tungsten sample increases at the beginning (Curve 3); it is only at concentrations above 40 per cent that the rate of dissolution is greater than the rate of oxide formation. After removal of the oxide layer from the surface we found that formation of oxide and dissolution proceeded at highest rates between concentrations of 25 and 30 per cent (Curve 4) and then decreased considerably.

The triangular diagram in Fig. 2 maps the characteristic concentration domains into which, within noted limits, the dissolution rates of tungsten belong. The numerical values given refer to 100 °C, and to the dimension and order of magnitude 10^{-5} g · cm^{-2} · hour^{-1}. In the case of compositions located within the concentration domain marked A in Fig. 3, a yellowish layer of oxide can be seen on the tungsten surface at the time the corrosion process is interrupted;

within the domain marked B, however, the surface retains its metallic colour throughout. In the case of domain A the weight of the tungsten sample still decreases substantially after treatment in boiling sodium hydroxide that follows the corrosive treatment, in domain B the subsequent alkaline treatment causes practically no loss of weight any more.

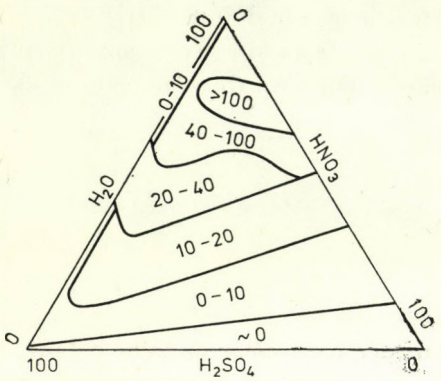

Fig. 2. Dissolution rate of tungsten in mixtures of various proportions (per cent by weight) of sulphuric acid, nitric acid and water. Temperature 100 °C. Dissolution rate 10^{-5} g · cm^{-2} · · hour^{-1}

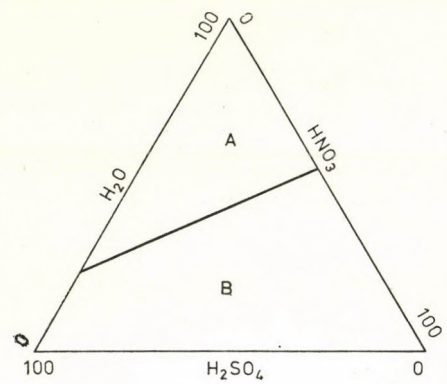

Fig. 3. Concentration domains delimited according to coverage by oxide of tungsten surfaces. A = tungsten surface, oxide-covered; B = tungsten surface, metallic

2. *Dissolution of molybdenum*

In contrast to tungsten, molybdenum is not attacked by sulphuric acid in any concentration, up to 100 °C; nitric acid, however, dissolves molybdenum by some orders of magnitude better. This feature can be utilized for the separation of molybdenum from tungsten. On the ascending section of the curves in Fig. 4, up to the point of maximum (at about 36 to 38 per cent), the sur-

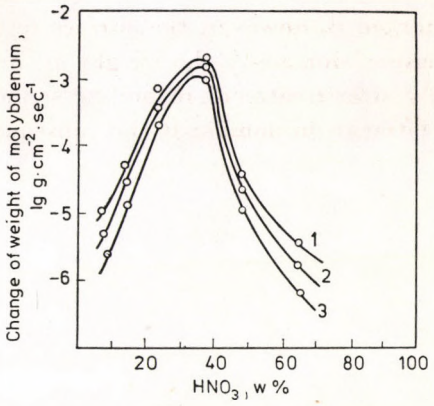

Fig. 4. Changes of weight of molybdenum in nitric acid and water systems. 1. 60 ± 0.5 °C; 2. 70 ± 0.5 °C; 3. 80 ± 0.5 °C

face of the molybdenum taken out of the acid is brown-black, at concentrations higher than these the surface has a clear metallic colour. The bulk of the dark surface layer is MoO_2, consequently it cannot be dissolved by alkaline treatment, therefore no curves as shown in Fig. 1 can be plotted for molybdenum.

In Fig. 5 the concentration domains delimited on the basis of dissolution rates noted for molybdenum have been drawn. These show that acid

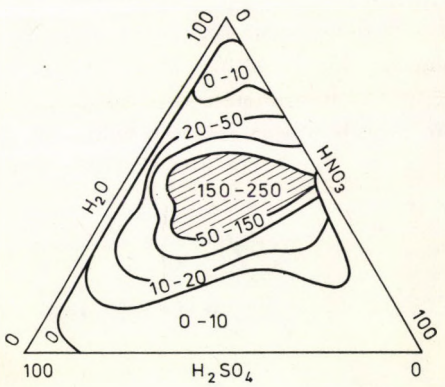

Fig. 5. Rate of dissolution of molybdenum in mixtures of various proportions (per cent by weight) of sulphuric acid, nitric acid, and water. Temperature 80 °C. Rate of dissolution 10^{-5} g · cm^{-2} · sec^{-1}

compositions indicated by the hatched part are the most suitable for the dissolution of molybdenum. At the interruption of the dissolution processes the oxide coating on the molybdenum surface is confined to a much smaller domain of concentrations than in the case of tungsten (*cf.* Fig. 6).

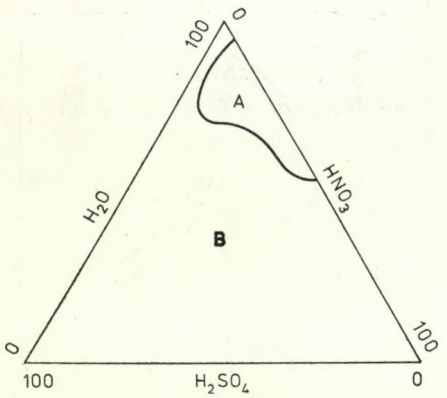

Fig. 6. Concentration domains delimited according to coverage by oxide of molybdenum surfaces. A = molybdenum surface, oxide-covered, B = molybdenum surface, metallic

3. *Simultaneous dissolution of tungsten and molybdenum*

In the presence of the much more readily dissolvable molybdenum the powerful oxidizing reaction products, *viz.* nascent oxygen and NO_2, significantly enhance the oxidation and dissolution of tungsten. Corrosion begins already at 60 °C, *i.e.* at a temperature where molybdenum begins to dissolve at a notable rate. In Fig. 7 we present rate domains recorded for the dissolution of tungsten when also molybdenum is present in the acid mixture. Juxtaposition of Figs 2, 5, and 7 informs us, according to expectation, that in the presence of molybdenum the location and shape of the concentration domains characteristic of the dissolution rate of tungsten approximate these features in Fig. 5, for molybdenum, rather than the corresponding ones in Fig. 2, for tungsten. At the same time we see that under the experimental

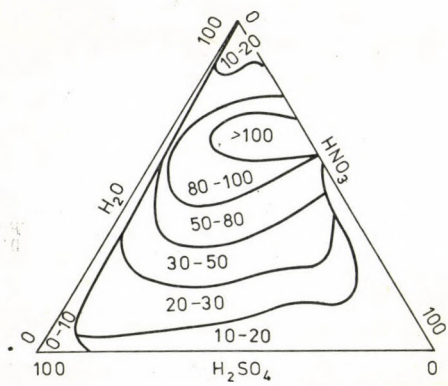

Fig. 7. Solution rate of tungsten at simultaneous dissolution of molybdenum in the same medium. Temperature 80 °C. Rate of dissolution 10^{-3} g · cm^{-2} · hour^{-1}

conditions described the rate of dissolution of tungsten increases by about two orders of magnitude.

We might state, generally, that the corrosion of tungsten is proportional to the dissolved quantity of molybdenum; in given cases the loss of weight can amount even to 10—12 per cent. Figures 8 and 9 contain corrosion data for

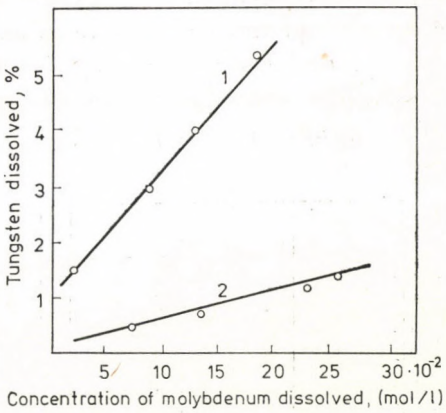

Fig. 8. The corrosion of tungsten as a function of the concentration of molybdenum dissolved at the same time in the same solvent. Temperature 80 °C. Duration of treatmenti 30 min

	1	2
Sulphuric acid	12.5%	16.6%
Nitric acid	19.5%	50.0%
Water	68.0%	33.4%

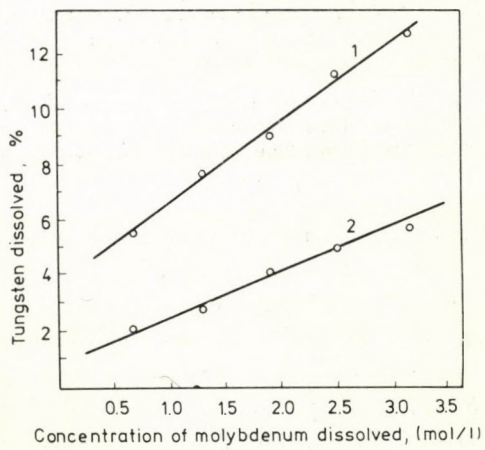

Fig. 9. The corrosion of tungsten as a function of the concentration of molybdenum dissolved at the same time in the same solvent. Temperature 80 °C. Duration of treatment 30 min

	1	2
Sulphuric acid	23.0%	35.0%
Nitric acid	30.0%	40.0%
Water	47.0%	25.0%

two concentration domains of dissolved molybdenum and two acid mixtures.

The measure of corrosion of the filaments tested can be demonstrated very well also by their change of resistance. In Fig. 10 we show the scatter of the resistance of pieces of tungsten untreated (1), treated in the absence (2), and in the presence (3) of molybdenum. This Figure shows very vividly that under otherwise identical experimental conditions an increase of resistance incidental to a significant diminution of cross-section occurs when aggressive nitrous gases evolved in the course of the dissolution of molybdenum enhance the corrosion of the tungsten surfaces.

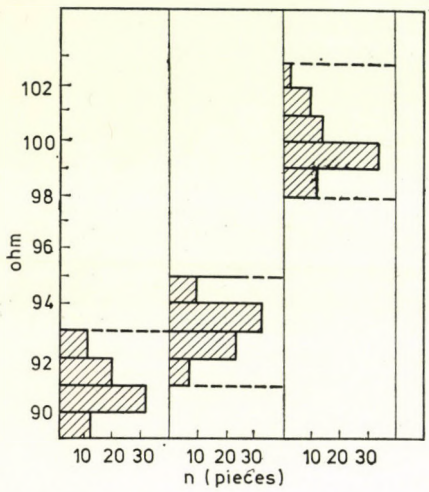

Fig. 10. Change of the resistance of tungsten filaments, due to corrosion. Temperature 80 °C. Duration of treatment 60 minutes. Final concentration of molybdenum 0.7 mole per litre. Acid mixture: sulphuric acid, 23.0%; nitric acid 30.0%; water 47.0%

As shown in Fig. 11, corrosion of tungsten is a linear function of temperature.

When the concentrations of the components of the acid mixtures were determined according to the method of STUCK [4] for states corresponding to points of measurements in Fig. 9, the process of the exhaustion of the acid mixture could be kept track of (*cf.* Fig. 12). As dissolution proceeds the concentration of the mixtures changes along a line parallel to the sulphuric acid axis or along a curve that does not deviate very far from it. Since the position of the concentrationdomains as shown in Fig. 7 is more or less horizontal, starting from a domain of a given dissolution rate it is generally feasible that in the course of the corrosion process passage through zones more and more dangerous for tungsten be evaded.

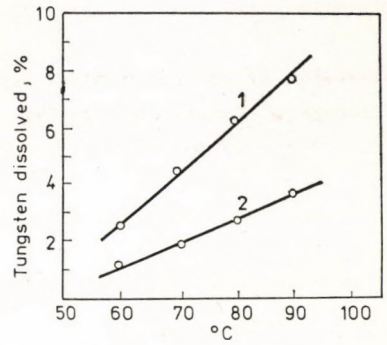

Fig. 11. Corrosion of tungsten as a function of temperature. Duration of treatment 30 minutes. Final concentration of molybdenum 1.25 mole per litre

	1	2
Sulphuric acid	23.0%	35.0%
Nitric acid	30.0%	40.0%
Water	47.0%	25.0%

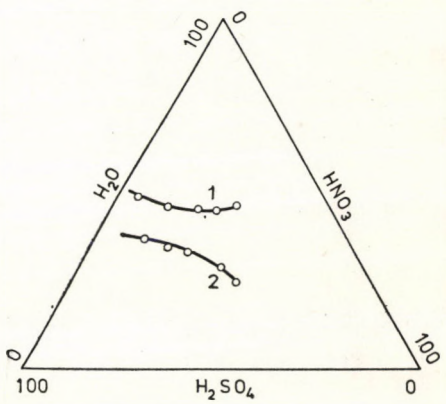

Fig. 12. Change of the concentration of the mixture of acids, in the course of dissolution processes

Taking Figs 5 and 7 as a basis, we can circumscribe the concentration domain wherein the two conflicting requirements, *viz.* quickest possible dissolution of molybdenum and least possible corrosion of tungsten, will best be satisfied by compromise (*cf.* Fig. 13).

4. *Calculation of the rate of dissolution for tungsten–molybdenum systems*

When these two metals are inseparably worked together then a determination of their initial masses is not feasible. In such cases it is expedient to proceed along the following lines.

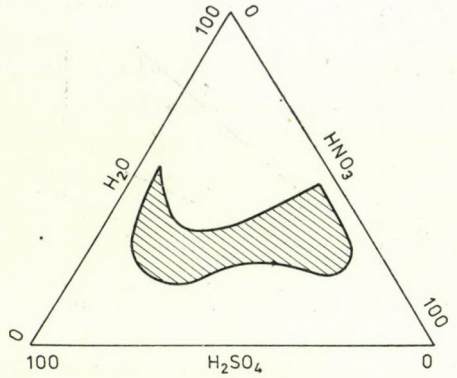

Fig. 13. The domain of concentrations most suitable for the prevention of the corrosion of tungsten

The overall weight of the tungsten and molybdenum common sample is noted and its density is determined in a pycnometer. With these data known, two equations are written, *viz.*

$$\frac{m_1}{\varrho_1} + \frac{m_2}{\varrho_2} = \frac{m_{1+2}}{\varrho_{1+2}}$$

and

$$m_1 + m_2 = m_{1+2},$$

where m_1 is the mass of tungsten, m_2 is the mass of molybdenum, m_{1+2} is the common mass; ϱ_1 is the specific weight of tungsten (19.35) [5], ϱ_2 is the specific weight of molybdenum (10.20) [6] and ϱ_{1+2} is the common specific weight of the sample with the mass $m_1 + m_2$.

When the term $K = 1 - \frac{\varrho_2}{\varrho_1}$ is introduced for substitution we get the initial mass of tungsten in the common sample, *i.e.*

$$m_1^{\mathrm{W}} = \left(\frac{1}{K} - \frac{\varrho_2}{K\varrho_{1+2}}\right) m_{1+2}$$

and for that of molybdenum we have

$$m_2^{\mathrm{Mo}} = \left(1 - \frac{1}{K} + \frac{\varrho_2}{K\varrho_{1+2}}\right) m_{1+2}.$$

Let it be supposed that the reaction is allowed to proceed till molybdenum is completely dissolved. By weighing the mass of tungsten left undissolved, respectively, by calculating the initial weight of tungsten as suggested, the difference between the two data represents the mass of tungsten gone into

solution; the surface area being known, also the rate of dissolution can be determined. No particular experimental support for the validity of this method is needed; the accuracy of the calculations depends on the accuracy of the determination of specific gravity, by pycnometry. We may note, however, that in view of the very low rate of dissolution of tungsten, a very high level of accuracy must be attained in the calculation of the initial weight of this metal in the sample.

The relative error in the initial weight of tungsten is a function of the relative error in ϱ_{1+2}.

$$\delta m_1^{\mathrm{W}} = \frac{\varrho_2}{\left(1 - \frac{\varrho_2}{\varrho_{1+2}}\right)\varrho_{1+2}}\,\delta\varrho_{1+2}\,.$$

Since in the case of tungsten and molybdenum the value of $\frac{\varrho_2}{\varrho_{1+2}}$ may vary between 1.0 and 0.527, the course of this function between these limits might be studied. According to Fig. 14 it is obvious that for the calculation of the initial mass m_1^{W} of tungsten the conditions are the more favourable the nearer the term $\frac{\varrho_2}{\varrho_{1+2}}$ approaches the value 0.5, *i.e.* the higher is the concentration of tungsten in the sample. In practice the cases most often met with are of systems to be exposed to corrosion in which the respective initial masses of molybdenum and of tungsten fall between the limits

$$m_1^{\mathrm{W}} \leq m_2^{\mathrm{Mo}} \leq 2m_1^{\mathrm{W}}\,.$$

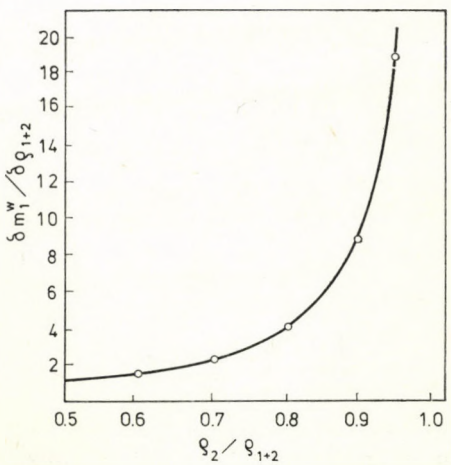

Fig. 14. Relative error of the calculation of m_1^{W} as a function of the relative error in ϱ_{1+2}

In this domain the values of $\frac{\varrho_2}{\varrho_{1+2}}$ fall between the limits 0.77 and 0.85; from this it follows that in order to arrive at a result for the initial mass m_1^W of tungsten within the limits of relative errors 1.0 and 1.5 per cent — and this is sufficiently accurate in most of the cases — the $\delta\varrho_{1+2}$ relative errors in pycnometric determinations must be limited between 0.15 and 0.5 per cent: this degree of accuracy is attainable without any difficulty.

REFERENCES

[1] VAN LIEMPT, J. A. M.: Rec. Trav. Chim. Pays-Bas, **45**, 508 (1926)
[2] KISS, B. A., NEUGEBAUER, J.: Acta Chim. Acad. Sci. Hung., **44**, 261 (1965)
[3] KISS, B. A.: Industr. Res. Inst. for Electronics, Budapest; Int. Res., Rept. 11009/1964. Classified.
[4] STUCK, W.: Z. Anal. Chem., **177**, 338 (1960)
[5] Handbook of Chemistry and Physics, 45th ed., B-234. The Chemical Rubber Co., Cleveland, 1965
[6] Handbook of Chemistry and Physics, 45th ed., B-195. The Chemical Rubber Co., Cleveland, 1965

András B. KISS
Éva SZALÁNCZY
H-1044 Budapest, Váci út 77.

Acta Chimica Academiae Scientiarum Hungaricae, Tomus 96 (2), pp. 95—103 (1978)

APPLICABILITY OF THE PPP AND CNDO/2 METHODS FOR THE STRUCTURAL INVESTIGATION OF ORGANOSILICON COMPOUNDS, II

J. RÉFFY, T. VESZPRÉMI, P. HENCSEI and J. NAGY

(Department of Inorganic Chemistry, Technical University, Budapest)

Received September 1, 1976

Calculations were carried out for the molecular structure of silicon-centered free radicals, para-substituted trimethylsilylbenzenes, *para*-substituted silylbenzenes, methyltrimethoxysilane and some compounds containing silicon–nitrogen bond. The correlation between various experimental physico-chemical data (ionization energy, dipole moment, ^{13}C and ^{29}Si NMR chemical shifts) of different organosilicon compounds and values calculated by the CNDO/2 method was investigated.

Introduction

In our previous paper [1] we have given an account of the PPP, IPPP and CNDO/2 calculations carried out for various organosilicon compounds. We have reported on the choice of parameters used in the calculations and on the structural investigation of phenylhalogenosilanes, phenoxysilanes and vinyl, allyl, phenyl, allyl derivatives of fourth main group elements. In the present paper the results for other organosilicon compounds are described. We report on calculations on silicon-centered free radicals and on the possibilities of applying the PPP and CNDO/2 methods in the interpretation of the results of various physico-chemical measurements.

Silicon-centered free radicals play an important role in several reactions. All the experimental evidence favours the pyramidal configuration for silyl (SiH_3), methylsilyl ($MeSiH_2$), dimethylsilyl (Me_2SiH) and trimethylsilyl (Me_3Si) radicals. To investigate these radicals CNDO/2 calculations were carried out for various assumed arrangements of hydrogen atoms and methyl groups bonded to the central silicon atom, and the conformations with minimum total energy were taken to be the most probable arrangements. According to the calculations at the energy minimum the H–Si–H bond angle is about 99° for the silyl radical, the bond angles are larger for the methylsilyl and dimethylsilyl radicals and the calculations indicate energy minimum at C–Si–C bond angle of 114° for the trimethylsilyl radical. With increasing methyl substitution the radical becomes more planar, but even the trimethylsilyl radical is non-planar. The same trend is concluded based on the measured ^{29}Si ESR splitting constants for trimethylsilyl and silyl radicals [2, 3].

In order to investigate the efficiency of the CNDO method in determining equilibrium bond distances and to study the change of silicon–carbon bond length as a function of bond order, CNDO/2 calculations were carried out for trimethylphenylsilane neutral molecule and the corresponding anion radical. In the calculations the silicon–carbon bond distance was varied in the range of 1.75—1.95 Å. Considering the energy minimum, the results indicate that the equilibrium bond distance is 1.886 Å for the neutral molecule and 1.848 Å for the anion radical. The calculated bond order between silicon atom and aromatic carbon atom is 1.09 and 1.35 in case of neutral trimethylphenylsilane and anion radical, respectively. As the bond order increases the equilibrium bond distance decreases. The bond distance obtained for neutral molecule is consistent with the bond distance data of silicon–aromatic carbon bond determined experimentally for phenylsilanes. According to the measurements this bond length is around 1.87 Å [4].

Calculations were carried out for *para-subsituted trimethylsilylbenzenes* and *para-substituted silylbenzenes* by the PPP and CNDO/2 methods. The investigated substituents were the following: H, CH_3, F, Cl, $N(CH_3)_2$, CN, NO_2. Out of our results the calculated and experimental dipole moments for the p-$XC_6H_4Si(CH_3)_3$ series are shown in Table I, the calculated and experimental electron transitions are summarized in Table II.

Table I

Calculated and experimental dipole moments of compounds p-$XC_6H_4Si(CH_3)_3$ in Debye

	$\mu_{calc.}$		$\mu_{exp.}$
	Del Re + PPP	CNDO/2	
H	0.09	0.32	0.25 [5]
CH_3	0.44	1.41	0.46 [6]
F	1.23	1.16	1.69 [7]
Cl	0.99	1.96	1.70 [7]
$N(CH_3)_2$	1.33	—	1.83 [6]
CN	2.89	—	4.34 [8]
NO_2	4.54	5.17	4.45 [8]

As far as the dipole moments are concerned the Del Re + PPP calculations show large deviations from the calculated values for the chloro and cyano derivatives, which can be explained by the difficulties in determining the Del Re parameters in the case of cyano group. The CNDO/2 method gives wrong results only for methyl substitution. The ultraviolet spectra are known only for three derivatives of the compounds investigated. The agreement between the singlet

Table II

Calculated and experimental transition energies for compounds p-$XC_6H_4Si(CH_3)_3$ in eV

	$^1E_{calc.}$ (PPP)	$\Delta E_{exp.}$
H	4.67	4.69 [9]
	5.69	5.77
	6.39	6.59
	6.43	
CH_3	4.78	4.70 [10]
	5.75	5.61
$N(CH_3)_2$	4.69	4.23 [11]
		4.69

electron transitions obtained by PPP calculations and transition energies corresponding to the maxima of experimental spectra of these derivatives seems appropriate.

NAGAI and his co-workers [12] determined the NMR chemical shift of hydrogens bonded to silicon and the J (^{29}SiH) coupling constants for some compound in the p-$XC_6H_4SiH_3$ series. Fig. 1 illustrates the correlation between the proton signs, the coupling constants and the δ_H partial charge of the corresponding hydrogen atoms. In both cases the point belonging to the unsubstituted compound lies farther from the regression line. The relative rate constants of the cleavage reaction of substituted trimethylsilylbenzenes by hydroxide [13] and the bond order values calculated for Si–C bonds are presented. Based on the results of the CNDO/2 calculations the values of bond orders were approximately determined by two methods (marked by A and B, respectively) [14]. Because of difficulties in carrying out calculations for larger molecules with many orbitals, CNDO/2 calculations could be performed for all the substituted compounds in question only for the p-$XC_6H_4SiH_3$ series and these calculated results were compared with the values of experimental rate constants. It can be seen clearly from the data of Table III that there exists a relationship between the relative rate constants and the Si–C bond orders. With the exception of unsubstituted derivatives the compounds follow the same order whether they are lined up according to decreasing rate constants or increasing bond orders. The strongly electron attractive nitro group weakens the Si–C bond, on the contrary, the dimethylamino group enhances the $(p-d)\pi$ character and the strength of this bond. The correlation of π bond orders calculated by the PPP method is generally worse with the relative rate constants.

The conformation analysis of *methyltrimetoxysilane* molecule was carried out by the CNDO/2 method. The geometry of the molecule was fixed by GERGŐ

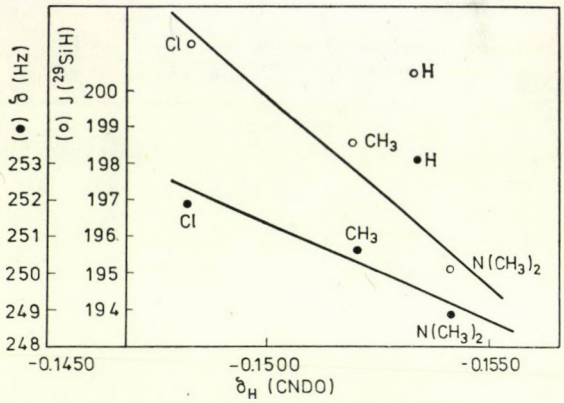

Fig. 1. Relationship between partial charges of hydrogens (δ_H) as well as chemical shifts (δ_{Si-H}) and coupling constants ($J(^{29}SiH)$) for compounds p-$XC_6H_4SiH_3$

et al., using electron diffraction method [15]. The minimum value of R factor was determined by least squares refinement, which gives the most probable state of the molecule from among the various possible conformers.

Figure 2 shows the change of R factor when the methyl groups are rotated along the Si–O axis keeping the C_3 symmetry of the molecule unchanged. The total energies calculated by the CNDO/2 method are also represented during the same rotational operations, and as it can be seen the agreement between the shapes of the two curves is good. This agreement raises the question whether the R factor can be regarded as the experimental measure of the potential energy of a molecule. The result has to be considered rather carefully since the R factor

Table III

Relative rate constants and Si–C bond orders for compounds p-$XC_6H_4Si(CH_3)_3$ and p-$XC_6H_4SiH_3$

	$k_{rel.}$ [13]	π-bond order PPP	Bond order (CNDO/2)			
			$-Si(CH_3)_3$		$-SiH_3$	
			method A	method B	method A	method B
NO_2	10 120	0.177	—	—	1.1241	0.9951
Cl	34.5	0.199	1.0938	0.9866	1.1389	1.0014
CN	—	0.187	—	—	1.1435	1.0034
F	8.0	0.197	1.1074	0.9920	1.1547	1.0082
H	1.0	0.193	1.0866	0.9770	1.1520	1.0095
CH_3	0.265	0.193	1.1143	0.9942	1.1593	1.0104
$N(CH_3)_2$	0.026	0.203	—	—	1.1736	1.0162

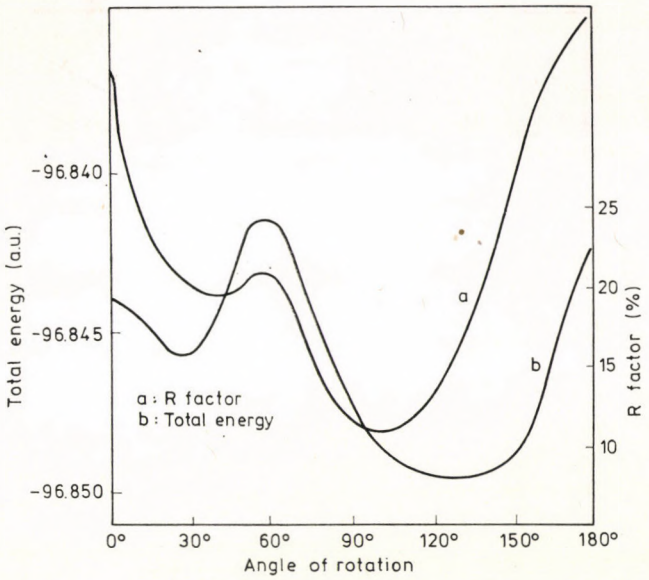

Fig. 2. Plot of total energy and value of R factor against the angle of rotation in the case of $CH_3Si(OCH_3)_3$

is sensitive, *e.g.* to the inscribing of background. In any case it is worth of carrying out similar calculations for other molecules.

The PPP and IPPP methods were used for the investigation of the following *compounds containing silicon–nitrogen bonds*: N-trimethylsilylaniline, N,N′-bis-(trimethylsilyl)-phenylenediamines, N-phenylhexamethyldisilazane, N-trimethylsilylpyrrole. To illustrate our results we chose the calculated electronic transitions and plotted in the function of the experimental values in Fig. 3.

It can be seen that the results obtained by the IPPP method show a better agreement with the data of experimental UV spectra than the values calculated by the PPP method.

In the following figures some results of our CNDO/2 calculations carried out for different organosilicon compounds are presented in comparison with the corresponding experimental data. The calculated orbital energies of the highest occupied molecular orbitals are plotted in the function of the experimental ionization energies in Fig. 4. The calculated values are larger than the experimental ones, but the correlation is good, more considerable deviation is indicated only for the SiH_4 molecule.

Figure 5 illustrates the calculated and experimental dipole moments. The points are scattered considerably; mainly molecules containing Si–H and Si–Cl bonds are farther from the straight line of 45°. The cause of this fact can possibly be attributed to the CNDO method which gives extremely high negative

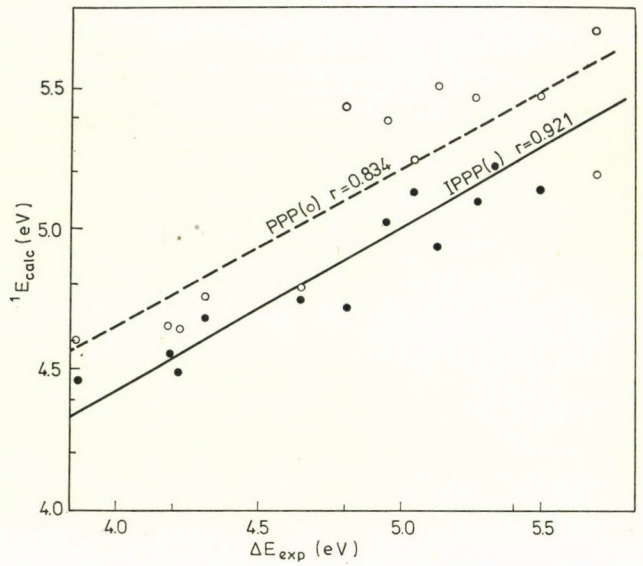

Fig. 3. Electronic transition energies calculated by the PPP and IPPP methods in the function of experimental values for compounds containing Si–N bond

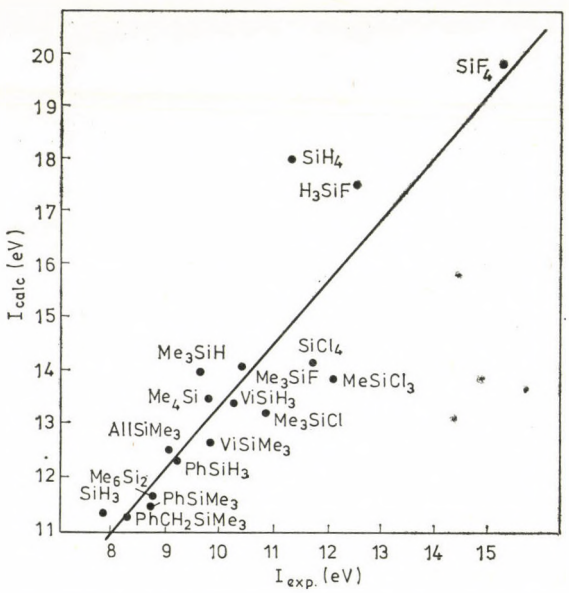

Fig. 4. Ionization energies calculated by the CNDO/2 method in the function of experimental values

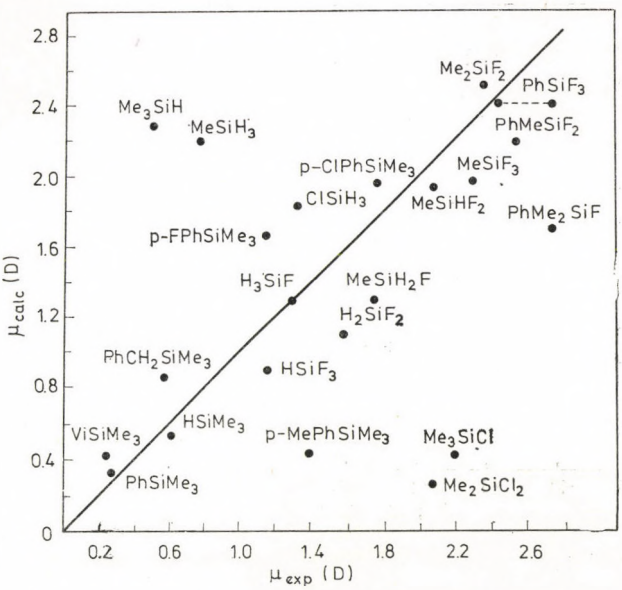

Fig. 5. Plot of dipole moments calculated by the CNDO/2 method against experimental values

charges to the hydrogen atoms and too low negative charges to the chlorine atoms attached to silicon.

The ^{13}C NMR chemical shifts of the aromatic carbon atoms in numerous phenylsilanes are compared with the calculated electron densities on the corresponding carbon atoms in Fig. 6. The experimental data were given by CHVALOVSKY *et al.* [16, 17]. For the carbon atoms in ortho, meta and para positions the correlation between the experimental data and calculated electron densities may be considered good, for the aromatic carbon atoms bonded to silicon the slope of the regression line is different, and the degree of correlation is much smaller.

We also investigated the correlation between the ^{29}Si NMR chemical shifts and the electron densities on silicon atoms, as it is illustrated in Fig. 7. The experimental data were taken from the works of ERNST [18] and SCHRAML [19]. The most considerable deviations can be observed for compounds containing Si—F bond, and for these compounds a separate regression line can be drawn.

The CNDO/2 method gives the bond energy of an investigated compound. This value can fairly be calculated according to the relatively simple SANDERSON method [20]. This method results in bond energies in accordance with the experimental heats of atomization. The values of the CNDO method are two to three times higher. The SANDERSON method was also applied using the charge distribution obtained by the CNDO method. This way the calculated bond energies were slightly larger than the experimental values. It is shown in Fig. 8 that *e.g.* in case of phenylmethylsilanes the bond energies obtained by the

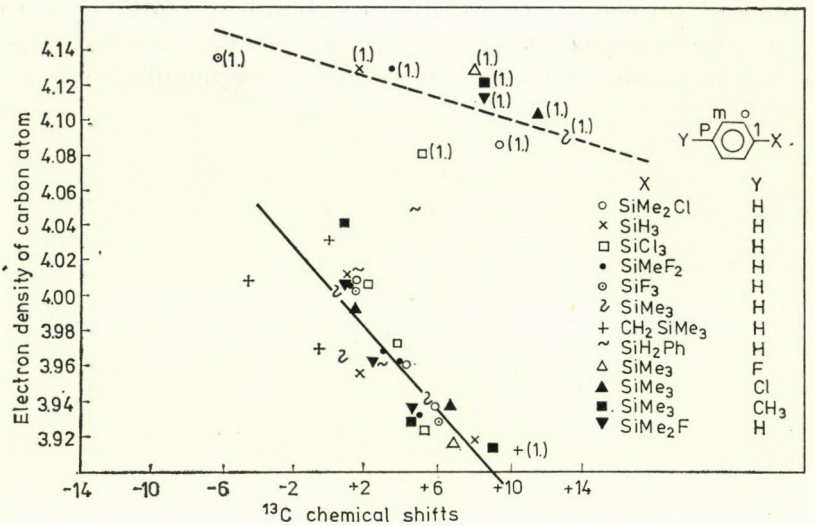

Fig. 6. Relationship between ^{13}C NMR chemical shifts of phenylsilanes and electron densities on the corresponding carbon atoms

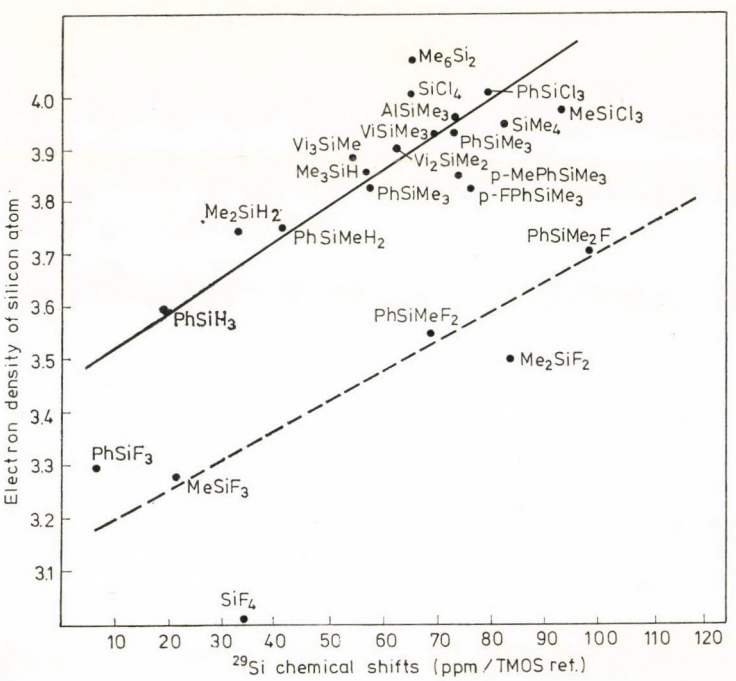

Fig. 7. Relationship between ^{29}Si NMR chemical shifts and electron densities on silicon atoms

CNDO method correlated well with those obtained by both the SANDERSON method and the modified SANDERSON method based on CNDO charge distribution. Similar relation holds for other series of compounds, too.

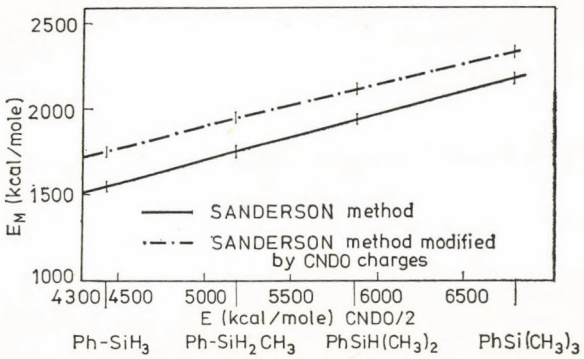

Fig. 8. Correlation of the bond energies calculated by various methods for phenylmethylsilanes

REFERENCES

[1] RÉFFY, J., VESZPRÉMI, T., HENCSEI, P., NAGY, J.: Acta Chim. (Budapest), **93,** 107 (1977)
[2] BENNETT, S. W., EABORN, C., HUDSON, A., JACKSON, R. A., ROOT, K. D. J.: J. Chem. Soc., A **1970**, 348
[3] JACKET, G. S., GORDY, W.: Phys. Rev., **176,** 443 (1968)
[4] DOMENICO, A., VACIAGO, A., COULSON, C. A.: Acta Cryst., B **31,** 1630 (1975)
[5] NAGY, J., FERENCZI-GRESZ, S., BECKER-PÁLOSSY, K., BORBÉLY-KUSZMANN, A.: Acta Chim. (Budapest), **61,** 149 (1969)
[6] SOFFER, H., DE VRIES, T.: J. Am. Chem. Soc., **73,** 5817 (1951)
[7] ROBERTS, J. D., MCELHILL, E. A., ARMSTRONG, R.: J. Am. Chem. Soc., **71,** 2923 (1949)
[8] LUCKIJ, A. E., OBUHOVA, E. M., VORONKOV, M. G., ALKSNE, V. N.: Teoret. Eksper. Khim., **9,** 123 (1973)
[9] RÉFFY, J., ÉLIÁS, P., NAGY, J.: Periodica Polytech., **14,** 47 (1970)
[10] NASIELSKI, J., PLANCHON, M.: Bull. Soc. Chim. Belg., **69,** 123 (1960)
[11] ALT, H., BOCK, H.: Tetrahedron, **27,** 4965 (1971)
[12] NAGAI, Y., OHTSUKI, M. A., NAKANO, T., WATANABE, H.: J. Organometal. Chem., **35,** 81 (1972)
[13] CRETNEY, J., WRIGHT, G. J.: J. Organometal. Chem., **28,** 49 (1971)
[14] RÉFFY, J., HENCSEI, P., NAGY, J.: Periodica Polytech., **20,** 279 (1976)
[15] GERGŐ, É., HARGITTAI, I., SCHULTZ, Gy.: J. Organometal. Chem. **112,** 29 (1976)
[16] SCHRAML, J., CHVALOVSKY, V., MÄGI, M., LIPPMAA, E.: Collect. Czech. Chem. Comm., **40,** 897 (1975)
[17] CHUY, N. D., CHVALOVSKY, V., SCHRAML, J., MÄGI, M., LIPPMAA, E.: Collect. Czech. Chem. Comm., **40,** 875 (1975)
[18] ERNST, C. R., SPIALTER, L., BUELLE, G. R., WHITE, D. L.: J. Am. Chem. Soc., **96,** 5375 (1974)
[19] SCHRAML, J., CHUY, N. G., CHVALOVSKY, V., MÄGI, M., LIPPMAA, E.: J. Organometal. Chem., **51,** C 5 (1973)
[20] SANDERSON, R. T.: Chemical Bonds and Bond Energy. Academic Press, New York and London, 1971.

József RÉFFY
Tamás VESZPRÉMI
Pál HENCSEI
József NAGY

H-1521 Budapest, Műegyetem

Acta Chimica Academiae Scientiarum Hungaricae, Tomus 96 (2), pp. 105—111 (1978)

CONFORMATIONAL STUDIES BY 300 MHz NMR SPECTROSCOPY: ROTATIONAL ISOMERISM ABOUT CO-CH_2 SINGLE BONDS

R. M. SINGH, C. K. RAO and S. M. VERMA*

(Department of Chemistry, Banaras Hindu University Varanasi-221005, India)

Received October 27, 1976

The 300 MHz NMR spectrum of N′,N′-dipropionyl-N-aminoimide of anthracene-maleic anhydride has revealed different conformations for the propionyl groups. The *exo*-propionyl group shows free rotation about the N–CO and CO–CH_2 bonds, while the *endo*-group has a preferred conformation about these bonds. An angular methyl group in the cage moiety gives an ABC_3 pattern for the *endo*-CO–CH_2CH_3, further supporting a preferred conformation. The observations on some substituted N′-acetyl derivatives are consistent with the proposed conformations.

Non-planar ground state conformations about the N–N bond in tetraacylhydrazine derivatives (**1**) have been observed [1—3] and interpreted in terms of repulsive interactions in the planar transition state between the two lone pair electrons in the *p*-orbitals of the N-atoms [4, 5]. High torsional barriers to the N–CO bond has been correlated [6] with the partial double bond character of the amide bond. However, preferred conformation about N–N and N–CO bonds has also been reported for certain acyclic N,N′-diacylhydrazines (**2**) [7]. The spectrum of the N′-monoacetyl derivative of N-aminocamphorimide (**3**) [8] at 44.5 °C indicates free rotation about the N–N′ bond and restricted rotation about the N′–CO bond, which has been characterized by the shielding constant of the β-methyl group. The NMR spectrum of compound (**4a**) [1] indicates hindered rotation about the N–N bond and the observed large shielding effect of the cage benzo ring (about 90 Hz in the 60 MHz spectrum) on the *endo*-N-acetyl protons can be expected from the preferred conformation about the N–CO bond, where the carbonyl group is oriented away from the cage benzo ring. We now report the observation of hindrance to rotation about the CO–CH_2 bond of the *endo*-(α-substituted) acetyl group in compounds of the type (**4**)

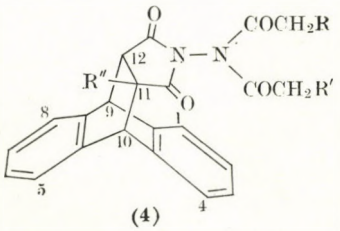

(**4**)

(4)

(4a)	R=H	R′=H	R″=H
(4b)	R=CH_3	R′=CH_3	R″=H
(4c)	R=CH_3	R′=CH_3	R″=CH_3
(4d)	R=H	R′=Cl	R″=H
(4e)	R=H	R′=Cl	R″=CH_3
(4f)	R=H	R′=$C_6H_4OCH_3$ (p)	R″=H
(4g)	R=H	R′=$C_6H_4OCH_3$ (p)	R″=CH_3

The 60 MHz NMR spectrum of compound (**4b**) in $CDCl_3$ (Table I) shows a quartet at δ 3.00 (2H) and a triplet at δ 1.10 (3H) for the *exo*-propionyl group and a complex multiplet at δ 0.80 (5H) for the *endo*-propionyl group. The other cage protons exhibit a normal pattern. Similarly, the spectrum of compound (**4c**) exhibited a complex pattern at δ 0.85 (5H) for the *endo*-propionyl group and a normal pattern for the other protons (Table I). 300 MHz spectra of these compounds revealed some evidence for the conformational preference about the CO–CH_2 bond in the *endo*-propionyl group. In the spectrum of compound (**4b**) in $CDCl_3$, the *exo*-propionyl protons appear as an A_2X_3 pattern, *i.e.* a sharp quartet at δ 2.93 (2H, J = 7.5 Hz) and a sharp triplet at δ 1.09 (3H, J = 7.5 Hz) while the *endo*-propionyl protons exhibit an A_2B_3 pattern [9] ($J_{AB} \simeq 7$ Hz and $\Delta\nu_{AB} = 42$ Hz) (Fig. 1). The other cage protons show the normal resonances. In the spectrum of compound (**4c**) in $CDCl_3$, the *exo*-propionyl protons exhibit a normal A_2X_3 pattern, while the *endo*-propionyl protons show an ABC_3 pattern (Fig. 2).

The cage moiety of compound (**4b**) possesses a plane of symmetry perpendicular to the succinimidyl plane and passing through the N–N bond. The two propionyl groups lie in the plane of symmetry in the non-planar ground state conformation about the N–N bond. The magnetic equivalence of the two methylene (geminal) protons of the propionyl groups suggests that (a) the

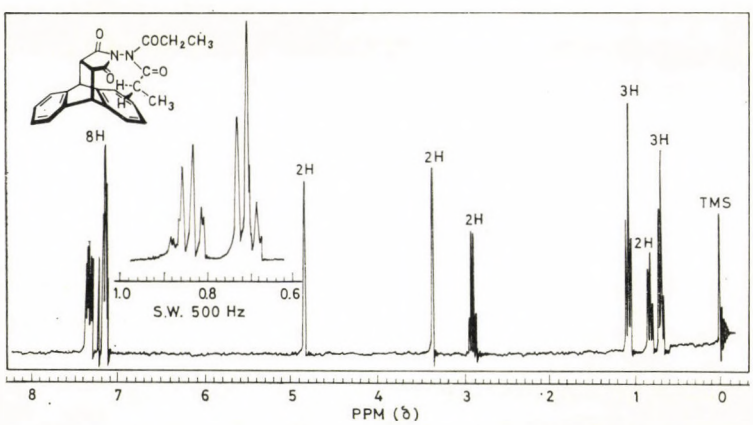

Fig. 1. 300 MHz NMR spectrum of compound (**4b**) in $CDCl_3$ at ambient temperature

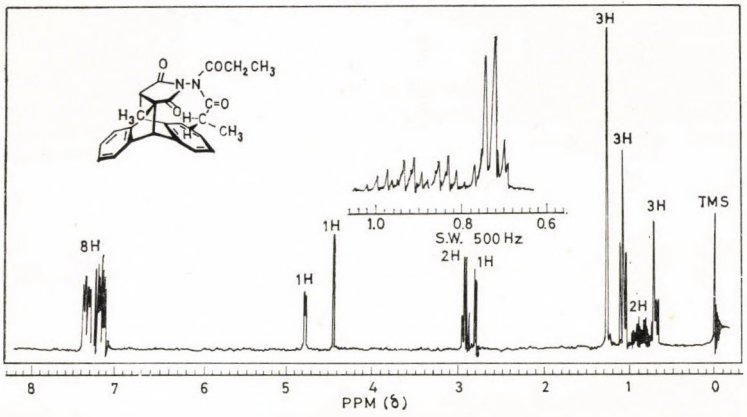

Fig. 2. 300 MHz NMR spectrum of compound (**4c**) in $CDCl_3$ at ambient temperature

propionyl group may freely change the conformation of the N–CO–CH_2 system, and (b) it may take up a preferred stable conformation like (**5**) or (**6**), which is symmetrical about the same plane of symmetry of the cage moiety. If any other conformation of the propionyl group were stable, it would make the geminal protons magnetically nonequivalent. The cage moiety of compound (**4c**) has no plane of symmetry and hence the two methylene (geminal) protons of any of the two propionyl groups may be expected to be magnetically nonequivalent [5]. However, the spectrum shows that the two methylene protons of the *exo*-propionyl group are magnetically equivalent, while those of the *endo*-propionyl group are nonequivalent. This observation could be explained by assuming stable conformation (**7**) about the N–CO–CH_2 system of the *endo*-propionyl group. The *exo*-propionyl group is free from any steric hindrance of the cage moiety and may rapidly change its conformations about the N–CO–CH_2 system. Thus, the methylene protons seem to be less sensitive to the cage asymmetry caused by the angular methyl group. The *endo*-propionyl seems to assume a preferred conformation of type (**7**), in which the two methylene protons are held rigidly in such a way that they are differently affected by the cage asymmetry due to the angular methyl group and may give rise to an ABC_3 pattern.

The possibility of the existence of conformation (**6**) may be eliminated on the basis suggested by RIGGS *et al.* [1]. The larger shielding effect of the cage benzo ring on the methylene protons relative to that on the methyl protons of the *endo*-propionyl group is also in accordance with conformations (**5**) or (**7**). In these conformations the methylene protons point to the cage benzo ring, while the methyl protons are slightly away from this ring.

In order to eliminate the spectral complexity due to vicinal couplings, compounds (**4d**)—(**4g**) have been prepared. The 60 MHz spectrum of compound

Table I

NMR data for compounds **(4a—4g)** *in* $CDCl_3$ *at 44.5 °C*

No.	CH_2R	CH_2R'	R″	C12	C10	C9	Aromatic protons
4b	3.00 (1H, q) 1.10 (1.5H, t); J = 7.2Hz and 0.80 (2.5H, complex)	3.00 (1H, q) 1.10 (1.5H, t); J = 7.2Hz and 0.80 (2.5H, complex)	3.46 (1H, t)	3.46 (1H, t)	4.97 (1H, t)	4.97 (1H, t)	7.42 (8H, m)
4c	3.05 (1H, q) 1.15 (1.5H, t); J = 7.5Hz and 0.85 (2.5H, complex)	3.05 (1H, q) 1.15 (1.5H, t); J = 7.5Hz and 0.85 (2.5H, complex)	1.33 (3H, s)	3.93 (1H, d) J = 3.5Hz	4.60 (1H, s)	4.94 (1H, d) J = 3.5Hz	7.50 (8H, m)
4d	1.72 (3H, ds) 3 : 2; 96Hz	3.68 (2H, ds) 2 : 3; 122Hz	3.41 (1H, m)	3.41 (1H, m)	4.87 (1H, m)	4.87 (1H, m)	7.31 (8H, m)
4e	1.73 (3H, ds) 1 : 1; 95.5Hz	2.66 (1H, ABq) 4.67 (1H, s)	1.27 (3H, ds) $\Delta\nu$ = 1.5Hz	2.84 (1H, d) J = 3.5Hz	4.45 (1H, s)	4.78 (1H, d) J = 3.5Hz	7.42 (8H, m)
4f*	2.49 (3H, s)	2.10 (2H, s) 3.78 (3H, s)	3.43 (1H, m)	3.43 (1H, m)	4.87 (1H, m)	4.87 (1H, m)	7.15 (12H, m)
4f**	1.75 (3H, ds) 1 : 1.2; 92Hz	3.16 (2H, ds) 1.2 : 1; 124Hz 3.79 (3H, ds) 2.5Hz	3.43 (1H, dt) $\Delta\nu$ = 4.5Hz	3.43 (1H, dt) $\Delta\nu$ = 4.5Hz	4.92 (1H, m)	4.92 (1H, m)	7.20 (12H, m)
4g*	2.52 (3H, s)	2.15 (2H, ABq) 3.82 (3H, s)	1.32 (3H, s)	2.91 (1H, d) J = 3.5Hz	4.50 (1H, s)	4.80 (1H, d) J = 3.5Hz	7.17 (12H, m)
4g**	1.73 (3H, ds) 1 : 2; 92Hz	2.15 (1.36H, ABq) 4.19 (0.64H, s) 3.79 (3H, ds); 2Hz	1.28 (3H, ds) 3.5Hz	2.85 (1H, dd) J = 3.5Hz	4.49 (1H, ds) 2.5Hz	4.82 (1H, bt)	7.17 (12H, m)

* Spectral data of the freshly prepared solution

** Spectral data of the solution after standing for 6 hrs

In case of multiplicity due to slow rotations, the ratio of the intensity of the upfield signal to that of the downfield signal and the separation (in Hz) are indicated

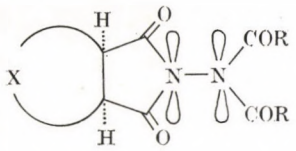

(1)

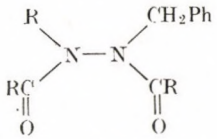

(2)

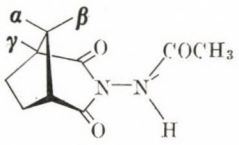

(3)

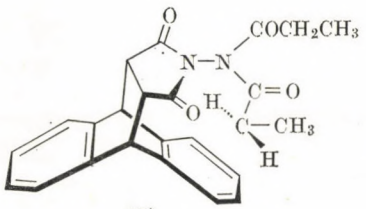

(5)

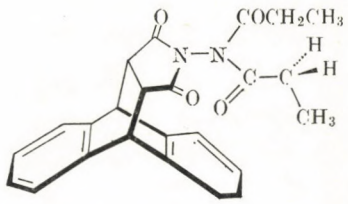

(6)

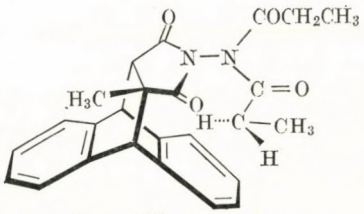

(7)

(**4d**) in $CDCl_3$ (Table I) shows conformational isomers about the N–N bond and two sharp singlets for the methylene protons corresponding to the two conformers. The 60 MHz spectrum of compound (**4e**) in $CDCl_3$ also reveals (Table I) two conformations about the N–N bond. But the methylene protons of the *exo*-$COCH_2Cl$ conformations appear as a sharp singlet, while those of the *endo*-$COCH_2Cl$ conformation appear as an AB pattern, the weak outer signals of which cannot be observed as the internal chemical shift of the two geminal

protons is very small. The 60 MHz spectra of freshly prepared solutions of compounds (**4f**) and (**4g**) in $CDCl_3$ (Table I) show that the *endo*-$COCH_2C_6H_4OCH_3$ (p) conformation about the N–N bond is preferred exclusively. The methylene protons of compound (**4f**) appear as a singlet while those of (**4g**) show an AB pattern. On standing, both conformations about the N–N bond were observed in the solutions of (**4f**) and (**4g**) (Table I).

Thus magnetic nonequivalence of the two methylene protons in the *endo*-(α-substituted) acetyl group and the absence of such nonequivalence in the *exo*-group may be considered as evidence for hindered rotation about the N–CO–CH_2 system. The hindrance to rotation about the –CO–CH_2 bond in these compounds is probably steric in origin.

Experimental

NMR spectra were recorded on a Varian A-60D NMR spectrometer and IR spectra were recorded on Perkin–Elmer 257 and 720 spectrophotometers. Chemical analyses, melting points and IR data are reported in Table II. All compounds were recrystallized from ethanol.

Table II

IR and physical data for compounds (**4b**)—(**4g**)

No.	M.p. (°C)	Analysis				IR ν_{max} (cm^{-1})
		Found		Calculated		
		C (%)	H (%)	C (%)	H (%)	
(4b)	259—61	71.41	5.58	71.63	5.51	1708 m, 1738 s, 1745 s, 1798 w
(4c)	237—39	71.89	5.75	72.10	5.81	1705 w, 1725 m, 1740 s, 1795 w
(4d)	231—33	64.52	4.08	64.63	4.16	1745 s, 1800 w, 1820 w
(4e)	191—93	65.46	4.38	65.32	4.50	1730 s, 1760 m, 1800 w
(4f)	202—04	72.16	4.89	72.49	5.03	1740 s, 1790 w
(4g)	188—90	72.92	5.14	72.86	5.30	1740 s, 1800 w
(10)	210—11	65.63	3.97	65.76	4.10	1690 m, 1730 s, 1795 w, 3175 m
(11)	259—61	66.43	4.35	66.23	4.47	1690 s, 1730 s, 1795 w, 3175 m
(12)	263—65	74.12	4.92	73.96	5.06	1665 s, 1730 s, 1795 w, 3180 m
(13)	266—88	74.18	5.18	74.34	5.35	1680 s, 1725 s, 1785 w, 3200 m

s = strong; m = medium; w = weak

Preparation of compounds (4b) and (4c)

Compound (**4b**) was prepared as follows: the adduct of anthracene and maleic anhydride [10] was treated with an equimolar amount of hydrazine hydrate in ethanol at room temperature to yield N-aminoimide (**8**) [1]. The latter was refluxed with propionyl chloride (more than 2 mol) and a few drops of pyridine for about 6 hrs. After removing the excess propionyl chloride, the solid obtained was washed with water and recrystallized.

Compound (**4c**) was prepared in a similar fashion from the N-aminoimide (**9**) [11] obtained from the adduct of anthracene and citraconic anhydride [12].

Preparation of compounds (4d), (4e), (4f) and (4g)

These compounds were prepared in two steps: N′-monoacyl derivatives **(10)**, **(11)**, **(12)** and **(13)** were obtained by the addition of the respective substituted acetyl chlorides (in dry benzene) dropwise to an equimolar amount of the corresponding N-aminoimides [**(8)** and **(9)**] in dry benzene under stirring. The reaction mixture was then refluxed for 1 hr. After removing the solvent, the products obtained were washed with water, recrystallized and characterized by their elemental analyses and IR spectra (Table II).

(10) = N′-monochloroacetyl of **(8)**
(11) = N′-monochloroacetyl of **(9)**
(12) = N′-p-methoxyphenylacetyl of **(8)**
(13) = N′-p-methoxyphenylacetyl of **(9)**

The monosubstituted derivatives [**(10)**, **(11)**, **(12)** and **(13)**] thus obtained were acetylated by heating with an excess of acetic anhydride on a water bath for about 2 hrs. After removing the excess of acetic anhydride, the products were recrystallized from ethanol.

*

The authors wish to thank Dr. J. N. SHOOLERY, NMR Applications Laboratory, Varian Associates, California, for providing 300 MHz NMR spectra of the two compounds. One of us (RMS) is grateful to the C.S.I.R. for the award of a Research Fellowship.

REFERENCES

[1] KORSCH, B. H., RIGGS, N. V.: Tetrahedron Lett., 5897 (1966)
[2] FOUCAUD, A., ROUDAUT, R., FAYAT, C.: Bull. Soc. Chim., 1915 (1972)
[3] VERMA, S. M., KOTESWARA RAO, C.: Tetrahedron, **28,** 5029 (1972)
[4] VERMA, S. M., SUBBA RAO, O.: Tetrahedron, **30,** 2371 (1972);
VERMA, S. M., KOTESWARA RAO, C.: Ind. J. Chem., **13,** 1278 (1975)
[5] VERMA, S. M., SINGH, R. M.: J. Org. Chem., **40,** 897 (1975)
[6] STEWART, W. E., SIDDAL III, T. H.: Chem. Rev., **70,** 517 (1970)
SPASSOV, S. L., DIMITROV, V. S., KANTSCHOVSKA, I.: Org. Magn. Resonance, **6,** 20 (1974)
[7] BISHOP, G. J., PRICE, B. J., SUTHERLAND, I. O.: Chem. Commun., 672 (1967)
[8] VERMA, S. M., PRASAD, R.: J. Org. Chem., **38,** 1004 (1973)
[9] EMSLEY, J. W., FEENEY, J., SUTCLIFFE, L. H.: High Resolution Nuclear Magnetic Resonance Spectroscopy, Vol. 1, pp. 351—356, Pergamon Press, 1965
[10] VOGEL, A. I.: A Text Book of Practical Organic Chemistry, p. 943. English Language Book Society and Longmans Green Co., Ltd., London 1968
[11] VERMA, S. M., SINHA, K. O. P.: Ind. J. Chem., **11,** 1138 (1973)
[12] BACHMANN, B. E., SCOTT, L. B.: J. Amer. Chem. Soc., **70,** 1458 (1948)

R. M. SINGH
C. KOTESWARA RAO
S. MOHAN VERMA
Department of Chemistry, Banaras Hindu University
Varanasi-221005, India.

Acta Chimica Academiae Scientiarum Hungaricae, Tomus 96 (2), pp. 113—126 (1978)

INHIBITION OF POSITRONIUM FORMATION BY SCAVENGER MOLECULES IN NONPOLAR LIQUIDS

B. LÉVAY* and Ole E. MOGENSEN

(Chemistry Department, Danish Atomic Energy Commission, Research Establishment Riso, DK-4000 Roskilde, Denmark)

Received December 6, 1976

o-Ps yields were determined in various liquid hydrocarbons, tetramethylsilane and mixtures thereof as a function of C_2H_5Br and CCl_4 concentration. These molecules are known to be good electron scavengers and positronium inhibitors as well. The spur reaction model of Ps formation predicts a correlation between the inhibition coefficient and the chemical rate constant of electrons with scavenger molecules. We found that the dependence of the inhibition coefficient on the work function (V_0) of eletrons in different liquids shows a very unusual behaviour, similar to that recently found for the chemical rate constants of quasifree electrons with the same scavenger molecules. The inhibition coefficient as a function of V_0 had a maximum for C_2H_5Br, while it increased monotonously with decreasing V_0 for CCl_4. The inhibition coefficient for C_2H_5Br in a 1 : 1 molar tetramethylsilane–*n*-tetradecane mixture was found to be greater than in both of the pure components. The clear correlation found between electron scavenging rate constants and positronium inhibition constitutes the severest test to date of the spur reaction model of positronium formation. The importance of the positron annihilation method from the point of view of radiation chemistry is also emphasized.

Introduction

For many years the excess electron in liquids (*e.g.* the hydrated electron [2]) has been an important subject of research in radiation chemistry. In particular the excess electron in nonpolar liquids is studied in much detail at present. It is probably less known that the properties of the two other light particles: the positron and the positronium (Ps) atom [3] in liquids are strongly correlated to those of the excess electron. We shall give an account of such correlation in this article.

When positrons, *i.e.* the antiparticles of electrons, are injected into a medium, they slow down mainly through ionization processes to nearly thermal energies, whereafter they annihilate into photons with the electrons of the medium [3]. Before this annihilation process, however, the positron can form — with a given probability (P) depending on the nature of the medium — a bound state with an electron, *i.e.* a so-called positronium (Ps) atom. Ps atoms are formed in two different states depending on whether the spins of the two

* Department of Physical Chemistry and Radiology, L. Eötvös University, Budapest, see [1]

particles are parallel (*ortho*-Ps or *o*-Ps) or antiparallel (*para*-Ps or *p*-Ps). In vacuum, *o*- and *p*-Ps have mean lifetimes of 1.4×10^{-7} and 1.25×10^{-10} sec, respectively. The lifetime of *o*-Ps is reduced to 0.5—5 nsec in condensed media. The theoretical formation probability of *o*-Ps is three times greater than that of *p*-Ps. Both the lifetime and the formation probability of *o*-Ps are strongly affected by the physical or chemical nature of its environment.

For many years, the behaviour of Ps in various molecular liquids and solids was investigated through measurements of the 2-γ angular correlation distributions and the positron lifetime spectra. In pure organic liquids the longest lifetime (τ_3) is normally ascribed to *o*-Ps pick-off annihilation with the outer electrons of the molecules. The rate of pick-off annihilation for the different pure liquids can be explained fairly well by the bubble model [4]. Chemical reactions of *o*-Ps atoms with solute molecules in liquids decrease the long lifetime. From the concentration dependence of this decrease, the chemical rate constants can be easily calculated and the results are now quite well interpreted.

However, the values of the Ps formation probabilities measured for different liquids, and the inhibition of Ps formation in them caused by different solutes, were very little understood until very recently [3] when one of the present authors (O.E.M.) proposed a new idea of Ps formation: the spur reaction model [5]. This model correlates the Ps-yields to the results of spur kinetics obtained in radiation chemistry. A spur formed due to the interaction of an ionizing particle with matter can be defined as a group of reactive intermediates which are so close together that there is a significant probability of their mutual reactions while they diffuse into the bulk of the medium. The positronium is assumed to be formed by a reaction between a positron and an electron in the positron spur. The positron spur is the group of reactive species (*e.g.* the positron, excess electrons, positive ions, etc.), which is created around the positron when it loses the last of its kinetic energy. Ps formation competes with the recombination of the electrons and their parent positive ions ('geminate recombination'), and also with the diffusion of electrons out of the spur. Reactions of the electrons or the positrons in the spur with the solvent molecules, or with scavengers, will also decrease the probability of Ps formation. Solvation of the electrons or the positrons in the spur may strongly influence the Ps formation on account of the increased dielectric shielding of the Coulomb forces between the particles. Chemical reactions between scavengers and the short-lived species in the spur, which would otherwise react with the electrons or the positron, may also influence Ps formation. The spur reaction model of Ps formation has been tested on several previous occasions [6] and proved to be very fruitful and predictive for interpreting Ps yield data. In particular, a general discussion of the model is found in references [5] and [6b]. Ps inhibition, explained as the result of electron scavenging in the positron spur, is discussed in detail in reference [6c].

Recently ALLEN *et al.* [7] measured the chemical reaction rates of quasi-free electrons in nonpolar liquids. They found that the chemical reaction rate of electrons with different scavenger molecules was strongly influenced by solvents. They correlated their results with the quantity V_0, the work function of the electrons in their mobile state in the liquids. For C_2H_5Br, the rate constants exhibited a pronounced maximum for a characteristic value of V_0, reminiscent of the resonant energy maximum in the dissociative attachment cross-sections for electron reaction shown by the same molecules in the gas phase. However, for CCl_4, the reaction rate constants increased monotonously with decreasing V_0. This kind of dependence of electron rate constants on V_0 was recently theoretically interpreted by HENGLEIN [8] and by SCHILLER and NYIKOS [9].

The purpose of our work was to measure the inhibition of Ps formation by C_2H_5Br and CCl_4 in nonpolar liquids and to correlate the strength of the Ps inhibition to the electron rate constants measured by ALLEN *et al.* [7]. Because of the spur model of Ps formation predicts strong correlation (*i.e.*, parallel trend) between Ps inhibition and electron rate constants, it is expected that the strength of the Ps inhibition *versus* V_0 will show a maximum at the same V_0-value as the electron rate constant in the C_2H_5Br case, while a monotonously increasing inhibition strength for decreasing V_0 is expected for CCl_4. The expected behaviour of the Ps inhibition was found. The Ps yields were correlated also to the steady state electron scavenging work of SCHULER *et al.* [10]. It seems to be quite difficult to explain these results in terms of the older Ps formation model [3, 11], the Ore model modified with hot Ps reactions.

Here we present positronium inhibition measurements for the following systems: C_2H_5Br in *n*-tetradecane (*n*-C_{14}), *n*-hexane (*n*-C_6), 2,2,4-trimethylpentane (iso-octane, iso-C_8), 2,2-dimethylpropane (neo-C_5) and tetramethylsilane (TMS); CCl_4 in *n*-C_{14}, iso-C_8 and TMS. In addition of these systems the inhibition function for C_2H_5Br were also determined in *n*-C_{14}-TMS (X_{TMS}= 0.49) and *n*-C_6-neo-C_5 ($X_{n-C_6} = 0.25$) mixtures (X represents the molar fraction of the component in the subscript).

Experimental

Lifetime measurements. About 40 μCi ^{22}NaCl deposited between two Kapton (Du Pont) polyimide foils of 1 mg/cm^2 constituted the positron sources. The positron lifetimes were measured as usual by determining the time interval between the detection of a 1.28 MeV photon, emitted simultaneously with the emission of a positron (start signal) and the detection of an 0.511 MeV annihilation photon (stop signal) [3]. A time-to-pulse-height converter generates output pulses with amplitudes proportional to the time interval between the start and stop signals. Then the pulse height distribution of output signals, *i.e.* the lifetime distribution of positrons, can directly be recorded by a multichannel analyzer. The time resolution function of our conventional lifetime spectrometer, determined by measuring the spectrum of a ^{60}Co source, could well be described as a sum of three Gaussian curves with a FWHM = 390 psec for the total curve. The lifetime spectra were analyzed by the Positronfit-Extended [12] computer program for three lifetimes [13] and intensities with 8% source correction. Details of the application of this program are discussed in reference [6c].

Materials. The chemicals were of analytical grade from Merck and were used without further purification. All the liquid samples were thoroughly degassed by the freeze-thaw method and afterwards distilled in vacuum into an ampoule containing the positron source. During the recording of the lifetime spectra the source and the sample were kept in this air-tight ampoule. The necessary amounts of neopentane and tetramethylsilane solvents and of solutes added to a given volume of solvent were determined by PV technique in the same apparatus as used for degassing the samples. All the measurements were performed at 20 °C.

Results

The analyses of the lifetime spectra gave the following results. The shortest lifetimes (τ_1) were found around 150 psec, the medium lifetimes (τ_2) around 500 psec, while the longest lifetimes (τ_3) for the pure solvents and mixtures were: n-C_{14} 3.35 nsec, n-C_6 3.94 nsec, iso-C_8 4.11 nsec, neo-C_5 5.17 nsec, TMS 4.77 nsec, TMS-n-C_{14} 3.75 nsec, n-C_6-neo-C_5 4.61 nsec and C_2H_5Br 3.23 nsec. By the lifetime results for their solutions, C_2H_5Br and CCl_4 proved to be practically pure inhibitors; hence, it was unnecessary to make any corrections to the intensity data due to quenching contributions. The relative Ps yield $P(c)$ is therefore

$$P(c) = I_3(c)/I_3(0) \tag{1}$$

where $I_3(c)$ is the intensity of the longest-lived component extracted from the lifetime spectrum at an inhibitor concentration c. The $I_3(0)$ values, *i.e.*, the o-Ps yields measured in the pure solvents or their mixtures where: n-C_{14} 37.5%, n-C_6 41.6%, iso-C_8 44.2%, neo-C_5 52.7%, TMS 55.5%, TMS-n-C_{14} 45.6% and n-C_6-neo-C_5 45.3% (C_2H_5Br 5.2%) (uncertainties $\simeq \pm 0.7$ absolute %) [13]. The values of $P(c)$ calculated from the experimentally found $I_3(c)$ values by Eq. 1 are presented in Fig. 1 with the inhibitor concentration (in mole/dm^3) on a logarithmic scale. Data found for C_2H_5Br in n-C_6-neo-C_5 mixtures followed a curve almost identical with that for n-C_6; hence, they were omitted for the sake of clarity.

The relative Ps yields from right to left correspond to increasing inhibition strengths, because it is obvious that stronger inhibitors decrease the Ps yield at lower concentrations. Even if the curves are compared in only this simple graphic way, the clear qualitative agreement with electron rate constant data [7] is immediately manifested.

Parameter fitting of the relative Ps yields

A discussion of the possibilities of obtaining a theoretical expression for the relative Ps yield $P(c)$ as a function of electron scavenger concentration in the framework of the spur reaction model of Ps formation has been published elsewhere [6c]. Here it was concluded that an application of a detailed spur

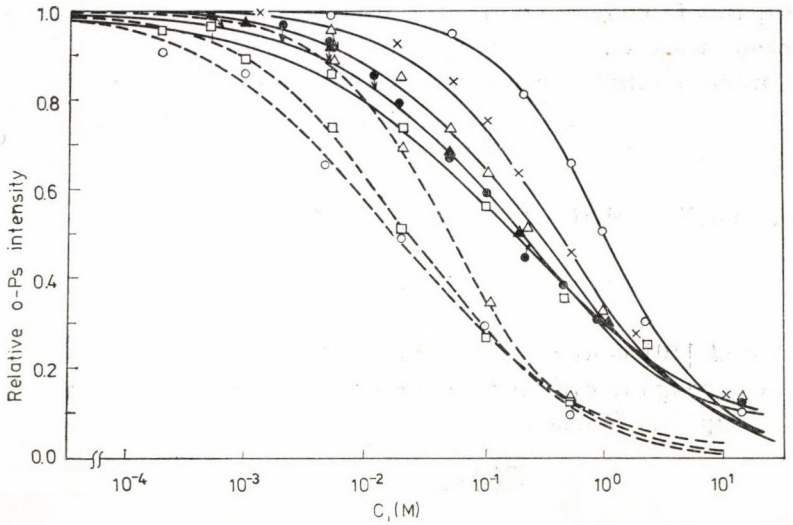

Fig. 1. Relative *p*-Ps intensities as a function of inhibitor concentration in various solvents. Symbols: △ *n*-C_{14}, ● *n*-C_6, □ iso-C_8, × neo-C_5, ○ TMS, ▲ TMS—*n*-C_{14} mixture. Solid curves for C_2H_5Br and dashed ones for CCl_4 are fit to Eq. 7 with σ and α values in Table I. (The solid curve for the TMS—*n*-C_{14} mixture is omitted)

diffusion theory to the positron spur problem is not promising at present. However, the Ps yield may be correlated to the electron spur results by use of the reasonable assumption that the relative electron—positron 'recombination' in the positron spur (*i.e.*, the Ps yield) is strongly correlated to the relative electron—ion recombination in the electron spur. The yield of a given product $G(p)$ of an electron reaction with a scavenger is normally described by

$$G(p) = G_{fi} + G_{gi}F(c)\,. \tag{2}$$

Here G_{fi} denotes the yield of 'free ions', while G_{gi} represents the yield of 'geminate ion pairs'. $F(c)$ is the scavenging function [10]. We may assume that

$$P(c) = (G_{fi} + G_{gi} - G(p))/G_{gi} = 1 - F(c)\,. \tag{3}$$

Thus the meaning of Eq. 3 is that the probability of Ps formation is proportional to the fraction of unscavenged 'geminate electrons'. $1 - F(c)$, *i.e.*, formally our $P(c)$, plays an important role in SCHULER's phenomenological scavenging model specifying the distribution function of the ion-pair lifetimes [10b].

With regard to the explicit analytical form of $F(c)$ and of the corresponding $P(c)$, three formulas have mainly been used in radiation chemistry. For very dilute solutions, several authors [14, 15] have theoretically derived the following expression:

$$F(c) = Kc^{1/2}\,. \tag{4}$$

However, this formula is totally inapplicable in our case, since we use high solute concentrations. Another scavenging function that can be theoretically derived using a simple, competitive kinetic model [10a] is:

$$F(c) = \frac{\sigma c}{1 + \sigma c} . \tag{5}$$

The corresponding relative Ps yield is:

$$P(c) = \frac{1}{1 + \sigma c} \tag{5a}$$

SCHULER *et al.* [10], however, found that Eq. 5 did not describe their scavenging results well enough in cyclohexane and *n*-hexane solvents. They proposed the use of an empirical function

$$F(c) = \frac{(\sigma c)^{1/2}}{1 + (\sigma c)^{1/2}} . \tag{6}$$

The relative Ps yields corresponding to Eq. 6 would be:

$$P(c) = \frac{1}{1 + (\sigma c)^{1/2}} . \tag{6a}$$

The analyses of our Ps yield results showed that fairly good fits could be obtained by use of (5a) in some solvents and (6a) in other solvents. To improve the goodness of the fit for all solvents we therefore fitted the results with a slightly modified empirical expression using a second adjustable parameter α in the exponent:

$$P(c) = \frac{1}{1 + (\sigma c)^{\alpha}} \tag{7}$$

which would correspond to the following scavenging function:

$$F(c) = \frac{(\sigma c)^{\alpha}}{1 + (\sigma c)^{\alpha}} . \tag{7a}$$

It is important to realize that we cannot expect a detailed quantitative correlation between the measured properties of the positron and electron spurs [5, 6]. The positron spur, being part of a 'high linear-energy-transfer' track, is very probably more dense than the normally studied electron spurs. The distribution of electron–positron distances at thermalization probably also differs from the distribution of electron–ion distances. Several other properties of the two spurs (*e.g.* yields of specific ions and radicals) may be different too. The experimentally determined Ps yield might also be influenced by the reaction of Ps with the reactive species in the spur. Another point of interest is that detailed tests of (5) or (6) seem not to have been performed in some of the

used solvents (see below). Hence, the fact that it was necessary to use a two-parameter formula (7) instead of the one-parameter formulas (5a) or (6a) to get good fits, is not surprising at all.

The fitting procedure with two adjustable parameters was carried out on a programmable table calculator (EMG 666) minimizing the RMS deviation between the measured and calculated points. The results of the fitting procedure are presented in Table I. The V_0 values for pure solvents are HOLROYD's [16] latest data for 20 °C, while for the mixtures they are calculated values assuming a linear relationship between V_0 and the molar fraction, as it was found by HOLROYD and TAUCHERT [17] to be valid for the TMS—n-C_6 and the neo-C_5—n-C_6 mixtures. The last column of Table I contains the goodness of the fit expressed as the RMS deviation between the measured and calculated points. The data in parentheses represent the results when only the upper part of the total inhibition curve ($P(c) > 0.6$) was involved in the fitting procedure. In the cases of C_2H_5Br in TMS and CCl_4 in all the three solvents investigated, the two fitting procedures gave practically identical results.

Table I

Summary of results obtained by parameter fitting of relative o-Ps yields measured in various liquids and liquid mixtures

Solvent	V_0 (eV)	Inhibitor	σ (M^{-1})	α	$\sqrt{\Delta^2}$
n-tetradecane (n-C_{14})	0.21	C_2H_5Br	3.9±0.4 (5.2)	0.61±0.01 (0.78)	0.032 (0.012)
		CCl_4	20.5±1	0.88±0.01	0.005
n-hexane (n-C_6)	0.00	C_2H_5Br	5.3±0.5 (8.2)	0.57±0.01 (0.74)	0.025 (0.005)
iso-octane (iso-C_8)	−0.26	C_2H_5Br	6.0±0.6 (10.3)	0.48±0.01 (0.62)	0.018 (0.005)
		CCl_4	46.0±1	0.67±0.01	0.006
neopentane (neo-C_5)	−0.35	C_2H_5Br	2.4±0.2 (2.8)	0.73±0.01 (0.83)	0.014 (0.004)
tetramethyl-silane (TMS)	−0.51	C_2H_5Br	1.04±0.1	0.94±0.01	0.011
		CCl_4	59.0±1	0.58±0.01	0.021
TMS + n-C_{14} ($X_{TMS} = 0.49$)	−0.14*	C_2H_5Br	4.8±0.5 (7.8)	0.56±0.01 (0.75)	0.021 (0.002)
n-C_6 + neo-C_5 ($X_{n-C_6} = 0.25$)	−0.26*	C_2H_5Br	4.3±0.5 (5.5)	0.55±0.01 (0.63)	0.014 (0.009)

* Calculated values from the V_0-values of the pure solvent components, assuming a linear relationship between V_0 and the molar fraction X

In the case of C_2H_5Br, one of the reasons for the difference between the two fitting procedures might be the high concentration of C_2H_5Br. At high concentrations the 'solute' molecules themselves contribute considerably to the primary processes of radiolysis. The spur size and rate constants of the electrons and the positron are probably also influenced by the solute molecules in high concentration, in particular in the high electron mobility (large spur) solvents: neo-C_5 and TMS. Although the RMS deviations for the upper-part fittings are better, those for the total curves are also within the accuracy of the method. Because of this fact, and since the qualitative features of the results are almost similar in both cases, the results are presented throughout this paper as they were evaluated from the total inhibition curves. The upper-part fittings might be useful in a detailed comparison with electron-spur scavenging results, which are normally only obtained at fairly low scavenger concentration.

In Fig. 1 the solid curves for C_2H_5Br and the dashed curves for CCl_4 are drawn using Eq. 7, with σ and α values calculated from the total curve fitting (Table I). The calculated curve for C_2H_5Br in the TMS—n-C_{14} mixture, which is practically identical with the n-C_6 curve, is omitted.

Discussion

General remarks. Although the correlation between the results of the present Ps inhibition measurements and those of the electron rate constant determinations [7] is clear by simply looking at Fig. 1, the comparison is more convincing in a figure presenting both sets of data. Figure 2 shows positronium inhibition constants (σ, left-hand scale) together with ALLEN, GANGWER and HOLROYD's electron rate constants [7] (k, right-hand scale) as a function of V_0. The solid and dashed lines are graphic fits for C_2H_5Br and CCl_4 data, respectively. In both cases the curves for C_2H_5Br exhibit a maximum for the same solvent (*i.e.*, for the same V_0), and both curves are very much steeper from the left to the maximum than from the right to the maximum. Very convincing is also the fact that the points for the solvent mixtures, the V_0 values of which were adjusted to be close to the maximum, are situated reasonably well on a common curve with the pure solvents. From this point of view, one must also consider the inaccuracy in calculating the V_0 values for the mixtures. The CCl_4 curves, on the other hand, increase with decreasing V_0 in both cases.

The prediction of the spur reaction model of Ps formation proved to be valid for this very unusual case, and this seems to be the severest test of this model to date. As discussed above the reaction rate of the spur electrons is only one factor affecting the process of Ps formation, and that there are several

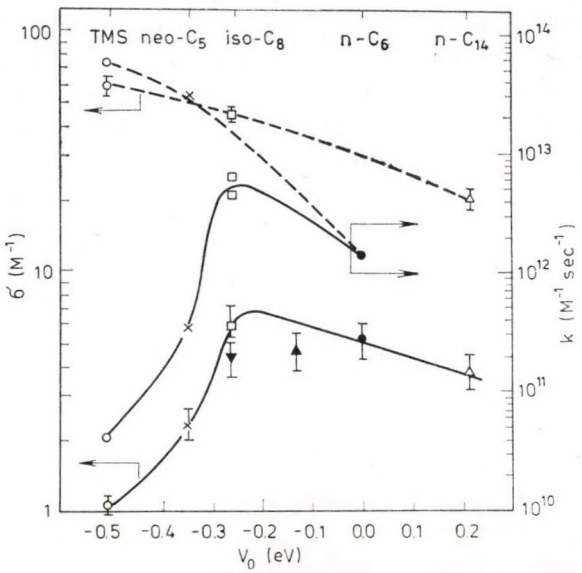

Fig. 2. Ps inhibition coefficients (σ, left-hand scale) and electron rate constants (k, right-hand scale) for reactions with C_2H_5Br (solid curves) and CCl_4 (dashed curves) as a function of V_0. Symbols: ▼ n-C_6—neo-C_5 mixture, others as in Fig. 1

others which may greatly modify the very complex and complicated situation in the spur. The good qualitative correlation between these two quantities (*i.e.* σ and k), however, demonstrates the important role of electron reaction rates in Ps formation, at least in these nonpolar liquids of high electron mobility.

With respect to the other models of Ps formation, namely the ORE model [11] and its modified version [18] or the 'hot-Ps' reaction model [19], these do not seem to be able to explain such unusual changes for the probability of Ps formation without the use of special assumptions and practically unavailable and unverifiable data for any system. The main problem is that all these models take into account positrons and Ps atoms of fairly large energies only, while it seems that very small changes in the work function of *thermalized* electrons are responsible for the great changes in electron rate constants or Ps inhibition properties. Although the spur reaction model itself is unable to make *a priori* predictions of Ps formation for every special case, its great advantage lies in the fact that, for explanations and predictions, it can use general principles and experiences originating from radiation chemistry.

Comparison with steady-state scavenging results. The basic idea of the spur reaction model of Ps formation is that Ps atoms are formed as a result of the scavenging of the spur electrons by the positrons. Thus any processes in

which spur electrons are involved compete with Ps formation [20] and a strong correlation must exist between scavenging and Ps inhibition experiments. This assumption gave the theoretical basis for using the scavenging function to fit the Ps inhibition functions and evaluate the inhibition coefficients (σ). Thus, in principle, the Ps inhibition coefficient has the same meaning as the relative scavenging constant in SCHULER's phenomenological model for scavenging in hydrocarbons [10] and the numerical values of these two quantities must be similar or at least comparable. Unfortunately, however, we have hardly any data with which to make this comparison. RZAD and BANSAL [21] measured the relative scavenging constant for C_2H_5Br in iso-octane and their 5 M^{-1} value is very close to ours: $\sigma = 6 \pm 0.6\ M^{-1}$. Although INFELTA and SCHULER's [22] value for C_2H_5Br in cyclohexane (7.8 M^{-1}) is not directly comparable since we have no data for this solvent, it seems to be quite reasonable because the V_0 of cyclohexane is close to that of iso-octane. The agreement of these results is promising, but the data are insufficient to prove the mutual identity of the two constants.

Correlation between σ and k. Through the phenomenological scavenging model, the ratio σ/k for a given solvent should be constant and equal to the mean lifetime of the geminate ion—electron pairs [10a]. ALLEN *et al.* [7] tested this correlation for rate constants and relative scavenging constants measured in cyclohexane and found it to be valid with the exception of CH_3I. Our Ps inhibition measurements, however, do not seem to support this prediction. Although the ratios σ/k for C_2H_5Br and CCl_4 in iso-octane (1.2×10^{-12} and 3.0×10^{-12} sec, respectively) are in quite reasonable agreement, the difference is more than one order of magnitude for TMS (26×10^{-12} and 1.1×10^{-12} sec), or other solvents. Thus the general validity of this theoretically predicted quantitative relation between σ and k does not seem to be proved as yet and the question requires further study.

We also tried to correlate our σ values measured for a given scavenger in different solvents to the k values for the same scavenger. In such a comparison a linear relationship between σ and k could not be expected. Nevertheless, we obtained a reasonable linear correlation for log k *vs.* σ:

$$\log k = a\sigma + b\,, \tag{8}$$

where $a = 0.45\ M$ and $0.065\ M$ for C_2H_5Br and CCl_4, respectively, and $b = 10$ for both scavengers from a graphic fit. Because of the very limited number of our data, this correlation is only tentative, and could be an exceptional case.

Correlation between α and V_0. We succeeded in fitting our Ps inhibition curves by making use of SCHULER's [10] empirical scavenging function if

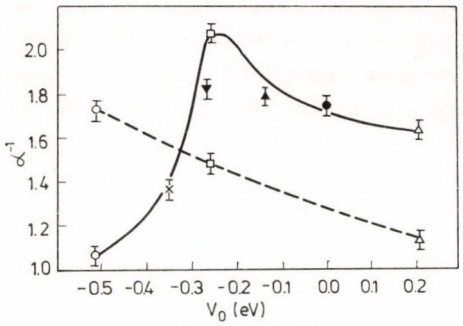

Fig. 3. α^{-1} as a function of V_0. Solid curve for C_2H_5Br and dashed curve for CCl_4. Symbols as in Fig. 2

only we used a new fitting parameter (α) instead of the constant value (0.5) in the exponent of concentration. SCHULER's scavenging function was tested for a great number of scavengers in cyclohexane [10], and the same expression was found to be valid for fitting scavenging data measured in iso-octane by RZAD and BANSAL [21]. The V_0 values for these solvents, however, are very close to each other and, as shown by ALLEN *et al.* [7] in this range of V_0 the reaction rates for quasifree electrons are also very close to each other. Thus a common behaviour for scavengers investigated in solvents of this narrow range of V_0 is not surprising. As a result of our fitting procedure, we also obtained a value of nearly 0.5 for our α in iso-octane. However, in other solvents of very different V_0, α has varied between 0.5 and 1. Surprisingly this α, or more exactly α^{-1}, could be correlated with V_0 in a way qualitatively similar to that found for the rate constants and Ps inhibition coefficients. As can be seen in Fig. 3, α^{-1} as a function of V_0 for C_2H_5Br exhibits a maximum for the same V_0 as was found for k or α, while for CCl_4 the α^{-1} *vs.* V_0 curve increase monotonously with decreasing V_0, again in a way similar to that found for k and σ. This correlation expresses the fact that our second fitting parameter (α) is strongly correlated to the reaction rate constant of electrons.

We should like to point out that in spite of the limited number of data, this correlation seems pronounced and emphasizes the decisive role of V_0 in the mechanism and kinetics of electron scavenging processes. New steady-state scavenging measurements at higher concentrations of C_2H_5Br and CCl_4 in neopentane, TMS, or in other solvents of low V_0, could test these, at present only tentative, correlations, and would be of great help in a more detailed interpretation of our results. The very few scavenging experiments carried out so far on neopentane [23] indicate great differences between the scavengers in this solvent and those in cyclohexane. However, these measurements are not directly comparable to ours, either because different scavengers were used and only

scavenging of the free ions was investigated at very low concentrations [23a], or because the high concentration scavenging results were treated and interpreted on a different theoretical basis [23b].

Correlation between α and σ. Because both σ and α^{-1} showed qualitatively similar dependence on V_0, it seemed obvious to look for possible interrelation. This search resulted in a simple linear relationship:

$$\alpha^{-1} = a'\sigma + b'. \tag{9}$$

where $a' = 0.21\ M$ and $0.015\ M$ for C_2H_5Br and CCl_4, respectively, and $b' = 0.81$ for both from a graphic fit (Fig 4). From Eqs (8) and (9) the interrelation between k and α can be easily calculated too. The advantage of a relation such as Eq. (9), if it proved to be valid also for other scavengers, would be the possibility of extracting a solvent-independent quantity for characterizing the 'scavenging or inhibition strength' of the scavengers. For example, $1/a' = 4.8$ and $67\ M^{-1}$ for C_2H_5Br and CCl_4, respectively, could express that the latter is a stronger scavenger or Ps inhibitor than the former.

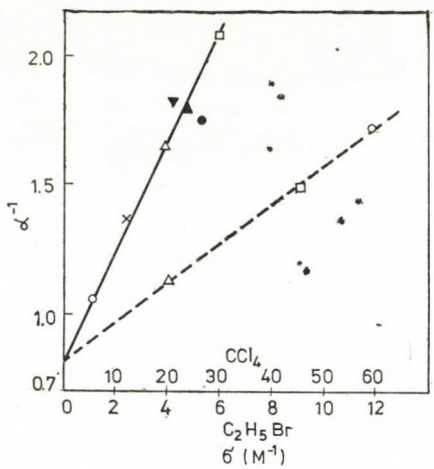

Fig. 4. Correlation between the two fitting parameters in Eq. 7. α^{-1} *versus* σ. Symbols as in Fig. 2

Conclusion

For the two good Ps inhibitors or electron scavengers studied by us (C_2H_5Br and CCl_4) the inhibition coefficients in nonpolar liquids can be correlated with V_0, the energy level of the mobile conduction electrons in various solvents. This correlation is similar to that found between V_0 and the electron reaction rate constants for the same scavengers. These Ps inhibition measure-

ments thus seem to be the severest test to date of the spur reaction model, which predicts a strong correlation between the formation probability of Ps and the electron scavenging rates in the positron spur. The analysis of the Ps inhibition curves resulted in the use of a new empirical fitting parameter instead of the constant used so far in the exponent of concentration. This new parameter can also be correlated with the work function (V_0) or with the scavenging rate constant of the quasifree electrons in nonpolar liquids. These and the other special correlations discussed in this paper are, however, at present only tentative, since the limited number of data are insufficient to prove their general validity. In order to test them, and to improve our understanding of the nature of matter, more experimental efforts are needed especially for extending the steady-state scavenging measurements to liquids of low V_0. For this purpose, Ps inhibition measurements can provide useful and important information both for radiation chemistry and for Ps chemistry.

*

The authors are grateful to P. JANSEN for stimulating discussions, and to R. A. HOLROYD for furnishing unpublished electron work function data. They are also much indebted to N. I. PEDERSEN for valuable technical assistance.

REFERENCES AND NOTES

[1] Visiting scientist from the Department of Physical Chemistry and Radiology, L. Eötvös University of Budapest, Hungary
[2] HART, E. J., ANBAR, M.: The Hydrated Electron. Wiley, New York, 1970
[3] (a) GREEN, J. H., LEE, J.: Positronium Chemistry. Academic Press, New York, 1964; (b) GOLDANSKII, V. I.: Atomic Energy Review, **6,** 3 (1968); (c) GOLDANSKII, V. I., FIRSOV, V. G.: Annual Rev. Phys. Chem. **22,** 209 (1971); (d) Positron Annihilation. A. T. STEWART and ROELLIG, L. (Eds). Academic Press, New York, 1967; (e) ACHE, H. J.: Angew. Chem., **84,** 234 (1972); (f) WEST, R. N.: Adv. Phys., **22,** 263 (1973); (g) MERRIGAN, J. A., GREEN, J. H., TAO, S. J.: in Physical Methods of Chemistry. A. Weissberger and B. W. Rositter (Eds). Wiley, New York, 1972, Vol. 1, Part III. D, p. 501
[4] (a) FERREL, R. A.: Phys. Rev., **108,** 167 (1957); (b) ROELLIG, L. O., KELLY, T. M.: Phys. Rev. Lett., **18,** 387 (1967); (c) BUCHIKHIN, A. P., GOLDANSKII, V. I., TATUR, A. O., SHANTAROVICH, V. P.: Zh. Eksp. Teor. Fiz., **60,** 1136 (1971) [Sov. Phys. — JETP, **33,** 615 (1971)]; (d) BUCHIKHIN, A. P., GOLDANSKII, V. I., SHANTAROVICH, V. P.: Pisma Zh. Eksp. Teor. Fiz., **13,** 624 (1971) [JETP Lett., **13,** 444 (1971)]; (e) TAO, S. J.: J. Chem. Phys., **56,** 5499 (1972); (f) LÉVAY, B., VÉRTES, A.: Radiochim. Radioanal. Lett., **14,** 227 (1973); (g) LÉVAY, B., VÉRTES, A., HAUTOJÄRVI, P.: J. Phys. Chem., **77,** 2229 (1973); (h) LÉVAY, B., VÉRTES, A.: J. Phys. Chem., **78,** 2526 (1974); (i) LÉVAY, B., VÉRTES, A.: J. Phys. Chem., **80,** 37 (1976)
[5] MOGENSEN, O. E.: J. Chem., Phys., **60,** 998 (1974)
[6] (a) JANSEN, P., ELDRUP, M., MOGENSEN, O. E., PAGSBERG, P.: Chem. Phys., **6,** 265 (1974); (b) MOGENSEN, O. E.: Appl. Phys., **6,** 315 (1975); (c) ELDRUP, M., SHANTAROVICH, V. P., MOGENSEN, O. E.: Chem. Phys., **11,** 129 (1975); (d) JANSEN, P., ELDRUP, M., SKYTTE, JENSEN, B., MOGENSEN, O. E.: Chem. Phys., **10,** 303 (1975)
[7] ALLEN, A. O., GANGWER, T. E., HOLROYD, R. A.: J. Phys. Chem., **79,** 25 (1975)
[8] HENGLEIN, A.: Ber. Bunsenges. physik. Chem., **79,** 129 (1975)
[9] SCHILLER, R., NYIKOS, L.: KFKI—75—74 (1975)
[10] (a) WARMAN, J. M., ASMUS, K.-D., SCHULER, R. H.: Advan. Chem. Ser., No. **82,** 25 (1968); (b) RZAD, S. J., INFELTA, P. P., WARMAN, J. M., SCHULER, R. H.: J. Chem. Phys., **52,** 3971 (1970); (c) SCHULER, R. H., INFELTA, P. D.: J. Phys. Chem., **76,** 3812 (1972)

[11] ORE, A.: Univ. i Bergen Årbok, Naturvitenskabelig, Rekke, Nr. **9** (1949)
[12] KIRKEGAARD, P., ELDRUP, M.: Computer Phys. Commun. **3,** 240 (1972), ibid., **7,** 401 (1974)
[13] The I_3-values correlate to several radiation chemistry quantities (*e.g.* the mobility μ, the "spur size constant" b, and the work function V_0). For example I_3 increases monotonously with increasing μ as discussed in references [5] and [6c]
[14] (a) HUMMEL, A.: J. Chem. Phys., **48,** 3268 (1968); (b) MOZUMDER, A.: J. Chem. Phys., **55,** 3026 (1971); (c) MAGEE, J. L., TAYLOR, A. B.: J. Chem. Phys., **56,** 3061 (1972)
[15] HUMMEL, A.: Adv. Radiation Chem. **4,** 1 (1974)
[16] HOLROYD, R. A.: (private communication)
[17] HOLROYD, R. A., TAUCHER, W.: J. Chem. Phys., **60,** 3715 (1974)
[18] TAO, S. J., GREEN, R. H.: J. Chem. Soc. A, 408 (1968)
[19] (a) BARTAL, L. J., NICHOLAS, J. B., ACHE, H. J.: J. Phys. Chem., **76,** 1124 (1972); (b) BARTAL, L. J., ACHE, H. J.: Radiochimica Acta, **17,** 205 (1972)
[20] On the other hand, reactions of solvated positrons (e_s^+) can also compete with Ps formation. Thus, for instance, the reaction of e_s^+ with Br^- or Cl^- ions, which are products of the reaction of electrons with scavenger molecules (C_2H_5Br and CCl_4), will probably result in the formation of e^+Br^- or e^+Cl^- bound states, as was recently pointed out by MOGENSEN and SHANTAROVICH [Chem. Phys., **6,** 100 (1974)].
The rate constant of the $e^+ + Cl^-$ reaction in water was found to be $2.5 \times 10^{10}\, M^{-1}\,\mathrm{sec}^{-1}$, but rate constants for nonpolar liquids are not known.
[21] RZAD, S. J., BANSAL, K. M.: J. Phys. Chem., **76,** 2374 (1972)
[22] INFELTA, P. P., SCHULER, R. H.: J. Phys. Chem., **76,** 987 (1972)
[23] (a) MORI, K., ITO, K., HATANO, Y.: J. Phys. Chem., **79,** 2093 (1975); (b) HORACEK, K., FREEMAN, G. R.: J. Chem. Phys., **53,** 4486 (1970)

Béla LÉVAY, H-1088 Budapest, Puskin u. 11—13.
Ole E. MOGENSEN, DK-4000 Roskilde, Denmark.

Acta Chimica Academiae Scientiarum Hungaricae, Tomus 96 (2), pp. 127–139 (1977)

SPONTANEOUS PROCESSES ON METAL SURFACE INDUCED BY ITS OWN METAL IONS, I

L. KISS and J. FARKAS

(Department of Physical Chemistry and Radiology, L. Eötvös University, Budapest)

Received December 24, 1976

The kinetics of the processes spontaneously proceeding in the $M–M^{z_1+}–M^{z_2+}$ system by the action of the own ions has been studied. The dependence of the rates and of the steady-state potential established at metal M on the concentration of M^{z_2+} and M^{z_1+} and on the hydrodynamic conditions of the electrolyte solution has been determined for a few characteristic cases.

The proceeding of spontaneous processes at the surface of a metal by the action of its own metal ions is to be expected, when the solution in contact with the metal contains ions with various oxidation number of the metal, and the concentration ratio of these ions is not the equilibrium one. In this case the system approaches the equilibrium while the following coupled electrode processes at the electrode, presuming a two-step process:

$$1. \quad M \underset{k_{k_1}}{\overset{k_{a_1}}{\rightleftharpoons}} M^{z_1+} + z_1 e$$

$$2. \quad M^{z_1+} \underset{k_{k_2}}{\overset{k_{a_2}}{\rightleftharpoons}} M^{z_2+} + n_2 e, \qquad \text{(I)}$$

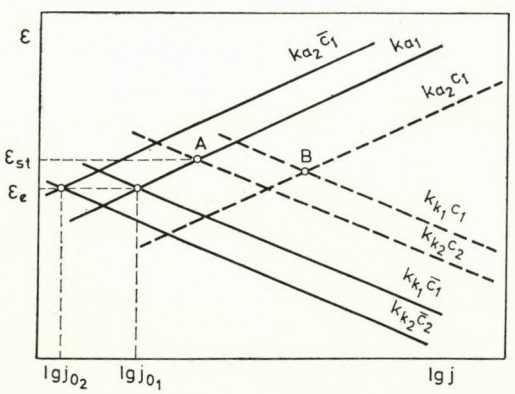

Fig. 1. Schematic polarization curves of the four part-processes of the electrode process (I); j_{01} and j_{02} are the exchange currents of steps 1 and 2 of process (I), ε_0 is the equilibrium potential

where k_{ai} and k_{ki} ($i = 1, 2$) are the rate constants of the respective reaction steps, depending on the electrode potential.

Figure 1 shows the schematic partial polarization curves of the four part-processes involved in process (I). Solid curves represent the case, when the concentration of M^{z_1+} and M^{z_2+} corresponds to equilibrium values ($\bar{c}_1$ and $\bar{c}_2$). When the concentration of the ion of charge z_2 is increased as compared to the equilibrium value ($c_2 \gg \bar{c}_2$), the straight line $k_{k_2}c_2$ shifts towards higher current density values (line $k_{k_2}c_2$). As can be seen, in this case the value of k_{a_1} or $k_{k_2}c_1$ at whatever potential is higher than that of the other partial rates. The same is true for the intersection of k_{a_2} and $k_{k_1}c_2$ (point A), when no current passes through the electrode from external current source, and the steady-state potential ε_{st} is established at the electrode. In the spontaneous process proceeding in this case, step 1 of process (I) will proceed mainly in the direction of the upper, while step 2 in the direction of the lower arrow. Thus, metal M is dissolved, and M^{z_2+} is reduced to M^{z_1+}.

If the concentration of the ion with charge z_1 is substantially increased as compared to the equilibrium value ($c_1 \gg \bar{c}_1$), then lines $k_{a_2}\bar{c}_1$ and $k_{k_1}\bar{c}_1$ symmetrically shift toward higher current densities (curves $k_{a_2}c_1$ and $k_{k_1}c_1$). Now the value of $k_{a_2}c_1$ or $k_{k_1}c_1$ will be higher at any potential than the other partial rates. The same holds true for the intersection of the lines $k_{a_2}c_1$ and $k_{k_1}c_1$ (point B). Now in the process proceeding spontaneously, step 1 of process (I) will proceed mainly in the direction of the lower, while step 2 mainly in the direction of the upper arrow, *i.e.* a disproportionation of M^{z_1+} takes place.

In the above considerations it has been neglected that the rate of process (I) may depend also on the diffusion of the components participating in the reaction.

Certain problems relevant to the kinetics and the equilibrium of process (I) have been discussed in an earlier publication [1]. Certain aspects of this problem have been studied also by MOLODOV and LOSEV and their co-workers [2, 3, 4] in their investigation of the dissolution of copper in methanolic medium. They studied also process (I) in conjunction with the etching [5] and dissolution [6, 7] of copper.

Process (I) may play an important role in the corrosion of metals [8], in the anodic dissolution and electrolytic deposition of metals and in the operation of chemical current sources. This justifies the more detailed study of this spontaneous process, and a fuller elucidation of its kinetic rules. This problem will be discussed in the following.

The rate of process (I), j, if it depends only on charge transfer, is the following:

$$j = k_{a_1} - k_{k_1} c_1 + k_{a_2}c_1 - k_{k_2}c_2 \qquad (1)$$

where c_1 and c_2 are the concentrations of ions M^{z_1+} and M^{z_2+} in the solution.

The rate of process (I), if it is influenced by both charge transfer and diffusion, is given by the following equation [9]:

$$j = \frac{k_{a_1}\left[z_1X_1 + \dfrac{\dfrac{z_2}{n_2}k_{a_2}}{1+\dfrac{k_{k_2}}{n_2X_2}}\right] - z_1X_1c_1\left[k_{k_1} - \dfrac{k_{a_2}}{1+\dfrac{k_{k_2}}{n_2X_2}}\right]}{z_1X_1 + k_{k_1} + \dfrac{\dfrac{z_1}{n_2}k_{a_2}}{1+\dfrac{k_{k_2}}{n_2X_2}}} - \frac{c_2}{\dfrac{1}{n_2X_2}+\dfrac{1}{k_{k_2}}} \cdot \frac{z_1X_1 + \dfrac{z_2}{n_2}k_{k_1}}{z_1X_1 + k_{k_1} + \dfrac{\dfrac{z_1}{n_2}k_{a_2}}{1+\dfrac{k_{k_2}}{n_2X_2}}} \tag{2}$$

where c_1 and c_2 are the concentrations of ions M^{z_1+} and M^{z_2+}, respectively, in the solution, and X_1 and X_2 are the 'rate constants' of the diffusion of M^{z_1+} and M^{z_2+}.

The dependence of k_{ai} and k_{ki} on the electrode potential ε is given by the following expressions [9]:

$$k_{a_i} = k'_{a_i}\exp\cdot\frac{\alpha_i n_i F\varepsilon}{RT}$$

$$k_{k_i} = k'_{k_i}\exp -\frac{(1-\alpha_i)n_i F\varepsilon}{RT} \tag{3}$$

where k'_{ai} and k'_{ki} are the values of the rate constants when $\varepsilon = 0$, α_i is the transfer coefficient while the other symbols are the usual.

The 'rate constant' of diffusion in the case of a rotated disc electrode is:

$$X_i = 0.62\, D_i^{2/3}\, \nu^{-1/6}\omega^{1/2} \tag{4}$$

D is the diffusion coefficient of the i-th ion, ν the kinematic viscosity of the solution, ω the angular velocity of the disc electrode ($\omega = 2\pi f$, where f is the speed of rotation).

Relationships (1) and (2) are valid also if no external source current passes the electrode, *i.e.* if $j = 0$.

If $j = 0$, that is to say, when the system $M - M^{z_1+} - M^{z_2+}$ is not in equilibrium, the part-reactions of process (I) proceed spontaneously in a direction so that the system approaches equilibrium (see Fig. 1). Using the relationships (1) and (2), below we give for a few limit cases the dependence of the rate of the spontaneous processes proceeding in this case, and of the electrode potential established at the electrode, on the concentration of the respective ions and on hydrodynamic conditions. Let us assume for simplicity that the solution volume is very large, so that the composition of the solution does not change with time.

1. Let the concentration of M^{z_1+} be much lower and the ion concentration of M^{z_2+} much higher than the equilibrium concentration, *i.e.*

$$c_1 \ll \bar{c}_1, \quad c_2 \gg \bar{c}_2 \quad \text{and} \quad c_1 \simeq 0 . \tag{5}$$

In this case, as has been seen in the discussion of Fig. 1, step 1 of process (I) proceeds mainly in the direction of the upper, while step 2 in the direction of the lower arrow with the same rate, *i.e.* metal M is dissolved and M^{z_2+} is reduced to M^{z_1+}.

1.a) If the process is influenced only by the charge transfer, as follows from Eq. (1), the rate of dissolution of metal M and of the reduction of M^{z_2+}, j_{st}, will be

$$j_{st} = k_{a_1} = k_{k_2} c_2 . \tag{6}*$$

Using the relationships (3), from (6) the following expression is obtained for the steady-state electrode potential ε_{st} of metal M:

$$\varepsilon_{st} = \frac{RT}{[z_1\alpha_1 + n_2(1-\alpha_2)]F} \ln \frac{k'_{k_2}}{k'_{a_1}} + \frac{RT}{[z_1\alpha_1 + n_2(1-\alpha_2)]F} \ln c_2 . \tag{7}$$

From relationships (7) and (6):

$$j_{st} = k'^{(1-\nu)}_{a_1} \cdot k'^{\nu}_{k_2} c_2^{\nu} \tag{8}$$

where

$$\nu = \frac{\alpha_1 z_1}{z_1\alpha_1 + n_2(1-\alpha)} . \tag{9}$$

* Between the rate of formation of M^{z_1+} (j'_{st}) and j_{st} since it is formed also by the reduction of M^{z_2+}, the following correlation exists:

$$j'_{st} = \frac{z_2}{n_2} j_{st} \tag{6a}$$

Accordingly, if $\alpha_1 = \alpha_2 = 0.5$ and $z_1 = n_2 = 1$, the order of reaction of the metal dissolution with respect to M^{z_2+}, $\nu = 0.5$. The rate of the process and the steady-state potential are independent of the hydrodynamic conditions.

1.b) Under the above conditions (5), let the relative numerical values of the constants in Eq. (2) be the following:

$$k_{k_1} \gg X_1 \gg k_{a_2};\ k_{k_2} \ll X_2 \tag{10}$$

This means that the process is influenced also by diffusion, and from (2), when $j = 0$ and under consideration that $c_1 \simeq 0$, the rate of ionization of the metal M is:

$$j_{st} = \frac{k_{a_1}}{k_{k_1}} \frac{n_2}{z_2} z_1 X_1 = k_{k_2} c_2 . \tag{11}$$

On the basis of (3), ε_{st} from (11) is:

$$\varepsilon_{st} = \frac{RT}{[z_1 + (1-\alpha_2)n_2]F} \ln \frac{k'_{k_1} k'_{k_2}}{k'_{a_1}} - \frac{RT}{[z_1 + (1-\alpha_2)n_2]F} \ln \frac{n_2}{z_2} z_1 X_1 + \\ + \frac{RT}{[z_1 + (1-\alpha_2)n_2]F} \ln c_2 \tag{12}$$

Thus, measured on a rotating disc electrode, the electrode potential is shifted with increasing speed of rotation in the negative direction.

From (11) and (12), the rate of ionization of metal M and the rate of reduction of M^{z_2+} to M^{z_1+} is:

$$j_{st} = k'^{(1-\nu)}_{a_1} k'^{-(1-\nu)}_{k_1} \left(\frac{z_1}{z_2} n_2 X_1 \right)^{(1-\nu)} k'^{\nu}_{k_2} c_2^{\nu} \tag{13}$$

where the order of reaction with respect to M^{z_2+} is:

$$\nu = \frac{z_1}{z_1 + (1-\alpha_2) n_2} . \tag{14}$$

According to (14), if $\alpha_2 = 0.5$ and $z_1 = n_2 = 1$, then the order of reaction with respect to M^{z_2+} is $\nu = 2/3$. When using a rotating disc electrode, the rate of ionization of the metal will be proportional to the 1/6 power of the speed of rotation. Relationship (13) corresponds to Eq. (7) published in the work of MOLODOV, JANOV and LOSEV [4].

1.c) Under condition (5), let the relative numerical values of the constants in Eq. (2) be the following:

$$k_{k_1} \ll X_1 \gg k_{a_2};\quad X_2 \ll k_{k_2} \tag{15}$$

Thus, from (2) for $j = 0$:

$$j_{st} = k_{a_1} = n_2 X_2 c_2 \tag{16}$$

The rate of the process will be determined by the limit current of the reduction of M^{z_2+}.

On the basis of (3), ε_{st} from (16) is:

$$\varepsilon_{st} = -\frac{RT}{z_1 \alpha_1 F} \ln k'_{a_1} + \frac{RT}{z_1 \alpha_1 F} \ln n_2 X_2 + \frac{RT}{z_1 \alpha_1 F} \ln c_2 . \tag{17}$$

Thus, measured on a rotating disc electrode, the steady-state potential of the electrode is shifted with increasing speed of rotation in the positive direction.

The rate of ionization of the metal is given by Eq. (16). Accordingly, the order of reaction of the process with respect to c_2, $\nu = 1$, and in the case of the rotating disc electrode the steady-state rate will be proportional to the square root of the speed of rotation.

1.d) Under condition (5), let the relative numerical values of the constants in Eq. (2) be the following:

$$X_1 \ll k_{k_1} \gg k_{a_2}; \quad X_2 \ll k_{k_2} . \tag{18}$$

Thus, from (2) for $j = 0$:

$$j_{st} = \frac{n_2}{z_2} z_1 X_1 \frac{k_{a_1}}{k_{k_1}} = n_2 X_2 c_2 . \tag{19}$$

Hence, the diffusion of M^{z_2+} to the electrode surface and of M^{z_1+} from the surface are both hindered.

The steady-state electrode potential is obtained from (19) and (3):

$$\varepsilon_{st} = \frac{RT}{z_1 F} \ln \frac{k'_{k_1}}{k'_{a_1}} + \frac{RT}{z_1 F} \ln \frac{z_2 X_2}{z_1 X_1} + \frac{RT}{z_1 F} \ln c_2 . \tag{20}$$

Therefore, in this case the steady-state potential is independent of the hydrodynamic conditions of the system (in the case of a rotating disc electrode, from the speed of rotation of the electrode). On the other hand, for the rate of ionization of the metal the same is valid according to (19) as in the preceding case 1.c).

1.e) A case relatively easy to discuss is realized also if condition (5) is fulfilled and equilibrium concentrations are rapidly set in at the electrode surface. This is to be expected when the rate constants of step 1 in process (I)

are high (large exchange current) and the 'rate constant' of the diffusion of the intermediate product, X_1, is relatively small, while for step 2 of process (I) the following conditions are fulfilled:

$$X_1 \ll k_{a_2} \ll k_{k_1}; \quad X_2 \gg k_{k_2}. \tag{21}$$

Under these conditions, the rate of dissolution of the metal and the rate of reduction of M^{z_2+} is obtained from Eq. (2):

$$j_{st} = \frac{n_2}{z_1} z_1 X_1 \frac{k_{a_1}}{k_{k_1}} = k_{k_2} c_2 - \frac{k_{a_1}}{k_{k_1}} k_{a_2} \tag{22}$$

Because of condition (21) from Eq. (22) we have:

$$k_{k_2} c_2 \simeq \frac{k_{a_1}}{k_{k_1}} k_{a_2} \tag{23}$$

From (23) and (3) the steady-state potential is:

$$\varepsilon_{st} = \frac{RT}{z_2 F} \ln \frac{k'_{k_1} k'_{k_2}}{k'_{a_1} k'_{a_2}} + \frac{RT}{z_2 F} \ln c_2 \tag{24}$$

It can be seen from Eq. (24) that the potential established at the electrode surface is actually an equilibrium potential and is independent of hydrodynamic conditions.

From (22) and (24) we have for the steady-state rate [3]:

$$j_{st} = \frac{n_2}{z_2} z_1 X_1 K^{1/z_2} c_2^{z_1/z_2} \tag{25}$$

where K is the equilibrium constant of process (I), which is given by the following expression [1]:

$$K = \left(\frac{k'_{a_1}}{k'_{k_1}}\right)^{n_2} \left(\frac{k'_{k_2}}{k'_{a_2}}\right)^{z_1} = \frac{\bar{c}_1^{z_1}}{\bar{c}_2^{z_1}} \tag{26}$$

As can be seen from (25), for $z_1 = 1$ and $z_2 = 2$, the order of reaction with respect to M^{z_2+} is 0.5, and, using a disc electrode, the rate of the process is proportional to the square root of the speed of rotation. Determining the value of j_{st} in the case of a rotating disc electrode at $f = \text{const.}$ as a function of c_2, or at $c_2 = \text{const.}$ as a function of $f^{1/2}$, the value of the equilibrium constant K can be calculated [3].

As can be seen also from inequalities (21) and (10), on increasing the speed of rotation of the disc electrode, gradually the conditions of case 1.b) are realized instead of those of case 1.e), and the rate of the process will depend only slightly on the speed of rotation.

2. In the following, let us assume that the concentration of M^{z_2+} is much lower, and the concentration of M^{z_1+} much higher than the equilibrium concentration, *i.e.*

$$c_1 \gg \bar{c}_1 \,;\; c_2 \ll \bar{c}_2 \,;\; \text{and}\; c_2 \simeq 0 \tag{27}$$

In this case, as has been mentioned also at the discussion of Fig. 1, step 1 of process (I) proceeds mainly in the direction of the lower arrow, while step 2 in the direction of the upper arrow, with the same rate. Thus, M^{z_1+} is spontaneously reduced to metal M and oxidized to M^{z_2+}. Thus, the disproportionation of M^{z_1+} takes place.

2.a) Under conditions (27), the diffusion of the components participating in the reaction is not to affect the process, and

$$k_{a_1} \ll k_{a_2} c_1 \tag{28}$$

Then, from Eq. (1)

$$j_{st} = k_{k_1} c_1 = k_{a_1} c_1 \tag{29}$$

j_{st} gives in this case the rate of formation of the metal M and of M^{z_2+}. From Eq. (29) the steady-state potential [1, 2] is:

$$\varepsilon_{st} = \frac{RT}{[z_1(1-\alpha_1) + \alpha_2 n_2] F} \ln \frac{k'_{k_1}}{k'_{a_2}} \tag{30}$$

Accordingly, if the conditions stipulated above are fulfilled, the steady-state potential of the electrode does not depend on the concentration of M^{z_2+} and M^{z_1+}.

Considering (3), the value of j_{st} from Eqs (29) and (30) is

$$j_{st} = k'^{(1-\nu)}_{a_2} k'^{\nu}_{k_1} c_1 \,, \tag{31}$$

where

$$\nu = \frac{\alpha_2 n_2}{z_1(1-\alpha_1) + \alpha_2 n_2} \tag{32}$$

The disproportionation is according to (31) a first-order reaction with respect to $M^{z_1+}1$. If disproportionation would proceed according to the so-called chemical mechanism by the following reaction:

$$z_2 M^{z_1+} \rightleftharpoons n_2 M + z_1 M^{z_2+} \tag{II}$$

then the order of reaction of the disproportionation reaction of M^{z_1+} would be z_2 with respect to M^{z_1+}. (In the case of a chemical mechanism the order of reaction could not be lower than 2.) Thus, if the order of reaction obtained experimentally for M^{z_1+} is 1, this proves that disproportionation proceeds by reaction (I) [2].

2.b) Under condition (27), the diffusion of the components participating in the reaction similarly does not influence the process, but:

$$k_{a_1} \gg k_{a_2} c_1 \,. \tag{33}$$

In this case, from (1):

$$j_{st} = k_{a_1} - k_{k_1} c_1 = k_{a_2} c_1 \tag{34}$$

Since on the basis of (33) $k_{a_2} c_1 \ll k_{a_1} \simeq k_{k_1} c_1$, the following expression is obtained for the steady-state potential:

$$\varepsilon_{st} = \frac{RT}{z_1 F} \ln \frac{k'_{k_1}}{k'_{a_1}} + \frac{RT}{z_1 F} \ln c_1 \tag{35}$$

When condition (31) is fulfilled, (34) and (35) give the following relationship for the rate of disproportionation (*i.e.* the formation of metal M and M^{z_2+}):

$$j_{st} = k'_{a_2} k'^{\nu}_{k_1} k'_{a_1} c_1^{(\nu+1)} \tag{36}$$

where $\nu = \frac{n_2 \alpha_2}{z_1}$. Accordingly, if $z_1 = 1, z_2 = 2, n_2 = 1$ and $\alpha_2 = 0.5$, then $\nu = 1/2$. Thus, the order of reaction with respect to M^{z_1+} is 1.5. If $z_2 = 3$ and $n_2 = 2$, the order of reaction will be 2.

2.c) Under condition (27), let the relative value of constant in Eq. (2) be the following:

$$k_{k_2} \ll X_2 \,, \quad k_{k_1} \gg X_1 \ll k_{a_2} \,, \quad k_{a_1} \ll X_1 c_1 \tag{37}$$

Then from (2):

$$j_{st} = z_1 X_1 \frac{k_{k_1}}{k_{k_1} + \frac{z_1}{n_2} k_{a_2}} c_1 = z_1 X_1 \frac{k_{a_2}}{k_{k_1} + \frac{z_1}{n_2} k_{a_2}} c_1 \tag{38}$$

As shown by Eq. (38), the rate of formation of metal M and of M^{z_2+} depends then on hydrodynamic conditions.

It follows from (38) that in this case $k_{k_1} = k_{a_2}$, so that the potential established at the electrode is given by Eq. (30), *i.e.* the electrode potential is independent of the concentration of M^{z_1+} and M^{z_2+}, and of hydrodynamic conditions.

When Eq. (38) is valid, $k_{k_1} = k_{a_2}$, hence, from (38):

$$j_{st} = \frac{z_1}{z_2} n_2 X_1 c_1 \tag{39}$$

As follows from Eqs (38) and (39), the order of reaction of the process with respect to M^{z_1+} is 1 also in this case.

2.d) In addition to condition (27) the following conditions are fulfilled:

$$k_{a_1} \gg X_1 c_1 ; \; k_{k_1} \gg X_1 \ll k_{a_2} ; \; k_{k_2} \gg X_2 \tag{40}$$

The steady-state rate of the formation of metal M and of M^{z_1+} is then:

$$j_{st} = n_2 X_2 \frac{k_{a_1} k_{a_2}}{k_{k_1} k_{k_2}} = \frac{n_2 z_1}{z_2} X_1 c_1 \tag{41}$$

Thus, the diffusion of M^{z_1+} to the electrode surface and that of M^{z_2+} from the surface are hindered processes.

From (41) the steady-state potential is:

$$\varepsilon_{st} = \frac{RT}{z_2 F} \ln \frac{k'_{k_1} k'_{k_2}}{k'_{a_1} k'_{k_2}} + \frac{RT}{z_2 F} \ln \frac{z_1 X_1}{z_2 X_2} + \frac{RT}{z_2 F} \ln c_1 \tag{42}$$

Hence, the rate of the process is dependent on the hydrodynamic conditions, while the steady-state potential is not.

On the basis of the above conclusions can be drawn from the kinetic parameters on the mechanism of the reactions, and on the rate-determining process.

Further information on the kinetics and mechanisms of the processes proceeding by the action of the own metal ions can be obtained when using the rotating ring-disc electrode. As is well known [10], the electroactive component formed at the disc, which does not react there chemically or electrochemically, can be voltametrically determined at the ring. If the electroactive component formed at the disc is absent in the solution, the limiting current which can be measured at the ring [10] is:

$$I_R = S_D N \frac{n}{z} j \tag{43}$$

where j is the current density expended at the disc for the production of the electroactive component, $S_D = r_1^2 \pi$ is the surface of the disc electrode (r_1 = radius of the disc), n is the change in charge number occurring (during the volta-

metric determination at the ring), z is the change in charge number of the electrode process taking place at the disc electrode, and N is the geometrical factor of the electrode.

In cases 1.a), b), c), d) and e) discussed above, the limiting current of the oxidation of M^{z_1+} formed at the M disc electrode to M^{z_2+} can be measured at the ring. In this case, j in Eq. (43) is equal to $j'_{st} = \frac{n_2}{z_2} j_{st}$ (see Eq. 6a), $n = n_2$ and $z = z_1$. Thus, in the case discussed, the limiting current to be measured at the ring electrode is:

$$I_{R_1} = S_D N \frac{z_2}{z_1} j_{st} \tag{44}*$$

From Eq. (44), j_{st}, the rate of dissolution of metal M, proceeding spontaneously under the given conditions, can be calculated from the oxidation limiting current I_{R_1}, easy to measure:

$$j_{st} = \frac{z_1}{z_2} \frac{I_{R_1}}{S_D N} \tag{45}$$

On the other hand, in cases 2.a), b), c) and d), when disproportionation takes place at the disc electrode, the limiting current I_{R_2} of the reduction of M^{z_2+} to M^{z_1+} can be measured at the ring. Now, the change in charge number occurring at the ring is $n = -n_2$, the change in charge number of the process proceeding at the disc is $z = n_2$, while j_{st} is to be written instead of j. Thus:

$$I_{R_2} = -S_D N j_{st} \tag{46}$$

For easier survey, Table I summarizes for the cases discussed above the I_{R_1} oxidation and the I_{R_2} reduction limiting currents to be measured at the ring of the rotating ring-disc electrode, as well as the values of the steady-state potentials to be measured at the M electrode.

According to the results of MOLODOV, JANOV and LOSEV [3, 4], obtained for rotating copper disc and platinum ring electrode in methanol solution containing $CuSO_4$, at low speed of rotation, case 1.e) discussed above is realized, *i.e.* I_{R_1} is proportional to the square root of the speed of rotation, and the steady-state potential is independent of stirring. With increasing speed of rotation case 1.b) begins to be realized, and accordingly, I_{R_1} changes more slowly with the speed of rotation, in the limit case proportional to its 1/6 power, while the steady-state potential is shifted in negative direction with increasing speed of rotation of the electrode.

* In the analogous expression in Ref. [4], the surface of the ring electrode, S_R, is erroneously written instead of S_D, the surface of the disc electrode.

Table I

Anodic (I_{R_1}) and/or cathodic (I_{R_2}) limiting currents measurable at the ring electrode, and steady-state potentials measurable at the M *electrode*

	Limiting current measurable at the ring electrode	Steady-state potential of metal, M	
1.a)	$I_{R_1} = \gamma_a k'^{(1-\nu)}_{a_1} k'^{\nu}_{k_2} c_2^{\nu}$	$\varepsilon_{st} = \frac{\nu RT}{\alpha_1 z_1 F} \ln \frac{k'_{k_2}}{k'_{a_1}} + \frac{\nu RT}{\alpha_1 z_1 F} \ln c_2$	$\nu = \frac{\alpha_1 z_1}{z_1 \alpha_1 + n_2(1-\alpha_2)}$
1.b)	$I_{R_1} = \gamma_a k'^{(1-\nu)}_{a_1} k'^{-(1-\nu)}_{k_1} \left(\frac{z_1 n_2}{z_2} X_1\right)^{1-\nu} k'^{\nu}_{k_2} c_2^{\nu}$	$\varepsilon_{st} = \frac{\nu RT}{z_1 F} \ln \frac{k'_{k_1} k_{k_2} z_2}{k'_{a_1} z_1 n_2 X_1} + \frac{\nu RT}{z_1 F} \ln c_2$	$\nu = \frac{z_1}{z_1 + (1-\alpha_2) n_2}$
1.c)	$I_{R_1} = \gamma_a n_2 X_2 c_2$	$\varepsilon_{st} = \frac{RT}{z_1 \alpha_1 F} \ln z_2 X_2 k'_{a_1} + \frac{RT}{z_1 \alpha_1 F} \ln c_2$	—
1.d)	$I_{R_1} = \gamma_a n_2 X_2 c_2$	$\varepsilon_{st} = \frac{RT}{z_1 F} \ln \frac{k'_{k_1} z_2 X_2}{k'_{a_1} z_1 X_1} + \frac{RT}{z_1 F} \ln c_2$	—
1.e)	$I_{R_1} = \gamma_a \frac{n_2 z_1}{z_2} X_1 K^{1/z_2} c_2^{z_1/z_2}$	$\varepsilon_{st} = \frac{RT}{z_2 F} \ln \frac{k'_{k_1} k_{k_2}}{k'_{a_1} k'_{a_2}} + \frac{RT}{z_2 F} \ln c_2$	—
2.a)	$I_{R_2} = \gamma_K k'^{(1-\nu)}_{a_2} k'^{\nu}_{k_1} c_1$	$\varepsilon_{st} = \frac{\nu RT}{\alpha_2 n_2 F} \ln \frac{k'_{k_1}}{k'_{a_2}}$	$\nu = \frac{\alpha_2 n_2}{z_1(1-\alpha_1) + n_2 \alpha_2}$
2.b)	$I_{R_2} = \gamma_K k'_{a_2} k'^{\nu}_{k_1} k'^{-\nu}_{a_1} c_1^{(\nu+1)}$	$\varepsilon_{st} = \frac{RT}{z_1 F} \ln \frac{k'_{k_1}}{k'_{a_1}} + \frac{RT}{z_1 F} \ln c_1$	$\nu = \frac{\alpha_2 n_2}{z_1}$
2.c)	$I_{R_2} = \gamma_K \frac{z_1}{z_2} n_2 X_1 c_1$	$\varepsilon_{st} = \frac{\nu RT}{\alpha_2 n_2 F} \ln \frac{k'_{k_1}}{k'_{a_2}}$	$\nu = \frac{\alpha_2 n_2}{z_1(1-\alpha_1) + n_2 \alpha_2}$
2.d)	$I_{R_2} = \gamma_K \frac{n_2 z_1}{z_2} X_1 c_1$	$\varepsilon_{st} = \frac{RT}{z_2 F} \ln \frac{k'_{k_1} k'_{k_2} z_1 X_1}{k'_{a_1} k'_{a_2} z_2 X_2} + \frac{RT}{z_2 F} \ln c_1$	
	$\gamma_a = S_D \frac{z_2}{z_1} N$		
	$\gamma_K = - S_D N$		

The rotating ring-disc electrode has in the given case the advantage that ε_{st}, the steady-state potential of the metal electrode M and the voltametric limiting current of the ring electrode can be easily and accurately measured. From the dependence of these quantities on metal ion concentration and on the speed of rotation of the electrode, unequivocal conclusions can be drawn on the mechanism of the process and on the rate determining step, and in certain cases (*e.g.* in case 1.e)) even on the equilibrium.

REFERENCES

[1] Kiss, L., Farkas, J.: Magy. Kém. Folyóirat **76,** 120 (1970); Acta Chim. (Budapest) **65,** 7 (1970)
[2] А. И. МОЛОДОВ, В. В. ЛОСЕВ: Итоги Науки, Электрохимия, Том 7. стр. 65 (1971)
[3] А. И. МОЛОДОВ, Л. А. ЯНОВ, В. В. ЛОСЕВ: Электрохимия, 57 **12** 513 (1976)
[4] А. И. МОЛОДОВ, Л. А. ЯНОВ, В. В. ЛОСЕВ: Защита металлов, **12** 578 (1976)
[5] Б. П. БОГДАНОВ, Р. С. БОЛОТИНА: Защита металлов, **11** 341 (1975)
[6] Pang, J., Ritchie, I. M., Giles, D. E.: Electrochim. Acta **20,** 923 (1975)
[7] Nicol, M. J.: J. S. Afr. Inst. Mining and Metals **75,** 291 (1975)
[8] Varsányi, M., Kiss, L., Farkas, J.: Symposium on Soil Corrosion, Siófok, Sept. 14—17, 1976.
[9] Л. ҚИШ, Й. ФАРҚАШ: Электрохимия, **7** 1744 (971)
[10] Л. Н. НЕКРАСОВ: Электрохимия, **11** 851 (1975)

László Kiss
József Farkas } H-1088 Budapest, Puskin u. 11—13.

Acta Chimica Academiae Scientiarum Hungaricae, Tomus 96 (2), pp. 141—150 (1978)

ELECTRON MICROSCOPIC STUDIES ON THE MORPHOLOGY OF POLY(VINYL ALCOHOL) HYDROGELS

T. VÁRADI,*** M. NAGY,* A. KALLÓ** E. WOLFRAM*

*(*Department of Colloid Science, L. Eötvös University, Budapest*
*** Research Institute for Plastics, Budapest*
**** BUDALAKK Paint and Synthetic Resin Works, Budapest)*

Received February 2, 1977

The morphology of PVA hydrogels of different supramolecular structures formed under various conditions has been studied by transmission electron microscopy. A method for the augmentation of the contrasts of supramolecular elements is described. There is a good agreement between structural features directly observable in the electron microscope and the physico-chemical properties of the gels as determined previously.

Introduction

The theoretical relationships connecting the structure of 3-dimensional networks and their physico-chemical properties are based on conformational models involving ideal networks with chains of a Gaussian distribution between junctions of the network. With certain modifications, the equation of the elastic state is valid for swollen 3-dimensional networks too [1, 2].

The structure of 3-dimensional macromolecular networks formed in solution is usually not ideal and depends primarily on the initial concentration of the polymer and on the degree of cross-linking.

Relative to the accepted fundamental model, the network structure may have defects on either the *macromolecular* or the *supermolecular* level. The first type (rings, closed and permanent loops, functional groups not reacted in stoichiometric proportions, etc.) does not alter strongly the original spatial distribution of segments and macromolecules. However, the second type brings about pronounced deviations from the ideal network since it affects the network elements formed by the arrangement of macromolecules on a higher level.

It seems reasonable to expect that deliberate alterations of the size, shape, inner structure and spatial distribution of the supramolecular network elements may lead to substances possessing a wide variety of properties. This is the basis of some practical applications of separation techniques. The biological implications of this topic are obvious.

In an earlier work [3, 4, 5] poly(vinyl alcohol) hydrogels of various structures were subjected to a systematic and complex study primarily to

elucidate the mechanism of their formation. We have found that, although the unreactive polymer of lower molecular weight continuously increases the concentration of supramolecular elements (as shown by the monotonic increase of the modulus of elasticity of the gels), it passes through a sharp maximum and the size of the elements through a minimum as a function of the additive concentration. Probably the extreme values of the physical properties are not due to size effects alone but also to changes in the shape and spatial distribution of the elements. However, the methods generally used for the study of gel structures do not provide information on these features.

Therefore, as a complement to previous optical, mechanical and swelling tests, we now report electron microscopic results for poly(vinyl alcohol) hydrogel. The method of sample preparation used in this work for soft, swollen gels may be applied in the study of wet biological specimens too.

Experimental

Materials. Poly(vinyl alcohol), PVA, hydrogels were prepared from commercial Rhodoviol 16/20 ($\overline{M}\eta = 1.0 \times 10^5$) *via* alkaline hydrolysis and fractionation. The unreactive polymeric additive was poly(vinylpyrrolidone), PVP (FLUKA K-30: $\overline{M}\eta = 4.0 \times 10^4$, and K-90 : $\overline{M}\eta = 3.6 \times 10^5$). PVA was cross-linked with glutaric dialdehyde (GDA) carefully purified by distillation.

Preparation of gels. The gel membranes were prepared as described earlier [5]. Some data of the gels prepared from PVP-containing solutions are listed in Table I.

Gel preparation for electron microscopic study. Considering the possibilities available, the so-called embedding technique was used for fixing the gel structure. This involved the exchange of the swelling fluid (water) for a monomer or a mixture of monomers which, after polymerization, turns into a substance with properties suitable for being cut into thin sections. It is very important that exchange for the monomer and its polymerization should not lead to structural changes. Since the electron densities of the loose, incompact gel structure and the embedding polymer do not differ strongly, the electron micrographs will not be rich in detail. In order to enhance the contrasts of supramolecular structural elements, we have devised a simple method based on the following considerations.

It is known that the colloidal stability of gold and silver sols can be substantially increased by the addition of suitable macromolecules [6], owing to the interaction of macromolecules and sol particles. Thus, if a high dispersity metal sol is prepared in a macromolecular system of fixed spatial structure, its particles will be bonded to the macromolecular matrix in densities depending on the local concentration of macromolecules. Consequently, electron-scattering should be weaker in low, and stronger in high segment density areas.

Based upon these suppositions, the samples were prepared in the following way. The gels were soaked in 0.02 *N* silver nitrate, followed by reduction to metallic silver by the slow addition of a 2.5 % aqueous hydrazine hydrate to the gel films. As a result, slightly yellow-brown gel membranes were obtained, which remained transparent if the original samples were transparent. This 'silvering' permits prior fixation of the structure under very mild conditions, which reduces the sensitivity of the gels to solvent replacement.

In the gels thus prepared water was replaced by anhydrous ethanol in four steps. After this ethanol was replaced, also in four steps, by a 1 : 1 mixture of methyl methacrylate and butyl methacrylate. The degree of gel swelling did not change significantly during these operations. The system was polymerized at 60 °C by the addition of 1% benzoyl peroxide.

From the embedded samples, having the shape of a pyramid, sections 60—80 nm thick were cut with a Reichert Om U2 type ultramicrotome.

The sections were placed on a microgrid specimen holder fitted with a formvar support membrane and exposed directly in an ELMI D2 Carl Zeiss Jena type transmission electron microscope.

Table I

Characteristics of the gels used

No.	c_{PVA}	c_{PVP}	n	q_{weight}
1	27.0	0	20	9.3
2	27.0	13.5	20	8.6
3	27.0	108.0	20	15.0
4	27.0	0	100	52.8
5	27.0	13.5	100	43.0
6	54.0	0	20	5.0
7	54.0	13.5	20	5.3
8	54.0	0	100	16.8
9	54.0	13.5	100	17.1
10	54.0	108.0	100	17.8
11*	27.0*	4.5*	20*	8.6*

c = concentration (g/dm^3) of the polymer in the initial system

$n = \frac{\text{PVA}}{\text{GDA}}$ to mole ratio

q_{weight} = degree of swelling of the sample at 25 °C in distilled water
Data marked with an asterisk refer to a system containing PVP of K-90 type

Results and discussion

Magnification by 12,000 was found to be the most suitable for the observation of the structures formed under various conditions. Figures 1 to 11 show the results of our electron microscopic studies.

The micrographs reveal that this technique of preparation with silver produces excellent contrasts between supramolecular elements and the embedding polymer. It is to be seen that the silver particles precipitated are in most cases very small indeed, perhaps smaller than 10 nm. The black spots (*cf.* Figs 2, 4, 9 and 10) are due to coarser grains of silver due to imperfect preparation.

It is useful to analyze these pictures by comparing the structure-determining factors (concentrations of the polymers present, degree of cross-linking) with the physico-chemical properties of the resulting structures.

In agreement with experimental results reported in the literature [2], we have shown earlier that the lower the concentration of the polymer that forms the three-dimensional network and the higher the degree of cross-linking, the more inhomogeneous the structure obtained [7]. With decreasing degree of cross-linking, the structural differences gradually disappear. The former statement is illustrated by samples 1 and 6 in Figs 3 and 9, and the latter by samples 4 and 8 in Figs 1 and 6.

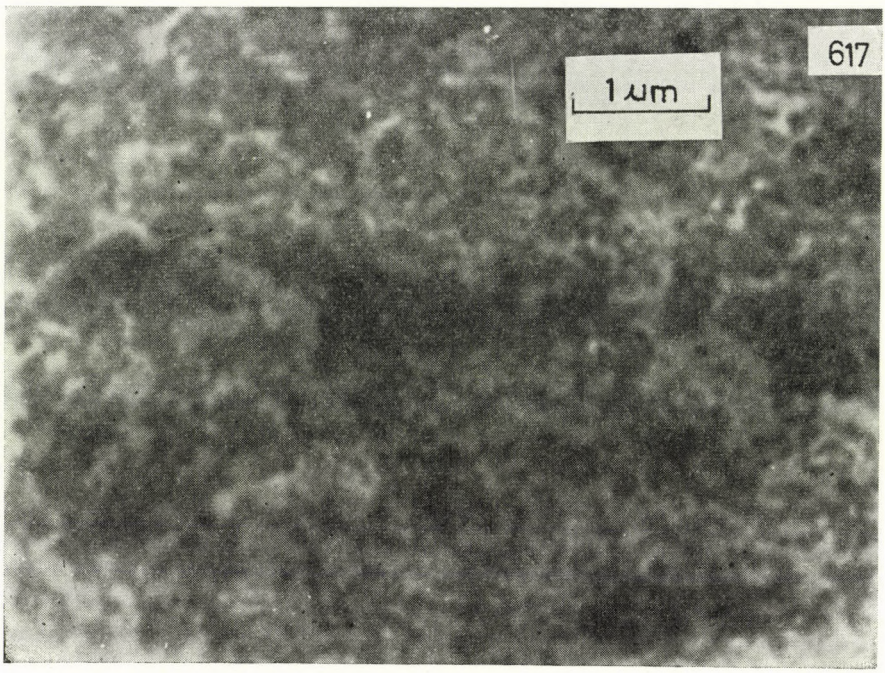

Fig. 1

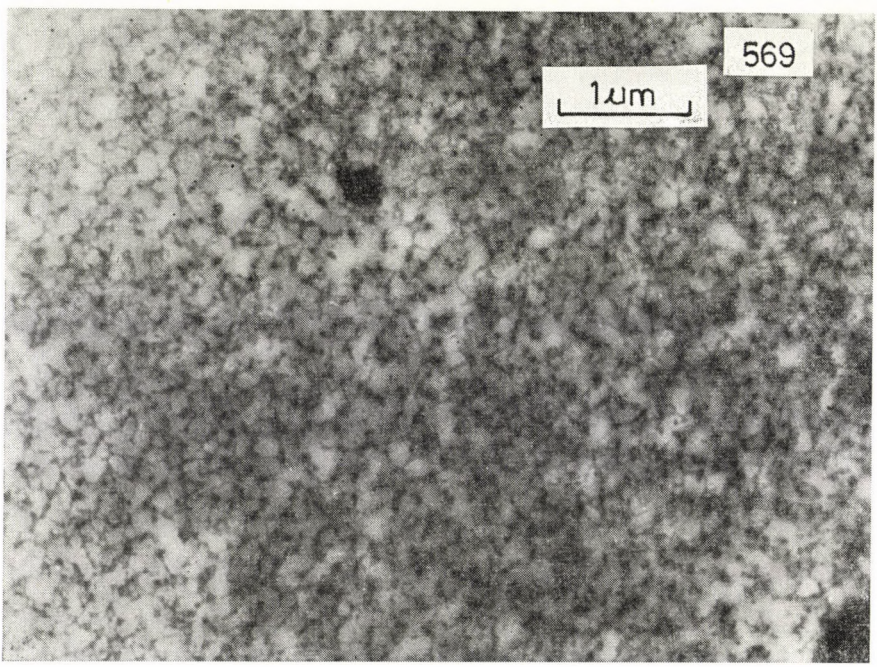

Fig. 2

Special attention should be paid to the reticular structure made up of very small globules, as shown in Fig. 3. Among the four samples, this exhibited the highest turbidity. Further we may mention that in gels of the lowest degree of cross-linking (Figs 1 and 6) the supramolecular elements are rather incompact, and that their size (a few hundred nm) agrees well with the results of structural studies [8] on moderately concentrated aqueous PVA solutions.

In connection with earlier studies the evaluation of the effect of the unreactive PVP additive upon the gel structure seems to be of special interest. Figures 3, 4 and 5 are the electron micrographs of gels prepared from mixtures with an initial PVA concentration of 27 g/dm^3 and the same degree of cross-linking ($n = 20$) but with various contents of PVP. Clearly, already at a concentration of 15 g/dm^3 PVP (Fig. 4) the spatial arrangement of the supramolecular elements is significantly changed. Compared with gels without PVP, this structure is apparently homogenized. Conversely, at a high concentration of PVP, *viz.* 120 g/dm^3 (Fig. 5), a very porous, incompact structure emerges. In agreement with these data the gels with the most compact structures show the highest modulus of elasticity. Essentially the same effect is in evidence in the case of samples with a lower degree of cross-linking ($n = 100$, *cf.* Figs 1 and 2); however, here smaller changes in both the mechanical properties and the structure are to be observed. Further, comparison of Fig. 1 with Fig. 2 explains our former finding that the size of the supramolecular elements initially decreases when PVP is added.

Essentially the same statements are valid for the electron microscopic structures of gels formed from solutions of higher PVA concentrations (Figs 6, 7 and 8).

As far as morphology is concerned, it is worth mentioning that in more dilute and strongly cross-linked PVA systems preferably globular structures are formed, whereas mixtures which contain more PVA and have a lower degree of cross-linking favour bundled structures (*cf.* Figs 5 and 8).

Strongly cross-linked systems with high concentrations of PVA significantly differ from those considered. The relatively homogeneous structure of the gel obtained in the absence of PVP (Fig. 9) turns highly porous when a small amount of PVP is added (Fig. 10). This is accompanied by the deterioration of the mechanical properties and a substantial reduction of the modulus of gel elasticity.

Special attention is directed to the electron micrograph shown in Fig. 11, which illustrates the efficiency of the preparation method.

This gel was made in the presence of PVP of a high molecular weight; here the three-dimensional network did not turn into an inhomogeneous structure but, owing to the incompatibility of the unreactive polymer with the network formed, the former separated and became fixed in the form of globules or droplets within the gel as a matrix. Other studies [5] have unequivocally

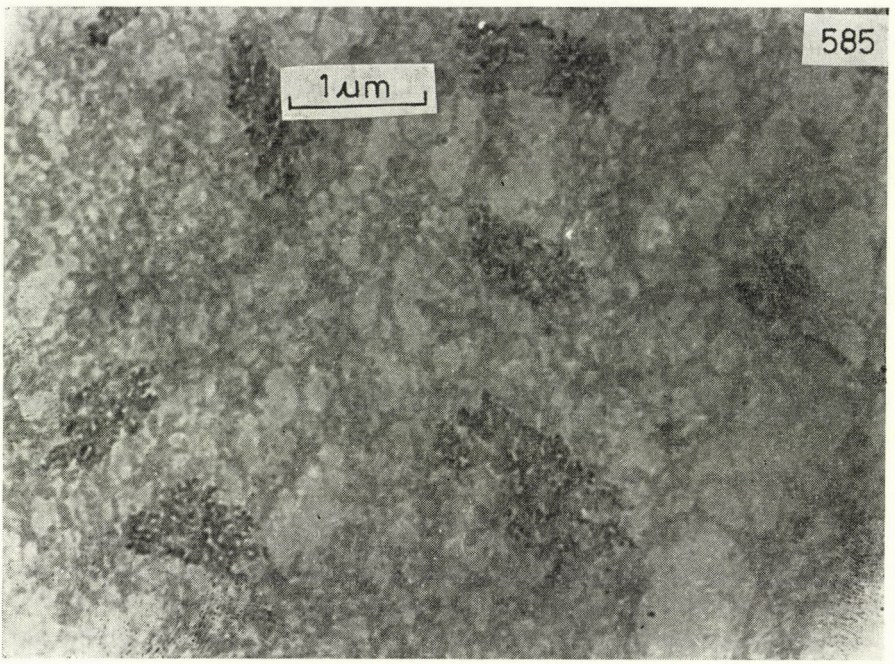

Fig. 3

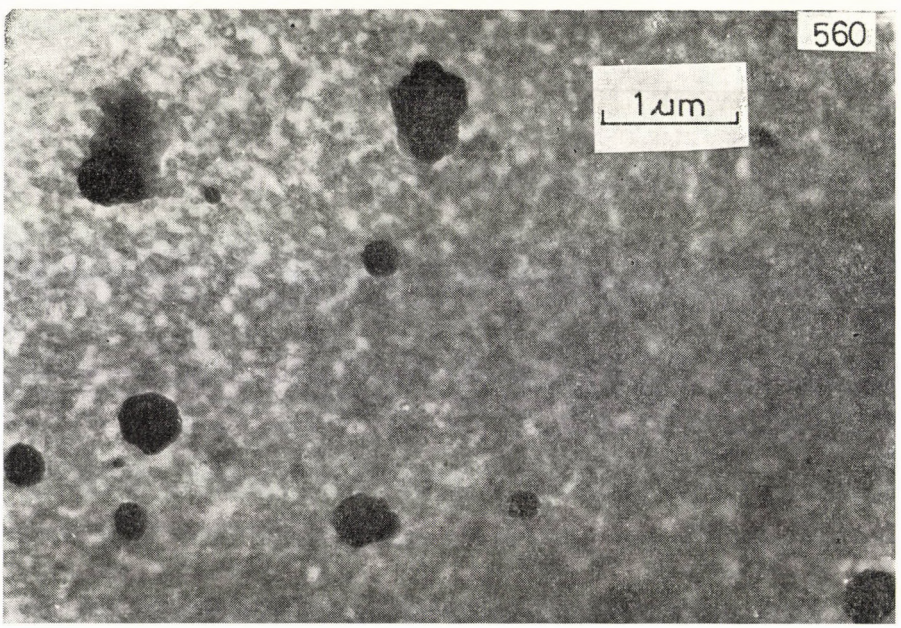

Fig. 4

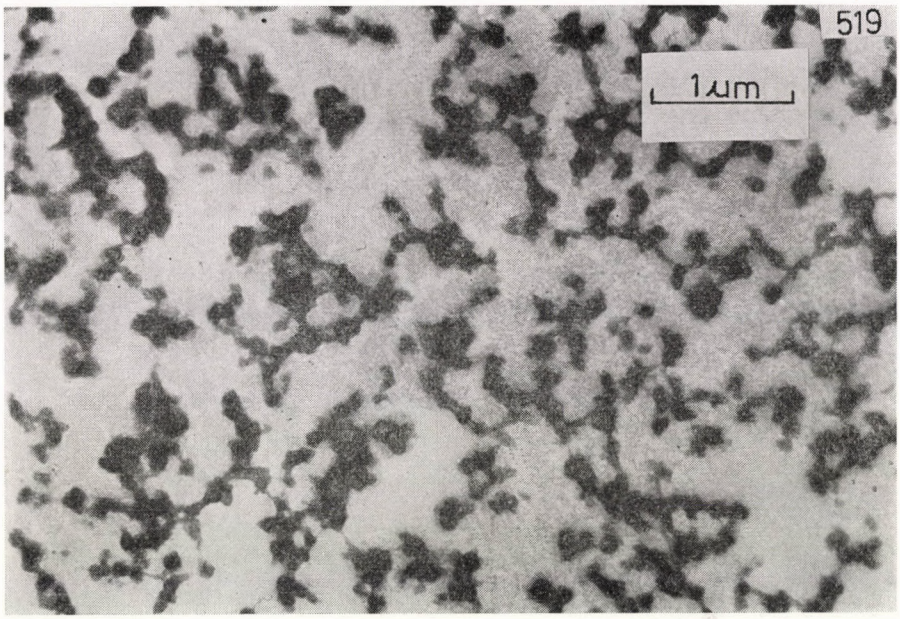

Fig. 5

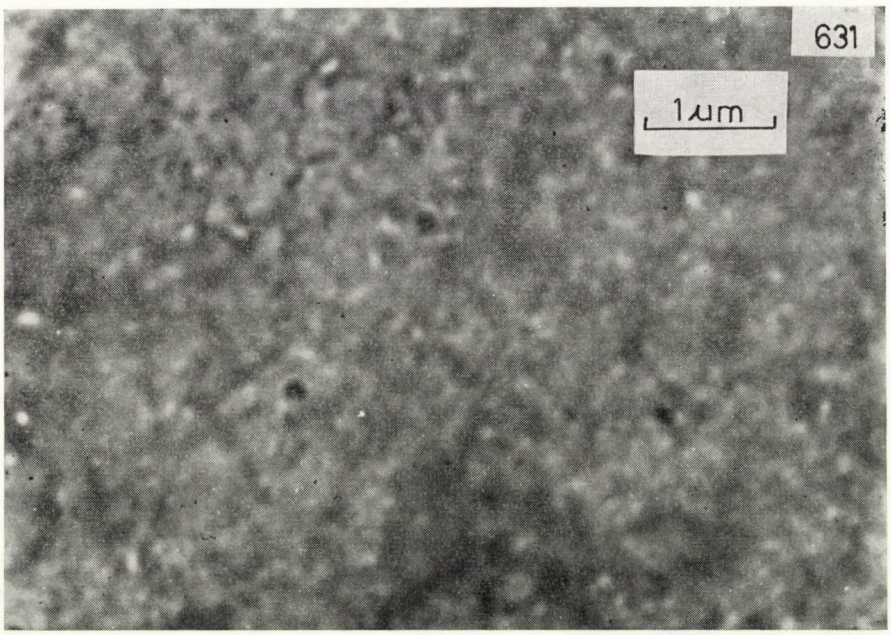

Fig. 6

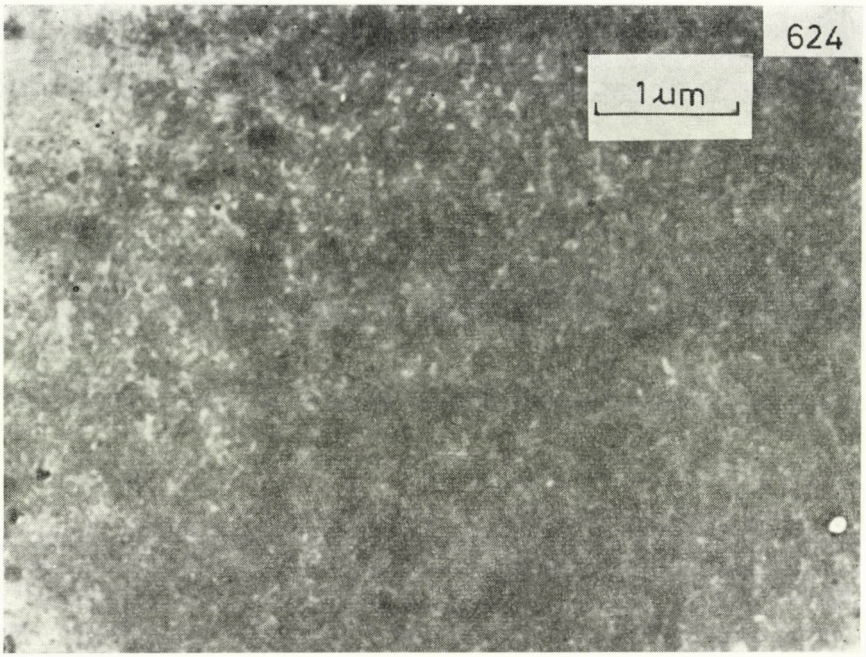

Fig. 7

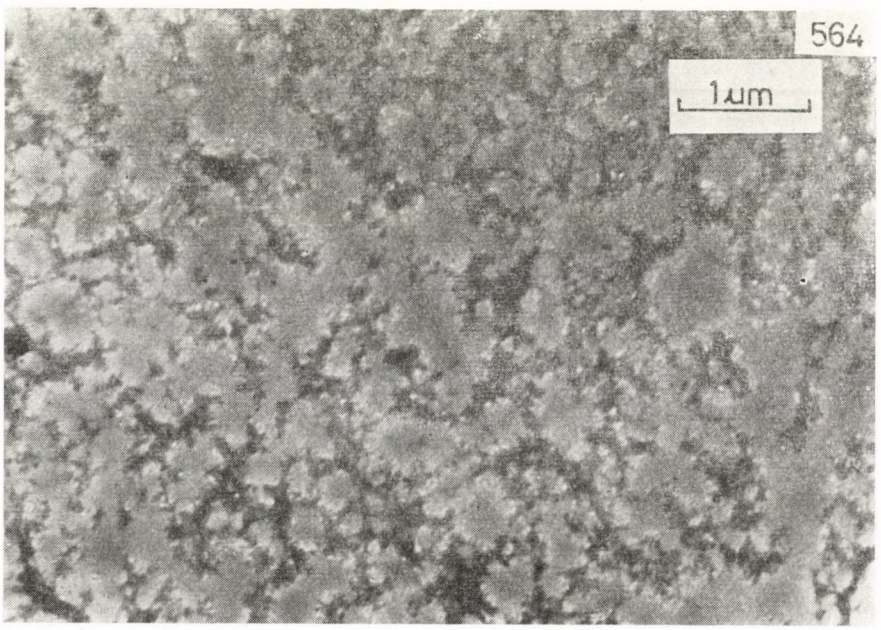

Fig. 8

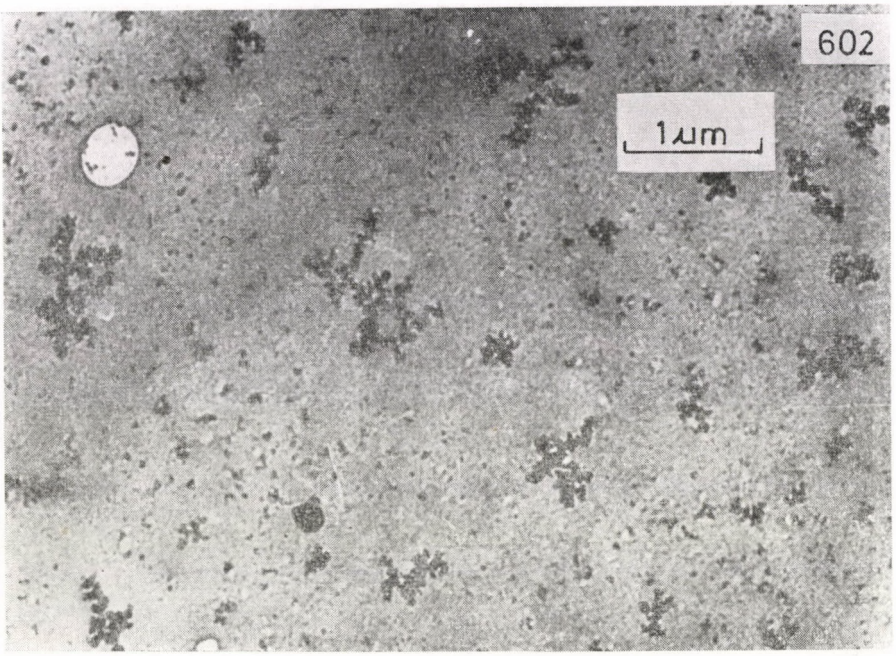

Fig. 9

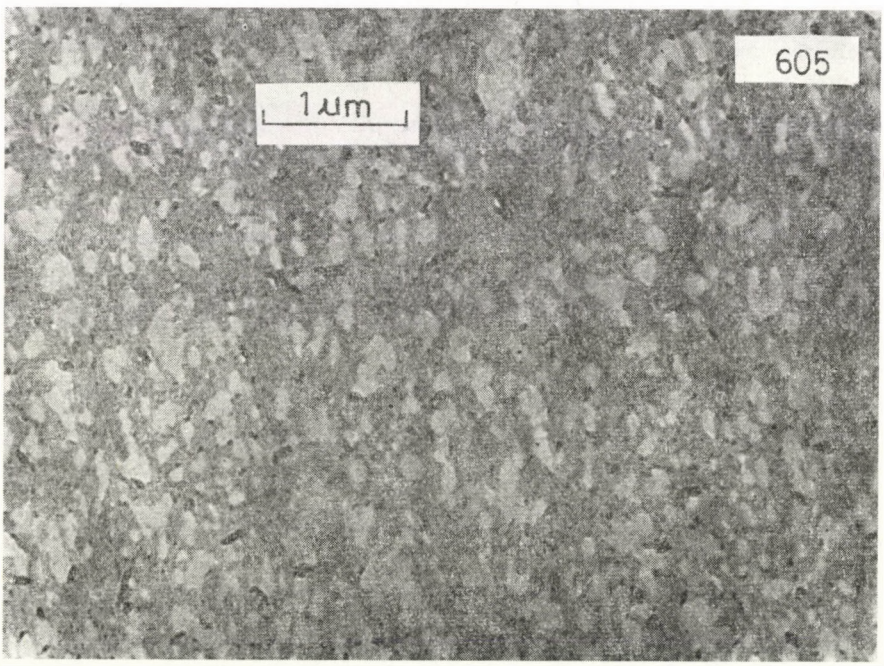

Fig. 10

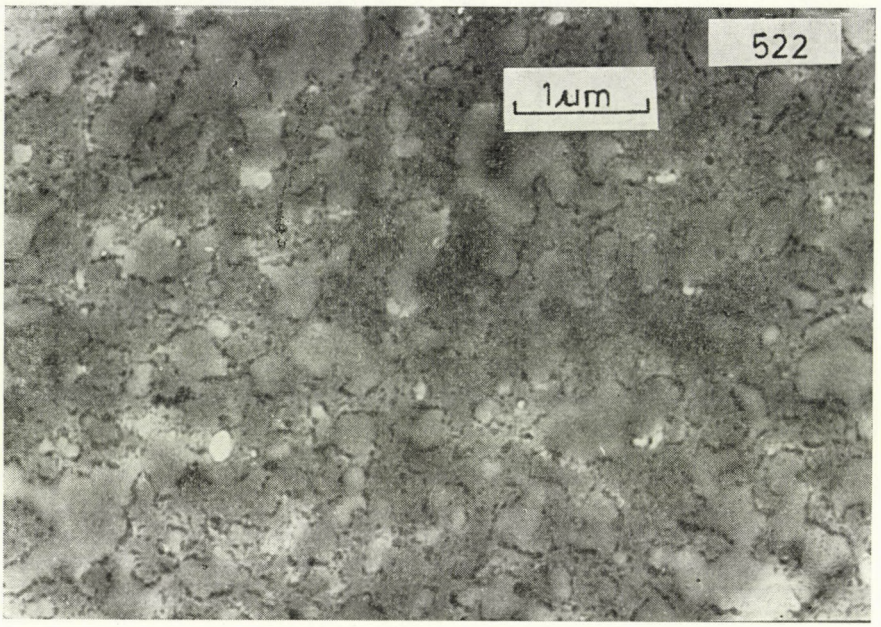

Fig. 11

shown that this process occurs. By the 'silver contrasting' method, it was thus possible to delineate the boundary surfaces of the microphases of a polymer solution embedded in a relatively soft gel matrix.

REFERENCES

[1] FLORY, P. J.: Principles of Polymer Chemistry. Oxford University Press, Ithaca 1953
[2] DUŠEK, K., PRINS, W.: Adv. Polymer Sci., **6**, 1—102 (1969)
[3] VÁRADI, T.: Thesis. L. Eötvös University, Budapest 1975
[4] NAGY, M., WOLFRAM, E., VÁRADI, T.: Proc. Internat. Conf. on Colloid and Surface Science, **1**, 447 (1975); **2**, 115 (1976)
[5] NAGY, M., WOLFRAM, E., VÁRADI, T.: Progr. Coll. and Polym. Sci., **60**, 138 (1976)
[6] WOLFRAM, E.: Kolloidika II/2 (in Hungarian). Tankönyvkiadó, Budapest 1965
[7] NAGY, M., WOLFRAM, E., MARTON, Gy.: Internat. Symp. on Macromolecules, Helsinki, July 1972; Preprint, Vol. 3, pp. 239.
[8] KLENIN, V. I., KLENINA, O. V., GALATINOV, V. V.: Vysokomolek. Soed., **8**, 1574 (1966)

Tibor VÁRADI
Miklós NAGY
Aranka KALLÓ
Ervin WOLFRAM

H-1088 Budapest, Puskin u. 11—13.

Acta Chimica Academiae Scientiarum Hungaricae, Tomus 96 (2), pp. 151—159 (1978)

DIAMAGNETIC STUDY OF MONOSUBSTITUTED NAPHTHALENES

V. SHANMUGASUNDARAM

(Department of Physics, Annamalai University, Annamalainagar 608101, Tamil Nadu, S. India)

Received December 22, 1976
In revised form June 8, 1977

The diamagnetic susceptibilities of several monosubstituted benzenes and isomeric monosubstituted naphthalenes were determined by the Curie method. The lower χ_M values for the α-isomers are explained on the basis of differences in the conjugation of the substituents in positions 1 and 2 with the ring. A comparison of the Van Vleck paramagnetism of monosubstituted benzenes calculated by the method of DORFMAN [19] with that of the respective naphthalene derivatives shows that the magnetic susceptibilities of the α-naphthyl derivatives are influenced largely by peri-methine steric hindrance.

As the π electron density at all positions in the naphthalene ring is unity, it may be expected that positions 1 and 2 in naphthalene would be attacked equally by reagents. However, such an attack also depends on the polarizability of these two positions. In naphthalene, position 1 has a larger polarizability [1] (0.44) than position 2 (0.41) and hence the different positions in naphthalene have different conjugating abilities. The magnitude of conjugation is represented by the contributions of the ionic structures to the resonance hybrid. There is considerable spectroscopic and chemical evidence to show the extent of conjugation of a substituent.

In general, substituents produce bathochromic shifts in the positions of the absorption bands of a compound, whose magnitude is determined by the extent of conjugation. The shifts in the wavelength of the absorption bands of α-substituted naphthalenes is always greater than that for isomeric β-substituted derivatives. DE LASZLÓ [2] has found from the spectral studies of various monosubstituted naphthalenes that the calculated moments of inertia are less for the α-isomers than those for the β-isomers. Dipole moment studies by NAKATA [3], EVERARD and SUTTON [4], and BATSANOV and PAKHONOV [5] on monosubstituted naphthalenes suggest that the moments of β-isomers are higher than those of the α-compounds. The molecular polarizabilities and Kerr constants [6] of monosubstituted naphthalenes suggest that rotational isomerism exists in all these compounds and that the β-isomers have higher Kerr constants than the α-isomers.

While a number of studies have been made to find structure-reactivity correlations for naphthalene derivatives, from absorption spectra, dipole

moments, etc., only a very limited amount of work has been done on these compounds regarding the effect of the position of the substituent on the diamagnetic susceptibility. PACAULT [7] has determined the diamagnetic susceptibilities of hydroxy, amino and acetyl derivatives of naphthalene and observed no significant variation in the molar susceptibilities of the isomeric compounds. However, LUFEROVA and SYRKIN [8] have concluded from similar studies that β-isomers show considerably greater values than the corresponding α-isomers. This result is of some significance. It is well known that the χ_{CH_2} increments obtained from benzene and toluene, chlorobenzene and chlorotoluene are less than the normal value of 11.66, which is generally found in aliphatic compounds [9]. This is due to several interaction terms that are introduced on disturbing the sixfold symmetry of the benzene ring by the replacement of a group or an atom, and other conjugation effects. Since the self-polarizabilities of positions 1 and 2 in the naphthalene ring are different, the interaction terms that modify the total diamagnetic susceptibility of the compound should also be different when substitution takes place in these positions. Therefore a systematic magnetochemical investigation of α- and β-substituted naphthalenes might be of interest. Naphthalene derivatives containing the following substituents in the α- and β-positions were chosen for the present study:

$-CH_3$, $-Cl$, $-Br$, $-OH$, $-OCH_3$, $-NH_2$, $-NHCOCH_3$, $-COCH_3$, $-SH$, $-SCH_3$ and $-NO_2$

The diamagnetic susceptibilities of the corresponding monosubstituted benzenes were also determined with a view to compare the effect of the substitution of those groups in the benzene ring and in the naphthalene ring.

Experimental and results

The substances were purified by standard methods and the purification was continued until they gave constant susceptibility values. The magnetic measurements were made by the Curie retorsion method as given in a previous publication [10].

The specific and molecular susceptibilities obtained for monosubstituted naphthalenes are given in Table I. In Table II the specific and molecular susceptibilities of the monosubstituted benzenes are listed. The standard deviation of the specific susceptibilities are also given along with the susceptibility values.

Discussion

On comparing the magnetic data for the α- and β-substituted naphthalenes, it is seen that the α-substituted compounds show a diminution in diamagnetism relative to the corresponding β-isomers. In interpreting the observed magnetic

Table I

Diamagnetic susceptibilities of monosubstituted naphthalenes*

No.	Substance	Molec. weight	$\chi_S \times 10^6$	$\chi_M \times 10^6$
1	Naphthalene	128.16	0.718±0.001	91.96
2	α-Methylnaphthalene	142.19	0.719±0.001	102.20
3	β-Methylnaphthalene	142.19	0.729±0.002	103.60
4	α-Naphthol	144.16	0.660±0.002	95.19
5	β-Naphthol	144.16	0.680±0.003	98.06
6	α-Naphthyl methyl ether	158.19	0.660±0.003	104.28
7	β-Naphthyl methyl ether	158.19	0.690±0.002	109.10
8	α-Chloronaphthalene	162.61	0.634±0.002	103.00
9	β-Chloronaphthalene	162.61	0.660±0.002	107.30
10	α-Bromonaphthalene	207.07	0.540±0.001	111.80
11	β-Bromonaphthalene	207.07	0.570±0.002	118.00
12	α-Naphthylamine	143.18	0.672±0.002	96.23
13	β-Naphthylamine	143.18	0.702±0.002	100.48
14	α-Naphthoic acid	172.17	0.604±0.002	104.00
15	β-Naphthoic acid	172.17	0.615±0.002	105.60
16	β-Thionaphthol	160.22	0.690±0.002	110.50
17	α-Acetamidonaphthalene	185.22	0.607±0.001	112.40
18	β-Acetamidonaphthalene	185.22	0.634±0.001	117.40
19	α-Acetylnaphthalene	170.20	0.628±0.001	106.80
20	β-Acetylnaphthalene	170.20	0.647±0.002	110.00
21	Methyl-α-naphthyl sulfide	174.26	0.677±0.001	118.00
22	Methyl-β-naphthyl sulfide	174.26	0.695±0.001	121.00
23	α-Nitronaphthalene	173.16	0.555±0.002	96.02

* The susceptibilities are given in this paper in CGS units. To convert them into SI units the susceptibilities should be multiplied by $4\pi \times 10^6$

susceptibilities of polyatomic molecules, different interacting terms that modify diamagnetism should be considered. This is more so in highly conjugated systems like naphthalene derivatives. Also, it is quite obvious that the contributions arising from different interactions are not strictly additive and therefore the magnitude of the individual contributions could not be sorted out. The problem becomes more complicated when the number of substituents in the ring is increased. However, in the monosubstituted naphthalenes, the interaction terms are reduced to a minimum. For a comparison between the two isomers, the conjugation of the substituents with the naphthalene ring should be considered.

Table II

Diamagnetic susceptibilities of monosubstituted benzenes*

No.	Substance	Molec. weight	$\chi_S \times 10^6$	$\chi_M \times 10^6$
1	Toluene	92.13	0.714 ± 0.003	65.78
2	Chlorobenzene	112.56	0.618 ± 0.002	69.56
3	Phenol	94.11	0.651 ± 0.002	61.27
4	Anisole	108.13	0.669 ± 0.001	72.34
5	Aniline	93.12	0.674 ± 0.002	62.76
6	Benzoic acid	122.12	0.579 ± 0.002	70.71
7	Acetophenone	120.14	0.603 ± 0.002	72.44
8	Bromobenzene	157.02	0.518 ± 0.003	81.34
9	Nitrobenzene	123.11	0.499 ± 0.002	61.44

* As given in Table I.

The application of dipole moment measurements as an analytical tool for the determination of configuration is now widely recognized. The dipole moments of α- and β-substituted naphthalenes reported by many investigators, pertinent to our present discussion are given in Table III.

It is evident from Table III that the moment of the β-isomers is generally greater than those of the α-isomers, irrespective of the nature of the substituent. This may be due to the differences in conjugation of the substituents in the two positions. This difference in the conjugation of the substituent groups with the naphthalene ring was explained by many authors in terms of steric inhibition of resonance due to the presence of the peri-methine group in the

Table III

Electric moments of α- and β-isomers*

Substituent	Solvent	Temperature, °C	Moment		Ref.
			α	β	
$-COCH_3$	C_6H_6	30	2.89	3.08	[11]
$-Cl$	C_6H_6	25	1.51	1.65	[12]
$-Br$	C_6H_6	20	1.58	1.71	[13]
$-CH$	C_6H_6	20	1.40	1.53	[14]
$-NO_2$	C_6H_6	20	3.88	4.36	[15]
$-NH_2$	C_6H_6	20	1.49	1.77	[15]

* The dipole moments are given in D units; to convert them into cm units these figures should be multiplied by 0.2998×10^{30}

case of α-derivatives. Therefore, it seems reasonable to assume that the lower χ_M obtained for the α-derivatives relative to the β-compounds may be due to this peri-methine hindrance. Also the lower susceptibility values of the α-derivatives may be due to the smaller sum-total of π^2 values of these molecules. A more thorough examination of the effect can be made by comparing the observed susceptibilities with the calculated values. Since the latter cannot be obtained easily by purely theoretical methods of evaluation, empirical and semi-empirical methods should be employed.

Different methods of obtaining the theoretical values and their relative advantages are discussed in detail elsewhere [16]. The χ_M values for the monosubstituted naphthalenes were calculated by different methods and are given in Table IV.

Table IV

Calculated and experimental diamagnetic susceptibilities of monosubstituted naphthalenes

No.	Compound	Theoretical $\chi_M \times 10^6$				Experimental $\chi_M \times 10^6$	
		Ingold [17]	Pascal [18]	Dorfman [19]	Yang [20]	α	β
1	Methylnaphthalene	103.5	104.95	101.53	103.83	102.20	103.60
2	Naphthol	96.30	98.00	94.23	98.33	95.19	98.06
3	Naphthyl methyl ether	108.10	110.25	105.53	109.11	104.28	109.10
4	Chloronaphthalene	106.00	109.20	105.03	106.15	103.00	107.30
5	Bromonaphthalene	115.30	115.85	112.53	117.55	111.80	118.00
6	Naphthylamine	100.20	103.70	98.58	100.46	96.23	100.48
7	Naphthoic acid	105.60	104.40	101.73	106.91	104.00	105.60
8	Thionaphthol	106.70	—	—	107.83	—	110.50
9	Acetamidonaphthalene	116.30	122.35	118.08	120.92	112.40	117.40
10	Acetylnaphthalene	107.00	111.35	109.03	112.40	106.80	110.00
11	Methyl naphthyl sulfide	118.50	—	—	119.71	118.00	121.00
12	Nitronaphthalene	97.60	97.55	96.08	98.53	96.05	—

Table IV suggests that fairly consistent values were obtained by different methods of evaluation. Generally, it may be seen that the experimental χ_M values of all the β-isomers studied agree closely with the theoretically calculated values.

Methylene increment

For the compounds studied it is possible to calculate the methylene increment from both α- and β-isomers (Table V).

Table V

Methylene increments in substituted naphthalene

Compound	CH_2 increment (χ_M)	
	α	β
$C_{10}H_8$		
$C_{10}H_7CH_3$	10.24	11.64
$C_{10}H_7OH$		
$C_{10}H_7OCH_3$	9.09	11.04
$C_{10}H_7SH$		
$C_{10}H_7SCH_3$	...	10.5

The replacement of a hydrogen by a CH_3 group in the β-position produces a methylene increment of 11.64, whereas in the α-isomer a methylene increment of 10.24 results. However, the methylene increments found on passing from —SH to $—SCH_3$ and from —CH to $—OCH_3$ for the α-position are significantly lower. This is understandable if one takes into account the steric factors. The α-methoxy group is sufficiently bulky to interfere with the peri-hydrogen atom, so free rotation is inhibited, if not totally excluded.

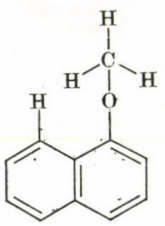

Fig. 1

This steric overlap of the substituent groups in the α-position with the hydrogen in position 8 strongly distorts the electron clouds and thus bring about changes in the Van Vleck paramagnetic term. The conjugation of the group with the ring is also affected to a large extent. However, the methylene increments for these groups in the β-positions are also significantly lower. Though this could not be adequately explained, it may probably be accounted for by considering the differences in the conjugation of these groups with the aromatic ring.

The conjugating abilities of different groups with the naphthalene ring can be better understood by comparing them with those for a benzene ring. The Van Vleck paramagnetic term in a polyatomic molecule arising due to the constraints involved in bond formation can be approximately calculated

by the method of DORFMAN. In this method, Langevin's diamagnetic term (χ_d) for many atoms and groups was calculated from polarizability data for a series of aliphatic compounds and then the paramagnetic contribution of the groups was computed by successively extending these values to more strongly conjugated systems. Therefore, it is clear that whereas this method should yield very consistent values for non-conjugated systems, the values obtained for highly conjugated systems such as those of benzene derivatives and other polynuclear aromatics will only be approximately true since the bond interaction terms introduced in the form of paramagnetic terms would vary with the differences in the conjugating abilities of the groups or atoms. Therefore, one method of studying the bond interactions that are involved in the conjugated systems is to find the apparent paramagnetic contributions of the compounds that are calculated by subtracting from the observed molecular susceptibilities, the diamagnetic susceptibilities (χ_d) obtained from polarizability data. The diamagnetic bond constants given by DORFMAN were derived mostly from polarizability data for the aliphatic compounds where conjugation effects are minimum and therefore these values can conveniently be used for the evaluation of $\chi_{p(apparent)}$. The apparent paramagnetic contributions for monosubstituted benzenes and monosubstituted naphthalenes can thus be calculated and compared.

The apparent χ_p values calculated by the above method for monosubstituted benzenes and for naphthalene derivatives are given in Table VI. The cumulative error involved in the calculation of χ_d by using the bond constants given by DORFMAN is ± 0.5 units.

Table VI

Apparent paramagnetic contributions of various monosubstituted benzenes and naphthalenes calculated by the method of Dorfman

No.	Substituent	Monosubstituted naphthalene			Monosubstituted benzene		$\chi_p \times 10^6$ for		
		Molar susceptibility $\times 10^6$		$\chi_d \times 10^6 \pm 0.5$	$\chi_M \times 10^6$	$\chi_d \times 10^6 \pm 0.5$	benzene derivatives	α-naphthalene	β-naphthalene
		α	β						
1	$-CH_3$	102.20	103.60	119.13	65.78	76.98	11.20	16.93	15.53
2	$-Cl$	103.00	107.30	124.63	69.56	82.48	12.92	21.63	17.33
3	$-OH$	95.19	98.06	116.13	61.27	73.98	12.71	20.94	17.07
4	$-OCH_3$	104.28	109.10	128.13	72.34	85.98	13.64	23.85	19.03
5	$-NH_2$	96.23	100.48	116.18	62.76	74.03	11.27	19.95	15.70
6	$-COOH$	104.00	105.60	132.13	70.71	89.98	19.27	28.13	26.13
7	$-COCH_3$	106.80	110.00	136.13	72.44	93.98	21.44	29.33	26.13
8	$-Br$	111.80	118.00	141.70	81.34	99.43	18.09	29.90	23.70
9	$-NO_2$	96.02	...	130.18	61.44	88.03	26.59	34.16	...

Considering the error involved in the calculation of these values, the paramagnetic values between of monosubstituted naphthalenes and the respective monosubstituted benzenes can be compared. DORFMAN attributed a paramagnetic value of 1.6 units to each C⋯C bond in the ring system and hence a difference of 8 units in χ_p value should normally be expected upon going from a benzene derivative to the corresponding naphthalene derivative. However, on passing from benzene to naphthalene, the observed paramagnetic increment is about 5 units. This apparently indicates the increased delocalization of the π electrons in the naphthalene rings. The delocalization of the π electrons depends strongly on the substituent. Further, the steric effect caused by the peri-hydrogen should also be taken into account. It can be seen from Table VI that the χ_p contribution on passing from a benzene derivative to the corresponding α-naphthalene derivative varies from about 5 to 12 units, whereas it is about 4—5 units in the β-isomers. This large difference in χ_p in the case of α-naphthalene derivatives could be accounted for only by taking into account the peri-interaction in the α-derivatives. The nuclear magnetic resonance studies of DUDEK [21], the dipole moment studies of LUTAKII and KOCHERGINA [22], RICHARDS and WALKER [23] and BALASUBRAMANIAN [11] on many substituted naphthalenes showed that the steric effect due to the peri-hydrogen affected largely the conjugation of the groups in position 1 with the ring.

From a study of the reaction rates of naphthalene derivatives, it has been shown by PACKER, VAUGHAN and WONG [24] that the peri C–H group of naphthalene has a slightly greater steric effect than an *ortho*-methyl substituent of a benzene derivative, since the strain in α-methyl naphthalene is measurably greater than that in *o*-xylene. These observations are consistent with the present magnetic studies.

A similar observation was also made by DIPPY, HUGHES and LAXTON [25] from dissociation studies of naphthoic and benzoic acids. The conjugation existing between the carbonyl group and the benzene ring, to be fully functional, demands the favoured position provided by coplanarity. If the latter is obstructed by bulky substituents in the adjacent position, by twisting of the carbonyl group out of the plane of the ring, the —M effect of the carboxy group is lowered and consequently the acid becomes stronger. Therefore, the greater the obstruction of resonance, the stronger will be the acid. HOOP and TEDDER [26] and FISHER *et al.* [27] also observed an increased dissociation constant for α-naphthoic acid relative to β-naphthoic acid. However, the strengths of β-naphthoic and benzoic acid are found to be closely similar. In line with these observations, it is found in the present magnetic investigations that the paramagnetic increment on passing from a benzene derivative to the corresponding β-naphthalene derivative is about 4—5 units in all compounds and this is again close to what is observed on passing from benzene to naphthalene.

Studying the effect of substituents on the ultraviolet absorption bands of naphthalene derivatives, OSKENGAENDLER and GENDRIKOV [28] have taken the displacement of the primary band ($\Delta\lambda$) as a measure of the magnitude of the peri-effect in α-substituted naphthalenes and arranged the groups in the order of peri-effect as $Br > Cl > OCH_3 > COOH$. Considering the magnitude of the paramagnetic increment upon going from a benzene derivative to the corresponding α-naphthalene derivative as an index of the extent of steric hindrance, the order of peri-effect is suggested to be $Br > OCH_3 > COOH > Cl$ from the present magnetic study. This order closely follows the one suggested by OSKENGAENDLER and GENDRIKOV.

REFERENCES

[1] FINAR,: Organic Chemistry, p. 610. Longmans Green and Co. 1955
[2] De LASZLÓ, H. G.: Proc. Roy. Soc. (London), **111A**, 355 (1926)
[3] NAKATA, N.: Bull. Chem. Soc. Japan, **10,** 318 (1935)
[4] EVERARD, K. B., SUTTON, L. E.: J. Chem. Soc. 2312 (1949)
[5] BATSANOV, S. S., PAKHONOV, V. T.: Vestan. Misk. Univ. Ser. Fiz. Mat. Estesven. Nauk, No. 1, 65 (1965)
[6] LE FEVRE, SUNDARAM, A.: J. Chem. Soc. 4756 (1962)
[7] PACAULT, A.: Ann. Chim., **12,** 527 (1946)
[8] LUFEROVA, M. A., SYRKIN, Ya. K.: Izv. Akad. Nauk. SSSR Ot del. Khim. Nauk 380 (1954)
[9] ANGUS, W. R., HOLLOWS, P. B. STOTT, G., KHANOLKAR, D. D., LEWELLYN, G. I. W.: Trans. Faraday Soc., **55,** 890 (1959)
[10] SHANMUGASUNDARAM, V., SABESAN, R., KRISHNAN, S.: Z. Phys. Chem. (Leipzig), **252,** 209 (1973)
[11] BALASUBRAMANIAN, V.: Thesis, Annamalai University 1964
[12] HAMPSON, G. C., WEISSEBERGER,: J. Chem. Soc., 393 (1936)
[13] PARTS,: Z. Phys. Chem., **10,** 264 (1930)
[14] HIGASHI,: Bull. Inst. Phys. Chem. Res. (Tokyo) **12,** 771 (1933)
[15] VASIL'EV, V. G., SYRKIN, Ya. K.: Acta Physicochimica URSSR **14,** 414 (1941)
[16] SRIRAMAN, S., SHANMUGASUNDARAM, V., SABESAN, R.: J. Annamalai Univ. Sci., **27,** 213 (1969)
[17] INGOLD, C. K.: Structure and Mechanism in Organic Chemistry, p. 193. Cornell University Press, Ithaca 1953
[18] PASCAL, P., PACAULT, A., HOARAU, J.: Compt. rend. **233,** 1078 (1951)
[19] DORFMAN, Y. A.: Diamagnetism and the Chemical Bond, p. 353. Edward Arnold Publishers Ltd. 1965
[20] YANG, T. Y.: J. Chem. Phys., **16,** 865 (1948)
[21] DUDEK, G. O.: Spectrochim. Acta., **19,** 691 (1963)
[22] LUTAKII, A. E., KOCHERGINA, L. A.: Zh. Fiz. Khim., **33,** 320 (1959)
[23] RICHARDS, J. H., WALKER, S.: Tetrahedron **20,** 841 (1964)
[24] PACKER, J., VAUGHAN, J., WONG, E.: J. Am. Chem. Soc. **80,** 905 (1958)
[25] DIPPY, J. F. J., HUGHES, S. R. C., LAXTON, J. W.: J. Chem. Soc., 1470 (1954)
[26] HOOP, G. M., TEDDER, J. M.: J. Chem. Soc., 4853 (1962)
[27] FISHER, A., MITCHELL, W. J., TOPSOM, R. D., VAUGHAN, J.: J. Chem. Soc., 2892 (1963)
[28] OSKENGAENDLER, G. M., GENDRIKOV, E. P.: Zh. Obshch. Khim., **29,** 3857 (1959)

V. SHANMUGASUNDARAM, Annamalainagar 608101, Tamil Nadu, S. India

Acta Chimica Academiae Scientiarum Hungaricae, Tomus 96 (2), pp. 161—166 (1978)

INFRARED STUDIES ON ANILS AND THEIR COMPLEXES, II

R. K. UPADHYAY,* RASHMI R. BANSAL, A. KUMAR and Arun K. BAJPAI

(N.R.E.C. College, Khurja-203131, India)

Received February 9, 1977
In revised form August 11, 1977

Ketoanils obtained by reacting 3-benzoylmethylglyoxal with different substituted primary aromatic amines have been characterized by infrared spectroscopy. The effect of the nature and position of substituents on the azomethine group of anils has been studied.

Four anils derived from *p*-dimethylamino-, *p*-diethylamino-*p*-bromo- and *p*-iodoanilines have been used for complexation with Os(VIII) and Au(III), and the sites of coordination, relative stabilities and structures of the complexes have been deduced from the IR spectra.

Introduction

In continuation of our previous work on infrared studies of anils [1—4] and their complexes [5—8], the present communication reports the extensive infrared studies of several new anil products of 3-benzoylmethylglyoxal and aromatic primary amines and their complexes. In this paper we deal with the influence of the nature and position of the substituent on the characteristic azomethine (C=N) groups of anils, the influence of electron repelling ability of the *para*-substituent on the complex stability, and stability orders and structural changes during complexation. Almost all the principal bands in each anil spectrum have been characterized.

Experimental

The methods of the synthesis and analysis of anils have been reported [9]. Complexes isolated following the method of UPADHYAY and BANSAL [10] were analyzed for their nitrogen and metal contents at C.D.R.I. Lucknow and the results are presented in Table II. The molar conductance (ΛM) of the complexes (Table II) was determined with Toshniwal's conductivity bridge. Infrared spectra of the anils in KBr pellets were recorded on a Perkin–Elmer infracord spectrophotometer; the frequencies with their tentative assignments [1—8, 11—14] are given in Table I. The IR spectra of the anils and their complexes were recorded on a Beckmann 621 spectrophotometer in Nujol mull using CsF optics.

Results and discussion

The influence of the nature and position of the substituents has been studied on the characteristic azomethine group of the anils. In order to study

* Postal address: 57, Chhatta Street, Khurja-203131, India

the effect of the nature of the substituent, *para*-substituted anils have been selected as this position is the most effective in establishing the characteristics of the molecules. In *para*-anils the azomethine group frequencies follow the order $OCH_3 < N(C_2H_5)_2 < OH < I < Br < C_6H_4—R < NO_2 < N(CH_3)_2 < Cl$, which is identical to the order of electron withdrawing nature of the substituents, except for the $N(CH_3)_2$ group, which shows a higher frequency than expected. This reveals that a weaker electron-withdrawing substituent will impart greater stability to the C=N bond. The effect of the position of the azomethine substituent has been studied on all the ternary and binary isomeric

Table II

Formulas, analyses and molar conductances of the complexes

Formula	Analysis				Molar conductance (electrolytic nature)
	Nitrogen (%)		Metal (%)		
	Calcd.	Found	Calcd.	Found	
$OsO_2A_2Cl_4$	5.87	5.71	20.13	20.00	37.27 (1 : 4)
$OsO_2B_2Cl_4$	5.54	5.44	19.01	19.20	30.51 (1 : 4)
$OsO_2C_2Cl_4$	2.73	2.61	18.72	18.60	28.73 (1 : 4)
$OsO_2D_2Cl_4$	2.50	2.44	17.14	17.00	27.80 (1 : 4)
$AuCCl_3$	2.21	2.13	31.13	31.00	18.25 (1 : 1)
$AuDCl_3$	2.05	1.93	28.98	28.74	18.05 (1 : 1)

sets of anils. In all the isomeric anils the azomethine group frequencies fall in the order $m < p \leqslant o$, except in nitroanils, which show a reverse order on account of the highest electron-withdrawing character of their substituted group. These results evidently show the maximum stability of *meta*-anils with C_6H_4-R, OH and OCH_3 substituents, whereas nitro substituents will impart maximum stability on *ortho*-anils.

The infrared data (Table III) of the anils derived from *p*-dimethylamino-*p*-diethylamino-, *p*-bromo- and *p*-iodoanilines (abbreviated as A, B, C and D, respectively) and their complexes reveal considerable perturbation in most of the frequencies of anils on complexation. Participation of the carbonyl and azomethine groups of anils in coordination with metal ions is quite obvious from the lowering of their frequencies on complexation. The appearance of new bands corresponding to M–O and M–N bonds in the complex spectra is in sup-

Table I

Infrared frequencies of anils in KBr with their tentative assignments

R–C_6H_4,NO_2(o–)	R–C_6H_4,NO_2(m–)	R–C_6H_4,NO_2(p–)	R_2–C_6H_4(o–)	R_2–C_6H_4(m–)	$R_2C_6H_4$(p–)	R–C_6H_4,OH(o–)	R–C_6H_4,OH(m–)	R–C_6H_4,OH(p–)	R–C_6H_4,OCH_3(o–)	R–C_6H_4,OCH_3(p–)	R–C_6H_4,I(p–)	R–C_6H_4,Br(p–)	R–C_6H_4,Cl(p–)	R–C_6H_4,$N(CH_3)_2$(p–)	R–C_6H_4,$N(C_2H_5)_2$(p–)	Assignment
3534 s	—	3509 w	—	3205 w	—	—	—	—	3472 w	—	—	—	—	3436 w	—	C–H Str. (alkyne + aromatic)
3390 s		3378 m														
—	—	—	—	—	—	3165 m	3155 m	3077 s	—	—	—	—	—	—	—	O–H Str. phenolic
—	3155 m	—	2976 w	—	3106 w	—	—	—	3012 w	—	3195 m	3175 m	3077 w	2899 w	3003 w	C–H Str. aromatic
1653 s	1712 sh, w	1650 s	1681 s	1667 sh, m	1675 sh, m	1725 sh, w	1667 sh, w	1667 sh, w	1629 s	1681 sh, w	1709 sh, w	1667 sh, m	1639 s	1667 sh, w	1626 s	C=O Str.
1592 s	1667 m	1610 s	1605 s	1587 s	1605 s	1600 m	1587 s	1587 m	1597 s	1570 s	1600 s	1600 s	1639 s	1613 s	1582 s	C=N Str.
—	1600 s	—	—	—	—	—	—	—	—	—	—	—	1563 s	—	—	
1527 s	1520 s	1481 s	—	—	—	—	—	1515 s	1506 s	1527 s	—	1481 s	1504 s	1541 s	1524 s	C=C Str.
1445 s	—	1456 m	1441 w	—	1439 w	1449 m	—	—	1453 s	1456 s	1449 m	—	1456 s	1443 m	1447 m	
—	—	—	1370 s	—	—	—	—	1375 m	1385 w	1387 w	1387 m	1389 w	1387 w	1377 m	1370 s	C–N Str. (tertiary aromatic)
1355 s	1348 s	1302 s	—	—	—	—	—	—	—	—	—	—	—	—	—	$C–NO_2$ Str.
—	—	—	—	—	—	—	—	—	1333 s	1342 s	—	—	—	1333 s	1333 s	CH_3 Symmetric bending
—	—	—	—	1316 m	1316 s	—	—	—	—	—	—	1323 m	1333 s	—	—	O–H Bending + C–O Str.
—	—	—	—	—	—	1316 w	1321 s	1325 m	—	—	—	—	—	—	1282 s	C–H in plane bending
1295 s	—	—	—	—	—	—	—	—	1292 s	1299 m	1282 m	—	1297 s	—	—	
1255 s	1258 m	—	—	—	—	—	—	—	—	—	—	—	—	—	—	N–O Str.
—	—	—	1258 m	—	1277 s	1267 m	—	1274 s	1256 s	1258 s	—	—	—	—	—	
—	—	—	—	—	1200 w	—	—	—	1214 m	1212 m	—	—	1206 m	—	—	
1185 s	1176 w	1195 m	1183 w	—	—	1183 w	—	1199 s	1182 m	1189 m	1183 w	1182 m	1189 m	—	—	
—	—	—	1156 w	—	—	—	1156 s	—	—	—	—	—	—	—	—	
1111 s	—	1121 s	1125 w	—	—	—	—	—	1130 s	—	—	1124 w	1124 w	—	—	
—	—	—	—	—	—	—	—	—	—	—	—	—	—	1214 s	1214 s	C–N Str. aliphatic
															1111 s	
—	—	—	—	1081 w	1089 w	—	—	—	1099 w	—	—	—	1098 m	1096 w	1091 m	
—	1073 w	—	1058 w	—	1063 w	—	1067 w	1075 w	1079 w	1075 w	1063 w	1071 s	1075 s	1075 w	1076 m	
1026 w	1028 w	—	1026 w	—	1029 w	1026 w	—	1031 w	1031 s	1042 s	1026 w	1030 m	1036 m	1035 m	1026 m	Benzene ring breathing
—	1004 w	1008 w	—	—	—	—	1004 m	1003 m	—	—	1005 m	1010 s	—	—	—	
970 w	—	—	986 w	—	—	—	—	—	966 w	—	—	—	985 w	967 m	—	C–H bending (*trans*-disubstituted alkene)
—	917 w	927 m	—	—	—	—	—	—	938 w	—	—	915 w	—	—	930 w	
882 w	—	—	—	—	—	—	—	866 w	858 s	866 w	—	—	864 w	862 m	864 w	C–H out-of-plane deformation
857 w	—	—	—	833 w	—	—	850 m	—	—	—	—	—	—	—	—	
—	—	—	—	—	855 m	—	—	833 m	—	847 m	828 w	—	847 s	835 m	833 w	C–H bending (two adjacent H-atoms)
—	800 w	—	—	—	—	—	—	—	—	—	—	—	—	—	—	
760 m	—	—	745 m	—	—	759 m	—	—	758 s	—	—	—	—	—	—	C–H bending (four adjacent H-atoms)
—	—	761 m	—	—	755 m	—	751 w	765 w	758 s	775 s	766 s	769 m	772 s	763 s	755 s	C–H bending (five adjacent H-atoms)
—	738 w	—	712 m	—	—	—	—	715 m	717 m	723 m	—	—	718 s	719 m	732 w	
706 w	694 m	704 w	—	694 m	707 w	696 w	701 m	—	698 w	698 w	693 m	692 m	694 m	694 w	698 w	C–H bending (*cis*-disubstituted alkene)
—	—	—	—	—	—	—	—	680 m	688 m	683 m	—	—	—	—	—	

s = strong; m = medium; w = weak; sh = shoulder;

$$R = CH_2 \begin{cases} COCH = N \\ COC_6H_5 \end{cases}$$

port of this fact. The shift for both the carbonyl and azomethine groups follows the order M—A > M—B > M—C > M—D (ligandwise) and Au(III) —L > Os (VIII) —L (metalwise) in agreement with the M–O and M–N bond frequency orders or stability orders, respectively. The shift of ligand bands corresponding to C=C (aromatic) to lower frequencies in their complexes indicates conju-

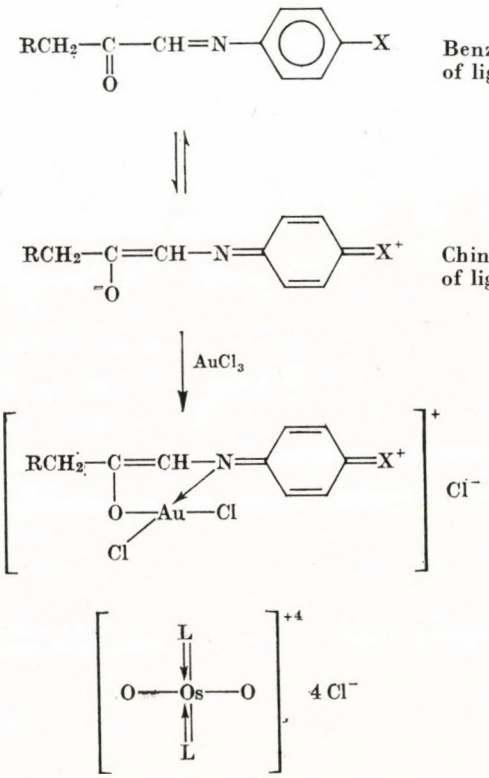

R = C_6H_5CO

X = $N(CH_3)_2$, $N(C_2H_5)_2$, Br or I

gation in the ligand upon chelation. If the doublet band appearing at 856, 834, 842 and 846 cm^{-1} in the ligands, respectively, is due to *para*-substitution, then its change to a singlet and its shift to lower values in the respective complexes may undoubtedly be attributed to the change from a benzenoide to a quinonoide structure upon chelation. A third new band, appearing only in the spectra of the Au(III) chelates in the frequency range of 314—342 cm^{-1}, has been assigned to the M–Cl bond.

Table III

Infrared frequencies of ligands and their

Ligand A	$AuACl_3$	$OsO_2A_2Cl_4$	Ligand B	$AuBCl_3$	$OsO_2B_2Cl_4$	Ligand C
						3525 m, d
3493 m, b	3429 m, b	—	—	—	3473 m	3413 m, b
—	—	—	—	—	3457 m, b	—
3109 m, b	—	—	—	3207 m	3277 m, b	3293 m
—	—	—	3165 w, b	—	—	—
1734 sh, m	1666 sh, m	1696 sh, m	1720 m	1656 sh, m	1696 m	1708 w
1708 sh, m	1640 sh, m	1660 m, b	1688 m	1624 m	1664 sh, m	1592 s
1636 s, b	1628 m	1608 m	1604 s	—	—	1626 s
—	1556 w	1580 m	1564 s, b	1596 m, b	1588 s	—
—	—	—	1508 s	1540 m	1552 s	1516 s
1240 s	—	—	—	—	—	—
1212 s	1232 w, b	1208 w	—	—	1204 w, b	—
1196 s	—	1176 w	1198 s	—	—	1172 s
—	—	1152 w	1154 s	—	1164 s	—
1128 s	1104 m, b	1132 m, b	1124 m	1142 m, b 1126 m	1108 s, b	1104 m
1066 s	1074 w	1048 w	1078 s	—	1074 m	1084 m
1026 s	—	1008 m	1026 s	1014 m	1014 s	1000 s
856 s	830 w	838 s	834 m	830 m	826 s	842 s
762 s	720 w	—	712 s	—	—	718 s
678 m	658 w	—	674 m	658 w	674 w	674 w
—	—	—	—	—	—	630 w
—	—	—	—	—	—	562 m
—	—	—	—	—	—	496 w
—	494 w	480 w		490 m	470 w	—
—	342 m	—	—	342 w	—	—
—	322 m	300 s	—	318 w	282 s, b	—

[sh = shoulder; s = strong; m = medium; w = weak;

It is worth noting that the medium may alter the ligand frequencies but not their frequency order. The intensity orders of the carbonyl, azomethine, M–O and M–N bonds are the same as the orders of chelate stability.

From the above it may be inferred that each ligand is bidentate, offering its adjacent carbonyl and azomethine groups for coordination. The benzoyl carbonyl group, being at a more remote position, does not form a coordinate bond with metal ions. The process of chelation and the chelate structures are shown on p. 163.

complexes in Nujol mull with assignments

$AuCCl_3$	$OsO_2C_2Cl_4$	Ligand D	$AuDCl_3$	$OsO_2D_2Cl_4$	Assignment
3429 m, b	—	—	3405 m, d	3549 m	C–H Str. (alkyene)
—	—	—	—	—	
—	—	3253 m	—	—	C–H Str. (aromatic)
		3189 m, b			
3101 w	3085 m	3133 m, b	3157 m	3127 s, b	
1648 m	1684 m	1688 w	1628 m	1680 m	C=O Str.
1564 m	1568 m	1584 s	1566 s	1574 m	C=N Str.
1600 m	1616 m	1620 s	1616 s	1628 m	C=C Str (aromatic)
—	—	—	1592 s	1604 m	
1504 m	1520 m	1522 m	1512 m	1552 m	
—	—	—	—	1248 w, b	C–N Str. (aliphatic)
1218 w, b	1202 m	—	1224 w	1200 m	
1196 w, b	1174 m, b	1190 s	1180 s	—	
1136 m	—	—	1140 m	—	
1100 m	1114 m	1122 m, b	1104 s	1108 w	
1068 s	1070 m	1090 m	—	1074 m	
1016 m	1014 m	1004 m	1000 s	1012 s	Benzene ring breathing
812 s	818 s	846 s	814 s	808 m	C–H bending (two adjacent H atoms) + 1,4 disubstitution
728 m	730 m, b	764 s	768 w	—	C–H bending (four adjacent H atoms)
676 w	—	678 m	652 w	660 m	C–H out-of-plane bending
612 m	626 m	—	—	—	C–Br Str.
—	530 m, b	570 m	—	520 m	C–Br Str. + C–I Str.
		512 m			
492 m	490 m	482 w	494 s, b	484 s, b	
468 w	462 w	—	462 m, b	448 s	M–N Str.
332 m	—	—	314 s	—	M–Cl Str.
296 m	282 m, b	—	290 m	268 m	M–O Str.

d = doublet; b = broad; M = metal

REFERENCES

[1] Upadhyay, R. K., Singhal, M. L., Saxena, A. K., Prasad, R.: Acta Chim. **83,** 299 (1974).
[2] Prasad, R.: Ph. D. Thesis, Meerut University, Meerut, India 1975
[3] Bansal, R. R.: Ph. D. Thesis, Meerut University, Meerut, India 1976
[4] Upadhyay, R. K., Bansal, R. R.: Indian J. Chem. (accepted for publication)
[5] Upadhyay, R. K., Singh, V. P.: Monatsh. Chem., **107,** 697 (1976)
[6] Upadhyay, R. K., Singh, V. P., Sharma, S. C.: J. Indian Chem., Soc., **51,** 781 (1974)
[7] Upadhyay, R. K., Singh, V. P.: Acta Chim. (In press)
[8] Upadhyay, R. K., Bansal, R. R.: J. Indian Chem. Soc. (In press)
[9] Upadhyay, R. K., Bansal, R. R.: Chromatographia, **9,** 582 (1976)
[10] Upadhyay, R. K., Bansal, R. R.: Monatsh. Chem., (in press)
[11] Dyer, J. R.: Applications of Absorption Spectroscopy of Organic Compounds, p. 37. Prentice Hall of India Pvt. Ltd., New Delhi 1969

[12] SAXENA, R. N., PANDEY, K. K.: J. Indian Chem. Soc., **49**, 782 (1972)
[13] NAKAMOTO, K.: Infrared Spectra of Inorganic and Coordination Compounds. John Wiley and Sons Inc. New York 1968
[14] MALIK, W. U., SAXENA, R. C.: J. Indian Chem. Soc., **45**, 307 (1968)

R. K. UPADHYAY
RASHMI R. BANSAL
A. KUMAR
ARUN K. BAJPAI
N. R. E. C. College, Khurja-203131, India.

Acta Chimica Academiae Scientiarum Hungaricae, Tomus 96 (2), pp. 167—181 (1978)

STEREOISOMERIC INDOLE ALKALOIDS OF QUEBRACHAMINE TYPE FROM *AMSONIA TABERNAEMONTANA* LEAVES

B. ZSADON, J. TAMÁS,* M. SZILASI, ZS. MAJER and P. KAPOSI**

*(Department of Chemical Technology, Eötvös Loránd University, Budapest, * Central Research Institute for Chemistry, Hungarian Academy of Sciences, Budapest, and ** Research Institute for Medical Plants, Budakalász)*

Received March 10, 1977

The alkaloid fraction A isolated from leaves (18 kg; air-dry) of *Amsonia tabernaemontana* collected before flowering was fractioned further by partition based on the base strength and by column chromatography: vincadine (3.45 g), epivincadine (64 mg), (+)-6,7-dehydrovincadine (670 mg) and (+)-6,7-dehydroepivincadine (545 mg) were obtained. The first two substances were subjected to fractional crystallization yielding crystalline (−)-vincadine (1.8 g), (±)-vincadine (850 mg) and crystalline (±)-epivincadine (22 mg). The products were identified by physical constants, chemical reactions, hemi-synthesis and mass spectrometry.

Furthermore, all stereoisomeric 3-hydroxymethylquebrachamine derivatives corresponding to the 3-carbomethoxyquebrachamine derivatives were prepared and their comparative mass spectrometric examination was carried out. The C_3-epimers could well be distinguished in these cases, too, and the results provided additional evidence for the usefulness of mass spectrometry in the identification of stereoisomers.

Earlier, isolation of quebrachamine [1] and vincadine (3-carbomethoxyquebrachamine) [2] from leaves of *Amsonia tabernaemontana* grown in Hungary was reported. Later, in a short communication [3] it was also published that in the slightly alkaline alkaloid fraction isolated from the leaves all the four possible stereoisomers of 3-carbomethoxyquebrachamine were identified; these are (—)-vincadine (**Ia**), (+)-vincadine (**IIa**) and their C_3-epimers (**IIIa** and **IVa**, respectively); furthermore, (+)-6,7-dehydrovincadine (**Va**) and its C_3-epimer (**VIa**) were isolated and their structures proved. Recently, WENKERT *et al.* [4] effected the conformational analysis of these quebrachamine derivatives by the use of the ^{13}C—NMR technique.***

In view of the phytochemical, theoretical and preparative importance of these natural indole alkaloids, details of our work not published up to now are reported in this paper.

*** In the present paper, the configurations of the C_3 and C_5 centres of asymmetry of quebrachamine derivatives will be denoted as suggested in Ref. [4], in accordance with the results of the conformational analysis.

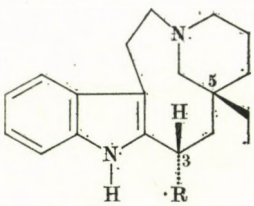

Ia: R=$COOCH_3$

Ib: R=CH_2OH

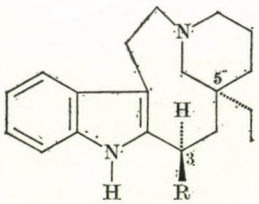

IIa: R=$COOCH_3$

IIb: R=CH_2OH

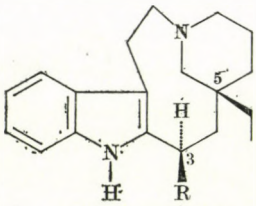

IIIa: R=$COOCH_3$

IIIb: R=CH_2OH

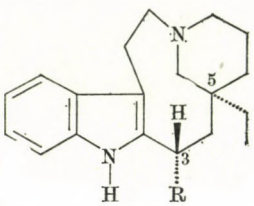

IVa: R=$COOCH_3$

IVb: R=CH_2OH

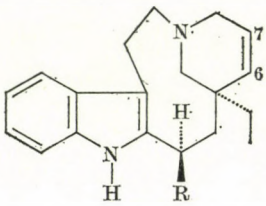

Va: R=$COOCH_3$

Vb: R=CH_2OH

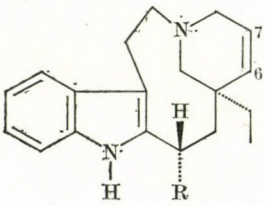

VIa: R=$COOCH_3$

VIb: R=CH_2OH

Methods of isolation and results

Amsonia tabernaemontana grown at the Research Institute for Medical Plants (Budakalász, Hungary) was used for our investigations. Since it had been observed that after having cut the shoots in the spring or early summer the fresh shoots appearing contained relatively higher amounts of alkaloids [5], in the present work the green plant material from the third cutting was used.

The raw material (18 kg of air-dry leaves) was exhaustively extracted with methanol as described earlier [1, 2]. The extract was purified and rutin and the raw alkaloid mixture was isolated from it (Fig. 1).

After clarification, the main alkaloid, (+)-vincadifformine [6, 5] (100 g), was isolated from the raw alkaloid mixture in the form of crystalline hydrochloride. The other alkaloids were isolated from the mother liquor in the form of a mixture of bases, and these were separated into two fractions by partition utilizing differences in the base strength. Fractions A and B had contained the weaker and the stronger bases, resp. (Fig. 2). Further on we shall deal with fraction A only (as for fraction B, see Ref. [1]).

Previously, fraction A was subjected to chromatographic separation on an alumina column and three sub-fractions were obtained (A_I, A_{II} and A_{III}). Sub-fraction A_{II} yielded tabersonine [1] and (+)-vincadifformine [6], while lochnericine and tetrahydroalstonine [7] were isolated from sub-fraction A_{III}.

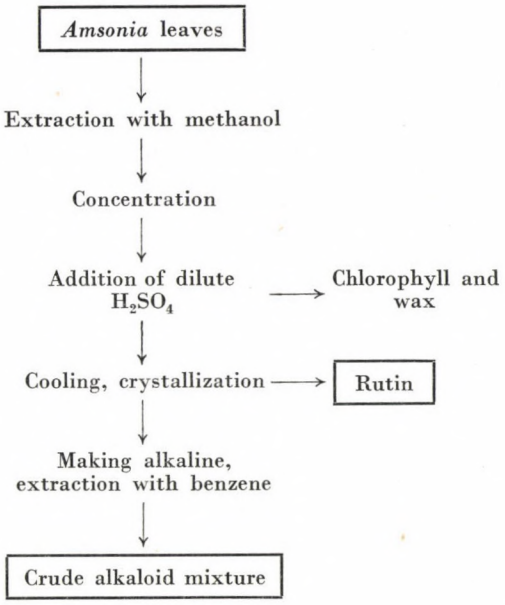

Fig. 1

Sub-fraction A_I containing the weakest bases yielded first only vincadine [2], however, it was found later [3] that this consisted of vincadine and (+)-6,7-dehydrovincadine isomers (Fig. 3).

The components of sub-fraction A_I were successfully separated on the basis of the differences in their base strengths (Table I) and their chromatographic behaviour, as shown in Fig. 4.

When, similarly to the present processing procedure, first the main alkaloid (+)-vincadifformine is separated from fraction A, there is no need for separating the A_I and the other sub-fractions, and the most advisable procedure is direct fractionation of fraction A according to Fig. 4. Of course, in this case the components of the sub-fractions A_{II} and A_{III} are present as

Table I

Alkaloid	pK_a (in 50% ethanol)
Vincadine	7.20
6,7-Dehydrovincadine	6.75
Epivincadine	5.20
6,7-Dehydroepivincadine	4.41

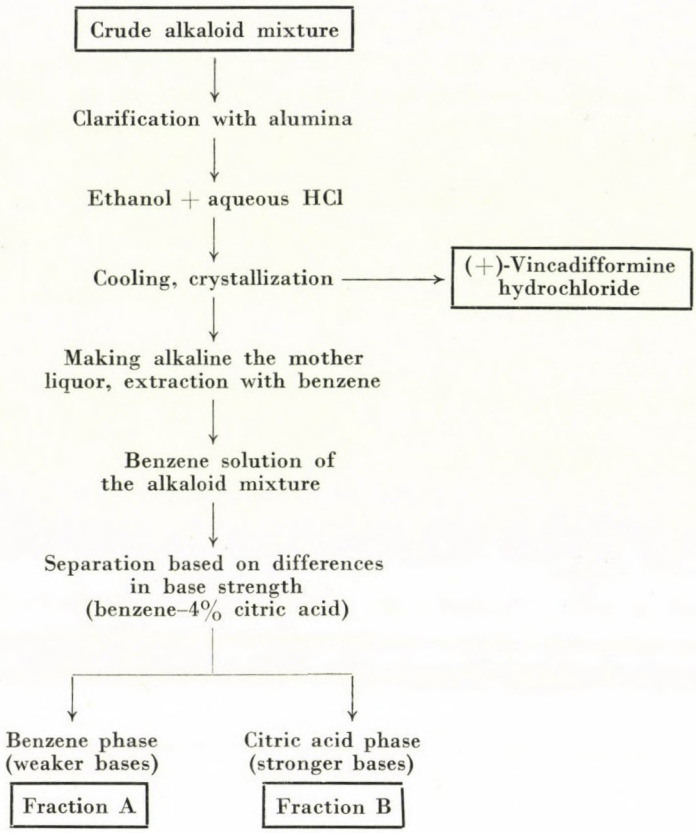
Crude alkaloid mixture
Clarification with alumina
Ethanol + aqueous HCl
Cooling, crystallization
(+)-Vincadifformine hydrochloride
Making alkaline the mother liquor, extraction with benzene
Benzene solution of the alkaloid mixture
Separation based on differences in base strength (benzene–4% citric acid)
Benzene phase (weaker bases)
Citric acid phase (stronger bases)
Fraction A
Fraction B

Fig. 2

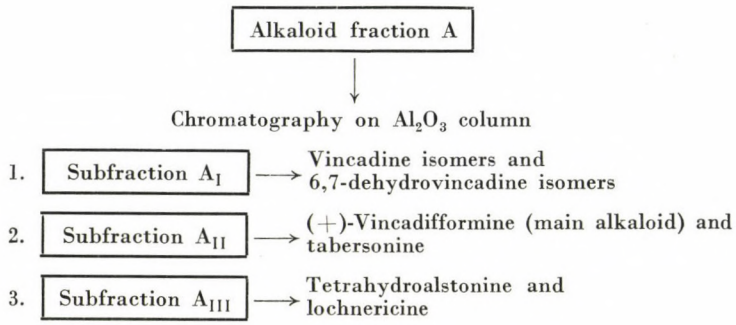
Alkaloid fraction A
Chromatography on Al_2O_3 column
1. Subfraction A_I → Vincadine isomers and 6,7-dehydrovincadine isomers
2. Subfraction A_{II} → (+)-Vincadifformine (main alkaloid) and tabersonine
3. Subfraction A_{III} → Tetrahydroalstonine and lochnericine

Fig. 3

contaminants, but can be removed relatively simply in the chromatographic purification procedure (which is anyway necessary). (See Experimental.)

When working according to the above scheme, 18 kg of green *Amsonia* leaves yielded 3.45 g of vincadine, 670 mg of (+)-6,7-dehydrovincadine (**Va**), 64 mg of epivincadine and 545 mg of (+)-6,7-dehydroepivincadine (**VIa**).

The products (+)-6,7-dehydrovincadine (**Va**) and (+)-6,7-dehydroepivincadine (**VIa**) were obtained as chromatographically pure amorphous solids (foamed, solidified evaporation residues). Both products were the pure dextrorotatory enantiomers, which could be confirmed unambiguously partly by hemi-synthesis starting from authentic natural tabersonine (**Xa**) [8], partly by their conversion in a catalytic hydrogenation process into (+)-vincadine (**IIa**) and (+)-epivincadine (**IVa**), respectively.

Vincadine isolated according to the scheme in Fig. 4 was a mixture of the two optical antipodes (**Ia** and **IIa**) where (—)-vincadine (**Ia**) was predominating (calculated to be about 85% of the mixture). Crystalline (—)-vincadine (1,8 g) and (±)-vincadine (850 mg) were obtained from the mixture by fractional crystallization.

Similarly to the above cases, the epivincadine isolated was also a mixture of the respective optical antipodes (**IIIa** and **IVa**) and the laevorotatory enantiomer was predominating. Crystallization of the mixture yielded only (±)-epivincadine in pure crystalline form (22 mg).

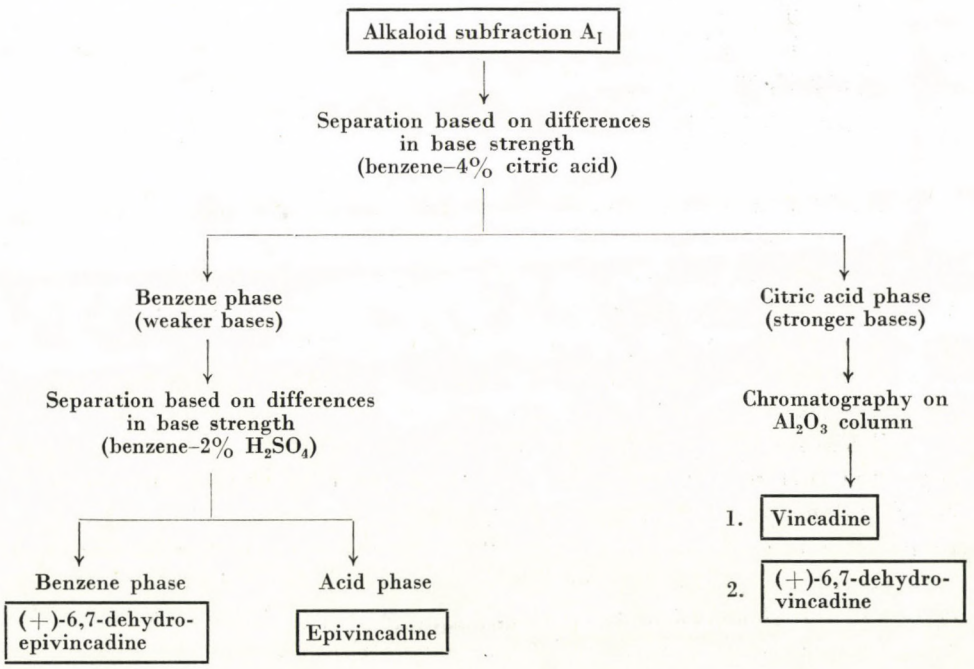

Fig. 4

Chemical conversions and hemi-syntheses

A common characteristic of the natural alkaloids described above is that the carboxylic acids formed in their acid hydrolysis can easily be decarboxylated. In this way, (—)-vincadine (**Ia**) was converted into (—)-quebrachamine (**VII**); (±)-vincadine and (±)-epivincadine into (±)-quebrachamine; and (+)-6,7-dehydrovincadine (**Va**) and (+)-6,7-dehydroepivincadine (**VIa**) into (+)-6,7-dehydroquebrachamine (**VIII**), in high yields.

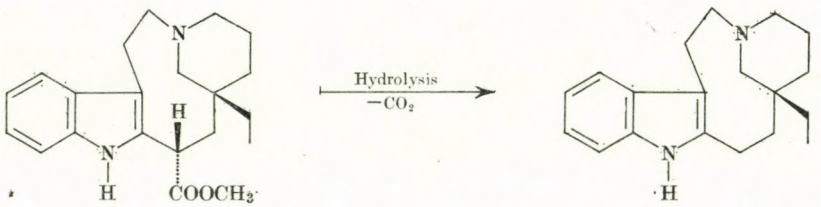

Ia **VII**

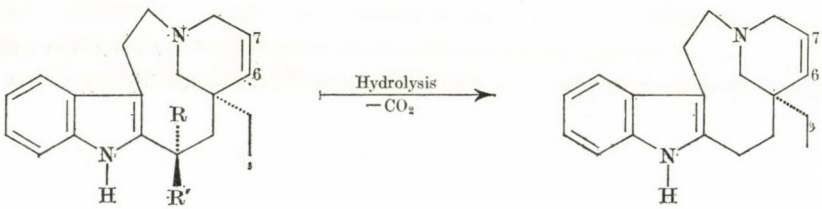

Va: R=H, R′=$COOCH_3$

VIa: R=$COOCH_3$, R′=H

VIII

Rapid decarboxylation of the carboxylic acids formed as a result of hydrolysis is strongly related to the fact that in these quebrachamine derivatives the carbomethoxy group is attached to C_3. The carboxylic acid of structure **IXa** can easily be protonated at the β carbon atom of the indole, with subsequent conversion into the β-iminocarboxylic acid **IXb**; this can release carbon dioxide in the well-known way [9] and the decarboxylated product **IXc** will rearrange into the tautomeric compound, **IXd**, by proton migration.

When starting from tabersonine and vincadifformine, the hemi-synthesis suggested first by HOIZEY *et al.* [10] was applied in the preparation of all 3-carbomethoxyquebrachamine derivatives isolated, and this is partly of preparative importance, partly constitutes additional evidence for the structures. Authentic [8] tabersonine (**Xa**) was converted into (+)-6,7-dehydrovincadine (**Va**) and the C_3 epimer (**VIa**); authentic [8] (—)-vincadifformine (**Xb**) gave (+)-vincadine (**IIa**) and the C_3 epimer (**IVa**); and authentic [6] (+)-vincadifformine (**XI**) was converted into (—)-vincadine (**Ia**) and the C_3 epimer

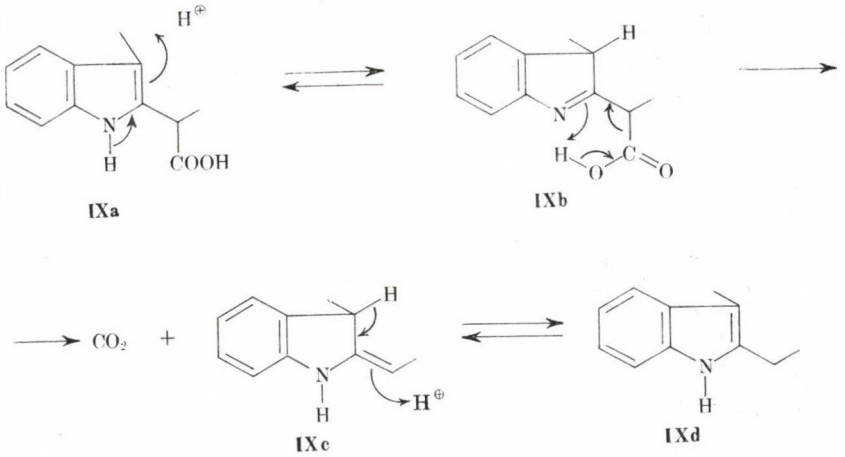

(**IIIa**), in high yields. The products obtained from the hemi-synthesis and the racemates prepared from them proved to be identical with the corresponding natural *Amsonia* alkaloids in all respects.

The 6,7-dehydroquebrachamine derivatives can be saturated by catalytic hydrogenation. In this way, (+)-6,7-dehydrovincadine (**Va**) was converted into (+)-vincadine (**IIa**) and (+)-6,7-dehydroepivincadine (**VIa**) was converted into (+)-epivincadine (**IVa**).

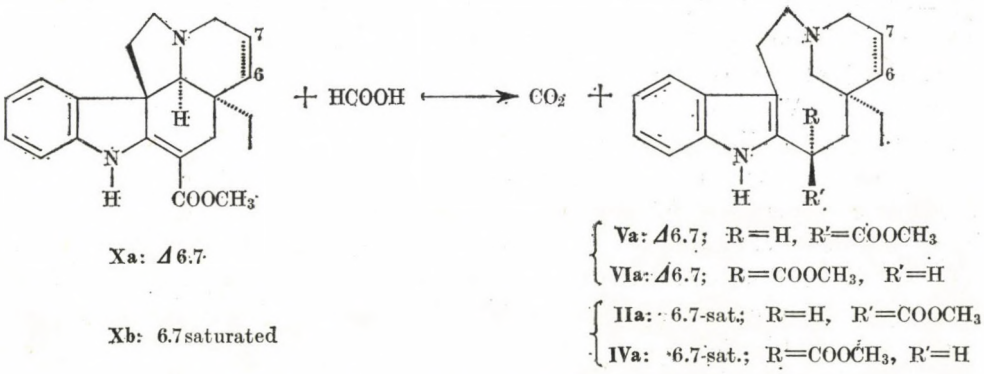

Xa: Δ6.7

Xb: 6.7 saturated

Va: Δ6.7; R=H, R′=COOCH$_3$

VIa: Δ6.7; R=COOCH$_3$, R′=H

IIa: 6.7-sat.; R=H, R′=COOCH$_3$

IVa: 6.7-sat.; R=COOCH$_3$, R′=H

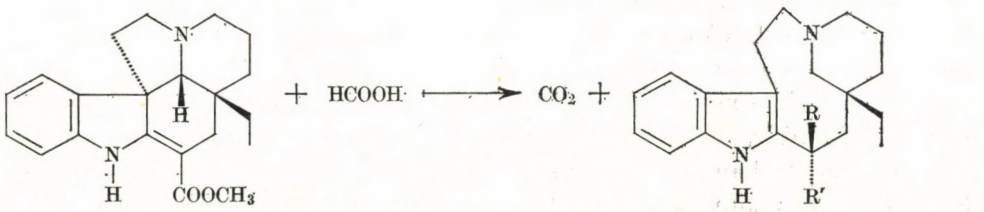

XI

Ia: R=H, R′=COOCH$_3$

IIIa: R=COOCH$_3$, R′=H

In methanol solution and in the presence of sodium methoxide, 3-carbomethoxyquebrachamine derivatives undergo epimerization. Particularly easily can this be achieved with the sensitive 6,7-dehydrovincadine. The conversion takes place also in benzene solution at room temperature in the presence of silica gel.

The 3-carbomethoxyquebrachamine derivatives can be converted quantitatively by reduction with lithium aluminium hydride into the corresponding 3-hydroxymethylquebrachamine derivatives. This fact is, besides its preparative importance, another evidence for the structure of the natural alkaloids isolated. In this way all the four stereoisomeric 3-hydroxymethylquebrachamines (**Ib, IIb, IIIb** and **IVb**), as well as the two epimeric 3-hydroxymethyl-6,7-dehydro-(+)-quebrachamines (**Vb** and **VIb**) were prepared. These derivatives played a role in the conformational analysis of alkaloids of quebrachamine type carried out by WENKERT *et al.*, too [4].

Mass spectrometric investigations

Mass spectrometric studies on vincadine isomers and 6,7-dehydrovincadine epimers have been reported in earlier papers [2, 3]. Data of the low-resolution and high-resolution mass spectra indicated unambiguously that each of the vincadine isomers corresponds to 3-carbomethoxyquebrachamine (**Ia—IVa**), while the 6,7-dehydrovincadine epimers correspond to 3-carbomethoxy-6,7-dehydroquebrachamine (**Va** and **VIa**). The enantiomers (**Ia** and **IIa**; **IIIa** and **IVa**) had identical spectra, the C_3 epimer pairs (**Ia** and **IIIa**; **IIa** and **IVa**; **Va** and **VIa**) have mass spectra with significant differences which also allowed making distinction between them.

The mass spectra of the products prepared by $LiAlH_4$ reduction from vincadine isomers and 6,7-dehydrovincadine epimers confirm unambiguously that all these compounds are 3-hydroxymethylquebrachamine derivatives (**Ib—VIb**), and their mass spectrometric behaviour is very similar to that of the analogous 3-carbomethoxy compounds. (Mass spectra of compounds **Ib—VIb** are shown in Fig. 5.)

Similarly to the case of vincadine enantiomers (**Ia** and **IIa**), the mass spectrometric behaviour of the 3-hydroxymethylquebrachamine enantiomers (**Ib** and **IIb**) prepared from them was also found identical. In their mass spectra an intense peak of molecular ions appears; the main fragments in the spectrum can be deduced by assuming splitting of the 9-membered ring, similarly to the case of quebrachamine [11] and 3-carbomethoxyquebrachamine [2] (see Scheme 5). The splitting of the 9-membered ring involves processes *a* and *c* being particularly important in the present case. Process *a* occurs practically only in the H-migration version, and both molecule parts can be observed as

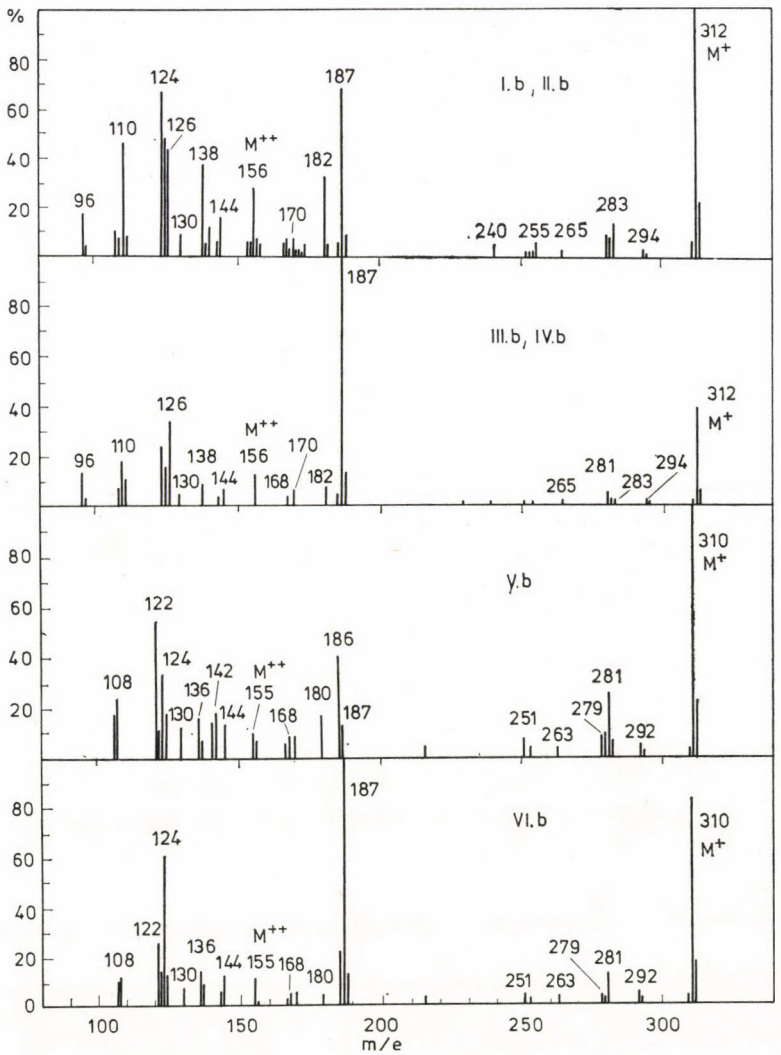

Fig. 5

charged particles (*m/e* 130 and 182). At the same time, process *c* occurs frequently without H-migration, too, and then the charge is localized at the *m/e* 187 fragment comprising the indole part, while in the H-migration version the fragment carrying the positive charge is primarily the piperidine part (*m/e* 126).

Mass spectra of the corresponding C_3-epimer antipodes (**IIIb** and **IVb**) are identical, and a significant difference exists between these and the former two compounds (**Ib** and **IIb**) in the relative abundances of several ions. The significantly lower stability of the molecular ion is particularly striking here, the

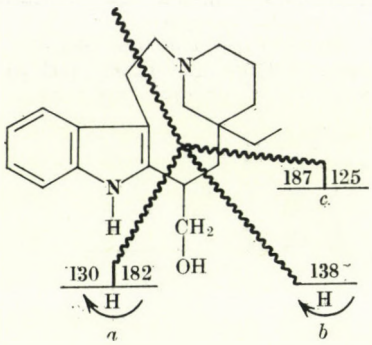

homolytic splitting *c* (formation of the ion *m/e* 187) comes into prominence, while process *a* (formation of the ion at *m/e* 182) is restricted. This property is entirely analogous to the observed behaviour of epimers of carbomethoxy compounds [3].

In the mass spectrum of the pair of epimers of 3-hydroxymethyl-6,7-dehydroquebrachamine (**Vb** and **VIb**) (lower part of Fig. 5) the mass number of the fragments containing the piperidine part is lower by 2, owing to the double bond at C-6,7. Otherwise, the processes are the same as with the 6,7-saturated compounds (**Ib**—**IVb**). The effect caused by the C_3-epimerism is also identical: the stability of the molecular ion decreases, and the formation of *m/e* 180 and 130 ions is restricted in **VIb**, as compared with the *m/e* 187 ions formed in process *c*. (The abundance ratios of the *m/e* 180 and *m/e* 187 ion species differ by one order of magnitude.)

This great change in the ratio of processes *a* and *c* seems to be characteristic of the C_3-epimers, irrespective of the nature of the substituent at C_3, thus it has a diagnostic value in studying these stereoisomers. (The preparation and mass spectrometric investigation of other C_3-epimeric quebrachamine derivatives are in progress.)

There is an interesting difference between the saturated (**Ib**—**IVb**) and unsaturated (**Vb**—**VIb**) compounds: in the case of the 6,7-dehydro derivatives, in the H-migration version of process *c*, the positive charge is often localized in both molecule parts. (Note the significant intensity of the ion *m/e* 187 besides the complementary ion *m/e* 124.)

Experimental

M.p.'s are uncorrected. Optical rotation was measured with a Schmidt–Haensch polarimeter, the UV and IR spectra were recorded with an Optica Milano CF 4R and a Spectromom 2000 instrument, respectively.

The mass spectra were recorded with a mass spectrometer of type AEI MS-902 (double focussing). This instrument was used in determining the exact masses, too. The sample was

introduced into the apparatus with a direct sampling system. The ionizing electron energy was 70 eV, the temperature of the ion source was 150 °C.

During isolation and the chemical reactions, the alkaloids were detected by means of TLC technique. Silica gel G layer, and benzene–ethanol (98 : 2) or benzene–ethyl acetate–methanol (40 : 40 : 20) developing solvent mixtures were used.

Isolation of alkaloids

In June, 1972, 20—30 cm green shoots, before flowering, were cut for processing; green shoots had been cut twice previously from the same stocks. The leaves were stripped and dried in air. A total amount of 18 kg of air-dry (8—9% moisture content) leaves was extracted in 1.2 kg portions.

The raw material was subjected to exhaustive extraction in Soxhlet extractor (Quickfit), and rutin, then a mixture of alkaloids was isolated from the extract in the manner described earlier [1, 2]. The raw alkaloid mixture obtained in the form of a benzene solution was 14—16 g from each 1.2 kg portion.

The benzene solutions containing the raw alkaloid mixture were concentrated to 70—80 ml under reduced pressure, mixed with an equal amount of petroleum ether and clarified on an aluminium oxide column (Brockmann II, 50 g). The column was rinsed with a mixture of benzene and petroleum ether (1 : 1, v/v) (600 ml); thus the weakly basic alkaloids (fraction A) could be completely eluted, together with the majority of more strongly basic alkaloids. The clarified solution was evaporated to dryness under reduced pressure, the residue (11—12 g from each portion) was dissolved in ethanol (25 ml), cooled to 0 °C and 1.25 N hydrochloric acid (100 ml) was added to it. Crystalline (+)-vincadifformine hydrochloride separated, which was found to be identical with an authentic sample [6] in all respects. In this way, a total of 100 g of (+)-vincadifformine hydrochloride was obtained from 18 kg of raw material.

The mother liquors were combined, the ethanol was evaporated at reduced pressure, the aqueous solution was made alkaline (pH 8) and the alkaloid bases were extracted with benzene (5 × 200 ml). The total extract content of the combined benzene phases was 76 g. The benzene solution was extracted with 4% aqueous citric acid solution (3 × 200 ml), the aqueous phases were then re-extracted with benzene (3 × 200 ml) in a counter-current procedure. The combined benzene solution contained the weakly basic alkaloid fraction A (14 g), while the more basic alkaloid fraction B (see Ref. [1]) (62 g) was in the citric acid solution.

Separation of the alkaloid fraction A

The benzene solution containing the alkaloid fraction A was concentrated to 200 ml under reduced pressure and the alkaloid mixture (14 g) was further fractionated by non-continuous counter-current extraction, in separatory funnels, with 1% aqueous citric acid (5 × 1000 ml) and benzene (5 × 200 ml). The benzene fractions Nos 1—3 contained the less basic components (4.8 g) consisting of epivincadine, 6,7-dehydroepivincadine and tabersonine, while in the citric acid fractions Nos 1—3 the relatively basic part was found, containing mainly vincadine and dehydrovincadine. The citric acid phases Nos 4 and No. 5 were made alkaline, extracted with benzene and the benzene solution was combined with the benzene phases No. 4 and No. 5. The 'residual' fraction obtained in this way had a total extract content of 3.6 g consisting of vincadine, dehydrovincadine, as well as vincadifformine, tabersonine and tetrahydroalstonine.

Isolation of epivincadine and (+)-6,7-dehydroepivincadine

The benzene solution of the less basic fraction (4.8 g) was concentrated to 100 ml under reduced pressure, then extracted with 2% sulfuric acid (25 × 100 ml). The benzene phase contained then no alkaloid; the total extract content was 1.95 g.

The combined sulfuric acid solution was made alkaline to pH 8, and the alkaloids were extracted with benzene (5 × 100 ml). After drying, the benzene solution (total extract content: 2.68 g) was concentrated to 50 ml under reduced pressure, then purified chromatographically on a silica gel column (60 g). The alkaloid mixture (660 mg) was eluted from the column with benzene (400 ml); it contained only epivincadine and 6,7-dehydroepivincadine according to

TLC. (Subsequently, 1.9 g of a mixture was eluted from the column with methanol; this contained coloured contaminants and tabersonine.)

The benzene eluate containing a mixture of epivincadine and dehydroepivincadine (660 mg) was concentrated to 100 ml under reduced pressure, then subjected to counter-current extraction, in separatory funnels, with 2% sulfuric acid (5 × 100 ml) and benzene (5 × 100 ml). In this process pure dehydroepivincadine appeared in the benzene phase; epivincadine and some dehydroepivincadine were found in the sulfuric acid phase. The latter phase was purified by repeated counter-current distribution again.

After drying, the benzene phases were evaporated to dryness under reduced pressure and (+)-6,7-dehydroepivincadine (545 mg) was obtained in the form of a nearly colourless amorphous residue (solidified foam); the substance was chromatographically homogeneous and pure. $[\alpha]_D^{20}$ +90° (ethanol, c = 0.5), $pK_a = 4.41$ (in 50% ethanol).

UV (methanol): λ_{max} 226, 285 and 292 nm; log ε 4.57, 3.94 and 3.91, respectively.

MS: molecular weight 338.1995; molecular formula $C_{21}H_{26}N_2O_2$.

The substance was very well soluble in organic solvents; it became brownish on standing in air. Attempts at crystallizing the substance have failed up to now.

The sulfuric acid solution (containing epivincadine) obtained in the counter-current distribution was made alkaline, extracted with benzene and the benzene phase was evaporated to dryness at reduced pressure. The evaporation residue (64 mg) was crystallized from hot methanol (1 ml) to obtain chromatographically pure, optically inactive (±)-epivincadine (22 mg), m.p. 156—157 °C; no melting point depression occurred with a sample obtained in the hemi-synthesis. $pK_a = 5.20$ (in 50% ethanol).

The molecular weight measured by mass spectrometry was 340.2150; molecular formula $C_{21}H_{28}N_2O_2$.

UV (methanol): λ_{max} 226, 285 and 292 nm; log ε 4.5, 3.96 and 3.93, respectively.

The evaporation residue of the mother liquor of epivincadine was dissolved in benzene and purified again by counter-current fractionation. The product obtained in this way (23 mg) was chromatographically pure, amorphous epivincadine; on the basis of the optical rotation it was a mixture of (−)-epivincadine and (±)-epivincadine; $[\alpha]_D^{20}$ −16° (ethanol, c = 0.5). The chromatographic behaviour, UV and IR spectra and mass spectrum of the product were identical with those of crystalline (±)-epivincadine.

Isolation of vincadine and (+)-6,7-dehydrovincadine

The alkaloid fraction containing mainly vincadine and dehydrovincadine (4.7 g) was dissolved in a mixture of benzene and petroleum ether (1 : 1, v/v) and subjected to chromatographic separation on an alumina column (300 g, Brockmann II). Pure vincadine (3.15 g) was eluted with a mixture (600 ml) of benzene and petroleum ether (1 : 1), and pure dehydrovincadine (480 mg) was then eluted with a further 500 ml portion of the same mixture.

Furthermore, the "residual" fraction containing vincadine, dehydrovincadine, vincadifformine and other alkaloids (3.6 g) was subjected to chromatographic separation on another alumina column (230 g). Pure vincadine (300 mg) was obtained with 350 ml of benzene–petroleum ether (1 : 1), and pure dehydrovincadine (190 mg) was eluted with further 400 ml of the eluent. (Subsequently, other alkaloids, among others, tetrahydroalstonine [7], were eluted from this column.)

The eluate fractions containing vincadine were then combined and evaporated to dryness under reduced pressure. The weight of the evaporation residue was 3.45 g; $[\alpha]_D^{20}$ −65° (ethanol, c = 0.5); $pK_a = 7.20$ (in 50% ethanol). Fractional crystallization of the substance [2] yielded optically inactive, crystalline (±)-vincadine (850 mg; m.p. 126 °C, from methanol) and crystalline (−)-vincadine (1.8 g; m.p. 76 °C, from heptane); $[\alpha]_D^{20}$ −92° (in ethanol). The crystalline products were found to be identical with the earlier isolated [2] and authentic samples prepared in hemisyntheses.

The eluates containing only dehydrovincadine were also combined and evaporated to dryness at room temperature at reduced pressure. An almost colourless, chromatographically pure evaporation residue (in the form of a solidified foam) (670 mg) was obtained; this was (+)-6,7-dehydrovincadine, $[\alpha]_D^{20}$ +65° (ethanol, c = 0.5), $pK_a = 6.75$ (in 50% ethanol).

UV (MeOH): λ_{max} 226, 284 and 292 nm; log ε 4.58, 3.90 and 3.86, respectively. The molecular weight measured by mass spectrometry was 338.1991, the molecular formula being $C_{21}H_{26}N_2O_2$. The substance was well soluble in organic solvents; it rapidly became brown suffering oxidation when exposed to air, particularly to sunshine. (Among others, lochnericine [7] was detected in the oxidation product.) Crystallization of the substance has failed up to now.

Acid hydrolysis and decarboxylation of 3-carbomethoxyquebrachamine derivatives

The 3-carbomethoxyquebrachamine derivatives isolated from the leaves of *Amsonia tabernaemontana* were refluxed in 1 N hydrochloric acid in nitrogen atmosphere for 1.5 hr. to hydrolyze and decarboxylate the compounds in the manner described earlier [2]. The results are summarized in Table II.

Table II

Starting material	Product of hydrolysis and decarboxylation			
	Name	Yield, %	M.p., °C	$[\alpha]_D^{20}$*
(−)-Vincadine (**Ia**)	(−)-Quebrachamine (**VII**)	96	147	−114°
(±)-Vincadine (±)-Epivincadine	(±)-Quebrachamine	100	113	0°
(±)-6,7-Dehydrovincadine (**Va**) (+)-6,7-Dehydroepivincadine (**VIa**)	(+)-6,7-Dehydroquebrachamine (**VIII**)	66—70	121	+125°

* in ethanol

Preparation of stereoisomeric 3-carbomethoxyquebrachamine derivatives by hemisynthesis

Vincadine isomers were prepared from vincadifformine, and (+)-6.7-dehydrovincadine and its C_3-epimer were made from tabersonine in a reaction with formic acid in the presence of formamide in the manner described earlier [2]. In each case, the product was a mixture of the corresponding C_3-epimers, which could be separated on the basis of the base strength by fractional partition. Some data of the products prepared by hemi-synthesis are given in Table III.

The properties of the racemates prepared from the optical antipodes obtained in the hemi-synthesis were identical with those of the natural racemates isolated.

Table III

Starting compound	Product of hemisynthesis			
	Name	Yield, %	M.p., °C	$[\alpha]_D^{20}$*
Tabersonine (**Xa**)	(+)-6,7-Dehydrovincadine (**Va**)	40—45	**	+65°
	(+)-6,7-Dehydroepivincadine (**VIa**)	25—30	**	+90°
(−)-Vincadifformine (**Xb**)	(+)-Vincadine (**IIa**)	70—80	76	+92°
	(+)-Epivincadine (**IVa**)	10—15	156	+24°
(+)-Vincadifformine (**XI**)	(−)-Vincadine (**Ia**)	70—80	76	−92°
	(−)-Epivincadine (**IIIa**)	10—15	156	−24°

* in ethanol
** amorphous

Epimerization of vincadine in the presence of sodium methylate

Vincadine (1.7 g; 5 mmoles) was dissolved in anhydrous methanol (100 ml) in which sodium metal (0.92 g) had been dissolved. The solution was refluxed for 1 hr., then evaporated to dryness in vacuum. Water (100 ml) was added to the residue; it was extracted with benzene (5 × 100 ml) and the combined benzene phases were concentrated to 100 ml, and the mixture of vincadine and the epivincadine formed were separated by counter-current extraction with citric acid (1%, 5 × 400 ml) and benzene (5 × 100 ml).

Unchanged vincadine was contained in the citric acid phases; these were combined, made alkaline and extracted with benzene. The evaporation residue of the benzene solution was vincadine (605 mg; 1.78 mmole; 35%).

The evaporation residue of the benzene phase obtained in the counter-current fractionation was epivincadine (615 mg; 1.81 mmole; 36%). (The spectral data and physical constants are given in the section dealing with the isolation and in Table III.)

Epimerization of (+)-6,7-dehydrovincadine (Va) in the presence of silica gel

(+)-6,7-Dehydrovincadine (**Va**) (405 mg; 1.2 mmole) was dissolved in anhydrous benzene (25 ml); finely ground silica gel (5 g) was added to it and the mixture was shaken at room temperature for 3 hrs. The solution was decanted and the silica gel washed with anhydrous methanol (3 × 25 ml). The evaporation residue of the combined solutions was a mixture of alkaloids (377 mg). This was separated as described above, by fractional distribution between benzene and citric acid solution. The evaporation residue of the benzene phase was (+)-6,7-dehydroepivincadine (**VIa**) (228 mg; 0.67 mmole; 56%); this was found to be identical with the products obtained by isolation and hemi-synthesis. (Spectral data and other values are given in the section on isolation and in Table III.)

Preparation of 3-hydroxymethylquebrachamine derivatives (Ib–VIb)

The method applied by us will be illustrated on the example of (−)-vincadine.

(−)-Vincadine (**Ia**) (2.38 g; 7 mmoles) was reduced with $LiAlH_4$ (2.12 g) in anhydrous ether solution (120 ml) refluxed for 2 hrs. The excess of the reducing agent was decomposed by cautious addition of water while cooling, then the ethereal solution was shaken with water (200 ml). After separation the aqueous phase was extracted with ether (3 × 100 ml), the combined ethereal solutions were washed with water, dried and evaporated to dryness. The evaporation residue was crystalline 3-hydroxymethyl-(−)-quebrachamine (**Ib**) (2.05 g; 6.57 mmoles, 94%); this was recrystallized from ethanol; m.p. 184 °C, $[\alpha]_D^{20}$ −154° (ethanol, c = 0.5). The molecular weight determined by mass spectroscopy was 312.2202; molecular formula $C_{20}H_{28}N_2O$.

UV (MeOH): λ_{max} 226, 283 and 291 nm; log ε 4.49, 3.88 and 3.85, respectively.

IR ($CHCl_3$): 3700 and 3450 cm^{-1} (OH and free NH); the band of non-conjugated ester group lacking at 1730 cm^{-1}.

The reduction of other 3-carbomethoxyquebrachamine derivatives was effected in a similar manner. In each case, the yield calculated for the raw product was higher than 90%. (The raw product was purified, when necessary, by clarification with alumina, in benzene solution.) In the UV and IR spectra of all products the characteristic maxima given above were found.

Some characteristic data of chromatographically pure 3-hydroxymethylquebrachamine derivatives are listed in Table IV.

Saturation of 6,7-dehydroquebrachamine derivatives

When the 3-carbomethoxy and 3-hydroxymethyl derivatives of (+)-6,7-dehydroquebrachamine (**Va** and **VIa**; **Vb** and **VIb**) were subjected to hydrogenation in methanol solution in the presence of Pd/C catalyst at room temperature and under atmospheric pressure, they were converted into the corresponding stereoisomeric (+)-quebrachamine derivatives (**IIa** and **IVa**; **IIb** and **IVb**, respectively).

Table IV

Starting compound	3-Hydroxymethylquebrachamine derivative		
	Formula	M.p., °C	$[\alpha]_D^{20}$*
(—)-Vincadine (**Ia**)	**Ib**	184	—154°
(+)-Vincadine (**IIa**)	**IIb**	184	+154°
(—)-Epivincadine (**IIIa**)	**IIIb**	amorphous	+ 10°
(+)-Epivincadine (**IVa**)	**IVb**	amorphous	— 10°
(+)-6,7-Dehydrovincadine (**Va**)	**Vb**	amorphous	+105°
(+)-6,7-Dehydroepivincadine (**VIa**)	**VIb**	amorphous	+ 70°

* in ethanol

*

The authors' thanks are due to Mrs. M. BARTA for the preparation of some of the compounds.

REFERENCES

[1] ZSADON, B., EGRY, É., SÁRKÖZI, M.: Acta Chim. (Budapest), **67,** 77 (1971); ZSADON, B., HUBAY, R., EGRY, É., RÁKLI, M., SÁRKÖZI, M.: Magyar Kém. Folyóirat, **76,** 466 (1970)
[2] ZSADON, B., TAMÁS, J.: Chem. Ind., **1972,** 32; ZSADON, B., TAMÁS, J., SZILASI, M., KAPOSI, P.: Acta Chim. (Budapest), **78,** 207 (1973)
[3] ZSADON, B., TAMÁS, J., SZILASI, M.: Chem. Ind., **1973,** 229.
[4] WENKERT, E., HAGAMAN, E. W., KUNESCH, N., WANG NAI-YI, ZSADON, B.: Helv. Chim. Acta, **59,** 2711 (1976)
[5] ZSADON, B., DÉCSEI, L., KAPOSI, T., TÉTÉNYI, P., SZILASI, M.: Hungarian Pat. 164.899 (1975)
[6] ZSADON, B., KAPOSI, P.: Tetrahedron Letters, **1970,** 4615; Acta Chim. (Budapest), **71,** 115 (1972)
[7] ZSADON, B., TAMÁS, J., SZILASI, M.: Magyar Kém. Folyóirat, **79,** 341 (1973)
[8] ZSADON, B., RÁKLI, M., HUBAY, R.: Acta Chim. (Budapest), **67,** 71 (1971)
[9] BARTLETT, M. F., DICKEL, D. F., TAYLOR, W. C.: J. Am. Chem. Soc., **80,** 126 (1958)
[10] HOIZEY, M. J., OLIVIER, L., LÉVY, J., LE MEN, J.: Tetrahedron Letters, **1971,** 1011
[11] BIEMANN, K., SPITELLER, G.: Tetrahedron Letters, **1961,** 299; J. Am. Chem. Soc., **84,** 4578 (1962)

Béla ZSADON
Mária SZILASI
Zsuzsanna MAJER
} H-1088 Budapest, Múzeum krt. 6—8.
József TAMÁS, H-1088 Budapest, Puskin u. 11.
Pál KAPOSI, H-2011 Budakalász, Pf. 11.

RECENSIONES

Structure and Bonding. Volume 31

Springer-Verlag, Berlin—Heidelberg—New York, 1976

This book is a new volume in the successful series "Structure and Bonding". It contains four studies of a review nature, dealing with various topics in structural chemistry.

The first article is "Paradoxical Violations of Koopmans' Theorem" by R. FERREIRA. One of the most important and descriptive tools of modern theoretical chemistry is the MO theory. The most generally used consequence of the MO theory is Koopmans' theorem, which means that the molecular orbital energies are assumed equal to the ionization energies. The ionization potentials thus calculated generally correlate well with the experimental results, but considerable differences are found at times. This brief, 23-page article discusses the causes of such differences. As paradoxical violations of Koopmans' theorem, the author lists those cases where the sequence of orbital energies differs from the assigned experimental values. In the first two chapters the causes of the contradiction are systematically discussed. Understanding is facilitated by some extremely illustrative diagrams. The final chapter, "MO energy level diagrams and the third revolution of the ligand field theory", presents concrete examples of the paradox, analyzing the causes in detail. The article is completed with 73 literature references. Its style is unusually vivid for a scientific work, and is indeed enjoyable.

C. BONNELLE writes on a special and rarely debated theme in "Band and Localized States in Metallic Thorium, Uranium and Plutonium and in Some Compounds, Studied by X-ray Spectroscopy". In the introductory chapters we find the principles of X-UV spectroscopy. The author describes the development of the characteristic peaks of absorption and emission spectra. The following chapter deals with the spectra of the rare earth metals. In chapter 4 analysis of the emission and absorption spectra of U, Th, and Pu M_{IV} and M_V is discussed. Energy diagrams are proposed for all three metals. The X-ray spectroscopic results on ThO_2, UO_2 and PuO_2 are reported. Finally, a valuable comparison is given between the X-ray spectroscopic and the photoelectron spectroscopic methods. The article is 23 pages in length and contains 50 literature references.

The next article is "Application of the Function Approach to Bond Variations under Pressure" by V. GUTMANN and M. MAYER. It is a well-known fact that, under sufficiently high pressure, materials crystallizing in ionic, atomic or molecular lattices are transformed into metallic lattices. In this process their physical and chemical properties undergo change. The authors give an account of the regularities in these changes. A brief description of the individual changes is first given, *e.g.* the connections between pressure and coordination number, the pressure—homologous series rule, the changes in the spectroscopic properties, and the pressure—atomic distance paradox. This latter is perhaps the most important; in the following an illustrated explanation of it is given with numerous examples (The Functional Approach). This brief, 18-page article is easy to read, its explanations are illustrative, and no special previous study is necessary for an understanding.

The article by J. K. BURDETT, "The Shapes of Main-Group Molecules; a Simple Semi-Quantitative Molecular Orbital Approach", deals with a very interesting theme: a possible explanation of the equilibrium geometry of molecules. At present, various methods are known and accepted for the explanation of the geometry of simple molecules. Examples are the VSEPR method developed by GILLESPIE and NYHOLM, the hybridization model, the qualitative explanation by WALSH, in which the electron–electron repulsion is completely neglected and the change in geometry is determined merely by the number of valency electrons, etc. The question is definitely important, as there is no possibility for an exact, quantitative explanation in university and college education. An improved variant of the WALSH diagrams is presented. Although the method is not so simple as the VSEPR method, and naturally cannot compete with the advantages given by the MO theory, it is nevertheless so illustrative that it can safely be recommended for reading by all those interested in structural chemistry.

Perhaps the only reason inhibiting its introduction in higher education is that it assumes certain group-theory knowledge. Molecules are classified according to the number of ligands (AB_2 . . . AB_7), and the utilizability of the theory is demonstrated on a rich collection of examples. The 38-page article is completed by 37 literature references.

J. NAGY

H. T. KERNER: *Foam Control Agents*

Noyes Data Corporation, Park Ridge, New Jersey, 1976 372 pages

Chemical Technology Review No. 75

This book in the series of Chemical Technology Review deals with a widely occurring problem, the control of foaming in various industrial processes and technologies on the basis of patents announced in the USA in the last 15 years.

The very broad subject-matter is discussed in groups formed according to the branches of industry and the various technologies. First the detergents and cleaning agents, paper industry, lubricants and fuels and different fields of the textile industry are examined for foaming phenomena. Then problems connected with foaming in phosphoric acid production, latex and photographic application, fermentation, and in the pharmaceutical and food industries are discussed. In the last three chapters of the book, problems involving foaming in various fields (polymerization, distillation, antifreezing fluids, etc.) are dealt with and chemical and technological aspects of foam control are discussed.

It is clearly seen in this short summary that the author provides information for experts working in widely different fields.

There are only few such summaries in the literature available, mainly theoretical (colloid chemical) papers and books have been published on foaming and control of foaming. The present book comprises the actual solutions of the problems which are or probably will be introduced in the industry, thus the information provided is important primarily for experts in the industry, but is considered to be useful for theoretical researchers, too.

The construction of the book is clear, it is well-written and contains a large number of tables.

The book is supplemented by a "Company Index", an "Inventor Index" and a "US Patent Number Index". Like the other members of the series, also here a carefully constructed, detailed list of contents supplement is given instead of a "Subject Index".

Special attention is called to the discussion of technical (mechanical) solutions reviewed in the last chapter: here the patents are discussed in connection with schematic diagrams of the apparatuses.

The book is a high-level, valuable work.

J. MORGÓS

NMR: Basic Principles and Progress

Editors: P. DIEHL, E. FLUCK and R. KOSFELD

Volume 13. Introductory Essays. Edited by M. M. PINTAR (University of Waterloo, Canada).

Springer Verlag, Berlin, Heidelberg, New York, 1976, 154 pp.

This latest volume of the series comprises the lectures delivered at the "School on Nuclear Magnetic Resonance" of the Waterloo University. The authors of the individual chapters and their topics are:

1. A Guide to Relaxation Theory. By A. G. REDFIELD
2. Thermodynamics of Spin Systems in Solids. An Elementary Introduction. By J. JEENER
3. Coherent Averaging and Double Resonance in Solids. By J. S. WAUGH
4. Macroscopic Dipole Coherence Phenomena. By E. L. HAHN
5. Nuclear Spins and Non-Resonant Electromagnetic Phenomena. By G. J. BENE
6. Nuclear Spin Relaxation in Molecular Hydrogen. By F. R. MCCOURT
7. Longitudinal Nuclear Spin Relaxation Time Measurements in Molecular Gases. By R. L. ARMSTRONG
8. Spin-Lattice Relaxation in Nematic Liquid Crystals *via* the Modulation of the Intramolecular Dipole Interactions by Order Fluctuations. By R. BLINC
9. NMR Studies of Molecular Tunnelling. By S. CLOUGH
10. Effect of Molecular Tunnelling on NMR Absorption and Relaxation in Solids. By M. M. PINTAR
11. How to Build a Fourier Transform NMR Spectrometer for Biochemical Applications. By A. G. REDFIELD

Publication of the topics of a course in the form of a book always presents certain difficulties. Although each of the lecturers is a well-known expert, there are great differences in the scientific level and manner of presentation of the individual chapters. Each chapter surveys an independent, separate field of research, thus the material of the book does not combine to form a consistent unit, and this fact is responsible for the high number of repetitions in the text. Essentially, the boom offers concise information about the fields of research of the individual lecturers. The primary aim of the series, that is treatment of the theoretical and physical aspects of the NMR technique, was seriously borne in mind in this case; however, this means that the book is of interest primarily for specialists, and much less useful for organic chemists, the most important group of users of NMR spectroscopy.

Certain chapters commanding wider interest must be mentioned here separately, such as the chapters written by A. G. REDFIELD (1 and 11). First, a short and very lucid picture of the theory of relaxation is given, and the most important relaxation mechanisms and their magnitudes expressed in frequency units are described.

Since the sensitivity of the NMR, technique is relatively low in comparison with other analytical methods, it has not become such an essential method for biochemists than for chemists. In his second lecture REDFIELD discussed the possibilities of the further development of high-resolution NMR spectrometers, as well as the results obtainable with them, particularly in the field of PMR spectroscopy. A short comparative evaluation of FTNMR and Correlation Spectroscopy is also given. The main problem in biochemical PMR studies is that the concentration of water used as solvent is usually 110 mole, while the sample is present only in sub-millimolar concentrations. Primarily the methods of Quadrature Detection and Optimal Filtering, Long Pulse Operation and Water Elimination FT (WEFT) can be utilized for overcoming this practical difficulty.

The chapter by R. BLINC (8) also deals with a very interesting topic: how spin-lattice relaxation measurement can be applied in studies of the structure of nematic liquid crystals.

NMR measurements accomplished at very low temperatures make possible the investigation of another region of molecular motion. In Chapter 9, S. CLOUGH discusses the relation forms of the methyl group, such as hopping rotation and tunnelling rotation, as well as the motion produced by their combination, and their effect on the NMR line shape.

In the hope that every inquiring researcher can find a chapter of special interest to him in the rich material of the book, the volume is recommended to those having a concern in the theory or practice of NMR spectroscopy.

G. TÓTH

Organic Conductors and Semiconductors
Proceedings of the International Conference, Siófok, Hungary 1976.
Edited by L. PÁL, G. GRÜNER, A. JÁNOSSY, J. SÓLYOM

Akadémiai Kiadó, Budapest and Springer-Verlag, Berlin, Heidelberg, New York 1977. 654 pages

Since superconduction at room temperature would revolutionalize energetics and technology it is a source of more than a little chagrin that theory and practice have indicated that the critical temperature, T_c, for superconducting metallic elements and alloys (maximum T_c being around 20 K) cannot be raised much further. In view of this, the search for new types of superconducting materials is understandable and, in spite of seemingly formidable difficulties, a necessity.

W. A. LITTLE originally suggested a mechanism according to which organic chains with highly polarizable groups on the spine can be superconductors. Research following up this line has been carried out since the early seventies initially leading to mood of over-optimism due to erroneous measurements and interpretations.

This book contains over 50 papers delivered at the Siófok Conference devoted to the theoretical and experimental achievements in the field of organic conductors. Most of the papers deal with quasi-one-dimensional charge transfer complexes and the effect of their structure on electrical, magnetic, thermal and other physical properties. A highly typical and mostly studied representative of these quasi-one-dimensional complex salts is TTF-TCNQ (tetrathiofulvalene-tetracyanoquino-dimethane). In salts of this type, because of electron transfer from the donors to the acceptors, half- or quarter-filled bands are formed making metallic-like conduction possible. This type of conduction disappears at critical temperature T_c due to structural changes in the stacks of donor and acceptor molecules. A substantial number both of theoretical and of experimental papers deal with the cause and mechanism of these metal-insulator or metal-semiconductor transitions taking place near T_c. The elimination of the critical temperature would be the first ray of hope for organic superconductors. There are papers in the book describing systems sustaining metallic-like conduction down to the lowest temperature, namely: (hexamethyltetraselenofulvalene) (HMTSF)-TCNQ, I-TCNQ and $(SN)_x$, the last-named becoming a superconductor at 0.3 K. The mechanism of superconduction is three-dimensional rather than one-dimensional in polysulphur nitride; thus proofs for a new mechanism are still awaited.

Roughly half of the papers are devoted to the theoretical problems of quasi-one-dimensional systems, the other half describe the results of experimental studies obtained on systems with TCNQ acceptor together with a great variety — in some cases systematically varied — donor molecules. Four chapters deal with theoretical aspects of quasi-one-dimensional CT complexes: I. One-dimensional models; II. Quasi-one-dimensional models; III. Impurity effects and disorder in one dimension; IV. Phase transition in TTF-TCNQ and related compounds. The next two chapters, V and VI, contain the experimental papers dealing with the properties of systems having TCNQ acceptor stacks; V. Experimental investigations on TTF-TCNQ salts and its derivatives; VI. Charge transfer salts other than TTF-TCNQ and its derivatives. (The explanation for the title of this chapter is that the donor molecules are other than TTF. Only one paper reports measurements on a system containing hexacyanobenzene, a new acceptor.) Chapter VII is headed: Polysulphur Nitride, $(SN)_x$ and Chapter VIII is concerned with metal complexes and organic semiconductors — containing three papers on organic semiconductors and two abstracts: the first on the structure and electrical properties of $C(NH)_2H_3\ _2Pt(CN)_4Br \cdot H_2O$ denoted GCP, a new pseudo-onedimensional compound, the second on the synthesis of linear chain planar metal complexes.

As follows from the papers of this volume, the hope for finding very good conductors or high temperature superconductors among organic charge transfer complexes, similar to those studied until now, is rather in vain because of the low free-electron density in the unit cell of this compound as compared to that of good metals. For enhancing conduction the interaction of electron orbitals of donor and acceptor molecules needs to be increased. A paper contained in this volume provides a re-analysis of LITTLE's suggested mechanism showing it to be sound, thus the synthesis of new types of organic conductors and the study of their conduction mechanism remains a challenging field in the years to come.

Both theory and experiment show the decisive role impurities play in conduction of quasi-one-dimensional CT complexes, indicating the necessity for more complete purification

and characterization of these materials to provide a firm basis for understanding the connection between molecular properties, structure, charge transfer and transport — achievable only with the coordinated and close cooperation of chemists and physicists, theorists and experimentalists from both sides.

The book — with the highly apposite summarizing remarks of Professor J. BARDEEN and excellent papers — is a very high level survey of the recent theoretical and experimental developments in the field of organic conductors. For the non-expert, the volume is a comprehensive guide to the subject; for those working with these compounds a very useful source of reference. There is little doubt that *Organic Conductors and Semiconductors* will go a long way towards achieving the synergetic cooperation between physicists and chemists necessary to face the formidable research challenge opened up by organic conductors.

I. KÓSA-SOMOGYI

INDEX

PHYSICAL AND INORGANIC CHEMISTRY

ORGANIC CHEMISTRY

Printed in Hungary

A kiadásért felel az Akadémiai Kiadó igazgatója — Műszaki szerkesztő: Zacsik Annamária

A kézirat nyomdába érkezett: 1977. XI. 8. – Terjedelem: 9,8 (A/5) ív, 50 ábra, 1 melléklet

78.5135 Akadémiai Nyomda, Budapest – Felelős vezető: Bernát György

ACTA CHIMICA

ТОМ. 96—ВЫП. 2

РЕЗЮМЕ

Исследование расствореня вольфрама и молибдена в системе H_2SO_4—HNO_3—H_2O

Б. А. КИШ и Е. САЛАНЦИ

Была исследована скорость растворения вольфрама и молибдена в системе H_2SO_4—HNO_3—H_2O. На основе измеренных скоростей растворения была построена концентрационная трехугольная диаграмма дла обоих металлов. Было обнаружено, что коррозия вольфрама значительно возрастает под влиянием сильноокисляющих продуктов реакции, образующихся при растворении молибдена, т. е. в случае, когда оба металла помещают в смесь кислот. Было установлено, что в трехугольной диаграмме положение и характер интервала концентраций для скорости растворения вольфрама в присутствии молибдена, ближе к молибдену, чем к вольфраму. В общем случае, скорость коррозии вольфрама пропорциональна количеству одновременно растворенного с ним молибдена.

Для расчета скорости растворения был разработан метод для того случая, когда оба металла механически не разделяемы и их начальные веса могут быть измерены лишь вместе ($M_1^W + M_2^{Mo}$). Была определена относительная погрешность измерения исходного веса вольфрама (M_1^W) в зависимости от относительной погрешности измерений общего удельного веса ($1 + 2$).

Применимость методов ППП и ЦНДО/2 для структурных исследований кремнеорганических соединений, II

Й. РЕФФИ, Т. ВЕСПРЕМИ, П. ХЕНЧЕИ и Й. НАДЬ

Проводились расчеты молекулярной структуры свободных радикалов с центральным атомом крешния, паразамещенных триметилсилилбензолов, паразамещенных силилбензолов, метилтриметоксилана и некоторых соединений, содержащих связь крешний-азот. Была исследована корреляция между различными экспериментальными физико-химическими данными ионизационная энергия, дипольный момент, химические сдвиги ЯМР для C^{13} и Si^{29}) и параметрами, рассчитаными с помощую ЦНДО/2 для различных кремнеорганических соединений.

Конформационные исследования с помощью ЯМР на 300 МГц: вращательный изомеризм вокруг связей -CO—CH_2

Р. М. СИНГ, С. К. РАО и Ш. М. ВЕРМА

Спектр ЯМР (300 МГц) N', N'-дипропионил-N-аминоимида антраценмалеинового ангидрида указывает на различные конформации пропиониловых групп. *Экзо*-пропиониловая группа имеет свободное вращение вокруг связей N—CO и CO—CH_2, в то время как *эндо*-группа обладает предпочтительными конформациями вокруг этих связей. Угловая метильная группа в клетке входит в структуру ABC_3 для *эндо*-CO—CH_2CH_3, подтверждая предпочтительную конформацию. Наблюдения с некоторыми замещенными N'-ацетильными производными находятся в согласии с предложенными конформациями.

Ингибирование образования позитрона молекулярными ловушками в неполярных жидкостях

Б. ЛЕВАИ и О. Е. МОГЕНСЕН

Выходы о-P_s были определены в различных жидких углеводородах, тетраметилсилане и их смесях в зависимости от концентраций C_2H_5Br и CCl_4. Эти молекулы известны как хорошие ловушки электронов, а также они ингибируют образование позитрона. Стимулирующая модель реакции образования P_s предсказывает корреляцию между коэффициентом ингибирования и константной скорости химической реакции электронов с молекулярными ловушками. Для зависимости коэффициента ингибирования от функции работы электронов (V_0) в различных жидкостях обнаружено весьма странное поведение, подобное недавно найденному для констант скорости химической реакции квазисвободных электронов с теми же молекулярными ловушками. Коэффициент ингибирования как функция от V_0 имеет максимум для C_2H_5Br, в то время как для CCl_4 он монотонно увеличивается с уменьшением V_0. Коэффициент ингибирования для C_2H_5Br в смеси тетраметилсилана с н-тетрадеканом с молярным отношением 1 : 1, оказался больше, нежели в том или другом чистом компоненте. Явная корреляция между константами скорости захвата электрона и ингибированием позитрона представляет собой наиболее строгую проверку существования стимулирующей модели реакции образования позитрона. Подчеркивается важность метода аннигиляции позитрона также и с точки зрения радиационной химии.

О спонтанных процессах, происходящих на поверхности металлов, под влиянием собственных ионов, I

Л. КИШ и И. ФАРКАШ

Изучалась кинетика спонтанных процессов, происходящих в системе $M - M^{z_1+} - M^{z_2+}$ под влиянием собственных ионов, в отсутствии равновесия. Для некоторых характерных случаев установлена зависимость скорости процессов, а также стационарный потенциал металла M от концентрации ионов M^{z_2+} или M^{z_1+} и от гидродинамических условий электролита.

Электрономикроскопические исследования морфологии гидрогелей поливинилового спирта

Т. ВАРАДИ, М. НАДЬ, А. КАЛЛО и Э. ВОЛЬФРАМ

Морфология гидрогелей ПВС с супрамолекулярной структурой, образующихся в различных условиях, была исследована с помощью трансмиссионного электронного микроскопа.

Был разработан способ повышения контраста супрамолекулярных элементов.

Было найдено хорошее согласие между структурными параметрами, наблюдаемыми непосредственно с помощью электронного микроскопа, и некоторыми физико-химическими свойствами этих гелей, определенными ранее.

Диамагнитные исследования монозамещенных нафталинов

В. ШАНМУГАСУНДАРАМ

Диамагнитные воспримичивости некоторых монозамещенных бензолов и изомерных монозамещенных нафталинов были определены с помощью метода Кюри. Более низкие величины χ_M для α-изомеров объясняются на основе различий в сопряжении заместителей с кольцом, когда они находятся в двух различных положениях. Сравнение парамагнетизма Ван Влека, рассчитанного методом Дорфмана, для монозамещенных бензолов с парамагнетизмом для соответствующих нафталиновых производных указывает, что магнитная восприимчивость соответствующих α-нафтиловых производных сильно зависит от стерических условий перименовой группы.

ИК исследования анилов и их комплексов, II

Р. К. УПАДХИАИ, Р. Р. БАНСАЛ, А. КУМАР и А. К. БАЙПАИ

Некоторые кетоанилы, являющиеся продуктами взаимодействия 3-бензоилметилглиоксаля с замещенными первичными ароматическими аминами были охарактеризованы на основе их ИК спектров. Был рассмотрен эффект природы и положения заместителя на характерную группу анилов- азометиновую группу.

Четыре анила, полученные из п-диметиламино-, п-диэтиламино-, п-бром- и п-иоданилинов, были использованы в образовании комплексов с ионами благородных металлов O_s(VIII) и Au(III). На основе ИК спектров этих комплексов были сделаны заключения относительно мест координации, их относительной стабильности и структуры.

Совместное нахождение стереоизомерных индолалкалоидов типа хибрахамина и изолирование их из листвы Amsonia tabernaemontana

Б. ЖАДОН, Й. ТАМАШ, М. СИЛАШИ и П. КАПОШИ

Из листвы (18 кг в воздушносухом состоянии), собранной перед цветением *Amsonia tabernaemontana* была изолирована алкалоидная фракция «А», из которой разделением на основе основности и дальнейшим фракционированием с помощью колонной хроматографии были изолированы винкадин (3,45 г), эпивинкадин (64 мг), (+)-6,7-дегидровинкадин (670 мг) и (+)-6,7-дегидроэпивинкадин (545 мг). Из двух первых веществ с помощью двухкратной фракционирующей кристаллизации были получены кристаллические (−)-винкадин (1,8 г) и (+)-винкадин (850 мг), а также кристаллический (±)-эпивинкадин (22 мг). Продукты были идентифицированы на основе физических постоянных, химических превращений, полусинтезов и данными масс-спектрометрии.

Были получены далее производные 3-карбометоксихибрахамина, все соответствующие им стереоизомерные производные 3-гидроксиметилхибрахамина, а также были произведены сравнительные масс-спектрометрические исследования. Эпимеры C_3 и в этом случае были легко различимы.

Полученные результаты свидетельствуют о том, что диагностическая величина в масс-спектрометрии может служить помощью в идентификации стереоизомеров.

Les *Acta Chimica* paraissent en français, allemand, anglais et russe et publient des mémoires du domaine des sciences chimiques.

Les *Acta Chimica* sont publiés sous forme de fascicules. Quatre fascicules seront réunis en un volume (4 volumes par an).

On est prié d'envoyer les manuscrits destinés à la rédaction à l'adresse suivante:

Acta Chimica
H-1521 Budapest, Hongrie

Toute correspondance doit être envoyée à cette même adresse.

La rédaction ne rend pas de manuscript.

Le prix de l'abonnement: $ 36,00 par volume.

Abonnement en Hongrie à Akadémiai Kiadó (1363 Budapest, P.O.B. 24, C.C.B. 215 11488), à l'étranger à l'Entreprise du Commerce Extérieur «Kultura» (H-1389 Budapest 62, P.O.B. 149 Compte-courant No. 218 10990) ou chez représentant à l'étranger.

Die *Acta Chimica* veröffentlichen Abhandlungen aus dem Bereich der chemischen Wissenschaften in deutscher, englischer, französischer und russischer Sprache.

Die *Acta Chimica* erscheinen in Heften wechselnden Umfanges. Vier Hefte bilden einen Band. Jährlich erscheinen 4 Bände.

Die zur Veröffentlichung bestimmten Manuskripte sind an folgende Adresse zu senden:

Acta Chimica
H-1521 Budapest, Ungarn

An die gleiche Anschrift ist jede für die Redaktion bestimmte Korrespondenz zu richten.

Manuskripte werden nicht zurückerstattet.

Abonnementpreis pro Band: $ 36,00.

Bestellbar für das Inland bei Akadémiai Kiadó (1363 Budapest, Postfach 24, Bankkonto Nr. 215 11488), für das Ausland bei »Kultura« Außenhandelsunternehmen (H-1389 Budapest 62, P.O.B. 149. Bankkonto Nr. 218 10990) oder seinen Auslandsvertretungen.

Acta Chimica издают статьи по химии на русском, английском, французском и немецком языках.

Acta Chimica выходит отдельными выпусками разного объема, 4 выпуска составляют один том и за год выходят 4 тома.

Предназначенные для публикации рукописи следует направлять по адресу:

Acta Chimica
H-1521 Budapest, BHP

Всякую корреспонденцию в редакцию направляйте по этому же адресу.

Редакция рукописей не возвращает.

Подписная цена — $ 36,00 за том.

Отечественные подписчики направляйте свои заявки по адресу Издательства Академии Наук (1363 Budapest, P.O.B. 24, Текущий счет 215 11488), а иностранные подписчики через организацию по внешней торговле «Kultura» (H-1389 Budapest 62, P.O.B. 149. Текущий счет 218 10990) или через ее заграничные представительства и уполномоченных.

Reviews of the Hungarian Academy of Sciences are obtainable at the following addresses:

AUSTRALIA
C.B.D. LIBRARY AND SUBSCRIPTION SERVICE, Box 4886, G.P.O., *Sydney N.S.W. 2001*
COSMOS BOOKSHOP, 135 Ackland Street, *St. Kilda (Melbourne), Victoria 3182*

AUSTRIA
GLOBUS, Höchstädtplatz 3, *1200 Wien XX*

BELGIUM
OFFICE INTERNATIONAL DE LIBRAIRIE, 30 Avenue Marnix, *1050 Bruxelles*
LIBRAIRE DU MONDE ENTIER, 162 Rue du Midi, *1000 Bruxelles*

BULGARIA
HEMUS, Bulvar Ruszki 6, *Sofia*

CANADA
PANNONIA BOOKS, P.O. Box 1017, Postal Station "B", *Toronto, Ontario M5T 2T8*

CHINA
CNPICOR, Periodical Department, P.O. Box 50, *Peking*

CZECHOSLOVAKIA
MAD'ARSKÁ KULTURA, Národní třida 22 *115 66 Praha*
PNS DOVOZ TISKU, Vinohradská 46, *Praha 2*
PNS DOVOZ TLAČE, *Bratislava 2*

DENMARK
EJNAR MUNKSGAARD, Norregade 6, *1165 Copenhagen*

FINLAND
AKATEEMINEN KIRJAKAUPPA, P.O. Box 128, *SF-00101 Helsinki 10*

FRANCE
EUROPERIODIQUES S. A., 31 Avenue de Versailles, *78170 La Celle St. Cloud*
LIBRAIRIE LAVOISIER, 11 rue Lavoisier, *75008 Paris*
OFFICE INTERNATIONAL DE DOCUMENTATION ET LIBRAIRIE, 48 rue Gay-Lussac, *75240 Paris Cedex 05*

GERMAN DEMOCRATIC REPUBLIC
HAUS DER UNGARISCHEN ÓULTUR, Karl Liebknecht-Strasse 9, *DDR-102 Berlin*
DEUTSCHE POST ZEITUNGSVERTRIEBSAMT, Strasse der Pariser Kommüne 3—4, *DDR-104 Berlin*

GERMAN FEDERAL REPUBLIC
KUNST UND WISSEN ERICH BIEBER, Postfach 46, *7000 Stuttgart 1*

GREAT BRITAIN
BLACKWELL'S PERIODICALS DIVISION, Hythe Bridge Street, *Oxford OX1 2ET*
BUMPUS, HALDANE AND MAXWELL LTD., Cowper Works, *Olney, Bucks MK46 4BN*
COLLET'S HOLDINGS LTD., Denington Estate, *Wellingborough, Northants NN8 2QT*
W.M. DAWSON AND SONS LTD., Cannon House, *Folkes-one, Kent CT19 5EE*
H. K. LEWIS AND CO., 146 Gower Street, *London WC1E 6BS*

GREECE
KOSTARAKIS BROTHERS, International Booksellers, 2 Hippokratous Street, *Athens-143*

HOLLAND
MEULENHOFF-BRUNA B.V., Beulingstraat 2, *Amsterdam*
MARTINUS NIJHOFF B.V., Lange Voorhout 9—11, *Den Haag*
SWETS SUBSCRIPTION SERVICE, 347b Heereweg *Lisse*

INDIA
ALLIED PUBLISHING PRIVATE LTD., 13/14 Asaf Ali Road, *New Delhi 110001*
150 B-6 Mount Road, *Madras 600002*
INTERNATIONAL BOOK HOUSE PVT. LTD., Madame Cama Road, *Bombay 400039*
THE STATE TRADING CORPORATION OF INDIA LTD., Books Import Division, Chandralok, 36 Janpath, *New Delhi 110001*

ITALY
EUGENIO CARLUCCI, P.O. Box 252, *70100 Bari*
INTERSCIENTIA, Via Mazzé 28, *10149 Torino*
LIBRERIA COMMISSIONARIA SANSONI, Via Lamarmora 35, *50121 Firenze*
SANTO VANASIA, Via M. Macchi 58, *20124 Milano*
D. E. A., Via Lima 28, *00198 Roma*

JAPAN
KINOKUNIYA BOOK-STORE CO. LTD., 17-7 Shinjuku-ku 3 chome, Shinjuku-ku, *Tokyo 160-91*
MARUZEN COMPANY LTD., Book Department, P.O. Box 5056 Tokyo International, *Tokyo 100-31*
NAUKA LTD., IMPORT DEPARTMENT, 2-30-19 Minami Ikebukuro, Toshima-ku, *Tokyo 171*

KOREA
CHULPANMUL, *Phenjan*

NORWAY
TANUM-CAMMERMEYER, Karl Johansgatan 41—43, *1000 Oslo*

POLAND
WĘGIERSÓI INSTYTUT KULTURY, Marszałkowska 80, *Warszawa*
CKP I W ul. Towarowa 28 *00-958 Warsaw*

ROMANIA
D. E. P., *Bucureşti*
ROMLIBRI Str. Biserica Amzei 7, *Bucureşti*

SOVIET UNION
SOJUZPETCHATJ — IMPORT, *Moscow*
and the post offices in each town
MEZHDUNARODNAYA KNIGA, *Moscow G-200*

SPAIN
DIAZ DE SANTOS, Lagasca 95, *Madrid 3*

SWEDEN
ALMQVIST AND WIKSELL, Gamla Brogatan 26, *101 20 Stockholm*
GUMPERTS UNIVERSITETSBOKHANDEL AB, Box 436, *401 25 Göteborg 1*

SWITZERLAND
KARGER LIBRI AG, Petersgraben 41, *4011 Basel*

USA
EBSCO SUBSCRIPTION SERVICES, P.O. Box 1943, *Birmingham, Alabama 35201*
F. W. FAXON COMPANY, INC., 15 Southwest Park, *Westwood, Mass, 02090*
THE MOORE-COTTRELL SUBSCRIPTION AGENCIES, *North Cohoc-on, N. Y. 14868*
READ-MORE PUBLICATIONS, INC., 140 Cedar Street, *New York, N. Y. 10006*
STECHERT-MACMILLAN, INC., 7250 Westfield Avenue, *Pennsauken* N.J. 08110

VIETNAM
XUNHASABA, 42, Hai Ba Trung, *Hanoi*

YUGOSLAVIA
JUGOSLAVENSKA KNJIGA, Terazije 27, *Beograd*
FORUM, Vojvode Mišiča 1, *21000 Novi Sad*

17. IV. 1978 HU ISSN 0001—5407 **Index: 26.007**

ACTA CHIMICA

ACADEMIAE SCIENTIARUM HUNGARICAE

TOMUS 96 FASCICULUS 3

AKADÉMIAI KIADÓ, BUDAPEST

1978

ACTA CHIM. ACAD. SCI. HUNG. ACASA2 96 (3) 189–320 (1978)

ACTA CHIMICA

A MAGYAR TUDOMÁNYOS AKADÉMIA KÉMIAI TUDOMÁNYOK OSZTÁLYÁNAK IDEGEN NYELVŰ KÖZLEMÉNYEI

Acta Chimica is a journal for the publication of papers on all aspects of chemistry, in the English, German, French and Russian languages.

Acta Chimica is published in 4 volumes per year. Each volume consists of 4 issues of varying size.

Manuscripts should be sent to

Acta Chimica
H-1521 Budapest, Hungary, BHP

Correspondence with the Editors should be sent to the same address. Manuscripts are not returned to the Authors.

Subscription rate $ 36.00 per volume.

Hungarian subscribers should order from Akadémiai Kiadó, 1363 Budapest, P.O. Box 24. Account No. 215 11488.

Orders from other countries are to be sent to "Kultúra" Foreign Trade Company (H-1389 Budapest 62, P.O. Box 149. Account No. 218 10990) or to its representatives abroad.

Acta Chimica Academiae Scientiarum Hungaricae, Tomus 96(3), pp. 189—199 (1978)

SOME CHEMICAL REACTIONS OF THE ELECTRODE GAP AND THEIR ROLE IN SPECTROCHEMICAL ANALYSIS, XXIII

BEHAVIOUR OF METAL OXIDES IN THE ARC. EXPERIMENTAL APPARATUS AND METHOD. PRELIMINARY EXPERIMENTS

Z. L. SZABÓ

(Department of Inorganic and Analytical Chemistry, Eötvös L. University, Budapest)

H. DOBOLYI-FEJÉRDY

(Hungarian Optical Works, Budapest)

Received November 15, 1976

A gas cell and an experimental method have been developed for investigating the reactions of the mixtures of various metal oxides with carbon powder in the arc and their effect on the results of spectrochemical analysis. According to preliminary experiments, the reactions are influenced by water vapour, the material of auxiliary electrodes, the composition of the powder mixture and the excitation current.

Chemical reactions in the arc can be divided into four groups [1]: high-temperature processes of the plasma, reactions taking place in the colder zones of the plasma, reactions on the electrode surfaces and reactions proceeding in the material of electrodes. The following series of papers is concerned with this latter group.

Carbon electrodes are often used as auxiliary electrodes in practical spectrochemical analysis. For the investigation of non-conducting powders, the sample, mixed in most cases with carbon powder, is filled into the boring of this electrode, and arced against carbon counterlectrode. As electrode material, carbon is very active chemically. In gas atmospheres containing oxygen the reactions on the electrode surface produce CO and CO_2 [2, 3], and their heat of formation is added to the electric energy of the arc thereby increasing the temperature of the electrode. Our previous investigations[4]have shown that the quality of carbon electrodes is relevant, and the reactions on the electrode surface are considerably influenced by the graphitic or non-graphitic nature of the electrode. More amorphous carbon electrodes are more reactive owing to their inferior heat conductance which causes the electrode warm up to higher temperatures during arcing. However, for structural reasons, their oxidation sets in at lower temperatures. This type of carbon is more porous, showing higher specific surface area in heterogeneous chemical reactions. Of course, the temperature and the reactions of carbon electrodes are also influenced by the mass of the electrode to be heated. In addition to thermal effects, the reac-

tions on electrode surface are also substantially affected by oxidation and reduction tendencies of purely electrical origin [5], depending on the polarity of electrode.

For non-conducting materials filled into the boring of electrodes, the chemical reactions induced by arcing and their effect on spectrochemical analysis have been studied to great extent. The role of thermochemical processes was first realized by LEUCHS [6]. The investigations of SCHROLL [7–10] have shown that mixtures filled into the borings of electrodes may undergo oxidation, reduction, decomposition, sulfide or carbide formation and halogenation. These reactions greatly affect the volatilities of the components of the sample. Since they also influence the results of spectrochemical analysis, their voluntary application may result in better analytical results and lower detection limits. The most thorough investigations have recently been carried out by NICKEL [11–17] and RAUTSCHKE [18–22]. These papers deal mainly with the reduction and carbide formation of transition metal oxides and boron(III) oxide. In parallel with spectrochemical analysis, the types of solid reaction products, formed in the mixtures of oxides and carbon powder filled into the borings of carbon electrodes, were investigated by means of X-ray diffraction and isotopic methods. The effect of their thermal behaviour on the subsequent volatilization of the sample and on the line intensities of the spectrum, and the material transport toward the counterelectrode were also studied. On the basis of the measured temperature distribution of the electrode, thermochemical calculations were made and the formation of expected and measured reaction products was compared.

These problems are discussed in several papers [23–29], studying the effect of these reactions on the results of spectrochemical analysis, mainly on the basis of the changes in line intensities.

In order to study the reactions occurring in the material of electrodes from another aspect, we applied gas analysis methods, developed in our earlier investigations [30]. Using mixtures of carbon powder and metal oxides as models, the amounts of carbon oxides formed in the reactions were measured, and the data were correlated with the results of spectrochemical analysis. Our aim was to study the role of the stabilities and reactivities of certain metal oxides in these reactions, the role of the amount of carbon powder used as diluent, and to study the effect of the quality of the carrier electrodes on the reactions. Another aim was to determine whether the above mentioned oxidation and reduction tendencies which depend on the polarity of the electrode, and control the reactions on electrode surfaces, do have a role in reactions proceeding in the electrode.

The investigations were carried out under Ar atmosphere in order to eliminate further parallel reactions caused by the gas phase. The parameters generally relevant in spectrochemical analysis, *i.e.* the flow rate of Ar (steady

and streaming atmosphere), the burning time of the arc, current, the quality and polarity of the carrier electrodes, and the composition of the mixture were varied. The purpose of these investigations was to acquire further pieces of information on the chemical side processes of the arc and on their role in chemical emission spectral analysis.

Apparatus and experimental conditions

The experiments were carried out in the apparatus shown in Fig. 1, which enables to perform measurements in steady and streaming gas atmosphere. The apparatus consists of the following parts.

1. Gas cell. The cell is a quartz tube, 35 mm in height and 38 mm in internal diameter, closed at the top and the bottom by stainless steel electrode holder assemblies by means of rubber seals. They broaden conically towards the interior of the cell. At the tips of either cone, in the bottom and top end of the cell, a steel gas inlet leads into the cell. The inner ends of the tubes are slightly conical, so that the two electrodes can be fixed in them by simply pressing. The ends of the tubes are closed by these electrodes. The gas is introduced and removed through perforated openings beside the conic ends. The tubes are mounted through rubber sealings, by means of ring clamps, in the two conic end plates, and they also play the role of electric leads. The end plates are held together by screws insulated with plexi glass. The cell can be disassembled and the electrodes replaced by loosening these screws. The two steel tubes can be moved in vertical direction, enabling the distance of the electrodes to be adjusted. In appropriately sealed state, the sealing of the cell is able to keep several tenths of atmosphere overpressure for prolonged time. Owing to the conical top and bottom ends of the cell the gas space can be flushed perfectly with pure argon.

2. Gas inlet system. Argon gas for the experiments is taken from cylinders through a finely adjustable reductor valve. To the reductor, a three-way cock is attached, with one branch connected to a balloon gasometer, and one for passing the gas from either the cylinder or the gasometer. This branch leads to another, six-way cock [31]. The role of this cock is to lead the gas directly into the cell or, by turning the tap by 180° with a single movement, pass it through a bubble flack filled with water. The direct path is for the introduction of dry gas, whereas reflushing can be checked by the bubble flask. In crossed position, the six-way cock closes one end of the cell, too. The gas is led by vacuum tubes and by simple, white rubber tubes.

3. Gas sampling system. The upper steel tube, which also holds the counterelectrode, is attached to another three-way cock by means of a rubber tube. One branch of the cock is connected to a soap-film gas flow meter. The third branch leads to an evacuated gas sampling

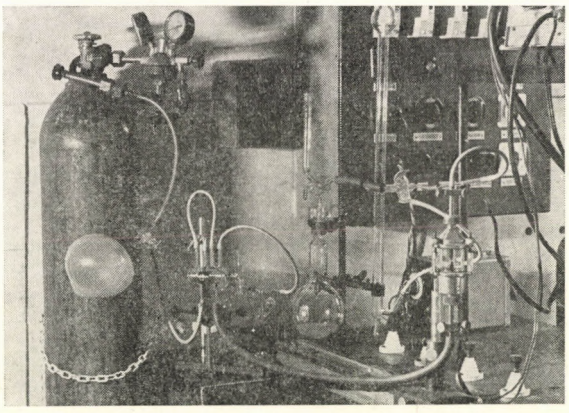

Fig. 1. Experimental apparatus

bottle containing appropriate reagents for gas analysis. The bottle is also used as a titration flask [30]. In experiments under steady gas atmosphere the outlet of the cell is closed by this three-way cock. In experiments using gas flow, capillary tubes varying in length and diameter are inserted between the three-way cock and the gas sampling bottle in order to control the flow rate of the gas into the evacuated bottle and thereby the flow rate in the cell, too. The capillary is protected from solid particles, carried by the gas from the powder sample, by a small piece of cotton wool. The flow rates produced by the various capillaries were calibrated with this piece of cotton wool inserted.

For the investigations welding argon of 99.96 % purity was used; the purity was checked by gas chromatography.* The gas contained 0.005 % of oxygen, also noted in the quality specification, 0.03 % of N_2, and minimum amounts of CO and methane. According to previous experiences, this quality is appropriate for the investigations, and no further purification is necessary.

The balloon gasometer was flushed several times with argon and then filled with ca. 1 l of the gas. Thereafter, the three-way cock was turned towards the cell, and it was flushed for 4 minutes with Ar flowing from the cylinder at a rate of 600 cm^3/min. The rate was measured with a flowmeter connected to the outlet of the cell.

In experiments under steady atmosphere the arc was initiated after stopping the gas flow and closing the cell. After arcing, the cell was connected to the gasometer and, by carefully opening the tap of the evacuated flask and the upper three-way cock, the gas content of the cell was passed into the flask and the cell was flushed with Ar from the gasometer. The completeness of sampling could be checked with the bubble flask at the six-way cock.

In experiments using gas flow, the gas cell was flushed in the above manner, then switched to the gasometer. To start the gas flow controlled by the capillary the upper cocks were opened. The arc was initiated 1 second after this operation, and burnt for 10 seconds in most experiments. The gas flow was maintained until the sampling flask reached the atmospheric pressure.

The complete flushing of the cell is ensured by the volume ratios of the cell and the sampling flask. The cell is only 50 cm^3 whereas the flask is 600 cm^3 in volume, *i.e.* the cell is flushed with more than tenfold amount of gas.

For the experiments an a.c. polarized arc, initiated at the maximum of voltage, was produced by a SZAKÁCS-type arc generator also controlled in the arc circuit [32]. Depending on the requirements, the current of the arc was varied between 3.5 and 18 A.

The powder specimens were filled into the boring of carrier electrodes (RW II or RW 0, produced by Ringsdorff Werke GmbH) of appropriate shape, and were used as the lower electrode (either anode or cathode) of an electrode pair opposite to a counter-electrode of the same type.

The spectra were photographed on Agfa-Gevaert 34 B 50 plates with an ISP 22 spectrograph, by directly illuminating the 20 μm slit of the instrument from a distance of 30 cm. For the calibration of the photographic plate, and to measure higher densities, a calibrated two-step filter of 100/20 % transmission was placed in front of the slit. The plates were developed in Agfa – 1 developer for 5 minutes at 20 °C. The densities were measured with an MF-2 microphotometer, and Y = log I and I values were calculated after P_x transformation and background correction.

The experiments are based on measuring the CO and CO_2 content of the gas passed from the cell into the titrating flask. Carbon monoxide was oxidized to CO_2 with potassium permanganate in the presence of silver nitrate as a catalyst, and the excess of potassium permanganate was measured. Carbon dioxide was measured separated by absorbing it in barium hydroxide solution and titrating the excess of alkali with hydrochloric acid [30].

The analytical and spectral data given in the tables and figures were obtained as a mean of 5 – 10 parallel measurements, the number of measurements depending on the actual scatter of data.

Preliminary experiments

No reference can be found in the literature on the measurement of gas products formed in reactions of non-conducting materials during spectroscopic analysis. Therefore, the first task was to determine whether the amount of

* The gas chromatographic measurements were made by Dr. J. TROMPLER and Dr. E. HOLLÓS-ROKOSINYI. The authors are much indebted for the measurements.

carbon oxides is detectable at all, and if so, to what extent it may vary with the parameters of spectrochemical analysis. To this end, some experiments were carried out with a medium current of 13 A using 1 : 1 mixtures of five metal oxides (Ag_2O, CuO, PbO, CoO and ZnO) and a graphitic carbon powder (type SU−601, prepared by Elektrokarbon Topolčany, Czechoslovakia). A boring, 4 mm in depth and 2.5 mm in diameter, was drilled into the long-stud end (length 4 mm, diameter 3.5 mm) of an RW II carbon electrode, and this boring was filled with the powder specimen. The filling was compacted with a glass rod, and the top was cleared off. The counterelectrodes were RW II carbon electrodes too, with long-stud ends (3.5 mm in diameter and 4 mm in length). The experiments were performed under steady Ar atmosphere.

The role of water vapour

Already in the first experiments, a lucky accident led to the recognition of the role of water vapour in the reactions. From the bubble flask, used to check the flow rate of gas, water entered the cell, and thus some experiments were carried out under water vapour atmosphere. This had increased the reaction, particularly the formation of CO_2. Connecting the carrier electrode as anode, 1.0 cm^3, with opposite polarity 0.7 cm^3 of CO_2 were measured, whereas in dry cell, with Ar bubbled through water, the results were 0.35 and 0.27 cm^3, respectively. Even this appeared to be too high, taking into account that a 1 : 1 mixture of CoO and carbon contains an about sevenfold excess of C, calculated for the possible reaction, and thus only CO was expected to form. To clarify the problem, the borings of the electrodes were filled with pure carbon powder to ensure that in a possible reaction only the oxygen of water should take place. Under Ar atmosphere bubbled through water, and thus saturated with water vapour, 0.15 cm^3 of CO_2 was measured with anodic, and 0.10 cm^3 with cathodic excitation. Under dry argon gas, however, no CO_2 could be measured, neither with pure carbon powder nor with CoO + C mixture. Therefore, in the subsequent experiments dry Ar was used and only carbon monoxide was measured.

The role of water vapour in the formation of CO was also investigated. With carbon powder filled into the boring of RW II carbon electrode, under dry Ar atmosphere, 0.75 cm^3 of CO was measured with either electrode polarity. Again, this appeared to be too high, taking into account that there could be practically no oxygen in the cell. Considering the porous surface of RW II carbon [3], we have concluded that adsorbed water vapour, or O_2, must be converted into CO in an electrode surface reaction. Therefore, the filled electrodes were dried at 135 °C, put into the cell in hot state, and argon-flow was started immediately. The results of these measurements are shown in Table I. In the heading of the table "a" and "c" refer to the polarity (anode or cathode) of the

carrier electrode during arcing. Graphite RW O electrodes with with smooth surfaces produced 0.06 and 0.04 cm^3 of CO if both electrodes of the pair were dried. The above data prove that the formation of CO is, indeed, due to materials adsorbed on the surface of electrodes. The variation of the amount of CO also shows that carbon powder filling with high specific surface area also adsorb reactive substances, since the drying of the filled carrier electrode decreases the amount of CO to a greater extent than the subsequent drying of the counter-electrode.

We have investigated this "remainder" reaction, still present when both electrodes are dried, as a function of current (Table II). In the experiments pure carbon powder was filled into RW II carrier electrodes. From the data obtained two conclusions can be drawn. (1) The reaction is caused by the adsorbed material, and it is essentially an electrode surface reaction. With increasing current the reaction zone also increases owing to the extending glowing area. (2) Drying at 135 °C does not remove the adsorbed substances completely. Stronger heating, however, may lead to a "spontaneous" reaction in the mixtures of less stable oxides. Therefore, we decided to dry the electrodes always at 135 °C, take the above values into account as the results of "blank" measure-

Table I

The role of drying the electrodes. RW II electrodes, carbon powder filling, current 13 A; a – anodic, c – cathodic excitation

Experimental condition	CO cm^3	
	a	c
Undried electrode pair	0.74	0.75
Carrier electrode dried	0.43	0.31
Both electrodes dried	0.16	0.13

Table II

The change of CO evolution with current, carbon powder filling; a – anodic, c – cathodic excitation

Current	CO cm^3	
	a	c
4	0.04	0.04
7	0.07	0.06
10	0.10	0.09
13	0.16	0.13
16	0.23	0.17

ments. According to our considerations this surface reaction runs parallel with, but independently of, the reactions proceeding in the material of the electrode, *i.e.* it can be regarded additive to good approximation, and simply subtracted from the results.

The role of the quality of auxiliary electrodes

On 1 : 1 mixtures of the five metal oxides given in the introduction with carbon powder SU – 601, we have studied the effect of the properties of carbon carrier electrodes (RW II and RW 0) on the reactions of the mixtures filled into the borings. It could be expected that these reactions also depend on the different heat conductances of the carrier electrodes and thus on the different extents of glowing in the arc, since RW II is more amorphous and RW 0 is more graphitic. For the sake of comparison, good heat conductor copper carrier and counter-electrodes were also applied. The current of the arc was 13 A, burning time 10 s. The results are given in Tables III and IV. On the basis of the data the following conclusions can be drawn.

1. The greatest reaction was obtained with carbon electrode RW II (amorphous), for which glowing is the strongest, and the smallest reaction was shown by good heat conductor copper electrodes.

Table III

The role of the material of auxiliary electrodes. Various metal oxide–carbon powder mixtures, 13 A, anodic excitation

Auxiliary electrode	CO cm³				
	Ag_2O	CuO	PbO	CoO	ZnO
RW II	1.84	2.75	1.23	2.15	1.76
RW O	1.89	1.12	0.56	0.59	1.15
Cu	1.04	0.88	0.36	0.36	0.34

Table IV

The role of the material of auxiliary electrodes. Various metal oxide–carbon powder mixtures, 13 A, cathodic excitation

Auxiliary electrode	CO cm³				
	Ag_2O	CuO	PbO	CoO	ZnO
RW II	1.84	1.72	1.30	1.35	1.12
RW O	1.80	1.13	0.71	0.85	1.04
Cu	0.62	0.41	0.36	0.25	–

2. With carbon electrodes RW II, the reaction is generally greater if this electrode is used as anode, in relationship with the visually observable fact that at the same current an RW II anode glows more strongly than a cathode of the same material.

3. Up to medium currents, graphitic electrode RW 0 glows more strongly when used as cathode. This is due to crystal structure reasons [3]. Therefore, greater reaction can usually be observed here with cathodic excitation.

4. The behaviour of copper electrodes can be interpreted in a different way. The filling is heated now through different mechanisms depending on the polarity of the electrode. With carbon electrodes at medium currents, the burning spot of the arc is located partly on the rim of the carrier electrode, but mainly on the filling itself. With copper electrodes this holds for anodic excitation only. On the cathode, the arc burns exclusively on the rim of the copper electrode, which can be explained in a simplified manner by the fact that copper has lower work function (4.38 eV) than carbon (4.83 eV). The electrons escape, therefore, from copper and the arc is localized on it. Accordingly, with cathodic excitation, the material filled into the boring of copper electrodes is heated only indirectly, through the copper carrier.

5. The results follow only partly the above series of metal oxides and their reactivity series. This may have two reasons. The mixtures, always 1 : 1 in weight ratio, contain different molar amounts of oxides and thus different amounts of reactive oxygen. Therefore, in the further experiments mixtures containing uniformly 3.45 % by weight of bound oxygen were studied. The other reason is that the various oxides have different specific weights. Thus, even when the mixtures contain the same percentage of oxygen, the practically identical volumes of borings contain different amounts of material. We have tried to eliminate this difficulty, with limited success only, by relating the results to the theoretically possible complete reaction that may take place in the given amount of material. However, the results obtained with copper carrier electrodes, corresponding to smaller reactions, follow the sequence of reactivity. Consequently, the strong glowing of carbon electrodes might lead to interfering side processes, *e.g.* increased spilling of sample, etc.

The role of metal oxide–carbon powder ratio

In the third series of experiments the influence of the ratio of metal oxide and carbon powder was investigated on CoO. Auxiliary electrodes were made of RW II carbon, current was 13 A and burning time 10 s. Measurements were made on mixtures of 1 : 1, 1 : 2, 1 : 3 and 1 : 5.2 ratio, corresponding to 50, 33, 25 and 16 % by weight of CoO. The results are summarized in Fig. 2. Labels *a* and *c* on the curves refer to the use of carrier electrode as anode or cathode. It can be seen that up to ca. 30 % by weight the formation of CO

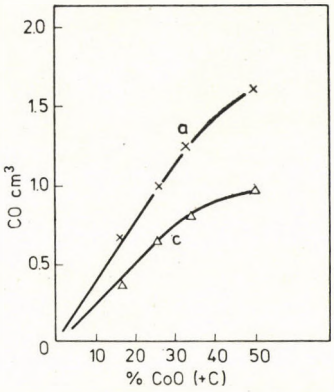

Fig. 2. The change of the amount of CO with the composition of CoO + C mixture; *a* – anodic, *c* – cathodic excitation

increases linearly with the reactive oxygen content of the mixture. At higher cobalt oxide concentrations, however, the curves incline downwards. It is worth extending the investigations to the complete 0–100 % range of metal oxide content, since this inclination can be expected to continue. This is due to the fact that at higher metal oxide concentrations the amount of the other reaction partner (carbon) decreases, thereby suppressing the reaction.

The role of the current

Our next experiments aimed at studying the role of the current of the arc in the reaction of metal oxide and carbon powder. Auxiliary electrodes were RW II carbon, burning time was 10 s. The experiments were performed on CoO of medium reactivity and on CuO of higher decomposition ability. The composition of the mixtures with carbon powder was chosen in a manner (1 part of CoO, 5.2 parts of C, and 1 part of CuO and 4.8 parts of C, respectively) that both mixtures contained 3.45 % by weight of bound oxygen. The curve pairs given in Figs 3 and 4 have saturation character. As at higher currents the material filled into the boring of the electrode glows to increasing extent, the reation can be regarded practically complete. In the anode, which glows to a greater extent, the reaction increases faster than in the cathode. It can also be seen that the curves of more easily decomposed CuO have steeper initial sections, and the amount of resulting CO is also higher than in the case of CoO. These data indicate the different reactivities of the two metal oxides. It can also be seen from the figures that, although the curves practically reach their saturation values, the reaction of the materials filled into the boring of electrode remains below 100 % even at a current of 18 A. Consequently, a part of the specimen is inaccessible for the reaction. The experiments have also

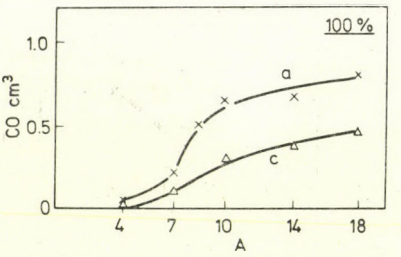

Fig. 3. The change of the amount of CO with current in CoO + C mixture; *a* – anodic, *c* – cathodic excitation

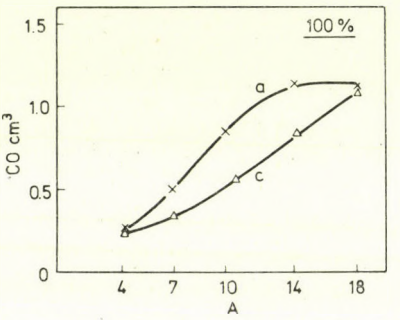

Fig. 4. The change of the amount of CO with current in CuO + C mixture; *a* – anodic, *c* – cathodic excitation

revealed that during arcing the material filled into the boring of the electrode spills to a remarkable extent. Spilling has two reasons. On one hand, the upper layer of the filling is looser than the bulk, which could be better compressed by means of a glass rod. This loose upper layer is very liable to spilling. On the other hand, after a certain extent of glowing, reactions involving gas evolution may also take place in the bulk of filling. The gas evolved may leave the material only upwards, thereby blowing out a part of the material above it. Taking these phenomena into account, the method has been modified in the following manner. Before filling in the sample, the walls of the carrier electrode were bored through horizontally with a driller 1 mm in diameter, 3 mm below the upper rim of the electrode, *i.e.* 1 mm above the bottom of the sample boring. Through these holes, the gas evolved in the bulk of the filling may leave the electrode sideways. These electrodes are called in the subsequent papers "ventillating" electrodes. The upper, loose layer of the filling was simply removed by turning the electrodes upside down and slightly tapping them. By this method spilling of the specimen during arcing could be reduced, and the results have also become more reproducible. We recommend this procedure, which has been applied successfully in other, specific analytical tasks, too.

REFERENCES

[1] SZABÓ, Z. L.: Kémiai Közlem., **44,** 357 (1975)
[2] SZABÓ, Z. L., TÓTH, I.: Spectrochim. Acta, **27/B,** 117 (1972)
[3] SZABÓ, Z. L., FEJÉRDY, H., BUZÁSI, A.: Acta Chim. (Budapest), **80,** 365 (1974)
[4] SZABÓ, Z. L., BUZÁSI, A., FEJÉRDY, H.: Acta Chim. (Budapest), **79,** 245 (1973)
[5] SZABÓ, Z. L.: Spectrochim. Acta **29/B,** 231 (1974)
[6] LEUCHS, O.: Spectrochim. Acta **4,** 237 (1950)
[7] SCHROLL, E.: Z. anal. Chem. **198,** 40 (1963)
[8] SCHROLL, E.: Proc. XIV. Coll. Spectr. Internat., Debrecen, 1967, p. 397
[9] SCHROLL, R., WENINGER, M.: Mikrochim. Technoanalyst. Acta (Wien) **1,** 378 (1965)
[10] SCHROLL, R., HEBER-SCHAUSBERGER, I., JANDA, J., SPATZEK, H.: Mikrochim. Acta (Wien), **3,** 649 (1968)
[11] NICKEL, H.: Z. anal. Chem. **198,** 55 (1963)
[12] NICKEL, H.: Spectrochim. Acta **21,** 363 (1965)
[13] NICKEL, H.: Paper on XIII. Coll. Spectr. Internat. Ottawa, 1967
[14] NICKEL, H.: Proc. XIV. Coll. Spectr. Internat., Debrecen, 1967, p. 467
[15] NICKEL, H.: Spectrochim. Acta **23,** 323 (1968)
[16] NICKEL, H.: Z. anal. Chem. **249,** 353 (1970)
[17] NICKEL, H.: Kémiai Közlem. **39,** 303 (1973)
[18] RAUTSCHKE, R.: Proc. XIV. Coll. Spectr. Internat., Debrecen, 1967, p. 487
[19] RAUTSCHKE, R.: Spectrochim. Acta **23,** 55 (1967)
[20] RAUTSCHKE, R.: Spectrochim. Acta **24,** 125 (1969)
[21] RAUTSCHKE, R., RENFELD, K. H.: Spectrochim. Acta **27,** 211 (1972)
[22] RAUTSCHKE, R., DOWE, CH.: Acta Chim. (Budapest), **80,** 147 (1974)
[23] ZAVOROTNOVA, G. I.: Zh. anal. Him. **20,** 671 (1965)
[24] GURNEY, I. I., ERLANK, H. J.: Analyt. Chem. **38,** 1836 (1966)
[25] BRILL, J.: Spectrochim. Acta **23,** 375 (1968)
[26] RAJIĆ, S.: Z. anal. Chem. **246,** 111 (1969)
[27] RAJIĆ, S.: Z. anal. Chem. **246,** 181 (1969)
[28] BONIFORTI, R., CIANCIA, A., DIGREGORIO, G.: Spectrochim. Acta **27/B,** 309 (1972)
[29] KRASNOBOEVA, N.: GTE lectures, 1966. IV. 15.
[30] SZABÓ, Z. L., TÓTH, I.: Acta Chim. (Budapest) **73,** 363 (1972)
[31] SZABÓ, Z. L., PÖPPL, L.: Acta Chim. (Budapest) **77,** 353 (1973)
[32] SZAKÁCS, O.: Proc. XIV. Coll. Spectr. Internat. Debrecen 1967, p. 997

Zoltán László SZABÓ, H-1088 Budapest, Múzeum krt 4/b.
Hajna DOBOLYI-FEJÉRDY, H-1126 Budapest, Csörsz u. 35–43.

Acta Chimica Academiae Scientiarum Hungaricae, Tomus 96(3), pp. 201—208 (1978)

SOME CHEMICAL REACTIONS OF THE ELECTRODE GAP AND THEIR ROLE IN SPECTROCHEMICAL ANALYSIS, XXIV

BEHAVIOUR OF METAL OXIDES IN THE ARC UNDER STEADY Ar ATMOSPHERE. ROLE OF CURRENT WITH RW II AUXILIARY ELECTRODES

Z. L. SZABÓ

(Department of Inorganic and Analytical Chemistry, Eötvös L. University, Budapest)

and

H. DOBOLYI-FEJÉRDY

(Hungarian Optical Works, Budapest)

Received November 15, 1976

The behaviour of materials in arc was studied on the mixtures of five metal oxides (Ag_2O, CuO, PbO, CoO and ZnO) with carbon powder. The amount of CO formed during arcing and, in the case of CuO and PbO, the line intensities of the spectrum were measured as a function of current. At low currents, the reaction sets in around the burning spot of the arc, causing greater reactions in cathodic excitation. The line intensities of the spectrum are also higher with cathodic excitation. With an increase in current the complete bulk of carrier electrode becomes glowing. With RW II carrier electrodes, the temperature of the anode increases to greater extent. At higher currents, therefore, anodic excitation leads to stronger reactions and higher line intensities.

Our previous paper [1] was concerned with a new experimental method for the investigation of the reactions of metal oxides and carbon powder, and reported some of our first results. We have found that practically only CO is formed during arcing when carbon powder is in large excess. The amount of CO depends, among other conditions, on the current of the arc. This paper deals with these correlations in greater detail, and also with the selection of an appropriate model material for further investigations.

Experimental results

On the basis of the considerations given in our previous paper [1], the experiments were performed with metal oxide–carbon powder mixtures in which the amount of oxygen bound in the metal oxide was uniformly 3.45 % by weight, corresponding to the 1 : 1 w/w mixture of the heaviest oxide, Ag_2O. In such mixtures there is a relatively large excess of carbon, and thus the formation of CO_2 could be practically neglected. The behaviour of five metal oxides, also used in the preliminary experiments (Ag_2O, CuO, PbO, CoO and ZnO),

was studied as a function of current. The measurements were carried out in a closed gas cell, *i.e.* under steady Ar atmosphere, using easily heatable RW II carbon auxiliary electrodes ("ventillating" electrodes [1]). The burning time of the arc was 10 s.

Ag_2O + C mixture. The results are shown in Fig. 1. The production of CO is in nearly linear relationship with the current, although in the anodic curve there is a slight saturation character. The data obtained with the carrier electrode as anode (curve *a*) and as cathode (curve *c*) give intersecting curves, and above ca. 8 A the anodic values are already higher. This indicates that at weaker currents the reaction sets in more readily in the cathode around the burning spot of the arc on the cathode, which has, according to the literature [2], higher temperature. At stronger currents, however, the complete bulk of the anode glows up more strongly, and this is decisive factor in the reaction. However, even with 18 A, complete reaction (100 % mark on the figure), as calculated from the initial weight of the specimen, could not be reached. In the case of easily decomposing Ag_2O, much more material is missing from the boring of the electrode than the amount calculated from the volume of CO formed. This may be due to the looseness of the material in the electrode, to the high reaction rate, or to the high volatility of silver. In Fig. 2, the measured deficiency is shown with solid line, and the deficiency calculated from the volume of CO with broken line. Upon excitation with different polarity, the magni-

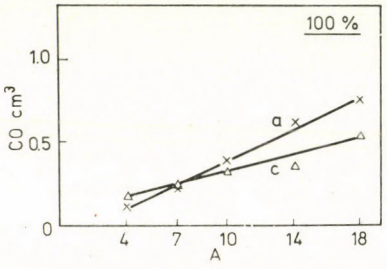

Fig. 1. The change of CO production with current. Ag_2O + C mixture; *a* – anodic, *c* – cathodic excitation

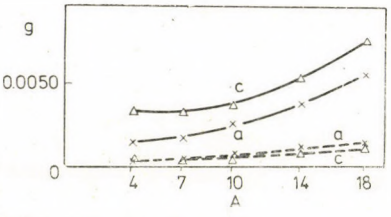

Fig. 2. The change of material consumed from the boring of the electrode with current. Ag_2O + C mixture. Solid line: measured, broken line: calculated value; *a* – anodic, *c* – cathodic excitation

tudes of the measured values are reversed at stronger currents, where the values obtained with cathodic excitation are always greater; the powder is obviously more liable to spilling under cathodic excitation.

CuO + C mixture. The CO curves are shown in Fig. 3. The runs of the curves are very similar to those obtained with the Ag_2O mixture. Although the results scatter strongly, the saturation character of curves is again observable. When compared with the maximum reaction calculated from the weight of sample placed into the boring of the carrier electrode (100 % mark in the figure), however, the reaction is now more complete. Since the reduction of both Ag_2O and CuO produces large amounts of good heat conductor metals in the boring of the electrode, the differences may be due to the different evaporation temperatures of the metals only. The boiling point of silver is 1950 °C, whereas that of copper is 2336 °C. The temperature of the burning spot of the arc, and thereby the temperature of the filling, is determined by the evaporation rates of metals formed in the reaction, and this is lower for silver, which transfers less heat to lower, undecomposed layers. Moreover, in the case of Ag_2O, containing two metal atoms in the molecule, a double amount of metal is formed at a given oxygen content, causing a stronger cooling effect. Finally, Ag_2O is less reactive although more unstable than CuO.

It can also be seen in Fig. 4 that the consumption of sample calculated from the CO production (broken line) and measured directly (solid line) is in better agreement in the case of CuO. Consequently, the spilling of sample is

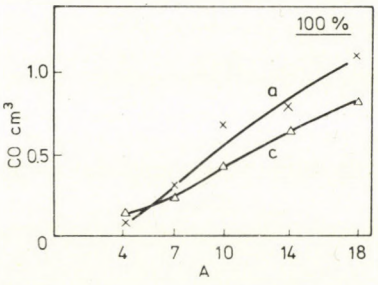

Fig. 3. The change of CO production with current. CuO + C mixture; *a* – anodic, *c* – cathodic excitation

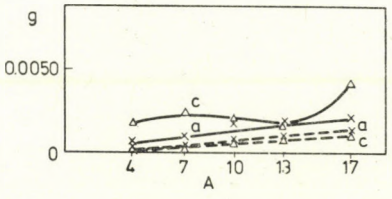

Fig. 4. The change of material consumed from the boring of the electrode with current. CuO + C mixture. Solid line: measured, broken line: calculated value; *a* – anodic, *c* – cathodic excitation

less, leaving more material in the boring for the reaction. Therefore, CuO appears to be a better model for further studies than Ag_2O, due to its fairly high reactivity, but relatively lower susceptibility to spilling.

PbO + C mixture. As shown in Fig. 5, the CO curves are similar to the previous ones. The spilling of the sample is, however, even stronger. If the amounts of CO are related to the weight of sample in the boring of the electrode, the reactions obtained with anodic excitation agree surprisingly well with those of CuO, and for lower currents the values are even slightly higher. On the other hand, the data obtained with cathodic excitation are always higher than those of CuO.

With CuO and PbO mixtures, spectra were also taken in parallel with gas analytical measurements. The intensities of atom line Cu 282.4 nm ($I_{Cu\ I}$) are shown in Fig. 6, while those of Pb 324.0 nm ($I_{Pb\ I}$) in Fig. 7. Since, according to previous investigations [3], the intensity of the atom line of the main component in a sample is characteristic of the evaporation of the sample, it is worth comparing these curves with the run of CO production. The intensities

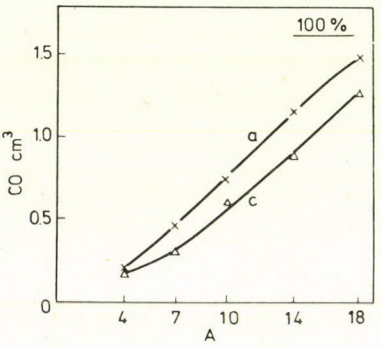

Fig. 5. The change of CO production with current. PbO + C mixture; *a* – anodic, *c* – cathodic excitation

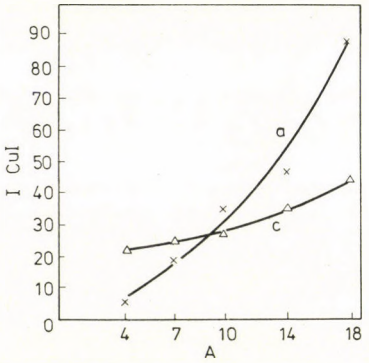

Fig. 6. The change of the intensity of atom line Cu 282.4 nm with current; *a* – anodic, *c* – cathodic excitation

obtained with anodic and cathodic excitation increase, of course, with current, *i.e.* with the electric energy used in excitation. Like CO curves, the intensity plots intersect one another, and at higher currents the anodic values are higher. It can be stated, therefore, that the evaporation of sample and the excitation of spectrum lines as well as the chemical reactions taking place in the boring of the electrode are governed by the same parameters, the energetical conditions of the arc, and these processes occur in parallel.

The data which define the character of spectra and pertain to the mean temperature of the plasm [4] were derived from ion line Cu 237.0 nm and atom line Cu 282.4 nm in the case of copper ($\Delta Y_{Cu\ II,\ I}$; Fig. 8), and from ion line Pb 262.8 nm and atom line Pb 324.0 nm in the case of lead ($\Delta Y_{Pb\ II,\ I}$; Fig. 9). The change of these values with current is slight, and can be observed

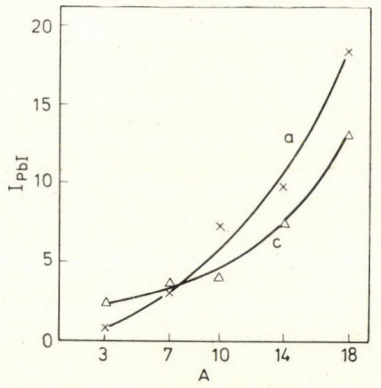

Fig. 7. The change of the intensity of atom line Pb 324.0 nm with current; *a* – anodic, *c* – cathodic excitation

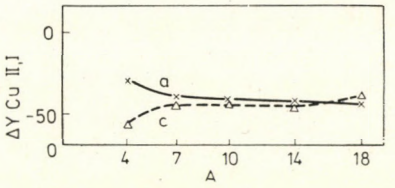

Fig. 8. The change of spectrum character ($\Delta Y_{Cu\ 237.0/Cu\ 282.4}$) with current; *a* – anodic, *c* – cathodic excitation

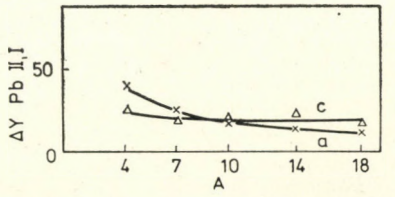

Fig. 9. The change of spectrum character ($\Delta Y_{Pb\ 262.8/Pb\ 324.0}$) with current; *a* – anodic, *c* – cathodic excitation

mainly below 7 A. This indicates again that at higher currents the effect of side processes is counterbalanced in tendency by the higher electric energy [5].

CoO + C mixtures. The CO curves (Fig. 10) show already more substantial differences. Although at higher currents the data obtained with the carrier electrode as anode are in fairly good agreement with those of CuO, at lower currents a well measurable "delay" can be observed in CO production. On the other hand, the CO volumes obtained with cathodic excitation are always below those of CuO. CoO is much more stable than the metal oxides discussed above, and thus its reaction in electrodes of lower temperature is significantly weaker. With anodic excitation, relatively low electrode temperatures may occur at weaker currents only, whereas with cathodic excitation they may occur in the complete range of current applied. The loss of material in the boring of electrode during arcing is relatively low, too.

ZnO + C mixture. The curves are shown in Fig. 11. The reaction curves of this compound, which is more stable than the previous oxides, are flatter than any of the previous curves. The extent of reaction in relation to sample weight is significantly lower. However, the spilling of sample is remarkable again, due probably to the low specific weight of ZnO and the looseness of filling.

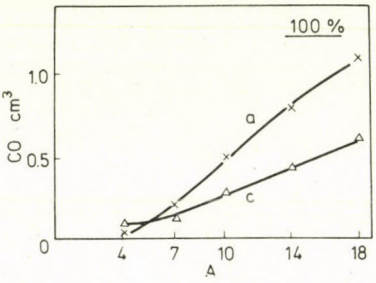

Fig. 10. The change of CO production with current. CoO + C mixture; *a* – anodic, *c* – cathodic excitation

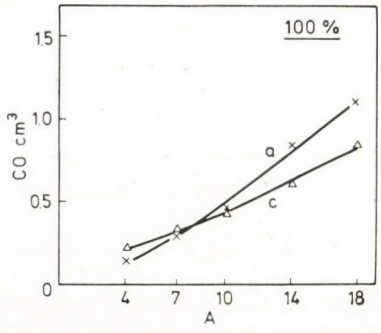

Fig. 11. The change of CO production with current. ZnO + C mixture; *a* – anodic, *c* – cathodic excitation

The character and, of course, the direction of the change of CO production with current is the same for the five metal oxides. In many cases, at high current intensities, even the magnitudes of experimental data are the same. With such a large excess of carbon, the heat conduction properties of carbon powder mixtures are evidently determined by the carbon component and the carrier electrode of the same material, and these effects are only modified by the physical and chemical properties of the various metal oxides. Thus, in mixtures containing different metal oxides in a large excess of carbon powder, the reaction zones in which the reduction of metal oxides takes place are roughy the same at strong currents. However, the lower colder boundary of the reaction zone, away from the arc, obviously varies with the sample. Carbon powder has, consequently, a buffer effect, and this is one of the reasons for its application as additive in the investigation of non-conducting materials. During arcing, however, the polarity of carrier electrode has an important role, since the electrodes may have different temperatures depending on polarity [6]. With RW II carbon, the temperature of anode is higher already at relatively low currents, and thus the reaction of materials filled into its boring is greater than in a cathode of the same material. It can be stated, therefore, that in the reactions of metal oxides, substantial differences can be expected at low and medium currents only. At higher electric energies, particularly in the case of anodic excitation, the complete bulk of sample filled into the boring of an RW II carbon carrier electrode glows up to such an extent that there may be no difference between the behaviour of various metal oxides. (The reaction heats evolved are, of course, different for the various materials.) Therefore, our further investigations with RW II auxiliary electrodes were carried out generally with a current of 7 A.

The reactivities of the five metal oxides decrease in the sequence given in Table I. However, this sequence was not reflected by the reaction curves, even if the reactions were evaluated as percentage of the maximum reaction pos-

Table I

Comparison of the metal oxide mixtures studied

Composition of mixture		Molecular weight of metal oxide	Weight of sample g	100% reaction CO cm^3
Part by weight	Mole fraction of metal oxide			
1 Ag_2O + 1.0 C	0.05	231.8	0.0331	1.60
1 CuO + 4.8 C	0.03	79.5	0.0251	1.22
1 PbO + 1.1 C	0.05	223.2	0.0348	1.68
1 CoO + 5.2 C	0.03	74.9	0.0264	1.26
1 ZnO + 4.7 C	0.03	81.4	0.0256	1.24

sible in the given sample instead of comparing simply the volumes of CO produced. The reasons for the weaker reaction of Ag_2O have already been discussed. The behaviour of PbO mixture was, however, also odd, producing slightly stronger reaction than the more reactive CuO. Therefore, by using the table, further comparisons were made. We have studied the possibility of complete, 100 % reaction calculated on the basis of sample weight. In the case of CuO, CoO and ZnO this corresponds to 1.24 cm^3 in average, whereas for Ag_2O and PbO to 1.64 cm^3 of CO in average, in accord with the average weights of sample able to fill the boring of electrode (0.0257 g and 0.0339 g, respectively). Consequently, of the mixture containing uniformly 3.45 % by weight of bound oxygen, there is a larger amount of reactive oxygen in the boring of the electrode for Ag_2O and PbO than for the former three oxides. Also, by expressing the compositions of the mixtures as the mole fractions of metal oxides, it could be discovered that these values were lower for CuO, CoO and ZnO. Owing to the nearly identical molecular weights, 3.45 % by weight of bound oxygen corresponds here to a mole fraction of 0.03, whereas for Ag_2O and PbO of higher molecular weights this fraction is 0.05, *i.e.* in the latter case there is more metal oxide in the mixture even when expressed as mole fraction. Considering the data pertaining to various CoO + C mixtures discussed in our previous paper [1], we feel probable that the reaction of PbO mixture is, among other reasons, stronger for the above reason. Consequently, it can be expected in principle that the behaviour of various metal oxides could be compared most reasonably by using mixtures which contain identical mole fractions of metal oxides, and by filling so much sample into the boring of electrode that the carrier electrode always contains the same weights of bound oxygen. Since this is quite difficult to achieve in practice, we will be satisfied in the following research with comparing the behaviour of mixtures of various metal oxides containing the same mole fraction of metal oxides.

REFERENCES

[1] SZABÓ, Z. L., DOBOLYI-FEJÉRDY, H.: Acta Chim. Acad. Sci. Hung. **96,** 189 (1978)
[2] ZALESSZKIJ, A. M.: The Electric Arc, Műszaki Könyvkiadó, Budapest, 1968
[3] SZABÓ, Z. L., TÓTH, I.: Spectrochim. Acta **27/B,** 107 (1972)
[4] LAQUA, K.: Spectrochim. Acta **4,** 446 (1952)
[5] SZABÓ, Z. L.: Papers presented on the "XII. Hungarian Emission Spectroscopy Conference" Aggtelek, 1969; p. 203
[6] PÖPPL, L., SZABÓ, Z. L.: Acta Chim. (Budapest) **79,** 27 (1973)

Zoltán László SZABÓ H-1088 Budapest, Múzeum krt 4/b.
Hajna DOBOLYI-FEJÉRDY H-1126 Budapest, Csörsz u. 35–43.

Acta Chimica Academiae Scientiarum Hungaricae, Tomus 96(3), pp. 209—216 (1978)

QUANTITATIVE DETERMINATION OF THE Pb AND Cu CONTENT OF HIGH PURITY GALLIUM BY SPARK SOURCE MASS SPECTROGRAPHY USING Hg INTERNAL STANDARD

J. KÜRTHY

(ALUTERV-FKI, Research, Engineering and Prime Contracting Centre of the Hungarian Aluminium Corporation, Budapest)

Received December 22, 1976

The aim of the present work was to develop an experimental technique to compare different high purity gallium samples and to reveal the relative changes in their impurity content. The applied evaluation method is based on a single exposure and on a properly chosen internal standard that possesses a useful isotopic distribution to calibrate the photographic plate. As internal standard, Hg proved to be useful for the quantitative determination of Pb and Cu in 99.9997 % Ga. The required amount of Hg in the samples added as a dilute alloy, is about 0.3 – 1.0 atomic ppm.

Considering the possible errors of the spark ion source technique, and closeness of the concentration range to the detection level, the precision attained is satisfactory. The method is to be extended to other elements in the future.

Introduction

After silicon and germanium, gallium is considered as the most important element in semiconductor technology. Therefore, the requirements on its preparation, refining and investigation are continuously increasing. Among the analytical methods those are preferred by which a number of impurities can be detected simultaneously in sub-ppm concentrations. In this respect spark source mass spectrography is considered as one of the most useful multi-element methods.

Ga has been analyzed by this method for about fiveteen years but only a few publications have appeared during this period. The analysis of Ga involves special difficulties related to

- sample preparation;
- ion source arrangement;
- considerable fluctuation of the ion current;
- lack of standards.

Quantitative analysis — practical considerations

According to the technique generally used in practice [1, 2] Ga is placed in the source as a self-supporting electrode between cooled clamps. In some experiments the sample is held in a graphite crucible facing a graphite electrode [3]. Recently an electrohydrodynamic ion source was designed in order

to avoid the instability of the spark source, however, the precision of the results did not improve [4].

Gallium analysis is performed by applying a double focusing mass spectrometer with a photographic detector. The advantages of this are the high sensitivity, the high resolution power and the integration of the fluctuating ion current. The technique of graded exposure* and the evaluation based on the visual comparison of the "just visible" lines are widely used [5].

Quantitative analysis can be accomplished only by making use of suitable standards. Ga standards, however, are not available, probably due to the difficulties of their production.

The impurities are inhomogeneously distributed in Ga samples as

- most of the impurities have low solubilities in Ga [6];
- in slow crystallization processes, the liquid phase is enriched in chemical elements characterized by $k_0 < 1$, where k_0 is the equilibrium distribution coefficient [7, 8];
- on oxidation of the sample, the oxide phase is enriched in certain elements (*e.g.* Pb, Zn, Al, Cu) [8].

The inhomogeneity can be left out of consideration if proper care is taken during the preparation of the high purity sample. However, the inhomogeneity becomes more important when doped samples or standards of large volume are handled.

The analysis can be accomplished most precisely on the basis of the internal standard principle. Thus the total amount of charge reaching a single line on the plate for the unknown impurity species (Q_x) should be compared with that amount the charge of which produces the reference line simultaneously on the plate (Q_{std}). Q_x and Q_{std} are calculated from the characteristic, or emulsion response curve [9]. The matrix element itself can be the reference. According to our experience, weaker matrix lines (multiply charged and polyatomic Ga lines) should not be used as internal standards because of the difficulty of keeping the Q_{std} at a constant values. The amount of such particles depends on the plasma conditions defined by the gap between the electrodes. For the maintenance of the sparkling the electrode position is to be altered frequently, however.

Experimental

In the Central Research Institute for Physics of the Hungarian Academy of Sciences the gallium is analyzed using an MS 702/R mass spectrometer (AEI). The method employed [10] is in many aspects similar to that of FITZNER's [2]. The standard deviation of the results calculated from a series

* According to the terminology of the SSMS literature [9]: "Exposure will refer to the total charge to which the plate has been subjected in a single exposure."

of 10 parallel measurements has been reviewed [10]. The plates were evaluated by a visual method and a microdensitometer. In both cases the considerable deviation of 200 – 300 % was found. Repeated investigations using a single exposure gave a markedly smaller scattering in the absorbance values.

The conclusions to be drawn are as follows:

1. As the impurity levels are probably the same or nearly the same in high purity Ga, graded exposures are not necessary. The analysis can be performed by means of the "single-exposure analysis technique" proposed by CHASTAGNER [11]. Repetition of the suitable exposure with as many parallel samples as possible is advisable.

2. A proper polyisotopic internal standard is to be chosen, by which the plotting of the characteristic curve is possible. For this purpose, mercury proved to be the most suitable element as

– the natural abundances of Hg isotopes, covering more then two orders of magnitude, make possible to complete the emulsion calibration curve over a very large dynamic range;

– Hg can be introduced into the sample as a dilute Ga/Hg alloy;

– a reliable titrimetric method is known for the determination of the Hg content above 1 ppm in Ga [12].

The quantity of the internal standards has to be adjusted to the expected concentration of the investigated impurities. In this case some isotopes of the internal standard and at least one isotope of the impurity will appear with suitable densities for measurement after an adequately chosen exposure.

The Hg concentration required for the determination of Pb and Cu in Ga was estimated and checked in the following way:

An alloy of 99.97 % Ga and 0.024 % Hg was chosen as sample A; two others were made by diluting A (samples B and C), thus their impurity content covered three orders of magnitude. The Ga applied in the dilution contained 3 ppm of total impurities, out of this Cu was 0.2 ppm, Hg and Pb were not detectable. Weighing was performed with an accuracy of 0.1 mg, the melt was mixed thoroughly with an ultrasonic shaker.

Mass spectra were taken with two series of graded exposure from all the samples. The parallels were made with a new pair of electrode on a new plate at every turn.

All the visible lines of the Hg isotopes were measured with a microdensitometer, making use of the peak heights of the recorded lines in per cent transmission. As is well known, the shape of a line depends on many variables. The peak height is influenced not only by the quantity and quality of the striking ions, by the plate developing process and the photometer technique, but also by the characteristics of the instrument and by the exposition as well. Therefore, a relatively better accuracy is expected when comparing the peak heights within a single exposure.

The evaluation was performed by a graphical method. The characteristic curve was plotted, using the W or SEIDEL transformation* suggested by CORNIDES [13], against the logarithm of the isotopic abundances of the Hg isotopes, instead of the logarithm of exposure, as was done in most former cases. The emulsion response curves obtained by the above method show a long linear section of $W = -1.0 \ldots +0.6$ (*i.e.* 20 – 90 % transmission). This statement is based on our experience obtained with different polyisotopic elements (Sn, Pb, Ba) in some other matrices [14].

Results and discussion

The characteristic curves for different exposures of samples A, B and C are illustrated in Figs 1 – 4 (symbols A/1, A/2 refer to parallel measurements). The direct lines are generally parallel to each other, *i.e.* they have the same slope. Those exposures were utilizable on which the lines of both impurities (Pb and Cu) appeared with a suitable density.

Making use of a chosen direct line – extrapolating it in the direction of weak blackenings if necessary – the relative concentration of the investigated impurity isotope can be calculated by means of the known Hg content (in

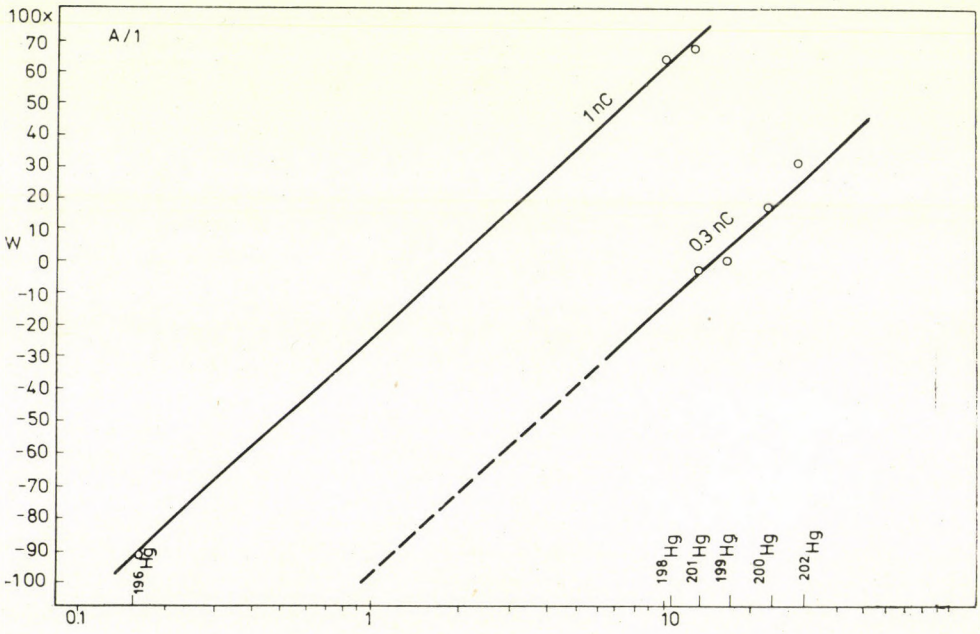

Fig. 1. Characteristic curves for sample A/1

* $W = \lg (1/T - 1)$, where T is transmission. This method was originally suggested for emission spectroscopy but is well adapted to mass spectrography.

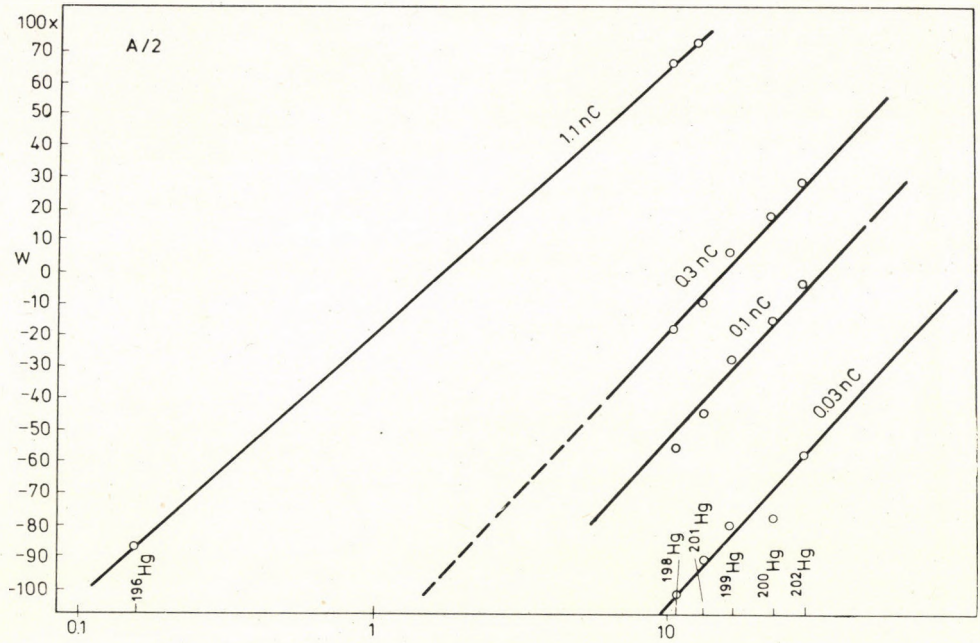

Fig. 2. Characteristic curves for sample A/2

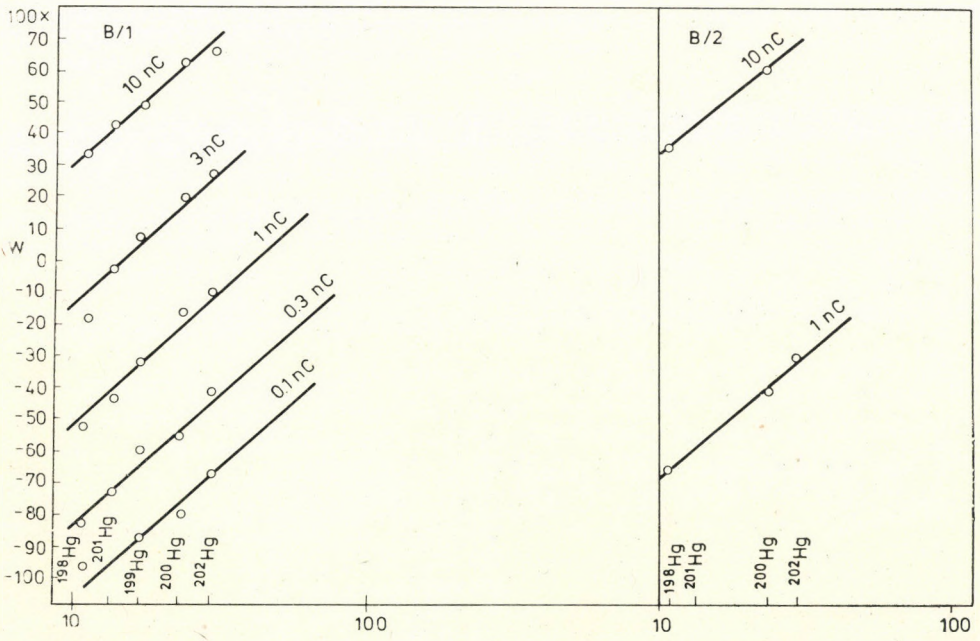

Fig. 3. Characteristic curves for samples B/1 and B/2

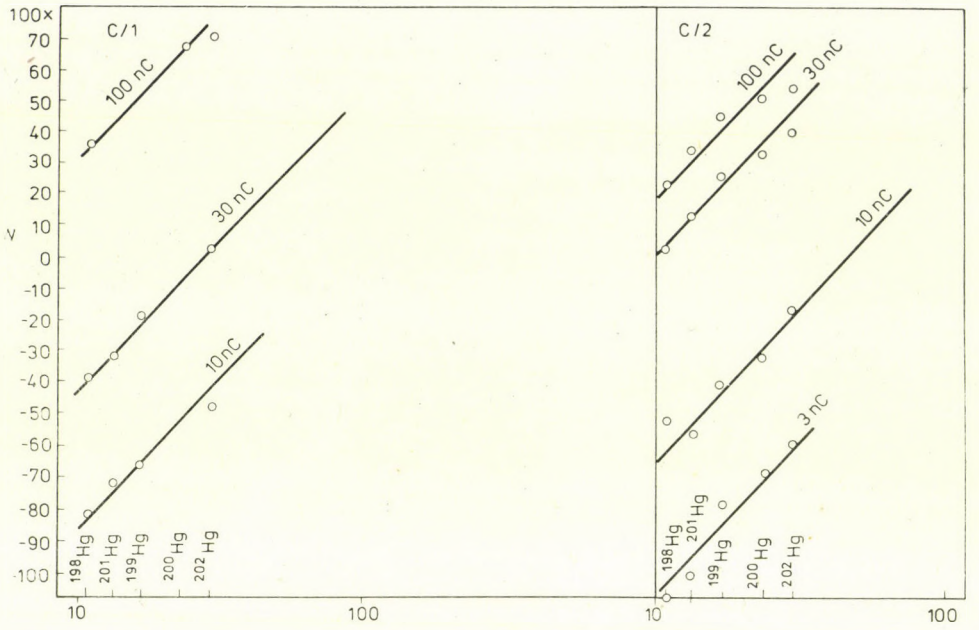

Fig. 4. Characteristic curves for samples C/1 and C/2

Abscissa: isotopic abundances of Hg (%)*
Ordinate: transformed density (W)

*Mass N⁰	*i* %	
196	0.153	
198	10.06	
199	16.92	
200	23.13	
201	13.19	
202	29.71	
204	6.80	(disturbed by 204 Pb)

atomic ppm). It is obvious that the concentration data obtained are relative if the relative sensitivity factors (RSF) referred to Hg are unknown.

We performed the quantitative analysis of Pb and Cu by the method outlined above. The results are summarized in Table I. The results were checked as the Pb and Cu contents of sample A had been determined by inverse polarography (stripping technique) [15], while those of samples B and C had been calculated on the basis of the dilutions.

Measurable impurity isotope lines were obtained with exposures 1 nC, 10 nC and 100 nC for samples A, B and high purity C, respectively. Two or three Pb isotope lines were found suitable for the evaluation, while weaker Cu isotope lines were not visible.

From Figs 1—4 it is seen that a lower concentration of the internal standard would have been more advantageous. The characteristic curves

Table I

Pb and Cu contents of high purity gallium samples (ppm)

Sample	Pb				Cu	
	1	2	3	4	5	6
A/1	3.00	1.65	2.25	2.25	3.70	0.65
A/2	3.00	3.00	3.15	2.25	3.70	0.45
B/1	0.30	0.50	0.45	0.45	0.60	
C/1	0.035	0.05		0.04	0.23	0.03
C/2	0.035	0.04		0.04	0.23	0.04

Columns 1, 5: expected values
Columns 2, 3, 4: measured values calculated from the Pb 206, 207, 208 isotope lines, respectively
Column 6: measured values calculated from the Cu 63 isotope lines.

could have been drawn from lines of more reliable weaker blackenings even at longer exposures if sample A had contained ca 30 atomic ppm Hg (instead of 84 atomic ppm Hg).

It is apparent from Table I that the agreement between results of parallel measurements is satisfactory especially if several well measurable isotope lines are applied. The ratio of the mean concentrations for A : B : C corresponds generally to the ratio calculated from the dilution.

The difference between the measured and expected concentration is probably positive and significant in the case of Pb. The correction factor for Cu amounts to about 6. This observation is in accordance with the finding of FITZNER [2] related to the different sensitivities of Cu and Pb in Ga matrices. Nevertheless enough statistical data are available for the determination of the RSF values.

*

The author wishes to thank Dr. I. CORNIDES and Dr. I. OPAUSZKY for valuable discussions, I. NYÁRI, J. FRECSKA and Mrs. CH. BÁRÁNY for help in the preparative work.

REFERENCES

[1] WOLSTENHOLME, W. A.: Appl. Spectroscopy, **17**, 51 (1963)
[2] FITZNER, E.: Chem. Rundschau, **13** (1965)
[3] NALBANTONGLU, M.: Chim. Anal., **48**, 148 (1966)
[4] EVANS, C. A.: Rev. Sci. Instr., **43**, 1527 (1972)
[5] BROWN, R., CRAIG, R. D., ELLIOT, R. M.: Spark source mass spectrometry as an analytical technique In Adv. in Mass Spectrometry, R. M. Elliot, Ed. Vol. 2, p. 141. Pergamon, Oxford 1963

[6] YATSENKO, S. P.: Gallii. Vzaimodeistvie s metallami. Nauka, Moscow 1974
[7] IVANOVA, R. V.: Khimiya i tekhnologiya galliya. Metallurgiya, Moscow 1973
[8] PAPP, E., SOLYMÁR, K., FARKAS, F., KOVÁCS, F.: FKI Közlemények, **6,** 109 (1962)
[9] KENNICOTT, P. R.: Trace analysis by mass spectrometry, A. J. Ahearn, Ed. p. 179. Academic Press, New York, London 1972
[10] KÜRTHY, J., OPAUSZKY, I., NYÁRI, I., FRECSKA, J.: 4. Int. Symp. Reinstoffe in Wiss. u. Technik. Dresden, Okt. (1975) Ausführliche Zusammenfassungen, 141
[11] CHASTAGNER, P.: Anal. Chem., **41,** 796 (1969)
[12] SZÜCS, P., LOVASI, J.: FKI Közlemények **7,** 431 (1964)
[13] CORNIDES, I.: Gyakorlati tömegspektroszkópia. Műszaki Könyvkiadó, Budapest 1975
[14] KÜRTHY, J., KÁNTOR, T.: to be published.
[15] LOVASI, J., TOMCSÁNYI, T.: Acta Chim. Acad. Sci. Hung., **54,** 21 (1967)

Judit KÜRTHY H-1389 Budapest, P. O. Box 128.

Acta Chimica Academiae Scientiarum Hungaricae, Tomus 96(3), pp. 217–222 (1978)

ULTRAVIOLET SPECTROSCOPICAL INVESTIGATIONS OF SILICON ISOCYANATE AND ISOTHIOCYANATE DERIVATIVES

T. VESZPRÉMI, J. NAGY and I. BARTA

(Department of Inorganic Chemistry, Technical University, Budapest)

Received September 24, 1976

The members of the series $(CH_3)_nSi(NCO)_{4-n}$ and $(CH_3)_nSi(NCS)_{4-n}$ were prepared, their ultraviolet spectra recorded and the observed bands assigned. Quantumchemical calculations were carried out in order to find an explanation for the largely differing spectra of the compounds containing Si–NCS and Si–NCO groups, respectively.

Introduction

The structure of isocyanates and isothiocyanates may be explained in the simplest way be the existence of two π bonds having four electrons and three centers. In the case of silicon derivatives the vacant *d*-orbital of the silicon atom contributes to the bond, giving a possibility for extending the conjugation (Fig. 1). In the course of our investigations $(CH_3)_nSi(NCO)_{4-n}$ and $(CH_3)_nSi(NCS)_{4-n}$ (where $n = 0, 1, 2, 3$) were prepared and the ultraviolet spectra of these compounds were recorded.

Quantumchemical calculations were also carried out with the aim to get an explanation for the rather different spectra of the Si–NCS and Si–NCO compounds, respectively.

The effect of the *d*-orbitals of the silicon atom was studied too.

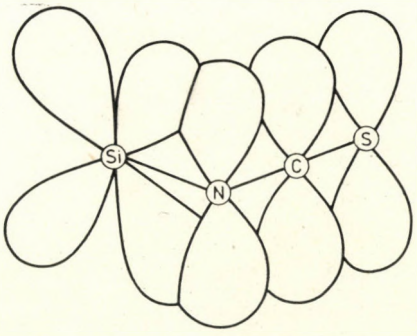

Fig. 1. The role of *d*-orbital in the Si–N–C–S system

Preparation of the compounds

The preparation of the isothiocyanate derivatives were performed as suggested by VORONKOV [1] from the appropriate methylchlorosilane and ammonium thiocyanate under stirring in boiling benzene. The mono- and difunctional compounds are liquids, the three- and tetrafunctional ones are solids at room temperature.

The series $(CH_3)_nSi(NCO)_{4-n}$ was prepared as described by ANDERSON [2], from silver cyanate and the chlorosilane of appropriate functionality. The reaction was carried out in a heterogeneous medium under stirring in the boiling solvent. As it has been mentioned, benzene was used as solvent, in all cases but at the preparation of trimethyl-isocyanatosilane where the solvent was isopropylbenzene. Each member of this series is liquid at room temperature. The purity of the products was determined by the argentometric titration according to EABORN [3], and by the comparison of the measured molar refractions and the calculated ones. In the latter case we applied the increments given by VOGEL [4]. For the solid derivatives the molar refraction was determined by extrapolation from cyclohexane solution.

In each case the measured and calculated molar refractions were in good agreement.

Ultraviolet spectroscopy

Ultraviolet spectra were recorded by Spektromom 201 using *n*-hexane as a solvent. Concentrations were in the range of $10^{-2}-10^{-4}$ mole/dm^3. The cell length was 1.0 and 0.2 cm, respectively. The spectra are presented in Figs 2, 3 and 4.

It can be seen, that the spectra of the compounds containing NCS and NCO groups differ significantly. Isothiocyanates show a maximum of medium intensity at 246–252 nm and an intensive band at 200 nm.

The maxima of isocyanates could be recorded in the far ultraviolet region, so merely the ascending part of the first band could be observed.

CRADOCK *et al.* [5] assigned the first band as a $\pi - \pi^*$ transition.

In our opinion the band in question is of $n - \pi^*$ type. This is supported by its relatively low intensity.

To verify our assumption the ultraviolet spectrum of trimethylisothiocyanatosilane was measured in dioxane too. It is known that the $n - \pi^*$ transitions show a hypsochrome shift when a polar solvent is used. Figure 5 demonstrates that in dioxane there is really a shift of 7 nm in comparison with the spectrum in cyclohexane.

We could not perform the measurements in methanol due to the rapid decomposition of trimethyl-isothiocyanatosilane in the mentioned solvent.

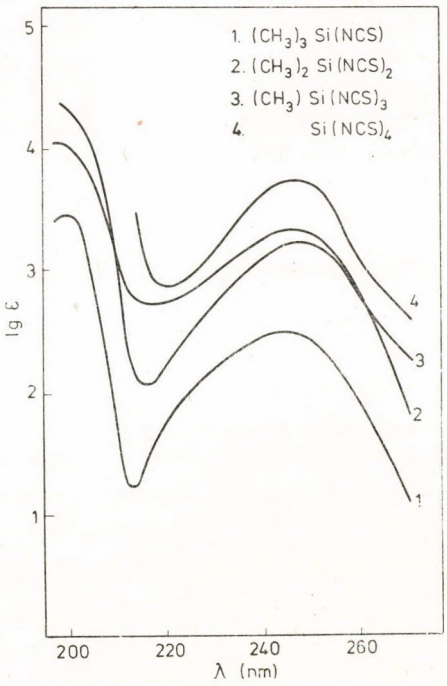

Fig. 2. **Ultraviolet spectra of isothiocyanatosilanes in *n*-hexane**

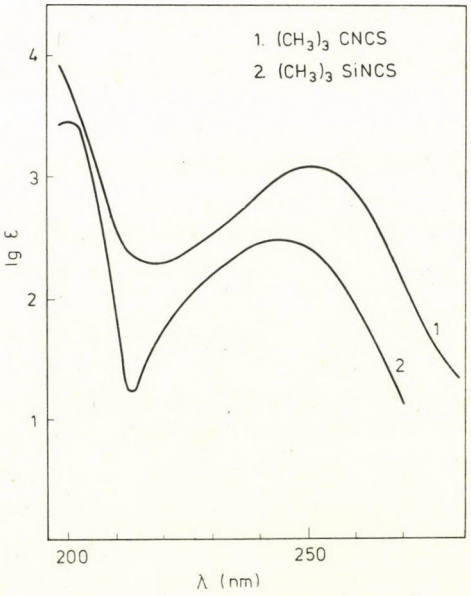

Fig. 3. **Ultraviolet spectra of tert-butylisothiocyanate and trimethylisothiocyanatosilane in *n*-hexane**

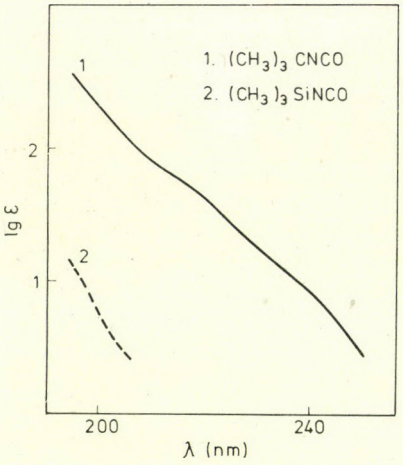

Fig. 4. Ultraviolet spectra of tert-butylisocyanate and trimethylisocyanatosilane in *n*-hexane

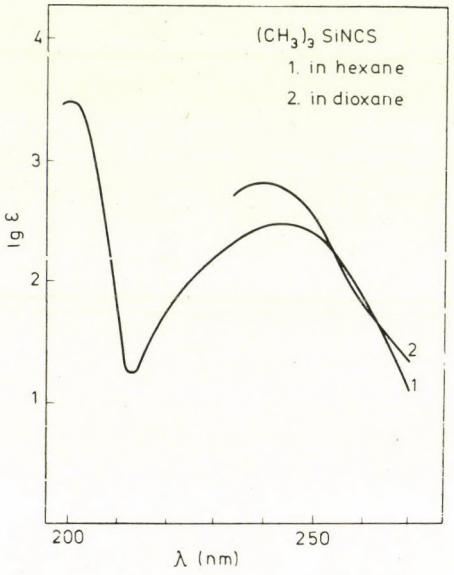

Fig. 5. Ultraviolet spectra of trimethylisothiocyanatosilane in *n*-hexane and dioxane

With increasing number of NCS groups in the $(CH_3)_nSi(NCS)_{4-n}$ series the position of the $n - \pi^*$ transition does not change, its intensity, however, increases. This fact indicates, that each NCS group responsible for the mentioned band seems to be independent from each other. An eventual conjugation can occur through the *d*-orbitals of the silicon atom. The bands reflecting the structure mentioned above may appear at shorter wave length with low intensity.

The effect of the silicon atom is demonstrated by the hypsochromic shift of 6 nm in the $n - \pi^*$ band of the $(CH_3)_3SiNCS$ derivative as compared to that of $(CH_3)_3CNCS$. Simultaneously the second $\pi - \pi^*$ band is shifted in bathochromic direction, the absolute intensity of the latter band could not be measured (Fig. 3).

Quantumchemical calculations

We tried to explain by quantumchemical calculations why the ultraviolet spectra of isocyanates and isothiocyanates differ so considerably. We used the PPP-method [6] in our calculations and assumed that the two π systems were independent from each other. This way the electron transitions for each π systems of $(CH_3)_3SiNCO$ and $(CH_3)_3SiNCS$ were calculated. The required parameters were taken from the tables of HINZE [8], using the MATAGA – NISHIMOTO relation [7].

The values of valence state ionization energy and the values of electron-affinity were interpolated for the hybridization given by the experimental geometry [9]. The appropriate parameters for silicon were taken from the publication of LEVISON and PERKINS [10].

Resonance integrals were calculated by applying the relation of WOLFSBERG and HELMHOLZ [11] (the proportionality factor k was 0.5 for the Si–N bond and 0.8 for all the other bonds). Table I contains the starting parameters.

Table I

Starting parameters

	$\dot{C}$	$\dot{N}$	$\ddot{N}$	$\dot{O}$	$\ddot{O}$	$\dot{S}$	$\ddot{S}$	Si
$I\mu$	11.19	14.12	31.69	17.70	33.16	12.70	23.72	1.10
$\gamma\mu\mu$	11.09	12.16	18.10	15.23	17.92	9.94	12.20	3.76

Resonance integrals

$Si-\dot{N} = -1.13$	$\dot{N}-C = -3.887$	$C-O = -3.617$
$Si-\ddot{N} = -1.09$	$\ddot{N}-C = -3.805$	$C-S = -3.498$

The calculated and measured electron transitions and oscillator strengths are summarized in Table II. The oscillator strengths were calculated from the measured spectrum by the relation $E = 41\,700\,f$, where E is the molar extinction coefficient, and f is the oscillator strength.

Table II

Calculated and measured electron transitions

	Calculated		Measured	
	ΔE [eV]	f	ΔE [eV]	f
$(CH_3)_3Si-\ddot{N}-\dot{C}-\dot{O}$	7.699	0.156		
$(CH_3)_3Si-\dot{N}-\dot{C}-\ddot{O}$	7.795	0.302		
$(CH_3)_3Si-\ddot{N}-\dot{C}-\dot{S}$	6.617	0.190	6.199	0.071
$(CH_3)_3Si-\dot{N}-\dot{C}-\ddot{S}$	6.940	0.372		

Although these results must be treated critically, because of the mentioned approximations, they demonstrate the tendency, that the electron transition of isocyanates appears at much shorter wave lengths than that of isothiocyanates.

According to our results the first $\pi - \pi^*$ transition is caused by the excitation of π system in which the nitrogen and sulphur atom participate with 2 and 1 electrons, respectively.

In the future we intend to widen our investigations on silyl isocyanates and isothiocyanates using all-valence electron methods, *i.e.* CNDO/S [12], and LCVO–MO [13].

REFERENCES

[1] Voronkov, M. G., Dolgov, B. N.: Zh. Obsch. Chim., **24,** 1082 (1954)
[2] Forbes, G. S., Anderson, H. H.: J. Am. Chem. Soc., **70,** 1222 (1948)
[3] Eaborn, C.: J. Chem. Soc., **1950,** 3077
[4] Vogel, A. I.: J. Chem. Soc., **1952,** 514
[5] Cradock, S., Ebsworth, E. A. V., Murdoch, J. D.: J. Chem. Soc. Faraday Trans. II. 1972., 86.
[6] Pariser, R., Parr, R. G.: J. Chem. Phys., **21,** 466, 767 (1953)
[7] Nishimoto, K., Mataga, M.: Z. Physik. Chem., **12,** 335 (1957)
[8] Hinze, J.: Ph. D. Dissertation, Univ. Cincinnati (1962)
[9] Kimura, K., Katada, K., Bauer, S. H.: J. Am. Chem. Soc., **88,** 416 (1966)
[10] Levison, K. A., Perkins, P. G.: Theoret. Chim. Acta **14,** 206 (1969)
[11] Wolfsberg, M., Helmholz, L.: J. Chem. Phys., **20,** 837 (1952)
[12] Del Bene, J., Jaffe, H. H.: J. Chem. Phys., **48,** 1807, 4050 (1968)
[13] Nagy, J.: Private communications

Tamás Veszprémi
József Nagy
István Barta
H-1521 Budapest

Acta Chimica Academiae Scientiarum Hungaricae, Tomus 96(3), pp. 223–233 (1978)

INVESTIGATIONS IN THE FIELD OF SOLID-STATE POLYMERIZATIONS XXXV [1]

SOLID-STATE POLYMERIZATION OF MONOALKYL ITACONATES

K. NYITRAI, N. L. NGUYEN,* F. CSER, E. TAKÁCS and GY. HARDY

(Research Institute for the Plastic Industry Budapest)

Received August 25, 1976; in revised form February 14, 1977

Solid-state direct and post-polymerizations of four β-monoalkyl itaconates (butyl, octyl, lauryl and cetyl) were studied. The phase diagrams of the monomer/polymer systems of butyl and octyl itaconate were determined. Polymerization was shown to take place at a high rate in the high-elastic state of the polymer plastified by the liquid monomer. On the basis of the highest identity period measured by X-ray diffractometry of the monomers, the crystal unit cells of the monomers studied were found similar. The solid-state heterogeneous reactivity of molecules in lattices of the same type decreases with increasing size of the molecule.

Investigations of the relations between the crystal structure of a monomer and the characteristics of its solid-state polymerization are encumbered by the fact that various crystal structures can usually be realized with different molecular structures. Very few works have been published on the solid state polymerization behaviour of different polymorphous forms of the same monomeric molecule (*e.g.* [2, 3]). Comparison of the behaviour of polymorphous modifications is particularly difficult since the polymer produced during the reaction interacts with the monomeric phase, and may transform the polymorphous modifications into each other.

The effects of the physical structure can be studied more readily by the investigation of homologous series. It is known of alkyl compounds that increasing chain length results in definite structural characteristics without any essential influence on the electron distribution of the functional groups [4, 5].

The present paper aims at an approximation of the effects of the structure on the solid-state polymerization characteristics by using monoalkyl itaconates. The relatively less considered mono-itaconates have been selected instead of the better-known diesters [6–10], since the hydrogen bond between the free carboxyl groups presumably fixes the functional groups of the two adjacent molecules thus the orienting effects of the ester chains certainly prevail. β-Butyl, β-octyl, β-lauryl, and β-cetyl itaconates were used. Polymerizations of the former two in the liquid phase were recently reported [11].

* Present address: Hanoi, Vietnam, Dem. Rep.

Experimental

Syntheses

Syntheses of β-monobutyl itaconate (MBI) and β-monooctyl itaconate (MOI) were described in a previous paper [11].

The syntheses of β-monolauryl itaconate (MLI) and β-monocetyl itaconate were the same; 0.5 mole of the alcohol and 0.6 mole of itaconic anhydride were heated to 67 °C (the melting point of the anhydride) on a water bath. Then 1 g of anhydrous $ZnCl_2$ dissolved in 10 ml of acetone was added. The mixture was heated at 95 – 98 °C for 4 – 5 hrs. After the addition of 200 ml of light gasoline, the mixture was boiled for 10 – 15 min then filtered. The filtrate was cooled to room temperature when in 24 hrs the crude product precipitated. After recrystallization from benzene the yields of MLI (m.p. 74 – 76°C) and of MCI (m.p. 83 – 84 °C) were cca. 60 %.

Polymerization

Polymerizations were initiated by a ^{60}Co γ-radiation source of 500 Cu. The samples were sealed into 6 mm diam. glass ampoules in oxygen free argon atmosphere. Polymerizations were carried out in the water-bath of an ultrathermostat. In post-polymerizations, samples were irradiated at room temperature.

The conversion was determined by precipitation using gravimetric methods. Samples containing the polymer were dissolved in a 10 % solution of benzoquinone in tetrahydrofuran. MBI and MOI were precipitated by light gasoline; for MLI and MCI methanol and acetone was used, respectively.

Determination of the polymer–monomer phase diagrams

The phase diagrams were determined by polarization microscopy, DTA and X-ray diffractometry. The thermomechanical behaviour of the samples was determined by consistometry. These methods are described in detail in [12].

The melting enthalpies of the monomers were measured by a DSC equipment (Perkin–Elmer) calibrated by In standard.

Results

Polymer–monomer phase diagrams

The phase diagram of poly-MBI and MBI is illustrated in Fig. 1. The diagram is similar to that of acenaphthylene–polyacenapthylene and N-vinylcarbazole–poly-N-vinylcarbazole reported previously [12]. The system of minimum melting point contains 34 % of monomer and 66 % of polymer with a glass transition temperature of 20 °C and a melting point of 36 °C. The polymer side of the phase diagram cannot be described by the fundamental equation of the plastification of polymer [13]; it is rather similar to the dissolution curves of eutectics. Its X-ray diffractogram shows a relatively sharp reflection at 13.6 Å. The average particle measure calculated from the line broadening is cca. 80 Å. The virtual degree of polymerization calculated from the melting point depression of monomer crystals with $\Delta H_m = 23.13$ kJ/mole is 9.

The phase diagram of poly-MOI is presented in Fig. 2. The phase conditions are identical to those shown in Fig. 1, although the variance in the measured values is higher. The composition with minimal melting point (M_{kr}) is in

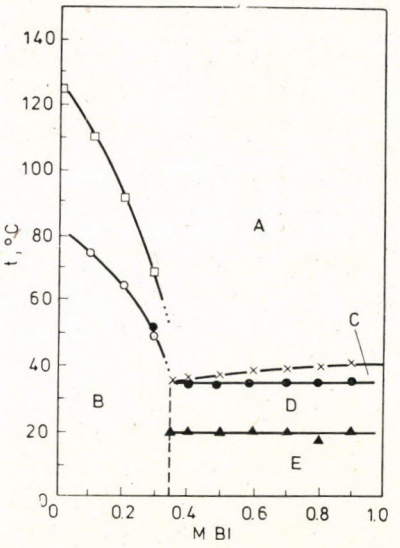

Fig. 1. Phase diagram of the polymer–monomer system of β-monobutyl itaconate. ▲ = Step on the DTA base line; ● = starting of the DTA peak (decrease in the light flux); × = DTA peak (light flux becomes zero); ○ = T_g; □ = T_f (plots obtained by consistometer). A = isotropic liquid; B = polymer plastified by its monomer in glassy state; C = liquid + crystalline monomer; D = crystalline monomer + plastified polymer in highly elastic state; E = crystalline monomer + plastified polymer in glassy state

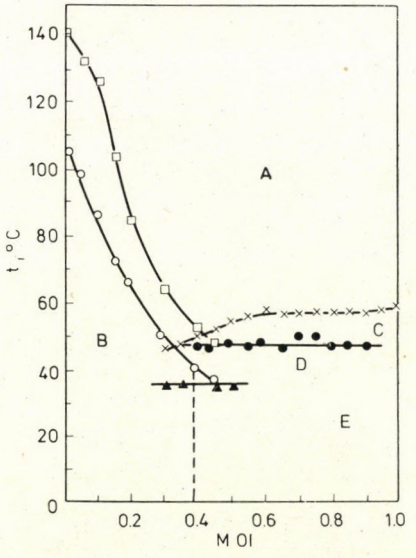

Fig. 2. Phase diagram of the polymer–monomer system of β-monooctyl itaconate. Marks and symbols are the same as in Fig. 1

the range of a monomer content of 36 to 40 % with a glass transition temperature of 35 °C and a melting point of 46 °C. The polymer side of the phase diagram can be well approximated by the equation of plastification. The virtual degree of polymerization is 5, using $\Delta H = 32.43$ kJ/mole for the melting heat of the monomer.

Polymerizations

Data for insource polymerization of MBI at 20, 25, 30 and 35 °C are shown in Fig. 3. Below 20 °C no detectable polymerization could be observed.

The accelerating kinetic curves for 25, 30 and 35 °C can be devided into two stages. The linear section of the first one gives an activation energy of 122 kJ/mole, while for the linear section of the second one 75 kJ/mole was calculated (see Fig. 4). The conversion limit is nearly 100 %. The initial rates for the kinetic curves were linear as a function of the first power of the dose rate (see Fig. 5). Figure 6 shows the insource polymerization of MBI in the presence of dimethyl oxalate. MBI forms an eutectic mixture with DMO of 0.32 MBI(DMO) (mole/mole) content having the melting point of 29 °C. The accelerating type kinetic curves turned linear in the eutectic mixture. Changes in the intrinsic viscosity against conversion are illustrated in Fig. 7. Viscosity decreases tending to a limiting value with increasing conversion. It increases with the polymerization temperature regardless of the dose rate. Figure 8 shows the kinetic curves for the post-polymerization of MBI at 25, 30 and 35 °C using 14.4 Mrad as a total dose of pre-irradiation at 20 °C. The conversion *versus* time curves for the polymerizations at 25 and 30 °C coincide up to 15 hours, when the polymerization at 30 °C gets accelerated. The molecular weight is practically independent of the conversion and the temperature, although the variance is high (see Fig. 7).

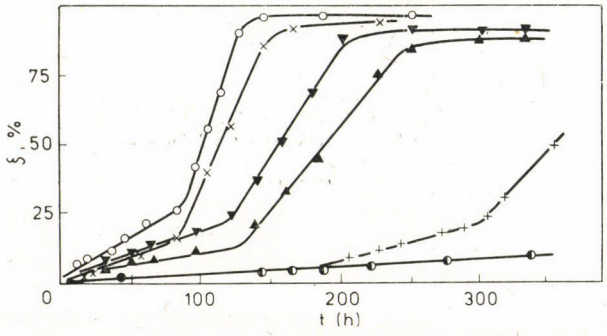

Fig. 3. Insource polymerization of MBI at a dose rate of $2.12 \cdot 10^4$ rad/h ◐ = 20 °C, + = 25 °C, × = 30 °C, ○ = 35 °C and at 30 °C with a dose rate of $1.43 \cdot 10^4$ (▲) and $1.05 \cdot 10^4$ (▼) rad/h

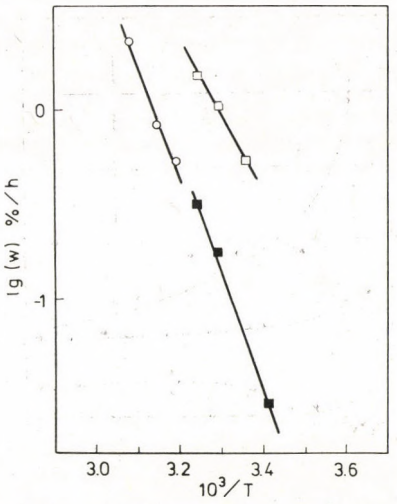

Fig. 4. The temperature dependence of the rate of polymerization in Arrhenius representation. ■ = MBI first linear part, □ = MBI second linear part, ○ = MOI linear part

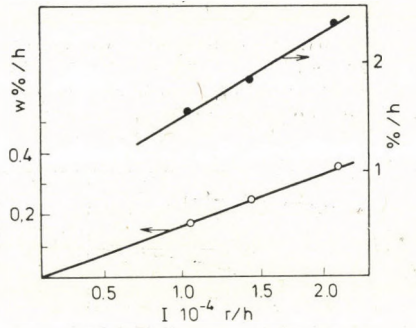

Fig. 5. The dependence of polymerization rate on the dose rate. MBI 30 °C = ● MOI 50 °C = ○

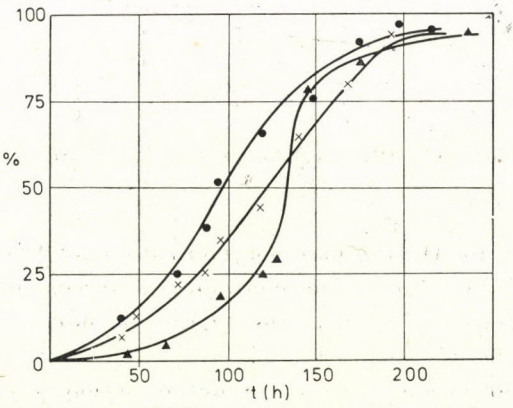

Fig. 6. Insource polymerization of MBI in the presence of dimethyl oxalate additive at 20 °C and at a dose rate of $1.5 \cdot 10^5$ rad/h, ▲ = 0, × = 0.2, ● = 0.32 (eutectic) mole/mole dimethyl oxalate

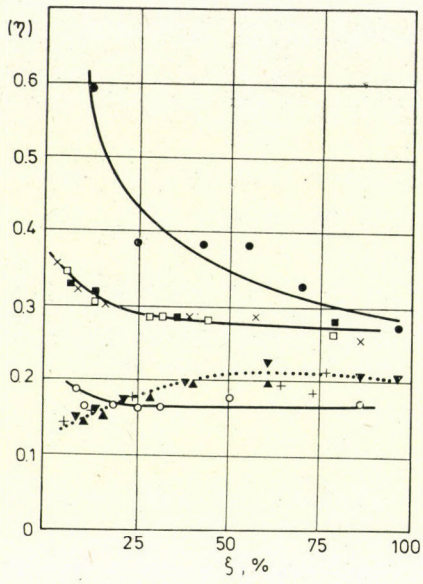

Fig. 7. Intrinsic viscosity of poly-MBI plotted against the conversion of insource polymerization at a dose rate of $2.12 \cdot 10^4$ rad/h (○ = 25 °C, × = 30 °C, ● = 35 °C, at 30 °C with a dose rate of $1.43 \cdot 10^4$ (□) and $1.05 \cdot 10^4$ (■) rad/h, and of post-polymerization irradiated by a total dose of 14.4 Mrad, polymerized at ▲ = 25 °C, + = 30 °C, ▼ = 35 °C

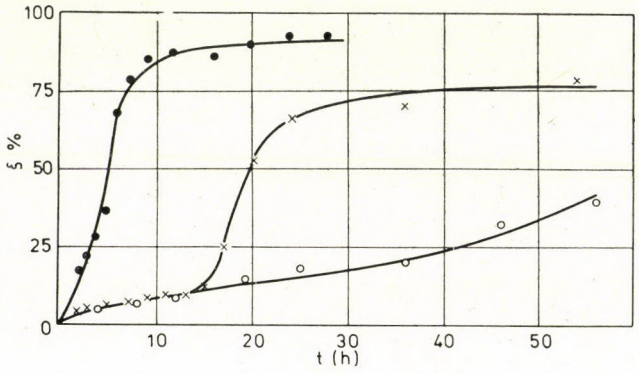

Fig. 8. Post-polymerization of MBI pre-irradiated by 14.4 Mrad at 20 °C. ○ = 25 °C, × = 30 °C, ● = 35 °C

Kinetic curves for the insource polymerizations of MOI are presented in Fig. 9. Kinetic curves of two systems containing different amounts of dimethyl oxalate (DMO) are also included in the Figure (63 mole- % of DMO in MOI forms an eutectic, the m.p. being 43 °C).

The kinetic curves start with an induction period; then a linear rate of polymerization can be observed. Below 35 °C practically no polymerization was observed. The activation energy calculated from the linear stages of the

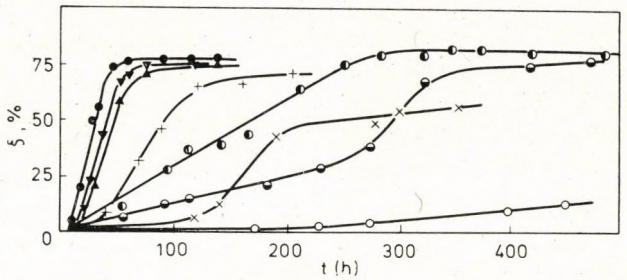

Fig. 9. Insource polymerization of MOI at a dose rate of $2.12 \cdot 10^4$ rad/h ○ = 35 °C, × = = 40 °C, + = 45 °C, ● = 50 °C, at 50 °C with a dose rate of $1.43 \cdot 10^4$ (▼) and $1.05 \cdot 10^4$ (▲) rad/h, ◐ = with 64 mole- % of dimethyl oxalate additive (eutectic) at 35 °C, ◒ = with 30 mole- % of additives at 35 °C

curves is 109 kJ/mole (see Fig. 4). The rate of the insource polymerization is proportional to the first power of the dose rate (Fig. 5).

In Fig. 10 the intrinsic viscosity is plotted against the conversion of insource polymerization. The nature of the curves is identical with that obtained for MBI. Kinetic curves for the post-polymerization of MOI are presented in Fig. 11. The kinetic character of the processes is not accelerating. The molecular weight is independent of the conversion and temperature (see Fig. 10).

Kinetic curves of insource polymerization and post-polymerization of MLI and MCI are shown in Figs 12 and 14. The corresponding intrinsic viscosity functions are illustrated in Figs 13 and 15. The intrinsic viscosities of

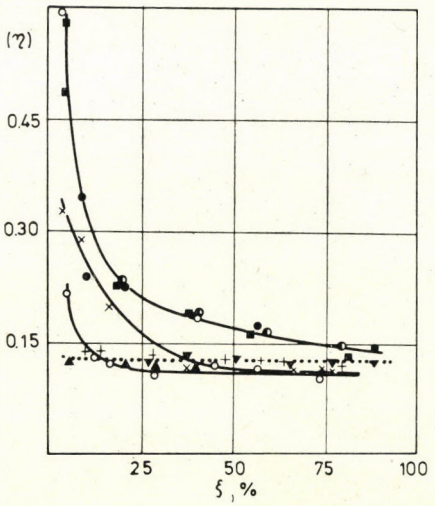

Fig. 10. Intrinsic viscosity of poly-MOI plotted against the conversion of insource polymerization at a dose rate of $2.12 \cdot 10^4$ rad/h. ○ = 40 °C, × = 45 °C, ● = 50 °C, at 50 °C with a dose rate of $1.43 \cdot 10^4$ (◐) and $1.05 \cdot 10^4$ (■) rad/h, and of post-polymerization irradiated at 20 °C by a total dose of 14.4 Mrad, polymerized at ▲ = 40 °C, + = 45 °C, ▼ = 50 °C

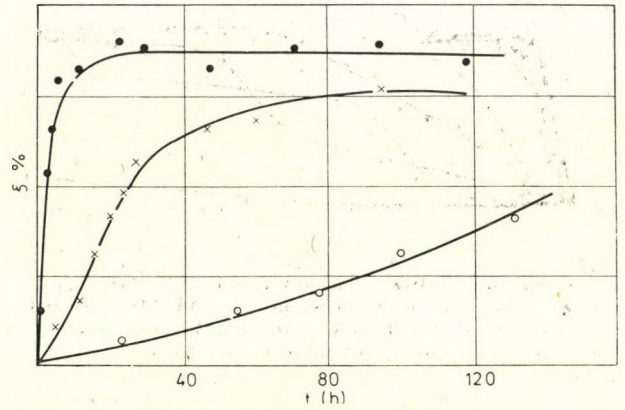

Fig. 11. Post-polymerization of MOI pre-irradiated by a total dose of 14.4 Mrad at 20 °C, polymerized at ○ = 40 °C, × = 45 °C, ● = 50 °C

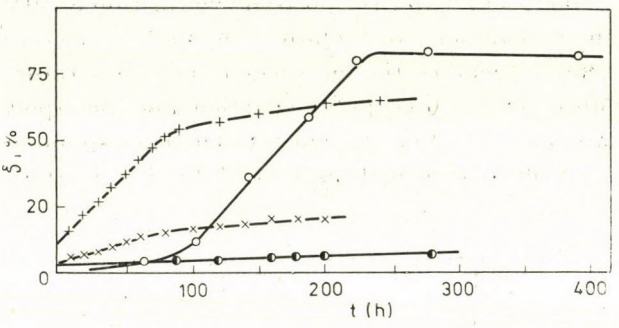

Fig. 12. Insource and post-polymerization of MLI. ○ = insource polymerization by a dose rate of $2.12 \cdot 10^4$ rad/h at 65 °C, post-polymerization after pre-irradiation at 20 °C by a total dose of 11.55 Mrad, at ◐ = 60 °C, × = 65 °C, + = 70 °C

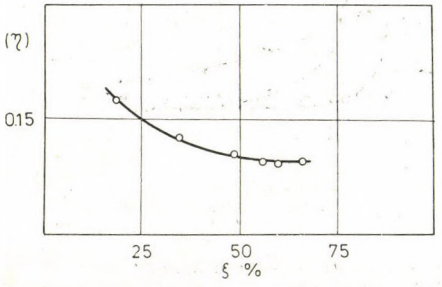

Fig. 13. Intrinsic viscosity of poly-MLI plotted against the conversion of insource polymerization by a dose rate of $2.12 \cdot 10^4$ rad/h at 65 °C

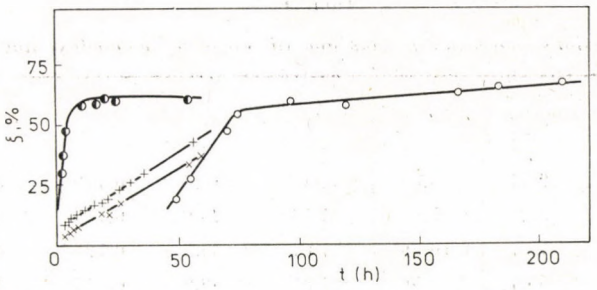

Fig. 14. Insource and post-polymerization of MCI. ○ = insource polymerization by a dose rate of $2.12 \cdot 10^4$ rad/h at 70 °C, post-polymerization after pre-irradiation at 20 °C by a total dose of 11.5 Mrad, at × = 68 °C, + = 73 °C, ◐ = 78 °C

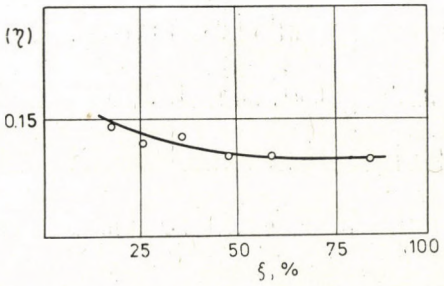

Fig. 15. Intrinsic viscosity of poly-MCI plotted against the conversion of insource polymerization by a dose rate of $2.12 \cdot 10^4$ rad/h

poly-MLI and -MCI obtained by post-polymerization at different temperatures were measured as 0.12 ± 0.02 gdm^{-3}. Characteristics of the kinetic curves and dependence of the molecular weight on the conversion are similar to those of the former two monomers.

Discussion

All the four monomers were classified by our previous system as having accelerating kinetic character. Additives enhance the rates of solid-state polymerizations. In post-polymerization, however, the kinetic character is getting retardant as the chain length of the monomeric molecules increases. In the insource polymerization, the molecular weight is higher during the initial conversion, then tends to a limiting value that depends on the temperature; while in post-polymerization it is independent of both the temperature and conversion.

Using powder records of X-ray diffractometry, the length of the crystal periods and, assuming extended chains, the size of the molecules were determined for the four monomers. These data are collected in Table I. The original diffractograms in schematic representation are shown in Fig. 16.

Table I

Cell dimensions, molecular lengths and tilt angles of monoalkyl itaconates

Compound	Length of dimer mol 1 Å	*a* Å	*b* Å	*c* Å	*c*/1 —	α degrees
MBI	25.7	5.64	7.14	18.7	0.779	50.5
MOI	35.7	5.67	7.54	25.9	0.786	48.8
MLI	45.7	10.39	7.87	33.3	0.727	48.6
MCI	55.7	5.56	7.57	39.9	0.715	47.2

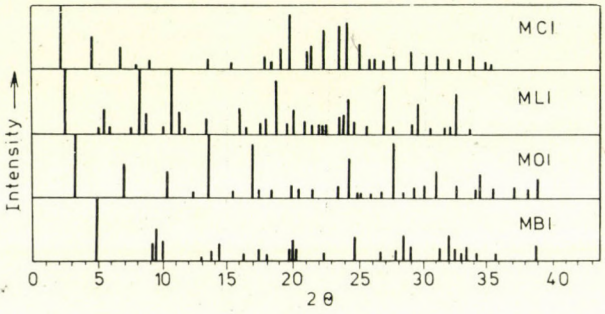

Fig. 16. X-ray diffractograms of monoalkyl itaconate crystals in schematic representation

It can be seen that the unit cell dimensions correspond to the monoclinic cell of substituted parraffins. The average spacing of the extended chain molecules is the same in all the four cases. The longest cell periods are proportional to the lengths of the monomeric molecules, but are higher than these. It means that there are two molecules in the asymmetric units bridged by hydrogen bonds and that the tilt angles of the coupled molecules (α) to the plane of the layers where they are arranged are just the same and decrease only slightly as the chain length increases. Therefore, it can be assumed that the topochemical behaviour of the monoalkyl itaconates should also be the same.

For MBI and MOI, close relations were observed between the kinetic character and the polymer–monomer phase diagram. Below the glass transition temperature of a polymer plastified by its monomer in a composition of M_{kr}, insource polymerization does not take place at a measurable rate. The initial topotactic reaction should, therefore, be regarded heterogeneous [14]. In the viscoelastic range, the polymerization has high activation energy which is commensurable with, or higher than, the estimated [15] heat of sublimation (107 and 123 kJ/mole, respectively). Above the melting point the polymerization rate is high. Thus the rapid polymerization is not brought about by the

reaction occurring in the solid state. It is reasonable, therefore, that the molecular weight of the polymer formed in the so-called solid state is commensurable with that obtained in the liquid phase [11]. The molecular weight of a polymer formed in the real topotactic processes dominating in the first stage of the polymerization should be higher than in the liquid or in the highly elastic state, as the intrinsic viscosity of the polymer rapidly decreases with increasing conversion and temperature.

The effect of increasing the chain length of the monomeric molecules cannot be interpreted unequivocally for the insource polymerization. In the post-polymerization, rates reduced to the same temperature are decreasing by increasing the chain length of the monomers. Obviously, it is not quite a good basis for comparison, since the phase conditions cannot be reduced to the same temperature. It can still be concluded that the increasing length of the monomeric molecules with identical structural conditions is less favorable for the non-homogeneous phase solid-state polymerization. This may be explained by the greater distance between functional groups as the tilt angle of the molecules to their sheet plane decreases, as well as by the higher binding energy by which the molecules are fixed to their sites as the length of the chain substituent is increased.

REFERENCES

[1] Part XXXIV: HARDY, GY., NYITRAI, K., CSER, F.: European Polymer J., **12,** 785 (1976)
[2] CHEN, C. S. H., GRABAR, D. G.: J. Polymer Science **C 4,** 848 (1946)
[3] HARDY, GY., VARGA, J., NAGY, G., JOBBÁGY, M.: Kinetics and Mechanism of Polyreactions. IUPAC Symposium, Abstr. No. 8/14, Akadémiai Kiadó, Budapest, 1969
[4] PLATE, N. A., SHIBAEV, V. P.: Macromol. Rev., **8,** 117 (1974)
[5] JORDAN, E. F.: J. Polymer Science, Polymer Chemistry **10,** 3347 (1972)
[6] COULSON, J.: J. Chem. Soc., **1932,** 2571
[7] DAINTON, F. S.: Trans. Farad. Soc., **56,** 1784 (1960)
[8] NAGAI, S.: Kobunshi Kagaku **15,** 550 (1958)
[9] ISHIDA, SH., SAITO, SH.: J. Polymer Science **5,** 689 (1967)
[10] HARDY, GY., KOVÁCS, G., FEDOROVA, N., BOROS-GYEVI, E.: J. Polymer Science **C 16,** 2675 (1967)
[11] NYITRAI, K., NGUYEN NGOC LAN, HARDY, GY.: Acta Chim. (Budapest) **88,** 195 (1976)
[12] HARDY, GY., CSER, F., KOVÁCS, G., SZATMÁRI, J., SAMAY, G.: Acta Chim. (Budapest) **79,** 143 (1973)
[13] BRAUN, G., KOVÁCS, A. J.: in Physics of Non-Crystalline Solids, p. 303. North Holland, Amsterdam, 1965
[14] WEGNER, G., MUNOZ-ESCALONA, A., KEGGENHOFF, B., VOIGT-MARTIN, I., FISCHER, E. W.: Proceedings of the Third Tihany Symposium on Radiation Chemistry (Ed.: DOBÓ, J. and HEDVIG, P.), p. 521. Akadémiai Kiadó, Budapest, 1972
[15] BONDY, A.: Physical Properties of Molecular Crystals, Liquids and Glasses. J. Wiley and Sons., New York 1968

Károly NYITRAI H-1950 Budapest, Hungária krt 114.
Ngoc Lan NGUYEN Hanoi, Vietnam.
Ferenc CSER
Erzsébet TAKÁCS } H-1950 Budapest, Hungária krt 114.
Gyula HARDY

Acta Chimica Academiae Scientiarum Hungaricae, Tomus 96(3), pp. 235—243 (1978)

INVESTIGATIONS IN THE FIELD OF SOLID-STATE POLYMERIZATIONS, XXXVI [1]

POLYMERIZATIONS OF N-HEXADECYL ACRYLAMIDE AND N-HEXADECYL METHACRYLAMIDE IN THE PRESENCE OF THEIR SATURATED ANALOGUES

F. Cser, K. Nyitrai, V. Dévényi and Gy. Hardy

(Research Institute for the Plastics Industry, Budapest)

Received August 25, 1976

It has been established that the solid-state polymerization of N-hexadecyl acrylamide and N-hexadecyl methacrylamide has accelerating kinetic character. They form isomorphous systems with their saturated analogues (N-hexadecyl propionamide and N-hexadecyl isobutyramide, respectively) which is proved by their phase diagrams and structure analyses. According to X-ray diffractometric investigations, the polymer of N-hexadecyl acrylamide remains in the lattice of the monomer, and the system undergoes a phase transition even at low conversions. The structure of this new phase is preserved in the course of the polymerization in spite of the fact that the structure of the polymer is different. This case is a new evidence for forced isomorphism. In the polymerization of N-hexadecyl methacrylamide, the polymeric product causes a phase transition at low conversions. The polymer becomes isomorphous with the monomer by dissolving the unreacted monomer into its own hexagonal phase. Polymerization takes place then in this loose-packed system.

Several studies have been devoted in our laboratories to the solid-state polymerizations of vinyl esters and ethers containing long-chain aliphatic [2—7] or cholesteryl [8—10] groups. It has been pointed out that these monomers are particularly capable of solid-state polymerization since their molecules are arranged in nodular and laminar structures within the crystal lattice. It follows from the latter that the vinyl groups are located in the same plane, which is a favourable pre-arrangement for solid-state polymerization. This pattern is also found in N-hexadecyl acrylamide and N-hexadexyl methacrylamide to be discussed in the present paper, but the acid amide group may give rise to some differences, owing to the presence of hydrogen bonds. These may, *e.g.* completely hinder longitudinal motion in contrast with the case of vinyl esters and ethers. Hydrogen bonds may interconnect the molecules at the vinyl plane influencing the structure of the polymer formed. These expected effects have been studied in the present work.

Experimental

N-Hexadecyl acrylamide (HAA) and N-hexadecyl methacrylamide (HMA) were prepared from cetylamine with acrylic and methacrylic chloride, respectively, according to Jordan *et al.* [11]. N-Hexadecyl propionamide (HPA) and N-hexadecyl isobutyramide (HIBA) were synthetized from cetylamine with propionic chloride and isobutyric chloride, respectively. The data of the materials prepared in this way are collected in Table I.

Table I

Properties of the substances used
$CH_3(CH_2)_{15}-NHCO-R$

Symbol	R	M.p., °C	Analysis					
			Calculated			Found		
			C	H	N	C	H	N
HAA	$-CH=CH_2$	48	77.40	12.52	4.75	77.51	12.41	4.82
HMA	$-\underset{\displaystyle CH_3}{\underset{\vert}{C}}=CH_2$	52	79.60	12.93	4.52	79.72	12.87	4.38
HPA	$-CH_2-CH_3$	45	76.82	13.14	4.73	76.74	13.21	4.92
HIBA	$-\underset{\displaystyle CH_3}{\underset{\vert}{CH}}-CH_3$	66	77.30	13.28	4.49	77.45	13.44	4.32

Polymerizations

Polymerizations of the monomers were initiated by the 500-Cu ^{60}Co γ radiation source of our Institute. The samples were sealed into 6 mm i.d. ampoules after expulsion of the oxygen by an argon stream. Conversion was determined by precipitation using gravimetric method. Polymer samples were dissolved in a 1 % solution of benzoquinone in chloroform and precipitated by methanol.

Phase diagrams were recorded by means of a polarizing microscope using a method described previously [12]. X-ray diffraction measurements were carried out with a Philips wide-angle powder diffractograph at a scanning rate of 1°/min in the range of 3 to 49° for 2Θ.

Results

Phase diagrams of monomer/inert material systems

Figure 1 shows the phase diagram of the binary system N-hexadecyl acrylamide (HAA) and N-hexadecyl propionamide (HPA). The melting point curve

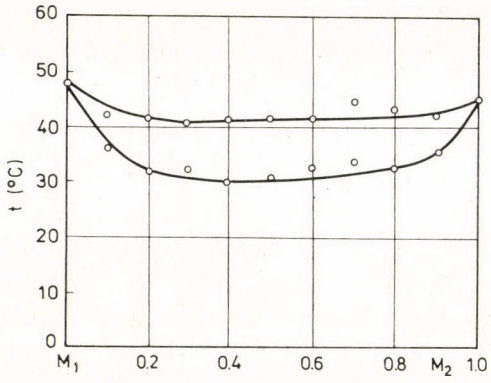

Fig. 1. Phase diagram of the system N-hexadecyl acrylamide (M_1)–N-hexadecyl propionamide (M_2)

starts at that of HAA at 48 °C and, after passing through a very flat minimum at about 40 °C, reaches the melting point of HPA at 45 °C. The course of the freezing point curve is similar, showing its minimum at 30 °C.

In Fig. 2 X-ray diffractograms for some compositions of HAA/HPA are presented schematically. Intesities of the reflexions are illustrated by the lengths of straight lines located at the place of the peak. For each composition, the height of the strongest reflexion is taken as unity, thus all other intesities correspond to its proportion. It can be seen that the characteristic reflexions of HAA are changed even at a molar ratio of 0.9 : 0.1 for HAA/HAP, indicating the appearance of a new phase. This phase can be detected up to the molar ratio 0.5 : 0.5, while the reflexion angles vary continuously. With HPA contents higher than 0.5 : 0.5, the reflexions of HPA are observed at angles varying monotonously with the composition. Comparing Figs 1 and 2 it can be established that HAA and HPA form partially miscible solid solutions. At high HPA contents, the structure of the solid solution corresponds to that of HPA itself, whereas at high HAA contents, the structure of the solid solution differs from that of pure HAA. The two phases, *i.e.* HAA containing HPA, and HPA

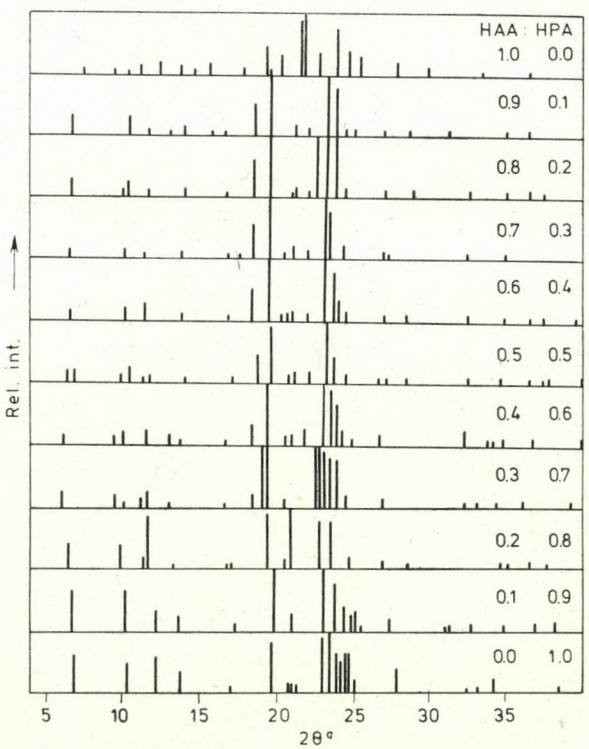

Fig. 2. X-ray diffractogram of N-hexadecyl acrylamide (M_1)–N-hexadecyl propionamide (M_2) mixtures

containing HAA, are not present simultaneously at ambient temperature; always the solid solution characteristic of the component of higher proportion can be detected. The liquidus and solidus curves decrease for both solid solutions by increasing the amount of the second component, and intersect at the composition where the structures of the solid solutions interchange.

The phase diagram of the system N-hexadecyl methacrylamide (HMA) and N-hexadecyl isobutyramide (HIBA) is illustrated in Fig 3. The shape of the solidus curve is convex from the melting point of HMA at 51 °C up to that of HIBA at 65 °C, and it shows a wide shallow maximum between HIBA contents of 0.6 to 0.9. In Fig. 4 schematic X-ray diffractograms are presented for several compositions of the HMA/HIBA system. The reflexions of HMA continuously approach to those of HIBA. For an interpretation of Figs 3 and 4 it can be stated that HMA and HIBA form a solid solution in spite of the slight differences in their structures. The structure of the solid solution depends on the composition and it corresponds to a transition structure between those of the pure components.

Polymerizations

Figure 5 shows the kinetic curves of solid-state in source polymerizations of HAA at 20 °C, in the presence of various amounts of HPA. It can be readily observed that both the polymerization rate and the conversion limit decrease as the concentration of the inert material increases. A physical hindrance of chain propagation of this kind was formerly observed in the binary system of cholesteryl propionate [8].

Kinetic curves of solid-state in source polymerizations of HMA in the presence of various amounts of HIBA are presented in Fig. 6. The inert material both changes the kinetic character and increases the initial rate of poly-

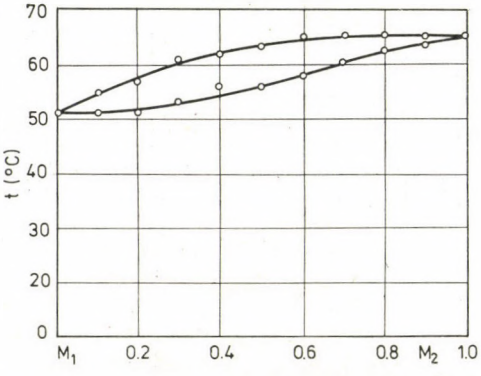

Fig. 3. Phase diagram of the system N-hexadecyl methacrylamide (M_1)–N-hexadecyl isobutyramide (M_2)

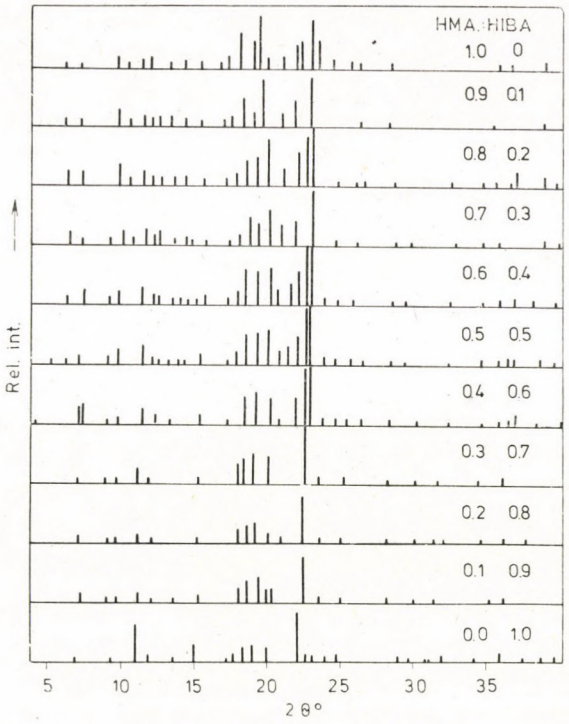

Fig. 4. X-ray diffractogram of N-hexadecyl methacrylamide (M_1)–N-hexadecyl isobutyramide (M_2) mixtures

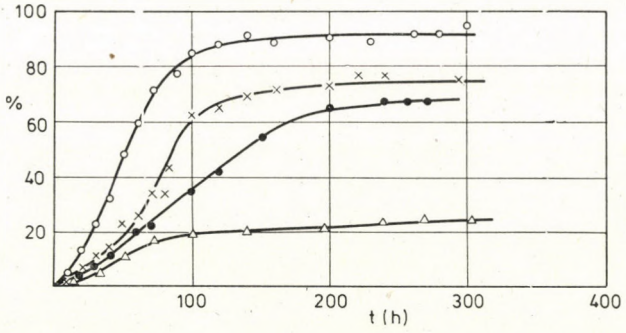

Fig. 5. Kinetic curves of solid-state polymerizations of N-hexadecyl acrylamide at a dose rate of $1.4 \cdot 10^5$ r/h at 20 °C; ○ = without additive; × = with 20 mole- % of HPA; ● = with 50 mole- % of HPA; △ = with 70 mole- % of HPA

merization. In this case the isomorphous diluent presumably alters the structure of the solid phase so that the polymer product can also be isomorphous with the originally isomorphous system consisting of the monomer and inert material.

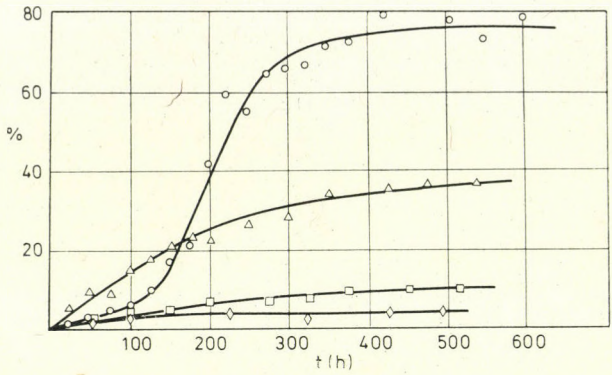

Fig. 6. Kinetic curves of solid-state polymerizations of N-hexadecyl methacrylamide at a dose rate of $1.4 \cdot 10^5$ r/h at 20 °C; ○ = without additive; △ = with 20 mole-% of HIBA; □ = with 50 mole-% of HIBA; ◇ = with 70 mole-% of HIBA

Interactions between the polymer and the monomer

Figure 7 shows the schematic diffractograms of HAA samples taken at various conversions. It can be established that the structure of the monomer changes considerably even at a low conversion. In the presence of the polymer the diffractograms remain characteristic of a crystalline material up to a conversion of 90 %, but the intensities of the reflexions are decreasing. In fact, the locations and relative intensities of the individual reflexions are changing with increasing conversion. The diffractogram of the precipitated pure polymer differs from that of the system of 90 % conversion suggesting a known hexagonal arrangement of the side chains [13]. The polymer/monomer system of 90 % conversion is hexagonal as well, but the reflexion corresponding to the attach-

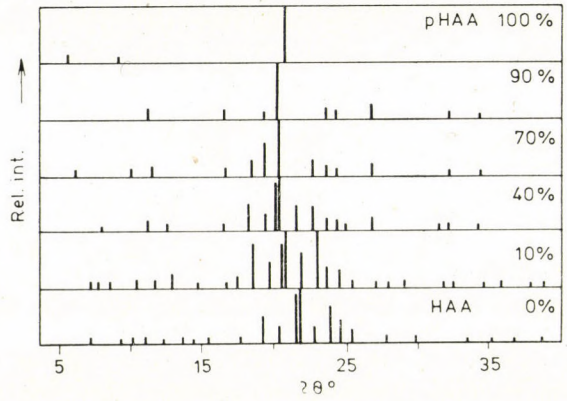

Fig. 7. Schematic illustrations of X-ray diffractograms of polymerizing HAA samples at different conversions

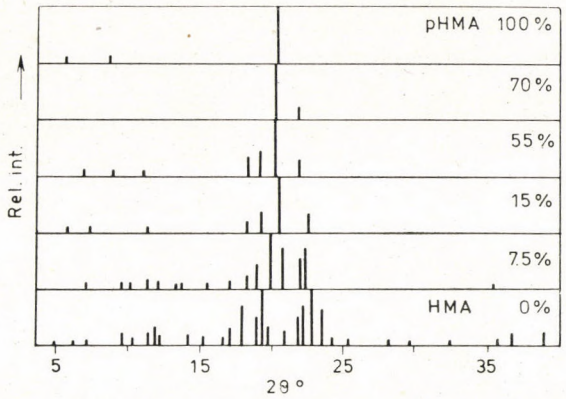

Fig. 8. Schematic illustrations of X-ray diffractograms of polymerizing HMS samples at different conversions

ment of the chains is shifted towards the lower angles (higher distances). This shift can also be observed in the course of the conversion.

In Fig. 8 X-ray diffractograms are schematically illustrated as a function of the HMA conversion. It can be stated that intensities of the crystalline reflexions decrease rapidly as compared with those of the original monomer. Even at a conversion of 7.5 %, the diffractogram indicates the formation of a new phase with crystalline orientation which latter becomes however, reduced with the progress of conversion. At conversions above 15 %, the diffraction pattern of the polymer is predominating. The polymer is characterized by a hexagonal structure and the monomer is transformed into that structure by the appearance of a relatively low amount of polymer.

Discussion of the phase conditions

For an interpretation of the above experimental results, it should be considered that an ideal solid solution of organic molecules is quite rare. According to KITAIGORODSKII [14], a solid solution can be expected when the molecular sizes of the components assure that their overlapping volume takes at least 90 % of the total volume, their crystalline structures are identical and none of the components has a group that could hinder setting into the molecular lattice of the other. Vinyl monomers generally do not form solid solutions with their saturated analogues. Ideal eutectics was obtained for the system acenaphthylene-acenaphthene [15]. The systems N-vinylphthalimide-N-ethylphthalimide [16] and N-vinylcarbazole-N-ethylcarbazole [17] form eutectics, too. Partial miscibility was found for the solid solutions of the monoallyl–monopropyl esters of norbornene-2,3-dicarboxylic acid [18] and cholesteryl meth-

acrylate–cholesteryl isobutyrate [10]. A partially miscible liquid crystalline solution was observed in the system cholesteryl acrylate–cholesteryl propionate [8].

Capability of isomorphism increases with the chain length of the substituent bonded to the vinyl group. It is impaired, however, by the fact that the vinyl group is planar, while its saturated analogue is non-planar. KITAIGORODSKII [14] made a theoretical study of the crystal structure of paraffins and found that the arrangement of the subcells of a long carbon chain related to the crystal lattice is determined by the attachment of the end-groups. This may explain the significance of the vinyl-to-alkyl change in the attachment of the layers in the crystal lattice. The difference observed between HAA and HMA in the present work may be attributed to the higher space requirement of the methyl group of the substituent in HMA (which is not entirely planar) as compared with that of the acryl group; the supplementary hydrogen atoms do not destruct the close packing of the lattice. Furthermore, it does not appear casual that no solid solution is formed in the lattice of HAA; instead, the system HAA/HPA of high HAA content creates a new structure, while HPA is able to dissolve HAA in its lattice with a higher space requirement.

A study of the polymerization of the monomers as a function of the conversion has shown that HAA undergoes a phase transition at a low conversion under the influence of the polymer remaining in the lattice. In the course of further polymerization, the polymer preserves the structure of this phase in spite of the fact that its own structure is different. This is an additional piece of evidence for forced isomorphism described previously [8]. The polymerization characteristics of mixed films of vinyl stearate–ethyl stearate studied by PUTERMAN *et al.* [19] can be explained similarly.

Phase transitions in HMA systems occur at lower conversions. The polymer becomes isomorphous with the monomer in such a way that the polymer dissolves the unreacted monomer in its hexagonal phase. Such a hexagonal phase is formed in smectic substances as well, characterized by chains perpendicular to the plane of the chain ends; the direction of the C – C – C planes within the chains is, however, statistical. Polymerization takes place in this loose-packed system. This pattern is related to the feature of the solid-state reaction. The reaction rate increases as the new phase has formed resulting in an accelerating kinetic character. In the presence of the isomorphous inert material the modifying effect of the polymer does not prevail, since the initial crystal structure differs from that of the pure monomer even if this difference is slight.

The highest periods of the monomeric crystals are 24.9 Å for HAA and 21.51 Å for HMA; those for the systems containing polymers are 31.2 and 31.1 Å, respectively. The estimated length of extended chain molecules is 27.5 Å. It means that the molecules are tilted to their sheet in monomeric crystals, but form sheets with perpendicular molecular chains in the presence

of polymer. Such a transformation of molecular orientation was not observed in monomers having no hydrogen bridges within the sheets. In all cases when forced isomorphism between a monomer and polymer was detected, the polymer was preserved by the lattice geometry of monomeric crystals. In the present cases this relation is reversed, which can be explained by hydrogen bonding forces coupling the molecules to each other within the sheets and preventing the formation of a separate polymeric phase.

REFERENCES

[1] Part XXXV: NYITRAI, K., NGUYEN, N. L., CSER, F., TAKÁCS, E., HARDY, GY.: Acta Chim. (Budapest) **96,** 223 (1978)
[2] HARDY, GY., NYITRAI, K., KOVÁCS, G., FEDOROVA, N.: Acta Chim. Acad. Sci., Hung., **43,** 121 (1965)
[3] HARDY, GY., NYITRAI, K., VARGA, J., PATHÓ, M.: Periodica Polytechnica **9,** 157 (1965)
[4] HARDY, GY., NAGY, L., CSER, F.: Acta Chim. Acad. Sci. Hung., **47,** 211 (1966)
[5] HARDY, GY., NYITRAI, K., CSER, F., CSELIK, GY., NAGY, L.: European Polymer J., **5,** 135 (1969)
[6] HARDY, GY., NYITRAI, K., CSER, F.: Acta Chim. Acad. Sci. Hung., **62,** 253 (1969)
[7] HARDY, GY., NYITRAI, K., CSER, F.: Macromolecular Synth., **5,** 91 (1974)
[8] HARDY, GY., CSER, F., KALLÓ, A., NYITRAI, K., BODOR, G., LENGYEL, B.: Acta Chim. Acad. Sci. Hung., **65,** 287 (1970)
[9] HARDY, GY., NYITRAI, K.: Acta Chim. Acad. Sci. Hung., **65,** 301 (1970)
[10] HARDY, GY., NYITRAI, K., CSER, F.: European Polymer J. **12,** 785 (1976)
[11] JORDAN, E. F., RISER, Jr. G. R., ARTYMYSHYN, B., PENSABANA, W., WRIGLEY, A. N.: J. Appl. Pol. Sci., **13,** 1777 (1969)
[12] HARDY, GY., CSER, F., KOVÁCS, G., SZATMÁRI, J., SAMAY, G.: Acta Chim. (Budapest) **79,** 143 (1973)
[13] Crystal structure and X-ray diffraction behaviour of paraffins, *cf.*: PLATE, N. A., SHIBAEV, V. P.: Makromol. Rev., **8,** 117 (1974); MOROSOFF, N., MORAWETZ, H., POST, B.: J. Am. Chem. Soc., **37,** 3035 (1965); SCHENER, A. A., BAYLE, G. G., MAZEE, W. M.: Rec. trav. Chim., **75,** 513 (1956) and Refs [14] and [19]
[14] KITAIGORODSKII, A. I.: in Organic Chemical Crystallography, Consultant B, New York, 1961
[15] ZURAKOWSKA-ORSZAGH, J., GOMULKA, A.: Proc. 2nd Tihany Symposium on Radiation Chemistry, p. 633. Akadémiai Kiadó, Budapest 1967
[16] VARGA, J.: Personal communication
[17] AZORI, M.: Personal communication
[18] HARDY, GY., NYITRAI, K.: Acta Chim. Acad. Sci. Hung., **52,** 105 (1967)
[19] PUTERMAN, M., FORT, T. Jr., LANDO, J. B.: J. Coll. Interf. Sci., **47,** 705 (1974)

Ferenc CSER
Károly NYITRAI
Veronika DÉVÉNYI
Gyula HARDY

H-1950 Budapest

Acta Chimica Academiae Scientarium Hungaricae, Tomus 96(3), pp. 245–258 (1978)

THE EFFECT OF ALLOYING ON THE SURFACE EXCESS FREE ENERGY OF NOBLE METAL CATALYSTS

T. MALLÁT, É. POLYÁNSZKY and J. PETRÓ

(Department of Organic Chemical Technology, Technical University of Budapest, Budapest)

Received April 30, 1977

Our previous studies have shown that the surface excess free energy of platinum, palladium, rhodium, ruthenium and iridium catalysts depends primarily on the nature of the catalyst, but it also varies with the method of preparation.

This work aims at investigating how the surface excess free energy of palladium and platinum catalysts varies upon alloying. The effect of alloying was studied on Pd–Ir and Pt–Au systems.

By extending the investigations to the measurement of hydrogen content, surface area and activity, we have found that the excess surface free energy remains essentially unchanged within the detection limit while the components of the alloy form a homogeneous solution and have similar physicochemical properties (*e.g.* lattice parameters) which enable the atoms of the alloying metal to replace easily those of the host metal in the lattice points.

Detectable changes occur in the excess free energy upon alloying only in those cases when new phases appear (Pt with an Au content of 10 – 15 atom %).

Introduction

According to the most generally accepted view, catalysts can be regarded as substances in a non-equilibrium state with excess free energy. The most important components of this excess free energy are, according to ROGINSKII [1], the phase defects, chemical and structural defects and the high dispersity.

In certain cases, there is a linear correlation between the excess surface free energy and other properties (*e.g.* catalytic activity) of the catalysts [2].

The excess free energy can be determined on the basis of several physicochemical properties of solids. Our measurements are based on an improved variant of the method of HÜTTIG and HERMANN [3] and ROGINSKII [1]. Accordingly, the excess free energy (ΔF) of noble metal catalysts is determined from the potential difference, E, of the active substance and the metal in equilibrium state, with respect to the ions of the given metal [4], by means of the equation

$$\Delta F = 23060\, n\, E \quad \text{(cal/mol)}$$

where n is the valence number of the metal ion in solution.

One of the basic features of the method developed in our laboratory is that, before the measurement, the catalyst is polarized galvanostatically to a

potential at which the catalyst can be regarded as practically free of gases. Otherwise, the oxygen or hydrogen gas on the surface of the catalyst interferes with the determination of the potential Me/Me^{n+}.

The excess free energy calculated from the electrochemical potential is characteristic of the surface of the catalyst, and thus it represents the excess free energy referred to unit surface area, an important property in catalysis.

We found [4] that the surface excess free energy of platinum, palladium, rhodium, ruthenium and iridium catalysts is a function primarily of the nature of the catalyst, but it can also be influenced by the method of preparation over a wide range. For a given metal, the higher the value of ΔF, the higher the catalytic activity obtained.

As an extension of this work, we have now studied how the changes occurring upon the alloying of the catalysts can be detected *via* the measurement of the surface excess free energy. The effect of alloying was studied on the Pd–Ir and Pt–Au systems.

In addition to the measurement of ΔF, the sorption of hydrogen was also investigated by galvanostatic and potentiodynamic methods, furthermore, the surface area and the catalytic activity were measured in liquid-phase hydrogenation reactions. On the basis of these measurements, we attempt to estimate the role of the components of ΔF in the surface excess free energy.

Experimental

1. Experimental methods

a) *The determination of surface excess free energy*

The surface excess free energies of palladium–iridium catalysts were measured in the following way. Thirteen to 50 mg samples of the catalyst were polarized to ca. 500 mV in 1 *N* HCl. The resulting degassed catalyst was transferred under liquid into the measuring electrode chamber of the apparatus described in our previous publication [4], containing a solution with a concentration of 1 *M* for HCl and 10^{-3} *M* for H_2PdCl_4. The flask was shaken to make the catalyst grains impact against a smooth platinum sheet electrode. The reference electrode was Ag/AgCl/HCl (1 *M*) system. The two electrode chambers communicated through ground joints. The measurements were carried out at 25 °C.

With this method, a possible source of error is that the catalyst may re-adsorb gases when transferred from the polarizing apparatus into the measuring chamber, or adsorb gases from the electrolyte fed into the latter. Therefore, an apparatus was developed (Fig. 1), which can be applied for both galvanostatic polarization and the measurement of ΔF. During the measurement, the electrolyte and the catalyst can be flushed with oxygen-free argon

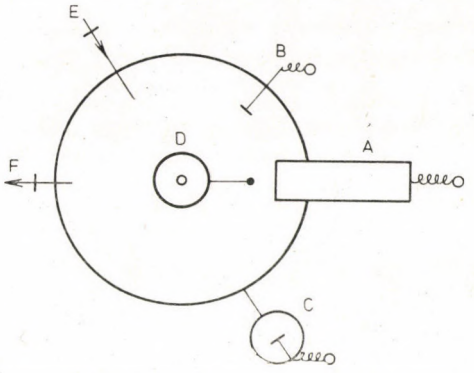

Fig. 1. Apparatus for the measurement of free energy. A – measuring electrode, B – auxiliary electrode, C – reference electrode, D – inlet and outlet of Ar gas, E – inlet of oxygen-free electrolyte, F – electrolyte drain

and between the two measurements the electrolyte can be replaced under an inert gas atmosphere.

The design of the measuring electrode is as follows. A ground piston moves in a sheath closed on the end with a sintered glass filter. The piston ends in a platinum sheet. The catalyst can be placed between the platinum sheet and the filter, and it is pressed against the latter by the piston. The polarizing auxiliary electrode is a smooth platinum sheet, and the reference electrode is Ag/AgCl immersed into 1 *N* HCl. The electrolyte can be stirred by argon gas or with a magnetic stirrer.

This apparatus was used to study Pt–Au catalyst systems.

b) *Galvanostatic and potentiodynamic studies*

The galvanostatic investigations of the catalysts containing palladium and the potentiodynamic measurements on all catalysts were performed in the three-electrode chamber described in our previous paper [4]. In this cell the measuring and polarizing electrodes are smooth platinum sheets, and the reference electrode is a platinized platinum hydrogen electrode. From the space of the reference electrode a Luggin capillary leads down to the catalysts.

The *galvanostatic* investigations of Pd-containing catalysts were performed at room temperature with 10 mg samples of catalyst in 1 *N* sulfuric acid. Current intensity was 2 mA. The catalyst samples were first saturated with hydrogen by cathodic polarization, and then the anodic curves were taken. In plotting the curves, the approximate value of the resistance polarization was also taken into account. The section of the curves below 50 mV was determined by extrapolation. In the evaluation of the charging curves, according to the approximation given in our previous paper [5], the amount of hydrogen

desorbed between 0 and 90 mV was regarded as dissolved, and that desorbed in the range of 90 – 300 mV as adsorbed. From the amount of adsorbed hydrogen, the surface area was calculated by the usual approximations [6], and it was also evaluated from the specific capacitance obtained from the double-layer sections of the curves [7]. (Since no data have been found in the literature on the specific capacitance of the alloys, the values pertaining to platinum were used in all cases.)

The galvanostatic curves of Pt–Au catalysts were measured in the apparatus shown in Fig. 1. The measurements were carried out at 25 °C with 20 – 30 mg of catalyst in 1 *N* HCl, at a current intensity of 1 mA. The amount of sorbed hydrogen was determined from the 0 – 300 mV section of the curves, whereas the surface area from the double-layer section.

In the *potentiodynamic* measurements 1 *N* sulfuric acid or 1 *N* hydrochloric acid was used as electrolyte. The measurements were carried out at room temperature between 50 and 300 mV with 1 – 10 mg of catalyst, using an AMEL 551/SU type potentiostat. To determine the potentials belonging to each of the maxima, the rate of the potential change was decreased until the peaks did not shift any more [5, 8].

c) *Activity measurements*

The apparent activities of the catalysts were investigated in liquid phase hydrogenation reactions at 20 °C under 1 atm, using nitrobenzene, eugenol and acetophenone as reactants. One hundred mg catalyst and 10 ml 90 % ethanol were charged into a 50 ml flask, and the reaction mixture was saturated with hydrogen under shaking. Thereafter, 2 ml of a 90 % alcohol solution containing 2 mmol of eugenol or acetophenone or 2/3 mmol of nitrobenzene, respectively, were injected into the system, and the consumption of hydrogen was measured.

Activity was defined as the amount of hydrogen (ml) consumed from the gas phase by 1 g catalyst in 1 min.

2. The preparation of catalysts

a) *Pd catalysts containing 0, 0.5, 2.5 and 4 atom % of Ir*

The pH of 30 ml of a 10 wt. % H_2PdCl_4 solution was adjusted to 9 – 10 with 30 wt. % NaOH solution. The precipitated oxide was boiled, and immediately hydrogenated under atmospheric pressure and shaking until the hydrogen uptake ceased. The catalyst was washed with hot distilled water, and dried at room temperature in a vacuum desiccator to constant weight.

The iridium containing catalysts were prepared in a similar manner, except that in the starting H_2PdCl_4 solution $(NH_4)_2IrCl_6$ was dissolved in amounts corresponding to 0.5, 2.5 and 4 atom % of iridium content.

b) *Pt–Au catalysts containing 0, 5, 10, 15 and 20 atom % of Au* were prepared by sodium borohydride reduction; 120 ml of a solution of 4.5 g Na_2PtCl_6 and an appropriate amount of $HAuCl_4$ and 300 ml 15 wt. % solution of $NaBH_4$ were dropped simultaneously, at 20–25 °C, into 150 ml of distilled water, in a manner always ensuring an excess of sodium borohydride. Thereafter, the reaction mixture was heated to boiling and then filtered. The catalysts were washed with 200 ml of 0.1 *N* hydrochloric acid and distilled water, and finally dried at 25 °C in vacuum.

Results

The effect of alloying was investigated on platinum catalysts containing gold and palladium catalysts containing iridium. These systems were selected on the basis of the following considerations. In the electrochemical measurement of the surface excess free energy, it must be taken into account that the potential of alloy catalysts is determined by the less noble component, but the alloying metal, in parallel with alloy formation, makes the standard potential of the less noble metal more positive. To be able to neglect the dissolution of the nobler component, the difference between the two standard potentials must be sufficiently large. These considerations have led to choosing iridium and gold for alloying palladium and platinum, respectively. (The corresponding metal/metal chloride complex standard potentials are as follows:

$$E^0_{Pd} = 0.64 \text{ V}$$

$$E^0_{Pt} = 0.76 \text{ V}$$

$$E^0_{Ir} = 0.86 \text{ V}$$

$$E^0_{Au} = 1.00 \text{ V})$$

The Pd–Ir system is homogeneous above 1500 °C, and separates into systems rich in palladium or iridium below this temperature. The heterogeneous range rapidly increases with a decrease in temperature: already at 700 °C only 3 atom % of iridium is dissolved in palladium [9]. According to the investigations of KHOMCHENKO *et al.* [10], pertaining to electrolytically precipitated Pd–Ir black, the system becomes heterogeneous only above 15 atom % of Ir. This might be due to the fact that at low temperatures the equilibrium state cannot be reached owing to slow diffusion. The concentrations of the Pt–Ir alloys chosen in our measurements were to ensure homogeneous alloys. Therefore, palladium was alloyed only with very small amounts of iridium (0.5, 2.5 and 4 atom %), suited for the investigation of the relative importance of chem-

ical defects according to the classification of ROGINSKII in the surface excess free energy.

Platinum and gold crystallize in the same system, and there is only a slight difference in their lattice parameters. Nevertheless, they are miscible to only a restricted extent due to some differences in their electronic structures. At room temperature, the equilibrium composition of the phase rich in platinum is, theoretically, almost 100 % platinum, which, however, cannot be reached in practice due to slow diffusion [11]. With this system, the concentrations of the alloys applied (5, 10, 15 and 20 atom % of Au) certainly reached the heterogeneous region, thereby it is possible to study not only the role of chemical defects but also that of phase defects occurring in the presence of the new phase.

For the calculation of the ΔF values of alloy catalysts it is also necessary to know, as a reference value for the potential of the catalyst, the standard potential of the metal–metal complex ion system of a given concentration, being at thermodynamic equilibrium in the alloy. In the case of Pd–Ir alloy this was calculated (for Pd) by assuming the presence of an ideal solution. In the case of Pt–Au alloys, the potential of Pt was calculated from the approximate equation given by BORELIUS [11]:

$$\frac{F}{R} = 950x^4(1 - x) + 7700\left[x^3(1 - x)^2 + x^2(1 - x)^3\right] + \\ + 2900x(1 - x)^4 + T\left[x \ln x + (1 - x) \ln (1 - x)\right]$$

where F is the free energy change of alloying referred to 1 g atom of the alloy;
$[F_{x=1} = 0$ and $F_{x=0} = 0]$;
x and $(1 - x)$ are the mole fractions of gold and platinum;
T is the temperature; and
R is the universal gas constant.

(a) The galvanostatic curves of Pd catalysts containing 0, 0.5, 2.5 and 4 atoms % of Ir were determined in 1 N sulfuric acid (Fig. 2). The sections corresponding to the processes which occur during anodic polarization, *i.e.* corresponding to hydrogen ionization, double layer charge inversion and oxygen adsorption are well distinguishable on the curves. In the range between 0 and 300 mV, the curve of palladium is more complex than those of other platinum metals owing to the large amounts of dissolved hydrogen. Below 100 mV a long, nearly horizontal section appears, which corrsponds essentially to the oxidation of dissolved hydrogen. The next, lower step can be attributed, according to the approximation mentioned above, to the ionization of the adsorbed amounts of hydrogen.

The potential of the first step of the curves decreases gradually upon alloying. For the catalyst containing 4 atom % iridium, the decrease reaches about 15 mV.

The hydrogen content and the surface area calculated from the galvanostatic curves are given in Table I. It can be seen that the amount of adsorbed hydrogen and the surface area calculated therefrom do not vary with the Ir content, whereas the dissolved and total amounts of hydrogen decrease.

Table I

Specific hydrogen content and surface area of palladium–iridium catalysts

Iridium content (atom %)	Hydrogen content (ml/g)			Surface area (m^2/g)
	Total	Dissolved	Adsorbed	
0	71.3	57.0	14.3	56.1
0.5	70.2	55.7	14.5	56.1
2.5	65.2	51.0	14.2	54.8
4.0	53.5	38.7	14.7	57.0

Upon the introduction of 4 atom % Ir, the apparent activities for the liquid phase hydrogenation of eugenol and nitrobenzene decrease only by 5 – 10 % with respect to that of pure palladium (84 and 79 ml H_2/min g catalyst).

The surface excess free energy of the catalysts remains practically unchanged upon alloying with Ir, being invariably in the range of 2.3 – 2.5 kcal/mol.

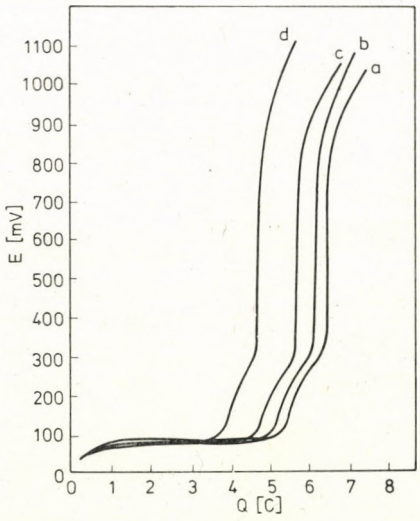

Fig. 2. Galvanostatic curves of Pd–Ir catalysts (1 *N* H_2SO_4, 10 mg catalyst, room temperature, i = 2 mA); *a* – pure Pd, *b* – 0.5 at. % Ir, *c* – 2.5 at. % Ir, *d* – 4 at. % Ir

The width of this range is the same as the probable scatter of the experimental results (± 0.1 kcal/mol).

According to X-ray diffraction measurements, the catalysts are homogeneous, and a new phase rich in iridium cannot be detected.

(b) The hydrogen content of platinum catalysts containing 0, 5, 10, 15 and 20 atom % gold was determined by galvanostatic and thermodesorption methods. The hydrogen content determined electrochemically (Fig. 3, curve b) decreases linearly between 0 and 10 atom %, increases in the range of 10 – 15 atom %, and then decreases again.

The surface areas calculated from the double layer capacitance on the basis of the galvanostatic curves also change abruptly, after a steady section, between 10 and 15 atom % (Fig. 3, curve c).

The hydrogen content referred to 1 m^2 of surface area determined by electrochemical methods (Table II) decreases by about 20 % upon the introduction of 20 % gold, *i.e.* the specific hydrogen sorption ability of the catalyst decreases.

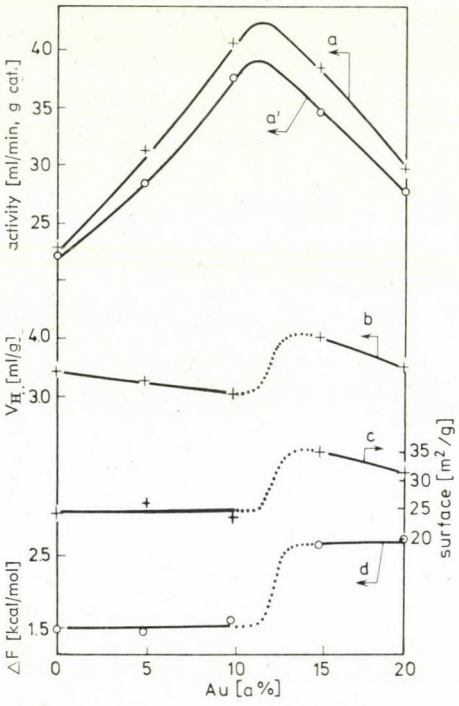

Fig. 3. The most important characteristics of Pt–Au catalysts as a function of composition. *a* and *a'* – activities in the hydrogenation of eugenol and nitrobenzene, *b* – hydrogen content determined electrochemically, *c* – surface area determined electrochemically, *d* – surface excess free energy

Table II

Hydrogen content and surface area of Au-containing Pt catalysts

Au (atom %)	Hydrogen content			Surface area
	From thermo-desorption (ml/g)	From electrochem. measurement		Electrochem. measurement (m^2/g)
		(ml/g)	(ml/m^2)	
0	1.4	3.42	0.140	24.3
5	–	3.22	0.122	26.3
10	0.9	3.01	0.126	23.9
15	1.3	3.95	0.114	34.8
20	0.7	3.45	0.110	31.3

The slight change in the potential dependence of hydrogen sorption is easy to observe on the $\frac{\Delta Q}{\Delta E}$ *vs.* E curves obtained by differentiation of the galvanostatic curves. The differential galvanostatic curves of the catalysts containing 0 and 5 % Au are shown in Fig. 4. (Owing to the different experimental conditions they are not identical to the potentiodynamic i *vs.* E curves.) It can be seen that with the introduction of gold (5 atom %), weakly bound hydrogen is desorbed at a potential by about 15 mV lower than in the case of pure platinum. The peak position of strongly bound hydrogen removed above 200 mV cannot be determined accurately enough due to the stepwise measurement of the galvanostatic curves. With samples of higher gold content, the first peak is already not shifted, and thus the corresponding curves are not reproduced here.

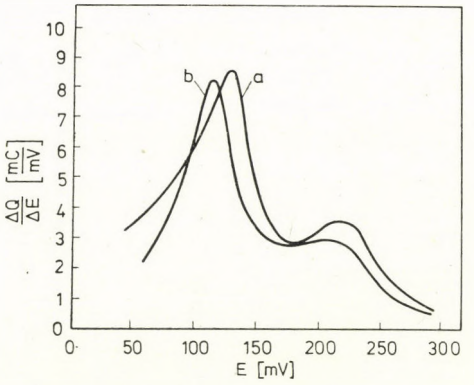

Fig. 4. Differential galvanostatic curves of Pt–Au catalysts (1 *N* HCl, 25 mg catalyst, 25 °C); *a* – pure Pt, *b* – 5 at. % Au

Potentiodynamic studies permit more detailed and accurate results to be obtained concerning the hydrogen adsorbed on the catalysts. The potentiodynamic curves of platinum catalysts containing gold exhibit two maxima due to hydrogen in all the cases, like those of pure platinum [12], but the spacing of maxima decreases with increasing gold content (Fig. 5). This is in agreement with the results of BREITER [13], according to which, if platinum is alloyed with increasing amounts of gold, only one, broad peak can be found above 40 % gold content.

The amount and nature of adsorbed hydrogen were also investigated by thermodesorption methods, in addition to electrochemical measurements. With an increase in gold content from 0 to 20 atom %, the termodesorption of hydrogen takes place at temperatures lower by about 100 °C. The decrease in the peak temperature corresponds to decreasing metal–hydrogen bond strengths. The amount of sorbed hydrogen as a function of the composition varies in a similar way as observed in the electrochemical measurements.

The structures of the catalysts were investigated by X-ray diffraction methods. The presence of a phase rich in gold could not be detected in any of the samples, only the two most intense peaks of platinum were broadened towards the value characteristic of gold. The asymmetric broadening of the two peaks of Pt and the invariance of the positions of the maxima can be attributed to the fact that upon the introduction of gold the amount of phases rich in platinum and containing gold in various amounts increases inside the grains at the expense of the pure platinum phase.

The apparent activities of the catalysts in the hydrogenation of eugenol and nitrobenzene (Fig. 3, curves *a* and *a'*) change quite similarly in the entire

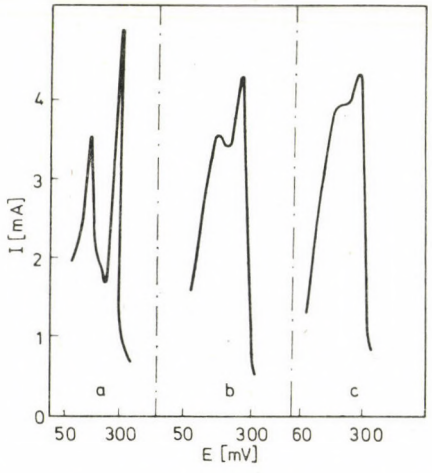

Fig. 5. Potentiodynamic curves of Pt–Au catalysts in 1 *N* sulfuric acid. Rate of potential change 200 mV/min; *a* – 0 at. % Au (17 mg), *b* – 10 at. % Au (17 mg), *c* – 20 at. % Au (15 mg)

concentration range studied. With both reactants, the probable maximum lies between 10 and 15 atom %.

The surface excess free energy (Fig. 3, curve *d*) was found to be constant between Au contents of 0 and 10 atom %, increasing only in the range of 10 – 15 atom % of Au by about 70 per cents. This increase occurs in the range where the other catalytic properties also show remarkable changes.

Discussion

The results obtained on the effect of alloying on the hydrogen content, surface area, activity and surface excess free energy of palladium–iridium and platinum–gold systems can be interpreted as follows.

(a) *Pd–Ir catalysts*

The lattice parameters of Pd and Ir are nearly identical (3.88 and 3.89 Å), making substitution in the crystal lattice possible, particularly in the alloys studied, containing 0 to 4 atom % of Ir. The structural homogeneity of the bulk of alloys is also proved by X-ray diffraction measurements, which failed to show the presence of phases rich in iridium. However, the bulk and surface compositions of alloy catalyst grains may be considerably different. According to the segregation theory [15], the component with a lower heat of sublimation is enriched on the surface of homogeneous alloys. In the Pd–Ir system, Pd has the lower heat of sublimation [16], and thus it can be expected to undergo enrichment in the surface layers. Therefore, the introduction of 4 atom % Ir may cause only minor changes in the surface characteristics as compared with palladium.

Accordingly, the surface excess free energy (ΔF) of the alloys was found to remain practically unchanged upon the introduction of iridium.

The invariance of ΔF leads to only insignificant changes in the catalytic activity (5 – 10 %), in agreement with our previous observations [4].

According to our electrochemical measurements, the effect of iridium is manifested primarily in a decrease of the metal–hydrogen bond strength (qualitative change) and in a slight decrease in the dissolved and total amounts of sorbed hydrogen (quantitative change). The amount of adsorbed hydrogen and the surface area were found to be independent of the iridium content.

The decrease in the amount and bond strength of dissolved hydrogen can be interpreted by assuming that iridium enters the lattice of palladium, *i.e.* an alloy is formed. The galvanostatic investigations of KHOMCHENKO *et al.* [10] on Pd–Ir catalysts have led to similar conclusions. Accordingly, the introduction of iridium changes primarily the *bulk structure* of the catalyst: alloy formation involves changes in the qualitative and quantitative parameters of the dissolution of hydrogen. In contrast, the surface characteristics

of the catalyst (amount of adsorbed hydrogen, surface area, activity and surface excess free energy) remain essentially unchanged.

(b) *Pt–Au catalysts*

In the alloys of platinum formed with gold substantial differences can be expected to occur between the surface and bulk properties of the grains. In this system the heat of sublimation of the alloying metal, gold, is much lower than that of the host metal [15]. Therefore, one can expect gold, or a phase rich in gold, to be enriched on the surface and in the nearby layers. Thus the surface of the alloy will probably separate into phases rich in platinum and gold. This surface inhomogeneity was detected by BREITER [17] in an electrochemical study of the surface composition of Pt–Au alloys.

Concerning the bulk structure of alloys, we have found by X-ray measurements that gold is built gradually into the lattice of platinum, as shown by the asymmetric broadening of the Pt maxima. The characteristic maximum of gold could not be detected in any of the alloys, but the X-ray diffractograms of the samples containing 15 and 20 atom % gold were already identical, suggesting that gold in a quantity above 15 atom % does not enter the phase rich in platinum, forming instead a new phase rich in gold which is amorphous in X-ray diffraction. A similar conclusion can be found in the literature [14] on electrolytically deposited Pt–Au black.

At low concentrations, when the alloy is homogeneous, alloying with gold causes only slight changes in the catalytic properties of platinum. More significant changes can be expected to occur in the concentration range in which the alloy is already heterogeneous, and contains a second phase rich in gold.

As shown by Fig. 3, there is an abrupt change in the surface area, hydrogen content, surface excess free energy and catalytic activity when the average gold content increases from 10 to 15 atom %. According to the above considerations, this is the range where the formation of a heterogeneous alloy begins on the surface.

The surface excess free energy increases by about 70 % in the above range, and the constancy of ΔF in the range above 15 atom % indicates that the character of the surface is essentially invariant with respect to the introduction of further amounts of gold. SACHTLER *et al.* [18, 19] obtained similar results by measuring the electronic work function and the adsorption ratio H_2/Xe.

The change in surface area can also be associated with the surface homogeneity or inhomogeneity of the alloy. The surface area is practically constant in the homogeneous range, it increases by about 25 – 30 % with the appearance of the second phase, and slightly decreases above a gold content of 15 atom %. The increase in surface area is presumably due to the ability of the new phase, similarly to supports, to readily disperse platinum. (The decrease above 15 atom % might be attributed to the fact that in the calculation of surface area

from the charging curves the specific capacity of platinum was used, and the error thereby introduced increases with increasing gold content.)

The variation of the hydrogen content of catalyst samples is essentially similar in tendency to that of the surface area. The amount of hydrogen sorbed on unit area shows a decreasing trend upon alloying. (Owing to the relatively great scatter of the ratio of the two quantities, no further conclusions can be drawn.) Gold decreases not only the amount but also the bonding energy of hydrogen. This is indicated by the shifts of the maxima in both the differential galvanostatic curves and the thermodesorption curves towards lower potentials and temperatures, respectively, upon alloying.

According to the potentiodynamic investigations, not only the metal hydrogens bond energy decreases with increasing gold content, but the two types of hydrogens also become less separated. Consequently, the surface area of the catalyst, at least with regard to hydrogen sorption, becomes energetically more homogeneous.

The apparent activities of the catalyst samples were similar in the hydrogenation of double bonds (eugenol) and nitro groups (nitrobenzene), and exhibited maxima between 10 and 15 atom % gold, *i.e.* in the range where the second phase occurs. The increase in activity between 0 and 10 atom % can be attributed presumably to a loosening effect of introduced gold on the platinum–hydrogen bond. The decrease in activity at higher concentrations can be associated with an enrichment of the inactive phase, rich in gold on the surface.

It appears from the above results that phase defects and changes in dispersity (surface area), two of the parameters considered by ROGINSKII as making the most important contribution to the surface excess free energy, need not be taken into account in the range between 0 and 10 atom % gold. Under the same conditions of preparation, the effect of structural defects is probably similar. The fact that the change in composition (chemical defects) is not accompanied by changes in the excess free surface energy can be attributed to the physicochemical similarity of the two components. The increase of ΔF in the range of 10 – 15 atom % gold can be ascribed equally to phase defects (formation of a new phase) and to increasing dispersity.

Conclusions

Our conclusions concerning the effect of alloying on the surface excess free energy of platinum–gold and palladium–iridium systems are as follows.

1. In the concentration range where the two components form a substitution alloy (0 – 4 atom % for Ir/Pd and 0 – 10 atom % for Au/Pt), the surface excess free energy is constant within the experimental error. Accordingly,

in such cases the role of "chemical defects" is negligible. (The introduction of increasing amounts of iridium, leads probably to its incorporation primarily into the bulk phase and Au may be enriched on the surface.)

2. In the range where the alloy becomes heterogeneous upon increasing the amount of one of the components (10 – 15 atom % for Au/Pt), the surface excess free energy of the catalyst, together with the other characteristics investigated, undergoes substantial changes. Since in this case the surface area also increases, the change in ΔF can also be attributed to an increase in dispersity and the formation of a new phase.

REFERENCES

[1] Roginskii, S. Z.: Zh. Fiz. Khim., **15,** 708 (1941)
[2] Tovbin, M. V., Yatsimirskii, V. K.: Katal. i Katal. Akad. Nauk Ukr. SSR., **3,** 24 (1967)
[3] Hüttig, G. F., Hermann, E.: Z. anorg. Chem., **247,** 221 (1941)
[4] Petró, J., Polyánszky, É., Csűrös, Z.: J. Catal., **35,** 289 (1974)
[5] Petró, J., Mallát, T., Polyánszky, É.: J. Catal., **44,** 345 (1976)
[6] Sokolskii, D. V.: Gidridovanie v rastvorakh. Izd. Akad. Nauk Kaz. SSR, Alma-Ata 1962
[7] Skopin, Yu. A., Sokolskii, D. V.: Katal. v. vysshei shkole. Tr. 1. Mezhd. sov. po katal. 1958 (1), Pt. 2.14 (pub. 1962)
[8] Will, F. G., Knorr, C. A.: Z. Electrochem., **64,** 258 (1960)
[9] Savitskii, E. M., Polyakova, V. N., Tylkina, M. A.: Splavy palladiya. Izd. Nauka, Moscow 1967
[10] Sutyagina, A. A., Kapteva, N. G., Khomchenko, G. P.: Vestn. Mosk. Univ., **11,** 562 (1970)
[11] Borelius, G.: Ann. Phys., **20,** 57 (1934); **24,** 489 (1935); **28,** 507 (1937); **33,** 517 (1938)
[12] Petró, J., Polyánszky, É.: Magy. Kém. Foly., **81,** 486 (1975)
[13] Breiter, M. W.: Trans. Faraday Soc., **61,** 749 (1965)
[14] Woods, R.: Electrochim. Acta, **16,** 655 (1971)
[15] Burton, J. J., Hyman, E., Fedak, D. G.: J. Catal., **37,** 106 (1975)
[16] Bond, G. C.: Catalysis by Metals. Academic Press, London 1962
[17] Breiter, M. W.: J. Phys. Chem., **69,** 901 (1965)
[18] Bouwman, R., Sachtler, W. M. H.: J. Catal., **19,** 127 (1970)
[19] Kuijers, F. J., Dessing, R., Sachtler, W. M. H.: J. Catal., **33,** 316 (1974)

Tamás Mallát
Éva Polyánszky
József Petró
H-1521 Budapest

Acta Chimica Academiae Scientiarum Hungaricae, Tomus 96(3), pp. 259–265 (1978)

STEREOCHEMISTRY OF PLATINUM METAL COMPLEXES OF BIURET

P. C. SRIVASTAVA* and B. K. BANERJEE

(Physical Research Wing, Planning and Development Division, Fertilizer Corporation of India Limited, Sindri, India)

Received December 14, 1976

in revised form June 6, 1977

The preparation and characterization of the complex of biuret with Pd(II), Pt(II), Pt(IV) and Rh(III) is described. Probable structures for the complexes are proposed on the basis of chemical analyses, magnetic susceptibility, electronic and infrared spectral data. The mode of co-ordination and force constants for M–O and M–Cl bonds are discussed. In every complex the ligand behaves as an oxygen donor. The order for K_{M-O} and K_{M-Cl} is Pt(II) > Pd(II) and Pt(IV) > Rh(III) for square planar and octahedral complexes respectively.

Introduction

The industrial application of platinum and Pt group metal catalysts is well known [1–6]. They play an important role not only in the fertilizer industry but also in many chemical manufacturing processes. The salient features of the modern trend of research on the aforesaid problems are the quick and precise analysis of the metal with some new organic ligands and their activity in relation to their electronic structure.

The versatility of biuret (BT) as a co-ordinating ligand is well recognized [7–11]. An extensive infrared study has been made on the most common nitrogen and oxygen bonded complexes. Recently, numerous papers dealing with the square planar and octahedral complexes of platinum metals have been published. The electronic energy levels of the complexes vary according to the oxidation state and nature of the ligand [12–17].

Moss [18] discussed the activity of heterogeneous platinum metal catalysts in terms of electronic configuration (d^n configuration). To circumvent the difficulty of describing the electronic structure of the surface itself, the electronic properties of the bulk have been assumed to be a fair approximation in an attempt to establish a correlation with the catalytic activity.

Keeping this in view we have made an effort to determine the stereochemical properties and crystallochemical characteristics of these metal biuret complexes. In the present study we report the preparation and properties of the Pd(II), Pt(II), Pt(IV) and Rh(III) complexes of biuret. Probable structures have been proposed which are consistent with spectral and magnetic susceptibility data and results of chemical analysis.

* Address all correspondence to this author.

Table I

Compound	Colour	m.p. (°C)	Metal (%)		Carbon (%)
			calcd.	obsd.	calcd.
$Pt(C_2H_5N_3O_2)Cl_2$	Orange	135	52.84	52.60	6.05
$Pt(C_2H_5N_3O_2)_2Cl_4$	Yellow	155	35.92	35.60	8.83
$Pd(C_2H_5N_3O_2)_2Cl_2$	Yellow	164	27.75	27.62	12.52
$Pd(C_2H_5N_3O_2)Cl_2$	Orange red	160	37.85	37.68	8.57
$[Rh(C_2H_5N_3O_2)Cl_3]_2$	Yellow	150	32.96	32.80	7.68

Experimental

(i) *Pd(BT)$_2$Cl$_2$*. Palladium(II) chloride and biuret in a 1 : 2 mole ratio were stirred together in a mixture of ethanol and water and concentrated on a water bath. A yellow product was obtained and recrystallized from alcohol and acetone and dried in vacuum; yield 60 %.

(ii) *Pd(BT)Cl$_2$*. An aqueous solution of palladium(II) chloride and biuret in a 1 : 1 mole ratio was concentrated on a water bath. The reaction mixture yielded an orange-red compound. The complex was washed with acetone and dried in vacuum; yield 70 %.

(iii) *Pt(BT)Cl$_2$* was obtained from sodium tetrachloroplatinate(II) and biuret in water–ethanol mixture after concentrating. Recrystallization from ethanol yielded a crystalline orange complex in 50 % yield.

Table II

Magnetic susceptibility and electronic spectra of the complexes

Complexes	$X_M \times 10^6$ (C.G.S. units at 297 K)	Position of the bands	Assignment	Ligand field parameters
$Pt(BT)Cl_2$	− 130.2	19600 cm^{-1}	$^1A_{2g} \leftarrow {}^1A_{1g}$	
		23000 cm^{-1}	$^1B_{1g} \leftarrow {}^1A_{1g}$	
		29120 cm^{-1}	$^1e_g \leftarrow {}^1A_{1g}$	
$Pd(BT)_2Cl_2$	− 85.6	21000 cm^{-1}	$^1A_{2g} \leftarrow {}^1A_{1g}$	
		24000 cm^{-1}	$^1B_{1u} \leftarrow {}^1A_{1g}$	
$Pd(BT)Cl_2$	− 103.5	20160 cm^{-1}	$^1A_{2g} \leftarrow {}^1A_{1g}$	
		24200 cm^{-1}	$^1B_{1u} \leftarrow {}^1Al_g$	
		31800 cm^{-1}	$L(\sigma^*) \leftarrow M$	
$Pt(BT)_2Cl_4$	− 88.32	25000 cm^{-1}		
		20500 cm^{-1}	$^3T_{2g} \leftarrow {}^1A_{1g}$	10 Dq = 22650 cm^{-1}
		16200 cm^{-1}*	$^3T_{1g} \leftarrow {}^1A_{1g}$	F_4 = 65 cm^{-1}
				B = 755 cm^{-1}
$[Rh(BT)Cl_3]_2$	− 96.34	24380 cm^{-1}	$^1T_{1g} \leftarrow {}^1A_{1g}$	10 Dq = 20880 cm^{-1}
		19050 cm^{-1}	$^3T_{2g} \leftarrow {}^1A_{1g}$	F_4 = 550 cm^{-1}
				B = 700 cm^{-1}
		15400 cm^{-1}*	$^3T_{1g} \leftarrow {}^1A_{1g}$	

* Calculated band position

	Nitrogen (%)		Hydrogen (%)		Chlorine (%)	
obsd.	calcd.	obsd.	calcd.	obsd.	calcd.	obsd.
6.32	11.38	11.40	1.35	1.51	18.97	18.72
8.72	15.46	15.20	1.84	1.90	26.14	25.96
12.38	21.90	22.00	2.60	2.58	18.50	18.62
8.62	15.00	14.78	1.78	1.30	25.35	24.96
7.72	13.43	13.21	1.60	1.71	34.08	33.82

(iv) $Pt(BT)_2Cl_4$. An aqueous solution of chloroplatinic acid and biuret in a mole ratio of 1 : 2 was refluxed on a water bath; on concentration the reaction mixture gave a yellow mass. The complex was washed with ethanol and finally with acetone; yield 60 %.

(v) $[Rh(BT)Cl_3]_2$ was prepared from $RhCl_3 .3H_2O$ and biuret in a mole ratio of 1 : 1, in an ethanol–water mixture and recrystallized from ethanol; yield 70 %.

The elemental analyses are given in Table I.

Physical measurements

Magnetic susceptibility measurements, UV, visible and IR spectral studies on solid complexes were made as described earlier [30]. The experimental results are given in Tables II and III.

Table III

Infrared spectra of biuret and its complexes

Assignment	Biuret	$Pt(BT)Cl_2$	$Pt(BT)_2Cl_4$	$Pd(BT)Cl_2$	$Pd(BT)_2Cl_2$	$[Rh(BT)Cl_3]_2$
Asym(NH_2)-bonded	3410 (vs)	3410 (bs)	3405 (bs)	3405 (bs)	3410 (bs)	3405 (bs)
Sym(NH_2)-bonded	3260 (bs)	3280 (bw)	3375 (m)	3255 (w)		
	3015 (w)		3200 (bw)	3200 (bw)	3200 (bw)	3170 (w)
Asym(C=O)	1720 (ms)	1690 (sh)	1680 (bw)	1725 (sh)		
Sym(C=O)	1670 (vs)	1670 (w)		1680 (ms)	1680 (bs)	1680 (bs)
		1650 (sh)		1650 (sh)	1650 (m)	1650 (sh)
(NH_2)sym deformation	1615 (m)	1615 (m)	1615 (m)	1615 (w)	1600 (bw)	1600 (bw)
(NH_2)asym deformation	1676 (s)	1575 (ms)	1575 (w)	1575 (m)		
		1555 (w)	1555 (sh)		1540 (sh)	1555 (sh)
Imide II band	1490 (w)		1540 (w)	1495 (m)	1500 (m)	
(C–N)	1420 (s)	1410 (s)	1410 (s)	1420 (sh)	1420 (w)	1410 (ms)
				1410 (s)	1350 (ms)	1350 (ms)
Imide III band	1325 (vs)	1320 (s)	1325 (s)	1325 (s)	1325 (sh)	
				1250 (m)		
(NH_2) rocking	1130 (ms)	1130 (s)	1130 (ms)	1130 (s)	1125 (m)	1130 (ms)
					1090 (m)	
(C–N) stretching	1075 (s)	1080 (s)	1075 (s)	1075 (s)	1080 (m)	1080 (m)
	975 (vw)					
	945 (w)	950 (w)		940 (w)	950 (w)	950 (w)
out-of-plane C=O	775 (ms)	800 (sh)				
deformation		760 (bw)	765 (bs)	760 (bs)	755 (w)	765 (s)
Skeletal out-of-plane	756 (ms)					
out-of-plane (NH_2)	713 (ms)	710 (s)	710 (s)	710 (s)	725 (m)	710 (s)
wagging	675 (w)		670 (w)	670 (w)	705 (s)	
Skeletal vibration	612 (ms)	605 (sh)	610 (s)	610 (sh)		610 (m)
	596 (ms)	580 (w)	590 (s)	595 (s)		

s: strong, bs: broad strong, m: medium, ms: medium strong, vs: very strong, w: weak, vw: very weak, sh: shoulder, bw: broad weak

Results and discussion

The synthesis of all metal complexes was essentially the same, involving the heating and stirring of stoichiometric amounts of the appropriate ligand and metal salt in a suitable solvent such as ethanol–water. All the metal chelates of this study are soluble in ethanol and water. The molar conductance (ΔM at 25 °C 1×10^{-3} M concetration) shows that these complexes are non-electrolytes except the Rh(III) complex, which behaves as a 1 : 1 electrolyte.

All the complexes are diamagnetic. This suggests that the metal ions are in the singlet ground state $^1A_{1g}$, which indicates a square planar geometry of the field around Pt(II) and Pd(II), and an octahedral geometry around Pt(IV) and Rh(III). These geometries are in accordance with the known preferences of Pd, Pt and Rh in their various oxidation states [19].

Electronic spectra

The band assignments of square planar complexes are based on the d-molecular orbital level ordering of $b_{1g}(X^2 - Y^2) > b_{2g}(xy) > e_g(xy, yz) > > a_{1g}(z^2)$. The ground state for low spin d^8 system is $^1A_{1g}$ ($a_{1g}2\ e_g4\ b_{2g}4$). The ligand field excited states are $^3A_{2g}$, $^1A_{2g}(b_{1g} \leftarrow b_{2g})$; ^3E_g, $^1E_g(b_{1g} \leftarrow e_g)$ and $^3b_{1g}$, $^2b_{1g}(b_{1g} \leftarrow a_{1g})$. Therefore, one should expect three spin-allowed and three spin-forbidden bands. The three bands are observed at 29120, 23000 and 19600 cm^{-1} in the electronic spectra of the Pt(II) complex. The first spin-allowed *d–d* transition $^1A_{2g} \leftarrow {}^1A_{1g}$ in the amine complexes has been reported to be about 18000 cm^{-1} higher in energy than in the halide complex [13, 20]. The corresponding transition in the present Pt(II) complex has been observed at 19600 cm^{-1}. According to the JÖRGENSEN [21], the band at 23000 cm^{-1} may be tentatively assigned to the $^1B_{1g} \leftarrow {}^1A_{1g}$ transition. The other band observed at 29120 cm^{-1} is due to the transition $^1E_g \leftarrow {}^1A_{1g}$. The absorption spectra of Pd BT_2 Cl_2 and Pd BT Cl_2 show a spin-allowed *d–d* transition ($^1A_{2g} \leftarrow {}^1A_{1g}$) band at 21000 and 20160 cm^{-1} in agreement with reported spectra of Pd(II) complexes [22]. The weak bands at 24000 and 24200 cm^{-1} are due to $^1B_{1u} \leftarrow {}^1A_{1g}$. The band at 31800 cm^{-1} in Pd BT Cl_2 is probably due to a metal–ligand transition. The spectral properties and diamagnetic character of the palladium complexes confirm the square planar stereochemistry around the Pd(II) ions. The ground state of the d^6 Pt(IV) and Rh(III) is $^1A_{1g}$. The ligand field transition $e_g t_{2g}^5 \leftarrow t_{2g}^6$ gives $^3T_{1g}$, $^3T_{2g}$ and $^1T_{1g}$ and $^1T_{2g}$ as excited states in increasing order of energy. The electronic spectra of Pt(IV) and Rh(III) complexes show absorption bands at 25000 and 20500, and 24380 and 19050 cm^{-1}, respectively. The bands at 20500 cm^{-1} in Pt(IV) and 19050 cm^{-1} in Rh(III) complexes are due to *d–d* transitions assigned to the singlet

triplet transition [21, 23, 24] $^3T_{2g} \leftarrow {}^1A_{1g}$. The assignment of the 24380 cm^{-1} band in the Rh(III) complex is uncertain. However, the theory of TANABE and SUGANO [25] implies that it is the band with the lowest wavenumber which should be assigned to the $^1T_{1g} \leftarrow {}^1A_{1g}$ transition. The first transition band of $^3T_{1g} \leftarrow {}^1A_{1g}$ is calculated and found to be appear at 16200 cm^{-1} in Pt(IV) and at 15400 cm^{-1} in Rh(III) complexes. The relevant ligand field parameters 10 Dq and β are calculated and found to be 22650 and 755 cm^{-1} in the Pt(IV) complex, and 22880 and 700 cm^{-1} in the Rh(III) complex, respectively. These values are in good agreement with other reported values for octahedral Pt(IV) and Rh(III) complexes.

Infrared spectra

Biuret co-ordinates either through two or one oxygen atom of the $-C=O$ group or through two or one nitrogen atom of the $-NH_2$ group, depending on the acidity [7, 9]. The infrared absorption frequencies of the ligand and complexes with their tentative assignment are given in Table III. The ν(NH) bands of biuret appearing in the 3500 – 3200 cm^{-1} region [7, 8] are not significantly shifted or deformed by co-ordination. Co-ordination to the metal through nitrogen should cause splitting of these bands and decrease their intensities. Since this is not the case, bonding through the oxygen of the $-C=O$ group can be inferred. The carbonyl group gives rise to two bands for the asymmetric and symmetric stretching frequencies [26, 27] at 1720 cm^{-1} and 1670 cm^{-1}. The asymmetric stretching frequency of free biuret is shifted in the complexes and the change observed for the $\nu(C=O)$ band suggests co-ordination through the oxygen. The C–N stretching frequency at 1420 cm^{-1} in biuret also shifts to higher frequencies in the complexes, corresponding to an increase in the double bond character due to oxygen co-ordination to the metal.

The far infrared spectra of the complexes (Table IV) show the presence of additional bands due to M–O and M–Cl stretching frequencies. These assignments are made according to NAKAMOTO. In the Rh(III) complexes a strong band at 325 cm^{-1} and a week band at 290 cm^{-1} appeared, which may be due to a dimeric complex. WALTON [29] observed a similar pattern for the dimeric complex of Rh(III) with 2,5-dithiohexane with a chloride-bridged structure.

A more quantitative comparison may be made between the force constant and stability order (the stability constant increases with increasing atomic number). If we arrange the metals in the order of ν(M–O) and ν(M–Cl), and K_{M-O} and K_{M-Cl}, we have Pt(II) > Pd(II) and Pt(IV) > Rh(III) in the case of square planar and octahedral complexes, respectively. Thus the force constants of the M–O and M–Cl bonds obey the stability order.

	Square planar complexes		Octahedral complexes	
	Pt(II)	Pd(II)	Pt(IV)	Rh(III)
νM–O (cm^{-1})	460	440	450	425
K_{M-O} (10^5 dyne/cm)	1.85	1.67	1.81	1.53
νM–Cl (cm^{-1})	350	315	340	305
K_{M-Cl} (10^5 dyne/cm)	2.102	1.597	2.0	1.58

The essential features of the bridged structure of the Rh(III) complex can be derived from (a) the chemical evidence given above (b) the maintenance of co-ordination number 6 for Rh(III), (c) the known bidentate character of biuret in relatively strong acid and (d) the molar conductivity corresponding to 1 : 1 electrolytes. The presence of a Rh–Cl band in the IR spectra support the bis structure. On the basis of this evidence, structure (I) is proposed for the Rh(III) complex.

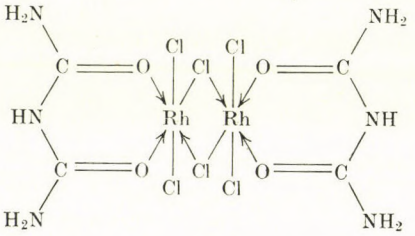

Fig. 1

Table IV

Far infrared spectra of the complexes

Biuret	$Pt(BT)Cl_2$	$Pt(BT)_2Cl$	$Pd(BT)Cl_2$	$Pd(BT)_2Cl_2$	$[Rh(BT)Cl_3]_2$
525 (sh)	540 (w)	525 (w)	525 (ms)	520 (w)	580 (w)
	520 (w)				540 (w)
478 (ms)	485 (w)				520 (vw)
	460 (w)	450 (w)	475 (s)	480 (w)	490 (w)
445 (ms)	430 (w)		440 (w)	445 (w)	450 (w)
428 (sh)	410 (sh)	410 (sh)	410 (sh)		425 (w)
	395 (sh)			355 (sh)	360 (w)
	365 (w)		360 (sh)		325 (s)
305 (sh)	350 (w)	340 (w)	315 (w)	310 (w)	305 (w)
298 (w)	315 (w)	280 (w)	270 (w)		290 (w)
288 (s)	275 (w)				

Conclusions

1. In all cases co-ordination occurs through the oxygen of the carbonyl group.

2. The Pd(II) and Pt(II) complexes have square planar geometries around the central metal ions, while the Rh(III) and Pt(IV) complexes show an octahedral arrangement.

*

We wish to thank Dr. B. J. ANSARI for recording the infrared spectra of the compounds.

REFERENCES

[1] BOND, G. C.: Catalysis by Metals, p. 141. Academic Press, London 1962
[2] BEECK, O.: Disc. Faraday Soc., **8,** 118 (1959)
[3] SHERIDAN, J., REID, W. D.: J. Chem. Soc., **1952,** 2962
[4] ANDERSON, J. R., KEMBALL, C.: Adv. Catal., **9,** 51 (1937)
[5] KEMBALL, C., MOSS, R. L.: Proc. Roy. Soc., **A238,** 107 (1956)
[6] KEMBALL, C., MOSS, R. L.: Proc. Roy. Soc., **A244,** 398 (1958)
[7] MCLELLAN, A. W., MELSAN, G. A.: J. Chem. Soc., (A) **1967,** 137
[8] BOUR, J. J., BIRKERAND, P. J. M. W. L., STEGGERED, J. J.: Inorg. Chem., **10,** 1202 (1971)
[9] MELSAN, G. A.: J. Chem. Soc., (A) **1967,** 669
[10] SANYAL, R. M., SRIVASTAVA, P. C., BANERJEE, B. K.: J. Inorg. Nucl. Chem., **37,** 343 (1975)
[11] SANYAL, R. M., SRIVASTAVA, P. C., BANERJEE, B. K.: Technology, **II,** 258 (1974)
[12] BASCH, H., GRAY, H. B.: Inorg. Chem., **6,** 365 (1967)
[13] MASON, W. R., GRAY, H. B.: J. Am. Chem. Soc., **90,** 5721 (1968)
[14] CHATT, J., GAMLEN, G. A., ORGEL, L. E.: J. Chem. Soc., **1958,** 486
[15] GRAY, H. B., BALLHAUSEN, C. J.: J. Am. Chem. Soc., **85,** 260 (1963)
[16] COTTON, F. A., HARRIS, C. B.: Inorg. Chem., **6,** 369 (1967)
[17] BALLHAUSEN, C. J., BJERRUM, N., DINGLE, R., ERIKS, K., HAIRE, C. R.: J. Am. Chem. Soc., **85,** 260 (1963)
[18] MOSS, R. L.: The Structure and Activity of Heterogeneous Catalysts. The Chemical Engineer, June CE 114 (1966)
[19] COTTON, F. A., WILKINSON, G.: Advanced Inorganic Chemistry. A comprehensive Text, p. 1024. Interscience, New York 1966
[20] JÖRGENSEN: Absorption Spectra and Chemical Bonding. Addison Wesley 1962
[21] JÖRGENSEN, C. K.: J. Inorg. Nucl. Chem., **24,** 1571 (1962)
[22] GRAY, H. B.: Transition Metal Chemistry, Vol. I. M. DEKKER, New York 1966
[23] JÖRGENSEN, C. K.: Acta. Chem. Scand., **10,** 500 (1958)
[24] FURLANI, C., LUCINAI, M. L.: Inorg. Chem., **7,** 1586 (1968)
[25] TANABE, Y., SUGANO, S.: J. Phys. Soc. Japan, **9,** 766 (1954)
[26] BULL, W. E., MADAN, S. K., WILLIS, J. W.: Inorg. Chem., **2,** 303 (1963)
[27] SIEBERT, H.: Z. Anorg. Allgem. Chem., **275,** 225 (1954)
[28] NAKAMOTO, K.: Infrared Spectra of Inorganic and Coordination Compound. John Wiley and Sons, Inc., New York 1962
[29] WALTON, R. A.: J. Chem. Soc., (A) **1967,** 1852
[30] SRIVASTAVA, P. C., BANERJEE, B. K.: Inorg. Chem., (submitted)

P. C. SRIVASTAVA
B. K. BANERJEE
Sindri-828122 India.

Acta Chimica Academiae Scientiarum Hungaricae, Tomus 96(3), pp, 267—273 (1978)

SYNTHESIS OF THE PROTECTED N-TERMINAL HEPTAPEPTIDE OF BOVINE PARATHYROID HORMONE

H. S.-VARGHA and K. MEDZIHRADSZKY*

(Research Group for Peptide Chemistry of the Hungarian Academy of Sciences, Budapest)

Received March 20, 1977

Boc-Ala-Val-Ser-Glu(O^{t}Bu)-Ile-Gln-Phe-OMe, the protected N-terminal heptapeptide fragment of bovine parathyroid hormone has been synthesized by the conventional solution technique. This peptide serves as intermediate in the synthesis of larger N-terminal fragments containing methionine residues, whose oxidation is supposed to be responsible for the cessation of the biological activity.

In the course of the isolation, structure elucidation and investigation of structure–activity relationships of polypeptide hormones it could be observed that some of them are sensitive to oxidation. In most cases this chemical change is accompanied by a marked decrease, or even by a total loss, of biological activity. Adrenocorticotropic hormone, for instance, is practically inactivated by treatment with hydrogen peroxide [1, 2], and the oxidation product of α-melanotropin also exhibits a melanocyte-stimulating potency which is significantly decreased compared with that of the parent hormone [3, 4, 5]. Moreover, it could be established that in both cases a single methionine residue was responsible for this sensitivity; mild oxidation converted the thioether group into the S-oxide derivative, which, in turn, could be reduced again to the methionine residue by incubation with mercapto compounds, with regeneration of the biological activity.

Like the hypophyseal hormones mentioned above, parathyroid hormon (parathormon, PTH), the proteohormone of the parathyroid gland is also sensitive to oxidation. RASMUSSEN [6], as well as RASMUSSEN and CRAIG [7] were the first who observed the biological inactivation of the hormone on treatment with hydrogen peroxide, and reactivation after incubation with cysteine. RASMUSSEN and CRAIG [8], and somewhat later TASHJIAN *et al.* [9] could establish that in the case of the parathyroid hormone again the reversible oxidation of the methionine residues was responsible for the disappearance of the biological activity. As the bovine hormone used in these experiments contains two methionine residues, it could not be decided with certainty whether both of them played a role in the inactivation process. Since, however, there is only

* To whom correspondence should be addressed.

one methionine residue in porcine parathyroid hormone in position 8 from the N-terminus, and this compound also loses its biological activity on oxidation, it is very likely that in the bovine and human hormone, both containing two methionine residues in positions 8 and 18, the oxidation of the first one contributes to the inactivation to a greater extent.

Like in the cases of the adrenocorticotropic and melanotropic hormones, the methionine residues of the parathyroid hormone can be substituted by amino acids possessing side chains of similar properties, without altering significantly the biological potency [10]. It is therefore obvious that the thioether grouping of methionine does not play any functional role in eliciting the hormonal activity. The fact that its oxidation greatly influences the biological activity can be explained by the effects exerted by the sulfoxide group on the conformation of the hormone molecule, or its binding to the receptor.

For eliciting the biological activity of the parathyroid hormone, the N-terminal 1 – 34 or 1 – 29 fragments of the whole molecule, consisting of 84 amino acids, are sufficient [11]. As the methionine residues are located in this part of the sequence, the inactivating effect of their oxidation can be studied in these N-terminal fragments (Fig. 1). Although smaller peptides are biologically inactive, conformational changes in consequence of oxidative modifications can be expected in even shorter N-terminal sequences. For this purpose the N-terminal dodecapeptide of bovine parathyroid hormone has been selected, which contains the methionine residue in position 8, whose oxidation plays a key role in the inactivation of the hormone. Preparation of the S-oxide derivative and comparison of its properties with those of the parent peptide allows the investigation of the possible effect of oxidation on the conformation of this hormone fragment. As the first part of this programme, in this paper details of the synthesis of the protected N-terminal heptapeptide are described.

	1 8
Human	H_2N-Ser-Val-Ser-Glu-Ile-Gln-Phe-Met-His-
Bovine	H_2N-Ala-Val-Ser-Glu-Ile-Gln-Phe-Met-His-
Porcine	H_2N-Ser-Val-Ser-Glu-Ile-Gln-Leu-Met-His-
	18
Human	-Asn-Leu-Gly-Lys-His-Leu-Asn-Ser-Met-Glu-
Bovine	-Asn-Leu-Gly-Lys-His-Leu-Ser-Ser-Met-Glu-
Porcine	-Asn-Leu-Gly-Lys-His-Leu-Ser-Ser-Leu-Glu-
Human	-Arg-Val-Glu-Trp-Leu-Arg-Lys-Lys-Leu-Gln-
Bovine	-Arg-Val-Glu-Trp-Leu-Arg-Lys-Lys-Leu-Gln-
Porcine	-Arg-Val-Glu-Trp-Leu-Arg-Lys-Lys-Leu-Gln-
	34
Human	-Asp-Val-His-Asn-Phe-COOH
Bovine	-Asp-Val-His-Asn-Phe-COOH
Porcine	-Asp-Val-His-Asn-Phe-COOH

Fig. 1. Primary structure of the biologically active N-terminal tetratriacontapeptide of the parathyroid hormones

The synthetic steps leading to the heptapeptide derivative are shown in Fig. 2. The conventional solution technique and a combination of the stepwise and fragment condensation methods have been used.*

Benzyloxycarbonyl-glutaminyl-phenylalanine methyl ester (**I**), prepared from benzyloxycarbonyl-glutamine *p*-nitrophenyl ester and phenylalanine methyl ester, was hydrogenolyzed in methanol in the presence of palladium-charcoal catalyst and an equimolar amount of hydrochloric acid. The dipeptide ester (**II**) was acylated with benzyloxycarbonyl-isoleucine 2,4,5-trichlorophenyl ester [12] to give the Z-Ile-Gln-Phe-OMe tripeptide ester (**III**), which could be crystallized from acetic acid. On catalytic hydrogenolysis in the presence of hydrochloric acid the crystalline H-Ile-Gln-Phe-OMe tripeptide ester hydrochloride (**IV**) was obtained, which, in turn, was coupled with benzyloxycarbonyl-glutamic acid γ-*t*-butyl-α-pentachlorophenyl ester [13]. The resulting protected tetrapeptide ester (**V**) was also crystalline; it gave on catalytic hydrogenolysis the pure H-Glu(O^{t}Bu)-Ile-Gln-Phe-OMe tetrapeptide (**VI**) in quantitative yield.

To synthesize the N-terminal tripeptide, first Z-Val-Ser-OMe dipeptide ester (**VII**) was prepared by the dicyclohexylcarbodiimide procedure. The protected ester was hydrogenolysed in methanolic hydrochloric acid to the crystalline valyl-serine methyl ester hydrochloride (**VIII**), and this compound was coupled with *t*-butyloxycarbonyl-alanine with the aid of dicyclohexylcarbodiimide. As neither extraction procedures, nor crystallization experiments were effective in purification of this material, column chromatography on silica gel

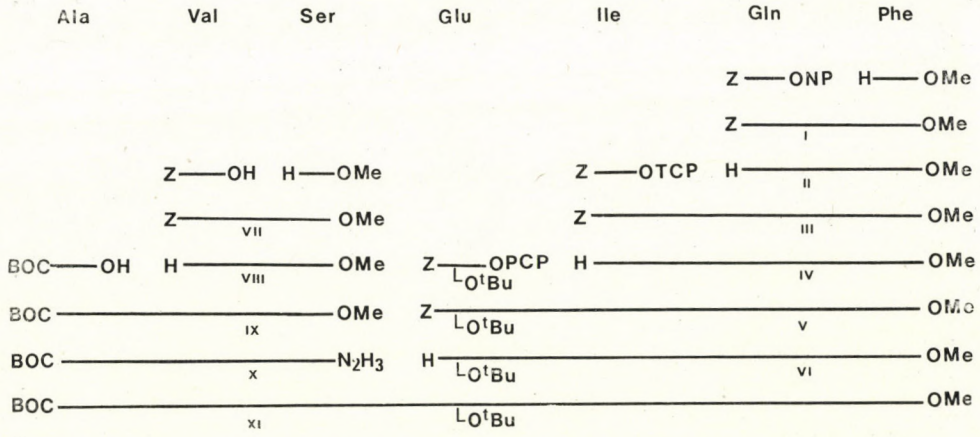

Fig. 2. Scheme for the synthesis of the protected N-terminal heptapep tide of bovine para thyroid hormone

* Abbreviations are used according to the recommendations of the IUPAC-IUB Commission on Biochemical Nomenclature, Symbols for Amino Acid Derivatives and Peptides J. Biol. Chem., **247**, 977 (1972).

was applied to obtain a homogeneous product. Finally, the resulting protected tripeptide methyl ester (**IX**) was converted into the crystalline hydrazide (**X**).

Coupling of these two compounds to the BOC-Ala-Val-Ser-Glu(O^tBu)-Ile-Gln-Phe-OMe heptapeptide (**XI**) was effected by the azide method, without isolating the intermediary azide. The resulting protected heptapeptide ester proved to be highly insoluble in a number of organic solvents; this could be expected on the basis of the amino acid composition. Amino acid analysis after total hydrolysis of the pure substance gave correct values.

Experimental

M.p.'s were determined on a Büchi apparatus (Switzerland) and are uncorrected.

R_F values refer to thin-layer chromatography on Kieselgel G, Merck, plates; detection with ninhydrin and chlorine-tolidine reagents. The following solvent systems were used (volumes):

1. Ethyl acetate–pyridine–acetic acid–water 30 : 20 : 6 : 11
2. Ethyl acetate–pyridine–acetic acid–water 60 : 20 : 6 : 11
3. Ethyl acetate–pyridine–acetic acid–water 120 : 20 : 6 : 11
4. Ethyl acetate–pyridine–acetic acid–water 240 : 20 : 6 : 11
5. Chloroform–methanol 9 : 1
6. Ethyl acetate–cyclohexane 1 : 1

Benzyloxycarbonyl-glutaminyl-phenylalanine methyl ester (I)

To a chilled solution of 2.15 g (10 mmoles) phenylalanine methyl ester hydrochloride in 30 ml dimethylformamide 1.45 ml (10 mmoles) triethylamine was added, followed by the addition of 4.01 g (10 mmoles) benzyloxycarbonyl-glutamine *p*-nitrophenyl ester to the stirred solution. The reaction mixture was kept at room temperature for 3 days, evaporated in vacuum, the residue dissolved in ethyl acetate and washed successively with dilute hydrochloric acid and water, then several times with aqueous triethylamine solution to remove *p*-nitrophenol. After a final washing with water, the ethyl acetate solution was dried over sodium sulfate, evaporated and treated with anhydrous ether to give a solid substance. Recrystallization from 60 % aqueous ethanol yielded 2.94 g (67 %) of dipeptide ester, m.p. 179 – 181 °C (lit. [14] m.p. 194 – 196 °C).

$C_{23}H_{27}O_6N_3$ (441.47). Calcd. C 62.57, H 6.16, N 9.52. Found C 62.56, H 6.80, N 9.55 %

Glutaminyl-phenylalanine methyl ester hydrochloride (II)

A suspension of benzyloxycarbonyl-glutaminyl-phenylalanine methyl ester (**I**) (2.20 g; 5 mmoles) in 50 ml methanol containing 0.84 ml (5 mmoles) of 6 *N* HCl was hydrogenated in the presence of 0.40 g Pd-charcoal catalyst for 1 hr. The catalyst was removed by filtration and the solution was evaporated to dryness.

The substance was homogeneous (R_F^3 0.28), and did not contain any starting material. It was used for the next coupling without purification.

Benzyloxycarbonyl-isoleucyl-glutaminyl-phenylalanine methyl ester (III)

The solution of glutaminyl-phenylalanine methyl ester hydrochloride (~5 mmoles, as described above) in 20 ml dimethylformamide was chilled to 0 °C, and under stirring 1.45 ml (10 mmoles) triethylamine, then, after 5 min 2.20 g (5 mmoles) benzyloxycarbonyl-isoleucine 2,4,5-trichlorophenyl ester were added. Stirring was continued for 2 hrs at 0 °C, and the reaction mixture was kept at room temperature overnight. The precipitated substance was filtered off and washed with water; it weighed after drying 1.66 g.

From the evaporated filtrate an additional 0.90 g of substance could be obtained; the combined materials were crystallized from acetic acid to give 2.07 g (75 %) of the pure tripeptide ester, m.p. 234 – 236 °C.

$C_{29}H_{38}O_7N_4$ (554.63). Calcd. C 62.80; H 6.91; N 10.10. Found C 62.68; H 7.21; N 10.10 %.

Isoleucyl-glutaminyl-phenylalanine methyl ester hydrochloride (IV)

The protected tripeptide ester (**III**) (1.10 g; 2 mmoles) was suspended in a mixture of 10 ml acetic acid and 10 ml anhydrous methanol containing 73 mg (2 mmoles) hydrochloric acid, and hydrogenated in the presence of 200 mg Pd-charcoal catalyst for 2 hrs. After removal of the catalyst, the solution was evaporated to dryness, giving the tripeptide ester in quantitative yield.

R_F^1 0.28. Analysis after crystallization from methanol–water (1 : 1) mixture gave N 12.15 %, calculated for $C_{21}H_{33}O_5N_4Cl$ (457.02), N 12.26 %.

Benzyloxycarbonyl-(γ-*t*-butyl)glutamyl-isoleucyl-glutaminyl-phenylalanine methyl ester (V)

To a chilled and stirred solution of isoleucyl-glutaminyl-phenylalanine methyl ester hydrochloride (0.92 g; 2 mmoles) in 6 ml dimethylformamide 0.29 ml (2 mmoles) triethylamine was added, followed after 5 min by the addition of 1.06 g (2 mmoles) of benzyloxyrbonyl-glutamic-acid-γ-*t*-butyl-α-pentachlorophenyl ester. The reaction mixture was kept for 1 day at room temperature, evaporated under reduced pressure, the residue powdered under anhydrous ether and collected on a funnel. The product was crystallized from ethanol–water (3 : 1) mixture, yielding 0.90 g (61 %) protected tetrapeptide ester, m.p. 228 – 232 °C. R_F^4 0.84.

$C_{38}H_{53}O_{10}N_5$ (739.84). Calcd. C 61.69, H 7.22, N 9.46. Found C 61.85, H 7.68, N 9.32 %.

γ-*t*-Butyl-glutamyl-isoleucyl-glutaminyl-phenylalanine methyl ester (VI)

The protected tetrapeptide methyl ester (**V**) (800 mg) was suspended in 20 ml anhydrous methanol and hydrogenated in the presence of 120 mg Pd-charcoal catalyst for 3 hrs. Dissolution of the peptide indicated the completion of the reaction. The catalyst was filtered of and the solvent evaporated. The residue was homogeneous to thin-layer chromatography, R_F^2 0.60. This substance was used for the synthesis of the heptatpeptide without purification.

Benzyloxycarbonyl-valyl-serine methyl ester (VII)

To a stirred solution of 15.5 g (0.1 mole) serine methyl ester hydrochloride in 200 ml dimethylformamide, chilled to 0 °C, slowly 14.5 ml (0.1 mole) triethylamine was added. After the addition of benzyloxycarbonyl-valine (25.1 g; 0.1 mole) and dicyclohexylcarbodiimide (20.6 g; 0.1 mole) the stirring was continued for 2 hrs at 0 °C, then the reaction mixture was kept in a refrigerator overnight. Dicyclohexylurea was removed by suction, washed on the filter with a few ml of dimethylformamide, and the combined filtrates were evaporated in vacuum (bath temperature 40 °C). The residue was taken up in a mixture of ethyl acetate and water, the organic layer was washed with dilute hydrochloric acid, water, saturated sodium bicarbonate solution and again with water, dried over sodium sulfate and evaporated. The crystalline residue was dissolved in hot ethyl acetate, and to this solution petroleum ether was added until turbidity appeared. After standing at room temperature for a few hours crystallization was completed by keeping the mixture in a refrigerator overnight. The crystals were filtered off and dried to yield 26.0 g (76 %) of the dipeptide ester, m.p. 164 – 166 °C (lit. m.p. 165 – 166 °C [15]).

$C_{17}H_{24}O_6N_2$ (352.38). Calcd. C 57.94, H 6.87, N 7.95. Found C 58.05, H 7.01, N 7.78 %.

Valyl-serine methyl ester hydrochloride (VIII)

Benzyloxycarbonyl-valyl-serine methyl ester (**VII**) (1.76 g; 5 mmoles) was suspended in 40 ml methanol, and to this suspension 0.84 ml (5 mmoles) of 6*N* HCl solution was added. Hydrogenation was performed in the presence of 0.22 g Pd-charcoal catalyst; the substance went into solution in about 4 hrs. After removal of the catalyst the solvent was evaporated in vacuum to obtain a crystalline substance (1.21 g; 95 %), m.p. 178 – 180 °C. The m.p. did not change on recrystallization from ethanol–ether.

$C_9H_{19}O_4N_2Cl$ (254.71). Calcd. C 42.43, H 7.52, N 11.00. Found C 42.40, H 7.71, N 10.89 %.

t-Butyloxycarbonyl-alanyl-valyl-serine methyl ester (IX)

Valyl-serine methyl ester hydrochloride (**VIII**) (1.52 g; 6 mmoles) was dissolved in 16 ml dichloromethane, chilled to 0 °C, and to the stirred solution triethylamine (0.88 ml; 6 mmoles) was added. After 10 min *t*-butyloxycarbonylalanine (1.14 g; 6 mmoles) and dicyclohexylcarbodiimide (1.26 g; 6 mmoles) were added and the mixture was kept in a refrigerator for 2 days. Dicyclohexylurea was filtered off, washed with a few ml of dichloromethane, and the combined solutions were evaporated. The residue was dissolved in 5 ml dimethylformamide and applied onto a column (15×1000 mm) filled with silica gel. Elution was performed with a 1 : 1 mixture of ethyl acetate and cyclohexane. The fractions containing the pure material were collected and evaporated to obtain 1.9 g (82 %) of the tripeptide ester, m.p. 171 – 173 °C; $R^6_F = 0.21$.

$C_{17}H_{31}O_7N_3$ (389.44). Calcd. C 52.43, H 8.02, N 10.79. Found C 52.42, H 8.27, N 10.67 %.

t-Butyloxycarbonyl-alanyl-valyl-serine hydrazide (X)

To a solution of the protected tripeptide ester (**IX**) (1.17 g; 3 mmoles) in 12 ml anhydrous methanol 0.75 ml (15 mmoles) of hydrazine hydrate was added, and the solution was allowed to stand at room temperature overnight. The separated hydrazide was filtered off, washed on the filter with methanol several times, and dried in desiccator over sulfuric acid. Recrystallization from ethanol–water (1 : 1) mixture gave 0.97 g (82 %) of the pure hydrazide, m.p. 228 – 229 °C.

On thin-layer chromatography (Solvent 6) the substance remained in the start, and no spot with R_F 0.21 (ester) was observed.

$C_{16}H_{31}O_6N_5$ (389.45). Calcd. N 17.99; hydrazide-N 7.19. Found N 17.73; hydrazide-N [16] 7.27 %.

t-Butyloxycarbony-alanyl-valyl-seryl-(γ-*t*-butyl)glutamyl-isoleucyl-glutaminyl-phenylalanine methyl ester (XI)

t-Butyloxycarbonyl-alanyl-valyl-serine hydrazide (390 mg; 1 mmole) was suspended in 4 ml dimethylformamide, and the suspension was chilled to – 20 °C. Under vigorous stirring a pre-cooled solution of 110 mg (3 mmoles) hydrogen chloride in 1.3 ml anhydrous tetrahydrofuran was added dropwise. In about 10 min a clear solution was obtained, to which 0.16 ml (1.2 mmoles) isoamylnitrite was added, maintaining the temperature at – 10 °C for 10 min. The resulting azide solution was poured, with stirring, into a mixture of 605 mg (1 mmole) of γ-*t*-butyl-glutamyl-isoleucyl-glutaminyl-phenylalanine methyl ester (**VI**) and 0.44 ml (3 mmoles) of triethylamine in 3 ml dimethylformamide at – 10 °C. Stirring was continued at the same temperature for 1 hr, then the reaction mixture was kept in a refrigerator overnight. Solvents were removed in vacuum, the residue triturated with water, filtered and washed with water to yield 920 mg of the crude heptapeptide ester.

For purification this substance was boiled with 3 ml anhydrous methanol, chilled and filtered, to obtain 710 mg (73 %) of the protected heptapeptide ester, R^5_F 0.28. The substance had m.p. above 240 °C.

$C_{46}H_{74}O_{14}N_8$ (963.12).

Amino acid analysis after total hydrolysis in 6*N* HCl in an evacuated tube at 105 °C for 24 hrs gave the following results: Ala 0.96, Val 1.02, Ser 1.00, Glu 2.00, Ile 0.96, Phe 1.05.

REFERENCES

[1] Dedman, M. L., Farmer, T. H., Morris, C. J. O. R.: Biochem. J., **66,** 166 (1957)
[2] Dedman, M. L., Farmer, T. H., Morris, C. J. O. R.: Biochem. J., **78,** 348 (1961)
[3] Lo, T. B., Dixon, J. S., Li, C. H.: Biochim. Biophys. Acta **53,** 584 (1961)
[4] Medzihradszky, K., Medzihradszky-Schweiger, H., Seprődi, J.: 9th Meeting of the Federation of European Biochemical Societies, 27 August 1974, Budapest; Abstract No. f. 12–15, p. 484.
[5] Medzihradszky, K.: Peptides 1976, Proc. Fourteenth European Peptide Symp., Wépion, 1976 (Ed. A. Loffet), p. 401 (1976)

[6] RASMUSSEN, H.: Science **128,** 1347 (1958)
[7] RASMUSSEN, H., CRAIG, L. C.: Recent Progr. Hormone Res., **18,** 269 (1962)
[8] RASMUSSEN, H., CRAIG, L. C.: Biochim. Biophys. Acta **56,** 332 (1962)
[9] TASHJIAN, A. H., ONTJES, D. A., MUNSON, P. L.: Biochemistry **3,** 1175 (1964)
[10] ROSENBLATT, M., GOLTZMAN, D., KEUTMANN, H. T., TREGEAR, G. W., POTTS, J. T., Jr.: J. Biol. Chem. **251,** 159 (1976)
[11] POTTS, J. T., Jr., TREGEAR, G. W., KEUTMANN, H. T., NIALL, H. D., SAUER, R., DEFTOS, L. J., DAWSON, B. F., HOGAN, M. L., AURBACH, G. D.: Proc. Natl. Acad. Sci. USA, **68,** 63 (1971)
[12] PLESS, J., BOISSONNAS, R. A.: Helv. Chim. Acta **46,** 1609 (1963)
[13] KOVÁCS, J., GIANOTTI, R., KAPOOR, A.: J. Am. Chem. Soc., **88,** 2282 (1966)
[14] MIROSHNIKOV, A. I., KIRJUSHKIN, A. A., OVCHINNIKOV, YU. A.: Zh. Obsch. Khim., **40,** 223 (1970)
[15] BODÁNSZKY, M., CHATURVEDI, N., HUDSON, D., ITOH, M.: J. Org. Chem., **37,** 2303 (1972)
[16] MEDZIHRADSZKY-SCHWEIGER, H.: Acta Chim. Acad. Sci. Hung., **34,** 213 (1962)

Helga SÜLI-VARGHA
Kálmán MEDZIHRADSZKY } H-1088 Budapest, Múzeum krt 4/b.

Acta Chimica Academiae Scientiarum Hungaricae, Tomus 96(3), pp. 275–293 (1978)

CHEMISTRY OF SULFUR DIIMIDES, 7*

ELECTRON IMPACT INDUCED FRAGMENTATION OF SULFUR DIIMIDES

I. LENGYEL,* G. KRESZE, M. BERGER, W. KOSBAHN und H. SCHÄFER

(Organisch-chemisches Laboratorium der Technischen Universität, München, Federal Republic of Germany)

Received April 14, 1977

The mass spectra of ten sulfur diimides are reported and discussed. The molecular ions of diaryl sulfur diimides undergo cyclization and, by loss of the *ortho* substituent from the phenyl ring, yield benzothiadiazole type even-electron ions. Diphenyl sulfur diimide also ejects sulfur, presumably from the diazathiirane valence-isomer of the molecular ion. Large skeletal rearrangement fragments are prevalent in the spectra, as substantiated by metastable peak analysis, high resolution mass measurement and substituent labeling. Cyclic sulfur diimides **IX** and **X** fragment by loss of CH_2N and $(CH_2)_2N$. A strong tendency of aromatization by dehydrogenation is noticed for **X**.

In view of our general interest in sulfur-nitrogen compounds [2], and in particular in sulfur diimides [1], we investigated the fragmentation of ten representatives of this class under electron impact. Eight of the compounds bear aromatic substituents, two are cyclic.

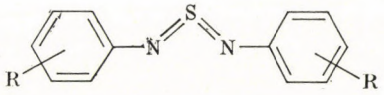

Compound	R
I	H
II	2-Me
III	2-Et
IV	4-Me
V	2-OMe
VI	4-OMe
VII	$4\text{-}NO_2$
VIII	4-Cl

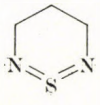

IX

X

Cumulated double bonds involving sulfur differ markedly from the corresponding carbon analogs [3]. It was of interest to determine how this is reflected in electron impact processes. There is no previous published report on the mass spectra of sulfur diimides. Generally, few reports are available on

* Alexander von Humboldt Senior Awardee, 1973–74, on leave from St. John's University, New York.

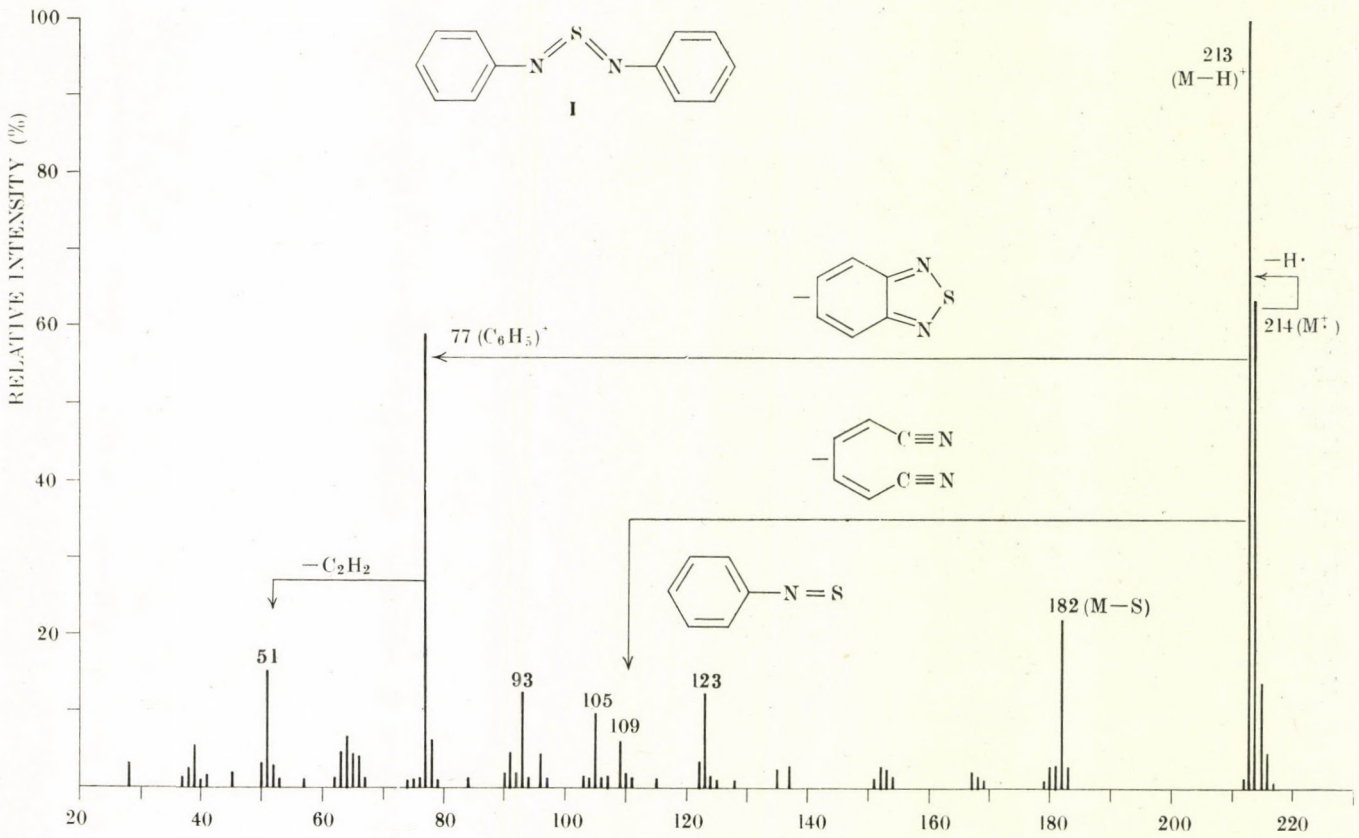
RELATIVE INTENSITY (%)
100
80
60
40
20
20
40
60
80
100
120
140
160
180
200
220
I
213
(M−H)⁺
−H·
214 (M⁺·)
77 (C₆H₅)⁺
−C₂H₂
51
93
105
109
123
182 (M−S)
N
S
C≡N
C≡N
N=S

Fig. 1

thiocumulenes. BROWN *et al.* uncovered [4] interesting rearrangements in arylsulphinylamines (Ar−N=S=O), which fragment by loss of CO and SO.

The mass spectrum of diphenyl sulfur diimide (R=H) is reproduced in Fig. 1. Most interestingly and quite unexpectedly, ion m/e 213 (M−1) is the base peak. The appropriate metastable ion for the loss of a hydrogen atom from the molecular ion is observed. The uncommon stability of the $(M-1)^+$ species can be accounted for by a resonance-stabilized cyclic structure. This process occurs in all other sulfur diimides with aromatic substituents (**I**−**VIII**), leading to $(M-1)^+$ ions of varying abundance.

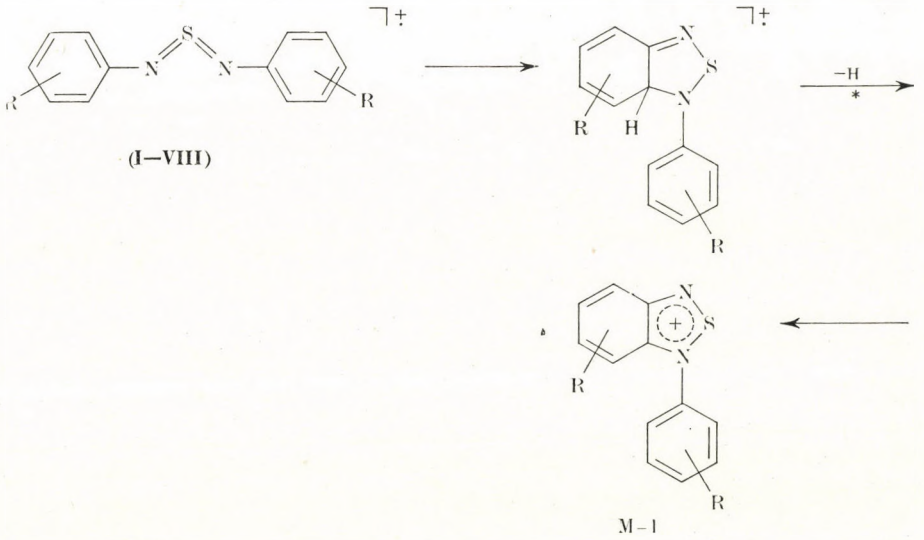

Cyclization reactions of this type leading to five and/or six membered rings, involving loss of an aromatic *ortho*-hydrogen or the *ortho*-substituent, have been observed for other classes of organic compounds [5−6]. A close analogy is described by GRÜTZMACHER [7] in the arylamidine series.

Further break-down of the M−1 ion in the aromatic sulfur diimides, supported by the appropriate metastable peak for **I**, **IV** and **VIII**, occurs by three paths, two of which involve skeletal rearrangement: ejection of 1. $(CH)_4(CN)_2$, 2. Benzothiadiazole, and 3. SH (S.p. 278). The elemental composition of ion *a* has been verified by accurate mass determination for **I** as C_6H_5S. A rearrangement analogous to 1 has been observed [4] in arylsulfinylanilines.

An interesting alternative decomposition path of the molecuar ion of diphenyl sulfur diimide (**I**) involves the loss of sulfur (S.p. 279). The analogous process − loss of carbon − is, of course, absent in the mass spectra of carbodiimides [8]. The N−S−N bond angle in sulfur diimides has been measured by X-ray diffraction [9] as 120°, and calculated by SCF MO-calculation [10] as

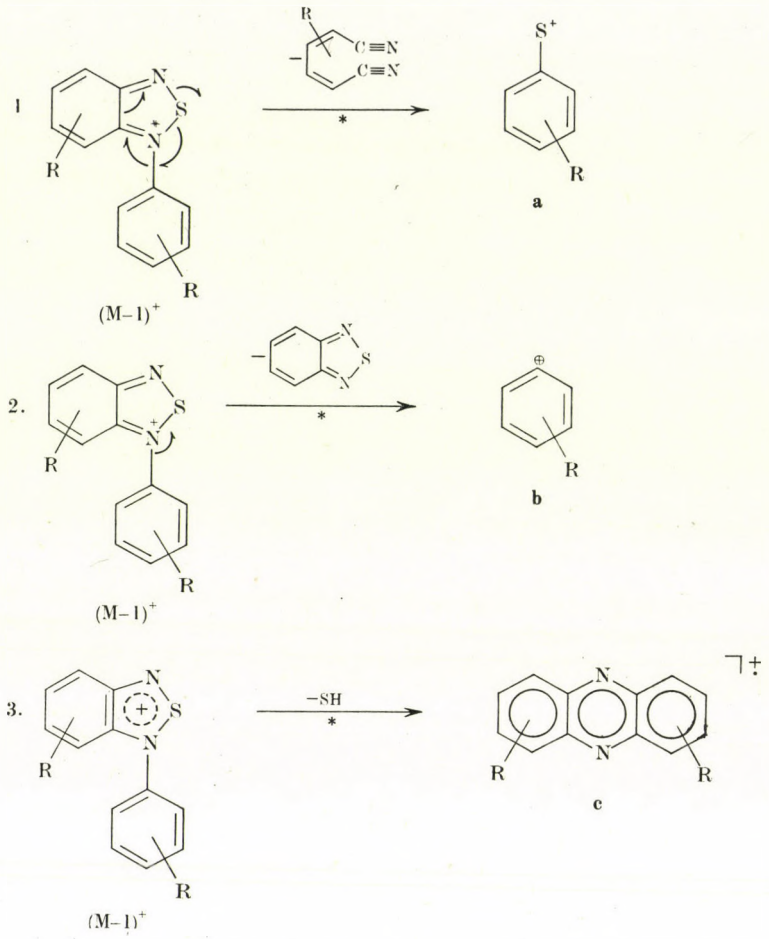

135 – 140°. It is convenient, therefore, to depict the loss of sulfur to occur *via* a valence-isomerized cyclic molecular ion (M') and to visualize the product ion as azobenzene. For comparison, the spectrum of azobenzene was recorded under identical conditions and the coincidental sequence 182 → 105 → 77 → 51 was found.

Substituents on the aromatic rings have a marked influence on the fragmentation. Especially strong "*ortho*-effects" are observed, as illustrated by the spectrum of the *bis-ortho*-tolyl derivative **II.** (Fig. 2.). Besides the M–H species, which is overshadowed by the M–CH_3 ion at m/e 227 (loss of the more stable methyl radical preferred), the main process is cyclization of the molecular ion with participation of one of the *ortho* methyl groups, with subsequent fragmentation leading either to m/e 135 or m/e 107. Further breakdown of ion m/e 135, depicted as benzoisothiazole, involves ejection of CS to m/e 91 or of HCN to m/e 108. Benzoisothiazole was synthesized for comparison and its mass

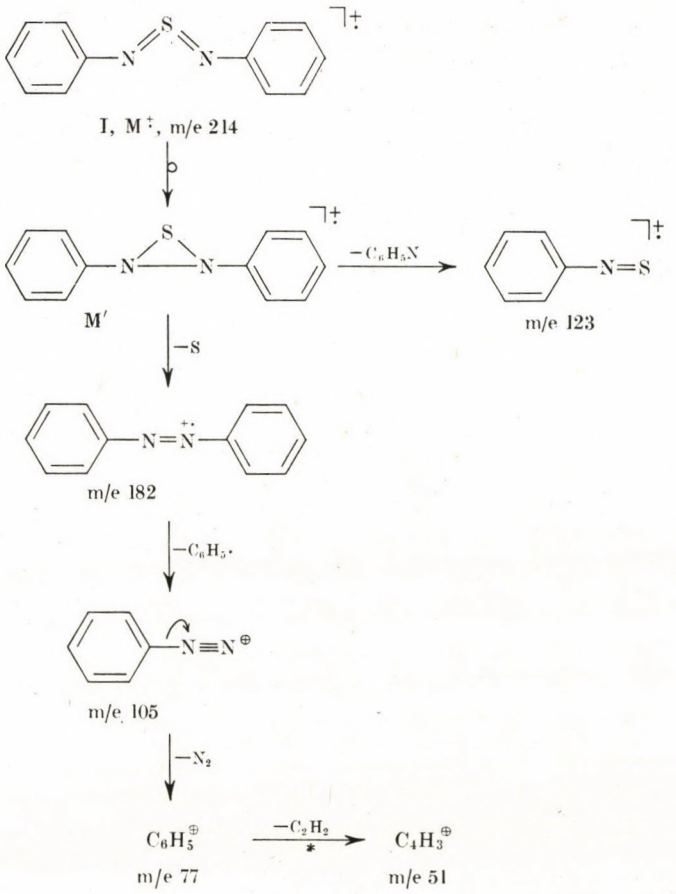

spectrum, recorded under identical conditions, showed the same fragments and the same mestastable ions for the loss of CS and HCN. Ion m/e 107 (*o*-toluidine) fragments by the sequence $107 \xrightarrow{-H\cdot} 106 \xrightarrow{-HCN} 79$. (S.p. 280) In order to investigate this point closer, substituent labeling was employed and *bis-ortho*-diethyl derivative **III** was synthesized. At 12 eV, the expected shifts were indeed observed (107 to 121, 135 to 149). However, at 70 eV, ion m/e 149 is supplanted by m/e 150, which is accompanied by an abundant peak at m/e 136. The spectrum is dominated by the familiar benzothiadiazolium ion m/e 241, derived by loss of an ethyl radical from the molecular ion. (S.p. 281)

It was now interesting to examine, what effect will be brought about by shifting the methyl group from the *ortho* to the *para* position. As shown in Fig. 3, (S.p. 285) ion m/e 135 is *absent* in the mass spectrum of the *bis*-para-tolyl derivative **IV**, a clear indication that the *o*-Me group is essential for the process leading to benzoisothiazole. Strong M–H and M–CH_3 peaks are apparent in the spectrum of **IV** (Fig. 3), and an intense metastable ion is present for the

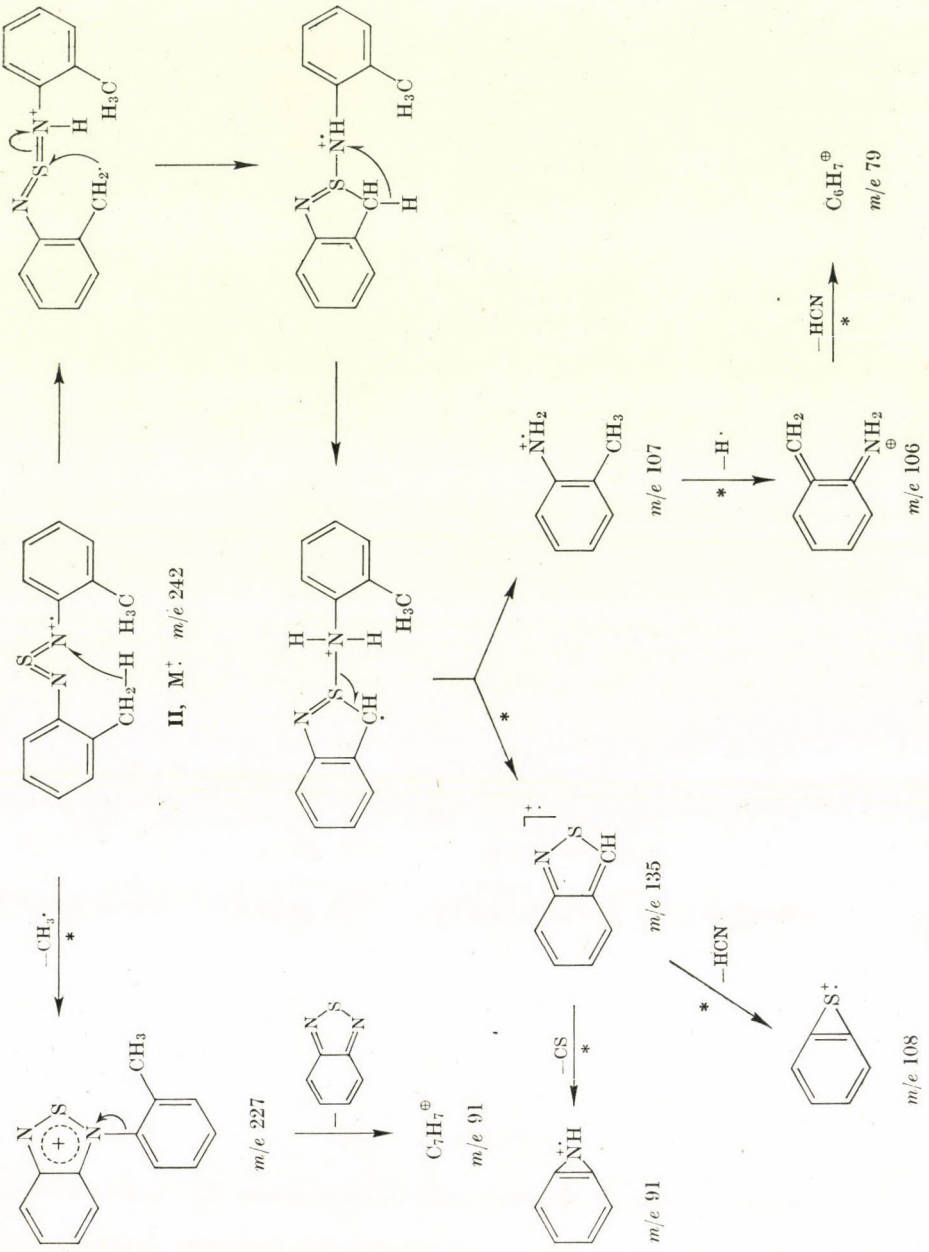
II, M·+ m/e 242
m/e 227
m/e 91
m/e 91
m/e 135
m/e 107
m/e 106
m/e 108
m/e 79
—CH3·
—CS
—HCN
—H·
—HCN

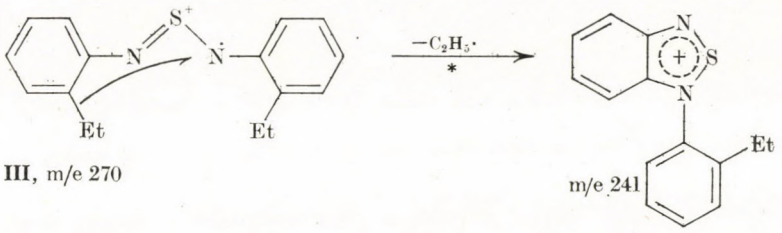

III, m/e 270 m/e 241

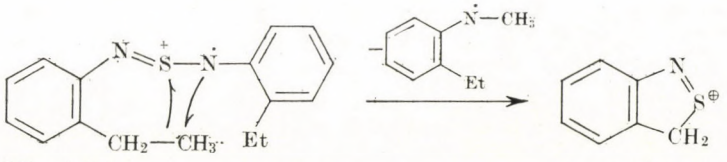

III, m/e 270 m/e 136

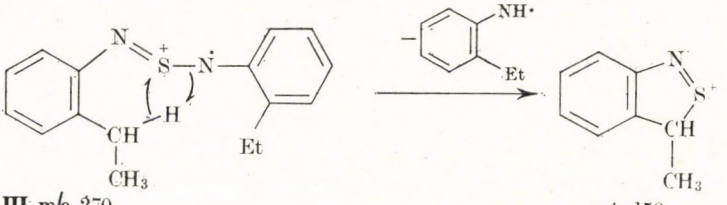

III, m/e 270 m/e 150

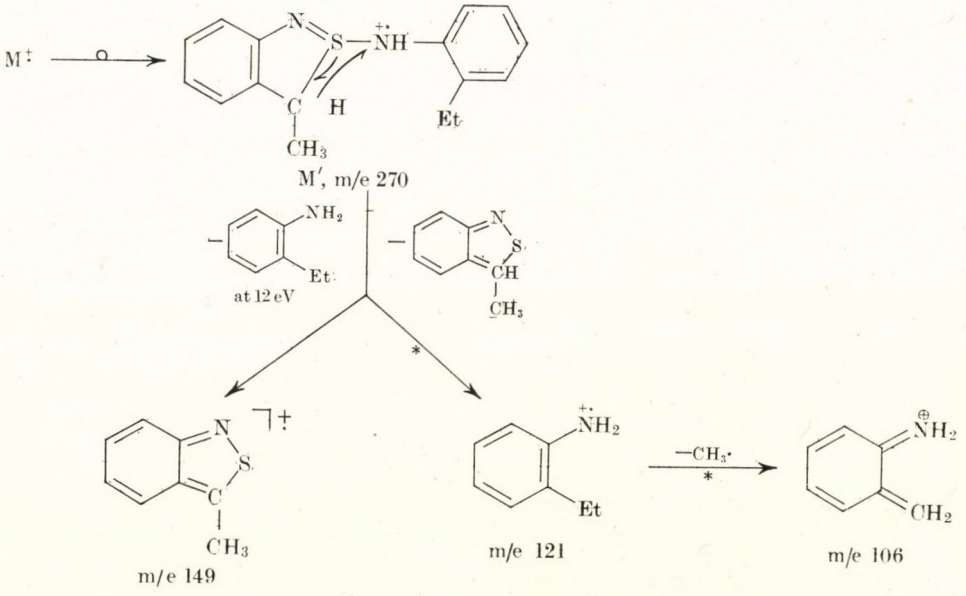

M′, m/e 270

m/e 149 m/e 121 m/e 106

Table I

Normalized 70 eV mass spectra of compounds **III**, **VII**, **IX**, **X** *and model compound* **XI**[a]

Bis [*o-ethylphenyl*] *sulfur diimide* (**III**)

28(17), 29(4), 30(1), 31(1), 32(10), 33(1), 34(1), 37(1), 38(2), 39(12), 40(2), 41(7), 42(3), 43(3), 44(3), 45(4), 50(4), 51(10), 52(6), 53(5), 54(1), 55(2), 59(2), 61(2), 62(3), 63(10), 64(5), 65(12), 66(3), 67(2), 69(2), 70(1), 75(2), 76(4), 77(22), 78(8), 79(8), 80(3), 81(2), 89(13), 90(12), 91(50), 92(10), 93(5), 94(3), 102(5), 103(8), 104(12), 105(7), 106(60), 107(5), 108(2), 109(11), 116(6), 117(30), 118(59), 119(20), 120(8), 121(56), 122(6), 123(2), 130(2), 134(3), 135(9), 136(51), 137(5), 138(3), 148(10), 149(18), 150(80), 151(11), 152(7), 167(2), 205(2), 237(2), 240(5), 241(100), 242(20), 243(6), 255(5), 256(2), 269(10), 270(26), 271(9), 272(7), 273(1).

Bis[*p-nitrophenyl*] *sulfur diimide* (**VII**)

28(1), 29(1), 30(12), 32(8), 37(2), 38(4), 39(17), 40(2), 41(2), 42(2), 44(3), 45(41), 46(3), 47(2), 48(1), 50(10), 51(9), 52(9), 53(2), 57(1), 58(2), 59(2), 60(1), 61(2), 62(5), 63(21), 64(12), 65(9), 66(4), 69(6), 70(2), 71(1), 73(3), 74(2), 75(5). 76(9), 77(3), 78(16), 79(2), 80(6), 82(2), 83(9), 84(2), 85(1), 88(2), 89(2), 90(12), 91(2), 92(8), 94(2), 95(4), 96(3), 103(4), 108(4), 109(8), 110(12), 111(2), 112(2), 120(2), 121(2), 122(10), 123(2), 134(2), 135(2), 136(2), 137(1), 138(16), 139(2), 140(2), 149(3), 150(2), 152(1), 153(1), 154(1), 166(1), 167(2), 168(11), 169(2), 179(2), 180(2), 184(3), 210(4), 211(19), 212(20), 213(4), 214(1), 229(2), 257(2), 258(100), 259(21), 260(8), 261(1), 276(2), 288(79), 289(15), 290(6), 291(1), 303(10), 304(24), 305(5), 306(2).

3,4-Dihydro-5H-1,2,6-thiadiazine (**IX**)

28(37), 29(3), 30(9), 32(9), 33(2), 34(1), 38(1), 40(2), 41(9), 42(35), 43(14), 44(6), 45(3), 46(22), 47(9), 48(3), 52(1), 54(1), 56(2), 57(1), 58(1), 59(4), 60(16), 61(4), 62(1), 73(8), 74(32), 75(3), 76(2), 86(2), 101(1), 102(100), 103(6), 104(6), 105(1).

3,4-Dihydro-1,2,5-thiadiazole (**X**)

28(68), 29(2), 30(2), 31(4), 32(57), 33(11), 34(4), 38(5), 39(6), 40(4), 42(3), 44(5), 46(22), 50(7), 51(9), 52(12), 53(3), 58(12), 59(81), 60(65), 61(16), 62(3), 70(4), 86(100), 87(10), 88(24), 89(2), 90(3).

Benzo [*c*]*isothiazole* (**XI**)

28(2). 37(1), 38(1), 39(2), 44(1), 45(9), 50(2), 51(2), 52(1), 54(2), 58(1), 62(1), 63(3), 64(2), 69(3), 75(1), 76(1), 77(2), 78(1), 81(1), 82(2), 84(1), 90(2), 91(7), 92(1), 93(1), 105(3), 107(1), 108(9), 109(1), 134(6), 135(100), 136(8), 137(4).

[a] Data presented as m/e-values followed by ion abundances in parentheses

227 → 91 transition S.p. (283). The latter suggests that the M–CH_3 ion (m/e 227) has the benzothiadiazolium structure for the *para* derivative **IV** too. This means that ejection of the methyl group from the *para* position is accompanied by loss of identity of the carbon atoms. Such a randomization of carbon atoms in substituted aromatics was first proved by RINEHART *et al.* [11] in 1968.

The predominant primary fragmentation process in *o*-anisyl derivative V is the ejection of an OMe group, leading to ion m/e 243 (S.p. 286). The latter undergoes an interesting even-to-odd electron ion transition by loss of the remaining methyl group to give ion m/e 228, the elemental composition of which has been verified as $C_{12}H_8N_2OS$. Through – conjugation in the product ion may be the driving force.

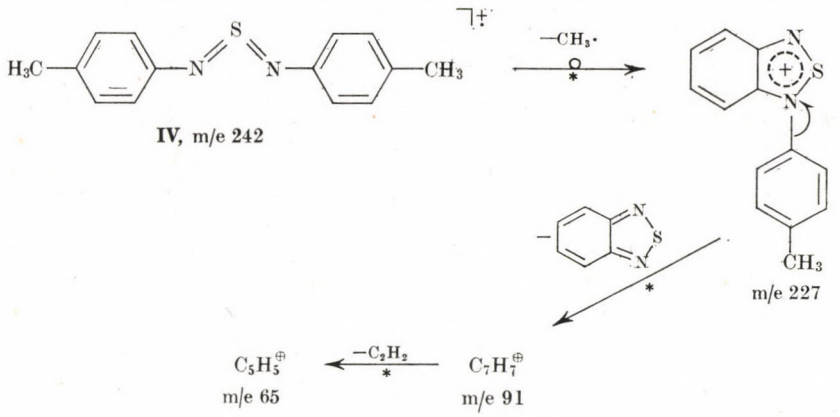

IV, m/e 242

Alternatively, the loss of both methyl groups from the molecular ion in consecutive steps leads to ion m/e 244. The unusual second loss of Me is rendered energetically favorable by the stable *ortho*-quinoid structure formed. Fission of the N – S bond yields ions m/e 106 and 138, elimination of CO from either leading to m/e 78 and 110, respectively. The process m/e 121 → 120 → 93 is similar to the one described by BROWN *et al.* [4] in the fragmentation of *o*-anisylsulfinylamine.

The *bis*-para-anisyl derivative **VI** exhibits a basically similar spectrum

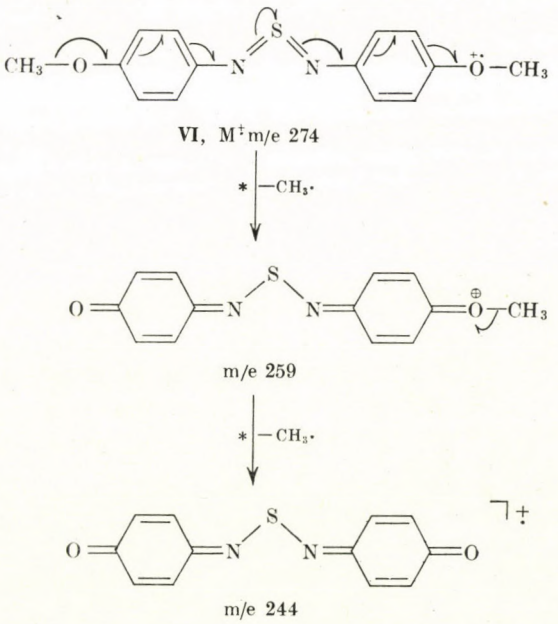

VI, M^{+} m/e 274

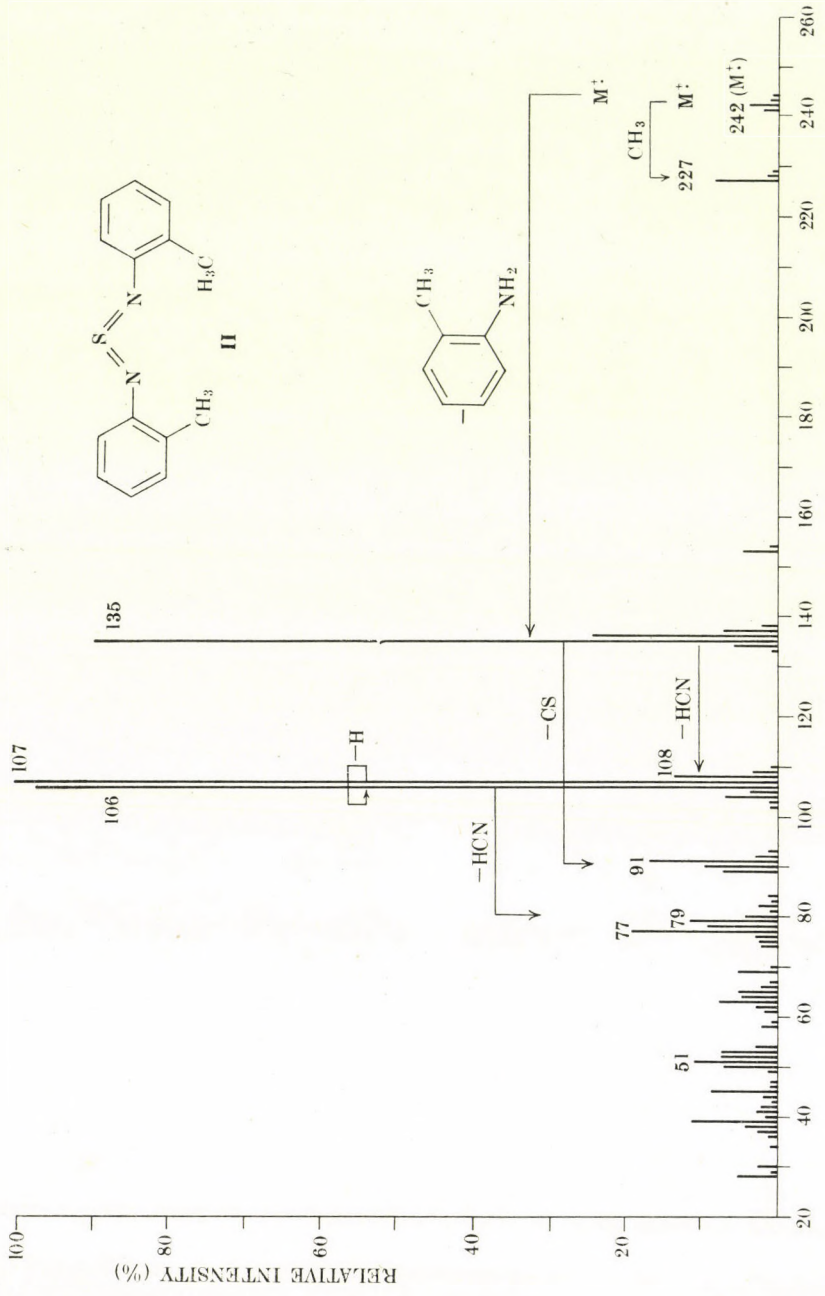
RELATIVE INTENSITY (%)
100
80
60
40
20
20
40
60
80
100
120
140
160
180
200
220
240
260
242 (M+)
M+
227
CH3
M+
135
107
106
108
91
79
77
51
-H
-HCN
-CS
-HCN
CH3
NH2
II
H3C
CH3
N
S
N

Fig. 2.

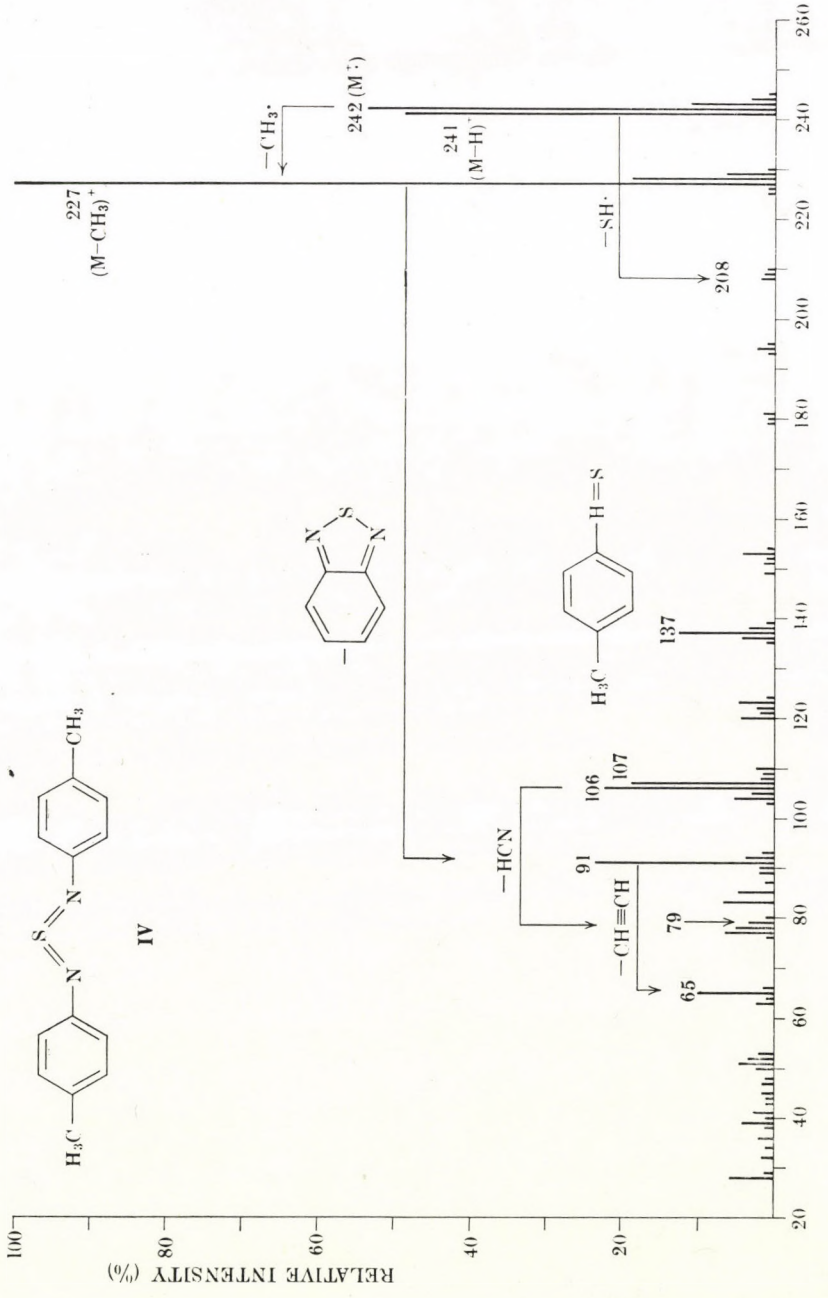
RELATIVE INTENSITY (%)
100
80
60
40
20
20
40
60
80
100
120
140
160
180
200
220
240
260
227
(M−CH3)+
242 (M+)
241
(M−H)
−CH3·
−SH·
208
137
106
107
91
79
65
−HCN
−CH≡CH
IV

Fig. 3

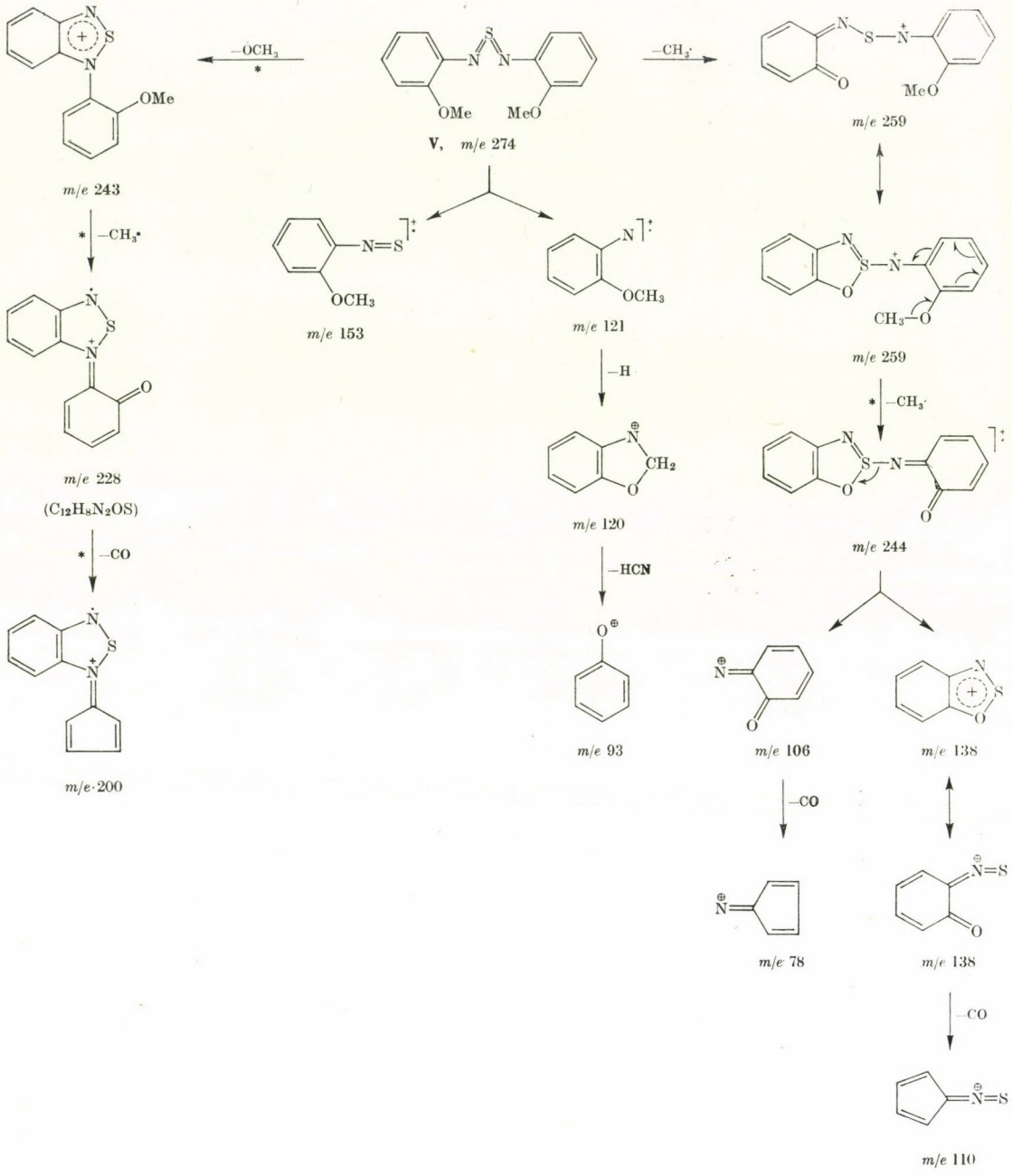
−OCH3
*
−CH3·
OMe
MeO
V, m/e 274
m/e 243
m/e 153
m/e 121
m/e 259
m/e 259
* −CH3·
m/e 228
(C12H8N2OS)
−H
m/e 120
m/e 244
* −CO
−HCN
m/e 93
m/e 106
m/e 138
m/e 200
−CO
m/e 78
m/e 138
−CO
m/e 110

but the relative abundances of ions are substantially different (Fig. 5). There are very intense $M-H$ and $M-CH_3$ ions while the $M-OCH_3$ peak is weaker and the m/e 244 ($M-2CH_3$) ion has only about 8 % rel. intensity. A main part of the ion current is carried by the following sequences: 153 → 138 → 110 and 123 → 108 → 80.

The origin of m/e 123 is not clear, there is no metastable evidence for its formation.

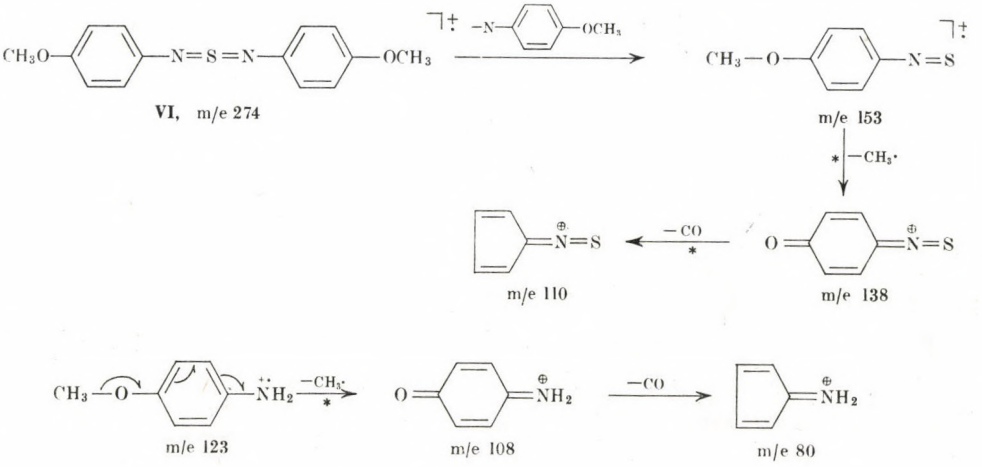

Bis-*para*-nitrophenyl sulfur diimide **VII** shows a complex and in some aspects unique spectrum. Besides the expected $M-H$ and $M-NO_2$ ions, there is an abundant m/e 212 peak. *A priori*, this could originate from the molecular ion by loss of the two NO_2 groups or by loss of NO_2 and NS. Exact mass measurement revealed that m/e 212 is homogeneous, $C_{12}H_8N_2S$, thus ($M-2NO_2$). For both steps, the appropriate metastable peak is present (S.p. 288).

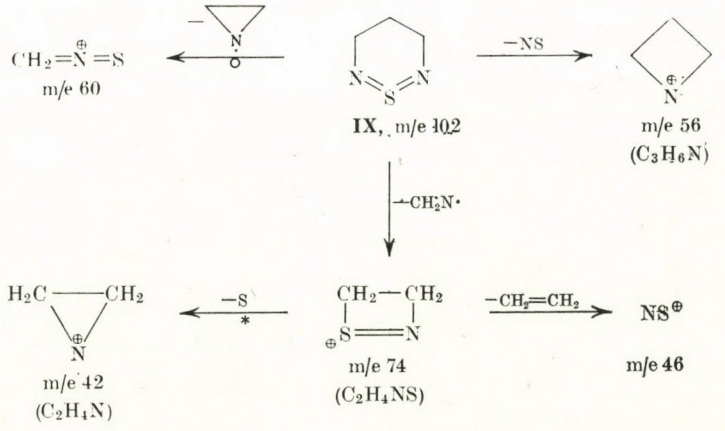

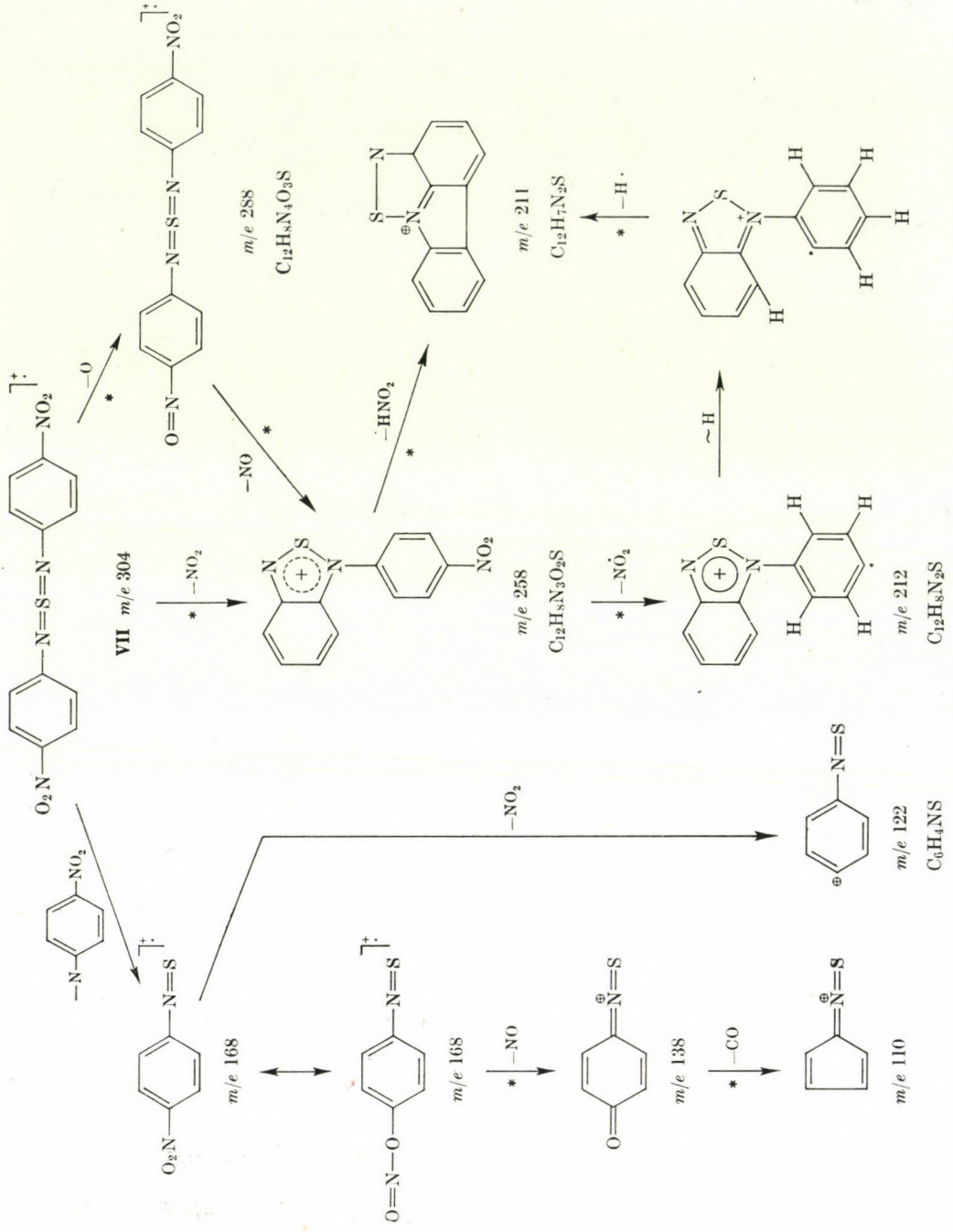
VII m/e 304
m/e 288
C12H8N4O3S
m/e 258
C12H8N3O2S
m/e 211
C12H7N2S
m/e 212
C12H8N2S
m/e 168
m/e 168
m/e 138
m/e 110
m/e 122
C6H4NS

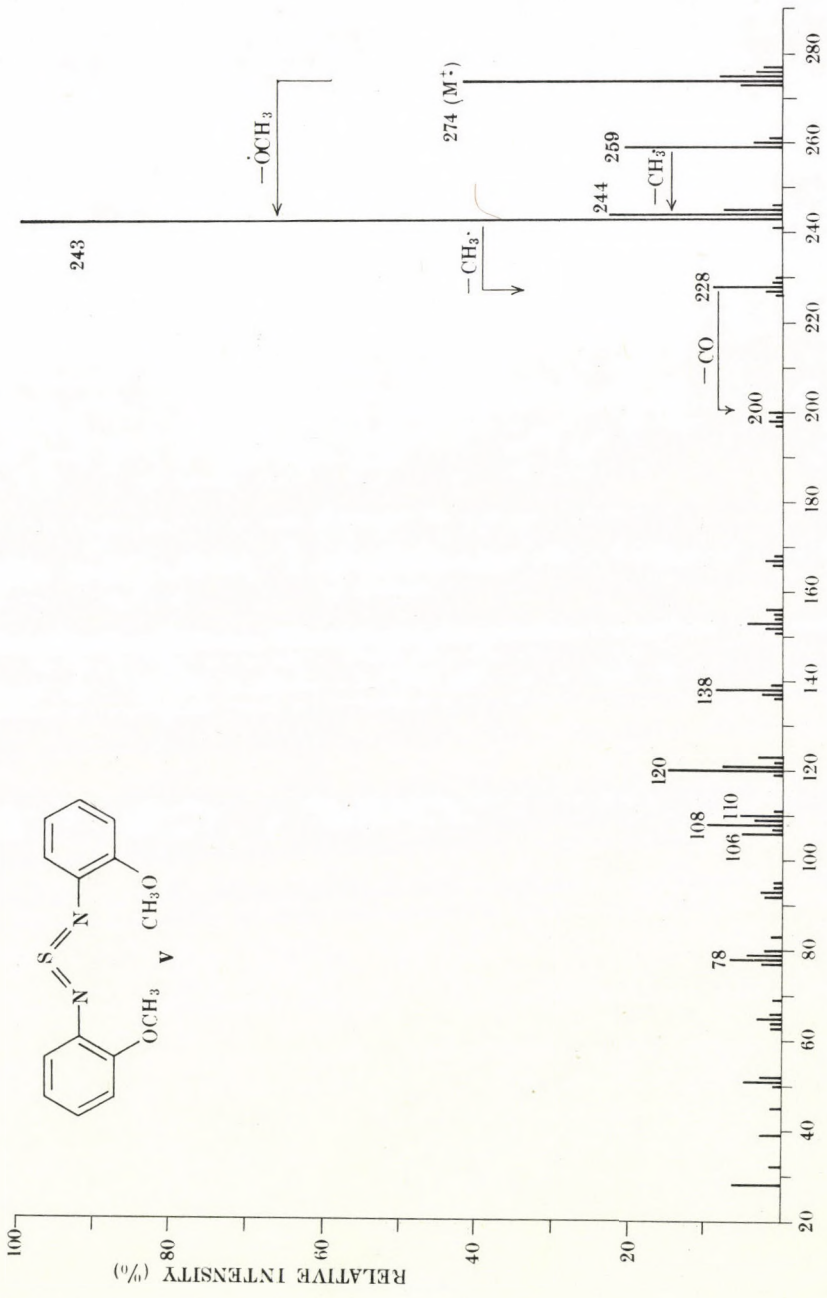
RELATIVE INTENSITY (%)
100
80
60
40
20
20
40
60
80
100
120
140
160
180
200
220
240
260
280
243
274 (M+)
259
244
228
200
138
120
108
110
106
78
—OCH3
—CH3·
—CH3
—CO
N
S
OCH3
CH3O

V

Fig. 4


RELATIVE INTENSITY (%)
100
80
60
40
20
274
(M+)
273
259
243
244
153
138
123
110
108
92
80
-H·
-OCH3·
-CH3·
-CO
VI
CH3O
OCH3
N=S

Fig. 5

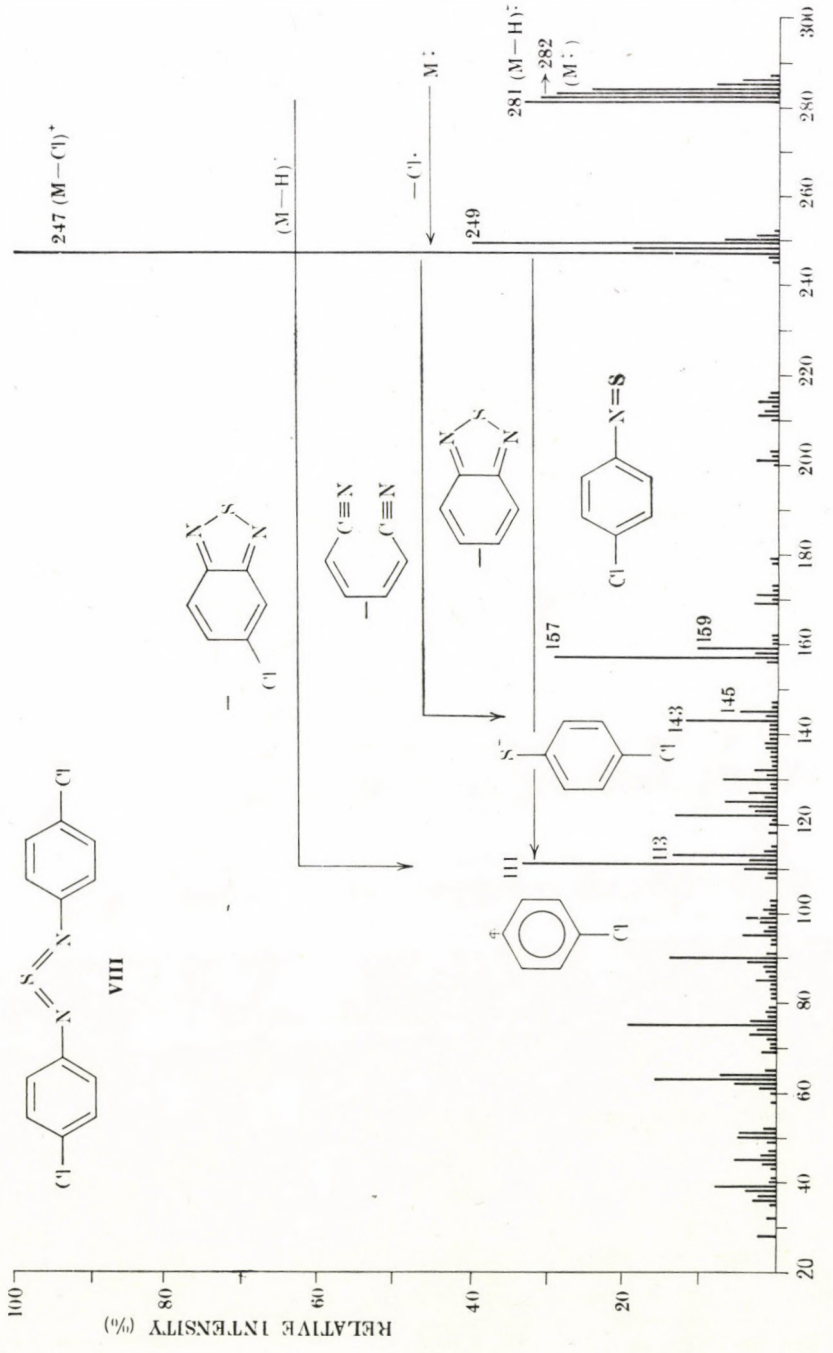
RELATIVE INTENSITY (%)
100
80
60
40
20
20
40
60
80
100
120
140
160
180
200
220
240
260
280
300
247 (M—Cl)+
(M—H)·
—Cl·
M·
249
281 (M—H)·
→282
(M·)
157
159
143
145
113
111
N≡C
N≡C
N=S
Cl
Cl
Cl
Cl
VIII

Fig. 6

According to metastable evidence, a second stepwise path also operates in the genesis of the $M-NO_2$ (m/e 258) ion: loss of oxygen followed by loss of NO.

The spectrum of 4,4'-dichlorodiphenyl sulfur diimide (**VIII**) shows the same fragmentation pattern as the other compounds discussed previously. All major processes except $M \rightarrow (M-H)$ are supported by the appropriate metastable transition (Fig. 6).

3,4-Dihydro-5H-1,2,6-thiadiazine, cyclic sulfur diimide **IX** [1], fragments by entirely different paths. Exact mass measurement was a necessity in this case, as multiple elemental compositions are possible for all major ions. (S.p. 287)

The highlight of the mass spectrum of 3,4-dihydro-1,2,5-thiadiazole (**X**) is the strong tendency to aromatize: the molecular ion ejects 2 H atoms to give ion m/e 86, which in turn loses HCN yielding ion m/e 59. The other paths observed are similar to six-ring compound **IX**.

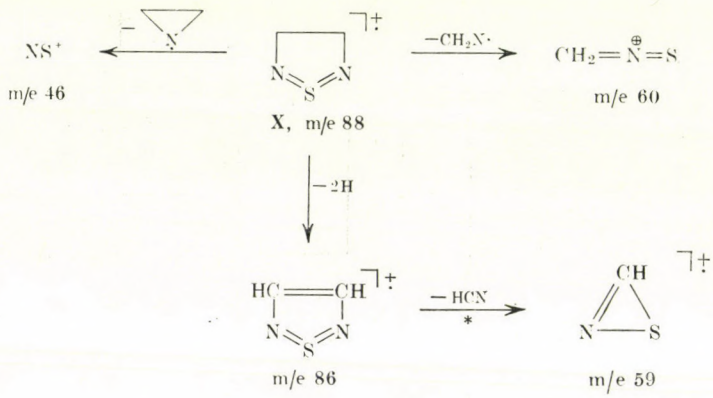

Experimental

A. Synthesis of compounds

The aromatic sulfur diimides have been prepared by treating the corresponding N-sulfinyl anilines with the appropriate base [12]. The liquid products were purified by column chromatography (Silica Merck 0.063 – 0.20), elution with benzene/hexane 1 : 1 and distillation (*c.f.*, Table II).

3,4-Dihydro-5H-1,2,6-thiadiazine (**IX**) and 3,4-dihydro-1,2,5-thiadiazole (**X**) have been synthesized by reaction of 1,3-diamino-propane and ethylene diamine, respectively, with bis-*p*-toluene sulfonyl sulfur diimide [13];

IX, b.p. 28°/6 – 8, **X**, b.p. 18 °C/6 – 8.

Benzo-1,2,5-thiadiazole, m.p. 44 °C (H_2O/EtOH), was prepared by treating *o*-phenylene diamine with $SOCl_2$ [14]. For the preparation of 4,5-benzoisothiazole the method of DAVIS and WHITE [15] was used, starting with *o*-toluidine and $SoCl_2$. The product was purified by hydrolysis of the by-product, N-sulfinyl *o*-toluidine, with dilute HCl, steam distillation, extraction of the distillate with dilute H_2SO_4, water and $NaHCO_3$ solution, drying with Na_2SO_4 and distillation, b.p. 60 °C/0.4. The product contains some (< 10 %) chloro-benzisothiazole.

Table II

Compound	*R*	Base/solvent	b.p. (°C) observed/ (b.p. reported[12])	m.p. (°C) observed/(m.p. reported[12])
I	H	KOtBu/benzene	98/0.1(126/0.5)	
II	2-CH_3	KOtBu/benzene	100/0.01(141/0.1)a)	
III	2-C_2H_5	KOtBu/benzene		
IV	4-CH_3	KOtBu/benzene		48.5 (hexane) (48)
V	2-OCH_3	KOtBu/benzene		89 (hexane) (89)
VI	4-OCH_3	NaOEt/isopropyl ether		47 (hexane) (47)
VII	4-NO_2	KOtBu/DMF		186 (benzene (P. E.) (187 – 189)
VIII	4-Cl	KOtBu/THF		60 (hexane) (61)

[a] Decomposed on distillation,
DMF dimethylformamide, PE petroleum ether b.p. 60 – 90 °C,
THF tetrahydrofuran.

B. Mass spectra

The conventional (low resolution) mass spectra were recorded on an A.E.I. MS9 mass spectrometer at 70 eV and 50 – 100 μA, ion source temperature between 40 and 100°. Samples **IX** and **X** were introduced *via* the reservoir at room temperature, the others using the solid probe. High resolution measurements were performed on a CEC 21 – 110 B mass spectrometer. The photoplate was processed automatically in conjunction with an IBM 1800 computer. The bar graph spectra were plotted on a Benson XY-plotter using a Fortran program written for the TR 440 computer.

*

Support of this work by the Fonds der Chemischen Industrie and the Alexander von Humboldt Foundation in the form of a Senior Award to I.L. is gratefully acknowledged. We thank Prof. Klaus BIEMANN, Cambridge, Mass., for the accurate mass measurements, carried out at the M.I.T. high resolution mass spectrometry facility, supported by National Institute of Health Research Grant No. FR 00317. We thank the Leibniz computer center, München for computer time.

REFERENCES

[1] SCHÖNBERGER, N., KRESZE, G.: Liebigs Ann. Chem., (**1975,** 1725)
[2] KRESZE, G., WUCHERPFENNIG, W.: Angew. Chem., **79,** 109 (1967)
[3] KRONER, J., STRACK, W., HOLSBOER, F., KOSBAHN, W.: Z. Naturforsch., **28b,** 188 (1973-
[4] BROWN, J. H., LARSSON, F. C. V., SCHROLL, G., LAWESSON, S.-O., COOKS, R. G.: Tetra) hedron **23,** 3743 (1967)
[5] *C.f.*, for example: CLAUSSEN, U., FEHLHABER, H.-W., KORTE, F.: Tetrahedron **22,** 3533 (1966)
[6] RONAYNE, J., WILLIAMS, D. H., BOWIE, J. H.: J. Am. Chem. Soc., **88,** 4980 (1966)
[7] GRÜTZMACHER, H. F., KUSCHEL, H.: Org. Mass spectr., **3,** 605 (1970)
[8] LENGYEL, I., ALESSANDRO, R. I.: Paper in preparation
[9] LEANDRI, G., BUSETTI, V., VALLE, G., MAMMI, M.: J. Chem. Soc., (D) **1970,** 413
[10] KOSBAHN, W.: paper in preparation
[11] RINEHART, K. L., BUCHHOLZ, A. C., VANLEAR, G. E., CANTRILL, H. L.: J. Am. Chem. Soc., **90,** 2983 (1968)

[12] [12] HÖRHOLD, H. H., BECK, J.: J. prakt. Chem., **311**, 621 (1969)
[13] GRILL, H.: Ph. D. Thesis, TU München, 1970.
[14] MICHAELIS, A., BUNTROCK, A.: Liebigs Ann. Chem., 274, 262 (1893)
[15] DAVIS, M., WHITE, A. W.: Chem. Commun., 547 (1968)

István LENGYEL
G. KRESZE
M. BERGER
W. KOSBAHN
H. SCHÄFER

8 München 2, Arcisstrasse 21
Federal Republic of Germany

Acta Chimica Academiae Scientiarum Hungaricae, Tomus 96(3), pp. 295–309 (1978)

BENZAZOLES, IX*

REACTION OF 2-MERCAPTO- AND 2-MERCAPTOALKYLBENZIMIDAZOLES WITH EPIHALOHYDRINS OR DIHALOGENOPROPANOLS AFFORDING SULFUR HETEROATOM-CONTAINING TRICYCLES

K. HIDEG, O. H. HANKOVSZKY, M. GAJDÁCS and F. ARADI

(Central Laboratory of Chemistry, University of Pécs, Hungary)

Received March 1, 1976; in revised form June 28, 1977

Benzimidazole-2-thiol, 2-mercaptomethyl-, 2(α-mercaptoethyl)-, 2-(β-mercaptoethyl)benzimidazole can be converted with epichlorohydrin or with dihalogenopropanols (2,3-dihalogeno-1-propanols or 1,3-dihalogeno-2-propanols), in alkaline medium, into tricycles: 3,4-dihydro-3-hydroxy-2*H*-[1, 3]thiazino[3,2-a]benzimidazole (**1**); 4,5-dihydro-4-hydroxy-1*H*,3*H*-[1,4]thiazepino[4,3-a]benzimidazoles (**3a – b**) and 1,2,5,6- tetrahydro-5-hydroxy-4*H*-[1,5]thiazocino[5,4-a]benzimidazole (**3c**). The 0-sulfonyl derivatives of **1** may enter elimination or substitution reactions with nucleophilic reagents.

The reactions of 3,4-dihydro-3-azido-2*H*-[1,3]thiazino[3,2-a]benzimidazole (**10d**) with asymmetric acetylenes into 1,2,3-triazole derivatives have been investigated.

Benzimidazole-2-thiol was converted with epibromohydrin in a mixture of N,N-dimethylacetamide and 2-butanone into a thiazine derivative (**1**) [1].

We effected this reaction in a simpler way, in an alkaline medium in ethanol, with epichlorohydrin at room temperature. When carrying out the reaction instead of halohydrin with 2,3-dihalogeno-1-propanols or 1,3-dihalogeno-2-propanols, similarly the formation of products having cyclic thiazine structure, but not cyclic thiazolidine structure, was experienced. From this we concluded that in all reactions a non-isolable epoxide had formed.

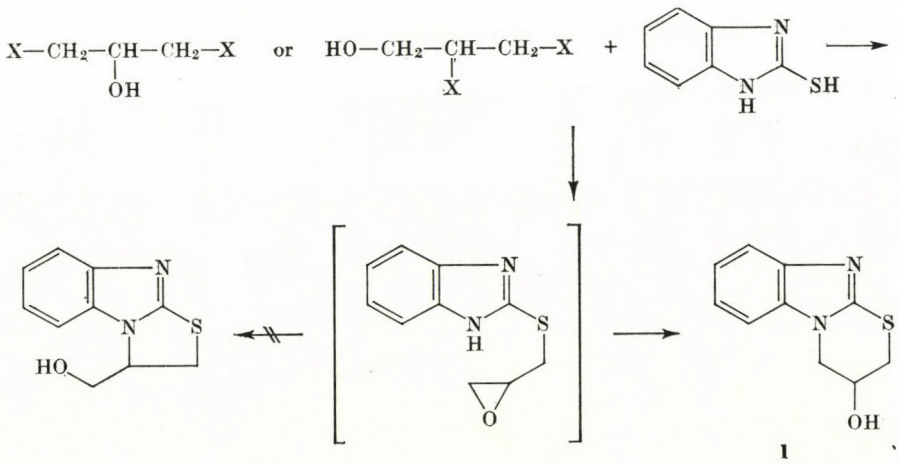

1

* Part VIII: O. H. HANKOVSZKY, K. HIDEG: Acta Chim. Acad. Sci. Hung., **63**, 447 (1970).

Acta Chim. Acad. Sci. Hung. 96, 1978

Table I

O-Acyl compounds of **1** *and* **3a – c**

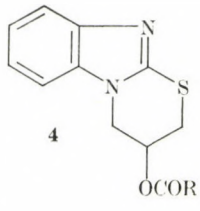

4

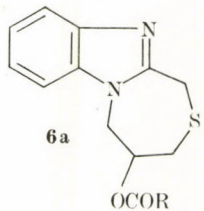

6a

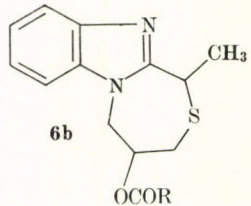

6b

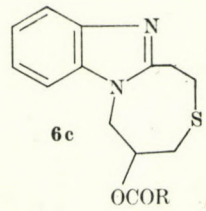

6c

No.	R	M.p., °C	Formula (Mol. wt.)	Analysis, % C	H	N	Cl	S	IR, cm^{-1} (Nujol)	NMR (ppm, δTMS=0 ppm)
				calcd./found						
4a	CH_3	137 – 138	$C_{12}H_{12}N_2O_2S$ (248.30)	58.05 58.28	4.87 4.97	11.28 11.39		12.91 12.85	1725 (CO)	2.04 (s, 3H, CH_3); 3.30 (d, 2H, SCH_2); 4.11 (d, 2H, NCH_2); 5.52 (q, 1H, CH); 7.1 – 7.8 (compl. 4H, Ar=CH) ($CDCl_3$)
		176 – 178	$C_{12}H_{12}N_2O_2S$ .HCl (284.76)	50.62 50.60	4.60 4.40	9.83 10.08	12.45 12.21	11.26 10.95	2800 – 2400 (NH) 1700 (CO)	
4b	CH_2CH_3	123 – 124	$C_{13}H_{14}N_2O_2S$ (262.33)	59.52 59.51	5.38 5.30	10.68 10.91	– –	12.22 12.17	1725 (CO)	1.06 (t, 3H, CH_3); 2.3 (m, 2H, $COCH_2$); 3.29 (d, 2H, SCH_2); 4.21 (d, 2H, NCH_2); 5.5 (m. 1H, CH); 7.0 – 7.8 (compl. 4H, Ar=CH) ($CDCl_3$)
4c	$CH_2CH_2CH_3$	118 – 119	$C_{14}H_{16}N_2O_2S$ (276.36)	60.85 60.93	5.84 6.09	10.14 10.24	– –	11.60 11.78	1725 (CO)	0.9 (t, 3H, CH_2); 1.6 (m, 2H, CH_2); 2.3 (t, 2H, CH_2); 3.32 (d, 2H, SCH_2); 4.15 (d, 2H, NCH_2); 5.54 (m, 1H, CH); 7.1 – —7.8 (compl. 4H, Ar=CH) ($CDCl_3$)
4d	$CH(CH_3)_2$	152 – 153	$C_{14}H_{16}N_2O_2S$ (276.36)	60.85 60.60	5.84 6.04	10.14 10.02	– –	11.60 11.93	1725 (CO)	1.06 (d, 3H, CH_3); 1.17 (d, 3H, CH_3); 2.52 (m, 1H, COCH); 3.32 (d, 2H, SCH_2); 4.15 (d, 2H, NCH_2); 5.52 (m, 1H, CH); 7.1 – 7.8 (compl. 4H, Ar=CH) ($CDCl_3$)

4e	$C(CH_3)_3$	197 – 198	$C_{15}H_{18}N_2O_2S$ (290.39)	62.04 62.02	6.25 6.34	9.65 10.03	– –	11.04 11.00	1715 (CO)	1.14 (s, 9H,3CH_3); 3.36 (d, 2H, SCH_2); 4.24 (d, 2H, NCH_2); 5.56 (m, 1H, CH); 7.1 – 7.8 (compl. 4H, Ar = CH) ($CDCl_3$)
4f	$(CH_2)_2COOCH_3$	147 – 148	$C_{15}H_{16}N_2O_4S$ (320.37)	56.24 56.34	5.03 5.12	8.74 8.82	– –	10.01 10.19	1710 (CO)	2.62 (s, 4H, CH_2CH_2); 3.38 (d, 2H, SCH_2); 3.62 (s, 3H, CH_3); 4.22 (d, 2H, NCH_2); 5.62 (m, 1H, CH); 7.2 – 7.8 (compl. 4H, Ar = CH) ($CDCl_3$)
4g	C_6H_5	165 – 166	$C_{17}H_{14}N_2O_2S$ (310.38)	65.79 65.93	4.57 4.49	9.03 8.93	– –	10.33 10.45	1730 (CO)	3.42 (d, 2H, SCH_2); 4.27 (d, 2H, NCH_2); 5.8 (m, 1H, CH); 7.0 – 8.1 (compl. 9H, Ar = CH) ($CDCl_3$)
4h	2-Cl – C_6H_4	168 – 169	$C_{17}H_{13}ClN_2O_2S$ (344.82)	59.22 60.08	3.80 4.01	8.12 7.99	10.29 10.47	9.29 9.39	1730 (CO)	3.50 (d, 2H, SCH_2); 4.35 (d, 2H, NCH_2); 5.85 (m, 1H, CH); 7.2 – – 8.0 (compl. 8H, Ar = CH) ($CDCl_3$)
4i	2-CF_3 – C_6H_4	173 – 175	$C_{18}H_{13}F_3N_2O_2S$ (378.38)	57.14 57.02	3.46 3.77	7.41 7.66	– –	8.48 8.61	1725 (CO)	3.52 (d, 2H, SCH_2); 4.38 (d, 2H, NCH_2); 5.85 (m, 1H, CH); 7.1 – – 7.9 (compl. 8H, Ar = CH) ($CDCl_3$)
4j	3,4,5-$(OCH_3)_3$ – – C_6H_2	186 – 188	$C_{20}H_{20}N_2O_5S$ (400.45)	59.99 60.17	5.03 5.05	6.99 6.68	– –	8.01 8.26	1720 (CO)	3.48 (d, 2H, SCH_2); 3.8 (s, 3H, OCH_3); 3.88 (s, 6H, 2OCH_3); 4.35 (d, 2H, NCH_2); 5.85 (m, 1H, CH); 7.2 – 7.8 (compl. 6H, Ar = CH) ($CDCl_3$)
4k	– CH = CH – – C_6H_5	162 – 164	$C_{19}H_{16}N_2O_2S$ (336.42)	67.84 67.51	4.80 5.02	8.33 8.25	– –	9.52 9.30	1720 (CO) 1630 (C = C conj.)	3.45 (d, 2H, SCH_2); 4.3 (d, 2H, NCH_2); 5.75 (m, 1H, CH); 6.44 (d, 1H, C*H* = CH, J 16.8 Hz); 7.2 – 7.55 (compl. 9H, Ar = CH); 7.79 (d, 1H, CH = C*H*, *J* 16.8 Hz) ($CDCl_3$)
6a	CH_3	161 – 162	$C_{13}H_{14}N_2O_2S$ (262.33)	59.52 59.61	5.38 6.01	10.68 10.48	– –	12.22 12.43	1740 (CO)	1.95 (s, 3H, CH_3); 3.0 (m, 2H, SCH_2); 4.0 (s, 2H, CCH_2S); 4.35 (d, 2H, NCH_2); 4.8 – 5.3 (m, 1H, CH); 7.2 – 7.8 (compl. 4H, Ar = CH) ($CDCl_3$)

Table I cont.

No.	R	M.p., °C	Formula (Mol. wt.)	Analysis, % calcd./found					IR, cm^{-1} (Nujol)	NMR (ppm, δTMS=0 ppm)
				C	H	N	Cl	S		
		217 – 219	$C_{13}H_{14}N_2O_2S$. HCl (298.79)	52.26 52.41	5.06 5.01	9.37 9.63	11.87 11.65	10.73 10.43		1.08 (s, 3H, CH_3); 3.2 – 3.6 (m, 2H, SCH_2); 4.4 (d, 2H, CH_2S); 4.8 – 5.1 (d, 2H, NCH_2); 5.2 – – 5.5 (m, 1H, CH); 7.68 (s, 4H, Ar=CH) (D_2O)
6b	CH_3	133 – 135	$C_{14}H_{16}N_2O_2S$ (276.35)	60.85 61.16	5.83 5.49	10.14 10.03	– –	11.60 11.94	1745 (CO)	1.85 (dd, 3H, CH_3); 2.1 (s, 3H, $COCH_3$); 3.06 (m, 2H, SCH_2); 4.2 – 5.1 (m, 4H, NCH_2CH, $CHCH_3$); 7.1 – 8.0 (compl. 4H, Ar=CH) ($CDCl_3$)
6c	CH_3	136 – 140	$C_{14}H_{16}N_2O_2S$ (276.35)	60.85 60.97	5.83 5.69	10.14 10.45	– –	11.60 11.41	1740 (CO)	2.1 (s, 3H, CH_3); 2.3 – 2.8 (m, 2H, SCH_2); 2.8 – 3.1 (m, 2H, $CH_2 - CH_2S$); 3.2 – 3.6 (m, 2H, CH_2CH_2S); 4.66 (d, 2H, NCH_2); 5.1 – 5.6 (m, 1H, CH); 7.2 – 7.9 (compl. 4H, Ar=CH) ($CDCl_3$)

The epoxide ring undergoes cleavage under the effect of the imidazole *NH* at the least substituted carbon atom.

The reaction of 2-mercaptoalkylbenzimidazoles [2, 3] with 1,2-epoxy-3-halogenopropane, 2,3-dihalogeno-1-propanols or 1,3-dihalogeno-2-propanols took place also on the terminal carbon atoms. This is proved by the NMR spectra: the proton of the hydroxyl group appears as a doublet (and not as a triplet) in the NMR spectrum of the solution of the product (**3a**—**c**) in DMSO-d_6.

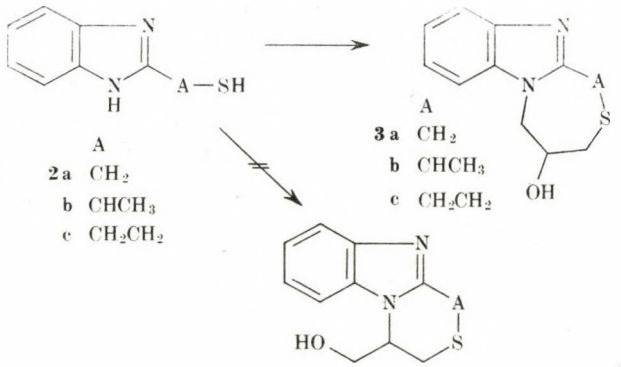

The hydroxyl group of the tricyclic compounds can be acylated to **4**, **6a**—**c** and sulfonated to **5**, **7a**—**c** (Tables I and II).

The sulfonic esters of type **5** are converted by an elimination reaction in aqueous ethanolic medium containing an alkali hydroxide, or with alkoxides (NaOEt, $KOBu^t$) in anhydrous media, into products of the type **8a** and **8b**.

Compound **8a** was formed in a fair yield (75 %) when the sulfonic ester (*e.g.* **5d**) was heated in pyridine while the formation of **8b** was detected in less

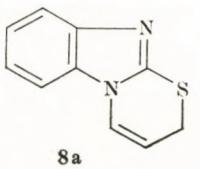
8a

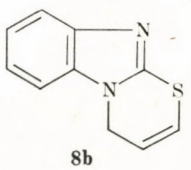
8b

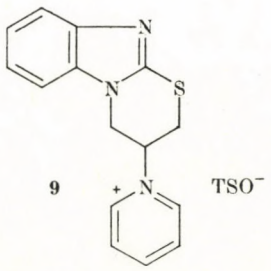

than 5—8 % only. This reaction takes place through an isolable intermediate: the pyridinium salt (**9**). On the effect of the highly nucleophilic sodium benzoate in dimethylformamide, the sulfonic ester undergoes elimination and

Table II

O-Sulfonyl compounds of **1** *and* **3a – c**

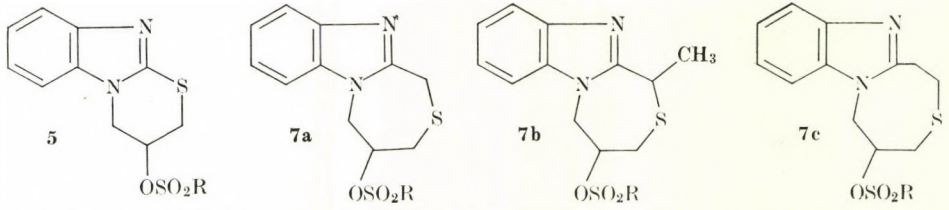

No.	R	M.p., °C	Formula (Mol. wt.)	Analysis, % C	H	N	S	NMR (ppm, δTMS=0 ppm)
				calcd./found				
5a	CH_3	173 – 174	$C_{11}H_{12}N_2O_3S_2$ (284.36)	46.46 46.48	4.25 4.19	9.85 9.92	22.55 22.31	3.3 (s, 3H, CH_3); 3.95 (m, 2H, SCH_2); 4.75 – 5.0 (m, 2H, NCH_2); 6.0 (m, 1H, CH); 7.72 (s, 4H, Ar = CH) (TFA)
5b	C_6H_5	148 – 150	$C_{16}H_{14}N_2O_3S_2$ (346.43)	55.47 55.28	4.07 4.25	8.09 7.84	18.51 18.69	3.30 (d, 2H, SCH_2); 4.19 (d, 2H, NCH_2); 5.36 (m, 1H, CH); 7.1 – 8.1 (compl. 9H, Ar = CH) ($CDCl_3$)
5c	4-BrC_6H_4	166 – 167	$C_{16}H_{13}BrN_2O_3S_2$ (425.33)	45.18 44.96	3.08 3.23	6.59 6.29	15.08 15.28	3.38 (d, 2H, SCH_2); 4.28 (d, 2H, NCH_2); 5.4 (m, 1H, CH); 7.3 (s, 4H, Ar = CH); 7.72 (s, 4H, Ar = CH) ($CDCl_3$)
5d	4-$CH_3C_6H_4$	189 – 191	$C_{17}H_{16}N_2O_3S_2$ (360.45)	56.65 56.68	4.47 4.57	7.77 7.76	17.79 17.88	2.5 (s, 3H, CH_3); 3.35 (d, 2H, SCH_2); 4.25 (d, 2H NCH_2); 5.2 – 5.45 (m, 1H, CH); 7.15 – 7.9 (compl. 8H, Ar = CH) ($CDCl_3$)
7a	CH_3	175 – 195[d]	$C_{12}H_{14}N_2O_3S_2$ (298.38)	48.31 48.21	4.73 4.54	9.38 9.42	21.49 21.67	3.0 (s, 3H, SO_2CH_3); 3.1 (d, 2H, SCH_2); 4.08 (s, 2H, $=CCH_2S$); 4.55 (d, 2H, NCH_2); 4.9 – 5.3 (m, 1H, CH); 7.2 – 7.9 (compl. 4H, Ar = CH) ($CDCl_3$)
7b	CH_3	202 – 204[d]	$C_{13}H_{16}N_2O_3S_2$ (312.41)	49.98 50.02	5.16 4.93	8.97 9.12	20.53 20.50	1.99 (dd, 3H, CH_3); 2.9 (s, 3H, SO_2CH_3); 2.7 – 3.2, (m, 2H, SCH_2); 4.0 – 5.5 (m, 4H, NCH_2CH, $CHCH_3$); 7.2 – 8.0 (compl. 4H, Ar = CH) ($CDCl_3$)
7c	CH_3	230 – 233[d]	$C_{13}H_{16}N_2O_3S_2$ (312.41)	49.98 50.15	5.16 5.25	8.97 8.73	20.53 20.39	3.1 (s, 3H, SO_2CH_3); 2.3 – 3.6 (m, 6H, $CH_2CH_2SCH_2$); 4.8 (d, 2H); 5.0 – 5.4 (m, 1H, CH); 7.2 – 7.9 (compl. 4H, Ar = CH) ($CDCl_3$)

[d] decomposition point

substitution. In the course of elimination **8b** is formed highly regioselectively (only 10 % of **8a** is obtained).

The esters **5** react readily with other nucleophilic reagents affording the corresponding substituted products (**10**).

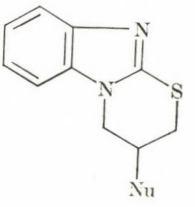

	Nu
10a	SH
b	SPh
c	SCN
d	N_3

The azido group of **10d** is reduced by sodium borohydride in 2-propanol to primary amine (**11a**). This primary amine can be converted with aldehydes, through the formation of Schiff bases into secondary amines, with acid chlorides or acid anhydrides into acid amides, whereas with 2-methyl-2-thiopseudourea sulfate into a guanidine derivative.

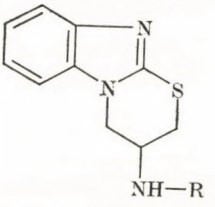

	R
11a	H
b	4-$ClC_6H_4CH_2$
c	CH_3CO
d	$C_6H_5CH{=}CHCO$
e	$C(=NH)NH_2$

We investigated also the products **12, 13** obtained in dipolar cycloaddition reactions of compound **10d** with various asymmetrically substituted acetylenes (Table III).

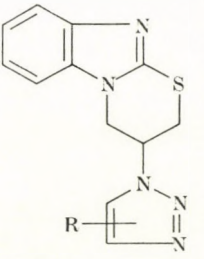

12 (4-R)
13 (5-R)

It was found that, in accordance with experiences of HUISGEN *et al.* [4, 5], in the examples chosen only the acetylene substituted with the strongly electron-attracting acetyl group exhibited regiospecificity. With acetylenes substituted by other groups, even by bulky substituents, both isomers were formed, similarly to the formation of **14a** and **14b** in the reaction between phenylacetylene and benzylazide [6].

Table III

2,3-Dihydro-3-(1,2,3-triazin-1-yl)-[1,3]thiazino-4H-[3,2-a]benzimidazoles **(12 – 13)**

No.	R	M.p., °C	Yield, %	Formula (Mol. wt.)	Analysis, %				NMR (ppm, δTMS=O ppm) in DMSO-d_6
					C	H	N	S	
					calcd./found				
12a	C_6H_5	240 – 241	27	$C_{18}H_{15}N_5S$ (333.42)	64.84 64.89	4.54 4.25	21.00 20.87	9.62 9.73	3.98 (d, 2H, SCH_2); 4.8 – 5.1 (m, 2H, NCH_2); 5.5 – 5.9 (m, 1H, CH); 7.1 – 8.0 (compl.9H, Ar = CH); 8.84 (s, 1H, N(CH =))
13a		178 – 180	43		64.84 64.79	4.54 4.34	21.00 21.32	9.62 9.42	3.0 – 5.5 (m, 5H, CH_2CHCH_2); 7.2 – 7.8 (compl. 9H, Ar = CH); 7.84 (s, 1H, N(CH =))
12b	$CH_2N(CH_3)_2$	163 – 165	49	$C_{15}H_{18}N_6S$ (314.42)	57.30 57.37	5.77 5.30	26.73 26.77	10.20 10.26	2.14 (s, 6H, $2CH_3$); 3.9 (d, 2H, SCH_2); 4.85 (m, 2H, NCH_2); 5.7 (m, 1H, CH);7.1 – 7.8 (compl. 4H, Ar = CH); 8.18 (s, 1H, N(CH =))
13b		237 – 238	33		57.30 57.28	5.77 5.96	26.73 26.85	10.20 10.32	2.16 (s, 6H, $2CH_3$); 3.62 (d, 2H, SCH_2); 4.73 (d, 2H, NCH_2); 5.4 – 5.8 (m, 1H, CH); 7.1 – 7.7 (compl. 4H, Ar = CH); 7.74 (s, 1H, N(CH =))
12c	$C(OH)(CH_3)_2$	226 – 227	81	$C_{15}H_{17}N_5OS$ (315.40)	57.12 57.00	5.43 5.09	22.20 22.15	10.16 10.32	1.46 (s, 6H, $2CH_3$); 3.95 (d, 2H, SCH_2); 4.8 (d, 2H, NCH_2); 5.7 (m, 1H, CH); 7.1 – 7.7 (compl. 4H, Ar = CH); 8.13 (s, 1H, N(CH =))
13c		185 – 186	14		57.12 57.09	5.43 5.40	22.20 22.48	10.16 10.26	1.60 (s, 6H, $2CH_3$); 3.9 (d, 2H, SCH_2); 4.8 (d, 2H, NCH_2); 5.65 (m, 1H, CH); 7.1 – 7.7 (compl. 4H, Ar = CH); 7.7 (s, 1H, N(CH =))
12d	$C(NH_2)(CH_3)_2$	193 – 195	47	$C_{15}H_{18}N_6S$ (314.42)	57.30 57.44	5.77 5.49	26.73 26.56	10.20 10.36	1.4 (s, 6H, $2CH_3$); 3.85 (d, 2H, SCH_2); 4.8 (d, 2H, NCH_2); 5.62 (m, 1H, CH); 7.1 – 7.7 (compl. 4H, Ar = CH); 8.36 (s, 1H, N(CH =))
13d		163 – 167	11		57.30 57.40	5.77 5.95	26.73 26.96	10.20 10.26	1.4 (s, 6H, $2CH_3$); 3.87 (d, 2H, SCH_2); 4.85 (d, 2H,NCH_2); 5.62 (m, 1H, CH); 7.1 – 7.7 (compl. 4H, Ar = CH); 8.15 (s, 1H, N(CH =))
12e	$C(NH_2)(C_2H_5)_2$	184 – 185	33	$C_{17}H_{22}N_6S$ (342.47)	59.62 59.15	6.48 6.46	24.54 24.66	9.36 9.49	0.69 (t, 6H, $2CH_3$); 1.6 (q, 4H, $C(CH_2)_2$); 3.82 (d, 2H, SCH_2); 4.8 (dd, 2H, NCH_2); 5.65 (m, 1H, CH); 7.1 – 7.7 (compl. 4H, Ar = CH); 8.12 (s, 1H, N(CH =))
13e		155 – 158	27		59.62 59.24 –	6.48 6.29	24.54 24.31	9.36 9.43	0.70 (t, 6H, $2CH_3$); 1.62 (q, 4H, $C(CH_2)_2$); 3.9 (d, 2H, SCH_2); 4.85 (m, 2H, NCH_2); 5.65 (m, 1H, CH); 7.1 – 7.7 (compl. 4H, Ar = CH); 7.62 (s, 1H, N(CH =))
12f	$COCH_3$	219 – 220	95	$C_{14}H_{13}N_5OS$ (299.35)	56.17 56.06	4.38 4.48	23.39 23.29	10.71 10.95	2.45 (s, 3H, CH_3); 3.98 (d, 2H, SCH_2); 4.7 – 5.1 (m, 2H, NCH_2); 5.6 – 6.0 (m, 1H, CH); 7.1 – 7.7 (compl. 4H, Ar = CH); 9.0 (s, 1H, N(CH =))

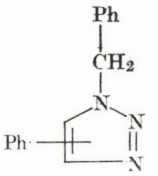

14a (4-Ph)
b (5-Ph)

In the NMR spectra of **14a** and **14b** (in DMSO-d_6) the sign of the triazole proton is at δ4CH = 8.0 and δ5CH = 8.7 ppm, respectively.

An investigation of the NMR spectra of compounds **12–13** has shown that the regularity δ4CH < δ5CH is valid also in this case.

Experimental

M.p.'s were determined with a Büchi instrument of type SMP – 20 and are uncorrected. IR spectra were recorded in a Specord 71 (Zeiss) spectrophotometer. NMR spectra were obtained with a Perkin – Elmer R – 12 instrument, using TMS as internal standard.

4,5-Dihydro-4-hydroxy-1*H*,3*H*-[1,4]thiazepino[4,3-a]benzimidazole (3a)

Method A

Sodium hydroxide (0.4 mole; 16.0 g) dissolved in water (about 40 ml) was added, with stirring, to a suspension of 2-mercaptomethylbenzimidazole (0.4 mole; 65.6 g) in ethanol (400 ml); the solid dissolved in the alkaline medium. Epichlorohydrin (0.4 mole; 37.0 g) was dropwise added with stirring, to the solution which was kept below 40 °C. Precpitation of a white crystalline solid started shortly. After allowing the mixture to stand for 3 hrs, it was filtered, and the crystals were washed with water to remove the inorganic salt, then with ethanol and ether, and dried to obtain 61.7 g (70 %) of the product, m.p. 231 – 233 °C (recrystallized from pyridine).

$C_{11}H_{12}N_2OS$ (220.29). Calcd. C 59.97; H 5.49; N 12.72; S 14.55. Found C 60.34; H 5.47; N 12.76; S 14.20 %.

IR (Nujol) ν_{max} = 3120 – 3070 (OH) cm^{-1}.

^{1}H-NMR (DMSO-d_6): δ = 3.03 (m, 2H, SCH_2); 3.6 – 4.1 (m, 1H, CH); 4.37 (m, 2H, NCH_2); 4.58 (d, 2H, SCH_2C=); 5.5 (d, 1H, OH, J = 4 Hz); 7.1 – 7.8 (compl., 4H, Ar = CH) ppm.

The following compounds were also prepared in the way specified above.

3,4-Dihydro-3-hydroxy-2*H*-[1,3]thiazino[3,2-a]benzimidazole (1)

3,4-Dihydro-3-hydroxy-2*H*-[1,3]thiazino[3,2-a]benzimidazole (**1**): Yield 70 %, m.p. 214 – 215 °C (lit. m.p. [1] 214 – 215 °C).

$C_{10}H_{10}N_2OS$ (206.26). Calcd. C 58.23; H 4.89; N 13.58; S 15.54. Found C 58.33; H 5.21; N 13.42; S 15.22 %.

IR (Nujol) ν_{max} = 3200 – 2800 (OH) cm^{-1}.

^{1}H-NMR (DMSO-d_6): δ = 3.3 (m, 2H, SCH_2); 4.20 (m, 2H, NCH_2); 4.3 – 4.8 (m, 1H, CH); 5.77 (d, 1H, OH, J = 4 Hz); 7.1 – 7.6 (compl., 4H, Ar = CH) ppm.

4,5-Dihydro-1-methyl-4-hydroxy-1*H*,3*H*-[1,4]thiazepino[4,3-a]benzimidazole (3b)*:

4,5-Dihydro-1-methyl-4-hydroxy-1*H*,3*H*-[1, 4]thiazepino[4,3-a]benzimidazole (**3b**):* Yield 55 %, m.p. 235 – 238 °C (from pyridine).

$C_{12}H_{14}N_2OS$ (234.32). Calcd. C 61.51; H 6.02; N 11.96; S 13.68. Found C 61.72; H 5.68; N 11.84; S 13.45 %.

* Isomers are possible because of chirality of the 1- and 4-carbon atoms. Existence of diastereomers are supported by two dublets for the hydroxyl proton at δ 4.98 and 5.68 ppm (for both isomers J = 4 Hz).

IR (Nujol) ν_{max} = 3400 – 2800 (OH) cm^{-1}.

^{1}H-NMR (DMSO-d_6): δ = 1.68 (d, 3H, CH_3); 2.4 – 2.7 (m, 2H, SCH_2); 3.3 – 4.7 (m, 2H, CH, CH); 4.4 (m, 2H, NCH_2); 4.98 d, 5.68 d (1H, OH); 7.1 – 7.8 (compl., 4H, Ar = CH) ppm.

1,2,5,6-Tetrahydro-5-hydroxy-4*H*-[1,5]thiazocino[5,4-a]benzimidazole (3c):

1,2,5,6-Tetrahydro-5-hydroxy-4*H*-[1,5]thiazocino[5,4-a]benzimidazole (**3c**): Yield 57 %, m.p. 276 – 277 °C (from pyridine).

$C_{12}H_{14}N_2OS$ (234.32). Calcd. C 61.51; H 6.02; N 11.96; S 13.68. Found C 61.88; H 5.78; N 11.77; S 13.48 %.

IR (Nujol) ν_{max} = 3120 – 3070 (OH) cm^{-1}.

^{1}H-NMR (DMSO-d_6): δ = 2.2 – 2.5 (m, 2H, SCH_2); 2.8 – 3.4 (m, 4H, SCH_2CH_2); 3.9 – 4.4 (m, 1H, CH); 4.5 (d, 2H, NCH_2); 5.4 (d, 1H, OH); 7.1 – 7.8 (compl., 4H Ar = CH) ppm.

Method B

Under the same reaction conditions as those applied in method A, two equivalents of potassium hydroxide were used instead of one equivalent, and dihalogenopropanol instead of epichlorohydrine. The reaction products obtained were identical in every respect with the corresponding products afforded by method A.

The yields were as follows: **1** 72 % from 1,3-dibromo-2-propanol; **3a** 62 % from 1,2-dibromo-3-propanol; **3b** 50 % from 1-chloro-3-bromo-2-propanol, **3c** 68 % from 2,3-dibromo-1-propanol.

The O-acyl and O-sulfonyl derivatives of **1** and **3a – c** were prepared by the usual routes and are listed in Tables I – II.

Reaction of sulfonates of type 5 with some nucleophilic agents*

(a) *With ethanolic sodium hydroxide*

A solution of 2,3-dihydro-3-(*p*-toluenesulfonyloxy-2*H*-[1,3]thiazino[3,2-a]benzimidazole **(5d)** (0.04 mole; 14.4 g) in ethanol (150 ml) was refluxed for 3 hrs, with stirring, with an aqueous solution (of about 5 ml) of sodium hydroxide (0.1 mole; 4 g). The solution was then evaporated, the residue diluted with water (100 ml) and extracted with chloroform (3 × 30 ml). The chloroform phase was washed with water (2 × 30 ml), dried over sodium sulfate and evaporated in vacuum. The solid residue was crystallized from ethanol. The product was a mixture of the isomers **2*H*-[1,3]thiazino[3,2-a]benzimidazole (8a)** and **4*H*-[1,3]thiazino[3,2-a]benzimidazole (8b)****. Yield 6.7 g (89 %), m.p. 136 – 137 °C.

Mass spectrum: m/e = 188 (M^+).

$C_{10}H_8N_2S$ (188.25). Calcd. C 63.80; H 4.28; N 14.88; S 17.03. Found C 63.75; H 4.10; N 15.14; S 16.41 %.

IR (KBr) ν_{max} = 1660 (C = C isolated) cm^{-1}.

^{1}H-NMR ($CDCl_3$): δ = 3.65 (q, 2H, SCH_2), 7.10 (d, NCH =); 4.80 (q, 2H, NCH_2); 6.20 (d, SCH =); 7.2 – 7.8 (compl., 4H, Ar = CH) ppm.

(b) *With sodium ethoxide*

Sodium ethoxide (0.02 mole; 1.36 g) was added to a solution of **5d** (0.01 mole; 3.6 g) in anhydrous ethanol and the mixture was boiled for 6 hrs, then processed as under (a). The product was a 1 : 1 mixture of the isomers **8a** and **8b**. Yield 1.5 g (80 %), m.p. 135 – 139 °C.

(c) *With potassium t-butoxide*

On boiling **5d** (0.01 mole; 3.6 g) with potassium *t*-butoxide (0.02 mole; 2.06 g) in *t*-butanol for 6 hrs, and processing the system as under (a), a 1 : 1 mixture of isomers **8a** and **8b** was obtained. Yield 1.6 g (85 %), m.p. 136 – 139 °C.

* Reaction of the sulfonates **6a – c** will be published in subsequent papers of this series.

** In gas chromatography the two isomers appear in a ratio of about 1 : 1. (GLC conditions were: 3 % SE – 30 column on Q 100 – 200 mesh; column temperature 200 °C; detected by flame ionization; N_2 carrier gas, 80 ml/min 29psi; Packard 7300 Gas Chromatograph.)

(d_1) *With pyridine (5 hours)*

The tosylate (**5d**) (0.01 mole; 3.6 g) was boiled in pyridine (15 ml) for 5 hrs, then the excess of pyridine was evaporated in vacuum and the residue crystallized from ethanol. The product was **3,4-dihydro-3-(1-pyridyl-)2H-[1,3]thiazino[3,2-a]benzimidazolium tosylate (9).** The yield was almost quantitative, m.p. 187 – 188 °C.

$C_{22}H_{21}N_3O_3S_2$ (439.56). Calcd. C 60.12; H 4.81; N. 9.56; S 14.59. Found C 60.51; H. 4.77; N 9.59; S 13.94 %.

^{1}H-NMR (D_2O): δ = 2.02 (s, 3H, CH_3); 4.0 – 4.3 (m, 2H, SCH_2); 4.5 – 5.2 (m, 3H, NCH_2CH); 6.8 – 8.9 (compl., 13H, Ar = CH) ppm.

On treating the ethanolic solution of **9** with ethanol saturated with hydrochloric acid, **3,4-dihydro-3-(1-pyridyl)-2*H*-[1,3]thiazino[3,2-a]benzimidazolium chloride,** m.p. 218 – 220 °C precipitated from the solution on cooling.

$C_{15}H_{15}Cl_2N_3S$ (340.28). Calcd. N 12.35; Cl 20.84; S 9.42. Found N 11.95; Cl 20.54; S 9.17 %.

^{1}H-NMR (D_2O): δ = 4.45 (d, 2H, SCH_2); 5.2 – 5.6 (m, 3H, NCH_2CH); 7.5 – 7.9 (compl., 4H, Ar = CH); 8.0 – 9.2 (compl., 5H, Py = CH) ppm.

(d_2) *With pyridine (50 hours)*

The tosylate (**5d**) (0.01 mole) was boiled for 50 hrs in pyridine (15 ml). The solvent was evaporated and the residue extracted with chloroform; the chloroform phase was dried over sodium sulphate and the solvent evaporated. The residual oil was crystallized from ethanol to yield 1.4 g (75 %) of the product: **2*H*-[1,3]thiazino[3,2-a]benzimidazole (8a),** m.p. 143 – 145 °C. According to gas chromatographic analysis and the NMR spectrum, the product was homogeneous consisting of the pure enamine isomer **8a.**

In repeated experiments, analysis of the crude product by GLC or NMR sometimes showed the presence of **8b** in less than 5 – 8 %.

The reaction was also carried with other sulfonates (**5a, b, c**) leading to **8a** which also contained a little (< 12 %) **8b** (detected by NMR).

$C_{10}H_8N_2S$ (188.25). Calcd. C 63.80; H 4.28; N 14.88; S 17.03. Found C 63.76; H 4.12; N 14.93; S 17.26 %.

IR (Nujol) ν_{max} 1660 (s) (NCH = CH) cm^{-1}.

^{1}H-NMR ($CDCl_3$): δ = 3.65 (q, 2H, SCH_2); 5.6 (q, 1H, $CH_2CH=$, J_{CH_2CH} 6 Hz); 7.1 (d, 1H, NCH =, $J_{CH=CH}$ 9 Hz); 7.2 – 7.8 (compl., 4H, Ar = CH) ppm.

(e) *With sodium benzoate*

The mesylate (**5a**) (0.01 mole; 2.84 g) was heated in dimethylformamide (20 ml) with sodium benzoate (0.11 mole; 1.6 g) for 4 hrs at 100 °C, and the solvent was then evaporated. The residue was diluted with water (30 ml), extracted with chloroform (3 × 10 ml), the chloroform phase dried and evaporated in vacuum. The residual pale yellow oil was dissolved in some ether (about 10 ml) and kept in a refrigerator. The precipitated white crystalline product was **4*H*-[1,3]thiazino[3,2-a]benzimidazole (8b)** (0.75 g; 40 %), m.p. 129 – 131 °C. After the elapse of a few hours further amounts separated from the mother liquor (0.20 g; 10 %). On the basis of the NMR spectrum this material was a 1 : 4 mixture of **8a** and **8b.**

Analysis of pure **8b**: $C_{10}H_8N_2S$ (188.25). Calcd. C 63.80; H 4.28; N 14.88; S 17.03. Found C 63.76; H 4.32; N 14.82; S 17.17 %.

^{1}H-NMR ($CDCl_3$): δ = 4.72 (q, 2H, NCH_2); 6.04 (q, 1H, $CH_2CH=$, $J_{CH_2CH=}$ 4 Hz); 6.14 (d, 1H, SCH =, $J_{CH=CH}$ 13 Hz); 7.1 – 7.8 (compl., 4H, Ar = CH) ppm.

The mother liquor was evaporated to half of its original volume, and the residue allowed to stand for 2 days in a refrigerator. The resulting white crystalline substance was filtered off. On the basis of the IR and NMR spectra it proved to be **3-benzoyloxy-2,3-dihydro-2*H*-[1,3]-thiazino[3,2-a]benzimidazole (4g)** (1.0 g; 34 %), m.p. 165 – 167 °C.

The reaction carried out from **5d** gave essentially the same results in respect of both the ratios and yiels of the products.

No **8a** $\rightleftharpoons$ **8b** isomerisation was observed when the pure isomer (**8a** or **8b**) was heated in several solvents (pyridine, EtOH, aqueous EtOH, or $CHCl_3$) for 24 hrs.

(f) *With sodium hydrogen sulfide*

A suspension of the mesylate (**5a**) (0.01 mole; 2.84 g) in methanol (50 ml) was boiled for a day with sodium hydrogen sulfide hydrate ($9H_2O$) (0.02 mole; 4.36 g). The yellow solution was evaporated in vacuum and the residue was crystallized from ethanol. The product was

3-mercapto-2,3-dihydro-2*H*-[1,3]thiazino[3,2-a]benzimidazole (10a). Yield 1.5 g (68 %), m.p. 196 – 198 °C (d.).

$C_{10}H_{10}N_2S_2$ (222.33). Calcd. N 12.60; S 28.85. Found N 12.32; S 28.35 %.

(g) *With thiophenol*

To a suspension of the benzenesulfonate (**5b**) (0.01 mole; 3.46 g) in anhydrous ethanol (50 ml), sodium ethoxide (0.015 mole; 1.02 g) and thiophenol (0.015 mole; 1.65 g) were added. After boiling for 34 hrs, the reaction mixture was evaporated to dryness and the residue extracted with chloroform (3×30 ml). The oily residue of the chloroform solution was dissolved in ethanol saturated with hydrochloric acid, and diluted with ether. On cooling the mixture, the monohydrochloride of the product: **3,4-dihydro-3-(phenylthio)-2*H*-[1,3]thiazino[3,2-a]benzimidazole (10b)** crystallized in a few days. Yield 2.26 g (76 %), m.p. 105 – 107 °C.

$C_{16}H_{14}N_2S_2$.HCl (334.89). Calcd. C 57.38; H 4.67; N 8.36; S 19.14; Cl 10.58. Found C 57.25; H 4.67; N 8.21; S 19.04; Cl 10.62 %.

^{1}H-NMR (CD_3OD): δ = 3.04 – 4.2 (m, 5H, CH_2CHCH_2); 6.8 – 7.6 (Compl., 9H, Ar=CH) ppm.

(h) *With sodium thiocyanate*

To a suspension of the tosylate (**5d**) (0.05 mole; 18.2 g) in ethanol (150 ml), an aqueous solution (30 ml) of sodium thiocyanate (0.075 mole; 6.07 g) was added, and the mixture was boiled for 60 hrs, then evaporated to dryness in vacuum and the residue extracted with chloroform (3×60 ml). The chloroform phase was dried, evaporated to dryness in vacuum and the residue crystallized from ethanol. The product was **3,4-dihydro-3-thiocyanato-2*H*-[1,3]thiazino[3,2-a]benzimidazole (10c)**, a white crystalline substance. Yield 9.9 g (80 %), m.p. 132 – 138 °C.

$C_{11}H_9N_3S_2$ (247.35). Calcd. C 53.41; H 3.67; N 16.99; S 25.93 %. Found C 53.67; H 3.92; N 16.95; S 25.88 %.

IR (Nujol) ν_{max} = 2175 (SCN) cm^{-1}.

^{1}H-NMR [$(CD_3)_2CO$: CD_3OD, 1 : 1]: δ = 3.66 (d, 2H, SCH_2); 4.62 (d, 2H, NCH_2); 4.7 – 5.2 (m, 1H, CH); 7.0 – 7.8 (compl., 4H, Ar=CH) ppm.

On acidifying the ethanolic solution of the base to pH 3 with ethanol saturated with hydrochloric acid and diluting it with ether until crystallization started, the hydrochloride of the product precipitated, m.p. 173 – 176 °C (d.).

$C_{11}H_9N_3S_2$.HCl (283.81). Calcd. C 46.55; H 3.55; N 14.81; S 22.60; Cl 12.49. Found C 46.58; H 3.48; N 15.05; S 22.25; Cl 12.20 %.

(i) *With sodium azide*

A suspension of the tosylate (**5d**) (0.05 mole; 18.2 g) in dimethylformamide (50 ml) was boiled for 70 hrs with an aqueous solution (8 ml) of sodium azide (0.1 mole; 6.5 g) under a stream of nitrogen gas. The solution was evaporated, the residue dissolved in some ethanol (10 ml), diluted with ether and allowed to crystallize in a refrigerator. The precipitated product was **3,4-dihydro-3-azido-2*H*-[1,3]thiazino[3,2-a]benzimidazole (10d)** (7.0 g; 60 %), m.p. 123 – 127 °C.

$C_{10}H_9N_5S$ (231.28). Calcd. C 51.93; H 3.92; N 30.28; S 13.86. Found C 52.12; H 4.13; N 29.92; S 14.15 %.

IR (Nujol) ν_{max} = 2110 (N_3) cm^{-1}.

^{1}H-NMR ($CDCl_3$): δ = 3.2 – 4.6 (m, 5H, CH_2CHCH_2); 7.1 – 7.9 (compl., 4H, Ar=CH) ppm.

The acetone solution of base **10d** was acidified to pH 3 with ethanol saturated with hydrochloric acid and it was diluted with ether until crystallization started. The precipitated white crystals were filtered off, washed with acetone and dried to afford the hydrochloride of the product, m.p. 207 – 208 °C (d.).

$C_{10}H_9N_5S$.HCl (267.74). Calcd. C 44.86; H 3.76; N 26.16; S 11.98; Cl 13.24. Found C 44.66; H 3.64; N 25.92; S 12.08; Cl 13.40 %.

IR (Nujol) ν_{max} = 2090 (N_3) cm^{-1}.

Reduction of the azido compound 10d

The azido compound (**10d**) (0.1 mole; 23.13 g) was suspended in isopropanol (200 ml), sodium borohydride (12 g) was added, and the mixture boiled for 30 hrs. After evaporating the solvent in vacuum, the residue was diluted with water to decompose the complex, then

extracted with chloroform (3×10 ml). The extract was dried over anhydrous sodium sulfate and evaporated. The residue was crystallized from a mixture of ethanol and ether. The precipitated white crystalline product was **3,4-dihydro-3-amino-2*H*-[1,3]thiazino[3,2-a]benzimidazole (11a)** (15.4 g; 75 %), m.p. 115–118 °C.

$C_{10}H_{11}N_3S$ (205.28). Calcd. C 58.51; H 5.40; N 20.47; S 15.62. Found C 58.32; H 5.13; N 20.42; S 15.33 %.

IR (Nujol) ν_{max} = 3360, 3320 (NH_2) cm^{-1}.

^{1}H-NMR ($CDCl_3$): δ = 1.8 (s, 2H, NH_2); 3.07 (d, 2H, SCH_2); 3.5–4.3 (m, 3H, NCH_2CH); 7.0–7.8 (compl., 4H, Ar=CH) ppm.

The base (**11a**) was dissolved in methanol saturated with hydrochloric acid and diluted with ether until crystallization started. The white crystalline product was filtered off, washed with ether and dried to obtain the dihydrochloride of **11a**, m.p. 235–238 °C (d.).

$C_{10}H_{11}N_3S$ .2HCl (278.21). Calcd. C 43.17; H 4.71; N 15.10; S 11.53; Cl 25.49. Found C 43.15; H 4.00; N 15.09; S 11.43; Cl 25.54 %.

IR (Nujol) ν_{max} = 3400–2600 (NH_3) cm^{-1}.

Reactions of the amino compound 11a

(a) *p-Chlorobenzaldehyde*

A solution of the amino compound (**11a**) (0.02 mole; 4.1 g) and of *p*-chlorobenzaldehyde (0.02 mole; 2.81 g) in toluene (100 ml) was boiled for 3 hrs in the presence of catalytic amounts (2 drops) of boron trifluoride etherate, in an apparatus equipped with a Dean–Stark trap. During this period the theoretical amount of water (0.36 ml; 0.02 mole) accumulated in the water separator. The solution was concentrated to one quarter of its initial volume, and cooled. The precipitated crystals were filtered off, washed with ether until free of toluene, and dried. The product was **3,4-dihydro-3-[(4'-chlorobenzylidene)-amino]-2*H*—[1,3]thiazino[3,2-a]benzimidaziole** (5.2 g; 80 %), m.p. 174–176 °C.

$C_{17}H_{14}ClN_3S$ (327.84). Calcd. C 68.28; H 4.30; N 12.82; Cl 10.82 %. Found C 61.98; H 4.02; N 12.66; Cl 10.51 %.

IR (Nujol) ν_{max} = 1625, 1575 (N=CH conj.).

^{1}H–NMR (DMSO-d_6): δ = 3.45 (m, 2H, SCH_2); 4.1–4.6 (m, 3H, NCH_2CH); 7.1–8.0 (compl., 8H, Ar=CH); 8.74 (s, 1H, N=CH) ppm.

The Schiff base obtained as described above (0.02 mole; 6.6 g) was dissolved in ethanol (30 ml) and boiled for 3 hrs. with sodium borohydride (1 g). After decomposing the complex with water (15 ml), the mixture was extracted with chloroform, dried and evaporated. The residue was crystallized from a mixture of ethanol and ether. The product was **3,4-dihydro-3-[(4'-chlorobenzyl)amino]-2*H*-[1,3]thiazino[3,2-a]benzimidazole (11b)** in almost theoretical yield, m.p. 150–152 °C.

$C_{17}H_{16}ClN_3S$ (329.86). Calcd. C 61.90; H 4.89; N 12.74; S 9.72; Cl 10.75. Found C 62.13; H 4.88; N 12.78; S 9.60; Cl 10.61 %.

IR (Nujol) ν_{max} = 3300 (NH) cm^{-1}.

^{1}H-NMR ($CDCl_3$): δ = 3.0–3.7 (m, 3H, SCH_2CH); 3.84 (s, 2H, NCH_2); 4.02 (d, 2H, NCH_2); 7.1–7.4 (compl., 8H, Ar=CH); 7.45–7.8 (m, 1H, NH) ppm.

The acetone solution of the base (**11b**) was acidified with methanol saturated with hydrochloric acid, it was then diluted with some ether, the precipitated white crystalline salt filtered off, washed with ether and dried. The dihydrochloride thus obtained had m.p. 218–220 °C (d.).

$C_{17}H_{16}ClN_3S$ .2HCl (402.77). Calcd. C 50.70; H 4.50; N 10.43; S 7.96; Cl 26.41. Found C 51.06; H 4.60; N 10.07; S 7.60; Cl 26.50 %.

IR (Nujol) ν_{max} = 3100–2200 ($\overset{+}{N}H_2$) cm^{-1}.

(b) *With acetic anhydride*

The amino compound (**11a**) (0.05 mole; 10.25 g) was dissolved in hot pyridine (40 ml), acetic anhydride (7 ml) was added and the mixture was allowed to stand for 3 hrs. The solution was poured into ice (about 300 g). The precipitated white crystals were filtered off, washed with ethanol and ether, then dried. The product was **3,4-dihydro-3-acetamido-2*H*-[1,3]-thiazino[3,2-a]benzimidazole (11c)** (11.2 g; 90 %), m.p. 179–181 °C. On recrystallizing the crude product from ethanol its m.p. did not change.

$C_{12}H_{13}N_3OS$ (247.32). Calcd. C 58.28; H 5.30; N 16.99; S 12.96. Found C 58.11; H 5.60; N 16.80; S 13.06 %.

IR (Nujol) ν_{max} = 3430 – 3080 (NH), 1665, 1560 (CONH) cm^{-1}.

^{1}H-NMR (DMSO-d_6): δ = 1.98 (s, 3H, CH_3); 3.3 – 4.8 (m, 5H, CH_2CHCH_2); 7.1 – 7.7 (compl., Ar = CH); 8.5 (d, 1H, NH) ppm.

The acetone solution of the base was acidified to pH 3 with ethanol saturated with hydrochloric acid and diluted with ether until crystallization started. The white crystals were filtered off, washed with ether and dried to obtain the monohydrochloride of **11c**, m.p. above 245 °C.

$C_{12}H_{13}N_3OS$ .HCl (283.78). Calcd. C 50.79; H 4.97; N 14.81; S 11.30; Cl 12.49. Found C 51.13; H 4.21; N 14.44; S 11.09; Cl 12.23 %.

IR (Nujol) ν_{max} = 3220 – 3020 (NH), 1605, 1540 (CONH) cm^{-1}.

(c) *With cinnamoyl chloride*

The amino compound (**11a**) (0.01 mole; 2.05 g) was dissolved in pyridine (20 ml) and allowed to stand with cinnamoyl chloride (0.011 mole; 1.83 g) for 3 hrs at room temperature, then poured into crushed ice (about 100 g). The resulting white crystalline substance was filtered off, washed with water, ethanol and ether, then recrystallized from ethanol. The product was **3,4-dihydro-3-(cinnamoylamino)-2*H*-[1,3]thiazino[3,2-a]benzimidazole (11d)** (2.7 g; 80 %), m.p. 214 – 216 °C.

$C_{19}H_{17}N_3OS$ (335.43). Calcd. C 68.03; H 5.11; N 12.53; S 9.56. Found C 67.87; H 5.06; N 12.78; S 9.17 %.

^{1}H-NMR (DMSO-d_6): δ = 3.5 (m, 2H, SCH_2); 4.2 – 4.4 (m, 2H, NCH_2); 4.5 – 5.0 (m, 1H, CH); 6.76 (d, 1H, CH = CH, J 16 Hz); 7.1 – 7.8 (compl., 10H, CH = C*H*, Ar = CH); 8.6 – 8.8 (m, 1H, NH) ppm.

(d) *With 2-methyl-2-thiopseudourea sulfate*

The amino compound (**11a**) (0.02 mole; 4.1 g) and S-methyl-isothiocarbamide sulfate (0.01 mole; 2.78 g) were heated in aqueous ethanol (30 ml, 70 %) in a flask equipped with a reflux condenser and gas outlet tube for 10 hrs. When the evolution of methyl mercaptan ceased, the solution was evaporated in vacuum, then the residue was diluted with ethanol and crystallized. The white crystalline substance was filtered off and washed with ether. The product was **3,4-dihydro-3-guanyl-2*H*-[1,3]thiazino[3,2-a]benzimidazole (11e)** (4.3 g; 72 %), m.p. 230 – 231 °C. On recrystallizing the crude product from aqueous ethanol its m.p. did not change.

$C_{11}H_{13}N_5S$ .1/2H_2SO_4 (296.36). Calcd. C 44.58; H 4.76; N 23.63; S 16.23. Found C 44.30; H 4.35; N 23.24; S 16.15 %.

IR (Nujol) ν_{max} = 3300 – 3000 ($\overset{+}{N}H_2$), 1690, 1630 (guanidine).

^{1}H-NMR (D_2O): δ = 3.62 (d, 2H, SCH_2); 4.25 (d, 2H, NCH_2); 5.1 – 5.4 (m, 1H, CH); 7.2 – 7.7 (compl., 4H, Ar = CH) ppm.

Reaction of the azido compound (10d) with acetylene derivatives

General procedure for the preparation of triazole derivatives:

A solution of the azido compound (**10d**) (0.01 mole) and of the acetylene derivative (0.02 mole) in toluene (30 ml) was refluxed for 36 hrs. After evaporating the toluene in vacuum, the residue was subjected to fractional crystallization from ethanol.

The compounds prepared by this method are listed in Table III.

*

The authors express their thanks to Miss T. HUSZÁR for her valuable participation in the preparative work, to Mrs. M. OTT, A. HALÁSZ and L. LOVAS for their valuable participation in the microanalyses, and to Dr. L. KECSKÉS (Gas Chromatographic Laboratory) for the gas chromatographic investigations. Thanks are due to the Chemical Works of Gedeon Richter Ltd. for the financial support of these researches.

REFERENCES

[1] ALPER, H., KEUNG, E. C. H.: J. Org. Chem., **37**, 1464 (1972)
[2] PHILLIPS, M. A.: J. Chem. Soc., **1928**, 2303
[3] FRANZEN, H., FÜRST, B.: Ann., **412**, 28 (1916)

[4] HUISGEN, R., GRASHEY, R., SAUER, J.: in The Chemistry of Alkenes p. 739. ed. S. Patai Wiley-Intersience, New York 1964
[5] HUISGEN, R., SZEIMIES, G., MÖBIUS, L.: Chem. Ber., **100**, 2494 (1967)
[6] KIRMSE, W., HORNER, L.: Ann. **614**, 1 (1958)

Kálmán HIDEG
Olga H.-HANKOVSZKY
Mihály GAJDÁCS
Ferenc ARADI

H-7643 Pécs, Szigeti u. 12.

Acta Chimica Academiae Scientiarum Hungaricae, Tomus 96(3), pp. 311—313 (1978)

ONE-STEP SYNTHESIS OF 2, 3, 4-TRIACETYL-LEVOGLUCOSAN FROM 1, 2, 3, 4-TETRAACETYL-6-TRITYL-β-D-GLUCOPYRANOSE BY MEANS TITANIUM TETRACHLORIDE*

(PRELIMINARY COMMUNICATION)

E. ZÁRA-KACZÁN and Gy. DEÁK

(Research Institute of Experimental Medicine, Hungarian Academy of Sciences Budapest)

Recevied December 8, 1977

It is well known [1] that removal of the trityl group, used in carbohydrate chemistry for the selective protection of primary hydroxyl groups, can be achieved in acetic acid solution with hydrogen bromide.

In an attempt of effecting cleavage of the ether linkage of 1,2,3,4-tetraacetyl-6-trityl-β-D-glucose (**1**) with titanium tetrachloride, we expected to obtain 1,2,3,4-tetraacetyl-β-D-glucose, or its titanium complex (**2**); cyclization of the latter to 2,3,4-triacetyllevoglucosan (**6**) seemed improbable, as earlier investigations [2] have shown that titanium tetrachloride, in contrast with tin tetrachloride effecting cyclization, rather causes cleavage of the anhydro ring.

When carrying out the reaction under preparative conditions, it has been found that refluxing of **1** in chloroform solution with the stoichiometric amounts of titanium tetrachloride and ethanol (molar ratio 1:1:1) for 1 hr, gives pure triacetyllevoglucosane (**6**) in a yield of 50—70%. When the reaction is carried out with titanium tetrachloride in the absence of ethanol, the quantity of 2,3,4-triacetylglucosyl chloride (**4**), always present as a by-product, increases. The quantity of the by-product is considerably increased, when pure tetraacetylglucose is used as the starting compound for the cyclization. In this case **6** and **4** were present after 300 min in nearly identical quantities in the solution; the chlorine content of the latter product was 10% (calcd. for triacetylglucosyl chloride: 10.91%). In view of the yields, it is by all means more advantageous to start from the 6-trityl derivative.

In consideration of the fact that by the combination of the hydrogen bromide and tin tetrachloride methods triacetyllevoglucosan can only be prepared in a yield as low as 33%, the procedure used in our experiments is of preparative importance. Moreover, it has been found that the reaction is also suitable for the synthesis of tribenzoyllevoglucosan.

*Presented at the 173rd National Meeting (Friedel-Crafts Centennial Symposium) of the American Chemical Society, New Orleans, Louisiana, March 23 (1977).

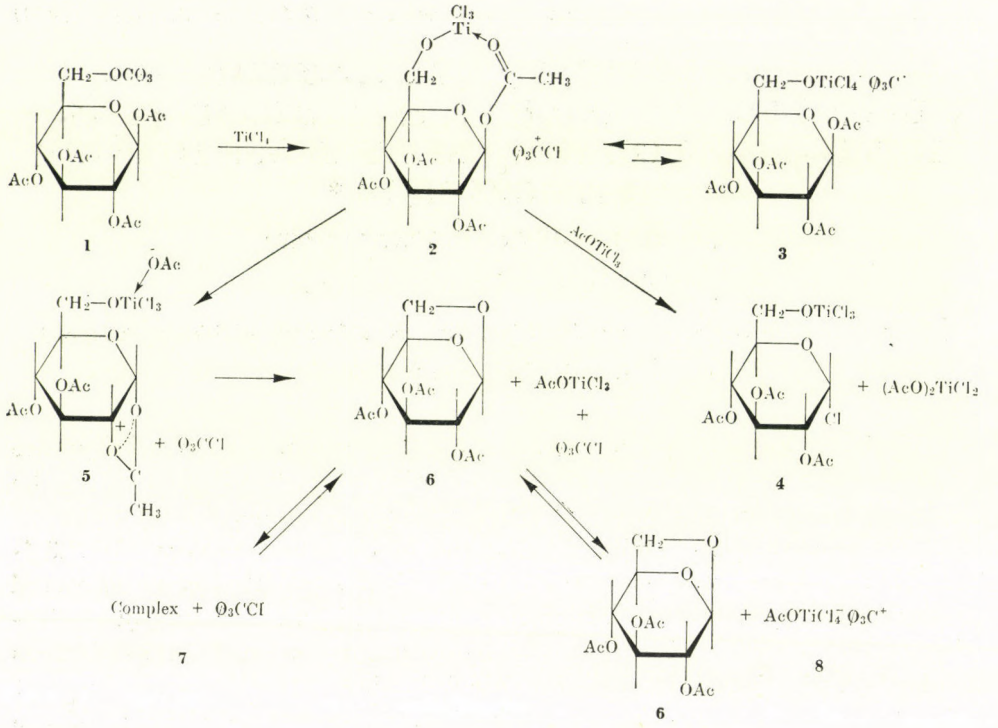

By lowering the temperature to 25 °C and the concentration of the reactants to 1/10, the reaction could be slowed down. It has been established that under these conditions too, detritylation proceeds very rapidly, and after 2 min **2** is the sole product that can be detected in the solution. The cyclization was then followed by TLC, by measurement of the change in optical rotation and on the basis of the IR spectra of the reaction mixture and the complexes precipitated by the addition of petroleum ether to the chloroform solution. On the basis of the composition and IR spectra, the so-called initial complex is the alkoxytitanium trichloride derivative of the detritylated tetraacetylglucose (**2**), the aqueous decomposition of which yields 1,2,3,4-tetraacetyl-β-D-glucopyranose. Noteworthy in the spectrum is the band at 1580 cm^{-1}, whose intensity gradually increases in the spectra of the complexes isolated with the progress of the reaction. On the basis of data reported in the literature for other Lewis acids [3] and according to our own experiments, this band can be assigned to the trityl cation formed in an equilibrium reaction from trityl chloride and **2**.

In the course of the ring closure acetoxytitanium trichloride is liberated, which, being also a Lewis acid, may form a coordinative bond with one of the carbonyl oxygens (**7**), but can also react with trityl chloride (**8**). As acetoxy-

titanium trichloride is a stronger Lewis acid than the starting compound **2** of alkoxytitanium trichloride type, the reaction of the former with trityl chloride is the preferred one, and this is indicated by the increase in intensity of the band at 1580 cm^{-1}.

As it has been stated previously, the formation of **4** is inevitable in the course of the reaction. We suggest that the by-product results from the reaction of acetoxytitanium trichloride, set free during ring closure, with the starting material **2**, still present. Starting from the trityl derivative, *i.e.* in the presence of trityl chloride, the amount of the "active" acetoxytitanium trichloride decreases (since one part of it is present as the anion **8** in the solution) and therefore the occurrence of the side reaction is decreased. The favourable effect of alcohol addition may be similarly interpreted: in this case, the actual reagent will be ethoxytitanium trichloride; acetoxyethoxytitanium dichloride is liberated during ring closure, and this has lesser chlorinating effect.

REFERENCES

1. HELFERICH, B.: Adv. Carbohydr. Chem., **3,** 79 (1948)
2. FENICHEL, L., DEÁK, Gy., BAKÓ, P., HOLLY, S., CSŰRÖS, Z.: Acta Chim. (Budapest) **85,** 313 (1975)
3. SHARP, D. W. A., SHEPPARD, N.: J. Chem. Soc., **1957,** 674

Erzsébet ZÁRA-KACZIÁN
Gyula DEÁK
} MTA KOKI 1083-Budapest

RECENSIONES

I. Inczédy: *Analytical Application of complex Equilibria*

Akadémiai Kiadó, Budapest, 1976, 415 pp.

The rapid development in the chemistry of coordination compounds during the last few decades has brought about significant changes in analytical chemistry. Unfortunately there is, however, a considerable lag between the appearance of fundamental relationships in the scientific literature and their general use in the common analytical praxis. The main aim of the author of the present book has been "to guide and aid the analytical chemist working in industrial and research laboratories in solving everyday problems, and by working through typical problems to show how rapid exploratory calculations may be performed with a slide rule. . ."

The book consists of four chapters. In Chapter 1. after a short repetition of the elements of complex chemistry the author deals in details with the various equilibria (complex-formation, acid-base, redox), with factors affecting and energy changes involved in complex formation reactions. A far too short subchapter gives some insight into the kinetics of the reactions of complexes.

Chapter 2. is an excellent compilation of the most widely used methods (potentiometric, spectrophotometric, polarographic, extraction and ion-exchange) for the determination of protonation constants, the stability constants of both mononuclear and polynuclear complexes.

Chapter 3. discusses the analytical applications of the various types of homogeneous and heterogeneous equilibria described in the previous chapters. The analytical applications include gravimetric analysis, acid-base, precipitation, complexometric and redox titrations, polarography, spectrophotometry, liquid-liquid extraction, ion-exchange separations and electrophoresis.

At the end of the chapters mentioned so far a large number worked examples are given. These help to comprehend the material described, and facilitate the solution of practical problems.

Tables of equilibrium constants (protonation, complex formation, precipitate formation, redox, extraction and ion-exchange) are compiled in Chapter 4. Finally 880 references refer to the most important publications.

The approach of the author to the various topics of analytical chemistry (acid-base, complexation, precipitation and redox reactions) is uniform and is based on the author's sound knowledge in coordination chemistry.

The book can be highly recommended to everybody interested and active in analytical chemistry. Both industrial and research chemists will find it a useful guide. Further it is a valuable book both to teach and to comprehend analytical chemistry. For this reason university and college teachers, undergraduate and research students should have it on their shelves.

E. Kőrös

Topics in Current Chemistry (Fortschritte der chemischen Forschung). Vol. 64. Inorganic Biochemistry

Springer-Verlag, Berlin, Heidelberg, New York, 1976. pp. 225

The 64. volume of Topics in Current Chemistry includes three monographies, each discusses some aspects of bioinorganic chemistry.

The first monography (112 pages with 559 references) is entitled "Molecular Mechanisms on Carbonate, Phosphate and Silica Deposition in the Living Cell" and written by E. T. DEGENS. The monography starts with the illustration on three examples the interaction of metal ions with organic compounds, which is important to understand how metal ions influence the structural organization of biochemical molecules and the functional processes operating in the genetic and metabolic apparatus. Then the author shows how epitaxis can be related to biocatalysis and points to the fact that organic matrices can act as morphological catalysts in the deposition of minerals. A short chapter is devoted to mineral equilibria (carbonate, phosphate and silica), then two enzyme systems — carbonic anhydrase and alkaline phosphatase — which have important roles in biomineralizations are discussed. The following chapter is on calcium transport and regulation. In the consecutive chapters the mechanisms of the deposition of carbonate, phosphate and silica are described in great details. Although the origin, nature and function of mineralized tissues are only tentatively known the author tries to coordinate the often contradictory results on mineral deposition processes. Also the author deals rather minutely with the organic matrices which serve as templates in the nucleation and oriented growth of biominerals, and with the evolution of biocarbonates, biophosphates and silica, respectively. Ample number of references close the monography.

"Water in Biological Systems" is the title of the second monography (67 pages with 303 references) and is written by W. A. P. LUCK. The purpose of the author of this article has been "to give a review on the present status of water research and on the first attempts to apply this to biological problems". The role of water in biological systems includes among others the stabilisation of higher structural organizations and the large free energy changes associated with the formation of water in a variety of chemical reactions. The first chapter deals with the structure of water and with its most important physical properties (density, specific heat, heat of melting, heat of vaporisation, surface tension and association structure). The next chapter is devoted to the structure of aqueous solutions, and this includes electrolyte solutions, non-electrolyte solutions with hydrophilic and hydrophobic solutes, respectively, and mixed aqueous systems hydrophilic–hydrophobic. Also a short description on entropy driven processes is given. The third chapter deals with the biological systems: lipids, polysaccharides, nucleic acids, peptides and protein, and the ion effects on the hydration of the three latters, and also with water in biological tissues. In the last chapter the author gives a short review on the strong effects of D_2O on biological systems, and both the most important biochemical and biological observations are summarized.

The third monography (36 pages with 192 references) written by D. D. PERRIN and entitled "Inorganic Medicinal Chemistry" deals with "the impact of pharmaceuticals on the mineral composition of cells and tissues, the use of metal containing agents in therapeutics, and the external control of the concentrations of essential and toxic metal ions in the living organisms". After a brief introduction and a short chapter on the topical applications of inorganic compounds the author deals rather extensively with the uptake of inorganic species (Na^+, K^+, Li^+, Ca^{2+}, halide ions, phosphate, trace metal ions and contrast media). The metal-organic complexes (arsenicals, antimonials, mercurials and the chelates, and organic compounds of some other metals) are described together with their mode of action in biosystems. A separate chapter is devoted to chelation therapy and this includes the most important and more widely used ligands, dimercaptopropanol, EDTA, D-penicillamine and desferrioxamine. The following chapters consider the antibacterial, antiviral, anticancer and antifungal action of the chelating agents. Also the antibacterial and anticancer activity of some inert metal complexes is described. In the last chapter the author deals briefly with a large variety of topics which include: applications based on selective binding, examples where chelation and activity may be unrelated, some untoward effect of chelating agents, macrocyclic ligands, and silicones.

The three monographies clearly show that there is an upsurge in the interest of the inorganic aspects of biochemistry, biology and medicine. This volume can be highly recommended to chemists (active in the field of inorganic chemistry and coordination chemistry) to biochemists and to biologists who are interested on molecular level in events occurring in the living systems.

E. KŐRÖS

P. DESLONGCHAMPS: *Stereoelectronic Control in the Cleavage of Tetrahedral Intermediates in the Hydrolysis of Esters and Amides*, Tetrahedron Report No 3.

Pergamon Press Oxford, New York (1976) pp. 1—28

The author presents a new stereoelectronic theory for the cleavage of the tetrahedral intermediate in the hydrolysis of ester and amides. In this new theory specific cleavage of a carbon–oxygen or a carbon–nitrogen bond in any conformer is allowed only if the other two hetero atoms (oxygen or nitrogen) each have an orbital oriented "antiperiplanar" to the leaving O-alkyl or N-alkyl groups. In other words, the precise conformation of the intermediate hemi-orthoester or hemi-orthoamide controls the nature of the hydrolysis products. The ejection of the leaving group is achieved with the assistance of a lone pair orbital properly aligned (antiperiplanar) on each of the two remaining heteroatoms.

The new theory originated in the author's earlier (1971—1974) studies on the oxidation of acetals to esters with ozone. First, the reaction is described, then the principle of stereoelectronic control, which provides and explanation for the formation of products in the osonolysis of acetales, is disclosed.

The main headings of the review are as follows: Stereoelectronic control in the cleavage of hemi-orthoesters; Hydrolysis of cyclic orthoesters; Concurrent istope oxygen exchange and hydrolysis of esters; Stereoelectronic control in the cleavage of hemi-orthoamides; Hydrolysis of N,N-dialkylated imidate salts; Stereoelectronic control and pH of the reaction medium; Conclusion.

DESLONGCHAMPS's review is interesting, concise and well arranged. However, it would have been useful to discuss briefly the quantumchemical basis of the principle of stereoelectronic control. It is felt that the theory of stereoelectronic control — just like other theories — is of value only if it provides a possibility for generalization and for making predictions. The author exercises true self criticism when writing: "The results that we have described on the hydrolysis of orthoesters and imidate salts constitute enough experimental evidence to take the stereoelectronic theory seriously. However, we believe that more experiments are still necessary to establish it completely". "This principle of conformation change can become a crucial point when the stereoelectronic theory is applied to the mechanism of hydrolysis by enzymes. For instance, it could lead to the prediction that conformation changes are necessary for the stereoelectronic assistance of hydrolysis by enzymes."

It should be noted that reviews of similarly high standard have recently become available in the form of "Tetrahedron Reports".

A. MESSMER

Metal Ions in Biological Systems, Vol. 6., Sigel, H. (ed.)

Marcel Dekker, Inc. New York and Basel, 1976. XIII + 453 pp.

Volume 6. of Metal ions in biological systems comprises six monographies.

The first monography written by J. F. CHLEBOUSKI and J. E. COLEMAN is on "Zinc and its role in enzymes". After a brief survey on the physiological role of zinc, the zinc metalloenzymes are characterized. This is followed by a chapter in which the most important methods used for the investigation of the role of zinc in catalysis are described. These include ligand and metal substitutions, respectively, absorption spectra, circular dichroism and magnetic circular dichroism, ESR and NMR spectroscopies. The next chapter is on the structure and function of well-characterized zinc metalloenzymes (peptidases, alkaline phosphatases, carbonic anhydrase, superoxide disumtase, alcohol dehydrogenases, aldolases, aspartate transcarbamylase, transcarboxylase, DNA polymerase I).

This monography clearly demonstrated that zinc metalloenzymes are highly important in living organism, since they catalyze metabolically important reactions including hydrolysis, hydration, oxidation-reduction and group-transfer. Zinc may also function by maintaining the required conformation of a protein or by participating in the binding of effector molecules to allosteric enzymes, and finally zinc is required for the function of the nucleotidyl transferase enzymes basic to DNA replication and transcription.

385 references are listed.

The second review written by W. R. BIGGS and J. H. SWINEHART is on "Vanadium in selected biological systems". This is a fascinating topic since there are organisms (mostly ascidi-

ans) which are speculator accumulators for vanadium (the concentration factor is over 10^6). In the introductory chapter the authors give information on the levels of vanadium in non-biological and biological environments, and on the equilibria of vanadium (V) species in aqueous solution. Then they list plants and animals which concentrate vanadium. These are some mushrooms, ascidians and holothurians. The final chapter is on the chemistry of vanadium in selected plants and animals. Although the uptake and transport mechanisms have not yet been revealed in details the monography summarizes the most important and in some respects conflicting suppositions. The monography is focussed on the vanadium-ascidian problem and the final conclusion is that "nearly seven decades of work on the problem of vanadium in biological systems has not resulted in the elucidation of its role".

147 references are given.

The third review written by P. W. SCHNEIDER is on a highly important biochemical and biological topic "The chemistry of nitrogen fixation". The author limits his discussion to the chemical aspects of the process, and emphasizes on the characteristics of the enzyme systems responsible for the reduction of nitrogen, their interactions with N_2 and other molecules which influence the rate of fixation. First the catalyst, nitrogenase, is characterized its purification and properties are described and the results of physico-chemical investigations on the Fe—Mo- and Fe-proteins given. Then the reaction itself ($N_2 \rightarrow NH_3$) is dealt with in detail: the requirement for activity (metals, pH optima, reductants, ATP), the subtrates, versatility and specificity of the catalyst. The final chapter is a survey of the suggestions on the mechanism of nitrogen fixation. At present not too much is known about the actual chemical pathway by which dinitrogen is activated and reduced by nitrogenaze, and about the chemical nature and location of the active site. There is, however, some hope that a biological approach to nitrogen fixation will cast further light to the mechanism of biological nitrogen fixation. A list of 286 references close the review.

The forth review written by D. W. DARNALL and E. R. BIRNBAUM is entitled "The metal ion acceleration of the activation of trypsinogen to trypsin". Trypsin catalyses the activation of a number of zymogens, however only the trypsinogen to trypsin conversion is accelerated by metal ions. In their review first the authors characterize both trypsinogen and trypsin, and then deal with the nature of the conversion of trypsinogen to trypsin. They discuss the products of conversion and the effects of calcium ion binding: stabilization of trypsin, activation of trypsinogen. The role of the metal ion in accelerating the activation of trypsinogen is regarded as a complex formation between metal ions and at least two aspartate carboxyl groups on the N-terminal hexapeptide of trypsinogen. The last chapter deals with the use of lanthanide ions as probes in biological systems especially for probing the calcium ion binding sites. Lanthanide ion binding to trypsin and trypsinogen is also discussed. 87 references are listed.

The fifth review written by K. S. RAJAN, R. W. COLBURN and J. M. DAVIS is entitled "Metal chelates in the storage and transport of neurotransmitters". In the introduction the authors outline the role of magnesium in monoamine uptake and that of calcium in monoamine release, and give information on metal ion levels of synaptic vesicles and several areas of brain. Then they discuss the metal-amine coordination (the amines are those which function as neurotransmitters), chelate formation, complex stability. It is followed by the description of the so called coordination hypothesis, which serves as a model for the explanation of the binding storage, and transport of neurotransmitters. Finally they examine the published data on the structure-activity relationships of a number of biogenic amines from the point of view of metal chelation.

A list of 45 references are given.

The final review "The role of divalent metals in the contraction of muscle fibers" is written by F. N. BRIGGS and R. J. GOLARO. The first part of the article deals with some bioelectrochemical problems connected to muscle contraction: *e.g.* effect of metals on membrane potentials, calcium current, voltage-calcium-tension relation. Then the authors discuss the interaction between divalent cations and the fundamental components of the contractile machine (myosin, actin, tropomyson, troponin) the sarcoplasmic concentrations of free calcium and magnesium, and the role of these ions in the cross-bridge cycle. The last chapter informs us how calcium is taken up by the sarcoplasmic reticulum (mechanism of the uptake and calcium transport, rate of uptake, calcium binding site).

347 references are listed.

Volume 6 of this excellent series of books on the role of metal ions in biological systems provides the reader with a wealth of information on the molecular basis of enzyme actions, metal accumulation, biosynthesis, conduction of nerve impulses and muscle contraction.

E. KŐRÖS

Recent Results in Chemistry (A kémia újabb eredményei). Vol. 29.

Akadémiai Kiadó, Budapest, 1976, 292 pp.

Volume 29 of the series comprises two monographies. The first monography is written by L. CSÁNYI and entitled: "Induced reactions in chemical analysis". In the first chapter of the monography, after a brief historical introduction, the author discusses the types of induced reactions (complex reactions, induced chain reactions, mutual induction etc.) and the relationship between induced reactions and catalysis. The second chapter deals with the role of induced reactions in volumetric analysis. Large number of examples draw the attention of the readers to the importance of induced reaction in analytical chemistry. Separate sub-chapters give information on induced reactions bring about with SO_4^--, SO_5^--, HO_2-, As(IV)-radicals, with Cr(V), Cr(IV), Tl(II) and with the informediate of the oxidation of SCN^-, and those of the reduction of MnO_4^-. Induced oxidation with molecular oxygen are also mentioned. This is followed by making known of analytical methods based on chemical induction. These include the determination of chlorate, perchlorate, chromate, tellurium (IV), manganese (II), cerium (III), plutonium (IV), and peroxosulphuric acid. Some examples are given how photochemically induced reactions can be utilized in quantitative analysis. Briefly mentioned are the test reaction based on chemical induction, and the catalytic polarographic waves. 201 references close the monography.

The second monography is written by I. KRAUSZ and entitled: "Recent problems of titrations in non-aqueous media".

The main aim of the author has been to give survey on the analytical chemistry in non-aqueous solutions excluding such topics as reactions in solid phases and in melts, and extraction.

After a short induction the author deals with some problems concerning non-aqueous solvent, laying emphasis on the classification and the composition of the solvents. This is followed by the discussion of the activity of solutions, their characteristic function, and the extension of the pH concept to non-aqueous media. A separate chapter deals with the conditions of non-aqueous titrations, acid-base equilibria, the method of BRUCKENSTEIN and KOLTHOFF, and that of IZMAILOV. Acid-base titrations in aprotic solvents, in solvent mixtures, and further redox titrations in various solvents (glacial acetic acid, acetonitril, dimethyl formamide, dimethyl sulfoxid etc.) are discussed. The last chapter deals with some problems of the solvation. 144 references are given.

Both monographies can be recommended to those who intend to widen their knowledge in analytical chemistry. Both analytical chemists in industrial and research laboratories will find useful informations in this volume for their practical and scientific activity. In addition both monographies can be valuable supplementary texts for university undergraduates and research students.

E. KŐRÖS

M. HARGITTAI and I. HARGITTAI: *The Molecular Geometries of Coordination Compounds in the Vapour Phase*

Akadémiai Kiadó, Budapest, 1977, 277 pages

There was a tremendeous development in the last two decades in field of structural investigations. Methods which provide structural data for molecules in the gaseous phase are of particular importance since no perturbation by intermolecular forces occurs. This book is an excellent critical treatment of molecular geometric studies of compounds in the gas phase.

The monograph consists of eight main chapters. 1. Chapter "General Concepts" gives a brief and lucid outline of the experimental methods, their limitations are clearly pointed out and the problems of concept of molecular geometry are treated. The considerations regarding the definition of coordination compounds seem a little bit awkward and superfluous.

The next seven chapters (Addition Compounds; Electron-deficient Molecules; Halogen Bridging Complexes; Salts of Oxycids; Polymeric Oxides; Hydrogen-bonded Complexes; Transition Metal Complexes) give a survey of the investigations. Apparently the classification

caused some problems to the Authors. The arrangement of the vast experimental material is logical and advantageous, although sometimes the same compounds could have been treated in different chapters.

The text is followed by a list of references (nearly 700 papers are cited, the literature is covered till 1974), by author and formula indexes. Date are summarized in 55 tables; the 76 figures are illustrative.

This book is an up-dated version of the monograph published in 1974 in Hungarian. The reviewer believes that the publisher made a good service to the chemists interested in the field of structural chemistry making available it in English.

M. T. BECK

INDEX

PHYSICAL AND INORGANIC CHEMISTRY

ORGANIC CHEMISTRY

Printed in Hungary

A kiadásért felel az Akadémiai Kiadó igazgatója — Műszaki szerkesztő: Zacsik Annamária

A kézirat nyomdába érkezett: 1978. I. 18. — Terjedelem: 11,90 (A/5) ív, 84 ábra

78.5403 Akadémiai Nyomda, Budapest — Felelős vezető: Bernát György

ERRATUM

Acta Chim. Acad. Sci, Hung. *93*, 43 (1977): in General method of syntheses after first line read: "10 ml of 2% solution of hydroxylamine hydrochloride was added and the mixture was heated on a water"

ACTA CHIMICA

ТОМ 96—ВЫП. 3

РЕЗЮМЕ

Некоторые химические реакции в электродной щели и их роль в спектрохимическом анализе, XXIII

Поведение окислов металлов в дуге. Экспериментальная устрановка, метод и предварительные опыты

З. Л. САБО и Х. ДОБОЛИНЕ-ФЕЙЕРДИ

Для исследований были разработаны экспериментальный метод и газовая ячейка Основной целью исследований было изучение реакций смесей разных окислов металлов с угольным порошком в дуге и влияние реакций на результаты спектрального анализа. На основе предварительных исследований выяснилось, что водяной пар, материал вспомогательных электродов, состав порошковой смеси и сила тока играют роль в протекающих реакциях.

Некоторые химические реакции в электродной щели и их роль в спектрохимическом анализе, XXIV

Проведение окислов металлов в дуге с неподвижной атмосферой аргона. Роль силы тока в случае вспомогательных электродов RW II

З. Л. САБО и Х. ДОБОЛИНЕ-ФЕЙЕРДИ

Было исследовано поведение смесей порошка угля с пятью различными окислами металлов (Ag_2O, CuO, PbO, CoO и ZnO). В зависимости от силы тока было определено количество CO, образующегося под влиянием дуги, а в случае CuO и PbO и изменение интенсивности спектральных линий. При небольших силах тока реакция начинается вблизи пламени дуги, поэтому более сильную реакцию получается при возбуждении, образца в качестве катода; в этом случае и интенсивность спектральных линий также оказываются более интенсивными. С повышением силы тока вся масса электрода-посителя накаляется. Температура электрода-носителя RWII, присоединенного как анод, повышается значительнее. Поэтому при повышенных силах тока именно при анодном возбуждении образца значительнее реакции и спектры более интенсивны.

Количественный анализ содержания Pb и Cu в галлии высокой чистоты с помощью масс-спекрографии с искровым источником, используя ртутный внутренний стандарт

Й. КЮРТИ

Цель настоящей работы заключалась в разработке экспериментальной техники сравнения образцов галлия с различной высокой чистотой и обнаружения относительных изменений в содержании примесей. Метод определения основан на единственной экспозии, а также на правильно выбранном внутреннем эталоне, обладающим таким распределением изотопов, который позволяет калибрацию фотопластинок. В качестве такого внутреннего стандарта для количественного определения Pb и Cu в 99,9996%-ом Ga наиболее удобней оказалась ктуть. Предлагаемое количество Hg, измеряемое в образце в качестве разбавляющего сплава, составляет около 0,1—0,3 атомных м. д.

Принимая во внимание погрешности тесники с искровым ионным источником, а также то, что область измеряемых концентраций находится близко к уровню детектирования, достигнутая точность является вполне удовлетворительной. В будущем метод будет распространен и на другие элементы.

УФ спектроскопическое исследование изоцианатных и изоцианатных производных силанов

Т. ВЕСПРЕМИ, Й. НАДЬ и И. БАРТА

Были приготовлены члены серии $(CH_3)_n$ Si $(NCO)_{4-n}$ и $(CH_3)_n$ Si $(NCS)_{4-n}$, сняты их УФ спектры и ассигнированы полосы поглащения. Были проведены квантово-химические расчеты с целью интерпретации сильных различий в спектрах соединений, содержащих группы Si—NCS и Si—NCO.

Исследования в области твердофазной полимеризации, XXXV

Твердофазная полимеризация моноалкил итаконатов

К. НИТРАИ, Н. Л. НГУЕН, Ф. ЧЕР, Э. ТАКАЧ и ДЬ. ХАРДИ

Была исследована прямая и пост-полимеризация четырех β -моноалкилитаконатов (бутил, октил, лаурил и цетил) в твердой фазе. Были определены диаграммы состояний мономер-полимер для бутил- и октилитаконатов. Было установлено, что полимеризация протекает с большой скоростью в жидкофазном выхокоэластичном полимере, пластифицированном мономером. На основе самого большого периода идентичности, измеряемого на рентгенодиффрактограмме мономера, было установлено, что элементарные ячейки кристаллов изучаемых мономеров подобны. Реакционная способность гетерогенной твердофазной полимеризации молекул, находящихся в решетках одинакового типа, уменьшается с увеличением размеров молекул.

Исследования в области твердофазной полимеризации, XXXVI

Полимеризация N-гексадецилакриламида и N-гексадецилметакриламида в присутствии насыщенных аналогов

Ф. ЧЕР, К. НИГРАИ, В. ДЕВЕНИ и ДЬ. ХАРДИ

Было установлено, что N-гексадецилакриламид (ГАА) и N-гексадециметакриламид (ГМА) полимеризуются в твердой фазе согласно кинетической кривой с ускорением. Эти мономеры образуют с их насыщенными аналогами (N-гексадецилпропионамид и амид N-гексадецилизомасляной кислоты) изморфную систему, которую характеризовали ее фазовыми диаграммами и структурными параметрами, полученными из них. На основе рентгенодиффракционных исследоавний, в случае ГАА было заключено, что полимер остается в решетке мономера после того, как система претерпевает фазовые превращения уже при небольших конверсиях. В ходе полимеризации полимер сохраняет новую образующуюся фазовую структуру, несмотря на то, что она отличается от его собственной структуры. Это явление представляет собой новое доказательство принужденной изоморфии. В случае ГМА фазовые превращения, происходящие при небольших конверсиях, приводят к структуре системы, подобной структуре полимера, так что мономер становится изоморфным с полимером за счет растворения в решетке полимера с упаковкой в виде гексагональных боковых цепочек. Полимеризация, по существу, протекает в этой разрыхленной системе.

Влияние сплавления на избыточную поверхностную свободную энергию катализаторов из благородных металлов

Т. МАЛЛАТ, Е. ПОЛЯНСКИ и Й. ПЕТРО

На основе более ранних исследований было установлено, что избыточная поверхностная свободная энергия катализаторов из платины, палладия, родия, рутения и иридия, в первую очередь, является функцией природы вещества, но изменяется и в зависимости от способа приготовления катализатора.

В настоящей работе было исследовано, каким образом влияет сплавление на избыточную поверхностную свободную энергию катализаторов из палладия и платины. Влияние сплавления было исследовано в системах Pd—Ir и Pt—Au.

Дополняя исследования измерениями содержания водорода, поверхности и активности, было установлено, что до тех пор пока компоненты дают гомогенный раствор в сплаве и их физико-химические свойства (напр., постоянная решетки) подобны, т. е. атомы сплава металла могут быть легко заменимы атомами основного металла в узгах решетки, избыточная поверхностная свободная энергия не изменяется заметно.

Лишь тогда может быть обнаружено изменение свободной энергии под влиянием сплавления, когда появляется новая фаза (в платине с 10—15 атом.%-ым содержанием Au).

Исследование стереохимии комплексов платиновых металлов с карбамилмочевиной

П. С. СРИВАСТАВА и Б. К. БАНЕРЙЕ

Описывается получение и характеристика комплексов карбамилмочевины с Pd(II), Pt(II), Pt(*IV*) и Rh(III). На основе химического анализа, измерений магнитной воспримичивости и данных электронных и ИК спектров предлагаются возможные структуры комплексов. Обсуждаются способ координирования и силовые постоянные связей M—O и M—Cl. В каждом комплексе лиганд ведет себя как кислородный донор. Порядок величин K_{M-O} и K_{M-Cl}: Pt(II) > Pd(II) и Pt(IV) > Rh(III) для крадратно-планарных и октаэдрических комплексов, соответственно.

Синтез защищенных *N*-концевых гептапептидов паратироидного гормона скота

Х. Ш. ВАРГА и К. МЕДЗИХРАДСКИ

Boc—Ala—Val—Ser—*G*lu(OtBu)—Ile—*G*ln—Phe—OMe—защищенный N-концевой гептапептидный фрагмент паратироидного гормона скота был синтезирован обычной техникой в растворе. Этот пептид представляет собой промежуточный продукт в синтезе более больших N-концевых фрагментов, содержащих метиониновые остатки, окисление которых, как полагается, является причиной обрыва биологической активности.

Химия серных диимидов, VII

Фрагментация серных диимидов, инициированная електронной бомбардировкой

И. ЛЕНДЬЕЛ, Г. КРЕСЕ, М. БЕРГЕР, В. КОСБАН и Х. ШАФЕР

Приводятся и обсуждаются масс-спектры 10 серных диимидов. Молекулярные ионы диарильных серных дииминов подвергаются циклизации, теряя орто-заместитель в фенильном кольце и образуя ионы бензотиаэольного типа с четным числом электронов. Дифенилсерный диимид также выделяет серу, вероятно, из диазотииранового валентного изомера молекулярного иона. В спектрах доминирует большие осколки скелетных перегруппиро-

вок, как это найдено из анализа метасабильных пиков, масс-измерений высокого разрешения и исследований с мечеными заместителями. Циклические серные диимиды IX и X фрагментируются с потерей CH_2N и $(CH_2)_2N$. В случае соединения X была найдена сильная тенденция к ароматизации за счет дегидрирования.

Бензазолы, IX

Получение серосодержаших трициклических соединений за счет реакции 2-меркапто- или 2-меркапто-алкилбензидазолор с эпигаогидринами иси дигалогенпропанолами

К ХИДЕГ, О. Х. ХАНКОВСКИ, М. ГАЙДАЧ и Ф. АРАДИ

Бензимидазол-2-тиол, 2-меркаптометил-, 2-(α-меркаптоэтил)-, 20(β-меркаптоэтил)-бензимидазолы с помощью эпихлоргидрина или дигалогеновых пропанолов (2,3-дигалоген-1-пропанолы или 1,3-дигалоген-2-пропанолы) в щелочной среде превращаются в трициклы: 3,4-дигидро-3-гидрокси-2*H*-[1,3]тиазино[3,2-а]бензимидазол (*1*), 4,5-дигидро-4-гидрокси-1*H*,3*H*-[1,4]тиазепино[4,3-а] бензимидазол (*3а—в*) и 1,2,5,6-тетрагидро-5-гидрокси-4*H*-[1,5] тиазоцино[5,4-а] бензимидазол (*3с*). О-Серные производные соединения *1* могут претерпевать элиминацию и/или вступать в реакции замещения с нуклеофильными реагентами.

Были исследованы реакции 3,4-дигидро-3-азидо-2*H*-[1,3] тиазино[3,2-а]-бензимидазола (*10*d) с асимметричными ацетиленами, приводящие к образованию производных 1,2,3-триазола.

Les Acta Chimica paraissent en français, allemand, anglais et russe et publient des mémoires du domaine des sciences chimiques.

Les Acta Chimica sont publiés sous forme de fascicules. Quatre fascicules seront réunis en un volume (4 volumes par an).

On est prié d'envoyer les manuscrits destinés à la rédaction l'adresse suivante:

Acta Chimica
H-1521 Budapest, Hongrie

Toute correspondance doit être envoyée à cette même adresse.

La rédaction ne rend pas de manuscript.

Le prix de l'abonnement est de $ 36,00 par volume.

Abonnement — en Hongrie l'Akadémiai Kiadó l'Entreprise pour le Commerce Extérieur « Kultúra » (1389 H-Budapest 62, P.O.B. 149 Compte-courant No. 218 10990) ou à l'étranger chez tous les représentants ou dépositaires.

Die Acta Chimica veröffentlichen Abhandlungen aus dem Bereich der chemischen Wissenschaften in deutscher, englischer, französischer und russischer Sprache.

Die Acta Chimica erscheinen in Heften wechselnden Umfanges. Vier Hefte bilden einen Band. Jährlich erscheinen 4 Bände.

Die zur Veröffentlichung bestimmten Manuskripte sind an folgende Adresse zu senden:

Acta Chimica
H-1521 Budapest, Ungarn

An die gleiche Anschrift ist auch jede für die Redaktion bestimmte Korrespondenz zu richten.

Manuskripte werden nicht zurückerstattet.

Abonnementpreis pro Band: $ 36,00.

Bestellbar für das Inland bei Akadémiai Kiadó (1363 Budapest, Postfach 24, Bankkonto Nr. 215 11488), für das Ausland Außenhandels-Unternehmen » Kultúra « (1389 Budapest 62, P.O.B. 149. Bankkonto Nr. 218 10990) oder bei seinen Auslandsvertretungen und Kommissionären.

«Acta Chimica» издает статьи по химии на русском, французском, английском и немецком языках.

«Acta Chimica» выходит отдельными выпусками разного объема, 4 выпуска составляют один том и за год выходит 4 тома.

Предназначенные для публикации рукописи следует направлять по адресу:

Acta Chimica
H-1521 Budapest,

Всякую корреспонденцию в редакцию направляйте по этому же адресу.

Редакция рукописей не возвращает.

Подписная цена — $ 36,00 за том.

Отечественные подписчики направляйте свои заявки по адресу Издательства Академии Наук (1363 Budapest, P.O.B. 24, Текущий счет 215 11488), а иностранные подписчики через организацию поз внешней торговле «Kultúra» (H-1389 Budapest 62, P.O.B. 149. Текущий кчет 218 10990) или через ее заграничные представительства и уполномоченных.

Reviews of the Hungarian Academy of Sciences are obtainable at the following addresses:

AUSTRALIA
C.B.D. LIBRARY AND SUBSCRIPTION SERVICE, Box 4886, G.P.O., *Sydney N.S.W. 2001*
COSMOS BOOKSHOP, 145 Ackland Street, *St. Kilda (Melbourne), Victoria 3182*

AUSTRIA
GLOBUS, Höchstädtplatz 3, *1200 Wien XX*

BELGIUM
OFFICE INTERNATIONAL DE LIBRAIRIE, 30 Avenue Marnix, *1050 Bruxelles*
LIBRAIRIE DU MONDE ENTIER, 162 Rue du Midi, *1000 Bruxelles*

BULGARIA
HEMUS, Bulvar Ruszki 6, *Sofia*

CANADA
PANNONIA BOOKS, P.O. Box 1017, Postal Station "B", *Toronto, Ontario M5T 2T8*

CHINA
CNPICOR, Periodical Department, P.O. Box 50, *Peking*

CZECHOSLOVAKIA
MAD'ARSKÁ KULTURA, Národní třida 22, *115 66 Praha*
PNS DOVOZ TISKU, Vinohradská 46, *Praha*
PNS DOVOZ TLAČE, *Bratislava 2*

DENMARK
EJNAR MUNKSGAARD, Norregade 6, *1165 Copenhagen*

FINLAND
AKATEEMINEN KIRJAKAUPPA, P.O. Box 128, *SF-00101 Helsinki 10*

FRANCE
EUROPERIODIQUES S. A., 41 Avenue de Versailles, *78170 La Celle St.-Cloud*
LIBRAIRIE LAVOISIER, 11 rue Lavoisier, *75008 Paris*
OFFICE INTERNATIONAL DE DOCUMENTATION ET LIBRAIRIE, 48 rue Gay-Lussac, *75240 Paris Cedex 05*

GERMAN DEMOCRATIC REPUBLIC
HAUS DER UNGARISCHEN KULTUR, Karl-Liebknecht-Strasse 9, *DDR-102 Berlin*
DEUTSCHE POST ZEITUNGSVERTRIEBSAMT, Strasse der Pariser Kommüne 3—4, *DDR-104 Berlin*

GERMAN FEDERAL REPUBLIC
KUNST UND WISSEN ERICH BIEBER, Postfach 46, *7000 Stuttgart 1*

GREAT BRITAIN
BLACKWELL'S PERIODICALS DIVISION, Hythe Bridge Street, *Oxford OX1 2ET*
BUMPUS, HALDANE AND MAXWELL LTD., Cowper Works, *Olney, Bucks MK46 4BN*
COLLET'S HOLDINGS LTD., Denington Estate, *Wellingborough, Northants NN8 2QT*
W.M. DAWSON AND SONS LTD., Cannon House, *Folkestone, Kent CT19 5EE*
H. K. LEWIS AND CO., 136 Gower Street, *London WC1E 6BS*

GREECE
KOSTARAKIS BROTHERS, International Booksellers, 2 Hippokratous Street, *Athens-143*

HOLLAND
MEULENHOFF-BRUNA B.V., Beulingstraat 2, *Amsterdam*
MARTINUS NIJHOFF B.V., Lange Voorhout 9—11, *Den Haag*
SWETS SUBSCRIPTION SERVICE, 373b Heereweg, *Lisse*

INDIA
ALLIED PUBLISHING PRIVATE LTD., 13/14 Asaf Ali Road, *New Delhi 110001*
150 B-6 Mount Road, *Madras 600002*
INTERNATIONAL BOOK HOUSE PVT. LTD., Madame Cama Road, *Bombay 400039*
THE STATE TRADING CORPORATION OF INDIA LTD., Books Import Division, Chandralok, 36 Janpath, *New Delhi 110001*

ITALY
EUGENIO CARLUCCI, P.O. Box 252, *70100 Bari*
INTERSCIENTIA, Via Mazzé 28, *10149 Torino*
LIBRERIA COMMISSIONARIA SANSONI, Via Lamarmora 45, *50121 Firenze*
SANTO VANASIA, Via M. Macchi 58, *20124 Milano*
D. E. A., Via Lima 28, *00198 Roma*

JAPAN
KINOKUNIYA BOOK-STORE CO. LTD., 17-7 Shinjuku-ku 3 chome, Shinjuku-ku, *Tokyo 160-91*
MARUZEN COMPANY LTD., Book Department, P.O. Boű 5056 Tokyo International, *Tokyo 100-31*
NAUKA LTD., IMPORT DEPARTMENT, 2-30-19 Minami Ikebukuro, Toshima-ku, *Tokyo 171*

KOREA
CHULPANMUL, *Phenjan*

NORWAY
TANUM-CAMMERMEYER, Karl Johansgatan 41—43, *1000 Oslo*

POLAND
WĘGIERSKI INSTYTUT KULTURY, Marszałkowska 80, *Warszawa*
CKP I W ul. Towarowa 28 *00-958 Warsaw*

ROMANIA
D. E. P., *Bucureşti*
ROMLIBRI, Str. Biserica Amzei 7, *Bucureşti*

SOVIET UNION
SOJUZPETCHATJ — IMPORT, *Moscow*
and the post offices in each town
MEZHDUNARODNAYA KNIGA, *Moscow G-200*

SPAIN
DIAZ DE SANTOS, Lagasca 95, *Madrid 6*

SWEDEN
ALMQVIST AND WIKSELL, Gamla Brogatan 26, *101 20 Stockholm*
GUMPERTS UNIVERSITETSBOKHANDEL AB, Box 346, *401 25 Göteborg 1*

SWITZERLAND
KARGER LIBRI AG, Petersgraben 31, *4011 Basel*

USA
ENSCO SUBSCRIPTION SERVICES, P.O. Box 1943, *Birmingham, Alabama 35201*
F. W. FAXON COMPANY, INC., 15 Southwest Park, *Westwood, Mass, 02090*
THE MOORE-COTTRELL SUBSCRIPTION AGENCIES, *North Cohocton, N. Y. 14868*
READ-MORE PUBLICATIONS, INC., 140 Cedar Street, *New York, N. Y. 10006*
STECHERT-MACMILLAN, INC., 7250 Westfield Avenue, *Pennsauken* N. J. 08110

VIETNAM
XUNHASABA, 42, Hai Ba Trung, *Hanoi*

YUGOSLAVIA
JUGOSLAVENSKA KNJIGA, Terazije 27, *Beograd*
FORUM, Vojvode Mišica 1, *21000 Novi Sad*

30. VI. 1978 HU ISSN 0001—5407 Index: 26.007

ACTA CHIMICA

ACADEMIAE SCIENTIARUM HUNGARICAE

TOMUS 96 FASCICULUS 4

AKADÉMIAI KIADÓ, BUDAPEST

1978

ACTA CHIM. ACAD. SCI. HUNG. ACASA2 96 (4) 321–412 (1978)

ACTA CHIMICA

A MAGYAR TUDOMÁNYOS AKADÉMIA KÉMIAI TUDOMÁNYOK OSZTÁLYÁNAK IDEGEN NYELVŰ KÖZLEMÉNYEI

Acta Chimica is a journal for the publication of papers on all aspects of chemistry, in the English, German, French and Russian.

Acta Chimica is published in 4 volumes per year. Each volume consists of 4 issues of varying size.

Manuscripts should be sent to

Acta Chimica
H-1521 Budapest, Hungary

Correspondence with the editors should be sent to the same address. Manuscripts are not returned to the authors.

Subscription: $ 36.00 per volume.

Hungarian subscribers should order from Akadémiai Kiadó, 1363 Budapest, P.O. Box 24. Account No. 215 11488.

Orders from other countries are to be sent to "Kultura" Foreign Trading Company (H-1389 Budapest 62, P.O. Box 149. Account No. 218 10990) or its representatives abroad.

Acta Chimica Academiae Scientiarum Hungaricae, Tomus 96 (4), pp. 321–332 (1978)

PRODUCT FORMATION IN THE PHOTOLYSIS OF *n*-BUTYRALDEHYDE

S. FÖRGETEG, T. BÉRCES and S. DÓBÉ

(Reaction Kinetics Research Group of the Hungarian Academy of Sciences, Szeged)

Received March 14, 1977

Experimental technique and preliminary results of a detailed study of the photolysis of *n*-butyraldehyde at 313 nm wavelength are described. Twenty photolysis products were identified in the vapour phase and in isooctane. Product quantum yields at 298 K and 3×10^{-10} mol photon $cm^{-2}\,s^{-1}$ light intensity are given, and the major routes of product formation discussed. Seven photochemical primary processes were established to occur both in the vapour phase and in solution.

Subsequent to the early paper by LEIGHTON *et al.* [1], the work carried out in the laboratory of F. E. BLACET elucidated most of the basic mechanistic features of the vapour phase photolysis of *n*-butyraldehyde [2, 3]. It was shown that propane, propylene, *n*-hexane and carbon monoxide were formed in a chain reaction; ethylene and acetaldehyde were assumed to be primary products, and hydrogen and methane were also detected. A kinetic study of the formation of the major reaction products supplied rate constants and Arrhenius parameters for some of the important free radical reactions [4].

Photolysis carried out in the presence of iodine vapour [5] has revealed that four primary processes occur; approximate values for the primary quantum yields could be determined.

Compared with the vapour phase results, very little is known about the photochemistry of *n*-butyraldehyde in solution. Cyclobutanol – a primary photochemical product – was detected by COYLE [6] and measured relative to acetaldehyde in benzene solution. LEMAIRE and co-workers studied the photolysis in *n*-heptane by observing the disappearance of the carbonyl group by a spectrophotometric method [7]. The major reaction was assumed to be triplet photoreduction. It has been concluded that photolysis is of non-chain character, and Norrish type II decomposition is of negligible importance.

The photolysis of several aldehydes, among them that of *n*-butyraldehyde, was studied by BLANK *et al.* [8] in solvents by Chemically Induced Dynamic Nuclear Polarization (CIDNP). Triplet photoreduction was found to be an efficient way of product formation and energy wastage for the systems studied.

The information available on the primary and secondary processes of the vapour phase photolysis of *n*-butyraldehyde [9] is based on the identification and measurement of simple hydrocarbons and permanent gases formed

in the reaction. Apart from acetaldehyde, no other oxygen-containing organic reaction product has been detected.

Regarding photolysis in solution, no detailed study of product formation has been attempted so far, thus neither the primary nor the secondary processes can be regarded as established. In this paper we report the analytical results of the study of product formation in the photolysis of *n*-butyraldehyde at 313 nm in the vapour phase and in isooctane at room temperature, at one aldehyde concentration and light intensity. A systematic study of the quantum yields of product formation at various aldehyde concentrations, light intensities and temperatures is in progress; the experimental results together with a detailed kinetic analysis of the primary and secondary processes will be reported in forthcoming papers [17, 18].

Experimental

Materials

n-Butyraldehyde was obtained from FLUKA AG and was purified by precipitation with sodium hydrogen sulfite. The recovered aldehyde was dried and further purified by 5-fold distillation in vacuum. The purified sample contained about 0.5 % isobutyraldehyde.

The isooctane solvent, obtained from FLUKA AG and purified by distillation on a high performance column, contained only saturated C_8 and some C_7 hydrocarbons as impurities.

Identification by gas chromatography and mass spectrometry was performed by comparison with retention times and mass spectra of authentic samples from the following sources. 1-Butanol was obtained from REANAL, cyclobutanol and 4-heptanol were prepared from the appropriate ketones by reduction with lithium aluminium hydride. 4-Heptanone and 5-hydroxy-4-octanone (butyroin) were synthesized by standard methods [10]. Dibutyril was obtained as a byproduct of the butyroin synthesis. 2-Ethyl-1-pentanal was prepared by aldol condensation of *n*-valeraldehyde and acetaldehyde and subsequent hydrogenation [11].

Preparation of the samples to be photolyzed

The vapour phase samples were prepared by direct expansion of the aldehyde vapour into the evacuated reaction cell.

Isooctane solvent containing isopentane (an internal standard) of known concentration (about 0.005 mol dm^{-3}) was thoroughly degassed via repeated freeze-thaw cycles. The solution of *n*-butyraldehyde was prepared in a vacuum line. The concentration of *n*-butyraldehyde was determined by chromatography.

Irradiation and light intensity measurements

Irradiation was carried out in cylindrical quartz cells equipped with greaseless Teflon valves and with plane-parallel ULTRASIL windows on both ends. The internal diameters of the cells used in the vapour phase experiments was 36 mm, while the optical path length was 25 and 50 mm. Irradiation of solution was carried out in a cuvette of 22 mm i.d. and 10 mm length. The cell temperature was kept constant by means of a thermostating jacket.

The irradiation line, installed on an optical bench, is outlined in Fig. 1. The light source was an OSRAM 200 W super pressure mercury lamp mounted in a metal house. ULTRASIL quartz lenses L_1, L_2 and L_3 as well as diaphragms D_1 and D_2 served to obtain a nearly parallel but slightly convergent beam. A third diaphragm D_3 cut the cross-section of the beam to the size adequate to fill almost completely the irradiation cell C. Irradiation could be started or interrupted by moving shutter S.

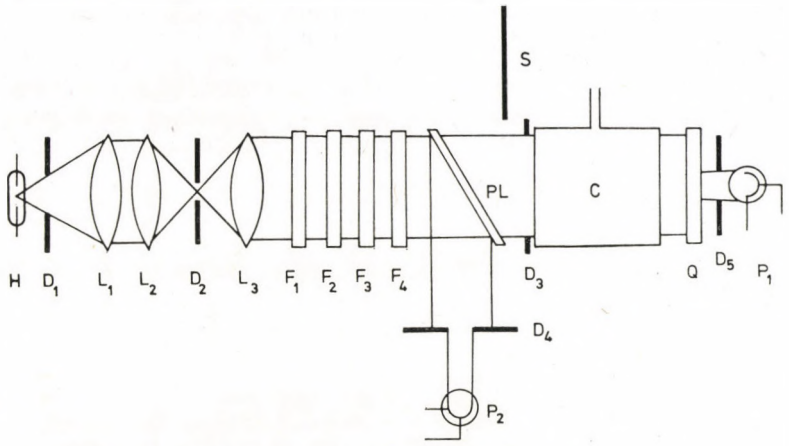

Fig. 1. Design of the irradiation line

A band in the 313 nm region was isolated using a combination of a 4 mm thick (SCHOTT UG 11) glass and three solution filters: (i) a $NiSO_4 - CoSO_4$ filter of 25 mm optical depth (64 g $NiSO_4.6H_2O$ + 10 g $CoSO_4.6H_2O$ + 100 cm^3 H_2O); (ii) a potassium chromate filter of 25 mm optical depth (5×10^{-4} mol dm^{-3} K_2CrO_4); (iii) a potassium biphthalate filter of 10 mm optical depth (0.0245 mol dm^{-3} $KHC_8H_4O_4$). The filtered light had a width of 3 nm at the half height of band.

Light intensities were measured by means of a PRESSLER DGL 490a vacuum photocell (P_1). In order to reduce the light intensity, a fluorescent screen (Q) was placed between C and P_1. This was similar to PARKER's quantum counter [12]. The whole quantum counter system was calibrated against a ferrioxalate actinometer [13]. The calibration was shown to be linear in the light intensity range used by us for irradiation ($2 \times 10^{-11} - 3 \times 10^{-9}$ mol photon cm^{-2} s^{-1}).

Much attention was paid to maintain constant light intensity during irradiation. Therefore, a power supply unit was developed for the mercury arc which regulated the lamp current to maintain the filtered light intensity constant at a pre-set value. This was accomplished by a feedback system, the sensing element of which was photocell P_2 (type DGL 490a) placed behind the beam splitter PL. With this controlling system the long range drift of the intensity of the exciting light was kept within ± 2 %. The short range stability was better than the accuracy of the readings, corresponding to about ± 0.2 % of the intensity.

Identification of the products and quantitative analyses of the irradiation samples

Taking into consideration the different character and large number of the products to be analyzed, a pre-separation of the irradiated sample was carried out and various analytical methods were used.

The reaction cell containing the irradiated sample was attached to a vacuum line. The whole content of the cell (vapour or solution) was led through a trap cooled to liquid air temperature where the condensable compounds were trapped, while the non-condensable products were collected at the end of the line by a TOEPLER pump and their volume was measured in a gas burette. The condensable compounds were transferred to a small tube attached to the bottom of the trap, and the tube was sealed off. In handling irradiated vapour samples, this attached small tube was filled prior to the whole procedure with a known amount of deaerated isooctane containing isopentane and cyclohexanone as internal standards (of known concentration).

With the exception of the determination of the CO content of the gas fraction – which was measured by the classical gas analysis method of BLACET, MCDONALD and LEIGHTON [14] – the products were analyzed by gas chromatography. Nitrogen carrier gas was used and flame ionization detection was applied, except for hydrogen measurements. Peak areas were

measured against that of an internal standard (either isopentane or cyclohexanone) or against the peak area of a product the amount of which in the sample was already known from another analyses. Altogether six column were required for quantitative and qualitative analysis:

(i) 2.5 m Molecular Sieve 5A, stainless steel tube of 6 mm i.d. at 343 K (for H_2);
(ii) 1.8 m Alumina, stainless steel tube of 6 mm i.d. at 373 K (for gaseous hydrocarbons);
(iii) 3.0 m Porapak QS deactivated with 0.5 % Apiezon L, stainless tube of 2.5 mm i.d. at 443 K (for hydrocarbons and aldehydes);
(iv) 30 m SCOT column with Carbowax 20M stationary phase, 0.25 mm i.d. at 383 K (oxygen containing compounds);
(v) 3.6 m 20 % Carbowax 20M column, stainless steel tube of 2.5 mm i.d. at 403 K (for butyroin);
(vi) 1.6 m 15 % Carbowax 20M terephthalic acid terminated, stainless steel tube of 6 mm i.d. at 403 K (for preparative work).

The hydrocarbons were identified by comparing their retention times with those of the corresponding pure substances. Identification of the oxygen-containing compounds was carried out by mass spectrometry, by comparing their spectra with those of authentic samples. Samples subjected to mass spectrometric analysis were concentrated by preparative gas chromatography. Mass spectra were taken on a FINNIGAN 1015 SL instrument. The columns used to separate the components before the mass spectrometer were identical with those used in routine quantitative analyses.

Different procedures for handling after irradiation and for analysis had to be applied in the case of formaldehyde and glyoxal. These compounds were extracted from the irradiated vapour or solution samples under air-free conditions by shaking with 3 cm^3 degassed water: chloroform was added in order to diminish the solubility of formaldehyde and glyoxal in isooctane. Unreacted *n*-butyraldehyde was removed by shaking the aqueous extracts with 1.5 cm^3 chloroform. Formaldehyde was determined by the procedure of BRICKER and JOHNSON [15]. Analysis of glyoxal was carried out by the 2.4-dinitrophenilhydrazine method [16]; extraction with 3×1 cm^3 benzene was made before the spectrophotometric measurement.

Results and discussion

Measurements were made at room temperature, 313 nm wavelength, 3×10^{-10} mol photon cm^{-2} s^{-1} light intensity and at 5.4×10^{-3} mol dm^{-3} and 1.1×10^{-2} mol dm^{-3} *n*-butyraldehyde concentrations in the vapour phase and in isooctane. The quantum yields of product formation are given in Tables I and II where each figure is the average of 2 or 3 determinations.

Altogether 20 products were identified. The formation of a higher molecular weight polymeric compound (or compounds) was detected by observing small drops or solid particles on the wall of the cuvette in which several experiments had been carried out. Indirect evidence for polymer formation is obtained from the comparison of the quantum yields of the products given in Tables I and II with the quantum yields of *n*-butyraldehyde consumption. The reproducibility of the yield of aldehyde consumption was poor in the vapour phase experiments, indicating that the surface may play a part in polymer formation; the quantum yield obtained was around 1.8 ± 0.6. A value of 0.9 ± 0.2 could be determined for aldehyde consumption in isooctane solution. These figures should be compared with 0.80 ± 0.01 and 0.68 ± 0.03, *i.e.* the yields of aldehyde consumption in the vapour phase and in isooctane, respectively, accounted for by the products indicated in the tables.

The products of *n*-butyraldehyde photolysis are formed with very different efficiencies, the quantum yields varying over four orders of magnitudes. In order to be able to measure the minor products with sufficient accuracy, the conversion had to be increased up to about 15 %. Therefore, the knowledge of the possible dependence of the quantum yields on conversion was required. In Tables I and II, the product quantum yields are given at various extents

Table I

Quantum yields of product formation in the vapour phase photolysis of n-butyraldehyde at $\lambda = 313$ *nm,* $I_0 = 3.1 \times 10^{-10}$ *mol photon* cm^{-2} s^{-1}, $[C_3H_7CHO]_0 = 5.4 \times 10^{-3}$ *mol* dm^{-3}, $T = 298$ *K*

Product \ Conversion	2.8%	6.7%	11.4%	18.0%
C_2H_4	0.17	0.16	0.17	0.17
CH_3CHO	0.17	0.16	0.16	0.16
cyclo-C_4H_7OH	0.025	0.025	0.026	0.026
CO	0.51	0.56	0.55	0.55
C_3H_8	0.34	0.32	0.35	0.33
C_3H_6	0.018	0.020	0.017	0.019
C_6H_{14}	0.09	0.11	0.09	0.10
$C_3H_7COC_3H_7$	0.005	0.008	0.007	0.007
$C_3H_7COCOC_3H_7$			0.00004	0.00005
$C_3H_7CH(C_2H_5)CHO$	0.002	0.003	0.003	0.002
H_2	0.011	0.011	0.012	0.012
CH_2O	0.023	0.022	0.021	0.020
$(CHO)_2$	0.001	0.001	0.001	0.002
CH_4	0.0003	0.0005	0.0003	0.0005
C_2H_6	0.0002	0.0002	0.0002	0.0003
n-C_4H_{10}	0.002	0.0007	0.0008	0.0006
n-C_5H_{12}	0.0001	0.0001	0.0004	0.0005
n-C_4H_9OH	0.013	0.014	0.016	0.016
$C_3H_7CH(OH)C_3H_7$	0.014	0.010	0.015	0.012

of reaction from 3 to 18 % conversion. (The conversions indicated were obtained from the yields of the reaction products.) With the exception of *n*-pentane formation in the vapour phase, the products are seen to be formed with an efficiency independent of conversion. The determination of the quantum yields for the major hydrocarbon products C_2H_4 and C_3H_8 were extended down to 0.2 % conversion with the same results as indicated in the tables.

Table II

Quantum yields of product formation in the photolysis of n-butyraldehyde in isooctane at $\lambda = 313$ nm, $I_0 = 3.4\times10^{-10}$ mol photon $cm^{-2}\,s^{-1}$, $[C_3H_7CHO]_0 = 1.1\times10^{-2}$ mol dm^{-3}, $T = 298$ K

Product \ Conversion	2.9%	6.5%	13.2%	16.5%
C_2H_4	0.14	0.12	0.11	0.13
CH_3CHO	0.13	0.12	0.12	0.13
cyclo-C_4H_7OH		0.025	0.03	0.02
CO	0.46	0.49	0.41	0.39
C_3H_8	0.44	0.43	0.39	0.43
C_3H_6	0.008	0.008	0.006	0.008
C_6H_{14}	0.006	0.003	0.004	0.003
$C_3H_7COC_3H_7$		0.003	0.006	0.003
$C_3H_7COCOC_3H_7$		0.001	0.001	0.001
$C_3H_7CH(C_2H_5)CHO$		traces	traces	traces
H_2		0.001	0.001	0.001
CH_2O		0.004		
CH_4		0.0003	0.0004	0.0004
C_2H_6		0.0004	0.0006	0.0008
n-C_4H_9OH		0.06	0.08	0.04
$C_3H_7CH(OH)C_3H_7$		0.02	0.02	0.01
$C_3H_7CH(OH)COC_3H_7$		0.01	0.01	0.01

Primary photochemical processes

The average values of the product quantum yields obtained in the vapour phase and in isooctane solution are summarized in Table III. It may be seen from the table that the products formed in photolysis in the vapour phase and in isooctane are essentially the same and the distribution of the products is similar too. Seven primary processes have to be assumed to explain the experimental results:

$$C_3H_7CHO \rightarrow \dot{C}_3H_7 + \dot{C}HO \qquad (I)$$

$$C_3H_7CHO \rightarrow C_3H_8 + CO \qquad (I')$$

$$C_3H_7CHO \rightarrow C_2H_4 + CH_3CHO \qquad (II)$$

$$C_3H_7CHO \rightarrow \text{cyclobutanol} \qquad (II')$$

$$C_3H_7CHO \rightarrow \dot{C}H_3 + \dot{C}H_2CH_2CHO \qquad (III)$$

$$C_3H_7CHO \rightarrow \dot{C}_2H_5 + \dot{C}H_2CHO \qquad (III')$$

$$C_3H_7CHO + C_3H_7CHO \rightarrow C_3H_7\dot{C}HOH + \dot{C}_3H_7CO \qquad (IV)$$

Table III

Quantum yields of product formation (average values) in the photolysis of n-butyraldehyde in the vapour phase and isooctane at 313 nm and room temperature

Products	Vapour phase	Isooctane
C_2H_4	0.17	0.12
CH_3CHO	0.16	0.12
cyclo-C_4H_7OH	0.026	0.025
CO	0.55	0.44
C_3H_8	0.34	0.42
C_3H_6	0.019	0.008
C_6H_{14}	0.10	0.003
$C_3H_7COC_3H_7$	0.007	0.004
$C_3H_7COCOC_3H_7$	0.00005	0.001
$C_3H_7CH(C_2H_5)CHO$	0.003	trace
H_2	0.012	0.001
CH_2O	0.021	0.004
$(CHO)_2$	0.001	
CH_4	0.0004	0.0004
C_2H_6	0.0002	0.0006
n-C_4H_{10}	0.0007	
n-C_5H_{12}	0.0001 – 0.0005	
n-C_4H_9OH	0.02	0.06
$C_3H_7CH(OH)C_3H_7$	0.02	0.02
$C_3H_7CH(OH)COC_3H_7$		0.01

Reaction I, the decomposition of *n*-butyraldehyde into *n*-propyl and formyl radicals, is a major primary photochemical process both in the vapour phase and in isooctane as indicated by the formation of various combination and disproportionation products of C_3H_7 and CHO radicals (see below). The occurrence of type I decomposition in vapour phase photolysis was thoroughly established by BLACET and CALVERT [3, 5], however, there is hardly any evidence available so far for process I in solution. Since any radical-sensitized decomposition of the aldehyde may give most (but not all) of the products formed in the secondary reactions initiated by type I decomposition, a detailed study of product formation is being carried out at various aldehyde concentrations, light intensities and temperatures in the vapour phase and in solution in order to determine the primary quantum yields for reaction I [17, 18].

Reaction I' cannot be proved on the basis of our results, however, experiments carried out by BLACET and CALVERT in the presence of iodine [5] have

provided convincing evidence for the occurrence of this reaction in the vapour phase. The process was found to be of minor importance at 313 nm where a primary quantum yield of 0.02 was obtained.

Reaction II is the well-known Norrish type II decomposition characteristic of the photolyses of carbonyl compounds with γ-hydrogen atoms. The quantum yields for ethylene and acetaldehyde formation were found to be equal both in the vapour phase and in isooctane as expected for this type of process. Norrish type II decomposition was shown to occur *via* a 1,4-biradical intermediate [19].

Reaction II' is a primary process analogous to type II decomposition; both occur *via* the same 1,4-biradical formed in intramolecular γ-hydrogen transfer. Cyclobutanol has been detected as a photolysis product of *n*-butyraldehyde in benzene solution by COYLE [6], however it has not been observed so far in the vapour phase.

Reaction between an excited state of a carbonyl compound and a ground state hydrogen donor molecule yielding photoreduction products was shown [8, 20] to play an important role in the photochemistry of aliphatic aldehydes at higher concentrations in solution. LEMAIRE and co-workers [7] demonstrated the occurrence of photoreduction in the photolysis of *n*-butyraldehyde in *n*-heptane, although the reaction products were not identified. The *n*-butanol, 4-heptanol and 5-hydroxy-4-octanone (butyroin) detected in this work prove that process IV — the reaction between an excited and a ground state *n*-butyraldehyde molecule — does occur both in the vapour phase and in solution.

The quantum yield of reaction IV is expected to increase with increasing aldehyde concentration. Thus the higher quantum yield of *n*-butanol and 4-heptanol formation found in isooctane may be accounted for by the higher *n*-butyraldehyde concentration used in our solution experiments. (It is to be pointed out, however, that excited aldehyde molecules may react with the solvent in a reaction analogous to process IV.) On this basis one may conclude that the increased efficiency of reaction IV in isooctane is responsible for the lower quantum yield of the type II decomposition in solvent compared with that in the vapour phase.

Two more primary processes have to be assumed on the basis of our experimental results, in which alkyl radicals are split off from the propyl group of *n*-butyraldehyde. Reaction III was shown to occur in vapour phase photolysis by BLACET and CALVERT [3, 5], while reaction III' has not been assumed so far. The analytical and kinetic evidences supporting primary processes III and III' will be given below.

Primary processes II and II' produce stable products being characteristic of these reactions, however, radicals are formed in primary reactions I, III, III' and IV, which are followed by secondary photochemical processes. The elucidation of the mechanism of the secondary processes and the determi-

nation of the primary quantum yields will be possible only on the basis of a kinetic treatment of experimental results obtained at various aldehyde concentrations, light intensities and temperatures [17, 18]. In the rest of this paper we intend to outline the major routes of product formation, to point out some characteristic differences between free radical reactions in the vapour phase and in isooctane, and to reveal certain data which support the primary processes assumed.

Reactions of n-propyl and formyl radicals

The main radical source in the photolysis of *n*-butyraldehyde at low aldehyde concentrations is primary reaction I, in which *n*-propyl and formyl radicals are formed. Two formyl radicals may react in three different ways forming carbon monoxide, hydrogen, formaldehyde and glyoxal. It is expected, however, that most formyl radicals disproportionate with propyl radicals forming CO and C_3H_8.

Almost half of the secondary products identified are formed in various combination and abstraction reactions of the *n*-propyl radical. It is to be taken into account, however, that in addition to reaction I, *n*-propyl radicals may be formed in reaction chains initiated by the abstraction of the formyl hydrogen of *n*-butyraldehyde by a free radical, and subsequent decomposition of the butyryl radical into C_3H_7 and CO.

Apart from the small amount of C_3H_8 directly formed in reaction I', propane is produced in hydrogen abstraction and disproportionation reactions of n-C_3H_7 radicals. Self-disproportionation and combination of *n*-propyl radicals are responsible for the formation of propylene and *n*-hexane, respectively. The disproportionation to combination ratio calculated from the propylene and *n*-hexane quantum yields measured in the vapour phase is $\Delta(n\text{-}C_3H_7, n\text{-}C_3H_7) = 0.19 \pm 0.01$. This is close to the literature value [21], indicating that self-disproportionation of *n*-propyl radicals is the only significant source of propylene in the vapour phase. On the other hand the ratio of the quantum yields of propylene and *n*-hexane in isooctane is more than an order of magnitude higher, suggesting the occurrence of some other major source of propylene in the liquid phase. The most probable reaction is the cross-disproportionation reaction between *n*-propyl and isooctyl radicals.

One observes a very significant difference in the quantum yields of *n*-hexane formation in the two phases which clearly demonstrates that the propyl radical concentration is much lower in isooctane than in the vapour phase. The low propyl radical concentration in isooctane may be caused by the reaction of these radicals with the solvent.

Reactions of the butyryl radicals

Butyryl radicals are formed in the primary process IV and mainly in the reaction chain. In addition to the decomposition into C_3H_7 and CO, the butyryl radicals enter various combination reactions (dibutyryl, 4-heptanone and butyroin formation). Taking into account the cross-, and self-combination products of *n*-propyl and butyryl radicals, one can calculate the cross-combination ratio $[C_3H_7COC_3H_7]/[C_6H_{14}]^{1/2}\,[C_3H_7COCOC_3H_7]^{1/2}$. Values of 3.1 and 2.3 are obtained for the vapour phase and for isooctane, respectively. The cross-combination ratio for alkyl radicals has been shown to be close to the value of 2 [21, 22], however, very little is known of these ratios for other radicals. In spite of the considerable error limits that may be estimated for our values given above, the cross-combination ratio for the *n*-propyl and butyryl radical pairs seems definitely higher than 2.

The efficiency of recombination of butyryl radicals, like that of *n*-propyl radicals, is very different in the vapour phase and in isooctane. The quantum yield of dibutyryl formation was found to be considerably higher in isooctane than in the vapour phase (as opposed to that found for *n*-hexane), which indicates higher butyryl concentration in isooctane compared with the vapour phase.

Formation and reaction of the $CH_3CH_2\dot{C}HCHO$ radical

The identification of 2-ethyl-pentanal-1, formed by the combination of $CH_3CH_2\dot{C}HCHO$ and C_3H_7 radicals, shows that beside formyl hydrogens the hydrogen atoms in the α-position to the carbonyl group may also be abstracted. The low quantum yield of 2-ethyl-pentanal-1 formation in isooctane is a consequence of the low concentration of propyl radicals.

Reactions of the 1-hydroxy-1-butyl radical

The *n*-butanol, 4-heptanol and 5-hydroxy-4-octanone (butyroin) are undoubtedly hydrogen abstraction and combination products of 1-hydroxy-1-butyl radicals. This radical is formed in primary process IV, *via* hydrogen atom abstraction by an excited aldehyde molecule from a ground state aldehyde molecule (and to some extent from isooctane in the solution experiments). Other possibilities of the formation of 1-hydroxy-1-butyl radicals may be considered, thus hydrogen atom transfer from a formyl radical to the carbonyl oxygen of *n*-butyraldehyde, or the hydrogen atom abstraction reactions of the 1,4-biradical intermediate of primary processes II and II'. While the first possibility is not compatible with the detailed kinetic analysis of the results

obtained at various aldehyde concentrations in isooctane [18], the latter possibility may be ruled out on the basis of the results of deuterium labelling experiments [17].

Reactions of CH_3 and C_2H_5 radicals

Finally, the evidence supporting the assumption of the minor primary processes III and III' have to be considered. The formation of low molecular weight hydrocarbon products indicates the presence of simple alkyl free radicals such as CH_3 and C_2H_5.

Methane is obviously formed in reactions of methyl radicals originating from primary process III. The possibility of methyl radical production (with a commensurable rate) by secondary photolysis or radical sensitized decomposition of acetaldehyde may be rejected as the methane yield was found to be independent of conversion.

Ethane may either be formed in reactions of the ethyl radicals originating from primary process III' or by combination of methyl radicals. On the other hand the *n*-butane identified is undoubtedly the result of combination of C_3H_7 and CH_3 radicals. (The contribution of ethyl recombination to *n*-butane formation cannot be significant since the concentration of C_3H_7 radicals is seen from the corresponding product yields to be several orders of magnitude higher than that of the C_2H_5 radicals.) If ethane is a recombination product of methyl radicals then the cross-combination ratio for the methyl-*n*-propyl radical pair should be close to the value of 2 established for alkyl radicals [21, 22]. The ratio $[C_4H_{10}]/[C_2H_6]^{1/2}\,[C_6H_{14}]^{1/2}$ calculated from the product quantum yields obtained in the vapour phase is 0.15 ± 0.04, one order of magnitude lower than the literature value. This means that an ethyl radical source, *i.e.* reaction I, II', has to be assumed to account for the experimental yield of ethane.

n-Pentane is expected to be formed as a result of combination of C_3H_7 and C_2H_5 radicals. However, the definite dependence of the *n*-pentane quantum yield on the conversion indicates that there is a significant contribution to n-C_5H_{12} formation by secondary reactions with the participation of reaction products. We suggest that these secondary reactions are the addition of *n*-propyl radicals to ethylene and subsequent hydrogen abstraction by the *n*-pentyl radicals.

Strong support for the suggestion that *n*-propyl radicals play a part in the formation of n-C_4H_{10} and n-C_5H_{12} is provided by the fact that in isooctane, where the propyl radical concentration is low, these products are not detected.

*

The authors are indebted to Dr. I. SZILÁGYI for the mass spectrometric analyses and to Dr. Á. NACSA for help in the syntheses of compounds used for identification.

REFERENCES

[1] LEIGHTON, P. A., LEVANS, L. D., BLACET, F. E., ROWE, R. D.: J. Amer. Chem. Soc., **59**, 1843 (1937)
[2] BLACET, F. E., CRANE, R. A.: J. Amer. Chem. Soc., **76**, 5337 (1954)
[3] BLACET, F. E., CALVERT, J. G.: J. Amer. Chem. Soc., **73**, 661 (1951)
[4] KERR, J. A., TROTMAN-DICKENSON, A. F.: Trans. Faraday Soc., **55**, 572 (1959)
[5] BLACET, F. E., CALVERT, J. G.: J. Amer. Chem. Soc., **73**, 667 (1951)
[6] COYLE, J. D.: J. Chem. Soc (B), **1971**, 2254
[7] LEBOURGEOIS, P., ARNAUD, R., LEMAIRE, J.: J. Chim. Phys., **71**, 481 (1974)
[8] BLANK, B., HENNE, A., LAROFF, G. P., FISCHER, H.: Pure Appl. Chem., **41**, 475 (1975)
[9] BÉRCES, T.: The Decomposition of Aldehydes and Ketones, in Comprehensive Chemical Kinetics (Ed.: C. H. BAMFORD and C. F. H. TIPPER), Vol. V, p. 234. Elsevier Publ. Co., Amsterdam 1972
[10] BLATT, A. H. (Editor): Organic Syntheses, Collective Volume 2. John Wiley and Sons, London 1943
[11] MÜLLER, E. (Editor): Methoden der organischen Chemie (Houben-Weyl), Sauerstoffverbindungen II, Teil I, Aldehyde, p. 82, 4. Aufl., Georg Thieme Verlag, Stuttgart 1954; SKITA, A.: Ber. deutschen chem. Ges., **48**, 1491 (1915)
[12] PARKER, C. A.: Photoluminescence of Solutions, p. 204. Elsevier Publ. Co., Amsterdam 1968
[13] HATCHARD, C. G., PARKER, C. A.: Proc. Roy. Soc., A, **235**, 518 (1956); BAXENDALE, J. H., BRIDGE, N. K.: J. Phys. Chem., **59**, 783 (1955)
[14] BLACET, F. E., MCDONALD, G. D., LEIGHTON, P. A.: Ind. Eng. Chem. Anal. Ed., **5**, 272 (1933)
[15] BRICKER, C. E., JOHNSON, H. R.: Ind. Eng. Chem. Anal. Ed., **17**, 400 (1945)
[16] SANDERS, E. B., SCHUBERT, J.: Anal. Chem., **43**, 59 (1971)
[17] FÖRGETEG, S., BÉRCES, T., DÓBÉ S.: to be published
[18] FÖRGETEG, S., BÉRCES, T.: to be published
[19] WAGNER, P. J., ZEPP, R. G.; J. Amer. Chem. Soc., **94**, 287 (1972); WAGNER, P. J., KELSO, P. A., ZEPP, R. G., *ibid.*, **94**, 7480 (1972)
[20] CHEN, H. E., COCIVERA, M., VAISH, S. P.: Canad. J. Chem., **53**, 2548 (1975)
[21] TERRY, J. O., FUTRELL, J. H.: Canad. J. Chem., **45**, 2327 (1967)
[22] KERR, J. A., TROTMAN-DICKENSON, A. F.: in Progress in Reaction Kinetics (Ed.: G. S. Porter), p. 107. Pergamon Press, New York 1961.

Sándor FÖRGETEG
Tibor BÉRCES
Sándor DÓBÉ

H-6701 Szeged, P. O. Box 105.

Acta Chimica Academiae Scientiarum Hungaricae, Tomus 96 (4), pp. 333–336 (1978)

ULTRASONIC INVESTIGATION OF MOLECULAR INTERACTIONS IN THE LIQUID STATE

SH. PRAKASH, O. PRAKASH, K. S. DWIVEDI and S. SINGH

(Chemical Laboratories, University of Allahabad, Allahabad, India)

Received April 13, 1977

The molecular interactions in the binary systems **(I)** *n*-butanol–ethyleneglycol (303.15 K), **(II)** *n*-butanol–isoamyl alcohol (303.15 K) were studied by ultrasound velocity measurements. Adiabatic compressibility, intermolecular free length, molar volume and available volume variations with the composition have been determined. The results are discussed in the light of molecular interactions.

Introduction

Attempts have been made by several workers [1–5] to study the behaviour of binary liquid mixtures by measuring ultrasound velocity and calculating related parameters. The variation of velocity and adiabatic compressibility is not always linear. The non-linearity may be explained on the basis of molecular dimensions and forces acting between the molecules. BHIMSENACHAR *et al.* [6] have calculated the excess free length and correlated it with the strength of interaction.

In the present paper we have calculated the adiabatic compressibility, intermolecular free length, molar volume and available volume from velocity and density data for the systems (I) *n*-butanol–ethyleneglycol (II) *n*-butanol–isoamyl alcohol. Sound velocity, density and compressibility variations are shown graphically.

Theory and calculations

JACOBSON [7] has introduced the concept of intermolecular free length in order to explain the ultrasound velocity in pure liquids and liquid mixtures. The intermolecular free length L_f, is the distance covered by a sound wave between the surfaces of the neighbouring molecules and is given by the equation

$$L_f = K\sqrt{\beta}$$

where K is a temperature dependent constant. Adiabatic compressibility was calculated from $\beta = v^{-2}\varrho^{-1}$; V_a, the available volume has been computed using the relation

$$V_a = V\left(1 - \frac{v}{v_\alpha}\right)$$

where V is the molar volume, v is the ultrasound velocity and $v_\alpha = 1600\,\text{m/s}$. Molar volume V has been evaluated from the equation

$$V = \frac{X_1M_1 + X_2M_2}{X_1 + X_2} \cdot \frac{1}{\varrho}$$

where X_1 and X_2 are the mole fractions of the two components, M_1 and M_2 are the molecular weights of the respective components, and ϱ is the density of the mixture.

Experimental

All the chemicals used were of BDH Analar grade and were further purified by standard methods described by WEISSBERGER [8]. Solutions of different compositions were prepared by mixing appropriate volumes of liquids in cleaned and dry flasks and were left to stand for some time to attain equilibrium. Care has been taken to minimize losses due to evaporation of components during mixing. Solutions were transferred to the ultrasonic cell for velocity measurements. The instrument and method of velocity measurements have been described before [9]. The frequency used was 5 MHz and the temperature was maintained at 303.15 K. Densities were measured in pyrex pyknometers and compared well with literature values. The probable error in velocity was 0.2 % and the accuracy of density was 1 in 10^4.

Results and discussion

Figure 1 shows the density, ultrasonic velocity and compressibility of *n*-butanol–ethyleneglycol mixtures as a function of the mole fraction of *n*-butanol. Figure 2 gives the density, ultrasonic velocity and compressibility of the *n*-butanol–isoamyl alcohol system. The density decreases with increasing mole fraction of *n*-butanol in both the cases but the mode of decrease is different in the two systems. The velocity curve is concave upwards in both cases. In the *n*-butanol–isoamyl alcohol system, there is some increase in velocity at higher concentrations of *n*-butanol. On the basis of the mode of sound propagation given by EYRING *et al.* [10], an increased free length in solution due to the process of mixing results in the lowering of sound velocity, which gives the velocity *vs.* mole fraction plot a concave upward shape. Our results are in conformity with this fact. As expected, the compressibility increases with increasing mole fraction of *n*-butanol in both cases. The free length,

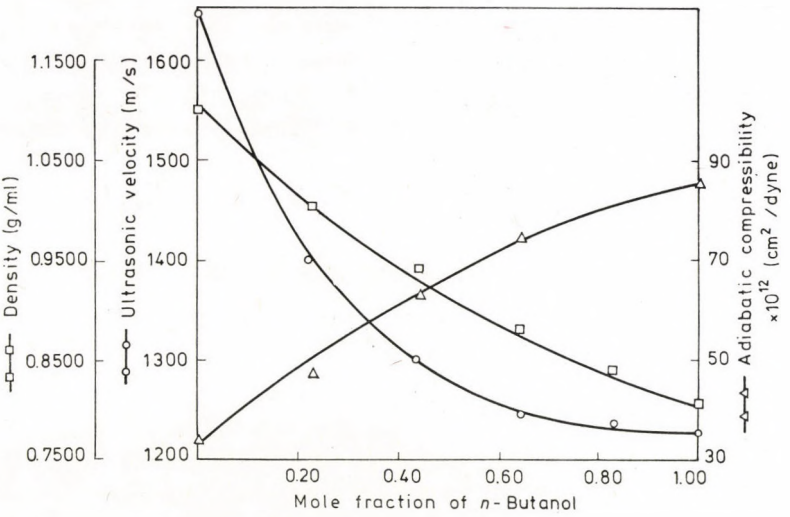

Fig. 1

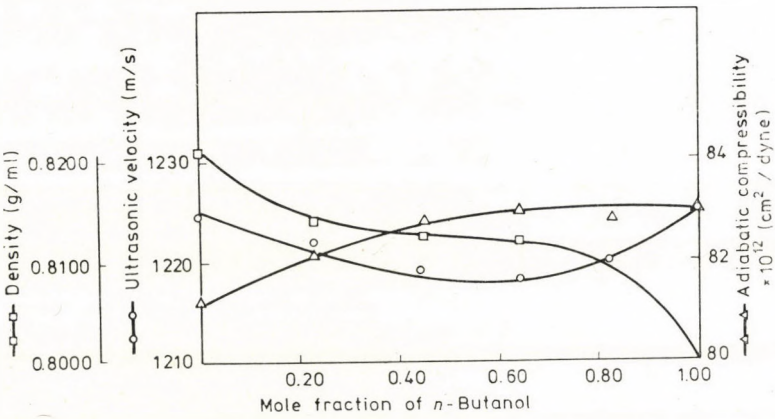

Fig. 2

molar volume and available volume for the two systems is presented in Tables I and II. The free length increases with increasing mole fraction of *n*-butanol. This increase is less in *n*-butanol–isoamyl alcohol. The molar volume and available volume increase with mole fraction for the former but decrease with mole fraction in the latter system. The liquids used are polar and associating in nature. The dissociating effect of the second liquid on *n*-butanol should result in the decrease of free length and hence compressibility. However, because of the decrease in cohesive energy due to the interaction between the components of the mixture, the overall effect is that of increase in free length and compressibility as has been observed here.

Table I

n-Butanol–ethyleneglycol, Temperature 303.15 K

No.	Mole fraction of *n*-butanol	Free length (A°)	Molar volume (ml/mol)	Available volume (ml/mol)
1	0.0000	0.3650	56.10	1.58
2	0.2274	0.4271	63.83	7.94
3	0.4396	0.5008	71.50	13.50
4	0.6397	0.5426	78.73	17.87
5	0.8252	0.5585	85.73	19.72
6	1.0000	0.5751	92.39	21.65

Table II

n-Butanol–isoamyl alcohol, temperature 303.15 K

No.	Mole fraction of *n*-butanol	Free length (A°)	Molar volume (ml/mol)	Available volume (ml/mol)
1	0.0000	0.5689	107.40	25.24
2	0.2291	0.5720	104.20	24.61
3	0.4422	0.5735	100.80	24.02
4	0.6408	0.5738	97.66	23.32
5	0.8263	0.5744	94.45	22.44
6	1.0000	0.5751	92.39	21.65

REFERENCES

[1] FORT, R. J., MOORE, W. R.: Trans. Faraday Soc., **61,** 2102 (1965)
[2] PRAKASH, S., SRIVASTAVA, S. B., PRAKASH, O.: J. Chim. Phys. **12,** 115 (1975)
[3] PRAKASH, S., PRASAD, N., SINGH, R., PRAKASH, O.: J. Pure Appl. Phys., **14,** 676 (1976)
[4] KAULGUD, M. V., PATIL, K. J.: Ind. J. Pure Appl. Phys., **13,** 322 (1975)
[5] NURMI, V., TUOMIKOSKI, P.: Comment. Phys. Maths., **10,** 11 (1940)
[6] REDDY, K. C., SUBRAHMANYAM, S. V., BHIMSENACHAR, J.: J. Phys. Soc. Japan, **19,** 559 (1964)
[7] JACOBSON, B.: Acta Chem. Scand., **6,** 1485 (1952)
[8] WEISSBERGER, A.: Techniques of Organic Chemistry, Vol. 7, Interscience, New York
[9] CHATURVEDI, C. V., PRAKASH, S.: Acta Chim. (Budapest) **72,** 289 (1972)
[10] EYRING, H., KINCAID, J. F.: J. Chem. Phys. **6,** 620 (1938)

Sheo PRAKASH
O. PRAKASH
K. S. DWIVEDI
S. SINGH

Chemical Laboratories, University of Allahabad, Allahabad, India.

Acta Chimica Academiae Scientiarum Hungaricae, Tomus 96 (4), pp. 337—354 (1978)

ON THE CORRELATION OF GEOMETRIC AND VIBRATIONAL PARAMETERS OF THE SO_2 GROUPS IN SULFONE MOLECULES

J. BRUNVOLL* and I. HARGITTAI

(Central Research Institute of Chemistry, Hungarian Academy of Sciences, H-1025 Budapest)

Received April 30, 1977

Revised empirical correlations are given between geometric and vibrational parameters of a series of simple sulfone molecules. Force constant calculations and the averaging of the S=O stretching frequencies are commented upon.

Introduction

Empirical correlations between geometric and vibrational parameters of relatively simple sulfone molecules have been established for a number of years and used extensively, see *e.g.* [1—3]. At the time of establishing the relationships [1] involving bond lengths and stretching frequencies, relatively few S=O bond lengths were available and they were considered in most cases to be less accurate than the corresponding frequencies. The same could be said for bond angles O=S=O. Because of the usefulness of the empirical relationships between the geometric and vibrational data, and since up-to-date and consistent geometric data have recently become available for a relatively large series of simple sulfone molecules (see Table I), we decided that a revision of the empirical relationships was timely. This investigation is described here and supplemented with some comments on the force constant calculations and on the averaging of the S=O stretching frequencies.

Geometric data

Vapour-phase geometric data only were used in establishing the revised relationships in order to achieve greater consistency. The vapour-phase data are usually more accurate than those from crystal-phase X-ray diffraction determinations, and they are also more well-defined since the molecule in the vapour phase can be considered unperturbed by intermolecular interactions which may well take place in the crystal phase. Electron diffraction studies have been performed for all but one ($(CH_2)_2SO_2$) molecules listed in Table I

* On leave from The University of Trondheim.

Table I

Bond distances, bond angles, symmetric and antisymmetric stretching and bending frequencies of SO_2 groups in sulfone molecules

Compounds	$r_g(S=O)$[a] (Å)	O=S=O[b] (°)	$\nu_s(S=O)$[c] (cm^{-1})	$\nu_{as}(S=O)$[c] (cm^{-1})	$\delta(SO_2)$[c] (cm^{-1})
SO_2F_2	1.398(2)[d]	125.1(2)[e]	1269	1502	544[f]
SO_2Cl_2	1.405(4)[g]	123.5(10)[g]	1182	1414	560[h]
SO_2FBr	[1.407][i]	[123.7][j]	1205	1437	564[k]
SO_2FCl	[1.408][l]	123.7(10)[m]	1228	1455	480[f]
CH_3OSO_2F	1.410(3)[n]	124.4(7)[n]	1235	1465[o]	
CH_3SO_2F	1.411(3)[ø]	123.1(15)[ø]	1223	1415	531[ö]
$C_6H_5SO_2Cl$	1.418(12)[p]	122.5(36)[p]	1186	1377	572[q]
CH_3OSO_2Cl	1.420(4)[r]	122.2(15)[r]	1192	1404	588[s]
$(CH_3)_2NSO_2Cl$	1.422(4)[t]	122.7(23)[t]	1182	1395	572[u]
CH_3SO_2Cl	1.425(3)[v]	120.8(8)[v]	1173	1378	533[w]
SO_2	1.432(2)[z]	119.3(10)[x]	1151	1362	518[y]
$(CH_3)_2NSO_2N(CH_3)_2$	1.433(10)[aa]	[120.2][bb]	1150	1335	526[u]
$(CH_3)_2SO_2$	1.436(3)[cc]	119.7(11)[cc]	1165	1343	510[dd]
$(C_6H_5)_2SO_2$	1.439(12)[ee]	[119.3][bb]	1149	1305	580[ff]
$(CH_2)_2SO_2$	1.439(6)[gg]	121.4(5)[gg]	1159	1309	446[hh]
$(CH_2=CH)_2SO_2$	1.440(4)[ii]	[119.2][bb]	1124	1320	550[jj]
$(CH_2)_4SO_2$	1.45(1)[kk]	114.6(30)[kk]	1147	1301	567[ll]

[a] Unless indicated otherwise, r_g was calculated from the electron diffraction r_a value according to the good approximation $r_g = r_a + l^2/r_a$, where l is the mean amplitude of vibration; [b] Unless indicated otherwise, determined in the electron diffraction analysis; [c] Unless indicated otherwise, liquid-phase infrared data; [d] Ref. [4]; [e] Calculated from the electron diffraction bond distance [4] and the O...O distance determined by microwave spectroscopy [5]; [f] Raman, Ref. [6]; [g] Ref. [7]; [h] Ref. [8]; [i] Assumed [9]; [j] Calculated from the assumed r(S=O) and the O...O distance determined from the microwave spectrum [9]; [k] Raman, Ref. [10]; [l] Assumed [11]; [m] Calculated from the assumed r(S=O) and the O...O distance determined from the microwave spectrum [11]; [n] Ref. [12]; [o] Ref. [13]; [ø] Ref. [14]; [ö] Ref. [15]; [p] Ref. [16]; [q] Ref. [17]; [r] Ref. [18]; [s] Ref. [19]; [t] Ref. [20]; [u] Solution, Ref. [21]; [v] Ref. [22]; [w] Ref. [23]; [z] Ref. [24]; [x] Microwave spectroscopy, Ref. [25]; [y] Gaseous phase, Ref. [26]; [aa] Ref. [27]; [bb] Calculated from r_g(S=O) and an assumed value of 2.484 Å for the O...O distance; [cc] Ref. [28]; [dd] Ref. [29] [ee] Ref. [30]; [ff] Ref. [31]; [gg] Microwave spectroscopy, r_0 parameters, Ref. [32]; [hh] Raman, Ref. [33]; [ii] Ref. [34]; [jj] Ref. [35]; [kk] Ref. [36]; [ll] Ref. [37].

and in most cases they originated from the same laboratory. In some cases microwave spectroscopic data were also utilized in the analysis (CH_3SO_2F, CH_3OSO_2F, $(CH_3)_2SO_2$), or could be used for later testing (CH_3SO_2Cl, SO_2Cl_2).* The results from both electron diffraction [4] and microwave spectroscopic [5]

* References for the microwave spectroscopic studies: CH_3SO_2F, Ref. [38]; CH_3OSO_2F, Ref. [12]; $(CH_3)_2SO_2$, Refs. [38], [39]; CH_3SO_2Cl, Ref. [40]; SO_2Cl_2, Ref. [41].

analyses were available for SO_2F_2. For reasons discussed later in more detail, the values for the S=O distance and O...O distance were taken from the electron diffraction and microwave studies, respectively, and the O=S=O bond angle was thus calculated. Although the physical meaning of the internuclear distance parameters determined by the two techniques is different, the sulfone molecules under consideration are relatively rigid systems and accordingly the electron diffraction and microwave spectroscopic distance parameters are thought to be little different as a consequence of intramolecular motion. In any case the S=O distances listed in Table I are consistent in this respect, while the O=S=O bond angles have no strictly defined physical meaning even if they come from only electron diffraction data. But again, this indeterminacy is of no great importance here, partly because of the mentioned relative rigidity,* and partly because of the large uncertainties with which these angles were determined from the electron diffraction data. Some of the O=S=O angles are especially ill-determined, since it is usually very difficult to determine reliably and accurately the O...O distance from electron diffraction. The difficulty is caused by the strong correlations among the nonbond distances around the sulfur atom and their mean amplitudes of vibration. On the other hand, the microwave spectra, although usually inadequate for a complete structure determination of the sulfone molecule, provide highly accurate information on r(O...O). All of them are, in fact, in the vicinity of 2.48 Å. It is then comforting that most O=S=O bond angles, and accordingly O...O distances, determined from electron diffraction data only, although more uncertain, are consistent with the microwave results. Some bond angles could not be determined in the electron diffraction analyses at all. For such molecules, *viz.* $(CH_2=CH)_2SO_2$, $(C_6H_5)_2SO_2$, CH_3OSO_2Cl, the O...O distance can be assumed as the average value of the accurately determined O...O distances, and accordingly the O=S=O bond angles can be calculated. They are also shown in Table I though these parameters were not then used in establishing the correlations. Three electron diffraction analyses reported O...O distances far below the 2.48 Å value. Of these, the calculations based on molecular intensities were repeated for $(CH_3)_2NSO_2N(CH_3)_2$ with assumed values for r(O...O), among them 2.48 Å. It was shown [43] that the experimental distributions could be approximated about as well as when r(O...O) refined to 2.42 Å [27]. Significantly, the other parameters showed no appreciable changes as compared with those reported [27]. The bond angle for this compound was not included into the present calculations, neither was that of $(CH_2)_4SO_2$ as it was seen to be unrealistically low.

* Calculated $K = \langle(\Delta x)^2 + (\Delta y)^2\rangle/2\,r$ correction terms may give some idea about the effects of the perpendicular vibrations. We quote here some data for $SOCl_2$ [42] at 323 K K(S=O) = 0.0014 Å, K(S−Cl) = 0.0004 Å, K(Cl...O) = 0.0002 Å, and K(Cl...Cl) = = 0.0001 Å.

Vibrational frequencies

The symmetric and antisymmetric stretching S=O and bending SO_2 frequencies used in our calculations are listed in Table I. They are similar to those used by GILLESPIE and ROBINSON [1]. They refer to liquid-phase infrared measurements unless otherwise stated. Although we would have preferred vapour-phase data, they are too scarce. It is difficult to predict the changes in frequencies corresponding to the transition from the vapour phase to the pure liquid or a dissolved state. It has been noted (see *e.g.* [2]) that the stretching frequencies in liquids are often displaced to lower frequencies and the bending frequencies to higher frequencies as compared with the vapour-phase data. Infrared gaseous and liquid data are quoted below from a study by SPOLITI *et al.* [29] showing that no trend can be established indeed with certainty, at least for the stretching frequencies

		Gas	Liquid (condensed)	Difference
CH_3SO_2F	$\nu_{as}(S=O)$, cm^{-1}	1451	1443	8
	$\nu_s(S=O)$, cm^{-1}	1225	1233	−8
	$\delta(SO_2)$, cm^{-1}	534	543	−10
CH_3SO_2Cl		1404	1386	18
		1192	1185	7
		543	548	−5
$CH_3SO_2CH_3$		1355	1343	12
		1162	1165	−3
		496	510	−14

The changes are relatively small, and significantly, the data originate from concurrent experiments. Referring to the dimethyl sulfone data, the above values are confronted below with some which refer to solid-state infrared and solution Raman spectroscopy [46]:

	Infrared	Raman
$\nu_{as}(S=O)$, cm^{-1}	1307	1289
$\nu_s(S=O)$, cm^{-1}	1143	1138
$\delta(SO_2)$, cm^{-1}	504	502

A final example, for gas-liquid comparison with considerable differences (infrared [35]) for divinyl sulfone

	Gas	Liquid	Difference
$\nu_{as}(S=O)$, cm^{-1}	1352	1310	−42
$\nu_{s}(S=O)$, cm^{-1}	1150	1124	−26

Thus we may conclude that the next step for a future refinement of the relationships between geometric and vibrational parameters may necessitate a consistent set of vapour-phase vibrational spectroscopic data.

The S=O stretching force constants

Even if all vibrational frequencies are known for a molecule, approximations have to be introduced, as a rule, to determine a force field. The valence force constants are therefore, to a certain extent, dependent on the approximations used. For several of the molecules discussed here, not even a complete set of experimental frequencies is available. Accordingly, further simplifications were necessary. The SO_2 group was looked upon as a separate entity, for which the well-known expressions for a bent XY_2 model were used (*cf.* CYVIN's book [47]).

The G matrix elements for bent XY_2 are as follows

$$G_1(A_1) = 2\mu_X \cos^2 A + \mu_Y$$

$$G_{12}(A_1) = -\sqrt{2}\,\mu_X \sin 2A$$

$$G_2(A_1) = 4\mu_X \sin^2 A + 2\mu_Y$$

$$G(B_1) = 2\mu_X \sin^2 A + \mu_Y$$

where $\mu_X = 1/m_X$, $\mu_Y = 1/m_Y$, m is the atomic mass, and 2A is the bond angle Y−X−Y.

The force constants are then

$$F_1(A_1) = f_r + f_{rr}$$

$$F_{12}(A_1) = \sqrt{2}\, f_{r\alpha}$$

$$F_2(A_1) = f_\alpha$$

$$F(B_1) = f_r - f_{rr}\,.$$

If the interaction force constant is put equal to zero, $F_1(A_1)$ and $F_2(A_1)$ can be found by means of the G matrix and the experimental frequencies for symmetric S=O stretching and for O=S=O bending. $F(B_1)$ is found from the antisymmetric S=O stretching frequency:

$$F(B_1) = \frac{\lambda_{as}}{G(B_1)} .$$

Finally,

$$f_r = \frac{1}{2} [F_1(A_1) + F(B_1)] .$$

The above outlined approach was used to obtain the results given in Column (1) of Table II.

Table II

Calculated stretching force constants f_r(S=O)

Molecule	Approximations (1)[a] f_r(S=O) mdyn Å^{-1}	Approximations (2)[b] f_r(S=O) mdyn Å^{-1}
SO_2F_2	12.081	12.202
SO_2Cl_2	10.540	10.680
SO_2FBr	10.927[c]	11.068[c]
SO_2FCl	11.329[c]	11.421[c]
CH_3OSO_2F		11.574
CH_3SO_2F	10.942	11.063
$C_6H_5SO_2Cl$	10.281	10.432
CH_3OSO_2Cl	10.520	10.683
$(CH_3)_2NSO_2Cl$	10.380	10.530
CH_3SO_2Cl	10.175	10.305
SO_2	9.856	9.980
$(CH_3)_2NSO_2N(CH_3)_2$	9.654[c]	9.782[c]
$(CH_3)_2SO_2$	9.850	9.967
$(C_6H_5)_2SO_2$	9.393[c]	9.560[c]
$(CH_2)_2SO_2$	9.608	9.690
$(CH_2=CH)_2SO_2$	9.228[c]	9.376[c]
$(CH_2)_4SO_2$	9.349[c]	9.507[c]

[a] Approximations: (i) G-matrix elements corresponding to kinematic coupling between the SO_2 group and the rest of the molecule are ignored; (ii) All force constants for interaction between the SO_2 group and the rest of the molecule are equal to zero; (iii) The force constant for the SO_2 group stretching-bending interaction $F_{12}(A_1) = 0$.

[b] Approximations: Same as (i), (ii), (iii), and (iv) $G_{12}(A_1)$ connected with kinematic coupling between symmetric S=O stretching and O=S=O bending is ignored.

[c] Bond angles used in these calculations were partly based on assumptions (*cf.* Table I).

Another, still rougher approximation might be to ignore $G_{12}(A_1)$ in addition to putting $F_{12}(A_1) = 0$. The condition $G_{12}(A_1) = 0$ means that kinematic coupling between symmetric S=O stretching and O=S=O bending is ignored. Then one gets

$$F_1(A_1) = \frac{\lambda_s}{G_1(A_1)}$$

and

$$f_r = \frac{1}{2}[F_1(A_1) + F(B_1)]$$

with the new $F_1(A_1)$.

This method gave the values listed in Column (2) of Table II.

Comparison of the data in Columns (1) and (2) of Table II shows that f_r(S=O) is increased by an amount between 0.08 and 0.17 mdyn Å^{-1} (1 mdyn Å^{-1} = 10^2 Nm^{-1}) when $G_{12}(A_1)$ is ignored. The removal of the G-ma-

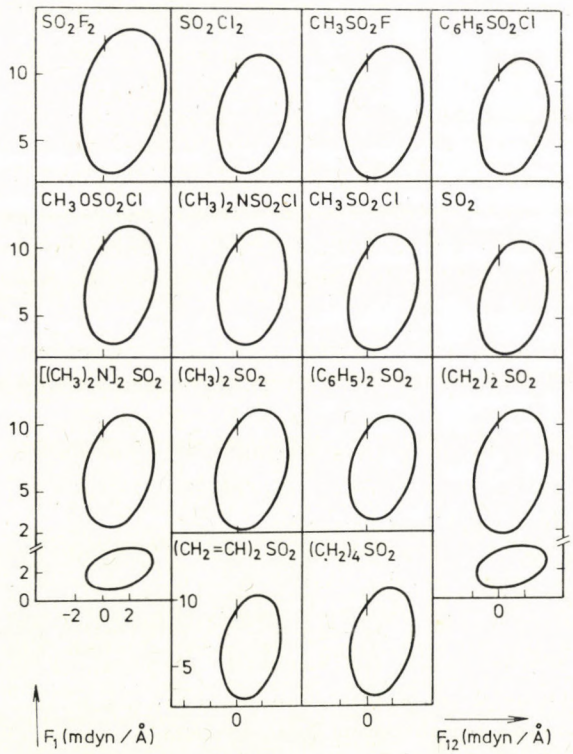

Fig. 1. $F_1(A_1)$ as a function of $F_{12}(A_1)$ from the approximation where the SO_2 group was looked upon as a separate entity. For $[(CH_3)_2N]_2SO_2$ and $(CH_2)_2SO_2$ also $F_2(A_1)$ is shown as a function of $F_{12}(A_1)$. The vertical mark shows the $F_1(A_1)$ value chosen at $F_{12}(A_1) = 0$ (and the corresponding $F_2(A_1)$ values for the two molecules mentioned)

trix elements corresponding to kinematic coupling between the SO_2 group and the rest of the molecule would also be expected to give similar effects.

A vibrational analysis of one complete molecule, SO_2Cl_2, also showed that force constants connected with the rest of the molecule influence the frequencies assigned to S=O stretching. When all non-diagonal valence force constants except f_{rr} were kept equal to zero, a value of $f_r = 10.33$ mdyn Å^{-1} was found (the triatomic model value was 10.54 mdyn Å^{-1}). With another set of force constants [45] found a value of 10.52 mdyn Å^{-1}. If molecules R'RSO$_2$ are considered, R' and R give different contributions, of course, both for the removed G-matrix elements and force constants. But the results obtained for SO_2Cl_2 should give an indication of the effects.

Finally, we examine the effect caused by ignoring the force constant for the SO_2 group stretching-bending interaction ($F_{12}(A_1) = 0$). Fig. 1 shows the ellipses for $F_1(A_1)$ as a function of $F_{12}(A_1)$. A change in $F_{12}(A_1)$ of ± 0.10 mdyn Å^{-1} in the vicinity of $F_{12}(A_1) = 0$ results in a change of 0.10 to 0.15 mdyn Å^{-1} in $F_1(A_1)$. When f_r is expressed as $f_r = 1\ [F_1(A_1) + F(B_1)]$, and $F(B_1)$ is constant, the change in f_r is half as much as the change in $F_1(A_1)$.

On averaging the S=O stretching frequencies

Gillespie and Robinson [1] used the average value of the antisymmetric and symmetric stretching frequencies in determining various correlation relationships, *e.g.* ν(S=O) vs. r(S=O). Szmant [3] argued, however, that certain phenomena should caution us to do so, *e.g.*, the two kinds of stretching frequencies are influenced to different extent by changes in the substituents on the sulfone group. Accordingly, it was decided to examine the correlation of the antisymmetric and symmetric stretching frequencies and the influence of averaging them.

Consider the S=O group as a diatomic X−Y molecule. For this model $G = \mu_X + \mu_Y$ and the force constant $F = f_r$. For a given force constant the vibrational frequency may be found from

$$\lambda = G_{XY} \cdot F, \quad \lambda = 4\pi^2 c^2 \nu^2, \quad \nu \text{ in } \mathrm{cm}^{-1}, \text{ or}$$

$$\lambda = (\mu_X + \mu_Y) f_r \tag{1}$$

The f_r values found for the XY_2 group can be used to find vibrational frequencies for X−Y groups with the same force constants.

By ignoring $G_{12}(A_1)$ for XY_2, f_r is found to be

$$f_r = \frac{1}{2}\left[F_1(A_1) + F(B_1)\right] = \frac{1}{2}\left[\frac{\lambda_s}{G_1(A_1)} + \frac{\lambda_{as}}{G(B_1)}\right]. \tag{2}$$

Using this expression of f_r, and the G matrix elements and inserting all these into equation (1), we obtain

$$\lambda = (\mu_X + \mu_Y)\frac{1}{2}\left(\frac{\lambda_s}{2\mu_X \cos^2 A + \mu_Y} + \frac{\lambda_{as}}{2\mu_X \sin^2 A + \mu_Y}\right). \tag{3}$$

Then, with $\lambda = 4\pi^2 c^2 \nu^2$ the result is:

$$\nu = \left\{\frac{1}{2}(\mu_X + \mu_Y)\left[\frac{\nu_s^2}{2\mu_X \cos^2 A + \mu_Y} + \frac{\nu_{as}^2}{2\mu_X \sin^2 A + \mu_Y}\right]\right\}^{1/2}. \tag{4}$$

For the sulfone group we have $\mu_Y \approx 2\mu_X$ if X = S and Y = O. If this is used in Eq. (4), we have

$$\nu \approx \frac{1}{2}\left[3\left(\frac{\nu_s^2}{\cos^2 A + 1} + \frac{\nu_{as}^2}{\sin^2 A + 1}\right)\right]^{1/2}. \tag{5}$$

If for the XY_2 model $G_{12}(A_1)$ is put equal to zero, then

$$\lambda_s = G_1(A_1)F_1(A_1) = (f_r + f_{rr})\,[2\mu_X \cos^2 A + \mu_Y]$$
$$\lambda_{as} = G(B_1)F(B_1) = (f_r - f_{rr})\,[2\mu_X \sin^2 A + \mu_Y].$$

From $\frac{1}{2}(\lambda_s + \lambda_{as})$, and (1), and ignoring f_{rr},

$$\frac{1}{2}(\lambda_s + \lambda_{as}) = f_r(\mu_X + \mu_Y) = \lambda_{XY}.$$

For the frequencies:

$$\nu_{XY} = \left[\frac{1}{2}(\nu_s^2 + \nu_{as}^2)\right]^{1/2}. \tag{6}$$

For simplicity one may use $\nu_{av} = \frac{1}{2}(\nu_s + \nu_{as})$, and the connection between ν_{XY} and ν_{av} is

$$\nu_{XY}^2 - \nu_{av}^2 = \left[\frac{1}{2}(\nu_{as} - \nu_s)\right]^2. \tag{7}$$

The ν values computed by the expression (1) using the f_r values in Column (1) of Table II are given in Column (1) of Table III. Column (2) of Table III gives the corresponding frequencies from the f_r values in Column (2) of Table II.

The same results were obtained by means of expression (5). The data of Column (3), Table III, were obtained according to expression (6). Finally, the average values, $\frac{1}{2}(\nu_s + \nu_{as})$ are listed in Column (4), Table III.

The difference between corresponding values in Columns (1) and (2) of Table III are between 5 and 11 cm^{-1}. The frequencies found by means of the average λ values (expression (6)), given in Column (3) of Table III are all smaller than or equal to the frequencies of Column (2) of the same Table. The average frequencies, Column (4), Table III, all should be smaller than the corresponding values of Column (3) according to equation (7). At the same time most of them are larger than the corresponding values of Column (1). Exceptions are SO_2F_2 and CH_3SO_2F (1 cm^{-1} lower), and $(CH_2)_2SO_2$ (3 cm^{-1} lower).

Table III

Calculated averages of the stretching frequencies

Molecule	ν(S=O) (cm^{-1})			
	(1)[a]	(2)[b]	(3)[c]	(4)[d]
SO_2F_2	1387	1394	1390	1386
SO_2Cl_2	1295	1304	1303	1298
SO_2FBr	1319	1327	1326	1321
SO_2FCl	1343	1348	1346	1342
CH_3OSO_2F		1357	1355	1350
CH_3SO_2F	1320	1327	1322	1319
$C_6H_5SO_2Cl$	1279	1289	1285	1282
CH_3OSO_2Cl	1294	1304	1302	1298
$(CH_3)_2NSO_2Cl$	1286	1295	1293	1289
CH_3SO_2Cl	1273	1281	1280	1276
SO_2	1253	1261	1261	1257
$(CH_3)_2NSO_2N(CH_3)_2$	1240	1248	1246	1243
$(CH_3)_2SO_2$	1252	1260	1257	1254
$(C_6H_5)_2SO_2$	1223	1234	1229	1227
$(CH_2)_2SO_2$	1237	1242	1236	1234
$(CH_2=CH)_2SO_2$	1212	1221	1221	1217
$(CH_2)_4SO_2$	1220	1230	1226	1224

[a] Corresponding to expression (1) and using the f_r values in Column (1) of Table II.
[b] Corresponding to expression (1) and using the f_r values in Column (2) of Table II.
[c] Corresponding to expression (6).
[d] Average values, $\frac{1}{2}(\nu_s + \nu_{as})$.

No values deviate more than 5 cm^{-1} from the corresponding frequencies of Column (1). Thus the simple approach of taking the average frequency does not give a much different result from the method of looking upon the SO_2 group as a separate entity (cf. the approximations described in the section on the S=O stretching force constants and listed as (i), (ii) and (iii) in Table II), and computing the frequencies from the corresponding stretching force constants (*cf.* eq. (1) of this section). The frequencies found from the average values of the λ's are within 6 cm^{-1} from the results obtained by means of the S=O stretching force constants when in addition of the above approximations, $G_{12}(A_1)$ was also ignored (*cf.* the section on the S=O force constants and (iv) under Table II).

Correlation relationships

A standard least-squares procedure [48] was used to establish the correlation relationships among the geometric and vibrational parameters. The geometric data were used with weights inversely proportional with the standard deviations parenthesized in Table I. The vibrational data were given equal weights.

The coefficients determined are listed in Table IV for 10 relationships, second degree, linear and logarithmic in each case. They are believed to be useful *within the* rather narrow *intervals covered by the data.* The linear relationships are certainly preferred for extrapolation rather than the second degree expressions. Unfortunately, the parameter r(S=O) of SO_2Cl_2 was seen not to be consistent with the other data and thus sulfuril chloride was not considered in establishing the relationships listed in Table IV (except that between the symmetric and antisymmetric frequencies). Inversely, 1.420 Å can be predicted for r_g(S=O) in SO_2Cl_2.* Since the value of r(S=O) was estimated for SO_2FCl in its microwave spectroscopic study by HOLT and GERRY [11] it was interesting to observe that the present correlation relationship provides firm support for their estimate.** On the other hand, 1.413 Å can be estimated for r_g(S=O) of SO_2FBr on the basis of the stretching frequency *vs.* bond length relationship. The data on $(CH_2)_2SO_2$ were also left out of our final calculations. Their poorer agreement with the relationships for the other parameters may be connected with different bonding peculiarities in this rather strained system.

The relationships established are given in Table IV and shown in Figs 2–7. Some comments follow below.

* Comparing the earlier [49] and further refined [7] values of r_g (S=O), it is suspected that this parameter was strongly influenced by the empirical background used. A reinvestigation is warranted in any case.

** The value of 1.408 Å was estimated as to be between 1.405 Å as given for SO_2F_2 in the microwave paper [5] and 1.409 Å as given for SO_2Cl_2 in the earlier electron diffraction paper [49]. By fortunate coincidence, the value of 1.408 Å is still between the electron diffraction value of 1.398 Å for SO_2F_2 (Table I) and the one (1.420 Å) estimated now for SO_2Cl_2.

Table IV

The constants A_0, A_1 and A_2 for $y = A_0 + A_1x + A_2x^2$ found by the least-squares method. 2A is the O=S=O bond angle, R the S=O bond length

y	x	A_0	A_1	A_2	Standard deviation
2A	R	−3040.52	4632.13	−1693.57	0.56
2A	R	358.373	−166.525		0.61
lg 2A	lg R	2.37969	−1.92899		0.62[a]
ν_s	R	79031.6	−106631	36487.8	9.8
ν_s	R	5404.21	−2962.62		12.5
lg ν_s	lg R	3.61213	−3.50857		11.9[a]
ν_{as}	R	42738.9	−53962.3	17500.0	14.0
ν_{as}	R	7426.24	−4241.64		14.5
lg ν_{as}	lg R	3.80090	−4.29674		14.2[a]
ν_s	ν_{as}	3888.88	−4.48191	0.00182282	11.2
ν_s	ν_{as}	375.297	0.583985		13.0
lg ν_s	lg ν_{as}	0.947270	0.676814		13.1[a]
$\frac{\nu_s}{\nu_{as}}$	2A	−10.8438	0.193229	−0.000797861	0.0079
$\frac{\nu_s}{\nu_{as}}$	2A	1.06171	−0.00172407		0.0083
lg $\left(\frac{\nu_s}{\nu_{as}}\right)$	lg (2A)	0.442553	−0.245630		0.0083[a]
f_r^b	R	1369.14	−1854.11	631.889	0.132
f_r^b	R	95.1364	−59.5477		0.193
lg f_r^b	lg R	6.88854	−69.1779		0.131[a]
f_r^c	R	1200.76	−1615.04	547.123	0.158
f_r^c	R	97.1161	−60.8273		0.196
lg f_r^c	lg R	2.25034	−8.01743		0.176[a]
ν^d	R	74537.8	−99527.7	33763.6	8.4
ν^d	R	6464.12	−3639.05		11.3
lg ν^d	lg R	3.71703	−3.97072		10.4[a]
ν^e	R	64356.1	−85096.5	236559	9.8
ν^e	R	6551.91	−3693.87		14.9
lg ν^e	lg R	3.72614	−4.00854		10.9[a]
ν^f	R	61159.2	−80683.0	27130.3	9.8
ν^f	R	6432.34	−3614.05		11.3
lg ν^f	lg R	3.71379	−3.94097		10.7

[a] This standard deviation does not correspond to $y = \lg z$ but to z itself, for better comparison with the other values.

[b] These force constants correspond to Column (1) of Table II.

[c] These force constants correspond to Column (2) of Table II.

[d] These frequencies correspond to Column (1) of Table III.

[e] These frequencies correspond to Column (2) of Table III.

[f] These frequencies correspond to Column (4) of Table III.

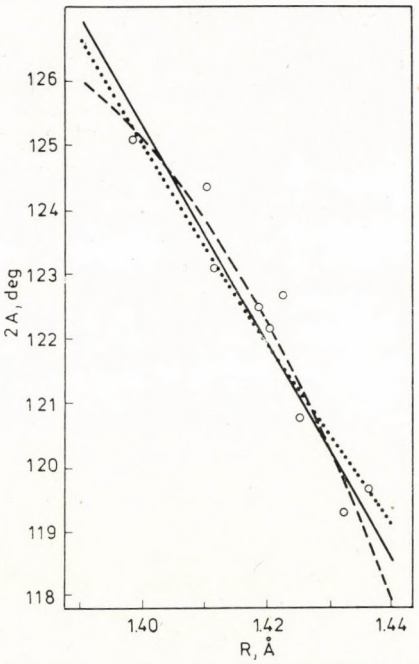

Fig. 2. The O=S=O angle (2A) as a function of the S=O bond length (R). + experimental values, —— linear equation, least-squares result, Table IV, - - - - second degree equation, least-squares result, Table IV, ... 2A = 2 arc sin (2.483/2R)

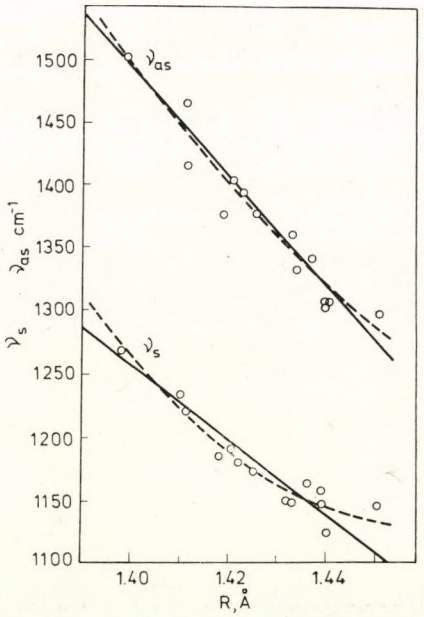

Fig. 3. The symmetric S=O stretching frequency (ν_s) and the antisymmetric S=0 stretching frequency (ν_{as}) as function of the S=O bond length (R). + experimental values, —— linear equations, least-squares result, Table IV, - - - - second degree equations, least-squares result, Table IV

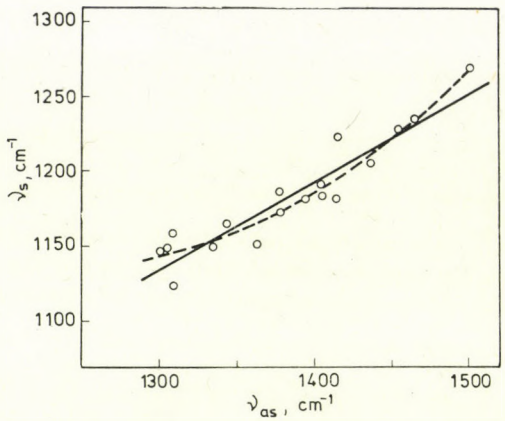

Fig. 4. The symmetric S=O stretching frequency (ν_s) as a function of the antisymmetric S=O stretching frequency (ν_{as}). + experimental values, ——— linear equation, least-squares result, Table IV, - - - - second degree equation, least-squares result, Table IV

The O=S=O angle (2A) as a function of the S=O bond length (R)

As mentioned earlier (*cf.* section on the geometric data), the experimentally determined O...O distances appear to be remarkably constant (average value 2.483 Å) in these molecules. If this is utilized, then the relationship between the O=S=O bond angle and the S=O bond distance is found from

$$2A = 2 \arcsin (2.483/2\ R).$$

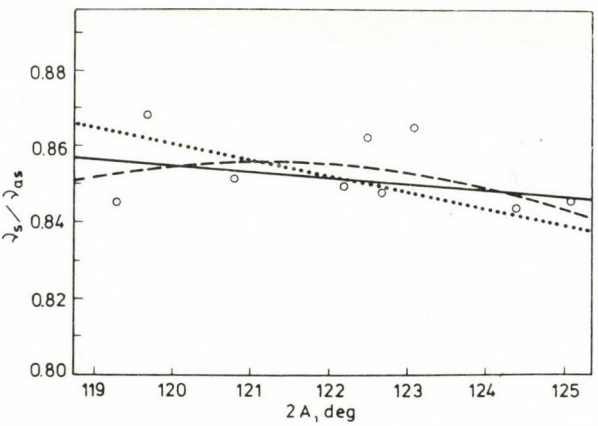

Fig. 5. ν_s/ν_{as} as function of the O=S=O angle (2A). + experimental values, ——— linear equation, least-squares result, - - - - second degree equation, least-squares result, ... $\frac{\nu_s}{\nu_{as}} =$

$$= 1.018 \left(\frac{\cos^2 A + 1}{\sin^2 A + 1} \right)^{1/2}.$$

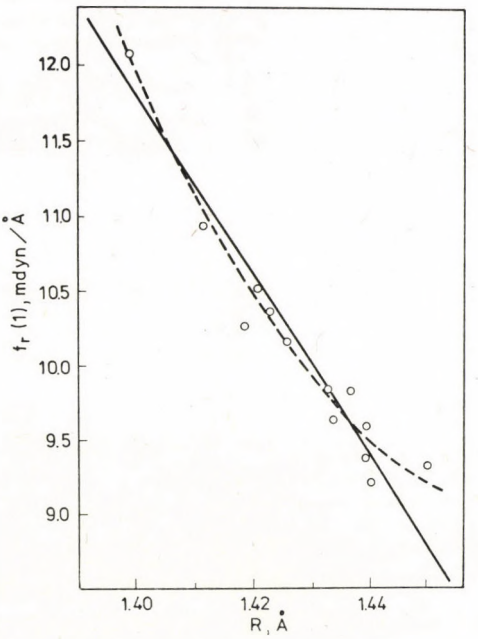

Fig. 6. The S=O force constant f_r found according to approximations i, ii, and iii of Table II and given in Column (1) of the same table as function of the S=O bond length (R). + values found from experimental results, ——— linear equation, least-squares result, Table IV, - - - second degree equation, least-squares result, Table IV

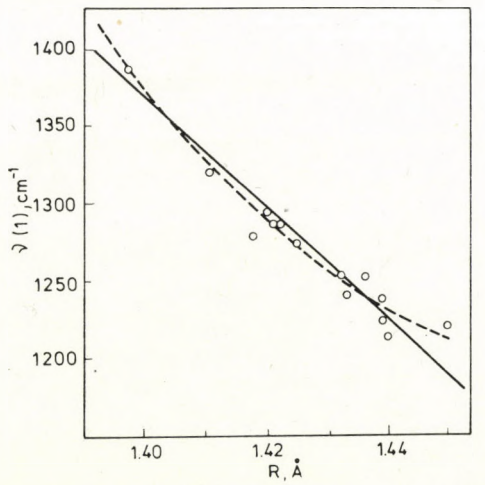

Fig. 7. Average S=O stretching frequencies from Column (1) of Table III as function of the S=O bond length (R). + values found from experimental results, ——— linear equation, least-squares result, Table IV, - - - - second degree equation, least-squares result, Table IV

It is seen in Fig. 2 that the curve from this function differs very little indeed from the curves found by the least-squares procedure.

It is interesting to note that the relationship obtained directly from the data on 2A and R is consistent with similar relationships between these two parameters as obtained through a third parameter. Thus, through the symmetric stretching frequencies:

$$2A = 342.993 - 155.395\ R$$

the antisymmetric stretching frequencies:

$$2A = 343.371 - 155.520\ R$$

the force constants, $f_r(1)$:

$$2A = 353.663 - 163.242\ R$$

ν_s/ν_{as} *as function of the* $O=S=O$ *angle* (2A)

From the approximation where $G_{12}(A_1)$ is ignored for the XY_2 model, we obtain

$$\frac{\nu_s}{\nu_{as}} = \left[\frac{G(A_1)\,F_1(A_1)}{G(B_1)\,F(B_1)}\right]^{1/2}.$$

Putting $\mu_X = \frac{1}{2}\mu_Y$ when inserting the expressions for the G-matrix elements, we get

$$\frac{\nu_s}{\nu_{as}} = \left(\frac{\cos^2 A + 1}{\sin^2 A + 1}\right)^{1/2} \left(\frac{F_1(A_1)}{F(B_1)}\right)^{1/2}$$

A least-squares adjustment of $\frac{\nu_s}{\nu_{as}} = k\left(\frac{\cos^2 A + 1}{\sin^2 A + 1}\right)^{1/2}$ gave $k = 1.0182$, while the weighted average of $\left[\frac{F_1(A_1)}{F(B_1)}\right]^{1/2} = 1.0184$, the two values being in excellent agreement (k had a standard deviation of 0.0029 in the least-squares calculation).

This form of $\frac{\nu_s}{\nu_{as}}$ as a function of the $O=S=O$ angle is shown together with the linear and quadratic relationships in Fig. 3.

Frequencies derived from the f_r *values*

$f_r(1)$: the SO_2 group is treated as a three-atomic molecule with $F_{12}(A_1) = 0$.

$$f_r(1) = \frac{1}{2}\,[F_1(A_1) + F(B_1)]$$

$\nu(1)$ is found as $\nu(1) = \frac{1}{2\pi c}[f_r(1)\,(\mu_S + \mu_O)]^{1/2}$

$f_r(2)$: the SO_2 group is treated as a three-atomic molecule with $F_{12}(A_1) = 0$, and also ignoring $G_{12}(A_1)$

$$\nu(2) = \frac{1}{2\pi c}[f_r(2)\,(\mu_S + \mu_O)]^{1/2}.$$

*

One of the authors (J. B.) wants to thank the Hungarian Institute for Cultural Relations for a Scholarship in the framework of the Hungarian-Norwegian Cultural Agreement.

REFERENCES

[1] Gillespie, R. J., Robinson, E. A.: Can. J. Chem. **41,** 2074 (1963)
[2] Banister, A. J., Moore, L. F., Padley, J. S.: Structural Studies on Sulphur Species in Nickless, G. (ed.): Inorganic Sulphur Chemistry. Elsevier, Amsterdam—London—New York, 1968
[3] Szmant, H. H.: The Sulfur-Oxygen Bond in Senning, A. (ed.): Sulfur in Organic and Inorganic Chemistry, Vol. 1., Dekker, New York, 1971
[4] Hagen, K., Coussens, V. R., Hedberg, K.: to be published
[5] Lide, D. R., Mann, D. E., Fristrom, R. M.: J. Chem. Phys. **26,** 734 (1957)
[6] Birchall, T., Gillespie, R. J.: Spectrochim. Acta **22,** 681 (1966)
[7] Hargittai, I.: Acta Chim. Acad. Sci. Hung. **60,** 231 (1969)
[8] Gillespie, R. J., Robinson, E. A.: Can. J. Chem. **39,** 2171 (1961)
[9] Raley, J. M., Wollrab, J. E., Lovejoy, L. W.: J. Mol. Spectroscopy **48,** 100 (1973)
[10] Reed, P. R., Lovejoy, R. W.: Spectrochim. Acta **24A,** 1795 (1968)
[11] Holt, C. W., Gerry, M. C. L.: Chem. Phys. Lett. **9,** 621 (1971)
[12] Hargittai, I., Seip, R., Nair, K. P. R., Britt, Ch. O., Boggs, J. E., Cyvin, B. N.: J. Mol. Structure **39,** 1 (1977)
[13] Dudley, F. B., Cady, G. H., Eggers, D. F.: J. Amer. Chem. Soc. **78,** 290 (1956)
[14] Hargittai, I., Hargittai, M.: J. Mol. Structure **15,** 399 (1973)
[15] Geiseler, G., Nagel, B.: J. Mol. Structure **16,** 79 (1973)
[16] Brunvoll, J., Hargittai, I.: J. Mol. Structure **30,** 361 (1976)
[17] Uno, T., Machida, K., Hanai, K.: Spectrochim. Acta **24A,** 1705 (1968)
[18] Hargittai, I., Schultz, Gy., Kolonits, M.: J. C. S. Dalton Transactions 1299 (1977)
[19] Nagel, B., Stark, J., Fruwert, J., Geiseler, G.: Spectrochim. Acta **32A,** 1297 (1976)
[20] Hargittai, I., Brunvoll, J.: Acta Chem. Scand. A **30,** 634 (1976)
[21] Török, F., Páldi, E., Dobos, S., Fogarasi, G.: Acta Chim. Acad. Sci. Hung. **63,** 417 (1970)
[22] Hargittai, M., Hargittai, I.: J. Chem. Phys. **59,** 2513 (1973)
[23] Cyvin, S. J., Dobos, S., Hargittai, I., Hargittai, M., Augdahl, E.: J. Mol. Structure **18,** 203 (1973)
[24] Clark, A. H., Beagley, B.: Trans. Faraday Soc. **67,** 2216 (1971)
[25] Morino, Y., Kikuchi, Y., Saito, S., Hirota, E.: J. Mol. Spectroscopy **13,** 95 (1964)
[26] Shelton, R. D., Nielsen, A. H., Fletcher, W. H.: J. Chem. Phys. **21,** 2178 (1953)
[27] Hargittai, I., Vajda, E., Szőke, A.: J. Mol. Structure **18,** 381 (1973)
[28] Hargittai, M., Hargittai, I.: J. Mol. Structure **20,** 283 (1974)
[29] Spoliti, M., Chackalackal, S. M., Stafford, F. E.: J. Amer. Chem. Soc. **89,** 1092 (1967)
[30] Rozsondai, B., Hargittai, I., Moore, J.: unpublished results
[31] Nagel, B., Steiger, Th., Fruwert, J., Geiseler, G.: Spectrochim. Acta **31A,** 255 (1975)
[32] Nakano, Y., Saito, S., Morino, Y.: Bull. Chem. Soc. Japan **43,** 368 (1970)
[33] Кузьянц, Г. М., Алексанян, В. Т.: Журн. структ. химии **13,** 617 (1972)
[34] Hargittai, I., Rozsondai, B., Nagel, B., Bulcke, P., Robinet, G., Labarre, J.-F.: J. C. S. Dalton Transactions, in the press
[35] Bulcke, P.: Diplomarbeit, KMU Leipzig, 1975

[36] Наумов, В. А., Семашко, В. Н., Шайдулин, С. А.: Журн. структ. химии **14,** 595 (1973)
[37] Katon, J. E., Feairheller, W. R.: Spectrochim. Acta **21,** 199 (1965)
[38] Jacob, E. J., Lide, D. R.: J. Chem. Phys. **54,** 4591 (1971)
[39] Saito, S., Makino, F.: Bull. Chem. Soc. Japan **45,** 92 (1972)
[40] v. Eijck, B. P., Korthoff, A. J., Mijlhoff, F. C.: J. Mol. Structure **24,** 222 (1975)
[41] Dubrulle, A., Boucher, D.: Compt. Rend. Acad. Sci. Paris **278,** Ser. B 211 (1974)
[42] Cyvin, S. J., Hargittai, I.: Unpublished results as communicated in Ref. 43
[43] Hargittai, I.: The electron diffraction interatomic distance (in Hungarian). A kémia újabb eredményei (Advances in Chemistry, ed.: Csákvári, B.), Vol. 21 pp 7—173, Akadémiai Kiadó, Budapest, 1974
[44] Hargittai, I., Vajda, E.: unpublished results
[45] Hargittai, I., Cyvin, S. J.: Acta Chim. Acad. Sci. Hung. **61,** 51 (1969)
[46] Uno, T., Machida, K., Hanai, K.: Spectrochim. Acta **27A,** 107 (1971)
[47] Cyvin, S. J.: Molecular Vibrations and Mean Square Amplitudes. Universitetsforlaget, Oslo and Elsevier, Amsterdam, 1968
[48] Kuo, S. S.: Numerical Methods and Computers. Addison-Wesley, Reading, Massachusetts, 1965
[49] Hargittai, I.: Acta Chim. Acad. Sci. Hung. **57,** 403 (1968)

Jon Brunvoll
István Hargittai } H-1525 Budapest, Pf. 17.

Acta Chimica Academiae Scientiarum Hungaricae, Tomus 96 (4), pp. 355—371 (1978)

THE STRUCTURAL MODEL OF WATER, II

THE STRUCTURE OF AMORPHOUS ICE AND STRUCTURAL RELATIONS BETWEEN WATER AND SOME ICE POLYMORPHS ON THE BASIS OF THE TETRAGONAL CLUSTER MODEL

F. HAJDU

(Central Research Institute for Chemistry, Hungarian Academy of Sciences, Budapest)

Received June 9, 1977

The basic ideas of the tetragonal cluster model of water (HAJDU, 1977) have been applied to amorphous (vitreous) ice. The experimental results of NARTEN, VENKATESH, and RICE (1976) can be well interpreted in terms of a cubic cluster model.

A qualitative physical picture is given to explain the temperature sequence and the transformations of the two types of vitreous ice, crystalline ices I_c, I_h and liquid water. The changes in the geometrical arrangement of molecules are deduced from the variations in the relative strength of hydrogen bonds between the first and van der Waals bonds between the second, third, etc. neighbours.

Introduction

In our previous papers [1, 1a], [2], some results obtained by an X-ray diffraction study on liquid water and on the tetragonal cluster model of water, have been reported respectively. In the present paper, the adaptation of the model to amorphous ice(s) is shown and a qualitative picture proposed for the tetragonal water structure, as well as for the mutual structural and physical relations (formation and transformation) existing between some ice polymorphs, supercooled and ordinary water.

1. *Amorphous ice*

1.1. *Some properties of amorphous (vitreous) ice*

The starting point of our investigations on amorphous ice was the working hypothesis of D. OLANDER and S. A. RICE according to which amorphous (vitreous) ice could be regarded as a frozen model of liquid water [3]. We have tried to adapt the tetragonal model of water to this metastable form of ice.

The necessary experimental data became available for us in the paper of NARTEN, VENKATESH and RICE [4]. From their reports it became clear that amorphous ice has at least two modifications each of which is prepared in vacuo by the slow deposition of water from the vapour phase onto a deeply

cooled target. The first modification was prepared on a copper plate cooled below 10 K and the sample was being kept at this temperature during the X-ray and neutron diffraction study. A second modification was obtained by a similar procedure, but at 77 K. A third sample has lastly been studied which had been prepared from the 10 K version by warming it afterwards to 77 K and submitted to diffraction experiments at this temperature. Below we shall refer to the three samples with the notations 10 K/10 K, 77 K/77 K, and 10 K/77 K, respectively.

The X-ray scattering curves and the pair correlation functions derived from them are similar to those of liquids and unambiguously exclude the presence of a crystalline phase. They show that the structure of both samples prepared at 10 K strikingly resembles that of liquid water. An outstanding feature in their pair correlation curves is a peak at $r = 3.3$ Å between the two maxima belonging to the first (2.76 Å) and second (4.5 Å) tetrahedral neighbour distances; the second tetrahedral peak exhibits a subsidiary maximum (a "shoulder") at about 3.9 Å, thus it seems to be composed of two overlapping maxima. At the same time, the density of these samples — as reported in the paper referred to — is 1.1 gcm^{-3}, *i.e.*, by 18 % higher than that of crystalline ordinary ice (I_h) and cubic ice (I_c) at the same temperature and pressure (0.93 gcm^{-3}). All these features are similar to those observed on liquid water [1]; the most important difference between the numerical data is the first neighbour distance which is about 2.83 Å in liquid water in the vicinity of the melting point, whereas it has the "ice value", 2.76 Å in the amorphous ices. All other abscissa values of the peaks in the pair correlation curves are also smaller than the corresponding ones of water. The maxima are sharper owing to the restricted thermal motion of the molecules.

The pair correlation curve of the amorphous ice sample 77 K/77 K differs from the other two mainly in that the peak at 3.3 Å is almost absent, the maximum around 4.5 Å exhibits no discernible "shoulder" and at the same time, the density approaches the crystalline value ($d = 0.94$ gcm^{-3}). The first peak is even sharper than in the former cases, but the character of the intensity and pair correlation functions is still liquid-like.

It seemed to us an obvious opportunity to attempt the adaptation of the tetragonal cluster model to the above amorphous ice forms making use of the tabulated intensity and pair correlation functions given by NARTEN, VENKATESH and RICE [4]. The trial seemed the more justifiable as our model differs radically from the interstitial water model of NARTEN, DANFORD and LEVY (see *e.g.* [5]) as well as from its version proposed for amorphous ice by the above authors in ref. [4]. In these models, the ice I_h lattice is claimed to be valid for both water and amorphous ice; the network is treated as being practically infinite. The increase of density and the "interstitial" peaks are explained by the assumption of the existence of free, gas-like water molecules

occupying a certain fraction of the cavities of the ice lattice without forming hydrogen bonds with the network molecules.*

The tetragonal cluster model is based on opposite assumptions. As pointed out in ref. [2], the topology of the ice I_h lattice is inconsistent with a large fluctuation of the bond angles $O-\widehat{HOH}-O$, or with an even slight deviation of their mean value from the tetrahedral 109.47°. Contrary to this, the ice I_c lattice can go over into tetragonal by a simple deformation by which the mean bond angle value may become $\leqslant 109.47°$, simultaneously preserving the mirror symmetries of the water molecule. We emphasize this feature of the model by reminding of well-known facts about the formation and transformations of amorphous, cubic, and hexagonal ices as follows. (See, *e.g.* [13], [17].)

The conditions of formation of the amorphous ices have been described above. Crystalline cubic ice I_c can be produced either from amorphous ice by warming it above 110 K, or directly by a similar procedure as discussed above but raising the temperature of the target over 110 K. Under similar conditions, ordinary ice I_h is formed only above 150 K, or alternatively, by a spontaneous and irreversible transformation of ice I_c at about 150 K. These experiments have been reproduced and described by the above authors [4]. The experimental facts are hardly reconcilable with the presumption of the hexagonal lattice structure in the amorphous states.

A second statement of the interstitial model which seems to us physically unlikely is that of the coexistence of two sharply different states of the water molecules in the same phase: fully hydrogen-bonded network molecules on one part and completely free interstitial ones on the other. The tetragonal cluster model, in turn, assumes finite clusters with a hydrogen-bonded tetragonal lattice structure and the aggregation of the clusters with the formation of more closely packed layers in the adjacent boundaries. In the interior of the clusters, the molecules are 4-bonded, in the boundary layers mostly 3- and 2-bonded and the number of 1- and 0-bonded molecules is regarded negligibly small. (The word "bonded" stands here for "hydrogen-bonded", not implying van der Waals interactions.)

1.2. *Fitting of the pair correlation functions*

The adaptation of the tetragonal cluster model to the amorphous ices – similarly to the procedure applied to liquid water [2] – took place in several steps.

* In the paper referred to an alternative model is also proposed, namely a network similar to that of ice II or ice III, or a mixture of the two. Since both are high-pressure ice forms, we cannot regard them as the basis of a physically more plausible hypothesis than that mentioned first.

(i) *Distinction between intra-lattice and interstitial distances*

The separation of the observed pair distances into the groups of lattice-point distances and interstitial ones, was facilitated by the available three independent data sets. As already mentioned, in the pair correlation curves of both 10 K samples (density 1.1 gcm^{-3}), a very sharp peak is found at 3.3 Å, and there is an unresolved peak (a "shoulder") around 3.9 Å. These features are almost absent from the curve of the 77 K sample (density 0.94 gcm^{-3}). The main peak of the latter at 2.76 Å is even sharper than in the two former instances indicating that the 77 K sample stands nearer to a crystalline form (presumably to ice I_c) than do the two former ones. The above observations led us to establish empirically two important interstitial distance values at 3.3 and 3.93 Å. Taking into account the results of cluster simulation (see below), some farther interstitial distances were introduced also at r-values between 5 and 6 Å and above 6 Å. It is a remarkable feature of the model that within the range $4 \leq r \leq 5$ Å, no interstitial distances were found neither by the semi-empirical approximation, nor by computer simulation of the cluster aggregates.

(ii) *Determination of the lattice parameters*

As shown earlier [2], the tetragonal lattice is characterized by the first neighbour distance, R, and the bond angle, 2α, subtended by the H-bond lines connecting 3 neighbouring oxygen atoms. In accordance with NARTEN *et al.* [4], $R = 2.76$ Å.

Establishing the optimal value for the bond angle, 2α, proved to be a more difficult task, because of the overlap of some network and interstitial distances. After several trials, it has been found that it is the tetrahedral angle, $2\alpha = 109.47°$, which results not only in a sufficiently good fit of the functions $g(r)$, but also the sets of radial distances and coordination numbers it yields can be best interpreted by the model. Recalling the angle $2\alpha = 97°$ found for water (departure from the tetrahedral angle: $-12.5°$), we may now state that the amorphous ices cannot be treated as simply the frozen models of liquid water reduced by a factor of $\frac{2.76}{2.83} = 0.975$. Although the main difference between them is determined by the first neighbour distance, this difference involves further physical and geometrical consequences. A difference in the R value affects the absolute and relative strengths of the H-bond between first neighbours, and of van der Waals forces between the others, which causes alterations in the geometry. It seems, as if the ice-like value of R ($= 2.76$ Å) involved the same also for the bond angle 2α ($= 109.47°$). On substituting these parameters, the tetragonal lattice becomes identical with the ice I_c lattice, hence the symmetry of the clusters gets cubic.

(iii) *Fitting the pair correlation functions*

Having defined the internal structure of the clusters by fixing R and α, and having established empirically the most characteristic interstitial distances (*i.e.*, the most frequent intermolecular separations between two neighbouring clusters), the range of fitting was chosen. As the lower limit, we took $r_{\min} = 2$ Å, since in the $g_{00}(r)$ Tables of ref. [4], the first non-zero values are found at $r_{\min} = 2.09$ Å. Although the Tables extend to $r_{\max} = 15.09$ Å, we have terminated the range of fitting at about 8 Å. A farther expansion would have greatly increased the computer time without adding important pieces of information on the structure. Having voluntarily neglected the structure above $r \sim 8$ Å, (*i.e.*, terminated the series of discrete intermolecular distances below this limit and taken $g(r) \equiv 1$ above it,) a rectangular jump of $g(r)$ from 0 to 1 has been eliminated by the introduction of an artificial transition term, $g_c(r)$ (where subscript "c" stands for "continuous"), in the following way.

$$g(r) = \sum_i g_d(r_i, r) + g_c(r_c, r)$$

whith

$$g_d(r_i, r) = C_i \times [(32\pi^3)^{1/2} l_i^2 r_i r]^{-1} \times \left\{ \exp\left[-\frac{(r_i - r)^2}{2l_i^2} \right] - \exp\left[-\frac{(r + r)^2}{2l_i^2} \right] \right\}$$

and

$$g_c(r_c, r) = \exp\left[-\frac{(r_c - r)^2}{2l_c^2} \right], \text{ if } r < r_c ;$$

$$g_c(r_c, r) \equiv 1, \text{ if } r \geq r_c$$

where $g_d(r_i, r)$ denotes the terms each of which represents the contribution of a distinct distance r_i; the parameters r_c and l_c^2 denote the inner radius of the "structurless sphere" (or the "correlation radius"), and the m.s. fluctuation of this length, respectively. The latters were refined by the least squares fitting procedure.

The number of distances defined by the lattice geometry was 6, that of empirically chosen "interstitial" ones 7. The 13 distance values fixed, the varied parameters for the fitting procedure were the coordination numbers, C_i, the m.s. amplitudes l_i^2 ($i = 1, \ldots, 13$), r_c and l_c^2, altogether 28 variables.

1.3. *Estimated mean cluster volume and computer simulated cluster aggregates*

(i) In modelling liquid water [2], the estimation of mean cluster volumes was based on the volume effect, *i.e.*, on the difference between the molecular volume in an ideal infinite tetragonal network (defined by R and α) and in real water, the temperature dependence of both volumes taken into account.

Considering the densities of the amorphous samples, we see that both of the 10 K samples exhibit a volume decrease of 15 % as compared with the ices I_h, or I_c. Since this effect is approximately equal to that found for liquid water, we have assumed that the mean cluster volume is also similar to that of a "water cluster" [2]. A volume containing 388 molecules ($N_c = 388$) proved to be suitable as the basis of the simulated model of cluster aggregates. The shape of the cluster is approximately a quadratic prism of dimensions $18 \times 18 \times 25$ Å^3.

NARTEN *et al.* have also made an estimation of the correlation length and for the corresponding edge length of a cube taken as structural unit. For the latter they found 24 Å [4].

(ii) The final result of cluster simulation is a distance statistics, *i.e.*, a list of the occurring pair distances, their occurrency numbers, and the average

Table I

Parameters of fitted pair correlation functions, g(r), of amorphous ice samples on the basis of the cubic cluster model

		Notation of amorphous ice samples						
		10K/10K		10K/77K		77K/77K		
		R = 2.76 Å α = 54.735°						
i	r_iÅ	C_i	l_i Å	C_i	l_i Å	C_i	l_i Å	$C_{i\infty}$
1	2.76	4.25*	0.15*	4.32**	0.155*	3.88*	0.11*	4
2	4.507	9.12	0.30	10.89	0.28	11.25	0.34	12
3	5.285	7.47	0.37	6.15	0.28	6.66	0.80	12
4	6.374	4.42	0.38	4.68	0.46	3.13	0.30	6
5	6.946	7.91	0.38	8.02	0.38	7.91	0.33	12
6	7.80	15.53	0.65	15.46	0.62	14.76	0.42	24
7	2.80	added to C_1	–	added to C_1	$r_7 = 2.70$ Å	added to C_1	–	
8	3.30	1.56	0.09	1.56	0.10	0.18	0.10	
9	3.93	4.37	0.30	2.95	0.18	1.02	0.20	
10	5.64	2.85	1.00	2.30	0.90	2.00	0.35	
11	6.14	7.05	0.32	7.34	0.35	6.13	0.75	
12	6.70	1.95	0.24	2.02	0.24	2.40	0.24	
13	7.50	15.07	0.90	15.14	1.20	14.31	1.40	
ΣC_i		81.55		80.83		76.53		
r_c Å		9.45		9.39		8.96		
l_c Å		1.20		1.20		0.73		
σ		0.031		0.026		0.036		

* Contracted with the parameters of the interstitial 2.80 Å.
** Contracted with the parameters of the interstitial 2.70 Å.
Distances No 1, . . ., 6 are lattice point separations, 7, . . ., 13 are interstitial.

coordination numbers (=2× occurence number/number of molecules). The list of distances and average coordination numbers is directly comparable with the corresponding parameters of the semi-empirical fit.

The simulated model and particularly the comparison of the distance statistics of a cluster aggregate with that of the individual cluster, illuminates the different roles played by the lattice-point distances and the interstitial ones. Those belonging to the first group are present in the single cluster as well as in the aggregate. Some items of them, however, are figuring with greater coordination numbers in the aggregate owing to a coincidence with an interstitial distance value.

The interstitial distances — those coinciding with neither of the lattice-point distances — are present only in the aggregates. With regard to the great number of such items as yielded by the simulation of the aggregates, we have contracted them into smaller sub-groups in order to get synoptical tables and to make an easier comparison with the semi-empirical fit. In Table II, the sub-groups are characterised with the range of distances they cover, and the sum

Table II

Distance statistics of a simulated cubic cluster and its aggregate
Cluster parameters: $R = 2.76$ Å, $\alpha = 54.735°$, $N_c = 388$

i	r_i Å	$C_{i\infty}$	C_i in the individual cluster	$C_i/C_{i\infty}$	C_i in the aggregate	C_i in the semiempirical model fitted to $g(r)$ of the 10K/10K sample
1	2.76	4	3.40	0.850	3.40	4.25*
2	4.507	12	8.94	0.745	8.94	9.12
3	5.285	12	8.35	0.696	8.75	7.47
4	6.374	6	4.05	0.675	4.05	4.42
5	6.946	12	7.26	0.605	7.67	7.91
6	7.80	24	13.57	0.565	15.83	15.43
7	2.8 – 3.0				0.62	– **
8	3.2 – 3.5				2.17	1.56
9	3.7 – 4.3				2.57	4.37
10	5.3 – 5.5				0.67	–
11	5.5 – 5.8				3.73	2.85
12	5.9 – 6.3				6.97	7.05
13	6.4 – 6.8				1.15	1.95
14	7.2 – 7.7				14.99	15.07
			ΣC_i		81.51	81.55

* Contracted with the coordination number C_7 pertaining to the interstitial 2.80 Å.
** Involved in C_1.

of the coordination numbers belonging to them. (The weighted average distance values within each sub-group agree fairly well with the interstitial distances established empirically for the least squares fit.)

1.4 *Results*

Table I. contains the parameter values that yield the best fits of the model pair correlations to the experimental $g_{oo}(r)$ functions of the three different amorphous ice samples. The goodness of the fits is characterized by the standard deviation, σ, according to

$$\sigma = \left[\frac{\sum_{j=1}^{N_p} [g_e(r_j) - g_m(r_j)]^2}{N_p} \right]^{1/2}$$

where $g_e(r_j)$ denotes the experimental, and $g_m(r_j)$ the model pair correlation function values at the points r_j where subtraction has been performed; N_p is the number of such points. N_p was 73, the r_j's ranging from 2.0 to 9 Å. We can add the following comments to the data figuring in Table I. Distances No. 1 to 6 represent the lattice points within the cluster, their values defined by the parameters R and α. The only exception is the first one which comprises also an overlapping inter-cluster distance. The best fit has been obtained when the latter was taken 2.80 Å in the case of the samples 10 K/10 K, and 77 K/77 K, while 2.70 has been found as optimal for the 10 K/77 K specimen.

Items No. 7 to 13 are purely interstitial distances found semi-empirically. We emphasize the significance of the average coordination numbers. In the last column, the ideal numbers corresponding to an infinite lattice are given. The actual figures are less than the ideal ones by a decreasing ratio, due to the existence of finite clusters. The two exceptions are the first coordination numbers referring to both denser phases, *i.e.* samples 10 K/10 K, and 10 K/77 K. The excess is evidently due to the contribution of the overlapping interstitial distances as mentioned before, thus yielding $C_1 > 4$. For the 77 K/77 K sample, $C_1 = 3.88$ (where the contribution by the interstitial is ~ 0.2), in accordance with our assumption that this version of amorphous ice consists of large clusters aggregated in such a way that the majority of the "cavities" is no more filled in.

In the present status of elaboration of the model we cannot attribute a great importance to the exact values, and the sequence of the amplitudes or fluctuations for several reasons.

(i) The lattice point distances and the interstitial ones must form two independent series of the amplitudes.

(ii) Within each group, the figures are by and large increasing together with the radial distance. The exceptions may be due to the overlap of the two types of distances, or/and, naturally, to imperfections of the fitting procedure. From general considerations one would expect even a linear increase of the squared amplitudes ([4], [6]) within the clusters, but this is not the fact. This simple rule holds for a system of particles vibrating independently and isotropically. In the present model, the clusters mean finite molecular ensembles held together by strongly oriented intermolecular forces. For such a system, independent and isotropical displacements of the molecules cannot be presumed.

By simulating clusters and cluster aggregates, we have succeeded to reproduce both types of intermolecular distances and the average coordination numbers from an *a priori* model.

The distance statistics of the model is shown in Table II. In this Table, four series of coordination numbers are compared with each other. The figures of the infinite lattice (3rd column) are comparable with those of the single cluster (4th column), their decreasing ratios given in column 5, showing the effect of finite dimensions. The figures of the 6th column representing the final result, are yielded by the aggregation of clusters. The comparison with column 4 demonstrates the effect of aggregation. Finally, the adequacy of the model can be seen by comparing column 6 to 7 where the corresponding data of the semi-empirical fit for sample 10 K/10 K are repeated from Table I.

In Figs 1 and 2, the fits of the pair correlation functions, $g_{00}(r)$, and of the reduced, modified intensities $i(s) \cdot M(s)$ (or, with and other notation, the structure functions $\bar{h}_{00}(s)$ in ref. [4]) are presented in graphical form.

Let us remark that the $i(s) \cdot M(s)$ $[= \bar{h}_{00}(s)]$ functions have been computed from $g_{00}(r)$ by Fourier transformations and not inversely which is the natural routine way in experimental diffraction studies.* For the sake of comparison, the same procedure was applied to the $g_{00}(r)$ functions of NARTEN *et al.*, but the original $\bar{h}_{00}(s)$ functions of the same authors are also drawn in Fig. 2. The small deviations between the latter two must be due to termination effect of the inverse Fourier transformation.

It should be mentioned finally that a certain kind of a "sum-rule" and an "integral test" can also be applied in order to check the adequacy of the model.

(i) The accordance between the semi-empirical and the simulated model can be shown by summing up the coordination numbers in both models within

* The Fourier transformation has been performed without the explicit use of atomic $[f_0(s), f_H(s)]$, or molecular $[F_{H_2O}(s)]$ amplitudes. This simplification had been based on the assumption that there exists a molecular scattered intensity function, $F^2_{H_2O}(s)$ that accurately represents the scattering by one independent molecule, in the given phase. In this case, the factor is cancelled out of the transformation formula by the intervention of $M(s) = [F^2_{H_2O}(s)]^{-1}$.

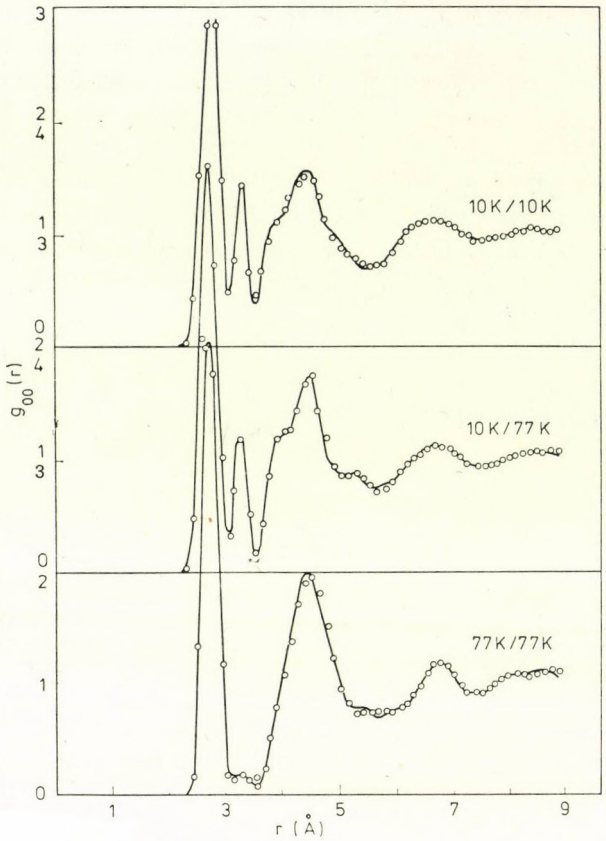

Fig. 1. Oxygen-oxygen pair correlation functions $g_{00}(r)$, of amorphous ice samples ——— calculated from the cubic cluster model; $\overline{\text{OOOO}}$ calculated from experimental X-ray diffraction data according to NARTEN *et al.* (1976) [4]

the same range $r_{j\,\min} \leq r_j \leq r_{j\,\max}$. This test can be made with the data pertaining to the 10 K/10 K, and 10 K/77 K samples, because the present model is primarily intended to explain the origin of densities higher than that of the crystalline phase. Thus, by calculating the sum $\sum_{r_{j\min}}^{r_{j\max}} C_j(r_j)$, we obtain

81.55 from the semi-empirical fit of the 10 K/10 K,

80.83 from that of the 10 K/77 K samples, and

81.51 from the simulated model. The deviation between the "semi-empirical" and the "simulated" figures amounts to $0.05 - 0.8$ %.

(ii) By integrating the radial density function $[D(r) = 4\pi\varrho_0 r^2 \cdot g(r)]$ over a sphere of radius R_m $(R_m \geq r_c)$, we can check, how accurately the model $g(r)$ conforms with the experimental mean density, ϱ_0, of the samples. With a good approximation

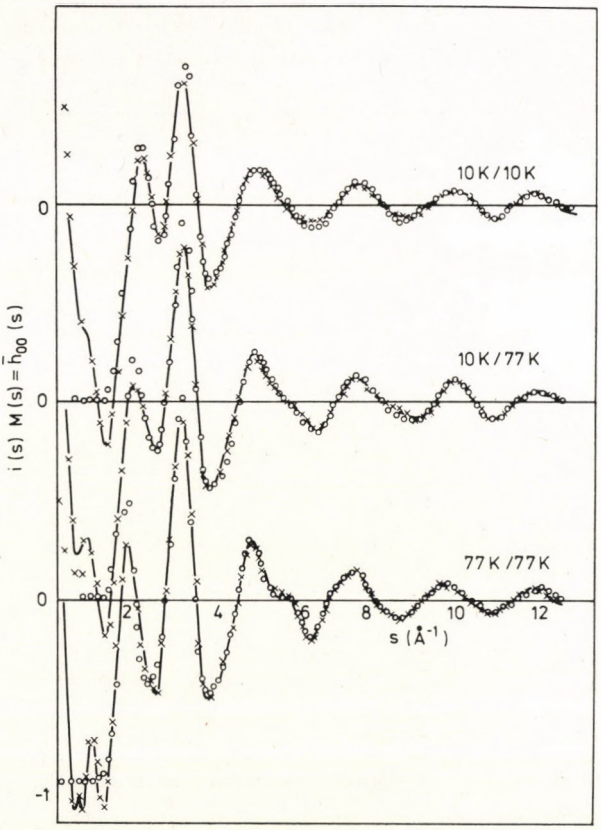

Fig. 2. Reduced modified intensity functions, $i(s).M(s)$, of amorphous ice samples (other notation: structure functions, $\bar{h}_{00}(s)$). ——— calculated from the model $g_{00}(r)$ function (by Fourier transformation); ×××××× calculated from the experimental $g_{00}(r)$ function (by Fourier transformation); ○○○○ obtained directly from X-ray diffraction data by NARTEN *et al.* (1976) [4]

$$4\pi\varrho_0 \int_0^{R_m} r^2 \cdot g(r)\,\mathrm{d}r \approx N_R - 1\,,$$

and

$$4\pi\varrho_0 \int_0^{R_m} r^2 \mathrm{d}r = \frac{4\pi\varrho_0}{3} \cdot R_m^3 = N_R\,.$$

where N_R denotes the number of molecules actually present in the given sphere. In this way, we have compared the experimental and the model $g(r)$'s with each other and with the expected value. Denoting the integrals of the

experimental functions by $N_R^e - 1$, and those of the model functions (semi-empirical fit) by $N_R^m - 1$, we have got the following values.

Calculated values for $R_m = 10$ Å	Samples		
	10K/10K	10K/77K	77K/77K
N_R	156.58	156.58	133.54
N_R^e	156.96	156.62	132.97
N_R^m	159.64	160.54	137.84
$N_m^R - N_R$	+3.06	+3.96	+4.30

The deviations between the corresponding N_R and N_R^e values are negligibly small, the N_R^m figures, however, are by 2 – 3 % too high. We ascribe this error to the contribution of the range $7 < r \leq 10$ Å where the accurate fit had been terminated and the arbitrary term $g_c(r, r_c)$ produces an increasing contribution. The model $g(r)$ function exhibits here a small excess which appears magnified in the above integral because of the multiplying factor $4\pi\varrho_0 r^2$.

2. *Relations between the structures of water, ice I_h, I_c and the amorphous ices*

In our previous paper [2], it has been pointed out that the assumed tetragonal symmetry of water lattice stands nearer to the mm2 (C_{2v}) symmetry of the free H_2O molecule than those of ice I_h and I_c. The origin of the higher degree of symmetry of the latters cannot be understood by studying merely the H – O – H...OH_2 dimer, but the interactions between second and third neighbours must also be considered. In order to estimate second neighbour interactions, at least a pentamer (one central molecule with its four neighbours) must be taken into account, and to see third neighbours' effects, a considerably larger structural unit is needed. To do this quantitatively is beyond the limits of our possibilities, but we attempt to suggest a qualitative picture of the correlations between the dynamics and the geometry of some systems of water molecules.

2.1. *Water and ordinary ice I_h*

For symmetry reasons, it seems a plausible assumption to us that the H – O – H planes of the first neighbours should be mutually perpendicular. This assumption does not involve, however, that the O...$\overset{\frown}{\text{H–O–H}}$...O angle necessarily would have the tetrahedral value, 109.47°. It actually has this value in ice lattices I_h and I_c whereas two, exactly linear hydrogen bonds would subtend a smaller angle, 104°. The higher value in the ices can be achieved

by slightly bending the hydrogen bonds which means a deviation from the geometry of a hypothetical free "trimer". The bond bending must be assigned to the influence of second (evtl. third, etc.) neighbours. To see the origin of this effect, we have to take into account that the first neighbour distance is significantly shorter (2.75 – 2.76 Å) in the ices than in water (2.82 – 2.84 Å closely above 0 °C).

Consequently, the second neighbours are also closer to each other and the intermolecular forces are stronger in the ice lattices. This is the reason why we dare to state that the symmetrical configuration of the four neighbours round the center in ice is mainly due to the influence exerted by second neighbours' forces on the hydrogen bonds. The more so, since – as pointed out by MOMANY *et al.* [7] – attractive forces between the non-nearest neighbours in hydrogen-bonded crystals constititute a general compressive force which reduce even the equilibrium intermolecular first distance compared with that in a free dimer. In connection with water and ice the latter is claimed to be 2.86 Å, the former 2.75 Å, the difference of 0.10 Å being due to the attractive potential of the non-nearest environment, according to SHIPMAN and SCHERAGA [8]. In this light, shortness of the first distance in ice is not the cause, but rather the consequence of stronger attraction between second (and farther) neighbours. The two phenomena mutually enhancing each other, the equilibrium in crystalline ice is restored partly by the short-range repulsive forces, partly by the symmetrization of second neighbours involving the emergence of counter-forces against hydrogen bond bending.

The regular tetrahedral pentamers can be arranged in two alternative ways according to either of the hexagonal, or the cubic ice pattern. The first and second coordination spheres in these lattices are identical; outside these, a part of the coordination radii and all of the coordination numbers are different. One of the third neighbours in ice I_h is a very near one, its radial distance is hardly longer than that of the second neighbours (=4.56 Å), its coordination number is 1. This is the distance between the cis-positioned molecules in the six-membered puckered rings of "boat" conformation and since in ice I_c, all rings are of the "chair" type, this distance is not present in I_c. This explains that – in accordance with the above findings of MOMANY *et al.* – the O–O bonds parallel to this distance (and to the z-axis) are by 0.01 Å shorter than the others in ice I_h. (The c/a ratio in I_h is 1.629 instead of the "ideal" value 1.633 as found by LONDSDALE [9], LA PLACA and POST [10], BRILL and TIPPE [11].) Consequently, the energy difference in favour of I_h against I_c can be assigned to the contribution of a surplus pair interaction at the distance 4.56 Å and the shortening of all distances parallel to the z-axis causing also a slight volume effect. Later on, we shall try to give an explanation for the formation and maintenance of ice I_c under the special conditions known from the ice literature [13, 17].

As seen above, the tetrahedral symmetry in ice is due to the combined interaction of first, second, and farther neighbours. Even a small deviation of the $\overset{\frown}{O{-}O{-}O}$ angles from the tetrahedral value – with preservation of the mm2 symmetry – destroys the trigonal rotational symmetry and at the same time, the possibility of the hexagonal lattice. We may conclude from this that both ice lattices represent somewhat strained and compressed structures, all H-bond being slightly bent and shortened; they may be straightened or even bent in the opposite direction when ice is fused, because of the general increase of pair distances and the weakening of the secondary intermolecular forces. The kinetic energy of the molecules is naturally greater in liquid water, than in ice, but in the liquid phase, the mean hydrogen bond length, and the mean $\overset{\frown}{OHOHO}$ angle may stand nearer to their potential minimum values as valid for a hypothetical free trimer than they are in the solid state. Just the opposite assumption was made by POPLE [12] in his "distorted bond" water model – true, he regarded the water molecule as a regular tetrahedral quadrupole. POPLE's model agrees, nevertheless, with the present one in that it claims the bond angles in water to be, on the average, non-tetrahedral.

In terms of the present model, we can outline the following picture of the melting process. When starting from a lower temperature, the three components of the thermal expansion coefficient of ice I_h grow monotonously and isotropically with the rise of temperature; the growth of the expansion is naturally due to the increasing anharmonicity of thermal vibrations. The secondary, van der Waals forces between non-nearest neighbours decrease with increasing distances more rapidly than the strengths of the hydrogen bonds (for which the actual O–O distance in ice is even below the pair potential minimum value). According to the above assumptions, by the weakening of attraction between non-nearest neighbours, the main reason for the regular tetrahedral symmetry of the hydrogen bonds is cancelled, and the nearest neighbour distance is also allowed to expand to its equilibrium length. Hence the ice I_h lattice must collapse because of its incompatibility with the mm2 symmetry. Before this catastrophe, in the range $-10 < t < 0$ °C, the thermal expansion of the lattice is no more isotropical, since its z-component preceeds the perpendicular ones, as seen in the Table of expansion coefficients given by LA PLACA and POST [10]. This slight anisotropy of the expansion thus "predicts" the breakage of the lattice at 0 °C. The hydrogen bonds are, however, strong enough to be rearranged to a pattern which is consistent with the non-tetrahedral bond angles. The formation of a complete new lattice is hindered by the strong thermal motion, and the crystalline-like network of the bonds extends over small domains only.

On further heating, the sudden changes at the melting point are followed by two competing slow processes: the increase of the average O–O distance,

and the breakage of an increasing portion of the H-bonds which involves the diminution of the average cluster volume. The volume effect of the two processes has the opposite sign, resulting in the well known volume *vs.* temperature function of water with its minimum at 4 °C. (Naturally, a similar assumption is the common feature of all reasonable water models.) The range of the two processes certainly extends even below the ordinary melting point as shown by the volume-temperature function of supercooled water which is the smooth and monotonous continuation of that of ordinary water between 0° and +4 °C. On the other hand, the effect of both processes as far as the boiling point can be proved by the fact that the cubic expansion of water between 4° and 100 °C is significantly less than the treble of the observed linear expansion of the first neighbour distance. The actual volume increase from 4° to 100 °C amounts to 60 % of that calculated from the linear expansion of the lattice.

No variation of the mean bond angle in the range $4 \leq t \leq 50$ °C could be observed ($2\alpha = 97°$) [2]. It must be assumed therefore that the bond angle is not (or only very slightly) affected by temperature changes at ordinary pressure; we suspect however, that it may play a main role in the anomalous behaviour of water under high pressures. Bond angle change under pressure is a third parameter which causes volume change and it may contribute to the understanding of the observed anomalous phenomena.

The temperature dependencies of the density and the specific heat of *supercooled water*, are straightforward extensions of the corresponding functions of water above 0 °C [13]. Naturally, the abrupt change of these quantities on freezing supercooled water is also analogous with that at the normal freezing point. Hence, supercooled water cannot be considered as preformed ice. The present model can be extrapolated below 0 °C. We suppose that supercooled water also consists of tetragonal clusters the average volume of which grows with sinking temperature: this would explain the increase of the specific volume on cooling. Freezing — *i.e.* transition into the stable ice I_h phase — requires an amount of activation energy for temporarily breaking a part of the hydrogen bonds, thus making transformation possible. Once started, the crystallization process becomes self maintaining by the free enthalpy change of the new hydrogen bonds.

2.2. *Amorphous ices and crystalline ice polymorphs* I_c *and* I_h

On the basis of the present model, we are able to give a qualitative explanation for the temperature sequence of the existence and the transformations of amorphous ices and crystalline ices I_c, I_h.

(i) The formation of amorphous ice: At the beginning of the slow deposition process, the molecules reaching the cooled target are captured there by adhesion in randomly dispersed and oriented positions, acting as the nuclei

for numerous uncorrelated crystallites. The molecules impacting later, join them by hydrogen bonds. In the absence of a molecular environment, the O–O distances correspond to the pair-potential minimum, and the bond angles are not necessarily tetrahedral. Thus the crystalline fragments should exhibit the tetragonal lattice structure. Due to the very open structure of this lattice, the cavities of the network are also offered for further impacting molecules forming the nuclei of independent lattice fragments. At very low temperatures (10 K), the interstitial fragments do not migrate away from these – energetically non-optimal – positions onto sites of the neighbouring crystallite. Simultaneously with the formation of a macroscopic layer of ice, there arises the compressive forcefield of non-nearest neighbours mentioned above. This field contracts the OHO distances to the ice-like value, 2.76 Å, and the bond angles approach the tetrahedral value. The two factors together, namely the interpenetration of the lattice fragments and the short O–O distances, must yield a density greater than that of ordinary ice and of water.

This structure will not be essentially altered on warming the sample to 77 afterwards, although the distribution of distances is slightly modified, probably because of the displacement of the clusters (compare the two data sets in Table I).

The formation of the second amorphous modification above 77 K and of cubic ice above 110 K, as well as the transformations of these forms from one into the other, can be explained by the increasing kinetic energy of the molecules. Owing to their larger translation and libration amplitudes, the molecules are able to jump from the interstitial positions into the energetically more favourable lattice sites. Thus, the clusters are growing. In the 77 K/77 K amorphous modification, the number of short interstitial distances is small but the crystalline fragments are of submicroscopic dimensions and are randomly oriented. Their surface molecules are hardly closer packed than in the interior of the clusters and as a consequence, the first coordination number gets below 4. Above 110 K the fragments unite in real crystallites, or such are directly produced by condensation from vapour. The transformation amorphous → cubic needs an initial energy input only for surmounting van der Waals forces acting between the cluster surfaces, the total issue of the process is an energy gain by virtue of the formation of new hydrogen bonds. The enthalpy change amounts to $0.2-0.3$ kcal mol^{-1} according to GHORMLEY [14] and to DOWELL and RINFERT [15].

The transformation of cubic ice into hexagonal ($I_c \rightarrow I_h$) takes place in the range $160-200$ K. This process needs a higher activation energy than the former because it demands the breakage of 1/4 part of the existing hydrogen bonds which are reestablished after rearrangement in the hexagonal pattern. The energy gain of this transformation is very small, due only to the decrease of pair potentials between some non-nearest neighbours (as explained above).

The amount was estimated by BEAUMONT *et al.* [16] as 1.5 cal g^{-1} (0.024 kcal mol^{-1}), less by an order of magnitude than the enthalpy change of the transition amorphous → cubic.*

It follows from the above considerations that all transformations discussed here must be irreversible: the forms created and existing as metastable phases at lower temperatures represent "frozen in" states as compared with those which are more stable at higher temperatures. The low temperature forms necessarily go over into the more favourable ones on heating, but the reverse processes *i.e.* the transitions $I_h \rightarrow I_c \rightarrow$ *amorphous* have no physical motivation.

*

The author thanks Professor G. SCHAY for helpful comments on the original manuscript.

REFERENCES

[1] HAJDU, F., LENGYEL, S., PÁLINKÁS, G.: J. Appl. Cryst. **9,** 134 (1976)
[1a] HAJDU, F., LENGYEL, S., PÁLINKÁS, G.: Acta Chimica (Budapest) **91**/3, 273 (1976)
[2] HAJDU, F.: Acta Chimica (Budapest) **93**/(3-4), 371 (1977)
[3] OLANDER, D., RICE, S. A.: Proc. Natl. Acad. Sci. USA **69,** 98 (1972)
[4] NARTEN, A. H., VENKATESH, C. G., RICE, S. A.: J. of Chem. Phys. **64,** 1106 (1976)
[5] NARTEN, A. H., DANFORD, M. D., LEVY, H. A.: Disc. Faraday Soc. **43,** 97 (1967)
[6] BAGCHI, S. N.: Acta Cryst. **A28,** 560 (1972)
[7] MOMANY, F. A., CARRUTHERS, L. M., MCGUIRE, R. F., SCHERAGA, H. A.: J. Phys. Chem. **78,** 1959 (1974)
[8] SHIPMAN, L. L., SCHERAGA, H. A.: J. Phys. Chem. **78,** 909 (1974)
[9] LONSDALE, D. K.: Proc. Roy. Soc. **A247,** 424 (1958)
[10] LA PLACA, S., POST, B.: Acta Cryst. **13,** 503 (1960)
[11] BRILL, R., TIPPE, A.: Acta Cryst. **23,** 343 (1967)
[12] POPLE, J. A.: Proc. Roy. Soc. **A205,** 163 (1951)
[13] EISENBERG, D., KAUZMANN, W.: The Structure and Properties of Water, Clarendon Press, Oxford (1969)
[14] GHORMLEY, J. A.: J. Chem. Phys. **48,** 503 (1968)
[15] DOWELL, J. G., RINFERT, A. P.: Nature, **188,** 1144 (1960)
[16] BEAUMONT, R. H., CHIARA, M., MORRISON, J. A.: J. Chem. Phys. **34,** 1456 (1961)
[17] FLETCHER, N. H.: The Chemical Physics of Ice, University Press, Cambridge (1970)

Ferenc HAJDU, H-1431 Budapest, 8. Pf. 156.

* It may be worth noting in connection with the above transformation temperature ranges that studies on the specific heat-temperature function of ice I_h (e.g. LEADBETTER, 1965) have led to the following conclusions. i) Below 80K, the hindered translations are only excited; ii) between 80 and 150 K, hindered rotation modes (librations) are being gradually excited; iii) by 150 K, the librations also contribute significantly to the heat capacity of ice. [13].

Acta Chimica Academiae Scientiarum Hungaricae, Tomus 96 (4), pp. 373–383 (1978)

ISOBENZOPYRYLIUM SALTS, VIII

^{13}C-NMR-SPECTROSCOPIC AND QUANTUM MECHANICAL INVESTIGATION OF THE CONFORMATION OF ISOBENZOPYRYLIUM SALTS

M. FARKAS,* W. VOELTER,** and M. VAJDA

(Central Research Institute for Chemistry of the Hungarian Academy of Sciences, Budapest,
**Department of Pharmaceutical Organic Chemistry, Semmelweis Medical University, Budapest, and*
*** Chemical Institute of the Eberhard-Karl University, Tübingen, GFR)*

Received February 25, 1977

The ^{13}C-NMR chemical shifts of some alkoxy-substituted 1-aryl-isobenzopyrylium salts are correlated with the all-valence charge densities of the various atoms calculated by the Del Bene-Jaffe method. On the basis of the data obtained, some spectral assignments are corrected and it is shown that the charge densities and shifts are in a good correlation if an sp^3 valence orientation is assumed on C-1.

In continuation of our earlier work on 1-aryl-isobenzopyrylium salts (**I**) [1, 2, 3] we now report results of quantum chemical calculations by the Del Bene–Jaffe CNDO method [4] and the correlation of these results with the ^{13}C-NMR data. The purpose of this investigation was twofold. We wished to obtain corroborative quantum chemical data on the effect of substituents on the chemical shift values, and information on the spatial arrangement of the 1-aryl substituent relative to the condensed heterocyclic ring.

Experimental

The compounds investigated were prepared by us as previously reported [5, 6, 7]. Their purity was checked by infrared [8], UV-visible [9] spectra and elemental analysis. Pulse Fourier Transform (PFT) ^{13}C-NMR spectra of 1-aryl-isobenzopyrylium salts were recorded, on a Bruker HFX-90 spectrometer equipped with a PDP-8 computer, in dideuteroformic acid solution except in the case of 1-(*p*-methoxyphenyl)-3-methyl-4-ethyl-6,7-dimethoxyisobenzopyrylium sulfate, which was insoluble in pure dideuteroformic acid and therefore had to be dissolved in a mixture of 9 parts dideuteroformic acid and 1 part of hexadeuterodimethyl sulfoxide. The spectra of 1.3-dimethyl-6,7-dimethoxyisobenzpyrylium perchlorate (**II**)* were recorded on a Varian XL 100 spectrometer, equipped with a Varian 620L computer, in tetradeuteroacetic acid–deuterosulfuric acid.** The concentrations of the solutions were about 0.25 *M*. The spectra were measured using the solvent signals as internal reference and the shifts converted to the TMS scale using data in the literature [10] and also our own measurements of samples containing TMS in the solvents used. The two sets of data agreed within 0.1 ppm.

Both noise-decoupled and off-resonance decoupled spectra of the compounds were recorded to facilitate assignments.

The quantum chemical calculations were performed on a CDC 6000 and a CDC 3000 computer.

* Numbering of atoms in this formula corresponds to the numbering in Table I.

** We are indebted to M. PEREDY–KAJTÁR for recording these spectra.

Method of calculation

For the purpose of determining the geometry of the molecules on which our calculations had to be based, preliminary calculations were performed using the extended Hückel method [3]

These calculations were prompted by the fact that examination of formula **I** and models of this type of structure shows that the plane of the 1-aryl ring cannot be coplanar with the plane of the isobenzopyrylium ring system because in this case the H atoms attached to C-8 and C-16 would be too near to each other. The most probable geometry was found by calculating the all-valence electronic energy of the system, while rotating the aromatic ring around the C-1–C-11 axis, which was taken as the extension of the line connecting C-1 and C-4.

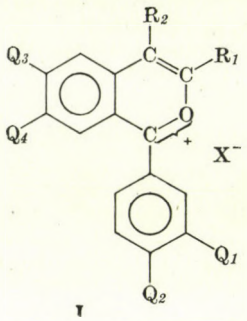

I

Substituents of the isobenzopyrylium salts (**I**)

	Q_3 3'	Q_4 4'	Q_1 6	Q_2 7	R_1 3	R_2 4
a	–	–	–	–	CH_3	C_2H_5
b	–	–	–	CH_3O	CH_3	C_2H_5
c	–	CH_3O	–	–	CH_3	C_2H_5
d	–	CH_3O	–	CH_3O	CH_3	C_2H_5
e	–	–	CH_3O	–	CH_3	C_2H_5
f	–	CH_3O	CH_3O	–	CH_3	C_2H_5
g	–	–	CH_3O	CH_3O	CH_3	C_2H_5
h	CH_3O	CH_3O	CH_3O	CH_3O	CH_3	C_2H_5
i	–	CH_3O	CH_3O	CH_3O	CH_3	C_2H_5
k	–	CH_3O	CH_3O	CH_3O	–	C_2H_5
l	–	CH_3O	CH_3O	CH_3O	CH_3	–
m	CH_3O	CH_3O	CH_3O	CH_3O	–	–
n	CH_3O	C_2H_5O	HO	C_2H_5O	CH_3	C_2H_5

This set of calculations showed that the energy minimum corresponds to a conformation where the plane of the condensed heterocyclic ring system and the plane of the 1-aryl group are at right angles to each other as shown in formula **Ip**.

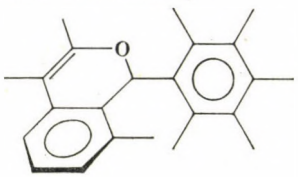

Ip

On the basis of previous experience [11] the Del Bene – Jaffe method was chosen for calculating the energy levels and wave functions,* and from this the all-valence electron charge densities (Coulson populations) were calculated. The paramagnetic contribution of the shielding factors were calculated by the average excitation energy approximation; the diamagnetic contribution was computed using Lamb's formula.

Results and discussion

NMR spectral assignments

Spectral data of the isobenzpyrylium salts investigated are collected in Table I. Assignment of the signals of carbon atoms was accomplished by using literature values, spectra of model compounds [2], prepared by us for this purpose, and also by comparison of the spectra of the various compounds of the isobenzopyrylium salt, isoquinoline and naphthalene series [1]. In some cases ambiguities could be removed and previous mistakes corrected by the use of the results of the quantum mechanical calculations which will be discussed later. These corrected assignments are marked with an asterisk.

Comparison of the spectra of the series of 1-aryl-naphthalene and its aza and oxa analogues, given in our previous communication [1], showed that the signal of C – 1 is shifted to progressively lower field if C – 2 is replaced by an N, N^+ or O atom. Even so the chemical shift of C – 1 in isobenzpyrylium salts of type **I** is substantially less than that of the classical carbonium ions studied by OLÁH *et al.* [15]. Although the difference in solvents (OLÁH used SO_2–SbF_5) should be taken into account, the difference is large enough to show that the positive charge is more delocalized in these compounds than in classical carbonium ions.

A more detailed discussion of assignments can be found in an earlier communication [2].

Quantum chemical calculations

It can be assumed that the differences in chemical shifts in the systems under discussion are mainly due to differences in the paramagnetic contribution, which is considered proportional to the charge density of the atom in question. This assumption should be valid in molecules with mobile electronic systems as the diamagnetic contributions are fairly constant.

Our first calculations by the Del Bene – Jaffe method were based on the conformation shown in **Ip**. In this formula, carbon valence angles were assumed to be the same as in naphthalene, and the C – O – C angle was also taken to be 120°. The results obtained: calculated all-valence electron densities (ΣQ) and measured shifts for compounds where the substituents on C – 6 and C – 7 are varied, are shown in Table II and in Figs 1 – 4.

* The overlay system in the program is the work of A. NESZMÉLYI.

Table I

^{13}C-NMR shifts (TMS=0) of various 1-aryl-isobenzopyrylium salts

Compound	Ia	Ib	Ic	Id	Ie	If	Ig	Ih	Ii	Ik	Il	Im
C–X pK	0.60	1.02	1.48	2.10	3.14	3.84	4.23	4.75	5.01	3.82	3.37	2.1
1	179.4	176.5	178.7	175.9	175.2	174.8	172.2	171.7	172.4	173.6	173.6	174.0
2	–	–	–	–	–	–	–	–	–	–	–	–
3	161.4	160.9	159.8	160.2	160.1	159.0	160.2	159.0	159.5	147.0	161.7	149.7
4	122.1	124.2	121.9	123.5	117.2*	116.9*	118.5*	117.8*	118.3*	118.4*	114.2	116.4
5	129.3	125.7	131.1	125.5	103.3	103.2	102.7*	103.2*	103.2*	107.8	107.8	108.8
6	142.3	135.0	141.7	133.4	171.0	170.5	162.9	162.2	164.3	164.2	165.2	165.0
7	123.8	160.9	123.8	159.0	122.5*	123.5*	152.5	151.7	152.6	152.6	152.7	153.2
8	132.5	108.2	132.9	108.8	135.4*	135.4*	108.0*	108.8*	108.8*	109.2*	105.6	106.6
9	128.6	129.3	128.9	129.2	127.5*	126.5*	127.5*	126.9*	127.3*	130.0*	117.4	118.0
10	140.9	138.5	141.7	137.5	145.1	144.9	141.6	140.8	141.2	140.1	142.2	140.7
11	130.6	131.0	121.3	121.5	128.8	121.2	129.6	122.0	122.1	121.5	121.7	121.6
12	129.3	129.3	134.5	133.4	128.9	133.5	127.9	112.6	133.3	133.0	132.8	113.3
13	131.5	131.0	115.2	115.1	130.8	114.4	129.5	149.8	115.3	114.9	115.0	149.1
14	134.5	134.2	165.4	164.8	133.7	164.4	133.4	155.3	162.7	162.3	163.0	155.7
15	131.5	131.0	115.2	115.1	130.8	114.4	129.5	111.5	115.3	114.9	115.0	111.9
16	129.4	129.4	134.5	133.4	128.9	133.5	127.9	125.6	133.3	133.0	132.8	126.3
17	16.9	18.6	16.7	16.5	16.7	16.5	16.8	16.5	17.2	–	18.1	–
18	19.6	19.8	19.6	19.5	19.4	19.4	19.7	19.4	20.7	20.1	–	–
19	12.2	12.4	12.2	12.2	11.3	11.4	11.7	11.5	12.2	11.3	–	–
20	–	–	–	–	56.6	56.5	57.2	56.9	57.5	57.1	57.0	55.9
21	–	55.6	–	55.2	–	–	55.8	55.7	55.6	55.1	55.0	54.9
22	–	–	–	–	–	–	–	55.2	–	–	–	54.9
23	–	–	55.5	55.5	–	55.1	–	55.2	56.2	55.8	55.8	55.2

* Assignments corrected on the basis of quantum chemical calculations.

Table II

Calculated all-valence charge densities (ΣQ) of atoms C-1 to C-10, based on planar valence orientation on C-1 and measured shifts of 6- and 7-alkoxy-substituted 1-phenyl-3-methyl-4-ethylisobenzpyrylium perchlorates; with regression data $\Sigma Q = A \cdot shift + B$; r = correlation coefficient

Substituent	–		6-Methoxy		7-Methoxy		6-7-Dimethoxy	
C–n	ΣQ	Shift	ΣQ	Shift	ΣQ	Shift	ΣQ	Shift
1	3.7798	179.4	3.7505	175.2	4.1037	176.5	4.1370	172.2
3	3.7193	161.4	3.9237	160.1	4.0234	165.5	4.0472	160.2
4	3.7568	122.1	3.5098	117.2	4.0311	124.2	3.4525	118.5
5	4.6765	129.3	4.8881	103.3	4.3599	125.7	4.2876	102.7
6	3.9471	142.3	3.8737	171.0	4.2448	135.0	3.8055	162.9
7	4.1405	123.8	4.3906	122.5	3.8614	160.9	3.7619	152.5
8	3.5395	132.8	3.6389	135.4	4.0691	108.2	4.0306	108.0
9	4.0569	128.9	3.8767	127.5	4.4200	129.3	4.3333	127.5
10	4.2035	142.3	4.2305	145.1	4.0635	138.5	4.2552	141.6
	$A = -0.0058$		$A = -0.00653$		$A = 0.00315$		$A = -0.00205$	
	$B = 4.7932$		$B = 4.9189$		$B = 4.5725$		$B = 4.2905$	
	$r = -0.325$		$r = 0.377$		$r = 0.397$		$r = 0.1845$	

It is obvious from the Figures and from the regression coefficients given in the Table that the conformation postulated is not quite correct.

The greatest discrepancies observed seem to be connected with carbons C–4 and C–8 and to a lesser extent with C–9 and C–5. It seemed plausible to assume a conformation where the aromatic ring attached to C–1 is closer to the plane of the heterocyclic ring and therefore a conformation was chosen where C–1 has a pyramidal valence orientation; *i.e.*, the three groups attached to it are arranged as if the carbon would be sp^3 hybridized and the δ^+ charge would occupy the direction of the fourth sp^3 orbital. In this case the valence angles between the three ligands on C–1 (O, C–11 and C–9) are 109°. The resulting conformation is shown by the spatial formula **It.**

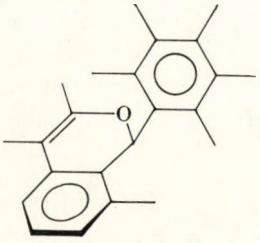

It

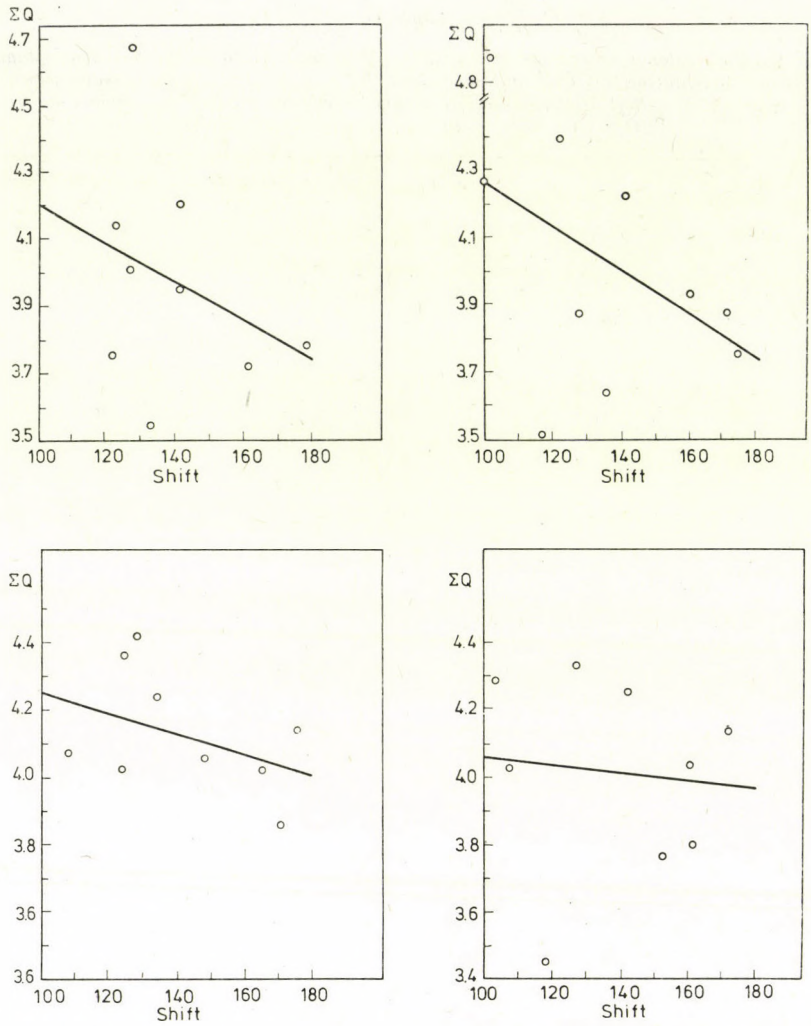

Figs 1—4. Calculated all-valence electron charge densities of 1-phenyl-3-methyl-4-ethylisobenzopyrylium perchlorate derivatives, assuming a *planar* (sp_2) valence orientation on C-1, plotted against the measured $^{13}C-NMR$ chemical shifts 1: Unsubstituted, 2: 6-methoxy, 3: 7-methoxy, 4: 6,7-dimethoxy derivatives

Unfortunately, no direct measurements of valence angles of such salts are available and therefore we have no independent evidence for the reality of this conformation apart from the results we obtained. These results are given in Table III and shown in Figs 5 – 8.

While the regression coefficients in the first set of calculations were between 0.3 – 0.47 for the regression line between the calculated all-valence charge densities and measured chemical shifts, the same regression coefficients for the second set are above 0.97.

Table III

Calculated all valence charge densities (ΣQ) of C atoms 1–10 based on tetrahedral valence orientation on C-1 and measured shift of 6,7-alkoxy substituted 1-phenyl-1-3-methyl-4-ethyl-isobenzpyriliumperchlorates with regression data: $\Sigma Q = A \cdot shift + B$; r = correlation coefficient

Substituent C–n	–		6-Methoxy		7-Methoxy		6,7-Dimethoxy	
	ΣQ	Shift	ΣQ	Shift	ΣQ	Shift	ΣQ	Shift
1	3.7443	179.4	3.6802	175.2	3.6815	176.5	3.6989	172.2
3	3.7762	161.4	3.7315	160.1	3.7375	165.5	3.7271	160.2
4	4.0425	122.1	4.0496	117.2	4.0432	124.2	4.0349	118.5
5	4.0317	129.3	4.0748	103.3	4.0207	125.7	4.0749	102.2
6	3.9447	142.3	3.7038	171.0	3.9692	135.0	3.7318	162.9
7	3.9939	123.8	4.0414	123.5	3.7567	160.9	3.7771	152.5
8	3.9880	132.5	3.9702	135.3	4.0437	108.2	4.0418	108.5
9	4.0024	128.9	4.0158	127.5	3.9932	129.3	4.0004	127.5
10	3.9189	142.3	3.9031	145.1	3.9220	138.5	3.9082	141.6
	$A = -0.00547$		$A = -0.00627$		$A = -0.00637$		$A = -0.00597$	
	$B = 4.7033$		$B = 4.7842$		$B = 4.7990$		$B = 4.7153$	
	$r = -0.970$		$r = -0.975$		$r = -0.971$		$r = -0.979$	

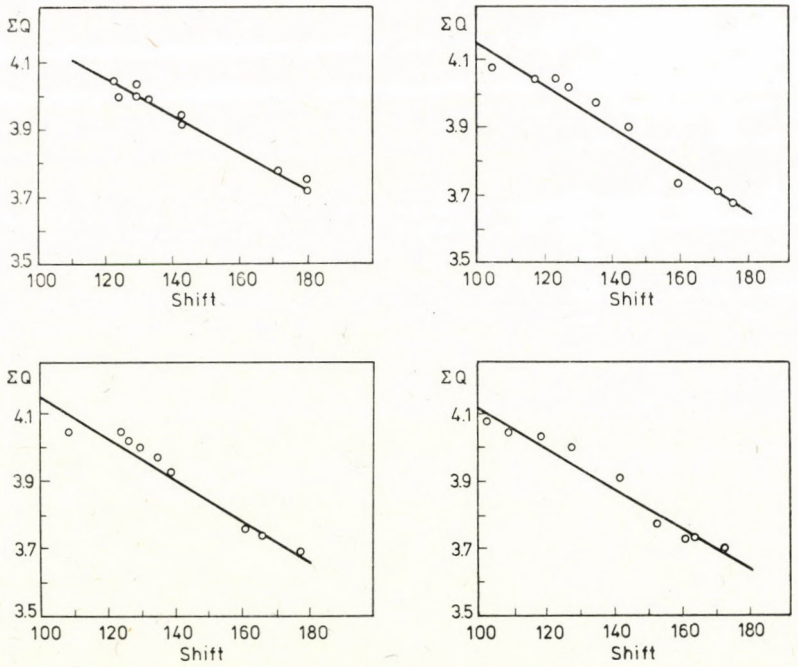

Figs 5–8. Calculated all-valence electron charge densities of 1-phenyl-3-methyl-4-ethyl isobenzopyrylium perchlorate derivatives, assuming a *pyramidal* (sp_3) valence orientation at C-1, plotted against the measured ^{13}C–NMR chemical shifts. 5: Unsubstituted, 6: 6-methoxy, 7: 7-methoxy, 8: 6,7-dimethoxy derivatives

This shows that the picture of the conformation is at least approximately correct. This would mean that a partially positively charged carbon atom in a quasi-aromatic system has a tetrahedral (pyramidal) valence orientation which is difficult to reconcile with our usual picture of an aromatic compound. On the other hand, the charges obtained are in reasonable agreement with the reactivity of the salts. It is found, *e.g.*, that C−1, C−3 and C−6 are positive, while the oxygen atom is a negative centre, and carbons 4, 5 and 10 are also slightly negative. The charges on carbons 7, 8 and 9 vary with the substituents on C−6 and 7, but C−8 and 9 are usually almost neutral. This distribution of electrons is in agreement with the reactivity of the salts. For instance, MÜLLER and LEMPERT-SRÉTER [12] showed that compounds with a free

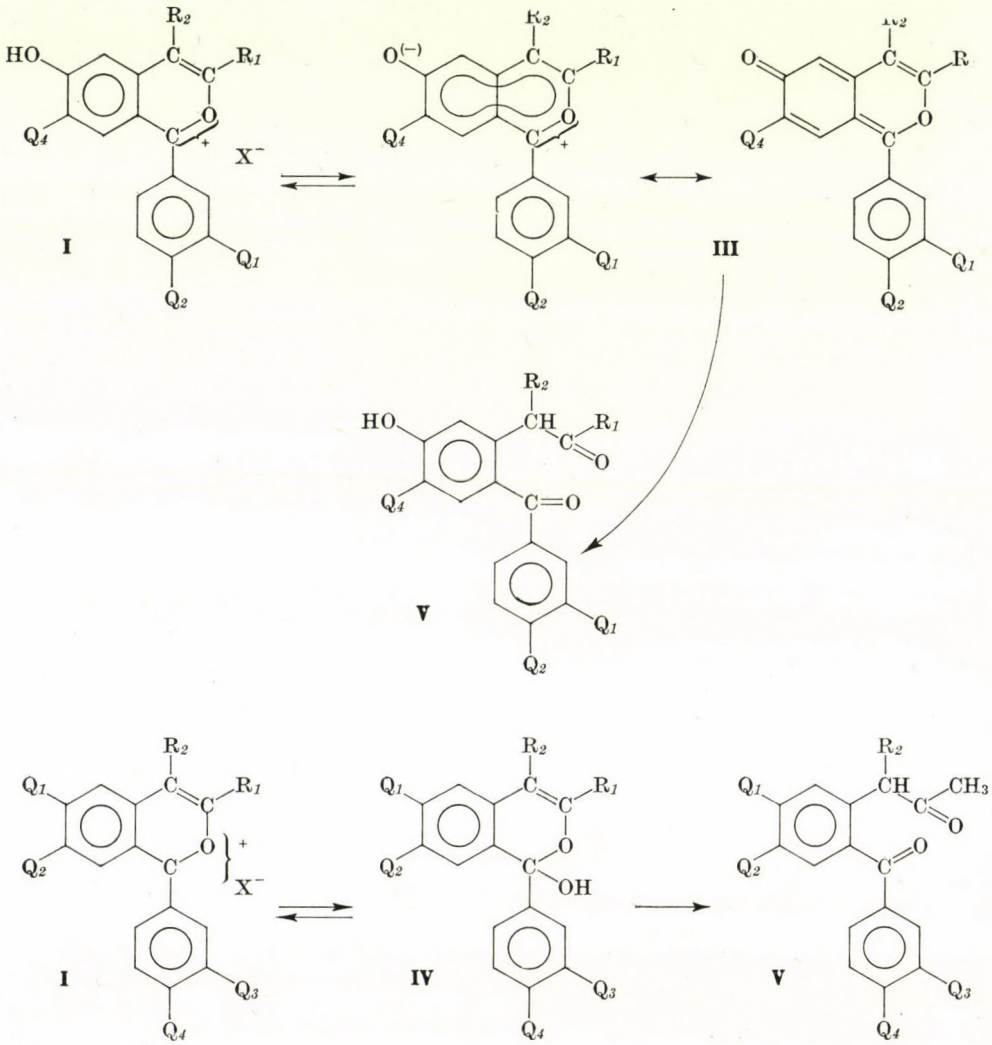

hydroxy group at C – 6 rearrange to a quinonoid structure (**III**) in neutral or slightly alkaline solution while the alkoxy compounds (**I**) undergo ring opening (**V**) at slightly acid or neutral pH values after forming an intermediate pseudobase **IV**. This base is very unstable if no alkoxy substituent is present on C – 6. Although independent evidence for the conformation suggested may be obtained by X-ray diffraction methods and we hope to be able to start such investigations in the near future, the obtaining of satisfactory single crystals is difficult as shown by preliminary experiments, since the crystals are prone to grow in clusters.

Therefore we decided to obtain indirect evidence on the conformation by recording the ^{13}C-NMR spectra of 1,3-dimethyl-6,7-dimethoxyisobenzpyrylium perchlorate (**II**) and comparing the data obtained with the results of the two sets of quantum mechanical calculations, where the first set is based on a geometry where the valence angles at C – 1 were 120°, while in the second set the bond between C – 1 and the methyl carbon was tilted out of the plane of the heterocyclic ring system.

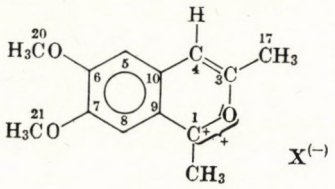

II

The results of this set of calculations are collected and illustrated in Figs 9 – 10 and Table IV. These show that the difference between the energy distribution of the two conformers is very small. The correlation is almost equally good, though the sp^3 case gives a slightly better fit ($r_{sp^2} = 0.98$, $r_{sp^3} = 0.99$).

This result can only be interpreted if we take into account that the large aromatic ring in close proximity of the heterocyclic ring obviously has a large

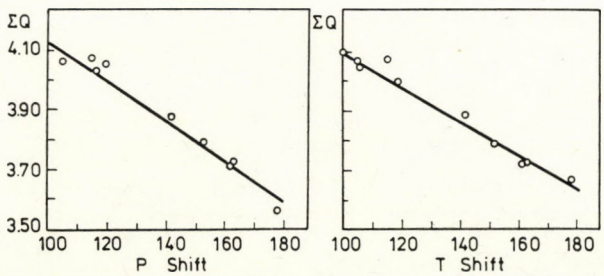

Figs 9 – 10. Calculated all-valence electron change densities of 1,3-dimethyl-6,7-dimethoxyisobenzopyrylium perchlorate plotted against the measured ^{13}C – NMR chemical shifts. 9: Planar valence orientation, 10: pyramidal valence orientation

Table IV

Calculated all-valence charge densities for planar (P) and tetrahedral (T) valence orientations and measured shifts of 1,3-dimethyl-6,7-dimethoxyisobenzpyrylium perchlorate

C–n	φQ		Shift
	P	T	
1	3.5601	3.6701	178.9
3	3.7236	3.7167	162.9
4	4.0749	4.0643	114.5
5	4.0608	4.0610	105.0
6	3.7198	3.7246	162.2
7	3.7952	3.7882	152.0
8	4.0280	4.0373	105.8
9	4.0458	3.9918	118.7
10	3.8780	3.8842	141.1

Regression data:

A =	−0.00661;	−0.00547
B =	4.7874;	4.6731
r =	−0.979;	0.987

shielding effect, whereas the small methyl group has almost no such effect. This result is, therefore, indirect evidence for the correctness of the conformation.

Further experiments in crystal growing for X-ray crystallographic work are in progress.

*

We would like to thank the Deutsche Forschungsgemeinschaft and the Hungarian Academy of Sciences for supporting this work and the Fonds der Chemischen Industrie for a fellowship granted to one of us (M. V.).

REFERENCES

[1] VAJDA, M., VOELTER, W.: Z. Naturforsch. **30**b, 943 (1975)
[2] VAJDA, M., VOELTER, W.: Organic Magnetic Resonance **8**, 324 (1976)
[3] FARKAS, M., BALOGH, K., VAJDA, M.: Computers and Chemistry. **1**, 125—127 (1976)
[4] DEL BENE, J., JAFFE, H. H.: J. Chem. Phys. **48**, 1807 (1969)
[5] VAJDA, M.: Acta Chim. Acad. Sci. Hung. **40**, 295 (1964)
[6] MÜLLER, A., MÉSZÁROS, M., EL SAAVI, M. M., RUFF, F.: Acta Chim. Acad. Sci. Hung. **52**, 267 (1967)
[7] DOROFEENKO, G. N., SEMENOV, A. D., DULENKO, V. I., KRIVUN, S. V.: Zh. Org. Khim. **2**, 1492 (1966)
[8] VAJDA, M., RUFF, F.: Acta Chim. Acad. Sci. Hung. **40**, 217 (1964)
[9] VAJDA, M., RUFF, F.: Acta Chim. Acad. Sci. Hung. **40**, 225 (1964)

[10] *Cf.:* E. BREITMAIER, W., VOELTER: ^{13}C-NMR Spectroscopy. Verlag Chemie, Weinheim/Bergstrasse, 1974
[11] FARKAS, M., NESZMÉLYI, A.: Paper presented at the Conference of the Hungarian Chemical Society, Pécs, 1973. Abstracts of Papers, p. 221
[12] MÜLLER, A., LEMPERT-SRÉTER, M.: Monatshefte **96**, 369 (1965)

Marianne FARKAS, H-1092 Budapest, Hőgyes Endre u. 7.
Wolfgang VOELTER, Chemisches Institut d. Eberhardt-Karl-Universität D-74 Tübingen, Auf der Morgenstelle 18
Miklós VAJDA,* H-1525 Budapest, P. O. Box 17.

* Requests for Reprints should be sent to this author.

Acta Chimica Academiae Scientiarum Hungaricae, Tomus 96 (4), pp. 385—391 (1978)

SYNTHESIS OF VINCA ALKALOIDS AND RELATED COMPOUNDS, IV*

SYNTHESIS OF BUTYL GROUP-CONTAINING (±)-VINCAMINE ANALOGUE

GY. KALAUS, P. GYŐRY, L. SZABÓ and CS. SZÁNTAY

(Institute for Organic Chemistry, Technical University, Budapest, and Central Research Institute for Chemistry, Hungarian Academy of Sciences, Budapest)

Received March 21, 1977

Addition of methyl α-acetoxyacrylate to the enamine of structure **7** and subsequent reduction afforded stereoselectively the alcohol ester **9b**. The oxidation of this latter compound gave racemic 16-deethyl-16-*n*-butylvincamine (**1b**).

The structural modification of vincamine (**1a**), which proved to be an excellent cerebral vasodilator, [2] appeared to be promising in the elucidation of the relationship between structure and biological action. An increase of lipoid solubility and consequent modification of the physiological effects was expected on exchanging the angular ethyl group against a butyl group (**1b**).

The substance of structure **1b** was prepared according to the scheme of our earlier synthesis [3] developed for vincamine.

On alkylating the diethyl (*n*-butyl)malonate with 1-bromo-3-chloropropane the derivative **2** was obtained [4] which behaved under the conditions of hydrolysis similarly to the corresponding ethyl analogue [3]. On heating **2** with sulfuric acid of a concentration of 70 % or higher, the five-membered lactone of structure **3** was formed which is, according to the investigations of OLLIS *et al.* [5], a 1 : 1 mixture of diastereomers.

The six-membered lactone **4** prepared by the alkaline hydrolysis of the diester **2** and subsequent acidification gave, on heating with 70—98 % sulfuric acid, similarly the compound of structure **3** with ring contraction.

In view of a similar conversion observed earlier [3] in the case of the ethyl analogue, ring contraction effected by sulfuric acid of a rather high concentration appears to be a quite general reaction of six-membered lactones carrying an alkyl group in the vicinity of the carbonyl carbon atom.

The reaction of lacton **4** with tryptamine afforded the hydroxypentanoyltryptamide derivative **5**, whose treatment with phosphoryl chloride resulted in ring closure replacement of the hydroxyl group by a chlorine atom. Treatment of the resulting compound **6** with alkali effected another ring closure affording the enamine **7**, to which methyl α-acetoxyacrylate was additioned in methylene chloride in the presence of some methanol as proton source, and the product was isolated as its perchlorate salt (**8**).

* For Part III, Sec Ref. [1].

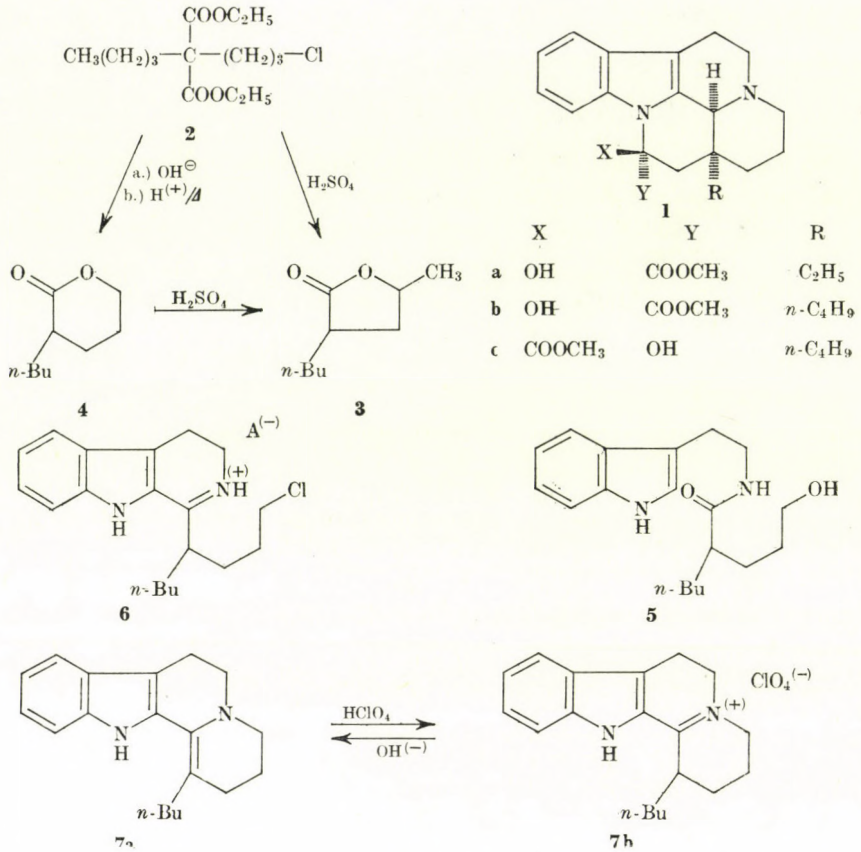

Fig. 1

On reducing the hexahydro derivative **8** either catalytically or with sodium borohydride, only one isomer could be isolated, as a perchlorate, from the reaction mixture.

We ascribe structure **9a** to the substance obtained in this way. It can be identified most conveniently after the hydrolysis of the acetyl group as the readily crystallizing compound **9b**. In the tetracycle **9** the hydrogen of annellation (12bH) and the butyl group are *cis*-positioned in respect to each ether. Thus the compound carrying the *n*-butyl group can be reduced with even better stereoselectivity than its ethyl analogue [3]. This supports again our observations according to which the higher the space requirement of the substituent attached to C−1, the greater will be the amount of *cis* isomer formed at the cost of the *trans* derivative, either in catalytic reduction or in that carried out with sodium borohydride.

The steric structure of compound **9b** is supported by the NMR data. It was found for the corresponding ethyl analogue in the compounds of *cis*-

type that the N*H* signal of indole appeared at a δ value of about 7.8 and that $COOCH_3$ at 3.6, whereas in the *trans* compounds these δ values were at about 9.0 and 3.8, respectively; this is explained by the geometry of the molecule [3]. In the NMR spectrum of **9b**, in turn, the chemical shift of the N*H* proton is 7.78, and that of the $COOCH_3$ proton 3.62, thus the data greatly support the structure suggested.

The alcohol **9b** was oxidized with Fétizon reagent. When the oxidation was carried out in benzene, the main product was the thermodynamically less stable 14-epivincamine analogue **1c**, whereas on performing the reaction at higher temperatures in xylene, the more stable vincamine analogue **1b** was obtained from the reaction mixture as the main product.

In a reaction catalyzed either by Ag ions or by sodium methoxide the epi-product **1c** is converted into the more stable derivative **1b**. Thus, the analogy with the equilibrium conversion observed in the case of vincamine is complete.

The epimeric relation existing between **1b** and **1c** is proved furthermore by the fact that on splitting off water, both compounds afford the same unsaturated compound (**10**).

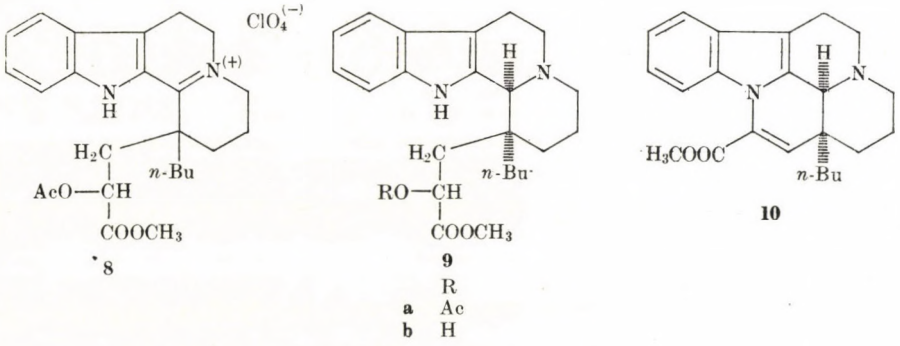

Fig. 2

Experimental

The IR spectra were obtained in KBr pills or in liquid films with a Spektromom 2000 spectro-photometer and the NMR spectra on a Perkin-Elmer R12 (60 MHz) instrument. The UV spectra were recorded with a Unicam SP 800 spectrophotometer.

Diethyl[n-butyl-3-(chloropropyl)]malonate (2)

Sodium metal (21.25 g; 924 mg-atom) was dissolved in 400 ml of anhydrous ethanol under stirring and external cooling with water. After the alkoxide solution had been cooled to room temperature, 200.00 g (924 mmoles) of diethyl (*n*-butyl)malonate was slowly added to the solution. On stirring for a few minutes, a solution of 146.80 g (936 mmoles) of 1-bromo-3-chloropropane in 80 ml of anhydrous ethanol was dropwise added during 30 min. Stirring at room temperature was continued for another 30 min., then the mixture was refluxed for 4 hrs. When the reaction was completed, the ethanol was evaporated in vacuum, the residue diluted with

300 ml of distilled water and extracted with benzene (200, 150, 100 ml). The combined organic phases were washed with 200 ml of distilled water and dried over magnesium sulfate. After filtration the benzene was evaporated in vacuum (water-pump). The viscous, oily residue was fractionated in high vacuum to yield 132.00 g (49.0 %) of a colourless oil, b.p. 137 – 138 °C at 0.6 torr; $n_D^{26} = 1.4412$.

$C_{14}H_{25}ClO_4$ (292.79). Calcd. C 57.42; H 8.60; Cl 12.10. Found C 56.96; H 8.63; Cl 11.94 %.

IR (film): ν_{max} 1727 cm^{-1} (>C=O).

NMR (in CCl_4): δ4.12 (q, 4H, $-\overset{\overset{O}{\|}}{C}-O-CH_2$); 3.52 (t, 2H, $-CH_2-Cl$); 1.21 (t, 6H, $-\overset{\overset{O}{\|}}{C}-CH_2-CH_3$); 0.89 (t, 3H, $-CH_2-CH_3$).

2-n-Butyl-5-pentanolide (4)

Potassium hydroxide (76.45 g; 1.36 mmole) was dissolved in 80 ml of distilled water, 100 ml of ethanol and 80.00 g (273 mmoles) of diethyl [*n*-butyl-3-(chloropropyl)] malonate (**2**) were added, and the reaction mixture was refluxed for 6 hrs. The ethanol was evaporated from the suspension in vacuum (water-pump) and the residue acidified to pH 5 with a 50 % solution of sulfuric acid. After the addition of 13.7 ml of conc. H_2SO_4, the mixture was kept and a bath of 120 – 140 °C until the evolution of carbon dioxide gas ceased (about 3 hrs). The cooled reaction mixture was diluted with 200 ml of distilled water and extracted with benzene (200, 100, 80 ml). The combined organic phases were washed with a 5 % solution of sodium hydrogen carbonate and dried over $MgSO_4$. The oily residue obtained on evaporation of the solvent was fractionated in vacuum, to yield 27.60 g (64.9 %) of a colourless oil, b.p. 104 – 106 °C at 0.7 torr; $n_D^{22} = 1.4511$.

$C_9H_{16}O_{22}$ (156.22). Calcd. C 69.19; H 10.32. Found C 68.86; H 10.08 %.

IR (film): ν_{max} 1730 cm^{-1} (>C=O).

NMR (in CCl_4): δ 4.24 (t, 2H, $-\overset{\overset{O}{\|}}{C}-O-CH_2-$); 0.92 (t, 3H, $-CH_2-CH_3$).

2-n-Butyl-4-pentanolide (3)

(*a*) Conc. sulfuric acid (173 ml) was slowly poured, with cooling, into 120 ml of distilled water, then 75.00 g (257 mmoles) of diethyl [*n*-butyl-3-(chloropropyl)]malonate (**2**) was added and the reaction mixture refluxed for 4 hrs. in a nitrogen atmosphere with vigorous stirring. The solution was cooled, 200 ml of distilled water was added and the mixture was shaken with benzene (100, 80, 50 ml). The combined organic phases were washed with a 5 % solution of $NaHCO_3$ then with distilled water and dried over $MgSO_4$. The residue obtained after evaporation of the solvent was fractionated to yield 19.70 g (49.2 %) of a colourless oil, b.p. 115 – 116 °C at 8 torr; $n_D^{20} = 1.4362$.

$C_9H_{16}O_2$ (156.22). Calcd. C 69.19; H 10.32; Found C 68.98; H 10.18 %.

IR (film): ν_{max} 1762 cm^{-1} (>C=O)

NMR (in CCl_4): δ 4.49 (s, 1H, $CH_3-\underset{|}{CH}-O-\overset{\overset{O}{\|}}{C}-$); 0.92 (t, 3H, $-CH_2-CH_3$).

(*b*) Conc. sulfuric acid (50 ml) was mixed slowly, with cooling, with 40 ml of distilled water then 15.00 g (96.5 mmoles) of 2-n-butyl-5-pentanolide(**4**) was added and the reaction mixture refluxed for 5 hrs.; it was poured then onto about 200 g of ice and extracted with benzene (200, 100, 50 ml). The combined organic phases were washed with a 5 % solution of $NaHCO_3$ distilled water and subsequently dried over $MgSO_4$. The dark oil which remained after evaporation of the solvent was fractionated in vacuum to obtained 7.80 (51.8 %) of a colourless oil, b.p. 142 – 146 °C at 21 Torr; $n_D^{26} = 1.4382$.

The product was in all respects completely identical with that prepared according to (*a*).

2-n-Butyl-5-hydroxypentanoyltryptamide (5)

Tryptamine (20.40 g; 127 mmoles) was dissolved in 140 ml of chlorobenzene, 23.85 g (152 mmoles) of 2-n-butyl-5-pentanolide (**4**) was added and the reaction mixture refluxed for 8 hrs. At the end of the reaction the solvent was distilled off in vacuum and the residue rubbed with petroleum ether. The solution was decanted from the solid portion, the residue dissolved

in 300 ml of dichloromethane and shaken with 100 ml of 1 : 4 dilute HCl solution. The organic phase was washed with distilled water until free of acid, than dried over $MgSO_4$. The slightly reddish solution was filtered, the filtrate evaporated in vacuum and the oily residue crystallized from twice its volume of dichloroethane to obtain 42.65 g (66.1 %) of a white crystalline substance, m.p.: 78 – 80 °C.

$C_{19}H_{28}N_2O_2$ (316.43). Calcd. C 72.11; H 8.92; N 8.85 Found C 71.80; H 9.18; N 8.92 %.

IR (KBr): ν_{max} 3250 cm^{-1} (indole-NH); 1622 cm^{-1} (>C=O).

NMR (in deuterochloroform): δ 8.95 (s, 1H, indole-NH); 7.56 – 6.98 (m, 4H, aromatic H); 3.60 (t, 2H, $-CH_2-OH$); 3.12 – 2.90 (m, 3H, $-CH_2-N-C-$ and $-CH-C-N-$).

1-n-Butyl-1,2,3,4,6,7-hexahydro-12H-indolo[2,3-a]quinolizin-5-ium perchlorate (7b)

2-*n*-Butyl-5-hydroxypentanoyltryptamide (**5**) (42.65 g; 135 mmoles) was dissolved in 250 ml (2.72 mmoles) of freshly distilled phosphoryl chloride and the solution refluxed for 8 hrs. The solution was then evaporated in vacuum and the residual dark brown oil dissolved in 300 ml of dichloromethane. The reaction mixture was diluted with 300 ml of distilled water and made alkaline to pH 11, under cooling, with 40 % NaOH solution. The organic phase was separated and the aqueous phase shaken with 2 × 100 ml of dichloromethane. The combined dichloromethane solution were dried over $MgSO_4$ and the residual red oil obtained after evaporating the solvent was dissolved in some methanol. On adding 70 % aqueous perchloric acid solution (up to pH 6), a yellow crystalline salt precipitated instantaneously. A second crop of crystals was obtained on allowing the mixture to stand in a refrigerator. The yield was 29.90 g (61.7 %) of a yellow crystalline powder; m.p.: 198 – 200 °C. On recrystallization from methanol the m.p.: rose to 201 – 202 °C.

$C_{19}H_{25}N_2ClO_4$ (380.86). Calcd. C 59.61; H 6.61; N 7.35. Found C 60.06; H 6.67; N 7.03 %.

IR (KBr): ν_{max} 3240 cm^{-1} (indole-NH); 1629 cm^{-1} ($>C=\overset{(+)}{N}-$).

UV (in methanol): λ_{max} 359 nm (log ε = 4.3598).

1-n-Butyl-1-{[2-(acetyloxy)]-(methoxycarbonylethyl)}-1,2,3,4,6,7-hexahydro-12H-indolo[2,3-a]quinolizin-5-ium perchlorate (8)

1-*n*-Butyl-1,2,3,4,6,7-hexahydro-12H-indolo[2,3-a]-quinolizin-5-ium perchlorate (**7**) (10.00 g; 26.6 mmoles) was suspended in 100 ml of dichloromethane, then 75 ml of distilled water and 20 ml of 2*N* NaOH were added. The mixture was stirred for 10 min. in an argon atmosphere and the organic phase was separated. The aqueous solution was shaken with 20 ml of dichloromethane, and the combined organic solutions dried over $MgSO_4$. After filtering off the drying agent, 10.0 ml of freshly distilled methyl [2-(acetyloxy)]acrylate was slowly added to the filtrate. The reaction mixture was rinsed with argon gas, sealed and allowed to stand for two days at room temperature. The solvent was evaporated in vacuum and the residual dark red oil rubbed with 3 × 50 ml of petroleum ether. The solidifying yellowish red substance was dissolved in 30 ml of hot methanol and slightly acidified (to pH 6) with a 70 % aqueous solution of perchloric acid, then the solution was allowed to stand in a refrigerator. The yellow salt which precipitated was filtered off with suction and washed with some cold methanol to obtain 4.20 g (30.0 %) of a yellow crystalline substance, m.p.: 210 – 212 °C. On recrystallizing the product from methanol, the m.p.: rose to 214 – 215 °C.

$C_{25}H_{33}N_2ClO_8$ (524.98). Calcd. C 57.19; H 6.33; N 5.34. Found C 57.40; H 6.21; N 5.19 %.

IR (KBr): ν_{max} 3320 cm^{-1} (indole-NH); 1758 cm^{-1} (acetyl >C=O); 1733 cm^{-1} (ester >C=O); 1629 cm^{-1} ($>C=\overset{(+)}{N}-$)

1α-n-Butyl-1-{[2-(acetyloxy)]-(methoxycarbonylethyl)}-1,2,3,4,6,7,12,12bα-octahydroindolo[2,3-a]quinolizine perchlorate (9a . $HClO_4$)

5 % palladium on bone black (about 1 g) was prehydrogenated in some methanol then a solution of 1.00 g (1.91 mmole) of the perchlorate salt **8** in 600 ml of methanol was slowly

added. The hydrogenation was carried out at room temperature and atmospheric pressure. The calculated amount (46 ml) of hydrogen was taken up by the substance in 6 hrs. At the end of the reaction the catalyst was filtered off and the solvent evaporated in vacuum. The residue was dissolved in some methanol and refrigerated to achieve crystallization. The product was filtered with suction to obtain 0.50 g (50.1 %) of white crystals, m.p. 218 – 219 °C.

$C_{25}H_{35}N_2ClO_8$ (527.00). Calcd. C 56.96; H 6.69; N 5.31. Found C 56.93; H 6.98; N 5.67 %.

IR ν_{max} (KBr): 1741 cm^{-1} (>C=O).

1α-n-Butyl-1-[2-hydroxy-(methoxycarbonylethyl)]-1,2,3,4,6,7,12,12bα-octahydroindolo[2,3-a]quinolizine (9b)

(*a*) The perchlorate **9a** (6.40 g; 12.1 mmoles) was dissolved in 150 ml of methanol saturated at 0 °C with hydrogen chloride and refluxed for 3 hrs. The acid solution was concentrated in vacuum, the residual solution was dissolved in 200 ml of a 1 : 1 mixture of acetone and water, and made alkaline to pH with a saturated solution of sodium carbonate. Distilled water (500 ml) was added to the solution, the resulting white precipitate was filtered off with suction and washed with distilled water to obtain 3.90 g (80.8 %) of white crystals m.p.: 207 – 208 °C.

$C_{24}H_{34}N_2O_3$ (398.53). Calcd. C 72.33; H 8.60; N 7.03. Found C 72.22; H 8.86; N 6.97 %.

IR (KBr): ν_{max} 1758 cm^{-1} (>C=O).

NMR (in deuterochloroform): δ 7.78 (s, 1H, indole-NH); 7.24 (m, 4H, aromatic H); 3.62 S, 3H, ester-CH_3).

(*b*) The adduct **8** (6.00 g; 11.4 mmoles) was suspended in 200 ml of methanol, and 4.00 g (106 mmoles) of sodium borohydride was added to the reaction mixture in small portions under cooling in ice-water. After the addition was completed, the solution was stirred for another hour at 0 °C, then acidified to pH 5 with 20 % acetic acid. The acidified solution was concentrated in vacuum 50 ml. The remainder was diluted with 150 ml of water, 200 ml of dichloromethane was added and the mixture was made alkaline (pH 10) with 40 % NaOH solution. After separation of the organic phase, the aqueous phase was repeatedly shaken with further 50 ml of dichloromethane, and the combined dichloromethane solutions were dried over $MgSO_4$. The drying agent was filtered off and the solvent evaporated vacuum to leave 4.80 g of a yellow oil. (During the reaction the product underwent partial deacetylation, therefore the crude product was processed without crystallization).

The oil was refluxed for 3 hrs. in 100 ml of methanol containing hydrochlorid acid, then methanol was removed by vacuum distillation, and the residual salt mixture dissolved in 100 ml of a 1 : 1 mixture of acetone and water. The solution was made alkaline (pH 10) with a saturated solution of sodium carbonate and 400 ml of water was added to complete the precipitation of the substance. The crystals were filtered off with suction to obtain 3.20 g (70.4 %) of a white flocculated substance, m.p.: 207 – 208 °C.

The product was in all respects identical with that prepared according to (*a*).

(±)-16-Deethyl-16-n-butyl-14-epivincamine (10)

The alcohol **9b** (1.00 g; 2.61 mmoles) was suspended in 80 ml of anhydrous benzene, 5.00 g of Fétizon reagent was added and the mixture refluxed for 72 hrs., with stirring. The progress of the reaction was followed by chromatography. The solution was filtered from the solid, half of the solvent was evaporated and the residue allowed to crystallize at room temperature. The product was 0.65 g (65.1 %) of colourless powdery crystals, m.p.: 186 – 187 °C.

$C_{23}H_{30}N_2O_3$ (382.49). Calcd. C 72.22; H 7.91; N 7.32. Found C 72.14; H 7.98; N 7.53 %.

IR (KBr): ν_{max} 1726 cm^{-1} (>C=O).

NMR (in deuterochloroform): δ4.56 (s, 1H, anellation-H); 3.71 (s, 3H, ester-CH_3).

(±)-16-Deethyl-16-n-butylvincamine (1b)

(*a*) The alcohol **9b** (1.00 g; 2.61 mmoles) was dissolved in 50 ml of hot anhydrous xylene, 5.00 g of Fétizon reagent was added and the suspension refluxed for 8 hrs., with stirring. The oxidation was complete in 3 – 4 hrs. On further heating, the first formed **12b** epimerized to the end product **12a**. The progress of the reaction was followed by thin-layer chromatography [adsorbent: alumina 60 F 254 neutral (Type E); developing solvent mixture of 10 ml dichloromethane and 0.05 ml methanol; detection in iodine vapour].

After the elapse of 8 hrs., which proved to be the optimum period of treatment, only traces of **12b** could be detected in the reaction mixture.

The solid was filtered off from the hot suspension, and the xylene solution was allowed to stand first at room temperature, and then in a refrigerator to yield 0.35 g (35.2 %) of chromatographically homogeneous (±)-16-deethyl-16-n-butylvincamine, m.p.: 202 – 203 °C.

$C_{23}H_{30}N_2O_3$ (382.49). Calcd. C 72.22; H 7.91; N 7.32. Found C 72.27; H 8.04; N 7.49 %.

IR (KBr): ν_{max} 1732 cm^{-1} (>C=O).

NMR (in deuterochloroform): δ 4.61 (s, 1H, anellation-H); 3.82 (s, 3H, ester-CH_3).

(*b*) (±)-16-Deethyl-16-n-butyl-14-epivincamine (**1c**) (0.20 g; 0.52 mmole) was dissolved in 15 ml of anhydrous methanol. 0.20 g (3.70 mmoles) of sodium methoxide was added and the mixture refluxed for 3 hrs. The methanol was then evaporated in vacuum and the residue dissolved in 15 ml of hot anhydrous benzene. The insoluble residue was filtered off and the solution concentrated to half of its volume. On standing for several hours a white powdery crystalline substance precipitated, which was filtered off with suction to yield 0.12 g (60.0 %) of **1b**, m.p.: 201 – 202 °C.

The product was in all respects identical with that prepared according to (*a*).

(*c*) (±)-16-Deethyl-16-n-butyl-14-epivincamine (**1c**) (0.20 g; 0.52 mmole) was refluxed with 1.0 g of Fétizon reagent in 40 ml of anhydrous xylene, with stirring. Epimerization was complete in 2 hrs. (The conversion can be well followed by thin-layer chromatography.) At the end of the reaction the catalyst was filtered off from the hot solution. The substance which separated on standing in a refrigerator was filtered off with suction to obtain 0.16 g (80.0 %) of a white crystalline substance, m.p.: 201 – 202 °C.

The product was in all respects identical with that prepared according to (*a*).

(±)-16-Deethyl-16-n-butylapovincamine (10)

(*a*) (±)-16-Deethyl-16-n-butyl-14-epivincamine (**1c**) or (±)-16-deethyl-16-n-butylvincamine (**1b**) (0.40 g; 1.04 mmole) was dissolved in 30 ml of acetic anhydride and the mixture refluxed for 24 hrs. The dark solution was then evaporated in vacuum, the residue dissolved in 50 ml of distilled water and made alkaline (pH 10 – 11) with a 40 % NaOH solution. It was then extracted with ether (30, 20, 10 ml), the organic phase dried over $MgSO_4$ and the solvent was evaporated in vacuum. The residual light coloured oil was dissolved in a minimum volume of methanol and acidified to pH 4 with a 70 % aqueous solution of perchloric acid. On scratching, white crystals precipitated which were filtered off with suction to obtain 0.35 (72.3 %) of the product, m.p.: 239 – 240 °C.

$C_{23}H_{29}N_2ClO_6$ (464.92). Calcd. C 59.41; H 6.29; N 6.03. Found C 59.64; H 6.12; N 5.89 %.

IR (KBr): ν_{max} 1726 cm^{-1} (>C=O); 1636 cm^{-1} (>C=C<); 1615 cm^{-1} (>C=C<).

*

The authors' thanks are expressed to the Gedeon Richter Pharmaceutical Factory for supporting our studies.

REFERENCES

[1] Kalaus, Gy., Szabó, L., Horváth, J., Szántay, Cs.: Heterocycles **6,** 321 (1977)
[2] Szporny, L., Szász, K.: Arch. Exp. Path. Pharm. **236,** 296 (1959)
[3] Szántay, Cs., Szabó, L., Kalaus, Gy.: Tetrahedron Letters **1973,** 191; complete paper: Tetrahedron **33,** 1803—1808 (1977)
[4] Sarkisyan, P. A., Zalanyan, M. G., Dangyan, M. T.: Arm. Khim. Zh. **1971** 24 (3), 245—251; C. A. **75,** 63050
[5] Hussain, S. A. M. T., Ollis, W. D., Smith, Ch., Stoddart, J. F.: J. Chem. Soc. Perkin I, **1975,** 1480

György Kalaus
Péter Győry
Lajos Szabó
Csaba Szántay

H-1521 Budapest, Gellért tér 4.

Acta Chimica Academiae Scientiarum Hungaricae, Tomus 96 (4), pp. 393—404 (1978)

THE SYNTHESIS OF SOME DIBENZO[a,d]-CYCLOHEPTENES, TRIBENZO[a,c,e]CYCLOHEPTENES AND HETEROCYCLIC ANALOGUES, MODEL COMPOUNDS FOR CONFORMATIONAL STUDIES

M. NÓGRÁDI

(Research Group for Alkaloid Chemistry of the Hungarian Academy of Sciences, Budapest)

Received April 1, 1977

The synthesis of dibenzo[*a*, *d*]cycloheptenes, dibenz[*b*,*f*]azepins, dibenzo[*b*, *f*]-oxepins, dibenzo[*b*,*f*]thiepins, and tribenzo[*a*, *c*, *e*]cycloheptenes with prochiral substituents as markers for conformational studies by ^{1}H-NMR is described.

The study of nuclear magnetic resonance spectra at variable temperatures is a powerful tool to collect information about intramolecular exchange processes [1]. Some years ago we reported the utilization of this technique in the investigation of the possibility of aromaticity and antiaromaticity in polycyclic systems containing seven-membered homocyclic or heterocyclic rings [2].

For our studies derivatives of dibenzo[*a*,*d*]cycloheptene, dibenzo[*b*,*f*]-oxepin, dibenzo[*b*,*f*]thiepin, dibenz[*b*,*f*]azepin, and tribenzo[*a*,*c*,*e*]cycloheptene, substituted with prochiral groups (*e.g.* benzyl, isopropyl, ethyl) were required and in this paper we are dealing with the synthesis of these compounds.

As the first member of this series 1-benzyldibenzo[*a*,*d*]cyclohepten-5-one (**1**) has been prepared by the adaptation of a known sequence of reactions.

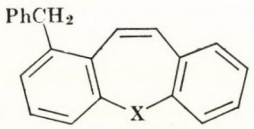

1 : X = CO
2 : X = CH_2

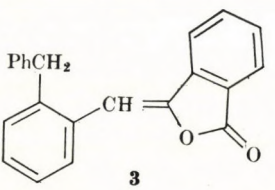

3

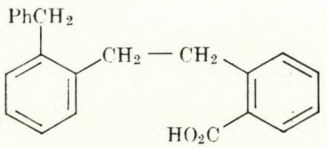

4

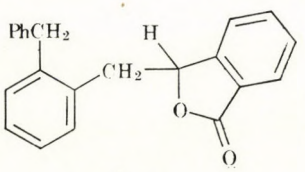

5

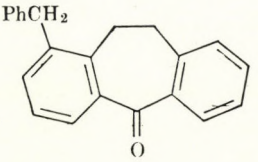

6

2-Benzylphenylacetic acid [3] was condensed [4] with phthalic anhydride to give the phthalide **3**, which was reduced with hydrogen iodide and red phosphorus [5] to the acid **4** that was accompanied by minor amounts of the partially reduced phthalide **5** and a condensed aromatic hydrocarbon, $C_{22}H_{18}$, of unknown structure. The acid was converted to its chloride and cyclized by heating with a trace of polyphosphoric acid [6] to yield the ketone **6** in moderate yield. In view of the presence of a susceptible diphenylmethyl moiety in the molecule, the usual bromination-dehydrobromination procedure was avoided and the double bond was introduced by dehydrogenation with palladium-on-charcoal. A by-product of this reaction was the hydrocarbon **2**, which has also been prepared by Wolf–Kishner reduction of the ketone **1**.

As the dibenzotropone **1** did not exhibit anisochrony of the protons of the methylene group, we turned our attention to analogues substituted on the ethylene bridge by the hydroxyisopropyl group.

Introduction of this function was conveniently performed by lithiation of the corresponding bromo compounds with butyllithium [7], followed by the addition of acetone.

The bromo compounds **7** [7], **8** [8], **10** [9] and **12** [10] have been reported in the literature, and we have described the preparation of **11** earlier [11].

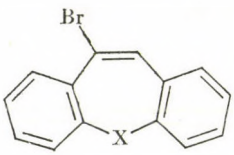

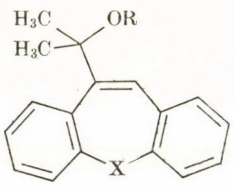

7: X = $>C(OMe)_2$

8: X = $>C{=}CH_2$

9: X = $>CH_2$

10: X = $>O$

11: X = $>S$

12: X = $>NCOCH_3$

13: X = $>NC_2H_5$

14: X = $>CO$, R = H

15: X = $>CO$, R = CH_3

16: X = $>CO$, R = n-C_3H_7

17: X = $>CH_2$, R = H

18: X = $>C{=}CH_2$, R = H

19: X = $>O$, R = H

20: X = $>NC_2H_5$, R = H

21: X = $>S$, R = H

22: X = $>SO$, R = H

23: X = $>SO_2$, R = H

9 has been prepared by bromination [12] followed by dehydrobromination of the appropriate unsaturated parent compound [12].

Lithiation of the bromo compounds **7**–**11** and addition of acetone generally proceeded smoothly giving the corresponding hydroxyisopropyl compounds in 30–70 % yield.

Removal of the ketal blocking group from the reaction product of **7** was accomplished by treatment with a mixture of isopropanol and dilute hydrochloric acid. The use of methanol for the same purpose gave rise to a mixture of the tertiary carbinol **14** and its methyl ether **15**. The carbinol gave the corresponding ethers when dissolved in methyl, ethyl or *n*-propyl alcohol containing a trace of acid. The rate of etherification decreased, however, rapidly with increasing chain length and the amount of by-products rose simultaneously. Since for our purpose it seemed to be useful to increase the size of the prochiral substituent, the *n*-propyl ether **16** was prepared on a preparative scale. The by-products in this case were identified as the elimination product **24** and the isomeric *n*-propyl ether **25** arising from the allylic rearrangement of the intermediate cation. The structure of the isopropylidene compound **25** was supported by its NMR spectrum showing a pair of methyl singlets at δ 1.60 and 1.65 ppm [$(CH_3)_2C=$], a broad singlet at δ 5.27 ppm (CH–O–), and the set of signals generated by the *n*-propyl group. On reacting **14** with isopropyl alcohol only dehydration to **24** took place.

The sulfoxide **22** and sulfone **23** have been prepared by oxidation of the sulfide **21** with one and two moles of perlauric acid, respectively.

As the amide **12** [10] did not react with *n*-butyllithium in the required way, it was reduced with lithium aluminium hydride to the amine **13** that underwent smooth reaction to give the hydroxyisopropylamine **20**.

Addition of acetophenone to the lithiation product of 10-bromodibenzo-[*b*,*f*]oxepin **10** produced the secondary alcohol **26**. Dehydration to **27** and subsequent careful hydrogenation afforded **28**.

Since the steric hindrance provided by a single substituent on the ethylene bridge of dibenzotropone proved to be insufficient to raise the energy barrier of the ring inversion process to a level that could be conveniently

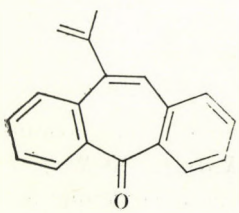

24

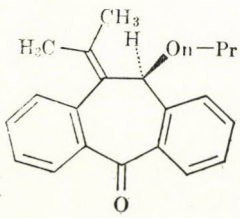

25

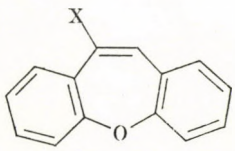

26: X = Ph–C(OH)CH_3

27: X = Ph–C=CH_2

28: X = Ph–CH–CH_3

studied by ^{1}H-NMR, attempts were made to synthesize derivatives having a pair of identical prochiral groups on the ethylene bridge.

The ketone **29** described by TOCHTERMANN, FRANKE and SCHÄFER [13] seemed to be a suitable starting material for this purpose. Oxidation with bromine in methanol, a reaction widely applied on simple furans [14] gave a mixture of *cis* and *trans* isomers of the cyclic diacetal **30**. Fractional crystallization afforded one of the isomers pure, to which the *trans* configuration has been tentatively assigned on the evidence of the relative positions of the acetal proton signals in the ^{1}H-NMR spectrum (stronger deshielding in the *trans* isomer owing to the through-space effect of the vicinal oxygen atom). The mixture of acetals was remarkably resistant to acid and could only be hydrolyzed by relatively strong acid at elevated temperatures. The product of this reaction was, however, not the expected dialdehyde. Though on one hand it furnished the expected composition and mass spectrum (M^+ 262 *m/e*, successive loss of CO and CHO fragments as the main breakdown pattern), but on the other it exhibited infrared absorption at 1750 cm^{-1} and a two-proton singlet at δ 5.62 ppm in the ^{1}H-NMR spectrum. Its extreme insolubility suggested that it was a dimer of the dialdehyde. Due to its insolubility it was difficult to bring about any reaction of this substance, so we turned our attention to the acetal **30** and found that it could be oxidized with chromium trioxide directly to the anhydride **31**. Unfortunately this compound was extremely unreactive and resisted hydrolysis, esterification or ketalisation, operations which would have been necessary for the conversion of the anhydride function to a pair of identical prochiral groups.

As according to TOCHTERMANN, SCHNABEL and MANNSCHRECK [15] the fusion of a third benzene ring to the dibenzotropene system considerably enhances the activation energy of ring inversion, compounds with prochiral substituents have been prepared in this series.

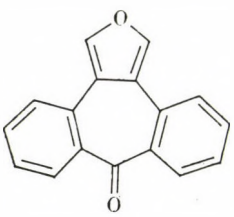

29

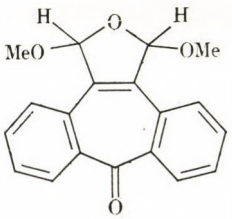

30

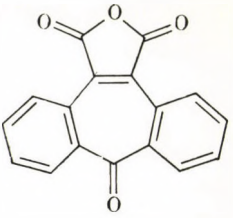

31

1-Ethyltribenzo[*a,c,e*]cyclohepten-9-one (**34**) was obtained by the adaptation of the elegant sequence described by TOCHTERMANN, OPPENLÄNDER and WALTER [16]. Diels-Alder addition of 2-ethylfuran [17] on dibenzo[*a,d*]cycloheptin-5-one, generated *in situ* from 10-bromodibenzo[*a,d*]cycloheptan-5-one [18]

gave the epoxide **32**, that was hydrogenated to **33** and subsequently dehydrated to yield **34**. It should be noted that dehydration with polyphosphoric acid at 150 °C for 2 hrs., as recommended [15], gave only very low yields of the tribenzoketone **34** and some of the fluorenone **38**, a reported type of by-product [15] of this reaction. Short boiling in toluene with *p*-toluenesulfonic acid produced **34** in high yield. Wolf–Kishner reduction of **34** and the known **35** [16] gave the hydrocarbons **36** and **37**, respectively.

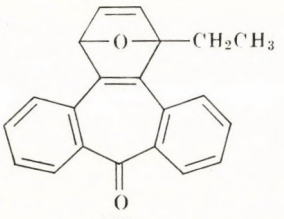

32

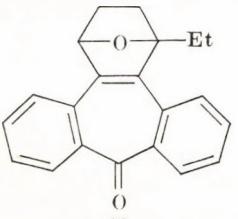

33

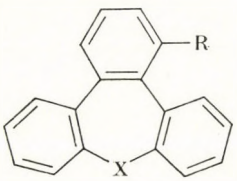

34: X = CO, R = Et

35: X = CO, R = H

36: X = CH_2, R = Et

37: X = CH_2, R = H

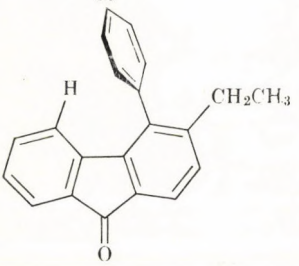

38

Experimental

M.p.'s were taken on a Kofler hot-stage and are uncorrected. IR spectra were recorded on a Perkin-Elmer Infracord instrument in chloroform solutions or, if stated, in KBr pellets. ^{1}H-NMR spectra were obtained on a Varian 60A or a Varian HA 100 spectrometer, if not otherwise stated, in $CDCl_3$ solutions with tetramethylsilane as internal standard. Chemical shifts are given in δ values.

2-(2-Benzylbenzylidene)phthalide (3)

An intimate mixture of 2-benzylphenylacetic acid [3] (15.6 g), phthalic anhydride (8.6 g) and anhydrous sodium acetate (1.1 g) was heated 90 min. at 260 °C bath temperature. The resulting gum was taken up in chloroform and extracted thoroughly with aqueous $NaHCO_3$ solution. The chloroform phase was evaporated and the residue crystallized from ethanol togive **3** (6.0 g, 37 %), m.p. 110–112 °C. Repeated recrystallization from ethanol gave colourless needles of the pure phthalide, m.p. 115–117 °C.

IR: ν_{max} 1780, 1650, 1500 and 960 cm^{-1}.

NMR: δ 7.13–8.30 (m, 8H), 6.58 (s, –HC=C), and 4.17 (s, CH_2).

$C_{22}H_{16}O_2$ (312.4). Calcd. C 84.59; H 5.16. Found C 84.51; H 5.21 %.

2-[2-(2-Benzylphenyl)ethyl]benzoic acid (4)

The phthalide **3** (8.0 g) and red phosphorus (3.0 g) were refluxed in 57% hydrogen iodide (40 ml) for 42 hrs. Additional amounts of red phosphorus (3.0 g each time) were added after 6 and 12 hrs. The reaction mixture was then poured into water, the precipitate filtered off and throughly extracted with ether. The ethereal solution was first extracted with aqueous $NaHCO_3$ and then with 10 % aqueous K_2CO_3 solution. Acidification of the K_2CO_3 extract gave the acid **4** (6.4 g; 78 %), m.p. 114 – 120 °C. Several recrystallizations from ethanol yielded colourless plates of m.p. 121 – 123 °C.

IR: ν_{max} 3000 – 2800, 2600, 1670, and 1580 cm^{-1}.

NMR: δ 10.53 (broad s, $-CO_2H$), 1.93 – 2.18 (m, 6-H), 6.96 – 7.52 (m, 12H), 4.03 (s, $-CH_2Ph$), and 2.70 – 3.44 (symmetrical m, $-CH_2CH_2-$).

$C_{22}H_{20}O_2$ (316.5). Calcd. C 83.51; H 6.37. Found C 83.87; H 6.42 %.

Evaporation of the ethereal solution gave a gummy mixture, part of which was separated on preparative TLC plates (Silica gel G, Merck; $CHCl_3$). The major component, m.p. 86 – 88 °C, colourless needles from ethanol, was identified as **3-(2-benzyl-benzyl)phthalide (5)**.

IR: ν_{max} 1750, 1580, and 1060 cm^{-1}.

NMR: δ 7.70 – 8.00 (m, 7-H), 6.95 – 7.68 (m, 12H), δ_X 5.46 (t), δ_A 3.15 (d), (J_{AX} 6.5 Hz, $-CH_2-CH_X=$), and 4.08 (s, CH_2Ph).

$C_{22}H_{18}O_2$ (314.4). Calcd. C 84.05; H 5.77. Found C 84.51; H 5.21 %.

1-Benzyl-10,11-dihydrodibenzo[a,d]cyclohepten-5-one (6)

The acid **4** (4.0 g) was converted to the acid chloride by treatment with $SOCl_2$. After evaporation of the excess reagent, polyphosphoric acid (0.25 g) was added to the residue and the mixture was heated at 200 °C for 25 hrs. It was diluted with chloroform, extracted with dilute alkali, the chloroform solution evaporated and the residue chromatographed on silica (80 g, benzene). The main fraction (2.1 g; 55 %; m.p. 80 – 84 °C) was purified for analysis by several recrystallizations from ethanol to obtain colourless hexagonal prisms of m.p. 92 – 93 °C.

IR: ν_{max} 1660, 1600 and 1300 cm^{-1}.

NMR: δ 7.73 – 8.25 (m, 6-H), 4.21 (s, CH_2Ph), and 3.17 (s, CH_2CH_2).

$C_{22}H_{18}O$ (298.4). Calcd. C 88.56; H 6.08. Found C 88.77; H 6.09; M (mass spectrum) 298.

On the front a hydrocarbon, $C_{22}H_{18}$, was eluted, colourless prisms from ethanol, m.p. 149 – 151 °C.

IR: ν_{max} 3000, 2900, 1700 (w), 1650 (w), 1600 (m), 1485 (s), 1450 (s), 1380 (w), 1360 (w), 1320 (w), 1260 (m), 1150 (w), 1100 (w), 945 (m), and 885 cm^{-1};

NMR (100 MHz): δ 6.97 – 7.52 (m, 11H, aromatic-H), 4.60 – 4.97 (m, 1H), 4.12 – 4.57 (m, 2H), 3.67 – 4.12 (m, 2H) and 3.22 (unsymmetrical t, 2H).

MS: *m/e* (rel. int.) 282 (100), 281 (24), 267 (17), 265 (23), 178 (19), 142 (11), 136 (11), 135 (11), 91 (30), 85 (17) and 83 (27).

$C_{22}H_{18}$ (282.4) Calcd. C 93.57; H 6.43. Found C 93.85; H 6.42 %.

1-Benzyl-5H-dibenzo[a,d]cyclohepten-5-one (1)

An intimate mixture of the ketone **6** (1.0 g) and 10 % palladium on charcoal (1.0 g) was heated under nitrogen at 220 °C for 2.5 hrs. After separation from the catalyst by extraction, the product was chromatographed on silica (40 g; benzene—ligroin (b.p. 40 – 60 °C) 1 : 1). The first product eluted was identified as 1-benzyl-5*H*-dibenzo[*a*,*d*]cycloheptene (**2**), after which fractions of the starting material and mixtures thereof with the product, and finally the pure ketone (**1**) were eluted (0.25 g; m.p. 109 – 112 °C). Thin colourless plates (from ethanol), m.p. 112 – 114 °C.

IR: ν_{max} 1640, 1580, and 1305 cm^{-1}.

NMR: δ 7.79 – 8.14 (m, 6-H), 6.90 – 7.61 (m, 7H), and 4.25 (s, CH_2).

1-Benzyl-5H-dibenzo[a,d]cycloheptene (2)

The ketone **1** (100 mg) and hydrazine hydrate (0.2 ml) were gently boiled in digol (2 ml) for 10 min. Potassium hydroxide (0.1 g) was added and boiling was continued for 1 hr. The mixture was diluted with water, extracted with benzene, the benzene solution evaporated and

the residue purified by preparative TLC (Silica gel G; benzene—ligroin (b.p. 40 – 60 °C), (1 : 1). The product was recrystallized from ethanol to obtain colourless hexagonal plates (27 mg) of m.p. 85 – 86 °C.

IR: ν_{max} 1570, 1460, and 1410 cm^{-1}.

NMR: δ 7.31 – 6.85 (m, 9H), 4.10 (s, 1-CH_2), and 3.69 (s, 5-CH_2).

$C_{22}H_{18}$ (282.4). Calcd. C 93.57; H 6.43. Found C 94.05; H 6.47 %. M (mass spectrum) 282.

10-(1-Hydroxisopropyl)-5H-dibenzo[a,d]cycloheptene-5-one (14)

To a solution of 10-bromo-5,5-dimethoxy-5*H*-dibenzo[*a,d*]cycloheptene (**7**) [17] (6.0 g) in dry ether (50 ml) butyllithium (11.3 ml of a 15 % solution in hexane) was added at – 70 °C. After stirring for 20 min., acetone (2 ml) was added. The reaction mixture was allowed to warm up to room temperature, extracted with water, and evaporated. In order to hydrolyze the dimethyl-ketal group, the residue was treated overnight with 80 % aqueous isopropanol (12 ml) containing hydrochloric acid (0.2 ml). After neutralization with sodium methoxide solution and evaporation, the crude product crystallized when triturated with *n*-hexane. Colourless rectangular prisms from ether, (3.24 g; 50 %), m.p. 133 – 135 °C.

IR: ν_{max} 3500, 3400, 1650, 1490, and 1300 cm^{-1}.

NMR: δ 8.35 – 8.68, (m, 9-H), 7.89 – 8.17 (m, 4,6-H), 7.50 – 7.89 (m, 6-H), 3.06 (s, broad, OH), and 1.95 [s, $(CH_3)_2C$)].

$C_{18}H_{16}O_2$ (264.3). Calcd. C 81.79; H 6.10. Found C 81.95; H 6.00 %. M (mass spectrum) 264.

10-[1-Methoxyisopropyl]-5H-dibenzo[a,d]cyclohepten-5-one (15)

To a solution of the hydroxyketone **14** (300 mg) in methanol (30 ml) conc. hydrochloric acid (0.2 ml) was added. After standing overnight, the solution was neutralized with sodium methoxide, evaporated and the residue chromatographed on silica (6 g, benzene). The ether **15** (200 mg) was eluted first, followed by some starting material, colourless prisms (from methanol), m.p. 102 – 104 °C.

NMR: δ 8.25 – 8.27 (m, 9-H), 7.63 – 7.95 (m, 4,6-H), 7.20 – 7.63 (m, 6H), 5.26 (s, OCH_3) and 1.54 [s, $(CH_3)_2COH$].

$C_{19}H_{18}O_2$ (278.3). Calcd. C 81.89; H 6.52. Found C 82.10; H 6.53 %. M (mass spectrum) 278.

10-(1-n-Propyloxy)-5H-dibenzo[a,d]cyclohepten-5-one (16)

A solution of the hydroxyketone **14** in propanol (13 ml) containing 5 drops of conc. hydrochloric acid was kept 3 days at room temperature.

After neutralization with sodium methoxide and evaporation, the resulting mixture was separated by preparative TLC (Silica gel G, Merck; benzene), giving two main products. The less polar fraction was the isopropenylketone **17** (50 mg), the next one the propyl ether **16** (120 mg), a colourless oil.

NMR: δ 8.33 – 8.59 (m, 9-H), 7.64 – 7.94 (m, 4,6-H), 7.19 – 7.64 (m, 6H), 3.35 (t, J 6.5 Hz, OCH_2-), 1.63 – 2.06 (m, 2'-CH_2) 1.54 [s, $(CH_3)_2C$] and 0.90 (t, J 6.5 Hz, 3'-CH_3).

$C_{21}H_{22}O_2$ (306.4). Found M (mass spectrum) 306.

16 was followed by its isomer, **10,11-dihydro-10-propyloxy-11-isopropylidene-5H-dibenzo-[a,d]cyclohepten-5-one (25)** (23 mg), colourless prisms from benzene–ligroin (b.p. 40 – 60 °C), m.p. 138 – 140 °C.

NMR: δ 8.14 – 9.07 (m, 8H), 5.27 (s, br., 10-H), 3.45 (t, J 6.7 Hz, OCH_2), 1.39 and 1.65 [pair of singlets, $(CH_3)_2C=$], and 1.01 (t, J 7 Hz, 3'-CH_3).

$C_{21}H_{22}O_2$ (306.4). Calcd. C 82.32; H 7.24. Found C 82.23; H 7.63 %.

10-Isopropenyl-5H-dibenzo[a,d]cyclohepten-5-one (24)

When the hydroxyketone **14** (200 mg) was treated with cold isopropanol containing a trace of hydrochloric acid, no reaction took place. Refluxing for 1 hr. gave rise to a complex mixture of products from which only the isopropenylketone **17** could be isolated in an amount sufficient for characterizing. The same product could be obtained in a simpler way by refluxing the hydroxyketone **14** with a mixture of ethanol and conc. hydrochloric acid (17 : 1) for 1 hr. Evaporation of the mixture gave the isopropenylketone **17** as a pale yellow oil.

IR: ν_{max} 1650, 1490, 1315 and 932 cm^{-1}.

NMR: δ 7.86 – 8.15 (m, 4,6-H), 7.14 – 7.75 (m, 6H), 7.13 (s, $-HC=$), 5.31 (s, br., $H_2C=$), and 1.94 (s, br., CH_3).

$C_{18}H_{14}O$ (246.1045). Found (mass spectrum) 246.1045.

10-(1-Hydroxyisopropyl)-5H-dibenzo[a,d]cycloheptene (17)

10,11-Dibromo-10,11-dihydro-5*H*-dibenzo[*a*,*d*]cycloheptene [12] (2.3 g) was refluxed for 1 hr. with a solution of sodium hydroxide (0.8 g) in methanol (40 ml). After acidification with acetic acid and evaporation, the residue was extracted with methylene chloride. Evaporation of the extract gave an oil (1.5 g) that was purified by chromatography on silica (20 g; benzene–hexane 1 : 1). The first fraction (0.8 g) afforded pure **10-bromo-5H-dibenzo[a,d]cycloheptene (9)** (0.2 g), as colourless plates of m.p. 128 – 131 °C.

NMR: δ 7.29 (s, 8H), 7.03 (s, $-HC=$) and 3.63 (s, CH_2).

Due to rapid decomposition, no satisfactory analyses could be obtained. A further amount of less pure material (0.4 g) was recovered from the mother liqour. The foregoing bromo compound (0.5 g) was treated with *n*-butyllithium and acetone in ether as described for the bromoketal **7**. The crude product was chromatographed on Silica gel G (5 g; $CHCl_3$) yielding an oil that crystallized from ether–hexane as colourless needles (200 mg), m.p. 88 – 91 °C.

IR: ν_{max} 3600, 3400, and 1490 cm^{-1}.

NMR: δ 7.70 – 8.00 (m, 9-H), 7.39 (s, HC=), δ_A 3.72 (d), δ_B 3.40 (d) (AB system, J 12.7 Hz, CH_2), 1.87 (s, OH), 1.62 and 1.68 [pair of singlets, $(CH_3)_2C$].

$C_{18}H_{18}O$ (250.3). Calcd. C 86.36; H 7.25. Found C 86.57; H 7.32 %. M (mass spectrum) 250.

5-Methylene-10-(1-hydroxyisopropyl)-5H-dibenzo [a,d]cycloheptene (18)

10-Bromo-5-methylene-5*H*-dibenzo[a,d]cycloheptene [8] (1.7 g) was treated with *n*-butyllithium and acetone as described for the bromoketal **7**. The crude product was chromatographed on silica (20 g) using for elution successively ligroin (b.p. 40 – 60 °C), benzene–ligroin (1 : 1) and benzene–chloroform (5 : 1). The last solvent eluted the heptafulvene **18**, colourless plates (0.62 g) from hexane–benzene, m.p. 120 – 122 °C.

IR: ν_{max} 3600, 3400, 1620, 1490, 910 cm^{-1}.

NMR: δ 8.81 – 9.07 (m, 9H), 7.21 – 7.35 (m, 8H), 5.26 (s, br., $CH_2=$), 1.87 (s, OH), 1.56 and 1.64 [pair of singlets, $(CH_3)_2C$]. NMR ($C_6D_5NO_2$) : δ_A 5.22 (d), and δ_B 5.16 (d) (AB system, J 1.8 Hz, $CH_2=$), 2.40 (s, OH), 1.63 and 1.72 [pair of singlets, $(CH_3)_2C$].

$C_{19}H_{18}O$ (262.3). Calcd. C 86.98; H 6.91. Found C 87.17; H 6.98 %. M (mass spectrum) 262.

10-(1-Hydroxyisopropyl)dibenzo[b,f]oxepin (19)

10-Bromodibenzo[*b*,*f*]oxepin [9] was treated with n-butyllithium and acetone as described for the bromoketal **7**. The crude product was crystallized from ether giving the hydroxyoxepin **19** (0.5 g) as colourless neddles of m.p. 118 – 121 °C.

IR: ν_{max} 3550, 3400, 1480, and 1435 cm^{-1}.

NMR: δ 7.81 – 8.06 (m, 9-H), 7.00 – 7.33 (m, 8H), 2.21 (s, OH), and 1.61 [s, $(CH_3)_2C$].

$C_{17}H_{16}O_2$ (252.3). Calcd. C 80.77; H 6.58. Found C 80.77; H 6.58 %. M (mass spectrum) 252.

5-Ethyl-10-bromodibenz[b,f]azepin (13)

To a solution of 5-acetyl-10-bromodibenz[*b*,*f*]azepin [10] (6.9 g) in dry ether (50 ml) lithium aluminium hydride (0.8 g) was added in portions. The reaction became soon vigorous and was complete within 10 min. The excess reagent was decomposed with wet ether, the ethereal solution washed with water, dried and evaporated. The crude product was crystallized from acetone–chloroform (1 : 1) giving the bromoazepin **13** as yellow rods (3.1 g) of m.p. 149 – 151 °C.

IR: ν_{max} 1580, 1560, 1460, and 1440 cm^{-1}.

NMR: δ 6.42 – 7.66 (m, 9H) 3.71 (q, J 7 Hz, CH_2), and 1.13 (t, J 7 Hz, CH_3).

$C_{16}H_{14}BrN$ (300.2). Calcd. C 63.97; H 4.70; Br 26.62; N 4.66. Found C 64.17; H 4.50; Br 24.64; N 4.99 %.

5-Ethyl-10-(1-hydroxyisopropyl)dibenz[b,f]azepin (20)

The bromoazepin **13** (0.9 g) was treated with *n*-butyllithium and acetone as described for the bromoketal **7**. Trituration of the crude product with hexane gave the almost pure hydroxyazepin **20** (0.6 g; 70 %), m.p. 126 – 129 °C. Colourless rectangular plates (0.42 g) when recrystallized from ether–pentane, m.p. 128 – 129 °C.

IR: ν_{max} 3600, 1590, 1575, 1470, and 1445 cm^{-1}.

NMR: δ 7.67 – 7.90 (m, 9-H), 6.88 – 7.30 (m, 8H), 3.40 – 4.04 (m, overlapping AB part of ABX_3 system, CH_2), 2.00 (s, OH), 1.63, and 1.59 (pair of singlets, $(CH_3)_2C$) and 1.17 (t, J 7 Hz, CH_3CH_2).

$C_{19}H_{21}NO$ (279.4). Calcd. C 81.86; H 7.58; N 5.01. Found C 82.07; H 7.40; N 5.29 %. M (mass spectrum) 279.

10-(1-Hydroxyisopropyl)dibenzo[b,f]thiepin (21)

10-Bromodibenzo[*b,f*]thiepin [11] (1.5 g) was treated with *n*-butyllithium and acetone as described for the bromoketal **7**. Chromatography of the crude product on silica (11 g, benzene) gave the hydroxythiepin **21** (0.9 g; 67 %) as a pale yellow oil.

IR: ν_{max} 3400, and 1460 cm^{-1}.

NMR (C_6F_6) : δ 7.69 – 7.92 (m, 9-H), 7.06 – 7.59 (m, 8H), 2.46 (s, OH), 1.54 and 1.13 (pair of singlets, $(CH_3)_2C$).

$C_{17}H_{16}OS$ (268.4) Calcd. C 76.10; H 6.0; S 12.93. Found C 76.51; H 6.11; S 12.84 %. M (mass spectrum) 268.

10-(1-Hydroxyisopropyl)dibenzo[b,f]thiepin-5-oxide (22)

To a solution of the hydroxythiepin **21** (400 mg) in benzene (10 ml) perlauric acid (80 %; 400 mg) was added. After standing overnight at 0 °C, the solution was evaporated and the residue triturated throughly with *n*-pentane. The product soon crystallized in colourless needles (360 mg; 130 – 147 °C).

Repeated crystallization from benzene gave the pure sulfoxide (**22**), m.p. 151 – 153 °C.

IR: ν_{max} 3500, 3350, and 1460 cm^{-1}.

NMR (100 MHz): δ 7.00 – 8.00 (m, 9H), 3.26 (s, OH), and 1.62 (s, $[CH_3)_2C]$.

$C_{17}H_{16}O_2S$ (284.4). Calcd. C 71.82; H 5.67; S 11.28. Found C 71.60; H 5.78; S 11.35 %. M (mass spectrum) 284.

10-(1-Hydroxyisopropyl)dibenzo[b,f]thiepin-5,5-dioxide (23)

To a solution of the hydroxythiepin **20** in benzene (5 ml), 80 % perlauric acid (230 mg) was added. After standing at room temperature overnight, the solution was evaporated, the residue triturated thoroughly with pentane and crystallized from ether–pentane. Colourless prisms (200 mg) of m.p. 138 – 140 °C.

IR: ν_{max} 1460, 1305 and 1165 cm^{-1}.

NMR: δ 7.97 – 8.25 (m, 4,6,9-H), 7.36 – 7.70 (m, 6H), 3.27 (s, broad, OH) and 1.66 [s, $(CH_3)_2C$].

$C_{17}H_{16}O_3S$ (300.4). Calcd. C 67.99; H 5.37. Found C 67.86; H 5.21 %. M (mass spectrum) 300.

10-(1-Hydroxyphenylethyl)dibenzo[b,f]oxepin (26)

To a solution of 10-bromodibenzo[*b,f*]oxepin [9] (1.09 g) in dry ether (20 ml) *n*-butyllithium (2.66 ml of a 15 % solution in hexane) was added at – 70 °C. After stirring for 20 min., acetophenone (0.72 g) was added and the reaction mixture was allowed to warm up to room temperature. The product (0.72 g; 57 %; m.p. 203 – 206 °C) that crystallized directly from the reaction mixture was separated and recrystallized from benzene to obtain long colourless prisms (0.63 g) of m.p. 208 – 208.5 °C.

IR: ν_{max} 3450, 1490, and 1440 cm^{-1}.

NMR (d_6-DMSO, 100 MHz): δ 2.99 – 1.57 (m, 7H), 2.63 – 2.89 (m, 4,6-H), 3.63 (s, OH), and 1.81 (s, CH_3).

$C_{22}H_{18}O_2$ (314.4). Calcd. C 84.05; H 5.77. Found C 84.01; H 5.68 %. M (mass spectrum) 314.

10-(1-Phenylvinyl)dibenzo[b,f]oxepin (27)

A suspension of the alcohol **26** (400 mg) in methanol (10 ml) containing four drops of conc. hydrochloric acid was stirred at room temperature until complete dissolution (60 hrs). The solution was evaporated and the residue crystallized from pentane. Colourless needles (106 mg) of m.p. 77 – 79 °C.

IR: ν_{max} 1590, 1560, 1430, and 896 cm^{-1}.

NMR (100 MHz): δ 8.93 – 7.60 (m, 16H), δ_A 5.72 (d), and δ_B 5.42 (d), (J_{AB} 2 Hz, AB-system, $CH_2=$).

$C_{22}H_{16}O$ (296.4). C 89.16; H 5.44. Found C 89.10; H 5.37 %. M (mass spectrum) 296.

10-(1-Phenylethyl)dibenzo[b,f]oxepin (28)

The crude vinyloxepin **27** (0.35 g) was hydrogenated in ethyl acetate in the presence of palladium on charcoal until the uptake of 1 molar equivalent of hydrogen. The usual work-up afforded long, colourless needles (from *n*-hexane) (0.20 g), m.p. 128 – 129 °C.

IR: ν_{max} 1595, 1560, 1475, and 1435 cm^{-1}.

NMR (100 MHz): δ 6.90 – 7.50 (m, 8H), 6.70 (s, $-HC=$), 4.29 (q, J 7 Hz, $HC\lessgtr$, and 1.61 (d, J 7 Hz, CH_3).

$C_{22}H_{18}O$ (298.4). Calcd. C 88.56; H 6.08. Found C 88.68; H 5.83 %. M (mass spectrum) 298.

1,3-Dihydro-1,3-dimethoxy-8H-dibenzo[a,e]furo[3,4-c]cyclohepten-8-one (30)

To a suspension of 8*H*-dibenzo[*a*,*e*]furo[3,4-*c*]cyclohepten-8-one (**29**) [13] (7.0 g) in methanol (150 ml) anhydrous potassium acetate (5.5 g) and bromide (5.0 g in 50 ml methanol) were added in portions at 0 °C. The starting material dissolved by the end of the addition and soon crystals (5.9 g; 67 %; m.p. 100 – 103 °C)precipitated, which proved to be a mixture of the *cis* and *trans* acetals.

NMR: δ 7.42 – 8.17 (m, 8H), 6.52 (s, *trans*-1,3-H), 6.39 (s, *cis*-1,3-H), 3.48 (s, *cis*-OMe) and 3.42 (s, *trans*-OMe).

Several recrystallizations from methanol gave the pure *trans* isomer as colourless cubes of m.p. 140 – 141 °C.

IR: ν_{max} 1650, 1490, and 1305 cm^{-1}.

NMR (100 MHz): δ 7.97 – 8.13 (m, 4.12-H), 7.77 – 7.97 (m, 7,9-H), 7.43 – 7.72 (m, 5.6.10. 11-H), 6.53 (s, 1.3-H), and 3.40 (s, OMe).

The mother liquor was evaporated, the residue taken up in chloroform and washed with water. On prolonged standing large pale yellow plates (1.4 g) of the hydrolysis product described next separated.

$C_{19}H_{16}O_4$ (308.3). Calcd. C 74.01; H 5.23. Found C 73.90; H 5.26 %. M (mass spectrum) 308.

Acid hydrolysis of 1,3-dihydro-1,3-dimethoxy-8H-dibenzo[a,e]furo[3,4-c]cyclohepten-8-one

The acetal **30** (500 mg) was refluxed with a mixture of ethanol (10 ml) and 10 % hydrochloric acid (2 ml) for 48 hrs. The crystalline product (410 mg; m.p. 236 – 238 °C) was separated and recrystallized from dimethyl sulfoxide to obtain colourless plates, m.p. 237 – 239 °C.

IR: ν_{max} 1750, 1650 and 1300 cm^{-1}.

NMR (CF_3CO_2H): δ 7.63 – 8.30 (m, 8H), and 5.62 (s, 2H).

MS: *m/e* (rel. int.) 262 (100), 234 (16), 233 (82), 205 (62), 177 (29) and 176 (30).

Found C 77.58; H 3.66. $(C_{17}H_{10}O_3)_x$ requires C 77.85; H 3.4 %.

5H-Dibenzo[a,d]cyclohepten-5-one-10,11-dicarboxylic anhydride (31)

A solution of the acetal **30** (3.75 g) in acetic acid (60 ml) was heated to 100 °C, 10 % sulfuric acid (10 ml) was added, followed immediately by an aqueous solution of chromium trioxide (6.0 g in 12 ml of water). After heating for about 5 min., the reaction mixture was cooled, whereupon a mixture of the anhydride (**31**) and the preceding hydrolysis product crystallized. After separation, the mixture was extracted several times with chloroform. Evaporation of the extract gave the anhydride (1.1 g; m.p. 197 – 205 °C). Colourless needles (from ethanol), m.p. 203 – 205 °C.

IR: ν_{max} 1840, 1760, 1560 and 1300 cm^{-1}.

NMR (100 MHz): δ 8.35 – 8.50 (m, 1,9-H), 7.90 – 8.07 (m, 4,6-H), and 7.65 – 7.86 (m, 2,3,7-H, 8H).

$C_{17}H_8O_4$ (286.3). Calcd. C 73.91; H 2.92. Found C 74.12; H 3.16 %. M (mass spectrum) 286.

1,4-Epoxy-1,4-dihydro-1-ethyl-9H-tribenzo[a,c,e]cyclohepten-9-one (32)

10-Bromo-5*H*-dibenzo[*a*,*d*]cyclohepten-3-one[18] (15 g), 2-ethylfurane [17] (24 ml) and potassium *t*-butoxide (8 g) were stirred in dry ether (100 ml) under nitrogen for 16 hrs. The reaction mixture was evaporated, the residue treated with water and extracted with chloroform. The chloroform solution was washed throughly with water, the solvent evaporated and the residue chromatographed on silica (150 g; $CHCl_3$). After some starting material, impure (10 g) and at last the pure epoxide (**32**) was eluted. Recrystallization from carbon tetrachloride gave, after processing of the mother liquors, a total yield of 7.75 g (50 %) of the pure epoxide, pale yellow needles, m.p. 148 – 150 °C.

IR: ν_{max} 1640, 1580 and 1495 cm^{-1}.

NMR: δ 7.83 – 8.15 (m, 8,10-H), 7.26 – 7.67 (m, 8H), 5.90 (s, br., 4-H), 2.50 (q, J 7 Hz, CH_2) and 0.97 (t, J 7 Hz, CH_3).

$C_{21}H_{16}O_2$ (300.3). Calcd. C 83.98; H 5.37. Found C 83.84; H 5.56 %. M (mass spectrum) 300.

1,4-Epoxy-1-ethyl-1,2,3,4-tetrahydro-9H-tribenzo[a,c,e]cyclohepten-9-one (33)

A solution of the epoxide (**32**) (2.1 g) in ethyl acetate (20 ml) was hydrogenated in the presence of palladium on charcoal until uptake of one molar equivalent of hydrogen. The usual work-up and recrystallization of the crude product from ethyl acetate gave **32** (1.7 g) as colourless rods of m.p. 169 – 171 °C.

IR: ν_{max} 1650, 1590 and 1305 cm^{-1}.

NMR (100 MHz): δ 7.87 – 8.06 (m, 8,10-H), 7.26 – 7.63 (m, 6H), 5.42 (d, J 5 Hz, 4-H), 1.70 – 2.70 (m, 6H), and 0.88 (t, CH_3).

$C_{21}H_{18}O_2$ (302.4). Calcd. C 83.42; H 6.00. Found C 83.73; H 5.85 %. M (mass spectrum) 302.

1-Ethyl-9H-tribenzo[a,c,e]cyclohepten-9-one (34)

The dihydroepoxide **33** (1.1 g) was refluxed in toluene (20 ml) with *p*-toluenesulfonic acid (0.2 g) for hr. The toluene solution was washed with water, evaporated and the residue recrystallized from ethanol to obtain **34** as colourless prisms or thin rectangular plates of m.p. 150 – 151.5 °C (0.93 g).

IR: ν_{max} 1670, 1600, 1295 and 930 cm^{-1}.

NMR (100 MHz): δ 7.00 – 7.80 (m, 10H), 1.50 – 1.86 (m, CH_2), and 1.11 (t, J 7 Hz, CH_3).

$C_{21}H_{16}O$ (284.3). Calcd. C 88.70; H 5.67. Found C 98.55; H 5.66 %. M (mass spectrum) 284.

Fractional crystallization of the mother liquor from carbon tetrachloride–cyclohexene gave rise to a small amount of **3-ethyl-4-phenylfluorenone (38)**, yellow prisms of m.p. 188 – 190 °C.

IR: ν_{max} 1700, 1490, 1395 and 970 cm^{-1}.

NMR (100 MHz): δ 7.00 – 7.82 (m, 11H), 6.00 (unsymm. quartet, 5-H), 2.45 (q, J 7 Hz, CH_2), and 1.06 (t, J 7 Hz, CH_3).

$C_{21}H_{16}O$ (284.3). Calcd. C 88.70; H 5.67. Found C 88.40; H 5.52 %. M (mass spectrum) 284.

9H-Tribenzo[a,c,e]cyclohepten-9-one (35)

1. 4- Epoxy- 1, 2, 3, 4-tetrahydro- 9*H*- tribenzo [*a*, *c*, *e*] cyclohepten-9-one [15] (1. 2g), [colourless prisms (from ethyl acetate), m.p. 163 – 165 °C

IR: ν_{max} 1640 cm^{-1}.

NMR (100 MHz): δ 8.00 – 8.14 (m, H-8,10), 7.20 – 7.70 (m, 6H), 5.62 (q, J_1 6 Hz, J_2 3Hz, 1,4-H), 2.00 – 2.60 (m, *exo*-2,3-H), and 1.50 – 2.00 (m, *endo*-2,3-H)*] was refluxed with *p*-

* Assigments were made by comparison with the spectrum of the *exo*-2,3-dideutero compound (singlets at δ 1.67 and 5.65).

toluenesulfonic acid (0.5 g) in toluene (20 ml) for 15 hrs. Evaporation and crystallization from ethanol gave rise to tribenzocycloheptenone (**35**) (0.85 g; 76 %), m.p. 175–177 °C (lit. [15] m.p. 176.5–177.5 °C).

$C_{19}H_{14}O_2$ (274.3). Calcd. C 83.20; H 5.17. Found C 83.57; H 5.34 %. M (mass spectrum) 274.

1-Ethyl-9H-tribenzo[a,c,e]cycloheptene (36)

The tribenzoketone **34** (1.1 g) was refluxed with hydrazine hydrate (1 ml) in ethanol (10 ml) for 3 hrs. The solution was evaporated to dryness and the residue stirred with potassium *t*-butoxide (1 g) in dimethyl sulfoxide (20 ml) for 3 hrs. and then heated slowly to 90 °C. After dilution with water the product was extracted with benzene, the benzene washed several times with water, evaporated and the residue chromatographed on silica (20 g; benzene–hexane 1 : 1), affording an oil (100 mg), that crystallized from methanol as colourless rods of m.p. 76–79 °C.

IR: ν_{max} 2950, 1480, 1420, 1290 and 840 cm^{-1}.

NMR (100 MHz, in diphenyl at 80°): δ_A 3.11, δ_B 2.90 and 1.11 (t), (ABX_3 system, $J_{AX} = J_{BX}$ 7.5 Hz, J_{AB} 15 Hz, CH_3CH_2).

$C_{21}H_{18}$ (270.4) Calcd. C 93.29; H 6.71. Found C 93.15; H 6.70 %. M (mass spectrum) 270.

9H-Tribenzo[a,c,e]cycloheptene (37)

Tribenzocycloheptenone (**35**) (2.72 g) in diethylene glycol (15 ml) was refluxed with hydrazine hydrate (3 ml) for 10 min. Potassium hydroxide (2.7 g) was added and boiling was continued for 1 hr. The product was extracted with benzene, the benzene solution washed, dried and evaporated to give crude **37** (1.4 g), which on recrystallization from ether yielded colorless crystals (0.6 g) of m.p. 118–119 °C.

IR: ν_{max} 3000, 1470, and 1430 cm^{-1}.

NMR: δ 7.18–7.80 (m, 12H), and 3.68 (s, CH_2); in $C_6D_5NO_2$ at 100° δ_A 3.16 and δ_B 3.41 (AB system, J 12.5 Hz, CH_2).

$C_{19}H_{14}$ (242.3). Calcd. C 94.18; H 5.82. Found C 94.29; H 5.91. M (mass spectrum) 242.

*

The author is grateful to Professor W. D. Ollis (Sheffield) and to Professor I. O. Sutherland (Liverpool) for their encouragement and for helpful discussions.

REFERENCES

[1] For reviews *cf.* (a) Sutherland, I. O.: Annual Reports of NMR Spectroscopy. **4,** 71 (1971); (b) Jackman, L. M., Cotton, F. A.: Dynamic Nuclear Magnetic Resonance, Academic Press, New York, 1975
[2] Nógrádi, M., Ollis, W. D., Sutherland, I. O.: Chem. Comm. **1970,** 158
[3] Corts, G. J. B., Nauta, W. T.: Rec. Trav. Chim. **85,** 395 (1965)
[4] Org. Synth. Coll. Vol. II, 61
[5] Cope, A. C., Fenton, S. W.: J. Am. Chem. Soc. **73,** 1673 (1951)
[6] Seidlova, V., Protiva, M.: Coll. Czech. Chem. Comm. **32,** 2826 (1967)
[7] Tochtermann, W., Oppenländer, K., Walter, U.: Chem. Ber. **97,** 1326 (1964)
[8] Belgian Patent 659.599; C. A. **64,** 5023 (1966)
[9] Bavin, P. M. G., Bartle, K. D., Jones, D. W.: J. Heterocyclic Chem. **5,** 327 (1968)
[10] Brit. Patent 943.277; C. A. **61,** 1815 (1964)
[11] Nógrádi, M., Ollis, W. D., Sutherland, I. O.: J. Chem. Soc. Perkin I **1974,** 621
[12] Cristol, S. J., Bly, R. K.: J. Am. Chem. Soc. **82,** 6155 (1960)
[13] Tochtermann, W., Franke, C., Schäfer, D.: Chem. Ber. **101,** 3122 (1968)
[14] Clauson-Kaas, N., Limborg, F.: Acta Chim. Scand. **1,** 622 (1974)
[15] Tochtermann, W., Schnabel, G., Mannschreck, A.: Ann. **705,** 169 (1967)
[16] Tochtermann, W., Oppenländer, K., Walter, U.: Chem. Ber. **87,** 1326 (1964)
[17] Armitage, A. K., Ing, H. R.: Brit. J. Pharmacol. **9,** 376 (1954)
[18] Treibs, W., Klinkhammer, H. J.: Chem. Ber. **84,** 671 (1951)

Mihály Nógrádi, H-1111 Budapest, Gellért tér 4.

RECENSIONES

Structure and Bonding. Volume **28.** *Electrons in Oxygen- and Sulphur-Containing Ligands*

Editors: J. D. DUNITZ, P. HEMMERICH, R. H. HOLM, J. A. IBERS, C. K. JØRGENSEN, J. B. NEILANDS, D. REINEN, R. J. P. WILLIAMS

Springer Verlag, Berlin, Heidelberg, New York. 1975

Volume 28 of this book series is of great interest from the aspect of structural chemistry, since it deals with compound types having oxygen- and sulphur-containing ligands in the framework of three smaller monographs.

R. W. ERSKINE and B. O. FIELD are presenting in their monograph entitled "Reversible Oxygenation" an evaluating survey of compounds of importance from both theoretical and practical aspects, of complexes of transition metals containing dioxygen ligands. Though from the aspect of bond theory the complexes containing dioxygen ligands are still not definitively satisfactorily treated, recently there was a possibility for drawing some general conclusions in relation to these compounds by the synthesis and structure investigation of a number of model compounds. One of the most important questions, the reversible or irreversible nature of oxygenation can be solved unequivocally according to our present knowledge. The reversible nature can be enhanced by increasing the electron density of the central atom, by substitution with a ligand of higher donor capacity or by an exchange of the central atom, and thus it is possible to plan previously the oxygen transferring catalysts. The bond distance O–O is a structural parameter by means of which the reversible-irreversible nature of a given dioxygen complex can be established almost unequivocally. The monograph deals briefly also with the oxygenation reaction of hemoglobin and synthetic porphyrin which reaction is of importance from the aspects of both theoretical and practical biology. On summarizing it can be stated that this short critical survey may be a useful reading for chemists and also for biologists.

K. DAHNICKE and A. F. SHIHADA are dealing in their short survey titled "Structural and Bonding Aspects in Phosphorus Chemistry – Inorganic Derivatives of Oxohalogeno Phosphoric Acids" with a compound type of great interest from the aspect of structural chemistry. Halophosphates with a smaller electrostatic charge show, in contrast to PO_4^{3-} having a symmetrical tetrahedral structure, an anisotropy of the bond system, and the structural difference of these species is due to this fact. The survey is a valuable source also for research workers studying problems of structural chemistry.

J. WILLEMSE, J. A. CRAS, J. J. STEGGERDA and C. P. KEIJZERS are discussing in their monograph titled "Dithiocarbamates of Transition Group Elements in 'Unusual' Oxidation States" a type of compounds of interest from the aspect of bond theory. It is known that the dithiocarbamate is a polydentate ligand stabilizing the central atoms of complexes of transition metals at a higher oxidation state. The monograph presents a summary of our knowledge concerning the theoretical interpretation of this effect, giving a concise but complete survey of the synthesis of the dithiocarbamate complexes of transition metals, and on our present knowledge concerning their redox properties and structure. The survey includes also the field of dithiocarbamate complexes containing also other ligands and having a central atom with a

lower oxidation number. The monograph is particularly valuable since it contains the complete literature of this special field of themes, and thus it represents an extremely useful work of reference.

B. CSÁKVÁRI

LANDOLT–BÖRNSTEIN: *Numerical Data and Functional Relationships in Science and Technology*

New Series, Editor in Chief: K.-H. HELLWEGE. Group II: Atomic and Molecular Physics. Vol. 7: Structure Data of Free Polyatomic Molecules. J. H. CALLOMON, E. HIROTA, K. KUCHITSU, W. J. LAFFERTY, A. G. MAKI, C. S. POTE; with the assistance of I. BUCK and B. STARCK. Eds.: K.-H. HELLWEGE and A. M. HELLWEGE

Springer-Verlag Berlin-Heidelberg-New York 1976

This volume presents a compilation of the geometric parameters – bond lengths, bond angles and angles of internal rotation – of free (vapour-phase) polyatomic molecules determined by experimental techniques. (The bond lengths of diatomic molecules are given in Landolt-Börnstein, New Series II/6.)

The book has been looked forward to for a long time, ever since the last similar work appeared in 1965 compiling the relevant data up to 1959 inclusive [1]. The present volume covers the period between 1960 and June 1974 with some later studies included as well. Some journals seem to fare better than others as regards the closing date. It is also true, however, that for some journals the date of actual publication is often delayed as compared with the cover date indicated on the journal.

The material collected is practically complete, with painstaking efforts I could find only three molecules which were ignored. They are ammonium chloride [2], 3-oxo-3-chloro-1,3-thiaphosphetane [3], and chloromethyl thiophosphonic dichloride [4].

The short and concise introduction is worth attention for users of structural information as well for those who are just interested. It summarizes the most important fundamentals of the experimental techniques employed for molecular geometry determination in the vapour phase. They are electron diffraction and spectroscopy (microwave, infrared, Raman, ultraviolet). Special emphasis is given to the physical meaning of the geometric parameters and to their uncertainties.

In addition to the ground state structures, those determined for excited states (electronic) are also collected.

The systematic compilation is divided into two parts. The first lists 355 molecules containing no carbon atom (inorganic). The second gives 848 molecules with one or more carbon atoms (organic).

The volume is concluded by a subject index referring not only to this volume but also to other data compilations on free molecules.

Each entry in the systematic parts provides the gross formula, name, symmetry, schematic structure formula, experimental technique(s), structure parameters with uncertainties and some comments. The comments usually concern the error estimation and conformational properties. It is also indicated if observed mean vibrational amplitudes are given in the original paper. Finally, the references follow. The first of them refers to the paper from which the data cited were taken. It is not described in detail how a selection was made when the same experimental technique was used by different groups on the same subject. Obviously critical considerations had to be applied. Although it is very difficult, if possible at all, to make such decisions without any bias, the emerging general picture seems to be convincing. A detailed checking would need tremendous work. In any case making these decisions, *i.e.* to select the structural parameters for the users, put a great responsibility onto the particular editor dealing with a given technique. The question occurs whether it would not be more appropriate, although certainly more troublesome, for these decisions to be made by a small group of scientists rather than by a single scientist.

By just glancing through the pages it appears how many interesting and often "surprising" structures have been determined especially among the inorganic and metal-organic compounds. It is also worth notice that some molecules continue to be repeatedly investigated, often by the same technique. This is seldom caused by parallel work. Most often repeated investigations are due to improved experimental techniques or scientific arguments.

The way the uncertainties of the structure parameters are given in this book calls for comments. To my knowledge it is unique in the authoritative Landolt-Börnstein series to subject the data to critical considerations in order to change the original uncertainties when felt necessary. Reviewing this volume it seems to me that I should not avoid to make a stand on this question.

The simplest cases are those, of course, when no numerical data are cited. There are polar molecules which had been earlier studied by infrared and Raman spectroscopy and later, more accurately, by microwave spectroscopy. In such cases the infrared and Raman data were not compiled. A relatively large number of electron diffraction studies are cited without data. Among them are all the studies by the visual technique. Although several visual determinations are known to have withstood comparison with up-to-date methods, it is true that generally they do not correspond to present requirements. Data were omitted also for several rather complicated molecules, usually with low symmetry even though the experiment was performed with up-to-date techniques.

Consider now those cases when the compilers changed the uncertainties of the cited parameters as compared with the original data. The different experimental techniques have to be examined separately.

Extremely high resolution may be achieved in microwave spectroscopy. The frequencies of rotational transitions and, accordingly, the rotation constants can be determined with great accuracy. Except for the simplest molecules, however, this is not the determining factor of the uncertainties. If data from the necessary number of isotopic species are available, the r_S substitution parameters can be determined and the uncertainties given for r_S reflect their consistency when data from more than the necessary number of isotopic species are available. The contribution of the vibrational–rotational interactions to the uncertainty is usually taken into account empirically. The compilers of this Volume have cited the original uncertainties of the r_S parameters without change. They have usually increased the uncertainties in those cases, however, where r_0 parameters could be obtained only, *viz.* when there were less isotopic species available than necessary for determining the substitution parameters. The uncertainties have also been increased in those cases where the experimental data had to be supplemented by certain assumptions to produce geometric parameters.

The caution is justified. The problem is that although the experimental errors of the rotation constants are small and well determined, it is very difficult to estimate the effect of various assumptions, and the error caused by them may be several times larger than the experimental one.

In a way the previous statement applies to electron diffraction as well as regards the uncertainties introduced by various assumptions. The choice of the molecular model may be the origin of erroneous results and its danger may be more probable for complicated molecules of low symmetry. Even with a correct model as regards the overall configuration, it may happen that a structure from a false minimum in the least-squares procedure is accepted. In this review, we are not dealing with the ways of avoiding such erroneous results but considering the way of critical reporting of the uncertainties only.

Although the experimental systematic error is determined in a straightforward manner in the electron diffraction structure analysis, and it is fairly constant in a given laboratory employing standard technique, nevertheless it happens quite often that this error is ignored in the error estimates and only the standard deviations from the least-squares procedure (they are in fact random errors) are considered. The compilers of this Volume aimed to cite uncertainties containing both systematic and random errors. They have often increased the errors given in the original papers, emphasizing at the same time, that even these 'reasonable' errors may not be free of hidden systematic errors. It is also pointed out that in the worst cases the original conclusions may be qualitatively wrong.

This is a very important warning. It is this very point, however, where to my view, the compilers were not consistent enough. The original errors were doubled in some cases or even tripled. To me, however, citing three times the original errors, indicates that the whole analysis is suspect and it would have been more consistent not cite the relevant parameters at all, similarly to some other cases mentioned above. My fear is that citing these parameters with three times the original errors creates a false feeling of security in the user of these structural data.

Since closing the data collection for this Volume, there have been performed reinvestigations and some of the cited results with three times the original errors may now be tested against the new results.

Two examples are given here to amplify the point made above. Item 17 among the organic molecules is trichloromethyl sulphonyl chloride. The geometric parameters from an electron diffraction study are cited with three times the original errors. Thus, *e.g.* $111 \pm 6°$ is given instead of the original $111 \pm 2°$ for the bond angle O=S=O. The experimental systematic error certainly played no role in increasing this error, since the experimental systematic error for a bond angle is probably negligible at an uncertainty of 2°. In the course of our own studies on other sulphone molecules, we have also become suspicious concerning the structural data communicated for this important molecule. Thus we also performed an electron diffraction analysis which yielded, among others, $< O=S=O = 121.5 \pm 0.9°$ [5].

In the other example, the authors of the original study have reanalyzed their own data, probably with good reason. Item 796 among organic molecules is bis(cyclopentadienyl)-zirconium dichloride. The original paper reported 2.309 ± 0.005 Å for the Zr – Cl bond length. This was changed to 2.309 ± 0.015 Å in the compilation. According to the reanalysis, $r(Zr-Cl) = 2.459 \pm 0.015$ Å [6].

The above examples are probably and hopefully extreme. Hopefully also, because a few carless studies may damage the credibility of many others. The above examples support the suspicion of the compilers in a dramatic way. They also demonstrate, however, that increasing the original errors even by drastic magnitudes does not solve the problem in such cases.

Unfortunately it would usually require a new investigation or at least reanalysis of the data, to establish quantitatively that the conclusions of a study are in error, or to estimate more realistic error limits. In case of suspicion, and provided that the parameters are nevertheless to be cited, the following approach might be considered: to cite the original conclusions and in addition to make comments and criticism. Checking the original conclusions and making further tests would be facilitated by depositing experimental intensity data, parallel to publishing a structure analysis, in suitable way to make them available for everybody.*

The considerations concerning the error reestimation are also meant to give weight to the importance of going back to critically examining the original papers, depending, of course, on the purposes of the user of structural data.

An important and some less important inaccuracies from the book are listed below.

A paper on the bond angle in $AlCl_3$ [7] is misrepresented in the discussion under item 4, inorganic molecules. The paper in question provides evidence *for* the planar or nearly planar bond configuration of the $AlCl_3$ molecules in disagreement with bond angles Cl – Al – Cl of $110 - 112°$ suggested in a spectroscopic study.

Item 45, organic molecules, $r_s(C-Se)$ is 1.708 Å in the original paper rather than 1.709 Å as cited.

Item 619, organic molecules, $r_a(C-H)$ is 1.100 Å in the original paper rather than 1.000 Å as cited.

Items 388, 611, 625, etc., organic molecules, for halogenated propane derivatives it is stated that the errors given are twice the original errors. However, the summaries of the original papers list the same errors as given in the compilation.

The above remarks do not by any means alter my opinion about *this Volume* as being *a unique compilation produced with exceptional care and effort.*

The book is an invaluable tool first of all for the structural chemists, but it is also a rich pool of useful data and references for workers in other branches of chemistry and physics. I would also like to call the attention of lecturers in both inorganic and organic chemistry to this book as a convenient source of up-to-date and interesting structural information.

Special appreciation is due to the compilers and editors of this Volume. The book is a worthy product grown from the activities of the Sektion für Strukturdokumentation, Universität Ulm directed by Barbara STARCK. Involving outstanding scientists from the special branches made this activity complete. It is felt that the critical revaluation of the original data was a tremendous task and Eizi HIROTA and Kozo KUCHITSU are mentioned here as those responsible for microwave spectroscopy and electron diffraction, respectively. The editors and compilers as well as the publisher are to be congratulated for this Volume.

* This is already practiced by some authors and some journals.

REFERENCES

[1] Tables of Interatomic Distances and Configuration in Molecules and Ions. Spec. Publ. No. 18. The Chemical Society, London, 1965
[2] SHIBATA, S.: Acta Chem. Scand., **24,** 705 (1970)
[3] НАУМОВ, В. А., СЕМАШКО, В. Н.: Докл. АН СССР, **200,** 882 (1971)
[4] ХАЙКИН, Л. С., ВИЛКОВ, Л. В., ВАСИЛЬЕВ, А. Ф., МЕЛЬНИКОВ, Н. Н., ТУЛЯКОВА, Т. Ф., АНАШКИН, М. Г.: Докл. АН СССР, **203,** 1090 (1972)
[5] BRUNVOLL, J., HARGITTAI, I., SEIP, R.: Z. Naturforsch., **33a,** 222 (1978)
[6] РОНОВА, И. А., АЛЕКСЕЕВ, Н. В.: Журн. структ. химии, **18,** 212 (1977)
[7] HARGITTAI, I., HARGITTAI, M.: J. Chem. Phys., **60,** 2563 (1974)

I. HARGITTAI

N. W. TIEZ (Editor). W. T. CARAWAY, E. F. FREIER, J. F. KACHMAR and H. M. RAWNSLEY (Editorial Committee)

Fundamentals of Clinical Chemistry

W. B. Sounders Company, Philadelphia–London–Toronto, 1976. 1263 pages

The book contains 15 chapters. The first five are devoted to general methodology: laboratory principles and procedures; statistics, normal values and quality control; analytical procedures and instrumentation; automation; laboratory computers.

In the remaining chapters the specific problems of clinical chemistry are discussed in great detail: carbohydrates; proteins and amino acids; hemoglobin, hemoglobin derivatives and myoglobin; porphyrins and related compounds; lipids and lipoproteins; vitamins; enzymes; endocrine function; thyroid function; blood gases and electrolytes; acid–base and electrolyte balance; renal function; analysis of calculi; liver function; gastric, pancreatic and intestinal function; analysis of drugs and toxic substances; amniotic fluid. Each part includes a brief biochemical, physiological introduction, a discussion of the chemical mechanism of the recommended assay(s), together with their detailed description and finally the evaluation of their clinical significance.

The book is completed with an appendix conatining very useful tables, conversion charts, nomograms, etc.

It is always a great pleasure to take in hand the new edition of a textbook, which has achieved an established reputation as a standard source of information. One is interested to see how far the new trends emerging during the time which elapsed between the two editions have been included and what could be omitted as superfluous. Naturally, the opinion, especially concerning the details, will be different of each reader. Therefore, only some points of general interest should be mentioned.

Owing to the rapid spread of automation, the most widely used systems are reviewed in considerable length together with a highly useful extension on laboratory computers. The other two additions describing the methods of radioactivity measurement and immunochemical principles testify how deeply radioimmuno-assays have become a part of the general clinical laboratory practice. Automation is only economic in big units. Smaller laboratories try to improve their services with the introduction of precise, simple micro methods. Interestingly, this development is not adequately represented in the book. Some of the recommended methods are old-fashioned, requiring several milliliters of serum; *e.g.* in the case of the creatinine method 2.0 ml protein free filtrate of plasma is needed.

In recent years all leading scientific organizations have accepted and decided the introduction of the new standardized S. I. system for expressing laboratory results. Enormous effort is needed to make the new units accepted in the general practice. Unfortunately the Editorial Committee did not take the full burden of this difficult task, thus frequently in the book, and throughout the most important tables of normal values the old system is used. The main help for the reader in this transition is a tabulation of factors used to convert traditional into new units.

In spite of these small shortcomings the book has maintained its high scientific standard and practical value. Therefore, it is warmly recommended to specialists of clinical chemistry.

S. KERPEL-FRONIUS

Stephen G. SCHULMAN: *Fluorescence and Phosphorescence Spectroscopy: Physicochemical Principles and Practice*

Pergamon Press, Oxford 1977

This book belongs to the series which aims at giving a review of the physical methods used in structure elucidation and determination of chemical composition. In writing his book, the author, who is associated with the Pharmaceutical Chemical Department of the University of Florida, has considered readers less exercised in higher mathematics and quantum chemistry. Neverheless, a detailed and illustrative interpretation is presented of the method based on the interaction of molecular matter in molecular environment with light.

The importance of fluorescence and phosphorescence spectroscopy lies in its high sensitivity and in the low prices equipments.

The book comprises 213 pages of text and 49 pages of tabulated data. It is divided into four chapters; at the and of each a detailed list of references is given, covering altogether 500 papers and 20 handbooks. There are 15 figures in the book. Photographic reproduction of the typewritten text and of the linear figures has been used.

The individual chapters are as follows:

1. *Photophysical processes in isolated molecules.* (The electronic structure of molecules, light absorption by molecules, vibrational relaxation and internal conversion, thermal equilibrium of molecules in excited electronic states, deactivation of the lowest excited singlet level in thermal equilibrium), 44 pages.

2. *Photophysical processes in molecules in solution.* (The effects of solvents on the electron spectra, acidity effects, photo-tautomerism, molecular luminescence, coordination with metal ions, influence of concentration, fluorescence and phosphorescence of nucleic acids, polarization of fluorescence and phosphorescence), 89 pages.

3. *Instrumentation.* (Excitation sources, monochromators, sample holders, detectors, readers, spectrum converters, low-temperature fluorescence and phosphorescence measurements, sample holders and solvents, measurement of fluorescence quantum yield, measurement of luminescent life-time, measurement of concentration, time-resolved fluorimetry, modulation separation method, microspectrofluorimetry, list of solvents for phosphorimetry), 39 pages.

4. *Application* (Examination of organic substances by direct and indirect methods, examination of inorganic compounds by direct and indirect methods, some special applications), 40 pages.

Tables (Direct and indirect fluorimetric methods for organic molecules, phosphorimetric methods for organic molecules, fluorimetric methods, both direct and indirect, for inorganic substances), 49 pages.

The book intends to provide a clear explanation of all the phenomena appearing in the field, and it is, in the main, successful in this respect. There are some misprints in some of the formulae (*e.g.*, (2.1), (2.4) and (2.12), but the general aim of the author, that is, offering an introduction to biochemists and analytical chemists into the use of fluorescence and phosphorescence methods, can be regarded as achieved within the given limits.

GY. VARSÁNYI

G. HENRICI-OLIVÉ and S. OLIVÉ: *Coordination and Catalysis*

Verlag Chemie, Weinheim – New York, 1977 310 pages

The book has been published in the series "Monographs in Modern Chemistry" (series editor: Hans F. EBEL) as the 9th volume. Each volume of the series deals with different special topics and recent problems in chemistry.

The general and theoretical introduction takes about one third of the review. In this part, all principles needed for later understanding are collected. This summary consists of six chapters, starting with an introduction (only 3 pages, with 13 references), which outlines the topics to be discussed. The basic principles are collected in Chapter 2 (18 pages) entitled as "Atomic Orbitals". This chapter is based on an excellent summary published in Journal of Chemical Education, but some additional readings are suggested, too.

Chapter 3 is a short survey, from theoretical point of view, of the transition metal ions, 14 pages with 7 references.

Chapter 4 (20 pages) deals with the problems of symmetry and group theory and has three special appendices, too: one about matrices and two tables, as "Character Tables of Some Relevant Groups" and "Splitting of Terms, arising from d^n Configurations".

The ligand field theory is well summarized in the next chapter, regarding first of all, of course, the problems of the electronic spectra and magnetic moments of transition metal complexes. These problems are discussed on 25 pages and the references (24) give further possibilities for better understanding.

The last (6th) chapter of this part, about the molecular orbital (MO) theory for transition metal complexes, has even higher number of pages (27), references (19) and suggested additional readings (8). Not only the concepts of MO theory and the MO description of relevant ligands and substrates are discussed, but the MO description of transition metal complexes and the (experimental) evidences for covalent bonding, too.

As it can be seen, the authors tried to demonstrate their special subject also in the general chapters. Between these and the later chapters, which summarize the different reactions catalyzed by complex compounds, Chapter 7 entitled as "General Aspects of Catalysis with Transition Metal Complexes" gives the transition. This is one of the biggest and best chapter of the book. It starts with the general questions of the coordinative bonding and catalysis, goes on with summaries of transition metal – carbon σ bonds; key reactions in catalysis; active species and ligand influences. These problems are discussed on 48 pages and have 124 well-selected references.

The further five chapters deal with special systems like Chapter 8, which summarizes the (catalyzed) reactions of olefines (54 pages with 108 references): their isomerization; hydrogenation; oxydation; dimerization, oligomerization, polymerization and disproportionation (metathesis).

In Chapter 9 (24 pages with 47 references), the reactions of conjugated diolefins are separately discussed, where the main topics are: selective hydrogenation to monoens; dimerization and oligomerization to open-chain products; codimerization with monoens; cyclodimerization and -oligomerization; polymerization.

Chapter 10 (32 pages with 60 references) summarizes the reactions of carbon monoxide, first of all the carbonylation reactions of unsaturated hydrocarbons and the hydroformylation.

The volumes of the two last chapters are smaller but they seem the most interesting parts of the book with the most recent results and references (some of them were published in 1976), summarizing the up-to-date knowledges on the dioxygen and dinitrogen complexes. The title of Chapter 11 is: "Activation of Molecular Oxygen" and it gives a good survey on the following problems: models for natural oxygen carriers; bonding of dioxygen to the metal; (non-catalytic and catalytic) reactions of coordinated dioxygen. This chapter takes only 23 pages, but the number of references is 78, so it is rather concentrated, similar to Chapter 12 (15 pages with 41 references) entitled as "Activation of Molecular Nitrogen". Two main problems are summarized: that of the dinitrogen complexes of transition metals (preparation, structure, etc.) and reactions of coordinated N_2. Regarding the importance of this type of complexes, the authors close this chapter (and the whole book) with an "Outlook".

The book is completed with subject and catalyst formula (only 23 compounds! indices.

The book is very interesting and a good survey. Its title, however is too general and regarding also its volume, it follows, that this book can not be a complete monograph: it is somewhere between a monograph and a textbook.

After all, the theoretical part is well summarized and the examples are well selected and important. It is worth to read for all those who are interested in the topics discussed or who want to be familiar with the given special problems.

L. BARCZA

Robert J. ANGELICI: *Synthesis and Techniques in Inorganic Chemistry*

W. B. Saunders Co., Philadelphia, London, Toronto 1977

This is the second edition of a notebook on laboratory practice.

The aim of this book and the attached laboratory practice is to familiarize advanced students in chemical engineering with modern methods of synthesis, research, purification and identification of inorganic compounds. At the same time this book helps the students to gain

an insight into fundamental theoretical knowledge and to acquire skills in observation, systematization and logical thinking, which is indispensable for research in chemistry.

The book provides a means of practice and training in the following methods.

a) Syntheses and techniques with the exculsion of air and moisture high-vacuum and high-temperature techniques work in non-aqueous media (NH_3, N_2O_4), reactions under high pressure in autoclaves and electrolytic oxidation

b) Methods of purification, *viz.* ion-exchange TLC and column chromatography vacuum sublimation, extraction, recrystallization, etc.

c) Characterization of compounds by IR, UV, NMR and mass-spectrometry, optical rotation magnetic susceptibility by the study of chemical reactivity, the determination of reaction rates; measurement of ionic conductivity.

The book present 20 increasingly difficult exercises. For the manual work in the laboratory about three hours are needed for one exercise, except when noted otherwise.

Each experiment is described according to the following scheme. A theoretical introduction is given, which explains the synthesis and the mechanism of the reaction that yields the desired compound. The properties of the compound obtained are then given, its structure is shown, and the theories of the physical and physicochemical methods of its analysis are reviewed. A very precise, stepwise direction concerning the experimental work to be done follows; figures of the apparatus needed are shown; the purification of the chemicals and solvents to be used is described. The spectroscopic method suitable for the determination of the structure of the product or methods for other tests are discussed. Finally the principal directions of how a laboratory notebook should be composed are given.

There are some ten questions in this book, to be answered after the completion of each exercise, concerning the product, its chemical and physical properties, structure and spectroscopic behaviour. If the preparation is a more difficult or somewhat hazardous process, important safety precautions in the laboratory are pointed out.

A selection of relevant matter summarized under the title: "Independent Studies" at the end of each part and supplemented with references to the literature invites the student to go more deeply into the problems raised.

Every description of an exercise in this book ends with a summary of references to the literature.

The book begins with safety regulations to be observed in the exercises and ends with tables of data most helpful in this work; indeed it is an indispensable help to students to carry out these experiments.

This book is also a very good guide to the teaching of applied inorganic chemistry. It stimulates factual thinking and purposeful activity, sharpens the power of observation and suggests combined application of the methods acquired. It will probably be of considerable interest to those engaged in teaching chemistry.

J. NAGY

INDEX

PHYSICAL AND INORGANIC CHEMISTRY

ORGANIC CHEMISTRY

Printed in Hungary

A kiadásért felel az Akadémiai Kiadó igazgatója. Műszaki szerkesztő: Zacsik Annamária

A kézirat nyomdába érkezett: 1978. I. 19. — Terjedelem: 8,4 (A/5) ív, 27 ábra

78.5407 Akadémiai Nyomda, Budapest — Felelős vezető: Bernát György

ACTA CHIMICA

ТОМ 96—ВЫП. 4

РЕЗЮМЕ

Образование продуктов фотолиза масляного альдегида

Ш. ФЕРГЕТЕГ, Т. БЕРЦЕШ и Ш. ДОБЕ

Описывается экспериментальная техника и приводятся первые результаты детального исследования фотолиза масляного альдегида при 313 нм. Было идентифицировано двадцать продуктов фотолиза в паровой фазе и в изооктане. Приводятся квантовые выходы образовании продуктов при температуре 298°К и интенсивности светооблучения $3 \cdot 10^{-10}$ моль фотон $см^{-2}сек^{-1}$, а также обсуждаются основные пути образования продуктов. Было установлено семь фотохимических первичных процессов, протекающих как в паровой фазе, так и в растворе.

Ультразвуковое исследование молекулярных взаимодействий в жидком состоянии

Ш. ПРАКАШ, О. ПРАКАШ, К. С. ДВИВЕДИ и С. СИНГ

Молекулярные взаимодействия в бинарных системах н-бутанол + этиленгликоль (при 303,15°К) и н-бутанол + изоамиловый спирт (при 303,15°К) были исследованы на основе измерений скорости ультразвука. Приводятся адиабатическая сжимаемость, межмолекулярная свободная длина, колярный объем и возможные изменения объема в зависимости от состава. Результаты обсуждаются в свете молекулярных взаимодействий.

Корреляция геометрических и колебательных параметров групп SO_2 в молекулах сульфонов

Й. БРУНВОЛ и И. ХАРГИТТАИ

Приводятся переработанные эмпирические корреляции между геометрическими и колебательными параметрами молекул серий простых сульфонов. С этой точки зрения рассматриваются расчеты силовых постоянных и усреднение частот валентных колебаний S = O.

Структурная модель воды, II

Структура аморфного льда. Структурные зависимости воды и отдельных модификаций льда на основе тетрагональной кластерной модели

Ф. ХАЙДУ

Основные идеи тетрагональной кластерной модели воды предложенной ранее (Хайду, 1977) оказались применимыми и для отдельных модификаций аморфного льда. Экспериментальные результаты Нартена, Венкатеша и Райса (1976) могут быть интерпретированы с помощью кубической кластерной модели. На основе предложенной модели

может быть построена качественная физическая картина и объяснение получают последовательность по температуре и превращения структур двух модификаций аморфного льда, модификаций I_c и I_h кристаллического льда и воды. Геометрические изменение в молекулярном строении вытекают из относительных изменений силы водородных мостиков между ближайшими соседами и вандервалсовских взаимодействий между вторыми и последующими соседами.

Исследование конформации изобразпирилиевых солей с помощью ^{13}C—ЯМР и на основе квантово-механических расчетов, VIII

Изобензпирилиевые соли

М. ФАРКАШ, В. ВЁЛЬТЕР и М. ВАЙДА

Химические сдвиги спектров ^{13}C— ЯМР некоторых алкокси-замещенных 1-арилизо бензпирилиевых солей коррелируются с плотностями заряда по всем валентностям для раз личных атомов, рассчитанными по методу Дэль Бене Джяффе. На основе полученных данных корригируются отдельные спектральные отнесения. Было также показано, что плотности заряда и сдвиги находятся в хорошей корреляции, при том условии, если валентная ориентация sp^3 находится на атоме С-1.

Синтез алкалоидов винка и родственных им соединений, IV

Синтез аналогов (±) винкамина, содержащих дутильные группы

ДЬ. КАЛАУШ, П. ДЬЁРИ, Л. САБО и Ч. САНТАИ

Присоединение метилового эфира α-ацетоксиакриловой кислоты к энамину со строением *7* с дальнейшим восстановлением. приводит к стереоселективному одразованию сложного эфира спирта *9b*. Окисление последнего соединения дает рацемат-16-дезетил-16-н-бутилвинкамина (*1b*).

Синтез дибензо(a, d)циклогептена, трибензо(a,c,e)циклогептена и гетероциклических аналогов с целью конформационных исследований

М. НОГРАДИ

Описывается синтез дибензо [a, d] циклогептена, дибензо [b, f] азепина, дибензо [b, f] оксепина, дибензо[b,f] тиепина и трибензо [a, c, e] циклогептена, содержащих прохиральный заместитель и используемых в качестве маркера в конформационных исследованиях методом ЯМР.

Синтетическое исследование 2-0-β-D-галактофуранозил-D-арабинитола (Умбилицина)

М. М. А. АБДЕЛЬ-РАХМАН

2-О-β-D-Галактофуранозил-D-арабинитол (умбилицин) был синтезирован взаимодействием 1,3,4,5-тетра-О-бензил-D-арабинитола (спиртового компонента в глюкозидном синтезе) с 3,5,6-три-О-ацетил-1,2-О-метилортоацетил-α-D-галактофуранозой в присутствии бромистой ртути с последующим удалением защищающих групп. С помощью этого синтеза была определена структура умбилицина.

Les Acta Chimica paraissent en français, allemand, anglais et russe et publient des mémoires du domaine des sciences chimiques.

Les Acta Chimica sont publiés sous forme de fascicules. Quatre fascicules seront réunis en un volume (4 volumes par an).

On est prié d'envoyer les manuscrits destinés à la rédaction à l'adresse suivante:

Acta Chimica
H-1521 Budapest, Hongrie

Toute correspondance doit être envoyée à cette même adresse.

La rédaction ne rend pas de manuscript.

Le prix de l'abonnement: $ 36,00 par volume.

Abonnement en Hongrie à l'Akadémiai Kiadó (1363 Budapest, P.O.B, 24. C.C.B. Compte en banque 215 11488 à l'étranger à l'Enterprise Commerce Extérieur «Kultura» (H-1389 Budapest 62, P.O.B. 149. Compte-courant No. 218 10990) ou chez ses représentants à l'étranger.

Die Acta Chimica veröffentlichen Abhandlungen aus dem Bereich der chemischen Wissenschaften in deutscher, englischer, französischer und russischer Sprache.

Die Acta Chimica erscheinen in Heften wechselnden Umfanges. Vier Hefte bilden einen Band. Jährlich erscheinen 4 Bände.

Die zur Veröffentlichung bestimmten Manuskripte sind an folgende Adresse zu senden:

Acta Chimica
H-1521 Budapest, Ungarn

An die gleiche Anschrift ist jede für die Redaktion bestimmte Korrespondenz zu richten.

Manuskripte werden nicht zurückerstattet.

Abonnementspreis pro Band: $ 36,00.

Bestellbar für das Inland bei Akadémiai Kiadó (1363 Budapest, Postfach 24, Bankkonto Nr. 215 11488), für das Ausland bei «Kultura» Außenhandelsunternehmen (H-1389 Budapest 62, P.O.B. 149. Bankkonto Nr. 218 10990) oder seinen Auslandsvertretungen.

«Acta Chimica» издает статьи по химии на русском, французском, английском и немецком языках.

«Acta Chimica» выходит отдельными выпусками разного объема, 4 выпуска составляют один том и за год выходит 4 тома.

Предназначенные для публикации рукописи следует направлять по адресу:

Acta Chimica
H-1521 Budapest, BHP

Всякую корреспонденцию в редакцию направляйте по этому же адресу.

Редакция рукописей не возвращает.

Подписная цена — $ 36,00 за том.

Отечественные подписчики направляйте свои заявки по адресу Издательства Академии Наук (1363 Budapest, P.O.B. 24, Текущий счет 215 11488), а иностранные подписчики через организацию по внешней торговле «Kultura» (H-1389 Budapest 62, P.O.B. 149. Текущий счет 218 10990) или через ее заграничные представительства и уполномоченных.

Reviews of the Hungarian Academy of Sciences are obtainable at the following addresses:

AUSTRALIA
C.B.D. LIBRARY AND SUBSCRIPTION SERVICE, Box 4886, G.P.O., *Sydney N.S.W. 2001*
COSMOS BOOKSHOP, 135 Ackland Street, *St. Kilda (Melbourne), Victoria 3182*

AUSTRIA
GLOBUS, Höchstädtplatz 3, *1200 Wien XX*

BELGIUM
OFFICE INTERNATIONAL DE LIBRAIRIE, 30 Avenue Marnix, *1050 Bruxelles*
LIBRAIRIE DU MONDE ENTIER, 162 Rue du Midi, *1000 Bruxelles*

BULGARIA
HEMUS, Bulvar Ruszki 6, *Sofia*

CANADA
PANNONIA BOOKS, P.O. Box 1017, Postal Station "B", *Toronto, Ontario M5T 2T8*

CHINA
CNPICOR, Periodical Department, P.O. Box 50, *Peking*

CZECHOSLOVAKIA
MAD'ARSKÁ KULTURA, Národní třida 22, *115 66 Praha*
PNS DOVOZ TISKU, Vinohradská 66, *Praha 2*
PNS DOVOZ TLAČE, *Bratislava 2*

DENMARK
EJNAR MUNKSGAARD, Norregade 6, *1165 Copenhagen*

FINLAND
AKATEEMINEN KIRJAKAUPPA, P.O. Box 128, *SF-00101 Helsinki 10*

FRANCE
EUROPERIODIQUES S.A., 41 Avenue de Versailles, *78170 La Celle St.- Cloud*
LIBRAIRIE LAVOISIER, 11 rue Lavoisier, *75008 Paris*
OFFICE INTERNATIONAL DE DOCUMENTATION ET LIBRAIRIE, 38 rue Gay-Lussac, *75240 Paris Cedex 05*

GERMAN DEMOCRATIC REPUBLIC
HAUS DER UNGARISCHEN KULTUR, Karl-Liebknecht-Strasse 9, *DDR-102 Berlin*
DEUTSCHE POST ZEITUNGSVERTRIEBSAMT, Strasse der Pariser Kommüne 3—4, *DDR-104 Berlin*

GERMAN FEDERAL REPUBLIC
KUNST UND WISSEN ERICH BIEBER, Postfach 46, *7000 Stuttgart 1*

GREAT BRITAIN
BLACKWELL'S PERIODICALS DIVISION, Hythe Bridge Street, *Oxford OX1 2ET*
BUMPUS, HALDANE AND MAXWELL LTD., Cowper Works, *Olney, Bucks MK46 4BN*
COLLET'S HOLDINGS LTD., Denington Estate, *Wellingborough, Northants NN8 2QT*
W.M. DAWSON AND SONS LTD., Cannon House, *Folkestone, Kent CT19 5EE*
H. K. LEWIS AND CO., 146 Gower Street, *London WC1E 6BS*

GREECE
KOSTARAKIS BROTHERS, International Booksellers, 2 Hippokratous Street, *Athens-143*

HOLLAND
MEULENHOFF-BRUNA B.V., Beulingstraat 2, *Amsterdam*
MARTINUS NIJHOFF B.V., Lange Voorhout 9—11, *Den Haag*
SWETS SUBSCRIPTION SERVICE, 347b Heereweg, *Lisse*

INDIA
ALLIED PUBLISHING PRIVATE LTD., 13/14 Asaf Ali Road, *New Delhi 110001*
150 B-6 Mount Road, *Madras 600002*
INTERNATIONAL BOOK HOUSE PVT. LTD., Madame Cama Road, *Bombay 400039*
THE STATE TRADING CORPORATION OF INDIA LTD., Books Import Division, Chandralok, 36 Janpath, *New Delhi 110001*

ITALY
EUGENIO CARLUCCI, P.O. Box 252, *70100 Bari*
INTERSCIENTIA, Via Mazzé 28, *10149 Torino*
LIBRERIA COMMISSIONARIA SANSONI, Via Lamarmora 35, *50121 Firenze*
SANTO VANASIA, Via M. Macchi 58, *20124 Milano*
D.E.A., Via Lima 28, *00198 Roma*

JAPAN
KINOKUNIYA BOOK-STORE CO. LTD., 17-7 Shinjuku-ku 3 chome, Shinjuku-ku, *Tokyo 160-91*
MARUZEN COMPANY LTD., Book Department, P.O. Box 5056 Tokyo International, *Tokyo 100-31*
NAUKA LTD., IMPORT DEPARTMENT, 2-30-19 Minami Ikebukuro, Toshima-ku, *Tokyo 171*

KOREA
CHULPANMUL, *Phenjan*

NORWAY
TANUM-CAMMERMEYER, Karl Johansgatan 41—43, *1000 Oslo*

POLAND
WĘGIERSKI INSTYTUT KULTURY, Marszałkowska 80, *Warszawa*
CKP I W ul. Towarowa 28 *00-985 Warsaw*

ROMANIA
D. E. P., *Bucureşti*
ROMLIBRI, Str. Biserica Amzei 7, *Bucureşti*

SOVIET UNION
SOJUZPETCHATJ — IMPORT, *Moscow* and the post offices in each town
MEZHDUNARODNAYA KNIGA, *Moscow G-200*

SPAIN
DIAZ DE SANTOS, Lagasca 95, *Madrid 6*

SWEDEN
ALMQVIST AND WIKSELL, Gamla Brogatan 26, *S-101 20 Stockholm*
GUMPERTS UNIVERSITETSBOKHANDEL AB, Box 436, *401 25 Göteborg 1*

SWITZERLAND
KARGER LIBRI AG, Petersgraben 41, *4011 Basel*

USA
EBSCO SUBSCRIPTION SERVICES, P.O. Box 1943, *Birmingham, Alabama 35201*
F. W. FAXON COMPANY, INC., 15 Southwest Park, *Westwood, Mass, 02090*
THE MOORE-COTTRELL SUBSCRIPTION AGENCIES, *North Cohocton, N. Y. 14868*
READ-MORE PUBLICATIONS, INC., 130 Cedar Street, *New York, N. Y. 10006*
STECHERT-MACMILLAN, INC., 7250 Westfield Avenue, *Pennsauken N. J. 08110*

VIETNAM
XUNHASABA, 32, Hai Ba Trung, *Hanoi*

YUGOSLAVIA
JUGOSLAVENSKA KNJIGA, Terazije 27, *Beograd*
FORUM, Vojvode Mišića 1, *21000 Novi Sad*

3. VII. 1978 HU ISSN 0001—5407 **Index: 26.007**